Oxidative Medicine and Cellular Longevity

Redox Homeostasis and Cancer

Special Issue Editor in Chief: Mithun Sinha
Guest Editors: Adil Mardinoglu, Jayeeta Ghose, and Kanhaiya Singh

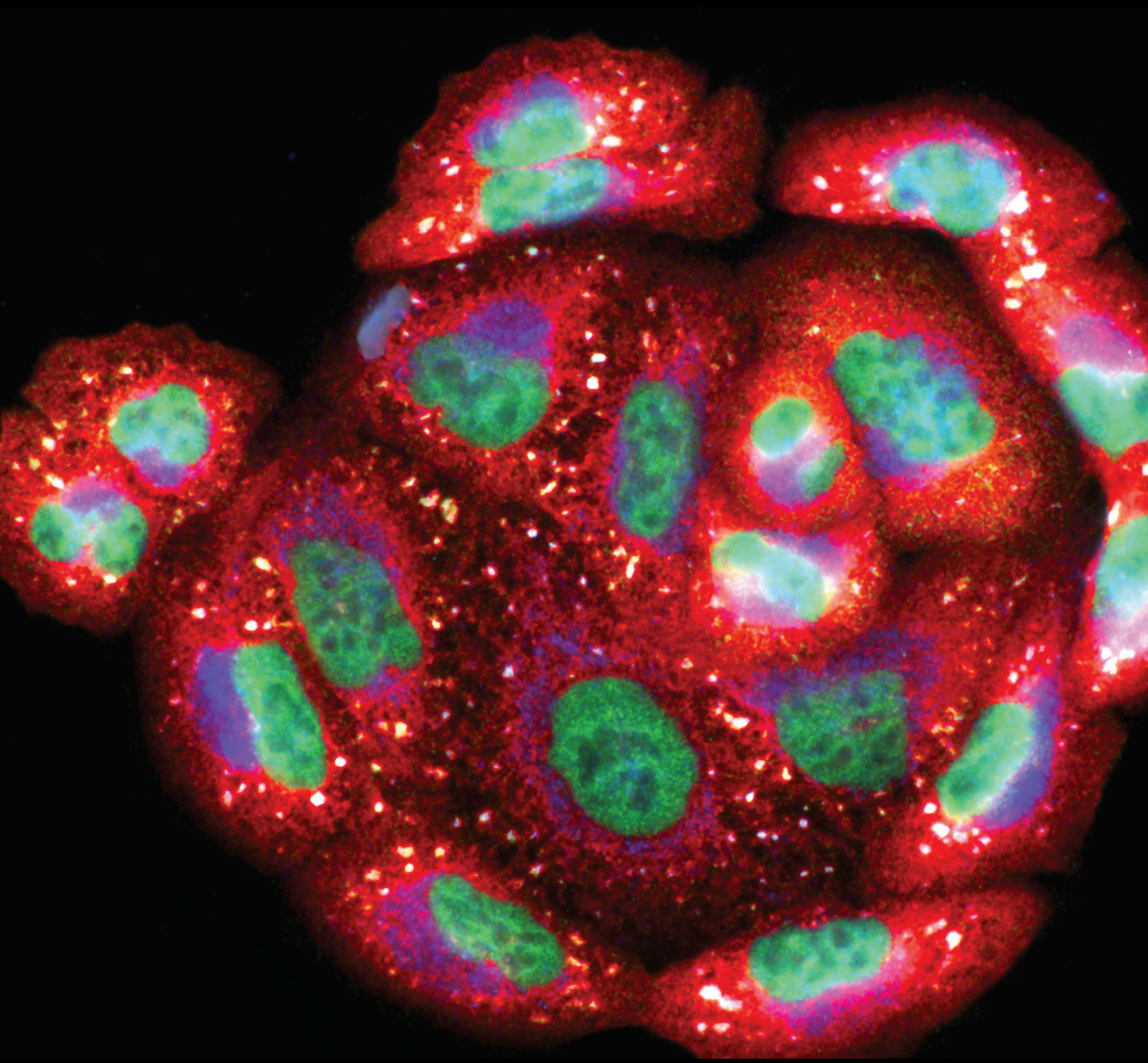

Redox Homeostasis and Cancer

Oxidative Medicine and Cellular Longevity

Redox Homeostasis and Cancer

Special Issue Editor in Chief: Mithun Sinha
Guest Editors: Adil Mardinoglu, Jayeeta Ghose, and Kanhaiya Singh

Contents

Contents

Hindawi
Oxidative Medicine and Cellular Longevity
Volume 2020, Article ID 5487381, 2 pages
https://doi.org/10.1155/2020/5487381

Editorial

Editorial: Redox Homeostasis and Cancer

Mithun Sinha,[1] **Adil Mardinoglu**,[2,3] **Jayeeta Ghose**,[4] **and Kanhaiya Singh**[1]

[1]*Indiana Center for Regenerative Medicine and Engineering, Indiana University School of Medicine, Indianapolis, Indiana 46202, USA*
[2]*Centre for Host-Microbiome Interactions, Department of Dentistry, Oral & Craniofacial Sciences, King's College London, London SE1 9RT, UK*
[3]*Science for Life Laboratory, KTH Royal Institute of Technology, Stockholm 17121, Sweden*
[4]*Comprehensive Cancer Center, Department of Radiation Oncology, The Ohio State University Wexner Medical Center, Columbus, Ohio 43210, USA*

Correspondence should be addressed to Mithun Sinha; mithun.sinp@gmail.com

Received 22 May 2020; Accepted 22 May 2020; Published 18 December 2020

Under physiological conditions, a balance between oxidants and antioxidants exists. Reactive oxygen species (ROS) are continuously generated by aerobic cells and eliminated through scavenging systems to maintain redox homeostasis. Disruption of redox homeostasis results in oxidative stress and altered ROS signaling. Higher ROS levels can lead to DNA mutation and genomic instability which can play causal role in cancer development and progression. These mutations coupled with distorted redox signaling pathways orchestrate pathologic events inside cancer cells, resulting in resistance to stress and death signals, aberrant proliferation, and inefficient repair mechanisms.

Cancer cells are energy intensive, owing to their high rate of proliferation. However, due to impaired TCA cycle and poor blood perfusion, cancer cells switch towards glycolytic pathway for energy generation termed as "Warburg effect." Such pathways lead to a higher oxidative environment. The oxidative environment is also enhanced by tumor-infiltrating macrophages and neutrophils. Thus, cancer cells are used to a high ROS environment. This redox imbalance allows for protumorigenic cell signaling. In this issue, we explore the relation between ROS and cancer. The issue comprises of twenty original articles and comprehensive reviews.

Reactive oxygen species (ROS) mediates cisplatin-induced cytotoxicity in tumor cells. However, when cisplatin-induced ROS do not reach cytotoxic levels, cancer cells may develop chemoresistance. Di Vito et al. reported the association of ferritin heavy subunit (FHC)-ROS axis with cisplatin resistance in ovarian cancer cells. Thus, implying that inhibition of FHC might be a potential approach for restoring cisplatin sensitivity of resistant ovarian cancer cells. The authors investigated whether the modulation of H-Ferritin might affect cisplatin-induced cytotoxicity in ovarian cancer cells. H-Ferritin knockdown strengthened cisplatin-mediated ROS increase and significantly restored sensitivity resistant ovarian cancer cells.

Studies by Zhao et al. in osteosarcoma cells found that metformin (drug for type 2 diabetes) suppressed the self-renewal ability of osteosarcoma stem cells (OSCs) and induced G0/G1 phase arrest by blocking the activity of cyclin-dependent kinases. Metformin triggered apoptosis in these cells, which promoted cell death *via* a ROS-dependent mitochondria-mediated pathway. Hämäläinen et al. investigated the expression of redox regulator nuclear factor erythroid-2-related factor (NRF)1 and NRF2 in skin lesions like naevi and melanoma from 172 patients. NRF1 and NRF2 are transcription factors essential for maintaining redox homeostasis and coordinating cellular stress responses. The study found the association of redox microRNAs (miRs) (miR-144, miR-212, and miR-510) with aggressive melanoma feature. This study opens up avenues to test these redox miRs as possible prognostic value in larger cohorts. The research article by Pires et al. described label-free mass spectrometry- (MS) based proteomics of breast cancer (BC)

plasma to investigate the differences between circulating proteins between chemoresponsive and chemoresistant luminal A breast cancer. Protein-protein interaction networks were created utilizing using *in silico* tools. The study reports interesting findings on differences in inflammatory, complement system, and oxidative stress pathways in both BC phenotypes which holds potential clinical implications. Moreira et al. presented their findings about the antitumor effect of celastrol, a natural pentacyclic triterpenoid, in colon cancer cells with acquired resistant to cytotoxic drugs. Yang et al. have evaluated the anticancer and anti-invasive properties of alpha-lipoic acid (ALA) in gastric cancer cells. ALA is a naturally occurring thiol antioxidant which is known to exhibit antiproliferative and cytotoxic effects on several cancers. The study found that the Mucin 4 (MUC4) gene was strongly expressed in human gastric cancer tissues. ALA administration reduced the proliferation and invasion of human gastric cancer cells by suppressing MUC4 expression. Helfinger et al. reported expression of Nox4 in macrophages and the role played by them in determining the polarization and the phenotype of macrophages. In the report by Acheva et al., authors showed epithelial to mesenchymal transition (EMT) in lung cancer cells postexposure to oxidative stress of gamma radiation. The authors conclude that induction of EMT in bronchial epithelial cells by radiation requires more than single acute exposure to gamma radiation and that the presence of stromal component might enhance the effect through free radical production and accumulation.

Gao et al. investigated the association of nitric oxide metabolites and lung cancer incidence through a matched case-control study based on the German ESTHER cohort. The study deduced that subjects with high urinary nitrite/nitrate concentrations had an increased risk of lung cancer. Butturini et al. highlighted plant-derived Sesquiterpene as a potential for cancer therapeutics. The authors exhibited that the compound downregulated STAT3 signaling leading to an antitumor effect and correlated the anti-STAT3 activity with their ability to decrease GSH levels in cancer cells. These properties make them lead compounds for the development of a new therapeutic strategy for cancer treatment.

In addition to these original works, Kim et al. listed a comprehensive report on the ROS-inducing strategy in anticancer therapy. The review by Xian et al. summarized the role of ROS in cutaneous carcinogenesis and skin cancer progression. Akanji et al. provides a comprehensive account of hypoxia-inducible factors (HIFs). In the review by Lv et al., the authors discussed recent understanding in the involvement of Glutathione (GSH) in cell death pathways such as apoptosis, necroptosis, ferroptosis, and autophagy. Goh et al. performed online literature search to identify studies reporting metabolic biomarkers of aerodigestive squamous cell carcinomas (ASCC). Akbari et al. have focused on the role of hydrogen sulfide in bladder, kidney, and prostate malignancies.

In the review by Tataranni et al., the authors have addressed the therapeutic potential of dichloroacetate (DCA) in cancer therapy. DCA is a 150 Dalton, water-soluble acid molecule, analog of acetic acid in which two of the three hydrogen atoms of the methyl group have been replaced by chlorine atoms. The authors have summarized recent reports suggesting the employment of DCA in cancer therapy, in combination with chemotherapy agents, radiotherapy, and other chemical or natural compounds showing anticancer properties. Paz et al. in their review have discussed the pharmacological effects and toxicogenetic impacts of omeprazole in context of cancer. This extensive report highlights that omeprazole therapy may induce genomic instability and increase the risk of certain types of cancer and hence advocates for taking adequate precautions, especially in long-term therapeutic strategies. The review by Fiocchetti et al. focused studies conducted on Neuroglobin (NGB), a globin primarily described in neurons as an oxidative stress sensor and cytoprotective factor against redox imbalance.

Although ROS sustain tumorigenesis and cancer progression, these can also be efficient therapeutic tools to fight cancer. Oxidative stress-based therapies like radiotherapy, chemotherapeutic agents, and photodynamic theory increase ROS levels in the tumor niche and take advantage of the cytotoxic face of ROS for killing tumor cells by a nonphysiologically sudden, localized, and intense oxidative burst. Clinical efficacy of anticancer therapies is often subdued by multidrug resistance (MDR). Redox therapy by using redox-active drugs or inhibitors of inducible antioxidant defense in tumor microenvironment has reported to be effective against MDR tumors. Further insight into such redox biology will enable precisely targeted manipulation of ROS for effective medical therapies against carcinomas.

Conflicts of Interest

The guest editors declare that this work was conducted in the absence of any commercial or financial relationships that could be construed as a potential conflict of interest.

Acknowledgments

We would like to thank all the authors who contributed to this special issue, as well as the reviewers who voluntarily participated in the review of manuscripts in a timely manner and provided their input to improve the manuscripts. Finally, we want to acknowledge the Editorial Board of Oxidative Medicine and Cellular Longevity for giving us this opportunity to publish this special issue.

Mithun Sinha
Adil Mardinoglu
Jayeeta Ghose
Kanhaiya Singh

Hindawi
Oxidative Medicine and Cellular Longevity
Volume 2020, Article ID 7095902, 15 pages
https://doi.org/10.1155/2020/7095902

Review Article

NOX2-Derived Reactive Oxygen Species in Cancer

Hanna Grauers Wiktorin,[1] Ebru Aydin,[1,2] Kristoffer Hellstrand,[1] and Anna Martner[1]

[1]*TIMM Laboratory, Salgrenska Center for Cancer Research, Department of Infectious Diseases, Institute of Biomedicin, Sahlgrenska Academy, University of Gothenburg, Sweden*
[2]*Molecular Genetics, German Cancer Research Center (DKFZ), Heidelberg, Germany*

Correspondence should be addressed to Anna Martner; anna.martner@gu.se

Received 2 August 2019; Accepted 21 October 2019; Published 30 November 2020

Academic Editor: Jayeeta Ghose

The formation of reactive oxygen species (ROS) by the myeloid cell NADPH oxidase NOX2 is critical for the destruction of engulfed microorganisms. However, recent studies imply that ROS, formed by $NOX2^+$ myeloid cells in the malignant microenvironment, exert multiple actions of relevance to the growth and spread of neoplastic cells. By generating ROS, tumor-infiltrating myeloid cells and $NOX2^+$ leukemic myeloid cells may thus (i) compromise the function and viability of adjacent cytotoxic lymphocytes, including natural killer (NK) cells and T cells, (ii) oxidize DNA to trigger cancer-promoting somatic mutations, and (iii) affect the redox balance in cancer cells to control their proliferation and survival. Here, we discuss the impact of NOX2-derived ROS for tumorigenesis, tumor progression, regulation of antitumor immunity, and metastasis. We propose that NOX2 may be a targetable immune checkpoint in cancer.

1. Introduction

1.1. Distribution and Function of NOX Enzymes. The NOX family of enzymes comprises seven structurally conserved isoforms, *i.e.*, NOX1-5 and DUOX1-2. The only known function of these transmembrane multicomponent enzymes is to catalyze the reduction of molecular oxygen to generate superoxide (O_2^-) or hydrogen peroxide (H_2O_2) [1, 2]. Superoxide is spontaneously or enzymatically converted to H_2O_2 that may be further converted to additional reactive oxygen species (ROS), including myeloperoxidase- (MPO-) derived hypochlorous acid and tyrosyl radical [3].

NOX enzymes differ in distribution between cell types in their subcellular localization and composition of subunits. NOX1 is mainly expressed in the colon, NOX2 on the lysosomal and plasma membranes of myeloid cells where it contributes to phagocyte killing of microbes, NOX3 in the inner ear and fetal tissues, NOX4 in the kidney, NOX5 in lymphoid tissue and testis, and DUOX1-2 in thyroid and gastrointestinal tissues [4, 5]. Low expression levels of NOX1 and NOX4 are also detected in myeloid cells [4, 6, 7], and NOX2 is minimally expressed by hematopoietic stem cells [8]. NOX2 is further expressed at low levels by B cells that may take up and, similar to myeloid cells, degrade microbial pathogens by generating NOX2-derived ROS [9]. Additionally, within dendritic cell (DC) phagolysosomes, NOX2 generates ROS in a process that consumes protons leading to alkalization of this compartment. This protects engulfed peptides from complete degradation by lysosomal proteases, which facilitates their presentation to cytotoxic T cells [10–12].

1.2. NOX Enzymes in Cancer. ROS formed from NOX enzymes have been implicated in carcinogenesis [13]. In addition, several NOX enzymes are expressed in malignant tissue and may contribute not only to cancer progression and spread but also to apoptosis of malignant cells. NOX1 is implicated in colon cancer where its ROS-producing activity may enhance tumor cell proliferation and metastasis [14, 15]. Myeloid leukemic cells express high levels of NOX2 that compromises destruction of malignant cells by triggering ROS-induced apoptosis of adjacent antileukemic lymphocytes [16–19]. Stem cell expression of NOX2 has been implicated in leukemogenesis by maintaining survival of leukemic stem cells [8]. NOX2 is further expressed by EBV-

Table 1: Tissue distribution, function, and cancer relevance of NOX enzymes.

Enzyme	Tissue expression (high to low)	Function	Cancer relevance
NOX1	Colon, uterus, prostate [24–28]	Repair of colon mucosa	Colon [14, 15, 29, 30] and prostate [31] cancers
NOX2	Myeloid cells [8, 32–34]	Host defense against pathogens, lymphocyte homeostasis, stem cell maintenance, myeloid cell differentiation	Myeloid leukemia [35, 36], melanoma [37, 38], lymphoma [32]
NOX3	Inner ear, fetal tissue [39–41]	Otoconia synthesis, organogenesis	Hepatocellular carcinoma [42]
NOX4	Kidney [43, 44]	Oxygen sensing*	Renal [45, 46] and ovarian [47] cancers, glioma [48], melanoma [49]
NOX5	Lymphoid tissue, testis [50, 51]	Lymphocyte differentiation, spermatozoa motility	Prostate cancer [52, 53], Barrett's esophageal adenocarcinoma [54]
DUOX1	Thyroid, respiratory tract [55–57]	Hormone synthesis, innate airway host defense	Thyroid [58, 59] and lung cancer[60, 61]
DUOX2	Thyroid, gastrointestinal tract [55, 62–65]	Hormone synthesis, regulation of gut microbiota/mucosa interactions	Thyroid [58, 66] and pancreatic cancer [67, 68]

infected gastric cancer cells to promote tumor progression [20] and by non-small-cell lung cancer cell lines, where it mediates tumor cell apoptosis [21]. NOX4 is overexpressed in several forms of cancer, including breast cancer, where it may enhance tumorigenesis [22], and prostate cancer, where it promotes apoptosis [23]. Table 1 summarizes the proposed physiological and pathophysiological functions of NOX enzymes.

Additionally, ROS from all cellular sources, including NOX-derived ROS, participate in redox signaling by oxidizing thiol groups on proteins, thus modifying cellular functions and activation status. For example, ROS may oxidize protein tyrosine phosphatases (PTPs) and protein kinase C (PKC) with ensuing effects on differentiation, proliferation, and survival of malignant cells [69–73].

1.3. The Myeloid NADPH Oxidase: NOX2. The first discovered and by far most extensively studied member of the NOX enzyme family, NOX2, is densely expressed by myeloid cells such as monocytes, macrophages, and granulocytes [2]. NOX2 is a complex of membrane-bound and cytosolic subunits that are spatially separated in resting cells. The membrane-bound subunits, $gp91^{phox}$ (also referred to as CYBB or NOX2) and $p22^{phox}$ (CYBA), constitute the catalytic core of the oxidase. The subunits $p47^{phox}$ (NCF1), $p67^{phox}$ (NCF2), and $p40^{phox}$ (NCF4) remain in the cytosol as a complex. Activation of NOX2 may be induced by pathogen-associated molecular patterns, danger-associated molecular patterns, bacterial peptides, growth factors, and cytokines, which trigger the cytosolic subunits $p47^{phox}$ (NCF1), $p67^{phox}$ (NCF2), and $p40^{phox}$ (NCF4) to translocate and assemble at the membrane [5, 74]. Two GTPases, Rac and Rap, are also critical for NOX2 activation [75, 76]. In its GTP-bound form, the cytosolic Rac interacts with $p67^{phox}$ and translocates to the membrane. Rap1 is a membrane protein with a partly unknown function that is required for optimal activation of NOX2 components [77] (Figure 1).

Phagocytes are stimulated to generate NOX2-derived ROS upon encountering microbes in a process referred to as a "respiratory burst." When the components of NOX2 assemble at the phagolysosome membrane, NOX2 generates intracellular ROS, while assembly at the plasma membrane leads to the formation of extracellular ROS [5, 78]. The respiratory burst is critical for phagocyte-mediated killing of microorganisms as highlighted by the susceptibility to bacterial and fungal infections in patients with chronic granulomatous disease, a rare genetic disorder caused by dysfunction of NOX2 [79–81], and by studies in mice that are genetically deprived of NOX2 [82]. NOX2 deficiency is also associated with hyperactive lymphocytes and autoimmunity in mice and humans, indicating that NOX2-derived ROS also participate in controlling lymphocyte reactivity [83–85]. Additionally, monocyte-derived DCs express NOX2, and the formation of NOX2-derived ROS by pathogen-activated DCs is proposed to reduce the potential transmission of pathogens to secondary lymphoid organs [86].

2. Redox Homeostasis

In addition to NOX-mediated formation of ROS, all cells generate ROS during mitochondrial ATP generation. In the process of oxidative phosphorylation, electrons pass through the electron transport chain where the final electron acceptor is oxygen, most of which is converted to water. Superoxide is produced as a byproduct in this process due to incomplete reduction of oxygen to water or premature electron leakage to oxygen [87, 88]. Intracellular levels of ROS affect cellular redox signaling and homeostasis, while ROS released into the surrounding, in particular H_2O_2 that is relatively stable and readily crosses cell membranes, may also affect adjacent cells [19, 89–91]. Under resting conditions, when there is a balance between ROS and antioxidants, redox signaling is reversible and regulates physiological processes due to the ability of ROS to reversibly oxidize cysteine residues to thus alter protein function [92, 93]. During environmental stress, infection, and inflammation, including cancer-related inflammation, the cell and tissue concentrations of ROS may increase beyond the capacity of the antioxidant defense systems. Such "oxidative stress" may result in irreversible oxidation and damage to proteins, lipids, and DNA [92]. Details

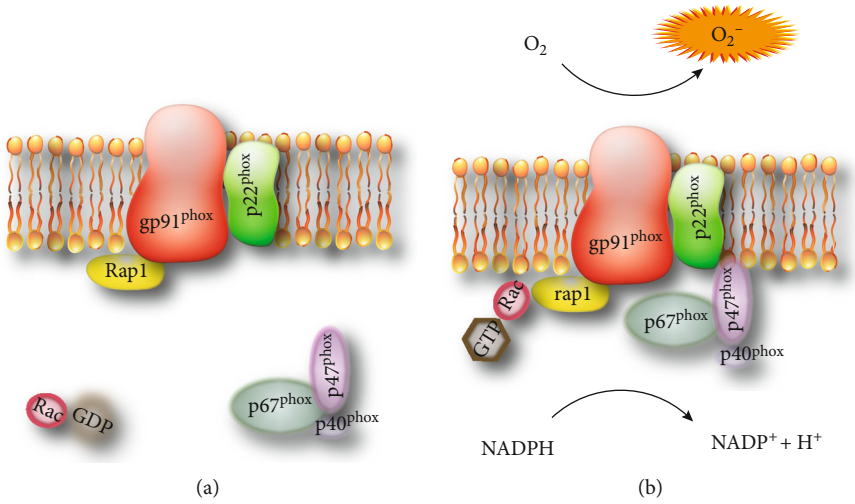

Figure 1: NOX2 in its resting and activated states. In its resting state (a), the membrane-bound and cytosolic subunits of NOX2 are spatially separated. Upon activation (b), the cytosolic subunits assemble with the membrane-bound subunits to generate O_2^-.

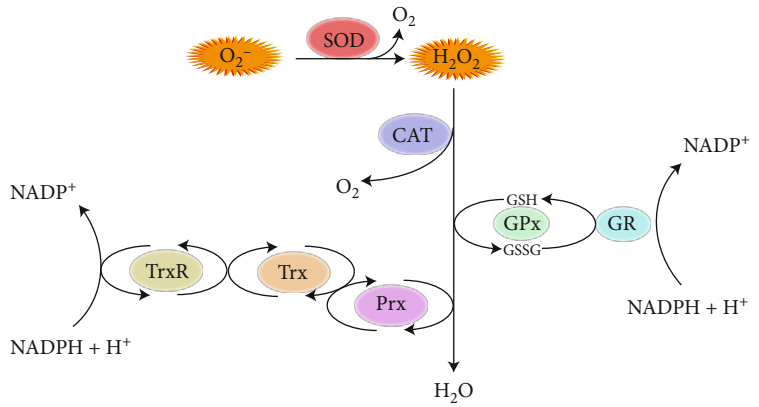

Figure 2: Mediators of redox homeostasis during the metabolism of O_2^-. Superoxide dismutase (SOD) catalyzes the conversion of O_2^- to H_2O_2. Catalase (CAT) metabolizes H_2O_2 into O_2 and H_2O. Glutathione peroxidase (GPx) detoxifies H_2O_2 by oxidation of reduced glutathione (GSH) to its oxidized form, GSSG. Intracellular GSH levels are regulated by glutathione reductase (GR). H_2O_2 is also metabolized by peroxiredoxin (Prx) that is recharged by thioredoxin (Trx). Trx is kept in a reduced state by thioredoxin reductase (TrxR).

regarding redox homeostasis and its impact on cancer have recently and comprehensively been reviewed [94, 95] and is beyond the major scope of this overview.

To avoid ROS-inflicted cell damage, several cellular systems that neutralize ROS are induced in an oxidative environment. The transcription factor Nrf2 is a key regulator of production of antioxidative enzymes within cells. In resting conditions, Nrf2 is bound to Keap1 in the cytoplasm, which prohibits Nrf2 from inducing gene transcription. Upon oxidation of cysteine residues in Keap1, Nrf2 is released and translocates to the nucleus where it binds to antioxidant response elements [96]. This process stimulates the transcription of Nrf2 target genes with cytoprotective functions. These include NAD(P)H quinone oxidoreductase 1, which catalyzes the reduction of reactive quinones that otherwise cause oxidative stress [97], heme oxygenase-1 (HO-1) that catalyzes the breakdown of heme [98], glutamate-cysteine ligase catalytic and modifier that catalyzes the rate-limiting step in synthesis of the endogenous antioxidant glutathione (GSH) [99], and thioredoxin reductase 1 that reduces peroxiredoxins of relevance to the detoxification of reactive peroxides, including H_2O_2 and peroxynitrite [100].

Other cellular antioxidant enzymes include superoxide dismutase, catalase, glutathione peroxidase-1, peroxiredoxins, and thioredoxin. Together with the nonenzymatic antioxidant GSH, these antioxidant enzymes are assumed to provide the most efficient protection from oxidative damage (Figure 2). Additional nonenzymatic scavengers of ROS include naturally occurring metabolites, vitamins (such as vitamins C and E) and iron chelators that prevent formation of hydroxyl radicals in the Fenton reaction [101, 102].

3. ROS and Cancer

3.1. Cancer-Related Oxidative Stress. Cancer may be associated with oxidative stress, *i.e.*, an imbalance between the

production and detoxification of ROS. Rapidly proliferating cancer cells have a high energy demand and therefore exhibit enhanced cellular respiration. Consequently, cancer cells generate enhanced levels of mitochondrial-derived ROS [89]. Growth factors and integrins, which are often produced at enhanced levels in cancer tissues, also contribute to enhanced NOX-derived ROS production [103] and, as reviewed above, several cancer histiotypes exhibit dysregulated expression of NOX enzymes [8, 14–17, 20–23]. Furthermore, solid and metastatic tumors are often infiltrated by $NOX2^+$ myeloid cells that may release ROS leading to an oxidized tumor microenvironment [104–108]. The extracellularly released ROS from myeloid cells affect redox regulation in adjacent tumor cells and may inactivate T cells and NK cells, thus compromising immune-mediated killing of malignant cells [19, 90, 91, 109–111]. Hypoxia is a common feature of the microenvironment of tumors that activates the hypoxia-inducible factor (HIF) family of transcription factors. HIFs mediate cellular adaptation to low oxygen levels and may influence several aspects of cancer such as promoting neovascularization [112], increasing cell survival [113], stimulating metastasis [114, 115], and conferring resistance to chemotherapeutics [116]. ROS may induce the activation of HIF-1α, a member of the HIF family of transcription factors, and thereby stimulate HIF-related cancer events [117].

The arguably most established role of ROS in cancer is its capacity to damage DNA with ensuing mutations and risk of cancer initiation and progression. Typically, deoxyguanosine is oxidized to 8-oxo-2-deoxyguanosine that may pair with adenine instead of cytosine, which promotes mutations in oxidatively stressed cells [118–121]. Overexpression of NOX enzymes, including NOX4, DUOX1, and DUOX2, has been shown to generate excessive H_2O_2 that may cause local tissue injury and DNA damage, thus resulting in the formation of a premalignant niche. NOX-derived ROS may thus contribute to tumor initiation and to tumor progression by inducing further DNA damage [122, 123].

Moreover, many cancer-related events, such as cell cycle proliferation, invasion, epithelial-to-mesenchymal transition, and metastasis are subject to redox regulation [47, 69–71, 73, 124–130]. For example, growth factors such as PDGF and EGF stimulate the PI3-K-AKT and RAS-MEK-ERK pathways, which are key regulators of cell proliferation and survival [131, 132]. These growth factors also stimulate NOX enzymes to produce ROS. The kinases in the PI3-K and RAS pathways phosphorylate target proteins, while PTPs serve to remove phosphate groups from proteins. This phosphorylation/dephosphorylation circuit alters protein function and controls cellular functions [133–135]. ROS may oxidize thiol groups in PTPs resulting in their inactivation. As a consequence, signaling along these pathways is boosted in an oxidative environment where PTPs are inactivated, and cancer cells may thus respond more vigorously to stimulation by growth factors [134, 135].

An additional example of the effects of ROS on PTPs is the inactivation of PTPs in pancreatic cancer cells that results in sustained activation of Janus kinase 2, which in turn activates signal transducer and activator of transcription (STAT) and antiapoptotic proteins to enhance tumor cell survival [72]. ROS may also oxidize and thus activate PKC; thereby, ROS modulate several PKC-dependent activities within cells [126, 136]. ROS have been proposed to enhance the tissue-invasive properties of cancer cells by modulating the function of mitogen-activated protein kinases via oxidation of PTPs and PKC [124–126]. However, as overproduction of ROS by cancer cells may trigger their apoptosis, the clinical efficacy of many therapies relies on induced ROS production in cancer cells, as further discussed below.

Tumor cells often show enhanced levels of antioxidative enzymes, presumably to resist the toxicity from the generation of NOX- and mitochondria-derived ROS [89]. In addition, tumor cells may acquire mutations that further boost antioxidative responses, thereby contributing to tumor cell resistance to oxidative stress. Approximately 30% of human lung cancers thus carry mutations in either Keap1 or Nrf2, resulting in Nrf2 stabilization and enhanced production of endogenous antioxidants [137]. One of the antioxidants controlled by Nrf2 is HO-1 that reduces intracellular levels of free heme; this, in turn, stabilizes the transcription factor BACH1 to activate transcription of genes that promote glucose uptake, glycolysis, and lactate secretion in the Warburg reaction [138]. Accordingly, BACH1 activation was shown to stimulate glycolysis-dependent metastasis of lung cancer cells [137, 138]. Thus, an antioxidative response by tumor cells, or antioxidative treatment strategies such as scavengers of ROS, may enhance tumorigenesis and metastasis by modulating tumor metabolism in favour of glycolysis.

3.2. Targeting NOX2 in Experimental Cancer Models. The development of knockout mice with NOX2 deficiency has been instrumental in studies on the role of ROS in cancer from sources other than mitochondria. Mice with deficiency in the NOX2 subunit Ncf1 show reduced growth or incidence of melanomas and the Lewis lung carcinoma tumors, whereas the growth of spontaneously arising prostate carcinoma or methylcholanthrene-induced sarcoma is not affected [38, 139].

Studies in knockout mice imply a role for NOX2 in metastasis. Mice deficient in the NOX2 subunit Cybb thus show reduced lung metastasis after intravenous inoculation of melanoma cells and a lower incidence of spontaneously formed metastases from surgically removed melanomas [37, 140, 141]. The targeting of NOX2 by systemic treatment with the NOX2 transduction inhibitor histamine dihydrochloride (HDC) reduced the formation of lung melanoma metastases in wild-type but not in *Nox2*-deficient mice. Effects of NOX2 repression on hematogenous metastasis were absent after the depletion of NK cells *in vivo* and absent also in interferon-γ- (IFN-γ-) deficient mice. These results thus imply that NOX2-derived ROS trigger the formation of melanoma metastasis by downmodulating NK cell functions, and that genetic or pharmacological inhibition of NOX2 restores tumor cell clearance exerted by IFN-γ^+ NK cells [37]. These results were confirmed and extended by Van der Weyden et al. showing that hematogenous metastasis was markedly reduced in mice genetically depleted of any of the major NOX2 subunits (Cyba, Cybb, Ncf1, Ncf2, and Ncf4) and that tumor tissues of NOX2-deficient mice showed

a marked increase of antineoplastic lymphocytes [141]. In accordance with the latter finding, treatment with the NOX2 inhibitor HDC resulted in enhanced NK cell counts in the lungs of wild-type mice with pulmonary melanoma metastases, but not in corresponding lungs from *Nox2*-deficient mice [37].

HDC suppresses ROS formation by exerting agonist activity at histamine type 2 receptors (H_2Rs) [18] and thus inhibits NOX2 signal transduction rather than directly inhibiting, *e.g.*, oxidase function or assembly. The detailed mechanisms of NOX2 inhibition and the ensuing protection of antineoplastic lymphocytes are incompletely understood. Myeloid cells deficient of MPO still exerted immunosuppression towards NK cells, which was reversible by HDC-treatment, thus suggesting that O_2^- and H_2O_2 are more likely mediators of NOX2-induced immunosuppression than MPO-derived ROS such as, *e.g.*, hypochlorous acid or tyrosyl radicals [142]. Additionally, circumstantial evidence links the NOX2-inhibitory properties of HDC to the PI3-K pathway. Activation of PI3-K thus activates Akt and PKC that triggers the assembly and ROS formation of NOX2 [143]. HDC suppresses NOX2-mediated ROS formation induced by fMLF and other bacterial peptides, but does not affect PMA-induced respiratory burst [144]. As fMLF activates the PI3-K pathway [145] whereas PMA directly induces the activation of PKC, these finding thus suggest that HDC, by activating H_2Rs, targets the PI3-K pathway upstream of PKC in myeloid cells. In support for this hypothesis, PI3-K inhibitors share the NOX2 inhibition exerted by HDC and equally efficiently protect antineoplastic lymphocytes from apoptosis and dysfunction induced by adjacent, ROS-producing myeloid cells [146].

Systemic treatment with HDC *in vivo* suppresses tumor growth in several models of experimental cancer [147]. While these antitumor effects of HDC are likely pleiotropic, it is noteworthy that beneficial effects of treatment with HDC in murine melanoma, lymphoma, and mammary cancer were only observed in NOX2-sufficient mice [32, 35, 37, 148] and that HDC only inhibited growth of $NOX2^+$ and not $NOX2^-$ leukemic cells in a xenograft setting [35]. Additionally, the efficacy of HDC in reducing murine tumor growth and metastasis relied on the presence of NOX2-expressing $Gr1^+$ myeloid cells since the effect was lost upon $Gr1^+$ cell depletion [37, 148]. Furthermore, experiments using single-cell suspensions from tumors, spleens, and lungs suggested that ROS formation was confined to the $Gr1^+$ cell fraction [37, 148]. These findings, along with results showing that HDC does not reduce metastasis after the depletion of NK cells, support the hypothesis that HDC provides a less immunosuppressive malignant microenvironment that favors NK cell-mediated clearance of tumor cells [37, 83]. Additionally, treatment with HDC was shown to increase the number of tumor-infiltrating effector $CD8^+$ T cells in murine lymphoma and to improve the antitumor efficacy of immune checkpoint inhibitors (anti-PD-1 and anti-PD-L1) [148], thus implying that HDC may facilitate also T cell-dependent elimination of tumor cells.

Monocytic leukemic cells recovered from patients with acute myeloid leukemia (AML) frequently express functional NOX2, and studies in xenografted mice support that NOX2 is relevant to the survival and expansion of monocytic AML cells [35, 149]. NOX2-derived ROS have been proposed to stimulate the transfer of prosurvival mitochondria from stromal cells to AML cells [149]. Furthermore, NOX2 inhibition by HDC reduced the expansion of xenografted $NOX2^+$ but not of $NOX2^-$ human AML cells, presumably by hindering S-phase entry of leukemic cells [35]. These results illustrate that the targeting of NOX2 may reduce malignant expansion independently of functional cellular immunity.

In addition, results obtained in a mouse model of Kras-induced myeloid leukemia showed that $Kras^+$ NOX2-deficient myeloid cells ($Nox2^{-/-}$M-$Kras^{G12D}$) expanded slower than their NOX2-sufficient counterparts. In this model, treatment of mice with *N*-methyl-histamine (an H_2R-selective analogue of HDC that shares the NOX2-inhibitory properties of HDC) reduced leukemic expansion and prolonged the survival of NOX2-sufficient but not of NOX2-deficient mice. *N*-Methyl-histamine-treated mice harbored leukemic cells with reduced intracellular ROS levels, reduced DNA oxidation, and reduced double-stranded DNA breaks [150]. These results thus imply that NOX2-derived ROS may promote genomic instability and malignant expansion in Kras-induced leukemia. NOX2 may also support myeloid expansion of murine $Bcr\text{-}Abl1^+$ cells as transplantation of $NOX2^+Bcr\text{-}Abl1^+$ cells into irradiated mice causes a more rapidly expanding and severe leukemia than the transfer of NOX2-deficient $Bcr\text{-}Abl1^+$ cells [8, 151].

4. Myeloid-Derived Suppressor Cells and NOX2

4.1. Myeloid Cells within the Tumor Microenvironment. The presence of cytotoxic lymphocytes, including $CD8^+$ T cells and/or NK cells, in the microenvironment of human cancer tumors is typically prognostically favorable, while the presence of infiltrating myeloid cells often, although not invariably, predicts poor survival [104–107, 152–159]. Hence, a high ratio of tumor-infiltrating T cells to myeloid cells entails favorable prognosis in several cancer forms including lung cancer, bladder cancer, glioblastoma, prostate cancer, and renal cell carcinoma [160–166]. In recent years, the neutrophil to lymphocyte ratio and the monocyte to lymphocyte ratio in peripheral blood have emerged as readily available and independent predictors of poor survival in several forms of solid cancer [167], thus underscoring that myeloid cell-induced immunosuppression may impact adversely on cancer prognosis.

Myeloid-derived suppressor cells (MDSCs) are immature and immunosuppressive myeloid cells that accumulate in the tumor microenvironment and in the periphery in patients with cancer. MDSCs comprise pathologically induced myeloid cells of the monocytic (M-MDSCs) and granulocytic (G-MDSC) linages that suppress T cells and NK cells by several mechanisms, including enhanced production of immunosuppressive NOX2-derived ROS, arginase, nitric oxide (NO), TGF-beta, and IL-10 [168]. MDSCs are thus assumed to favor immune escape in cancer [169, 170]. MDSCs and other myeloid cells are attracted to tumors in response to

cytokines such as CCL2 and CSF1 for M-MDSCs and CXCL1 and CXCL8 for G-MDSCs [171]. Once in the tumor microenvironment, M-MDSCs may differentiate into tumor-associated macrophages (TAMs) or DCs. TAMs may also originate from infiltrating monocytes and tissue-resident macrophages [172]. MDSCs and TAMs may release soluble molecules such as cytokines, prostaglandins, chemokines, interleukins, and growth factors into the tumor microenvironment that may contribute to the formation of premetastatic niches, promote angiogenesis, promote tumor cell survival, and enhance tumor cell invasion [173, 174]. These properties of MDSCs and TAMs may, in part, account for the unfavorable association between myeloid cell tumor infiltration and prognosis.

TAMs exhibit either M1 or M2 polarization. The M1-polarized TAMs express iNOS and TNF and are denoted proinflammatory, whereas the M2-polarized TAMs produce the L-arginine-depleting enzyme arginase and secrete IL-10 to compromise immune activation [171, 175]. M1 and M2 macrophages both express NOX2, although the expression level is higher in M1 macrophages [176]. Mice lacking NOX1 and NOX2 showed reduced M2 macrophage polarization, while single knockout of NOX1 or NOX2 did not [6]. Hence, in the Lewis lung carcinoma model, wild-type and NOX1/NOX2 double-knockout mice showed a similar degree of TAM infiltration, while the content of M2-TAMs was reduced in the double-knockout mice along with reduced tumor growth [6]. These results imply that inhibition of NOX enzymes may favor M1 polarization in cancer; however, studies of nonmalignant inflammation (spinal cord inflammation in mice) suggest that inhibition of NOX2 instead reduces M1 polarization [177], and further studies are required to define the impact of NOX enzymes on macrophage polarization.

In contrast to MDSCs and M2-TAMs, the intratumoral accumulation of other myeloid cells, such as DCs and M1-polarized TAMs, may indicate favorable cancer prognosis [178–181]. Tumor-infiltrating DCs initiate the induction of tumor-specific T cell responses and are thus critical to evoke antitumor immunity, and M1 polarized macrophages may contribute in the killing of tumor cells [182]. While the favorable impact of the presence of M1-polarized macrophages in cancer tumors is well established, the subdivision of macrophages into distinct populations is challenged by reports showing that TAMs often display features of both M1 and M2 subsets [183, 184].

4.2. Immunosuppression by MDSC-Derived ROS. Early studies showed that MDSCs displayed enhanced expression of NOX2 as a result of the activation of the transcription factor STAT3 [185, 186]. The formation of NOX2-derived ROS is considered a major immunosuppressive action mediated by MDSCs, in particular by G-MDSCs [148, 186, 187], and ROS-producing MDSCs or other immunosuppressive myeloid cells thus induce apoptosis or dysfunction in adjacent lymphocytes such as NK cells and T cells [19, 91, 188–190]. ROS induce activation of ERK1/2 in lymphocytes, which results in PARP-1-dependent accumulation of poly-ADP-ribose (PAR) and parthatanosis (a form of apoptosis) [191].

In addition, MDSC-derived ROS inhibit antigen-specific $CD8^+$ T cell responses and may thus selectively eradicate antitumor T cell clones [188]. The immunosuppression exerted by ROS towards T cells has been linked to nitration of the T cell receptor (TCR) and occurs when ROS react with NO to form peroxynitrite during MDSC-T cell interactions. Nitration was proposed to induce a conformational change of the TCR, and T cells thus display reduced affinity for MHC-peptide complexes [192]. This effect was linked to ROS as MDSCs with dysfunctional NOX2 did not suppress antigen-specific T cell responses [186]. On a similar note, MDSCs isolated from mice systemically treated with the NOX2 inhibitor HDC produced lower levels of ROS and were less prone to suppress T cells *ex vivo* [148].

4.3. ROS as Inhibitors of Myeloid Cell Differentiation. MDSCs isolated from mice with myeloid cells that cannot generate NOX2-derived ROS, *i.e.*, *Stat3* or *Nox2* knockout mice, are prone to differentiate towards mature macrophages and DCs [186, 193] suggesting that NOX2-derived ROS inhibit myeloid cell maturation and thus promote the accumulation of immature MDSCs. Furthermore, the antioxidant N-acetyl cysteine (NAC) was found to trigger differentiation of MDSCs [194]. Similarly, all-*trans*-retinoic acid (ATRA), which upregulates the antioxidant glutathione synthase and thus reduces intracellular ROS, stimulates the differentiation of MDSCs in murine tumor models and of MDSCs isolated from cancer patients [195–198]. In agreement with these reports, treatment with the NOX2 inhibitor HDC reduces the accumulation of tumor-infiltrating MDSCs in EL-4 thymoma-bearing mice. The reduction of tumor-infiltrating MDSCs was accompanied by augmented levels of intratumoral DCs and by improved maturation of human DCs from monocytes [32, 148]. Figure 3 summarizes aspects of NOX2-mediated regulation of myeloid cell differentiation in cancer.

5. Targeting ROS in Human Cancer

While low ROS levels in cells are reportedly mitogenic due to the activation of the PI3-K-AKT and RAS-MEK-ERK pathways [131, 132], high ROS levels are toxic to numerous cell types including cancer cells [92, 118–121]. Several chemotherapies, as well as radiotherapy and photodynamic therapy, trigger excessive ROS production within cells. Oxidants may thus contribute to the elimination of tumor cells and to the toxicity of chemotherapeutics [199]. In addition, several antitumor agents, including erlotinib and silibinin, trigger overproduction of ROS via NOX enzymes, which contributes to killing tumor cells [21, 23].

Despite that increased intracellular ROS levels may induce killing of malignant cells, ROS have also been ascribed protumorigenic properties. Antioxidative strategies have thus been evaluated for human cancer therapy and prevention. Such strategies include ROS scavengers such as NAC, vitamin E, and beta-carotene that are aimed at reducing oxidative stress [200–202]. These studies, as well as animal experiments comprising the administration of ROS scavengers in cancer treatment, have shown partly divergent results. Whereas some studies support that antioxidants reduce the

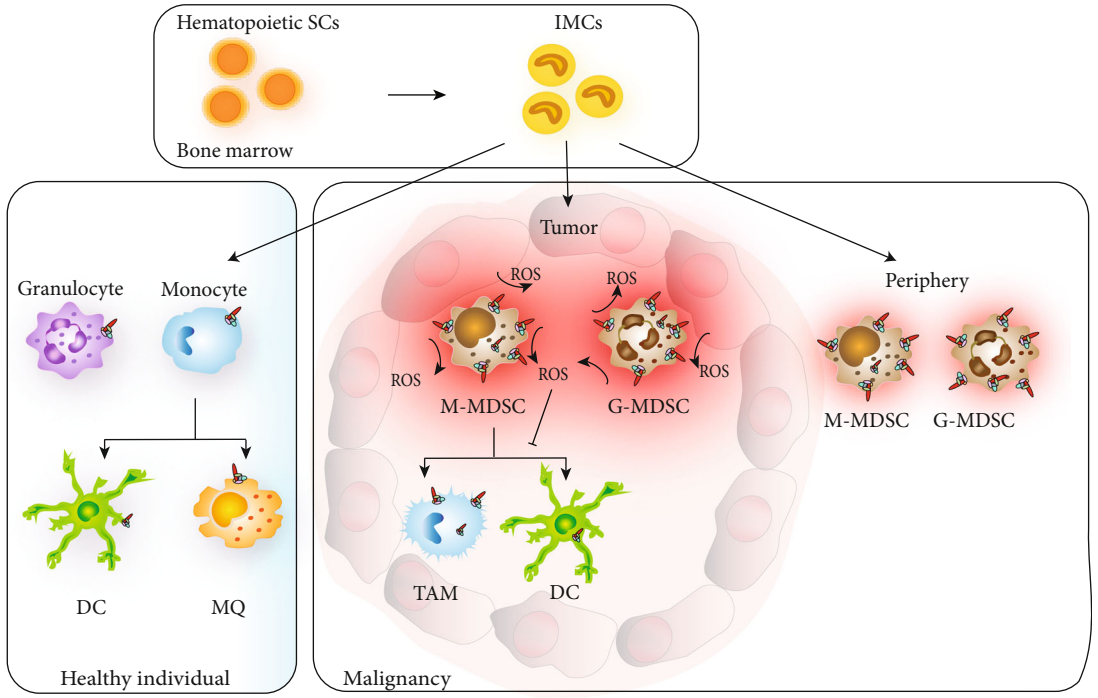

Figure 3: Myeloid cell differentiation in healthy individuals and in cancer patients. Hematopoietic stem cells (SC) differentiate into immature myeloid cells (IMCs) in bone marrow. In healthy individuals, IMCs rapidly differentiate into mature myeloid cell populations in the periphery. In cancer, however, myeloid cell differentiation is often impaired, and the IMCs may be activated to become monocytic or granulocytic myeloid-derived suppressor cells (M- and G-MDSCs, respectively) within tumors and in the periphery. MDSCs show upregulated NOX2 expression and increased production of reactive oxygen species (ROS), in particular in the G-MDSCs. The M-MDSCs may differentiate into tumor-associated macrophages (TAM) or dendritic cells (DC), and the differentiation may be inhibited by excessive intracellular ROS levels.

risk of cancer [200–202], other studies, in particular those involving the administration of antioxidants to smokers to prevent lung cancer, imply enhanced cancer risk by the administration of antioxidants[203].

The mechanisms explaining the partly opposing results in studies of broad antioxidants in cancer remain to be elucidated. Recent studies imply that antioxidants trigger the activation of the transcription factor BACH1 that stimulates a metabolic reprogramming of cancer cells in favor of glycolysis, which enhances their capacity to metastasize [137, 138]. These findings may appear counterintuitive in light of the abovereferenced reduction of metastasis induced by HDC and other NOX2 inhibitors that act by reducing ROS levels. However, a noticeable difference between global antioxidants and HDC is that HDC targets NOX2-derived ROS formation only in myeloid cells that coexpress H_2R and NOX2. HDC or other NOX2-inhibitory strategies are hence unlikely to alter metabolically generated ROS.

ATRA is used in the treatment of acute promyelocytic leukemia where the leukemic cells carry a PML-RARA translocation giving rise to a block in myeloid cell differentiation and development of leukemia. ATRA releases this block and allows the differentiation of immature leukemic promyelocytes into mature granulocytes [204]. ATRA may also promote the differentiation of MDSCs by neutralizing intracellular ROS [195–198]. ATRA exerts antitumoral effects in several murine models [205, 206] and has been investigated in combination with immunotherapies such as IL-2 and DC vaccines in renal cell carcinoma and non-small-cell lung cancer [205–207]. The efficacy of ATRA combined with ipilimumab is currently assessed in stage IV melanoma (ClinicalTrials.gov identifier: NCT02403778).

The NOX2-inhibitor HDC is used in conjunction with low-dose IL-2 within the EU to prevent relapse of AML in the postchemotherapy phase [208]. HDC acts on H_2Rs expressed on the surface of normal and leukemic myeloid cells to inhibit production of NOX2-derived ROS [208, 209]. *In vitro* studies support that HDC promotes cellular immunity by protecting subsets of cytotoxic lymphocytes against ROS-induced inactivation [19, 91] and that these effects of HDC are markedly enhanced by the coadministration of NK and T cell activators such as IL-2 [111]; however, complementary or alternative mechanisms are conceivable, including HDC-induced differentiation of AML cells [19, 35, 208]. While the side-effects of HDC/IL-2 were typically mild and transient with minimal impact on global health [208, 210], the incidence of grade 1/2 arthralgia and myalgia was slightly but significantly higher in treated patients. It may thus be speculated that HDC/IL-2 induces autoimmunity similar to that observed in NOX2-deficient CGD patients and in experimental animals that are devoid of functional NOX2 [83].

6. Conclusion

While details regarding the contribution by NOX2-derived ROS for the induction and progression of cancer remain to be elucidated, it seems likely that the impact of NOX2 is confined mainly to primary and metastatic tumors that are infiltrated by immunosuppressive $NOX2^+$ myeloid cells and to myeloid leukemias, where the malignant clone comprises $NOX2^+$ cells. In cancer, NOX2 may contribute to the immunosuppression exerted by myeloid cells, in part by producing extracellular ROS that trigger dysfunction in adjacent lymphocytes. Recent studies show that NOX2 promotes tumor growth and metastasis and that intact NOX2 is crucial for self-tolerance, thus fulfilling the criteria of an immune checkpoint [83]. Inhibition of NOX2-derived ROS may thus relieve immunosuppression in cancer and may act in synergy with cancer immunotherapies such NK and T cell-activating cytokines or checkpoint inhibitors.

Conflicts of Interest

Authors HGW, KH, and AM hold issued or pending patents that protect the use of NOX2-inhibitors in cancer.

References

[1] Y. Nisimoto, B. A. Diebold, D. Cosentino-Gomes, and J. D. Lambeth, "Nox4: a hydrogen peroxide-generating oxygen sensor," *Biochemistry*, vol. 53, no. 31, pp. 5111–5120, 2014.

[2] K. Bedard and K. H. Krause, "The NOX family of ROS-generating NADPH oxidases: physiology and pathophysiology," *Physiological Reviews*, vol. 87, no. 1, pp. 245–313, 2007.

[3] J. W. Heinecke, W. Li, G. A. Francis, and J. A. Goldstein, "Tyrosyl radical generated by myeloperoxidase catalyzes the oxidative cross-linking of proteins," *Journal of Clinical Investigation*, vol. 91, no. 6, pp. 2866–2872, 1993.

[4] K. H. Krause, "Tissue distribution and putative physiological function of NOX family NADPH oxidases," *Jpn J Infect Dis*, vol. 57, no. 5, pp. S28–S29, 2004.

[5] A. Panday, M. K. Sahoo, D. Osorio, and S. Batra, "NADPH oxidases: an overview from structure to innate immunity-associated pathologies," *Cell Mol Immunol*, vol. 12, no. 1, pp. 5–23, 2015.

[6] Q. Xu, S. Choksi, J. Qu et al., "NADPH oxidases are essential for macrophage differentiation," *Journal of Biological Chemistry*, vol. 291, no. 38, pp. 20030–20041, 2016.

[7] J. S. Moon, K. Nakahira, K. P. Chung et al., "NOX4-dependent fatty acid oxidation promotes NLRP3 inflammasome activation in macrophages," *Nature Medicine*, vol. 22, no. 9, pp. 1002–1012, 2016.

[8] B. Adane, H. Ye, N. Khan et al., "The hematopoietic oxidase NOX2 regulates self-renewal of leukemic stem cells," *Cell Reports*, vol. 27, no. 1, pp. 238–254.e6, 2019.

[9] I. Á. Kovács, M. Horváth, Á. Lányi, G. L. Petheő, and M. Geiszt, "Reactive oxygen species-mediated bacterial killing by B lymphocytes," *Journal of Leukocyte Biology*, vol. 97, no. 6, pp. 1133–1137, 2015.

[10] A. Savina, C. Jancic, S. Hugues et al., "NOX2 controls phagosomal pH to regulate antigen processing during crosspresentation by dendritic cells," *Cell*, vol. 126, no. 1, pp. 205–218, 2006.

[11] A. R. Mantegazza, A. Savina, M. Vermeulen et al., "NADPH oxidase controls phagosomal pH and antigen cross-presentation in human dendritic cells," *Blood*, vol. 112, no. 12, pp. 4712–4722, 2008.

[12] I. Dingjan, D. R. J. Verboogen, L. M. Paardekooper et al., "Lipid peroxidation causes endosomal antigen release for cross-presentation," *Scientific Reports*, vol. 6, no. 1, 2016.

[13] D. Xian, R. Lai, J. Song, X. Xiong, and J. Zhong, "Emerging perspective: role of increased ROS and redox imbalance in skin carcinogenesis," *Oxidative Medicine and Cellular Longevity*, vol. 2019, Article ID 8127362, 11 pages, 2019.

[14] H. P. Wang, X. Wang, L. F. Gong et al., "Nox1 promotes colon cancer cell metastasis via activation of the ADAM17 pathway," *European Review for Medical and Pharmacological Sciences*, vol. 20, no. 21, pp. 4474–4481, 2016.

[15] A. Juhasz, S. Markel, S. Gaur et al., "NADPH oxidase 1 supports proliferation of colon cancer cells by modulating reactive oxygen species-dependent signal transduction," *Journal of Biological Chemistry*, vol. 292, no. 19, pp. 7866–7887, 2017.

[16] J. Aurelius, F. B. Thorén, A. A. Akhiani et al., "Monocytic AML cells inactivate antileukemic lymphocytes: role of NADPH oxidase/gp91phox expression and the PARP-1/PAR pathway of apoptosis," *Blood*, vol. 119, no. 24, pp. 5832–5837, 2012.

[17] J. Aurelius, A. Martner, R. E. Riise et al., "Chronic myeloid leukemic cells trigger poly(ADP-ribose) polymerase-dependent inactivation and cell death in lymphocytes," *Journal of Leukocyte Biology*, vol. 93, no. 1, pp. 155–160, 2013.

[18] U. H. Mellqvist, M. Hansson, M. Brune, C. Dahlgren, S. Hermodsson, and K. Hellstrand, "Natural killer cell dysfunction and apoptosis induced by chronic myelogenous leukemia cells: role of reactive oxygen species and regulation by histamine," *Blood*, vol. 96, no. 5, pp. 1961–1968, 2000.

[19] K. Hellstrand, A. Asea, C. Dahlgren, and S. Hermodsson, "Histaminergic regulation of NK cells: role of monocyte-derived reactive oxygen metabolites," *Journal of Immunology*, vol. 153, no. 11, pp. 4940–4947, 1994.

[20] S. M. Kim, D. Y. Hur, S. W. Hong, and J. H. Kim, "EBV-encoded EBNA1 regulates cell viability by modulating miR34a-NOX2-ROS signaling in gastric cancer cells," *Biochem Biophys Res Commun*, vol. 494, no. 3-4, pp. 550–555, 2017.

[21] S. W. Hong, N. S. Park, M. H. Noh et al., "Combination treatment with erlotinib and ampelopsin overcomes erlotinib resistance in NSCLC cells via the Nox2-ROS-Bim pathway," *Lung Cancer*, vol. 106, pp. 115–124, 2017.

[22] B. Zhang, Z. Liu, and X. Hu, "Inhibiting cancer metastasis via targeting NAPDH oxidase 4," *Biochem Pharmacol*, vol. 86, no. 2, pp. 253–266, 2013.

[23] S. H. Kim, K. Y. Kim, S. N. Yu et al., "Silibinin induces mitochondrial NOX4-mediated endoplasmic reticulum stress response and its subsequent apoptosis," *BMC Cancer*, vol. 16, no. 1, p. 452, 2016.

[24] B. Bánfi, R. A. Clark, K. Steger, and K.-H. Krause, "Two novel proteins activate superoxide generation by the NADPH oxidase NOX1," *Journal of Biological Chemistry*, vol. 278, no. 6, pp. 3510–3513, 2003.

[25] X. L. Cui, D. Brockman, B. Campos, and L. Myatt, "Expression of NADPH oxidase isoform 1 (Nox1) in human placenta: involvement in preeclampsia," *Placenta*, vol. 27, no. 4-5, pp. 422–431, 2006.

[26] Y. A. Suh, R. S. Arnold, B. Lassegue et al., "Cell transformation by the superoxide-generating oxidase Mox1," *Nature*, vol. 401, no. 6748, pp. 79–82, 1999.

[27] M. Kato, M. Marumo, J. Nakayama, M. Matsumoto, C. Yabe-Nishimura, and T. Kamata, "The ROS-generating oxidase Nox1 is required for epithelial restitution following colitis," *Experimental Animals*, vol. 65, no. 3, pp. 197–205, 2016.

[28] I. Szanto, L. Rubbia-Brandt, P. Kiss et al., "Expression of NOX1, a superoxide-generating NADPH oxidase, in colon cancer and inflammatory bowel disease," *The Journal of Pathology*, vol. 207, no. 2, pp. 164–176, 2005.

[29] M. Fukuyama, K. Rokutan, T. Sano, H. Miyake, M. Shimada, and S. Tashiro, "Overexpression of a novel superoxide-producing enzyme, NADPH oxidase 1, in adenoma and well differentiated adenocarcinoma of the human colon," *Cancer Lett*, vol. 221, no. 1, pp. 97–104, 2005.

[30] E. Laurent, J. W. McCoy, R. A. Macina et al., "Nox1 is over-expressed in human colon cancers and correlates with activating mutations in K-Ras," *International Journal of Cancer*, vol. 123, no. 1, pp. 100–107, 2008.

[31] S. D. Lim, C. Sun, J. D. Lambeth et al., "Increased Nox1 and hydrogen peroxide in prostate cancer," *Prostate*, vol. 62, no. 2, pp. 200–207, 2005.

[32] A. Martner, H. G. Wiktorin, B. Lenox et al., "Histamine promotes the development of monocyte-derived dendritic cells and reduces tumor growth by targeting the myeloid NADPH oxidase," *The Journal of Immunology*, vol. 194, no. 10, pp. 5014–5021, 2015.

[33] B. M. Babior, J. D. Lambeth, and W. Nauseef, "The neutrophil NADPH oxidase," *Arch Biochem Biophys*, vol. 397, no. 2, pp. 342–344, 2002.

[34] A. R. Cross and A. W. Segal, "The NADPH oxidase of professional phagocytes—prototype of the NOX electron transport chain systems," *Biochim Biophys Acta*, vol. 1657, no. 1, pp. 1–22, 2004.

[35] R. Kiffin, H. Grauers Wiktorin, M. S. Nilsson et al., "Anti-leukemic properties of histamine in monocytic leukemia: the role of NOX2," *Front Oncol*, vol. 8, p. 218, 2018.

[36] J. Aurelius, A. Hallner, O. Werlenius et al., "NOX2-dependent immunosuppression in chronic myelomonocytic leukemia," *Journal of Leukocyte Biology*, vol. 102, no. 2, pp. 459–466, 2017.

[37] E. Aydin, J. Johansson, F. H. Nazir, K. Hellstrand, and A. Martner, "Role of NOX2-derived reactive oxygen species in NK cell-mediated control of murine melanoma metastasis," *Cancer Immunology Research*, vol. 5, no. 9, pp. 804–811, 2017.

[38] T. Kelkka, A. Pizzolla, J. P. Laurila et al., "Mice lacking NCF1 exhibit reduced growth of implanted melanoma and carcinoma tumors," *PLoS One*, vol. 8, no. 12, p. e84148, 2013.

[39] B. Bánfi, B. Malgrange, J. Knisz, K. Steger, M. Dubois-Dauphin, and K.-H. Krause, "NOX3, a superoxide-generating NADPH oxidase of the inner ear," *Journal of Biological Chemistry*, vol. 279, no. 44, pp. 46065–46072, 2004.

[40] R. Paffenholz, R. A. Bergstrom, F. Pasutto et al., "Vestibular defects in head-tilt mice result from mutations in Nox3, encoding an NADPH oxidase," *Genes & Development*, vol. 18, no. 5, pp. 486–491, 2004.

[41] G. Cheng, Z. Cao, X. Xu, E. G. V. Meir, and J. D. Lambeth, "Homologs of gp91 phox : cloning and tissue expression of Nox3, Nox4, and Nox5," *Gene*, vol. 269, no. 1-2, pp. 131–140, 2001.

[42] S. Carnesecchi, J. L. Carpentier, M. Foti, and I. Szanto, "Insulin-induced vascular endothelial growth factor expression is mediated by the NADPH oxidase NOX3," *Experimental Cell Research*, vol. 312, no. 17, pp. 3413–3424, 2006.

[43] M. Geiszt, J. B. Kopp, P. Varnai, and T. L. Leto, "Identification of renox, an NAD(P)H oxidase in kidney," *Proceedings of the National Academy of Sciences*, vol. 97, no. 14, pp. 8010–8014, 2000.

[44] A. Shiose, J. Kuroda, K. Tsuruya et al., "A novel superoxide-producing NAD(P)H oxidase in kidney," *Journal of Biological Chemistry*, vol. 276, no. 2, pp. 1417–1423, 2001.

[45] K. Block, Y. Gorin, P. Hoover et al., "NAD(P)H oxidases regulate HIF-2alpha protein expression," *Journal of Biological Chemistry*, vol. 282, no. 11, pp. 8019–8026, 2007.

[46] J. P. Fitzgerald, B. Nayak, K. Shanmugasundaram et al., "Nox4 mediates renal cell carcinoma cell invasion through hypoxia-induced interleukin 6- and 8- production," *PLoS One*, vol. 7, no. 1, p. e30712, 2012.

[47] C. Xia, Q. Meng, L. Z. Liu, Y. Rojanasakul, X. R. Wang, and B. H. Jiang, "Reactive oxygen species regulate angiogenesis and tumor growth through vascular endothelial growth factor," *Cancer Research*, vol. 67, no. 22, pp. 10823–10830, 2007.

[48] T. Shono, N. Yokoyama, T. Uesaka et al., "Enhanced expression of NADPH oxidase Nox4 in human gliomas and its roles in cell proliferation and survival," *International Journal of Cancer*, vol. 123, no. 4, pp. 787–792, 2008.

[49] M. Yamaura, J. Mitsushita, S. Furuta et al., "NADPH oxidase 4 contributes to transformation phenotype of melanoma cells by regulating G2-M cell cycle progression," *Cancer Research*, vol. 69, no. 6, pp. 2647–2654, 2009.

[50] B. Bánfi, G. Molnár, A. Maturana et al., "A Ca(2+)-activated NADPH oxidase in testis, spleen, and lymph nodes," *Journal of Biological Chemistry*, vol. 276, no. 40, pp. 37594–37601, 2001.

[51] B. Musset, R. A. Clark, T. E. DeCoursey et al., "NOX5 in human spermatozoa: expression, function, and regulation," *Journal of Biological Chemistry*, vol. 287, no. 12, pp. 9376–9388, 2012.

[52] W. C. Huang, X. Li, J. Liu, J. Lin, and L. W. K. Chung, "Activation of androgen receptor, lipogenesis, and oxidative stress converged by SREBP-1 is responsible for regulating growth and progression of prostate cancer cells," *Molecular Cancer Research*, vol. 10, no. 1, pp. 133–142, 2012.

[53] S. S. Brar, Z. Corbin, T. P. Kennedy et al., "NOX5 NAD(P)H oxidase regulates growth and apoptosis in DU 145 prostate cancer cells," *American Journal of Physiology-Cell Physiology*, vol. 285, no. 2, pp. C353–C369, 2003.

[54] J. Hong, M. Resnick, J. Behar et al., "Acid-induced p16 hypermethylation contributes to development of esophageal adenocarcinoma via activation of NADPH oxidase NOX5-S," *American Journal of Physiology-Gastrointestinal and Liver Physiology*, vol. 299, no. 3, pp. G697–G706, 2010.

[55] X. De Deken, D. Wang, M.-C. Many et al., "Cloning of two human thyroid cDNAs encoding new members of the NADPH oxidase family," *Journal of Biological Chemistry*, vol. 275, no. 30, pp. 23227–23233, 2000.

[56] A. W. Boots, M. Hristova, D. I. Kasahara, G. R. M. M. Haenen, A. Bast, and A. van der Vliet, "ATP-mediated activation of the NADPH oxidase DUOX1 mediates airway epithelial

responses to bacterial stimuli," *Journal of Biological Chemistry*, vol. 284, no. 26, pp. 17858–17867, 2009.

[57] R. Forteza, M. Salathe, F. Miot, R. Forteza, and G. E. Conner, "Regulated hydrogen peroxide production by Duox in human airway epithelial cells," *American Journal of Respiratory Cell and Molecular Biology*, vol. 32, no. 5, pp. 462–469, 2005.

[58] M. Pulcrano, H. Boukheris, M. Talbot et al., "Poorly differentiated follicular thyroid carcinoma: prognostic factors and relevance of histological classification," *Thyroid*, vol. 17, no. 7, pp. 639–646, 2007.

[59] R. Ameziane-El-Hassani, M. Talbot, M. C. de Souza Dos Santos et al., "NADPH oxidase DUOX1 promotes long-term persistence of oxidative stress after an exposure to irradiation," *Proceedings of the National Academy of Sciences*, vol. 112, no. 16, pp. 5051–5056, 2015.

[60] A. C. Little, D. Sham, M. Hristova et al., "DUOX1 silencing in lung cancer promotes EMT, cancer stem cell characteristics and invasive properties," *Oncogenesis*, vol. 5, no. 10, p. e261, 2016.

[61] S. Luxen, S. A. Belinsky, and U. G. Knaus, "Silencing ofDUOXNADPH oxidases by promoter hypermethylation in lung cancer," *Cancer Research*, vol. 68, no. 4, pp. 1037–1045, 2008.

[62] C. Dupuy, M. Pomerance, R. Ohayon et al., "Thyroid oxidase (THOX2) gene expression in the rat thyroid cell line FRTL-5," *Biochemical and Biophysical Research Communications*, vol. 277, no. 2, pp. 287–292, 2000.

[63] R. A. El Hassani, N. Benfares, B. Caillou et al., "Dual oxidase2 is expressed all along the digestive tract," *American Journal of Physiology-Gastrointestinal and Liver Physiology*, vol. 288, no. 5, pp. G933–G942, 2005.

[64] H. Grasberger, J. Gao, H. Nagao-Kitamoto et al., "Increased expression of DUOX2 is an epithelial response to mucosal dysbiosis required for immune homeostasis in mouse intestine," *Gastroenterology*, vol. 149, no. 7, pp. 1849–1859, 2015.

[65] F. Sommer and F. Backhed, "The gut microbiota engages different signaling pathways to induce Duox2 expression in the ileum and colon epithelium," *Mucosal Immunol*, vol. 8, no. 2, pp. 372–379, 2015.

[66] D. V. Bann, Q. Jin, K. E. Sheldon et al., "Genetic variants implicate dual oxidase-2 in familial and sporadic Nonmedullary thyroid cancer," *Cancer Research*, vol. 79, no. 21, pp. 5490–5499, 2019.

[67] Y. Wu, S. Antony, A. Juhasz et al., "Up-regulation and sustained activation of Stat1 are essential for interferon-gamma (IFN-gamma)-induced dual oxidase 2 (Duox2) and dual oxidase A2 (DuoxA2) expression in human pancreatic cancer cell lines," *Journal of Biological Chemistry*, vol. 286, no. 14, pp. 12245–12256, 2011.

[68] Y. Wu, J. Lu, S. Antony et al., "Activation of TLR4 is required for the synergistic induction of dual oxidase 2 and dual oxidase A2 by IFN-γ and lipopolysaccharide in human pancreatic cancer cell lines," *The Journal of Immunology*, vol. 190, no. 4, pp. 1859–1872, 2013.

[69] T. Mochizuki, S. Furuta, J. Mitsushita et al., "Inhibition of NADPH oxidase 4 activates apoptosis via the AKT/apoptosis signal-regulating kinase 1 pathway in pancreatic cancer PANC-1 cells," *Oncogene*, vol. 25, no. 26, pp. 3699–3707, 2006.

[70] E. C. Vaquero, M. Edderkaoui, S. J. Pandol, I. Gukovsky, and A. S. Gukovskaya, "Reactive oxygen species produced by NAD(P)H oxidase inhibit apoptosis in pancreatic cancer cells," *Journal of Biological Chemistry*, vol. 279, no. 33, pp. 34643–34654, 2004.

[71] J. K. Lee, M. Edderkaoui, P. Truong et al., "NADPH oxidase promotes pancreatic cancer cell survival via inhibiting JAK2 dephosphorylation by tyrosine phosphatases," *Gastroenterology*, vol. 133, no. 5, pp. 1637–1648, 2007.

[72] J. Li, T. Lan, C. Zhang et al., "Reciprocal activation between IL-6/STAT3 and NOX4/Akt signalings promotes proliferation and survival of non-small cell lung cancer cells," *Oncotarget*, vol. 6, no. 2, pp. 1031–1048, 2015.

[73] C. Zhang, T. Lan, J. Hou et al., "NOX4 promotes non-small cell lung cancer cell proliferation and metastasis through positive feedback regulation of PI3K/Akt signaling," *Oncotarget*, vol. 5, no. 12, pp. 4392–4405, 2014.

[74] R. Rastogi, X. Geng, F. Li, and Y. Ding, "NOX activation by subunit interaction and underlying mechanisms in disease," *Frontiers in Cellular Neuroscience*, vol. 10, 2017.

[75] B. A. Diebold and G. M. Bokoch, "Molecular basis for Rac2 regulation of phagocyte NADPH oxidase," *Nat Immunol*, vol. 2, no. 3, pp. 211–215, 2001.

[76] M. T. Quinn, C. A. Parkos, and A. J. Jesaitis, "[48] Purification of human neutrophil NADPH oxidase cytochrome b-558 and association with Rap 1A," *Methods Enzymol*, vol. 255, pp. 476–487, 1995.

[77] M. Takahashi, T. J. Dillon, C. Liu, Y. Kariya, Z. Wang, and P. J. S. Stork, "Protein kinase A-dependent phosphorylation of Rap1 regulates its membrane localization and cell migration," *Journal of Biological Chemistry*, vol. 288, no. 39, pp. 27712–27723, 2013.

[78] F. Kotsias, E. Hoffmann, S. Amigorena, and A. Savina, "Reactive oxygen species production in the phagosome: impact on antigen presentation in dendritic cells," *Antioxid Redox Signal*, vol. 18, no. 6, pp. 714–729, 2013.

[79] D. E. Arnold and J. R. Heimall, "A review of chronic granulomatous disease," *Advances in Therapy*, vol. 34, no. 12, pp. 2543–2557, 2017.

[80] R. L. Baehner and D. G. Nathan, "Leukocyte oxidase: defective activity in chronic granulomatous disease," *Science*, vol. 155, no. 3764, pp. 835-836, 1967.

[81] P. G. Quie, J. G. White, B. Holmes, and R. A. Good, "In vitro bactericidal capacity of human polymorphonuclear leukocytes: diminished activity in chronic granulomatous disease of childhood," *Journal of Clinical Investigation*, vol. 46, no. 4, pp. 668–679, 1967.

[82] A. Pizzolla, M. Hultqvist, B. Nilson et al., "Reactive oxygen species produced by the NADPH oxidase 2 complex in monocytes protect mice from bacterial infections," *The Journal of Immunology*, vol. 188, no. 10, pp. 5003–5011, 2012.

[83] A. Martner, E. Aydin, and K. Hellstrand, "NOX2 in autoimmunity, tumor growth and metastasis," *The Journal of Pathology*, vol. 247, no. 2, pp. 151–154, 2019.

[84] J. Zhong, L. M. Olsson, V. Urbonaviciute, M. Yang, L. Bäckdahl, and R. Holmdahl, "Association of NOX2 subunits genetic variants with autoimmune diseases," *Free Radical Biology and Medicine*, vol. 125, pp. 72–80, 2018.

[85] S. Stubelius, "Estrogen and 2-methoxyestradiol: regulation of arthritis, inflammation and reactive oxygen species," in *Department of Rheumatology and Inflammation Research*, University of Gothenburg, Gothenburg, 2014.

[86] M. Vulcano, S. Dusi, D. Lissandrini et al., "Toll receptor-mediated regulation of NADPH oxidase in human dendritic cells," *The Journal of Immunology*, vol. 173, no. 9, pp. 5749–5756, 2004.

[87] N. R. Madamanchi and M. S. Runge, "Mitochondrial dysfunction in atherosclerosis," *Circulation Research*, vol. 100, no. 4, pp. 460–473, 2007.

[88] M. Jastroch, A. S. Divakaruni, S. Mookerjee, J. R. Treberg, and M. D. Brand, "Mitochondrial proton and electron leaks," *Essays Biochem*, vol. 47, pp. 53–67, 2010.

[89] L. B. Sullivan and N. S. Chandel, "Mitochondrial reactive oxygen species and cancer," *Cancer Metab*, vol. 2, no. 1, p. 17, 2014.

[90] R. Kiessling, K. Wasserman, S. Horiguchi et al., "Tumor-induced immune dysfunction," *Cancer Immunology Immunotherapy*, vol. 48, no. 7, pp. 353–362, 1999.

[91] M. Hansson, A. Asea, U. Ersson, S. Hermodsson, and K. Hellstrand, "Induction of apoptosis in NK cells by monocyte-derived reactive oxygen metabolites," *Journal of Immunology*, vol. 156, no. 1, pp. 42–47, 1996.

[92] M. Schieber and N. S. Chandel, "ROS function in redox signaling and oxidative stress," *Current Biology*, vol. 24, no. 10, pp. R453–R462, 2014.

[93] C. C. Winterbourn and M. B. Hampton, "Thiol chemistry and specificity in redox signaling," *Free Radical Biology and Medicine*, vol. 45, no. 5, pp. 549–561, 2008.

[94] L. He, T. He, S. Farrar, L. Ji, T. Liu, and X. Ma, "Antioxidants maintain cellular redox homeostasis by elimination of reactive oxygen species," *Cell Physiol Biochem*, vol. 44, no. 2, pp. 532–553, 2017.

[95] B. Marengo, M. Nitti, A. L. Furfaro et al., "Redox homeostasis and cellular antioxidant systems: crucial players in cancer growth and therapy," *Oxidative Medicine and Cellular Longevity*, vol. 2016, Article ID 6235641, 16 pages, 2016.

[96] A. Kobayashi, M. I. Kang, H. Okawa et al., "Oxidative stress sensor Keap1 functions as an adaptor for Cul3-based E3 ligase to regulate proteasomal degradation of Nrf2," *Molecular and Cellular Biology*, vol. 24, no. 16, pp. 7130–7139, 2004.

[97] R. Venugopal and A. K. Jaiswal, "Nrf1 and Nrf2 positively and c-Fos and Fra1 negatively regulate the human antioxidant response element-mediated expression of NAD(P)H:-quinone oxidoreductase 1 gene," *Proceedings of the National Academy of Sciences*, vol. 93, no. 25, pp. 14960–14965, 1996.

[98] T. Jarmi and A. Agarwal, "Heme oxygenase and renal disease," *Current Hypertension Reports*, vol. 11, no. 1, pp. 56–62, 2009.

[99] W. A. Solis, T. P. Dalton, M. Z. Dieter et al., "Glutamate-cysteine ligase modifier subunit: mouse Gclm gene structure and regulation by agents that cause oxidative stress," *Biochem Pharmacol*, vol. 63, no. 9, pp. 1739–1754, 2002.

[100] C. A. Neumann, J. Cao, and Y. Manevich, "Peroxiredoxin 1 and its role in cell signaling," *Cell Cycle*, vol. 8, no. 24, pp. 4072–4078, 2014.

[101] J. Chaudiere and R. Ferrari-Iliou, "Intracellular antioxidants: from chemical to biochemical mechanisms," *Food Chem Toxicol*, vol. 37, no. 9-10, pp. 949–962, 1999.

[102] J. Limón-Pacheco and M. E. Gonsebatt, "The role of antioxidants and antioxidant-related enzymes in protective responses to environmentally induced oxidative stress," *Mutation Research - Genetic Toxicology and Environmental Mutagenesis*, vol. 674, no. 1-2, pp. 137–147, 2009.

[103] P. Chiarugi, "From anchorage dependent proliferation to survival: lessons from redox signalling," *IUBMB Life*, vol. 60, no. 5, pp. 301–307, 2008.

[104] M. R. Porembka, J. B. Mitchem, B. A. Belt et al., "Pancreatic adenocarcinoma induces bone marrow mobilization of myeloid-derived suppressor cells which promote primary tumor growth," *Cancer Immunology, Immunotherapy*, vol. 61, no. 9, pp. 1373–1385, 2012.

[105] L. Wang, E. W. Y. Chang, S. C. Wong, S. M. Ong, D. Q. Y. Chong, and K. L. Ling, "Increased myeloid-derived suppressor cells in gastric cancer correlate with cancer stage and plasma S100A8/A9 proinflammatory proteins," *Journal of Immunology*, vol. 190, no. 2, pp. 794–804, 2013.

[106] C. M. Diaz-Montero, M. L. Salem, M. I. Nishimura, E. Garrett-Mayer, D. J. Cole, and A. J. Montero, "Increased circulating myeloid-derived suppressor cells correlate with clinical cancer stage, metastatic tumor burden, and doxorubicin-cyclophosphamide chemotherapy," *Cancer Immunology, Immunotherapy*, vol. 58, no. 1, pp. 49–59, 2009.

[107] C. Bergenfelz, A. M. Larsson, K. von Stedingk et al., "Systemic monocytic-MDSCs are generated from monocytes and correlate with disease progression in breast cancer patients," *PLoS ONE*, vol. 10, no. 5, 2015.

[108] S. J. Antonia, N. Mirza, I. Fricke et al., "Combination of p53 cancer vaccine with chemotherapy in patients with extensive stage small cell lung cancer," *Clinical Cancer Research*, vol. 12, no. 3, pp. 878–887, 2006.

[109] Y. Tsuchiya, M. Igarashi, R. Suzuki, and K. Kumagai, "Production of colony-stimulating factor by tumor cells and the factor-mediated induction of suppressor cells," *Journal of Immunology*, vol. 141, no. 2, pp. 699–708, 1988.

[110] Y. Mao, I. Poschke, and R. Kiessling, "Tumour-induced immune suppression: role of inflammatory mediators released by myelomonocytic cells," *Journal of Internal Medicine*, vol. 276, no. 2, pp. 154–170, 2014.

[111] A. Martner, F. B. Thorén, J. Aurelius, and K. Hellstrand, "Immunotherapeutic strategies for relapse control in acute myeloid leukemia," *Blood Reviews*, vol. 27, no. 5, pp. 209–216, 2013.

[112] Y. Kondo, S. Arii, A. Mori, M. Furutani, T. Chiba, and M. Imamura, "Enhancement of angiogenesis, tumor growth, and metastasis by transfection of vascular endothelial growth factor into LoVo human colon cancer cell line," *Clinical Cancer Research*, vol. 6, no. 2, pp. 622–630, 2000.

[113] A. M. Roberts, I. R. Watson, A. J. Evans, D. A. Foster, M. S. Irwin, and M. Ohh, "Suppression of hypoxia-inducible factor 2 Restores p53 activity via Hdm2 and reverses chemoresistance of renal carcinoma cells," *Cancer Research*, vol. 69, no. 23, pp. 9056–9064, 2009.

[114] J. T. Erler, K. L. Bennewith, M. Nicolau et al., "Lysyl oxidase is essential for hypoxia-induced metastasis," *Nature*, vol. 440, no. 7088, pp. 1222–1226, 2006.

[115] A. K. Azab, J. Hu, P. Quang et al., "Hypoxia promotes dissemination of multiple myeloma through acquisition of epithelial to mesenchymal transition-like features," *Blood*, vol. 119, no. 24, pp. 5782–5794, 2012.

[116] B. Muz, P. de la Puente, F. Azab, and A. K. Azab, "The role of hypoxia in cancer progression, angiogenesis, metastasis, and resistance to therapy," *Hypoxia*, vol. 3, pp. 83–92, 2015.

[117] S. Movafagh, S. Crook, and K. Vo, "Regulation of hypoxia-inducible factor-1a by reactive oxygen species: new

developments in an old debate," *Journal of Cellular Biochemistry*, vol. 116, no. 5, pp. 696–703, 2015.

[118] E. Bolton-Gillespie, M. Schemionek, H. U. Klein et al., "Genomic instability may originate from imatinib-refractory chronic myeloid leukemia stem cells," *Blood*, vol. 121, no. 20, pp. 4175–4183, 2013.

[119] M. Sattler, S. Verma, G. Shrikhande et al., "The BCR/ABL tyrosine kinase induces production of reactive oxygen species in hematopoietic cells," *Journal of Biological Chemistry*, vol. 275, no. 32, pp. 24273–24278, 2000.

[120] U. E. Martinez-Outschoorn et al., "BRCA1 mutations drive oxidative stress and glycolysis in the tumor microenvironment: implications for breast cancer prevention with antioxidant therapies," *Cell Cycle*, vol. 11, no. 23, pp. 4402–4413, 2014.

[121] A. Salazar-Ramiro, D. Ramírez-Ortega, V. Pérez de la Cruz et al., "Role of redox status in development of Glioblastoma," *Frontiers in Immunology*, vol. 7, no. APR, 2016.

[122] K. Roy, Y. Wu, J. L. Meitzler et al., "NADPH oxidases and cancer," *Clin Sci (Lond)*, vol. 128, no. 12, pp. 863–875, 2015.

[123] J. L. Meitzler, M. M. Konate, and J. H. Doroshow, "Hydrogen peroxide-producing NADPH oxidases and the promotion of migratory phenotypes in cancer," *Arch Biochem Biophys*, vol. 675, p. 108076, 2019.

[124] N. Hempel, P. M Carrico, and J. A. Melendez, "Manganese superoxide dismutase (Sod2) and redox-control of signaling events that drive metastasis," *Anti-Cancer Agents in Medicinal Chemistry*, vol. 11, no. 2, pp. 191–201, 2011.

[125] P. Chiarugi, G. Pani, E. Giannoni et al., "Reactive oxygen species as essential mediators of cell adhesion," *Journal of Cell Biology*, vol. 161, no. 5, pp. 933–944, 2003.

[126] L. Tochhawng, S. Deng, S. Pervaiz, and C. T. Yap, "Redox regulation of cancer cell migration and invasion," *Mitochondrion*, vol. 13, no. 3, pp. 246–253, 2013.

[127] H. Peshavariya, G. J. Dusting, F. Jiang et al., "NADPH oxidase isoform selective regulation of endothelial cell proliferation and survival," *Naunyn-Schmiedeberg's Archives of Pharmacology*, vol. 380, no. 2, pp. 193–204, 2009.

[128] Y. Li, N. Han, T. Yin et al., "Lentivirus-mediated Nox4 shRNA invasion and angiogenesis and enhances radiosensitivity in human glioblastoma," *Oxidative Medicine and Cellular Longevity*, vol. 2014, 9 pages, 2014.

[129] M. Wang, J. S. Kirk, S. Venkataraman et al., "Manganese superoxide dismutase suppresses hypoxic induction of hypoxia-inducible factor-1α and vascular endothelial growth factor," *Oncogene*, vol. 24, no. 55, pp. 8154–8166, 2005.

[130] Z. A. Sibenaller, J. L. Welsh, C. du et al., "Extracellular superoxide dismutase suppresses hypoxia-inducible factor-1α in pancreatic cancer," *Free Radical Biology and Medicine*, vol. 69, pp. 357–366, 2014.

[131] C. R. Hoyal, A. Gutierrez, B. M. Young et al., "Modulation of p47PHOX activity by site-specific phosphorylation: Akt-dependent activation of the NADPH oxidase," *Proceedings of the National Academy of Sciences*, vol. 100, no. 9, pp. 5130–5135, 2003.

[132] B. Govindarajan, J. E. Sligh, B. J. Vincent et al., "Overexpression of Akt converts radial growth melanoma to vertical growth melanoma," *Journal of Clinical Investigation*, vol. 117, no. 3, pp. 719–729, 2007.

[133] S. K. Sastry and L. A. Elferink, "Checks and balances: interplay of RTKs and PTPs in cancer progression," *Biochem Pharmacol*, vol. 82, no. 5, pp. 435–440, 2011.

[134] H. J. Forman, F. Ursini, and M. Maiorino, "An overview of mechanisms of redox signaling," *Journal of Molecular and Cellular Cardiology*, vol. 73, pp. 2–9, 2014.

[135] K. Block and Y. Gorin, "Aiding and abetting roles of NOX oxidases in cellular transformation," *Nature Reviews Cancer*, vol. 12, no. 9, pp. 627–637, 2012.

[136] R. Gopalakrishna and S. Jaken, "Protein kinase C signaling and oxidative stress," *Free Radical Biology and Medicine*, vol. 28, no. 9, pp. 1349–1361, 2000.

[137] L. Lignitto, S. E. LeBoeuf, H. Homer et al., "Nrf2 activation promotes lung cancer metastasis by inhibiting the degradation of Bach1," *Cell*, vol. 178, no. 2, pp. 316–329.e18, 2019.

[138] C. Wiel, K. le Gal, M. X. Ibrahim et al., "BACH1 stabilization by antioxidants stimulates lung cancer metastasis," *Cell*, vol. 178, no. 2, pp. 330–345.e22, 2019.

[139] M. A. Ligtenberg, Ö. Çınar, R. Holmdahl, D. Mougiakakos, and R. Kiessling, "Methylcholanthrene-induced sarcomas develop independently from NOX2-derived ROS," *PLoS ONE*, vol. 10, no. 6, 2015.

[140] F. Okada, M. Kobayashi, H. Tanaka et al., "The role of nicotinamide adenine dinucleotide phosphate oxidase-derived reactive oxygen species in the acquisition of metastatic ability of tumor cells," *American Journal of Pathology*, vol. 169, no. 1, pp. 294–302, 2006.

[141] L. van der Weyden, A. O. Speak, A. Swiatkowska et al., "Pulmonary metastatic colonisation and granulomas in NOX2-deficient mice," *The Journal of Pathology*, vol. 246, no. 3, pp. 300–310, 2018.

[142] A. Betten, C. Dahlgren, U. H. Mellqvist, S. Hermodsson, and K. Hellstrand, "Oxygen radical-induced natural killer cell dysfunction: role of myeloperoxidase and regulation by serotonin," *Journal of Leukocyte Biology*, vol. 75, no. 6, pp. 1111–1115, 2004.

[143] S. Chatterjee, E. A. Browning, N. K. Hong et al., "Membrane depolarization is the trigger for PI3K/Akt activation and leads to the generation of ROS," *American Journal of Physiology-Heart and Circulatory Physiology*, vol. 302, no. 1, pp. H105–H114, 2012.

[144] A. Betten, C. Dahlgren, S. Hermodsson, and K. Hellstrand, "Histamine inhibits neutrophil NADPH oxidase activity triggered by the lipoxin A4 receptor-specific peptide agonist Trp-Lys-Tyr-Met-Val-Met," *Scand J Immunol*, vol. 58, no. 3, pp. 321–326, 2003.

[145] B. A. Babbin, A. J. Jesaitis, A. I. Ivanov et al., "Formyl peptide receptor-1 activation enhances intestinal epithelial cell restitution through phosphatidylinositol 3-kinase-dependent activation of Rac1 and Cdc42," *The Journal of Immunology*, vol. 179, no. 12, pp. 8112–8121, 2007.

[146] A. A. Akhiani, A. Hallner, R. Kiffin et al., "Idelalisib promotes anti CD20-mediated ADCC by inhibiting immunosuppressive ROS production in monocytes," in *International Congress of Immunology*, Melbourne, Australia, 2016.

[147] F. B. Thoren, J. Aurelius, and A. Martner, "Antitumor properties of histamine in vivo," *Nature Medicine*, vol. 17, no. 5, pp. 537–537; author reply 538, 2011.

[148] H. Grauers Wiktorin, M. S. Nilsson, R. Kiffin et al., "Histamine targets myeloid-derived suppressor cells and improves the anti-tumor efficacy of PD-1/PD-L1 checkpoint blockade," *Cancer Immunol Immunother*, vol. 68, no. 2, pp. 163–174, 2019.

[149] C. R. Marlein, L. Zaitseva, R. E. Piddock et al., "NADPH oxidase-2 derived superoxide drives mitochondrial transfer

from bone marrow stromal cells to leukemic blasts," *Blood*, vol. 130, no. 14, pp. 1649–1660, 2017.

[150] E. Aydin, A. Hallner, H. Grauers Wiktorin, A. Staffas, K. Hellstrand, and A. Martner, "NOX2 inhibition reduces oxidative stress and prolongs survival in murine KRAS-induced myeloproliferative disease," *Oncogene*, vol. 38, no. 9, pp. 1534–1543, 2019.

[151] H. Grauers Wiktorin, T. Nilsson, E. Aydin, K. Hellstrand, L. Palmqvist, and A. Martner, "Role of NOX2 for leukaemic expansion in a murine model ofBCR-ABL1+leukaemia," *British Journal of Haematology*, vol. 182, no. 2, pp. 290–294, 2018.

[152] N. E. Thomas, K. J. Busam, L. From et al., "Tumor-infiltrating lymphocyte grade in primary melanomas is independently associated with melanoma-specific survival in the population-based genes, environment and melanoma study," *Journal of Clinical Oncology*, vol. 31, no. 33, pp. 4252–4259, 2013.

[153] T. Donnem, S. M. Hald, E. E. Paulsen et al., "Stromal CD8+ T-cell density—a promising supplement to TNM staging in non-small cell lung cancer," *Clinical Cancer Research*, vol. 21, no. 11, pp. 2635–2643, 2015.

[154] M. V. Dieci, M. C. Mathieu, V. Guarneri et al., "Prognostic and predictive value of tumor-infiltrating lymphocytes in two phase III randomized adjuvant breast cancer trials," *Annals of Oncology*, vol. 26, no. 8, pp. 1698–1704, 2015.

[155] M. Okabe, U. Toh, N. Iwakuma et al., "Predictive factors of the tumor immunological microenvironment for long-term follow-up in early stage breast cancer," *Cancer Science*, vol. 108, no. 1, pp. 81–90, 2017.

[156] E. Sato, S. H. Olson, J. Ahn et al., "Intraepithelial CD8+ tumor-infiltrating lymphocytes and a high CD8+/regulatory T cell ratio are associated with favorable prognosis in ovarian cancer," *Proceedings of the National Academy of Sciences of the United States of America*, vol. 102, no. 51, pp. 18538–18543, 2005.

[157] G. Esendagli, K. Bruderek, T. Goldmann et al., "Malignant and non-malignant lung tissue areas are differentially populated by natural killer cells and regulatory T cells in non-small cell lung cancer," *Lung Cancer*, vol. 59, no. 1, pp. 32–40, 2008.

[158] S. Coca, J. Perez-Piqueras, D. Martinez et al., "The prognostic significance of intratumoral natural killer cells in patients with colorectal carcinoma," *Cancer*, vol. 79, no. 12, pp. 2320–2328, 1997.

[159] F. R. Villegas, S. Coca, V. G. Villarrubia et al., "Prognostic significance of tumor infiltrating natural killer cells subset CD57 in patients with squamous cell lung cancer," *Lung Cancer*, vol. 35, no. 1, pp. 23–28, 2002.

[160] L. Jiang, Z. Zhao, S. Jiang et al., "Immunological markers predict the prognosis of patients with squamous non-small cell lung cancer," *Immunologic Research*, vol. 62, no. 3, pp. 316–324, 2015.

[161] M. F. Chevalier, S. Trabanelli, J. Racle et al., "ILC2-modulated T cell-to-MDSC balance is associated with bladder cancer recurrence," *Journal of Clinical Investigation*, vol. 127, no. 8, pp. 2916–2929, 2017.

[162] S. Han, Y. Liu, Q. Li, Z. Li, H. Hou, and A. Wu, "Pre-treatment neutrophil-to-lymphocyte ratio is associated with neutrophil and T-cell infiltration and predicts clinical outcome in patients with glioblastoma," *BMC Cancer*, vol. 15, no. 1, p. 617, 2015.

[163] F. Donskov, M. Hokland, N. Marcussen, H. H. Torp Madsen, and H. von der Maase, "Monocytes and neutrophils as "bad guys" for the outcome of interleukin-2 with and without histamine in metastatic renal cell carcinoma—results from a randomised phase II trial," *British Journal of Cancer*, vol. 94, no. 2, pp. 218–226, 2006.

[164] M. D. Iglesia, J. S. Parker, K. A. Hoadley, J. S. Serody, C. M. Perou, and B. G. Vincent, "Genomic Analysis of Immune Cell Infiltrates Across 11 Tumor Types," *Journal of the National Cancer Institute*, vol. 108, no. 11, p. djw144, 2016.

[165] W. Q. Wang, L. Liu, H. X. Xu et al., "Infiltrating immune cells and gene mutations in pancreatic ductal adenocarcinoma," *British Journal of Surgery*, vol. 103, no. 9, pp. 1189–1199, 2016.

[166] T. M. Nywening, B. A. Belt, D. R. Cullinan et al., "Targeting both tumour-associated CXCR2(+) neutrophils and CCR2(+) macrophages disrupts myeloid recruitment and improves chemotherapeutic responses in pancreatic ductal adenocarcinoma," *Gut*, vol. 67, no. 6, pp. 1112–1123, 2018.

[167] A. J. Templeton, M. G. McNamara, B. Šeruga et al., "Prognostic role of neutrophil-to-lymphocyte ratio in solid tumors: a systematic review and meta-analysis," *JNCI: Journal of the National Cancer Institute*, vol. 106, no. 6, p. dju124, 2014.

[168] C. Groth, X. Hu, R. Weber et al., "Immunosuppression mediated by myeloid-derived suppressor cells (MDSCs) during tumour progression," *British Journal of Cancer*, vol. 120, no. 1, pp. 16–25, 2019.

[169] D. I. Gabrilovich and S. Nagaraj, "Myeloid-derived suppressor cells as regulators of the immune system," *Nature Reviews Immunology*, vol. 9, no. 3, pp. 162–174, 2009.

[170] A. H. Zea, P. C. Rodriguez, M. B. Atkins et al., "Arginase-producing myeloid suppressor cells in renal cell carcinoma patients: a mechanism of tumor evasion," *Cancer Research*, vol. 65, no. 8, pp. 3044–3048, 2005.

[171] E. Tcyganov, J. Mastio, E. Chen, and D. I. Gabrilovich, "Plasticity of myeloid-derived suppressor cells in cancer," *Curr Opin Immunol*, vol. 51, pp. 76–82, 2018.

[172] Y. Zhu, J. M. Herndon, D. K. Sojka et al., "Tissue-resident macrophages in pancreatic ductal adenocarcinoma originate from embryonic hematopoiesis and promote tumor progression," *Immunity*, vol. 47, no. 2, pp. 323–338.e6, 2017.

[173] T. Condamine, I. Ramachandran, J. I. Youn, and D. I. Gabrilovich, "Regulation of tumor metastasis by myeloid-derived suppressor cells," *Annual Review of Medicine*, vol. 66, no. 1, pp. 97–110, 2015.

[174] Y. Lin, J. Xu, and H. Lan, "Tumor-associated macrophages in tumor metastasis: biological roles and clinical therapeutic applications," *Journal of Hematology & Oncology*, vol. 12, no. 1, p. 76, 2019.

[175] K. Movahedi, D. Laoui, C. Gysemans et al., "Different tumor microenvironments contain functionally distinct subsets of macrophages derived from Ly6C(high) monocytes," *Cancer Research*, vol. 70, no. 14, pp. 5728–5739, 2010.

[176] K. Y. Gerrick, E. R. Gerrick, A. Gupta, S. J. Wheelan, S. Yegnasubramanian, and E. M. Jaffee, "Transcriptional profiling identifies novel regulators of macrophage polarization," *PLoS One*, vol. 13, no. 12, p. e0208602, 2018.

[177] G. Khayrullina, S. Bermudez, and K. R. Byrnes, "Inhibition of NOX2 reduces locomotor impairment, inflammation, and oxidative stress after spinal cord injury," *Journal of Neuroinflammation*, vol. 12, no. 1, p. 172, 2015.

[178] I. Truxova, L. Kasikova, M. Hensler et al., "Mature dendritic cells correlate with favorable immune infiltrate and improved prognosis in ovarian carcinoma patients," *Journal for ImmunoTherapy of Cancer*, vol. 6, no. 1, p. 139, 2018.

[179] R. A. Soo, Z. Chen, R. S. Yan Teng et al., "Prognostic significance of immune cells in non-small cell lung cancer: meta-analysis," *Oncotarget*, vol. 9, no. 37, pp. 24801–24820, 2018.

[180] M. Zhang, Y. He, X. Sun et al., "A high M1/M2 ratio of tumor-associated macrophages is associated with extended survival in ovarian cancer patients," *Journal of Ovarian Research*, vol. 7, no. 1, p. 19, 2014.

[181] C. E. Lewis and J. W. Pollard, "Distinct role of macrophages in different tumor microenvironments," *Cancer Research*, vol. 66, no. 2, pp. 605–612, 2006.

[182] A. H. Klimp, E. G. E. de Vries, G. L. Scherphof, and T. Daemen, "A potential role of macrophage activation in the treatment of cancer," *Critical Reviews in Oncology/Hematology*, vol. 44, no. 2, pp. 143–161, 2002.

[183] B. Z. Qian and J. W. Pollard, "Macrophage diversity enhances tumor progression and metastasis," *Cell*, vol. 141, no. 1, pp. 39–51, 2010.

[184] E. F. Redente, L. D. Dwyer-Nield, D. T. Merrick et al., "Tumor progression stage and anatomical site regulate tumor-associated macrophage and bone marrow-derived monocyte polarization," *American Journal of Pathology*, vol. 176, no. 6, pp. 2972–2985, 2010.

[185] T. Condamine, J. Mastio, and D. I. Gabrilovich, "Transcriptional regulation of myeloid-derived suppressor cells," *Journal of Leukocyte Biology*, vol. 98, no. 6, pp. 913–922, 2015.

[186] C. A. Corzo, M. J. Cotter, P. Cheng et al., "Mechanism regulating reactive oxygen species in tumor-induced myeloid-derived suppressor cells," *Journal of Immunology*, vol. 182, no. 9, pp. 5693–5701, 2009.

[187] T. Ando, K. Mimura, C. C. Johansson et al., "Transduction with the antioxidant enzyme catalase protects human T cells against oxidative stress," *The Journal of Immunology*, vol. 181, no. 12, pp. 8382–8390, 2008.

[188] S. Kusmartsev, Y. Nefedova, D. Yoder, and D. I. Gabrilovich, "Antigen-specific inhibition of CD8+ T cell response by immature myeloid cells in cancer is mediated by reactive oxygen species," *Journal of Immunology*, vol. 172, no. 2, pp. 989–999, 2004.

[189] J. Schmielau and O. J. Finn, "Activated granulocytes and granulocyte-derived hydrogen peroxide are the underlying mechanism of suppression of T-cell function in advanced cancer patients," *Cancer Research*, vol. 61, no. 12, pp. 4756–4760, 2001.

[190] G. Mantovani, A. Macciò, C. Madeddu et al., "Antioxidant agents are effective in inducing lymphocyte progression through cell cycle in advanced cancer patients: assessment of the most important laboratory indexes of cachexia and oxidative stress," *Journal of Molecular Medicine*, vol. 81, no. 10, pp. 664–673, 2003.

[191] A. A. Akhiani, O. Werlenius, J. Aurelius et al., "Role of the ERK pathway for oxidant-induced parthanatos in human lymphocytes," *PLoS One*, vol. 9, no. 2, p. e89646, 2014.

[192] S. Nagaraj, K. Gupta, V. Pisarev et al., "Altered recognition of antigen is a mechanism of CD8+ T cell tolerance in cancer," *Nature Medicine*, vol. 13, no. 7, pp. 828–835, 2007.

[193] C. Abad, H. Nobuta, J. Li, A. Kasai, W. H. Yong, and J. A. Waschek, "Targeted STAT3 disruption in myeloid cells alters immunosuppressor cell abundance in a murine model of spontaneous medulloblastoma," *Journal of Leukocyte Biology*, vol. 95, no. 2, pp. 357–367, 2014.

[194] Y. Nefedova, M. Fishman, S. Sherman, X. Wang, A. A. Beg, and D. I. Gabrilovich, "Mechanism of all-*trans* retinoic acid effect on tumor-associated myeloid-derived suppressor cells," *Cancer Research*, vol. 67, no. 22, pp. 11021–11028, 2007.

[195] B. Almand, J. I. Clark, E. Nikitina et al., "Increased production of immature myeloid cells in cancer patients: a mechanism of immunosuppression in cancer," *Journal of Immunology*, vol. 166, no. 1, pp. 678–689, 2001.

[196] D. I. Gabrilovich, M. P. Velders, E. M. Sotomayor, and W. M. Kast, "Mechanism of immune dysfunction in cancer mediated by immature Gr-1+ myeloid cells," *Journal of Immunology*, vol. 166, no. 9, pp. 5398–5406, 2001.

[197] M. Mohty, S. Morbelli, D. Isnardon et al., "All-*trans* retinoic acid skews monocyte differentiation into interleukin-12-secreting dendritic-like cells," *British Journal of Haematology*, vol. 122, no. 5, pp. 829–836, 2003.

[198] A. Gervais, J. Levêque, F. Bouet-Toussaint et al., "Dendritic cells are defective in breast cancer patients: a potential role for polyamine in this immunodeficiency," *Breast Cancer Research*, vol. 7, no. 3, pp. R326–R335, 2005.

[199] C. Hegedűs, K. Kovács, Z. Polgár et al., "Redox control of cancer cell destruction," *Redox Biology*, vol. 16, pp. 59–74, 2018.

[200] W. J. Blot, J. Y. Li, P. R. Taylor et al., "Nutrition intervention trials in linxian, China: supplementation with specific vitamin/mineral combinations, cancer incidence, and disease-specific mortality in the general population," *Journal of the National Cancer Institute*, vol. 85, no. 18, pp. 1483–1491, 1993.

[201] B. Li, P. R. Taylor, J. Y. Li et al., "Linxian nutrition intervention trials design, methods, participant characteristics, and compliance," *Annals of Epidemiology*, vol. 3, no. 6, pp. 577–585, 1993.

[202] S. M. Wang, P. R. Taylor, J. H. Fan et al., "Effects of nutrition intervention on total and cancer mortality: 25-year post-trial follow-up of the 5.25-year linxian Nutrition intervention Trial," *Journal of the National Cancer Institute*, vol. 110, no. 11, pp. 1229–1238, 2018.

[203] The Alpha-Tocopherol Beta Carotene Cancer Prevention Study, G, "The effect of vitamin e and beta carotene on the incidence of lung cancer and other cancers in male smokers," *New England Journal of Medicine*, vol. 330, no. 15, pp. 1029–1035, 1994.

[204] F. Lo-Coco, G. Avvisati, M. Vignetti et al., "Retinoic acid and arsenic trioxide for acute promyelocytic leukemia," *New England Journal of Medicine*, vol. 369, no. 2, pp. 111–121, 2013.

[205] S. Kusmartsev, F. Cheng, B. Yu et al., "All-*trans*-retinoic acid eliminates immature myeloid cells from tumor-bearing mice and improves the effect of vaccination," *Cancer Research*, vol. 63, no. 15, pp. 4441–4449, 2003.

[206] N. Mirza, M. Fishman, I. Fricke et al., "All-*trans*-retinoic acid improves differentiation of myeloid cells and immune response in cancer patients," *Cancer Research*, vol. 66, no. 18, pp. 9299–9307, 2006.

[207] C. Iclozan, S. Antonia, A. Chiappori, D. T. Chen, and D. Gabrilovich, "Therapeutic regulation of myeloid-derived suppressor cells and immune response to cancer vaccine in patients with extensive stage small cell lung cancer," *Cancer*

Immunology, Immunotherapy, vol. 62, no. 5, pp. 909–918, 2013.

[208] M. Brune, S. Castaigne, J. Catalano et al., "Improved leukemia-free survival after postconsolidation immunotherapy with histamine dihydrochloride and interleukin-2 in acute myeloid leukemia: results of a randomized phase 3 trial," *Blood*, vol. 108, no. 1, pp. 88–96, 2006.

[209] J. Aurelius, A. Martner, M. Brune et al., "Remission maintenance in acute myeloid leukemia: impact of functional histamine H2 receptors expressed by leukemic cells," *Haematologica*, vol. 97, no. 12, pp. 1904–1908, 2012.

[210] E. Wallhult, J. Whisnant, J. M. Rowe et al., "Impact on quality of life of postconsolidation immunotherapy with histamine dihydrochloride and interleukin-2 in acute myelogenous leukemia," in *American Society of Hematology 49th Annual Meeting and Exposition*, Atlanta, Georgia, 2007.

Hindawi
Oxidative Medicine and Cellular Longevity
Volume 2020, Article ID 3457890, 21 pages
https://doi.org/10.1155/2020/3457890

Review Article

Pharmacological Effects and Toxicogenetic Impacts of Omeprazole: Genomic Instability and Cancer

Márcia Fernanda Correia Jardim Paz,[1,2] **Marcus Vinícius Oliveira Barros de Alencar**,[3] **Rodrigo Maciel Paulino de Lima**,[3] **André Luiz Pinho Sobral**,[2,4] **Glauto Tuquarre Melo do Nascimento**,[5] **Cristiane Amaral dos Reis**,[4] **Maria do Perpetuo Socorro de Sousa Coêlho**,[5] **Maria Luísa Lima Barreto do Nascimento**,[2] **Antonio Luiz Gomes Júnior**,[2,6] **Kátia da Conceição Machado**,[1] **Ag-Anne Pereira Melo de Menezes**,[1] **Rosália Maria Torres de Lima**,[2] **José Williams Gomes de Oliveira Filho**,[2] **Ana Carolina Soares Dias**,[7] **Antonielly Campinho dos Reis**,[2] **Ana Maria Oliveira Ferreira da Mata**,[1] **Sônia Alves Machado**,[8] **Carlos Dimas de Carvalho Sousa**,[8] **Felipe Cavalcanti Carneiro da Silva**,[1,9] **Muhammad Torequl Islam**,[10,11] **João Marcelo de Castro e Sousa**,[12] **and Ana Amélia de Carvalho Melo Cavalcante**[1,2]

[1]*Postgraduate Program in Biotechnology (RENORBIO), Federal University of Piauí, Teresina, PI, Brazil*
[2]*Laboratory of Genetic Toxicity, Postgraduate Program in Pharmaceutical Sciences, Federal University of Piauí, Teresina, PI, Brazil*
[3]*University Centre UNINTA, Sobral, CE, Brazil*
[4]*University Hospital, Teresina, PI, Brazil*
[5]*Postgraduate Program in Pharmaceutical Science, Federal University of Piauí, Teresina, PI, Brazil*
[6]*University Centre UNINOVAFAPI, Teresina, PI, Brazil*
[7]*Laboratory of Genetics and Molecular Biology, Federal University of Maranhão, São Luís, MA, Brazil*
[8]*Getúlio Vargas Hospital, Teresina, PI, Brazil*
[9]*Department of Biological Sciences, Federal University of Piauí, Picos, PI, Brazil*
[10]*Department for Management of Science and Technology Development, Ton Duc Thang University, Ho Chi Minh City 700000, Vietnam*
[11]*Faculty of Pharmacy, Ton Duc Thang University, Ho Chi Minh City 700000, Vietnam*
[12]*Department of Biochemistry and Pharmacology, Federal University of Piauí, Teresina, PI, Brazil*

Correspondence should be addressed to Marcus Vinícius Oliveira Barros de Alencar; marcus.alencar@ufpi.edu.br and Muhammad Torequl Islam; muhammad.torequl.islam@tdtu.edu.vn

Received 15 August 2019; Revised 19 October 2019; Accepted 21 November 2019; Published 29 March 2020

Guest Editor: Kanhaiya Singh

Omeprazole (OME) is commonly used to treat gastrointestinal disorders. However, long-term use of OME can increase the risk of gastric cancer. We aimed to characterize the pharmacological effects of OME and to correlate its adverse effects and toxicogenetic risks to the genomic instability mechanisms and cancer-based on database reports. Thus, a search (till Aug 2019) was made in the PubMed, Scopus, and ScienceDirect with relevant keywords. Based on the study objective, we included 80 clinical reports, forty-six *in vitro*, and 76 *in vivo* studies. While controversial, the findings suggest that long-term use of OME (5 to 40 mg/kg) can induce genomic instability. On the other hand, OME-mediated protective effects are well reported and related to proton pump blockade and anti-inflammatory activity through an increase in gastric flow, anti-inflammatory markers (COX-2 and interleukins) and antiapoptotic markers (caspases and BCL-2), glycoprotein expression, and neutrophil infiltration reduction.

The reported adverse and toxic effects, especially in clinical studies, were atrophic gastritis, cobalamin deficiencies, homeostasis disorders, polyp development, hepatotoxicity, cytotoxicity, and genotoxicity. This study highlights that OME may induce genomic instability and increase the risk of certain types of cancer. Therefore, adequate precautions should be taken, especially in its long-term therapeutic strategies and self-medication practices.

1. Introduction

Cumulative reports suggest that a high prevalence of gastroesophageal diseases and drug-induced side effects may result in genomic instability (GI), leading to increased mutations and carcinogenesis [1–3]. Omeprazole (OME) therapy can alter the bacterial flora of the gastrointestinal tract, leading to malabsorption, enteric infections, and acute or chronic lesions in the stomach. This is due to the compensatory effect in response to decreased acid production, resulting in the destruction of the gastric glands and persistent hypergastrinemia, a denomination for atrophic gastritis [4].

Also, *Helicobacter pylori* infection and OME monotherapy can cause atrophic gastritis associated with an increased risk of mucosal dysplasia and gastric cancer [4]. Although these events may be derived by different mechanisms, a common theme is the involvement of reactive oxygen and nitrogen species (ROS/RNS) in the human stomach and oncoprotein production such as the cytotoxin-associated gene A (CagA) [5].

OME, especially for long-term use, may induce DNA damage [6, 7]. Genotoxicity assays have been shown that not only OME but all prazoles (e.g., esomeprazole, lansoprazole, pantoprazole, and rabeprazole) can induce chromosomal damages [8–11]. Upon understanding the overall fact, this review aimed to sketch a current scenario on the pharmacological effects and toxicogenetic risks of OME therapy in the context of genomic instability and cancer.

2. Methodological Strategies

We conducted a systematic review of published manuscripts to determine if exposure to OME during the treatment of gastric disorders increases the risk of genomic instability and cancer. The search criteria for this study includes publications in English using the keyword "Omeprazole," which was then paired with "genomic instability," "genotoxicity," "cancer," "gastritis," "gastric ulcer," and "gastric/stomach cancer," in the PubMed, Scopus, and ScienceDirect databases. We excluded irrelevant reports that are not meeting inclusion criteria, duplicated publications, and data dealing with other prazoles than OME. The data obtained are listed in Table 1. Out of the 6349 articles, only 202 met our inclusion criteria (80 clinical reports, forty-six *in vitro*, and 76 *in vivo* studies). The selected articles were read in full.

3. Characterization of Scientific Reports

We have analyzed studies based on doses, side effects, drug interactions, pharmacological effects, and toxicogenetic risks (Table 2). The therapeutic use of OME is related to the treatment of duodenal ulcers, gastric ulcers, gastric cancer, and especially to gastroesophageal pathologies (42.4%) and others (26.0%). Regarding *in vitro* studies, the models are more related to other pathologies (90.0%), while for *in vivo*, most studies are associated with the simulating gastric pathologies. Few studies emphasize the use of antioxidants during OME therapy. Also, the therapeutic use of OME in clinical, *in vivo*, and *in vitro* studies varies between 10 and 40 mg/kg, 40 mg/kg, and 40 μM to 25 mM, respectively.

Regarding mechanisms of OME therapeutic action, clinical studies emphasized mechanisms of proton pump inhibition (52.6%), acid and pH control (26%), and CYP219 and CP3AY enzyme inhibition, which are involved in the processes of OME metabolism. In a similar manner, *in vivo* studies are also correlated to proton pump inhibition (60%) and metabolizing enzymes (14.3%), although about 18% emphasized studies related to aryl hydrocarbon receptors (AhR). Around 27% of *in vitro* studies are about acid and pH control, and the same percentage for AhR and proton pump.

Clinical studies on toxicogenetic effects of OME are still limited (5.3%). However, about 89.5% of them point out to oxidative risks by ROS formation, which is also observed in *in vivo* studies. ROS-mediated cytotoxic effects on test systems were also seen in *in vitro* and *in vivo* studies (Table 3). In spite of the scarcity of toxicogenetic studies, the OME mechanisms of action were correlated to genotoxicity by applying bivariate correlation statistics, using the Spearman correlation factor of $r = 0.433^{*}$ and $p < 0.044$ in nonclinical studies and $r = 0.577^{*}$ and $p < 0.005$ in studies with cell cultures. At clinical doses, there were correlations with genomic instability ($r = 0.300^{*}$ and $p < 0.032$) and cytotoxicity ($r = 0.532^{**}$ and $p < 0.001$). In studies of drug interactions, toxicity was strongly correlated with the genomic instability ($r = 1.000$ and $p < 0.001$).

4. Anatomophysiological Characteristics of the Stomach

The stomach is divided into three portions: fundus, corpus, and antrum pylorus, where the processes of digestion, absorption, and protection take place. The lubrication and protection of the gastric mucosa are maintained by enzymatic activity, during digestive process that contribute to the maintenance of acidic pH by hydrogen ion secretion [12]. The pyloric and oxyntic glands act on the gastric mucosa. The former types are located in the antrum of the stomach and have the same cell types as the oxyntic glands, except the parietal cells that, when stimulated, release the gastrin, mainly responsible for the secretion of gastric acid [13]. The oxyntic glands, responsible for secreting hydrochloric acid (HCl), are located in the fundus and the corpus of the stomach. They consist of somatostatin-producing D cells; main cells, responsible for the secretion of pepsinogen; enterochromaffin-like cells responsible for secretion of histamine; parietal cells, which mainly secrete HCl and intrinsic

Table 1: Publications found in the databases.

Keywords (paired with OME)	Databases			Number of articles
	PubMed	*Scopus*	*ScienceDirect*	
Genetic instability	0	2	0	2
Genotoxicity	21	11	9	41
Cancer	94	1219	27	1340
Gastritis	605	2276	160	3041
Gastric ulcer	121	1311	87	1519
Stomach/gastric cancer	24	373	9	406
Total				6349

OME: omeprazole.

factors; and mucosal cells, responsible for the secretion of mucus and bicarbonate ions [14]. The enterochromaffin cells are stimulated by gastrin or acetylcholine, releasing histamine, which binds to H2 receptors found in the parietal cells, stimulating the secretion of acid by the proton pump [15, 16].

Acetylcholine stimulates pepsinogen secretion by peptic cells, HCl by parietal cells, and mucus by the mucous cells [17]. The parietal cells, present in the gastric mucosa, when stimulated, are responsible for the secretion of HCl through the H^+/K^+ adenosine triphosphatase (H^+/K^+/ATPase–proton pump) from the canalicular membrane [18].

4.1. Alteration of Gastric Mucosa

4.1.1. Inflammation. Gastritis is considered a superficial and inflammatory lesion that can also compromise the integrity of the stomach mucosa or duodenum and cause lesions in deeper layers, resulting in gastric ulcers [19] and stomach cancer [20]. The body has preepithelial defenses against gastric lesions and protective factors such as the production of bicarbonate and mucus, nitric oxide (NO), blood flow, prostaglandins, cell regulation, growth factors, nonprotein sulfhydryl groups (SHs), and antioxidant defenses.

It is noteworthy that the lesions may be caused by alterations in the balance between protection and aggression factors to the gastric mucosa [21]. Loss of mucosal protection, derived from the deficiency in mucus secretion and bicarbonate, favors the action of HCl [22]. Gastric secretion, pepsin, free radicals, bile reflux, and ischemic processes are aggressive factors to the tissue [23]. HCl and pepsin generate lesions in the gastric mucosa that destabilize the gastric barrier and cause acute inflammation [24].

Increased gastric HCl secretion is one of the most prominent lesion signals, and its reduction is the main strategy for preventing gastric lesions [25]. The unbalance between harmful (HCl and pepsin) and protector agents characterizes the acute inflammatory process [24, 26]. As a consequence of chronic gastritis and stomach inflammations, peptic ulcers and gastric cancer are the most frequent pathological alterations [20, 27], especially during *H. pylori* infections [27].

4.1.2. Infection by Helicobacter pylori. H. pylori is described as a bacterium whose reservoir is the human stomach [28, 29]. It is a gram-negative bacillus, with flagella, adhesion factors, urease enzyme, cytosines, and proteases as virulence factors [30]. *H. pylori* produces toxic enzymes, as well as induce the release of gastrin, leading to an increase in gastric acid secretion and pH, stimulating somatostatin release [26] and hypergastrinemia. *H. pylori* also triggers a trophic effect and hyperplasia of the enterochromaffin and parietal cells [31].

Infection with *H. pylori* may cause gastritis, gastric and peptic ulcers, and even gastric cancer [32]. Gastric ulcer is considered one of the major public health consequences that occur due to many factors, especially the harmful activity of gastric acid and pepsin [33]. Peptic ulcer is characterized by acid peptic lesions in the digestive tract, which result in mucosa ruptures (reaching the submucosa) that are generally found in the proximal stomach or duodenum [34]. Gastric lesions associated with *H. pylori*, with exposure to acid or pepsin, are amplified and more aggressive [27]. *In vivo* studies indicate that the presence of *H. pylori* may lead to the maintenance of chronic inflammatory responses, as well as to other pathological disorders in the stomach mucosa [35].

The use of nonsteroidal anti-inflammatory drugs (NSAIDs), stress, smoking, excessive alcohol consumption, and the presence of *H. pylori* in the gastrointestinal tract may reach the deeper layers of the muscular wall of the gastric mucosa and cause gastric ulcers [19, 36].

5. Therapies for Gastric Lesions

Proton pump inhibitors (PPIs), such as OME, are frequently used in gastric therapies [37, 38]. Other PPIs, such as lansoprazole, rabeprazole, pantoprazole, esomeprazole, and dexlansoprazole, are also used to inhibit HCl secretion [39]. These drugs are considered efficient in suppressing gastric acidity [40]. PPIs present chiral sulfur in their chemical structure and are activators of the AhR and inducers of CYP1A metabolism genes in human hepatoma cells and primary human hepatocytes [41]. The product of these genes may influence the pharmacokinetics and pharmacodynamics of OME [42, 43].

PPIs activate and release sulfonamide or sulfenic acid, thus inhibit gastric acid secretion by covalently (irreversible) binding to the sulfhydryl group of cysteine in the extracellular domain of H^+/K^+-ATPase [44]. A reduction in gastric acid secretion results in a faster lesion healing, depending on the dose administered [45].

OME is a first-line drug for inhibiting gastric acid secretion in the treatment of gastroesophageal reflux disease

Table 2: Omeprazole studies published in scientific databases in relation to therapeutic use, mechanisms of action, dose/concentration, and interactions with vitamins.

Parameters	Clinical % ($n = 80$)	Nonclinical %	
		In vitro ($n = 46$)[#]	*In vivo* ($n = 76$)[##]
Analysis objects			
Dose	15.8	—	13.3
Adverse effects	10.5	9.1	13.3
Drug interactions	26.3	9.1	—
Mechanisms of pharmacological action	42.1*	63.6*	53.4*
Toxicogenic risks	5.3	18.2	20.0
Therapeutic use			
Duodenal ulcer	15.8	—	26.7
Gastric ulcer	10.5	—	20
Gastroesophageal pathologies	42.4*	9.1	20
Gastric cancer	5.3	—	13.3
Other pathologies	26.0	90.9	20.0
Mechanism of action			
Proton pump inhibition	52.6*	27.3	60*
Acid and pH control	26.3	27.2	7.4
CYP219 and CP3AY enzyme inhibition	10.5	—	14.3
Effect of gastric distension	5.3	—	—
Apoptosis and protein p53	5.3	—	—
Activators of the receptor (AhR)	—	18.2	18.3
Regulation ATPase in tumor cells	—	9.1	—
Inhibition of interleukin- (IL-) 8	—	9.1	—
Inhibition of absorption of Na^+	—	18.2	—
Not reported	—	—	—
Dose/concentration			
10 mg/kg	5.3	—	—
20 mg/kg	66.7*	—	6.7
30 mg/kg	8.7	—	6.7
40 mg/kg	19.3	—	20.2*
20 mM	—	18.2	6.7
25 mM	—	18.2	6.7
40 mM/ml	—	—	20
100 mM	—	9.1	—
1 μM	—	7.28	1.26
2 μM	—	7.28	1.26
3 μM	—	7.28	1.26
4 μM	—	7.28	1.26
5 μM	—	7.28	1.26
40 μM	—	18.1	6.7
100 μm/kg	—	—	10.0
200 μm/kg	—	—	10.0
Interaction with vitamins			
Use of antioxidants	—	—	13.3
Without the use of antioxidants	100	100	86.7*

[#]Concentration/ml. [##]Dose/kg. CYP219 and CYP3AY (metabolizing enzymes). AhR: aryl hydrocarbon receptor; IL-8: interleukin 8. Chi-square test $^*p < 0.05$.

Table 3: Characterization of omeprazole studies in relation to toxicogenetic effect, oxidative damage, and cytotoxicity.

Parameters	Clinical % ($n = 80$)	Nonclinical %	
		In vitro ($n = 46$)	*In vivo* ($n = 76$)
Toxicogenetic effect			
Mutagenicity	5.3	—	—
Interaction with catalase	—	9.1	—
Activation of AhR	—	9.1	13.3
Not reported	94.7*	81.8*	86.7*
Oxidative damage			
Oxidation of thiols	10.4	18.2	20
Inhibition of cysteine interaction	—	9.1	—
Interaction and oxidation of cysteine residues	—	9.1	—
ROS induction	89.5*	63.6*	80*
Cytotoxicity			
Oxidation of thiols	50.5	18.2	20
Oxidation of cysteine residues	49.5*	18.2	-
ROS induction	—	45.4*	80*

AhR: aryl hydrocarbon receptors; ROS: reactive oxygen species. Chi-square test $^*p < 0.05$.

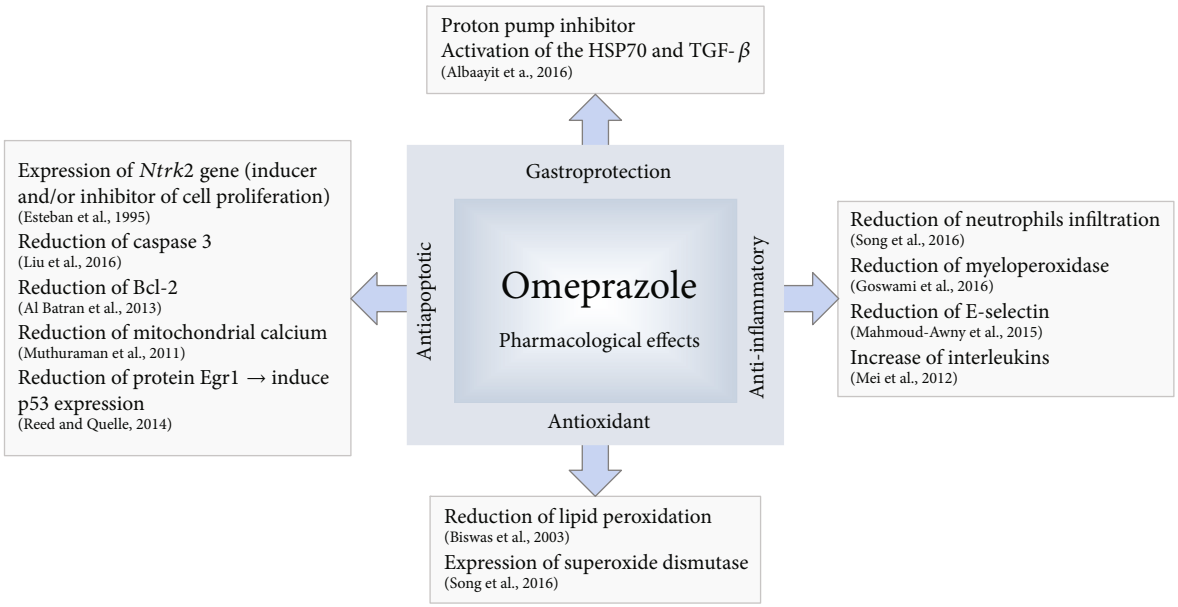

Figure 1: Pharmacological effects of omeprazole and suggested mechanisms of action.

(GERD), peptic ulcer, and *H. pylori* infection [46]. Its mechanisms of action occur from selective and covalent activation with H^+/K^+-ATPase, in particular of extracellular cysteine 813, leading to potent inhibition of gastric acid secretion and triggering changes in the stomach flora [38]. Another mechanism is by blocking the proton pump in the stomach parietal cells, activating the heat shock protein (HSP70), and the transforming growth factor beta (TGF-β) [47], with consequent relief of symptoms and lesion healing [48].

5.1. Therapeutic Effects of Omeprazole and Suggested Mechanisms. Several therapeutic effects have been suggested for OME, such as gastroprotection [49], antioxidant [50], anti-inflammatory [51], antinecrotic [52], and antiapoptotic [53]. The mechanisms of action of these effects are presented in Figure 1.

5.1.1. Gastroprotective Effect. OME gastroprotection is attributed to its ability to block the proton pump in the parietal cells of the stomach, activating the HSP70 and the TGF-β as mentioned above [47]. The expression of HSP70 mRNA was observed in the gastric tissue of rats pretreated with OME [54, 55]. This OME mechanism was reported for rats at doses that varied between 10 μM and 400 mg/kg, as well as 200 μM/ml in regular epithelial cell lines (MDCK) and mouse macrophage (RAW264.7) [55, 56].

Table 4: Gastroprotective effects of OME and mechanisms of action that may lead to protection and/or risk of genomic instability.

Dose/concentration	Study	Test system	Mechanisms of action	Prevention/risk of DNA damage	References
5-40 mg/kg	Clinical	Human ($n = 94558$)	H2 receptor antagonists and PPIs	Oxidative stress	[57]
20 and 40 mg/kg	Clinical	—	pH control	Not identified	[58]
20, 40, and 100 mg/kg	Clinical	Human ($n = 12$)	Inhibition of CYP2C19, pharmacokinetics, gastroprotection of microdoses	Oxidative stress	[42, 43]
10 mg/14 days	Clinical	Human ($n = 32$)	Gastroprotection	Not identified	[62]
20 mg/kg	Clinical	Human ($n = 75$)	Histamine blockage	Not identified	[59]
—	Clinical	Human ($n = 17489$)	Mechanisms involved in the gastric diseases	Oxidative stress	[63]
20 mg/kg	Clinical	Human ($n = 70$)	Pharmacokinetics-antiulceratives	Not identified	[64]
20 mg	Clinical	Human ($n = 199$)	Better action in patients with CYP 2 C1Q PM phenotype	Not identified	[65]
20 mg+amoxicillin 750 mg	Clinical	Human ($n = 268$)	Antacids, dose-dependent, CYP2C19 polymorphisms	Infection, oxidative stress	[66]
0.7, 1.4, and 4 mg/kg	*In vivo*	Horses	Pharmacokinetic and pharmacodynamic mechanisms	Not identified	[67]
15, 30, and 60 mg/kg	*In vivo*	Rats	Reduced necrotic damage, increased mucosal and gastric acid secretion reduction	Not identified	[52]
200 g/ml	*In vivo*	Rats	Increased prostaglandins synthesis and sulfhydryl compounds	Oxidative stress	[60]
40 mg/kg	*In vivo*	Rats	Inhibition of caspase 1, AC-YVAD-CMK, silencing of inflammasome NLRP3	Inhibition of apoptosis	[61]
40 mg/kg	*In vivo*	C57BL1 mice ($n = 6$)	Upregulation of BAX and caspase 3 → increased cell necrosis	Induction of apoptosis and necrosis	[61]
20 mg/kg	*In vivo*	Rats	Gastric protection, inhibition of H^+/K^+-ATPase system	Not identified	[68]
15 mg/kg	*In vivo*	Rats	Decreases blood flow, increased glycoproteins, prostaglandins, necrosis factor (TNF-α)	Not identified	[69]
1-100 μM	*In vitro*	Human hepatocyte cell line	Activation of AhR and induction of CYP1A	Catalytic activities	[41]

PPIs: proton pump inhibitors; TNF-α: tumor necrosis factor-alpha.

In clinical studies, there is evidence of the OME gastroprotective function at doses of 5 to 40 mg/kg by mechanisms associated with interaction with H2 receptors [57], pH control [58], inhibition of CYP2C19 enzymes [42, 43], and histamine blockade [59]. OME in *in vivo* studies increased prostaglandins and sulfhydryl compounds [60], increased expression of BAX and caspases [61], and AhR and CYP1A expression [41]. These mechanisms of action may be related to other pathways that eventually cause genomic instability. Table 4 shows the gastroprotective mechanisms of OME, including its possible association with apoptosis and necrosis, as well as the risk of genomic instability.

5.1.2. Antioxidant and Anti-Inflammatory Effects. Several *in vivo* studies indicate antioxidant activities of OME, due to mechanisms associated with reduction of lipid peroxidation at doses of 2 to 5 mg/kg [50], 10 mg/kg [70], and 20 mg/kg [56]. Antioxidant activities of OME were also reported considering gastric lesions in animals [51] and *in vitro* studies in epithelioid MDCK, RAW264.7 [71], and U-87 cells [72].

OME also has antioxidant activities (*in vitro*), by blocking hydroxyl radical ($^{\cdot}OH$), preventing apoptosis and necrosis [73], inducing nicotinamide adenine dinucleic acid (NADPH) kinase oxidoreductase production [74], and increasing endogenous antioxidants [72]. *In vivo* and *in vitro* studies report inhibition of necrosis by activation of TNF-α, interleukin B [75], and proinflammatory cytokines [76]. OME at 20 mg/kg presented antioxidant activity through mechanisms associated with increased superoxide dismutase (SOD) enzyme production [77, 78], as well as glutathione peroxidase (GPx) and reduced glutathione (GSH) at 30 and 40 mg/kg [51, 79]. In ethanol-induced gastritis rats, OME modulated mucosal lesions through its antioxidant and anti-inflammatory activity [80]. However, clinical studies regarding OME antioxidant activities have not yet been reported.

There are reports of *in vivo* studies, in which OME had effects over increased blood flow of the gastric mucosa and

Table 5: Antioxidant and/or anti-inflammatory activities of OME and its protective effects and/or risk of genomic instability.

Activities	Dose/concentration	Study	Test systems	Mechanism of action	Preventive approach	References
Antioxidant	2, 10, and 20 mg/kg	*In vivo*	Rats	Induction of CYP1A1, antihyperoxia	Prevention of oxidative damage	[92]
Antioxidant	10.0 μM	*In vitro*: cell culture	Human lung fetal cells	Upregulation of NADPH kinase oxidoreductase-1 *via* Nrf-2 expression not dependent on Nrf-2	Prevention of oxidative damage	[74]
Antioxidant	2 and 5 mg/kg (dose-dependent)	*In vivo*	Rats	$^{\cdot}$OH scavenging capacity, prevention of apoptosis by nuclear fragmentation	Prevention of oxidative damage and apoptosis	[73]
Antioxidant/ anti-inflammatory	8.49 g/ml	*In vivo*	Rats	Reduction of hemorrhages and inflammation, preserving the endoplasmic reticulum	Protection of oxidative stress	[80]
Antioxidant Antineuropathic	50 mg/kg	*In vivo*	Rats	Inhibits NF-κB, releases cytokines, protects cranial cruciate ligament (CCL) damage induction, reduces oxidative stress, increases several internal antioxidants	Protection of oxidative damages	[72]
Antitoxicity	5 μg/ml	*In vitro*	Tumor cells	Cytochrome P450 metabolism (CYP450), CYP2C19, CYP3A4, C4P2CY	Toxicity prevention	[93]
Anti-inflammatory	300 μM	*In vivo*	Mice	Inhibition of TNF-α and interleukin	Antiapoptosis prevention of oxidative stress	[75]
Anti-inflammatory	Not reported	*In vivo*	Microglia	Inhibition of proinflammatory cytokines	Prevention of oxidative damage	[76]
Anti-inflammatory	0.5, 1.5, and 10 μg/ml	*In vitro*	MRC-5 cells	Antibacterial effect	Protection from bacterial infection	[94]

expression of gastric glycoproteins [69] that is used as a precise and sensitive marker for the gastric mucosal status. Moreover, OME also plays a significant role as an antiacid, pepsin-resistant, and ulceration protector, which helps to protect the mucosal integrity [81] and reduces neutrophil infiltration [69].

Other mechanisms of action of OME, observed in animals and in cell cultures, relate to the anti-inflammatory marker cyclooxygenase (COX)-2 [77] and NSAIDs, which inhibit COX-1 and COX-2 that cause gastric ulcerogenic effects [82] and to the increase in the neurotrophic tyrosine kinase receptor type 2 (Ntrk2) [83]. OME also reduced TNF-α capacity (*in vivo*) [84]. OME can exert its anti-inflammatory effect through increasing the anti-inflammatory cytokines and autoimmune pathologies [85]. Proinflammatory cytokines, particularly TNF-α and nuclear factor kappa B (NF-κB), are inducers of apoptosis [86]. NF-κB pathway is correlated to gastric lesions in response to TNF-α and IL-1 signaling [77, 87]. TNF-α is involved in inflammatory induction, lesion, and carcinogenesis in several tissues, including the gastric mucosa [87].

In clinical studies, OME can also act in reducing the effects of proinflammatory markers, such as IL-1β [56, 72], monocyte chemoattractant protein-1 (MCP-1) [88], and IL-6 [87]. In cell cultures, esomeprazole has anti-inflammatory activity through mechanisms associated with suppression of proinflammatory proteins, including proteins of cell adhesion molecule 1, nitric oxide synthase, TNF-α, and interleukins (e.g., IL-1β and IL-6). The anti-inflammatory activity is associated with antioxidant activity by the induction of cytoprotective proteins induced by heme oxygenase-1 (HO-1), as well as by inhibition of fibroblast proliferation [89]. OME also has anti-inflammatory effects through reduction of E-selectin [56] and myeloperoxidase (MPO) [90], which can cause damage to proteins, lipids, and DNA through ROS formation [91]. In summary, other OME mechanisms of action as an antioxidant and/or anti-inflammatory and its protective effects and/or risk of genomic instability, as well as toxicity, are presented in Table 5.

5.1.3. Antiapoptotic and Antinecrotic Effects. Apoptosis induction is one of the mechanisms for inducing acute gastric lesion [95]. OME presented antiapoptotic effects (*in vivo*) associated with reduction of caspase 3 expression [90], as well as reduction of BAX [54] and mitochondrial calcium [96]. Other studies indicate that OME has antiapoptotic activity in

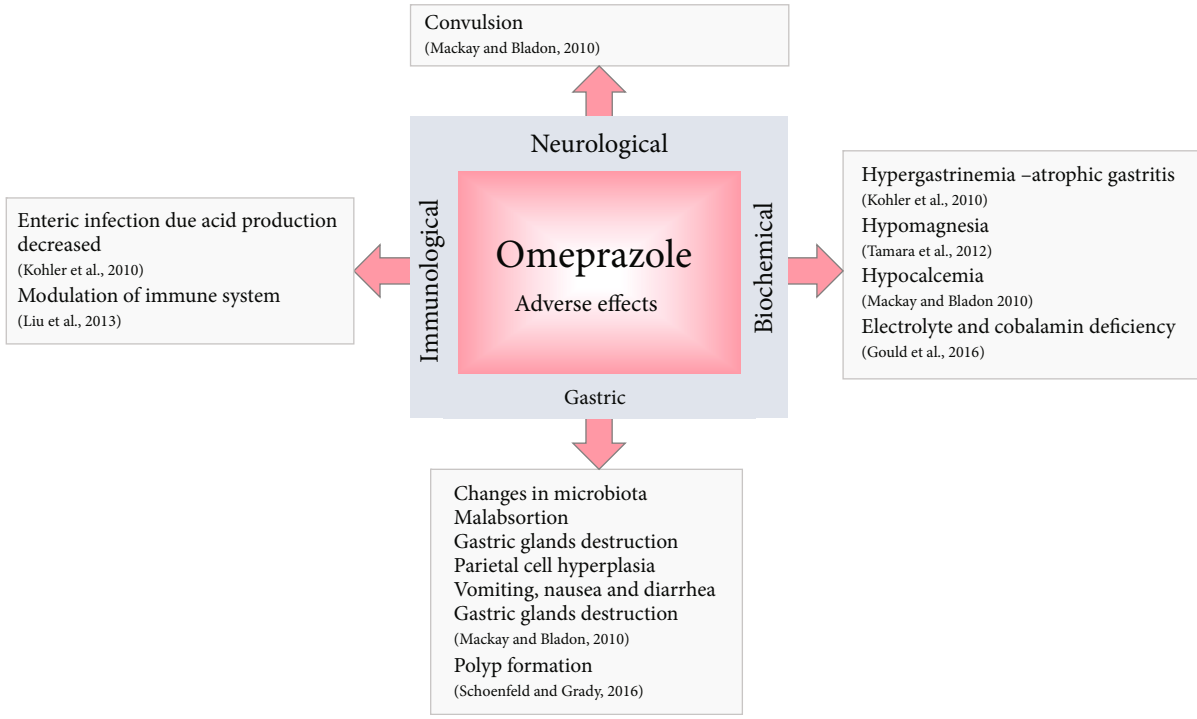

Figure 2: Adverse effects of omeprazole.

the gastric and intestinal tissues, showing reduction of lesions through antioxidant processes and anti-inflammatory activity through expression of *Ntrk2* gene (inductor/inhibitor of cell proliferation) [97] and reduction of protein Egr1, which influences the increase of protein p53 [98].

Mitochondrial permeability transition pore is associated with apoptosis due to free radical production, calcium accumulation [99], and increase in mitochondrial ATP, which is linked to the maintenance of cellular respiration [96] and reduction of mitochondrial cytochrome C [100]. OME in gastric lesion models reduced ulcerative lesions [50], the incidence of gastric hemorrhages [101], prevented visible lesions with edema, erosions, and necrosis in gastric endothelial cells [102, 103], and reduced vascular permeability [104]. OME exerted an antinecrotic effect in rats at 10 μM and 60 mg/kg doses [52] by increasing the gastric mucosal barrier [60] and reducing the necrotic area induced by skin suspension in the animal model [105].

5.2. Adverse Effects of Omeprazole and Suggested Mechanisms. Figure 2 shows the adverse effects of OME. Evidences suggest that OME treatment can alter the gastrointestinal bacterial flora in response to decreased acid formation [106, 107] and increased gastrin production that causes hypergastrinemia. These events can result in gastric polyps, increased risk of bacterial infection, especially *H. pylori*, and gastric cancer as a consequence of the decreased somatostatin release from D cells [108].

Chronic therapies can induce electrolyte and cobalamin deficiency, interrupted bone homeostasis, hypergastrin, and acid secretion (rebound effect) in humans [109]. Atrophic gastritis is characterized by the destruction of the gastric glands and persistent hypergastrinemia [4].

Several studies have been reported that long-term OME use in the treatment of gastritis causes anomalies in the gastric mucosa, such as parietal cell hyperplasia, dilatation of canaliculi in the stomach fundus, corpus and antrum, and projection of cytoplasmic protrusions into the canaliculus lumen [110]. Common side effects observed in the literatures include headache, diarrhea, nausea, constipation, abdominal pain, pruritus, rebound acid hypersecretion, malabsorption, vitamin B_{12} deficiency, and hypotension.

Long-term use of PPIs is also associated with pathological alterations, such as protrusions of parietal cells, dilation of oxyntic glands [110], and development of fundic gland polyps, resulting from a trophic effect on parietal cells [111]. PPIs induce bone fractures [112], enteric infections [113], destruction of gastric glands that induce atrophic gastritis [114], being capable of compromising the immunological system [115], and increasing the risk of morbidity and mortality of patients [116].

Adverse side effects subsequent to long-term OME exposure include severe hypomagnesia [117] and hypocalcemia associated with vomiting, nausea, diarrhea, muscle cramps, and seizures are in relatively low frequency [118]. OME has effects against ulcerative damages induced in the gastric mucosa of rats and mice [56, 61], being able to block the proton pump in the parietal cells of the stomach [47] and activating HSP70 [119].

In summary, OME gastroprotective activities may induce various adverse effects reported in clinical studies such as diarrhea, nausea, constipation, immune deficiencies, fracture induction, vitamin B_{12} deficiency [120], allergies, respiratory infections, hypo- and hyperglycemia, and electrochemical changes [121]. It is important to emphasize that therapeutic clinical studies highlighted toxicity due to

Table 6: Mechanisms of adverse effects of omeprazole, which may be associated with prevention and/or risk of genomic instability.

Dose/concentration	Study	Study model	Mechanisms of action	Prevention/risk for genetic material	References
10 and 20 mg/kg	Clinical	—	Proton pump and histamine receptors, hyperplasia, gastric atrophy, carcinoid tumors	Apoptosis, tumor induction	[125]
—	Clinical	Human ($n = 113$)	Characterization of *H. pylori* associated with gastritis, therapeutic complications	Not reported	[126]
—	Clinical	Meta-analysis review	Hypomagnesemia	Not reported	[42, 43]
5, 10, 20, and 40 mg/kg	Clinical	Human ($n = 764$)	Adverse effects: diarrhea, nausea, constipation, immune deficiencies	Immunological changes	[127]
5 and 40 mg/kg	Clinical	Human ($n = 170$) (review)	Induction of fractures, vitamin B_{12} deficiency, and diarrhea	Apoptosis	[120]
20 mg/kg	Clinical	Patients with gastric disorders, case studies	Induction of allergies, respiratory infection, hepatotoxicity, electrochemical changes, hypo- and hyperglycemia, diarrhea	Apoptosis	[121]
20 and 40 mg/kg	Clinical	Case study	Deficiency of vitamin B_{12}, anemia	Not identified	[128]
20 mg/kg	Clinical	Case study	Induction of gastroesophageal reflux	Metastases, hyperplasias, polyp	[129]
—	Several	Several	Intestinal nephritis, hepatitis, polyps, metaplasia, pneumonia	Cancer	[130]
—	Clinical	Human ($n = 298$)	Adverse effects on cysts and polyps	Lung cancer and pancreatic cancer	[131]
0.83–1.6 mg/kg	*In vivo*	Cats	Heartburn, hypergastrinemia, hypersecretions	Oxidative stress	[109]

increased liver enzymes [122], while in *in vivo* and *in vitro* studies, toxicity has been reported by the oxidation of thiols, sulfonamides [123], caspase 3, and PARP cleavage [124]. Adverse effects of OME may be associated with apoptosis and tumor induction, immune changes, hyperplasia, inflammation, and polyp formation, which may imply in genomic instability (Table 6).

6. Toxicological Risks and Genomic Instability Induced by Omeprazole

Genetic variations induced by genomic instability are involved in the processes of initiation, progression, and resistance to therapy [132]. In the treatment of gastrointestinal disorders, drugs are intermittently or long-term used, and genotoxic risks must be assessed [6, 7]. Toxicogenetic assessment plays an important role in human health [133] and many drugs can be carcinogenenic due to the mechanisms associated with genotoxicity [134]. Thus, it is important in any drug therapy to evaluate the benefits against the risks, especially long-term drug treatment [6, 7].

Studies in animals showed that some drugs induced genotoxicity through DNA damage, as well as micronuclei formation [10, 11, 135]. OME can induce DNA damage by mechanisms involved with oxidative damage, genotoxicity, and mutagenicity (Figure 3).

6.1. Oxidative Damage. Oxidative stress is an important parameter for chemical carcinogenesis [136]. ROS are continuously generated in cells through aerobic metabolism and exogenous sources, including drugs, pesticides, and other environmental factors [137]. This process occurs when the amount of substances responsible for oxidative damage exceeds the capacity of the endogenous antioxidant system [138]. As a consequence, there are alterations in the process of cell signaling, regulation, activation, apoptosis, and necrosis [139].

ROS can cause several types of damage in distinct biomolecules, including DNA, proteins, lipids, carbohydrates, and amino acids; cause ruptures, alterations in guanine and thymine bases, and translocations across the sister chromatids. These alterations can lead to inactivation of tumor-suppressing genes, such as *TP53* and *ATM*; or lead to increased protooncogenes gene expression [140]. ROS can also promote genomic instability and tumorigenesis through increased glucose metabolism and hypoxia adaptations and mutations, which contribute to the abnormal cell growth, angiogenesis, and apoptosis resistance [140].

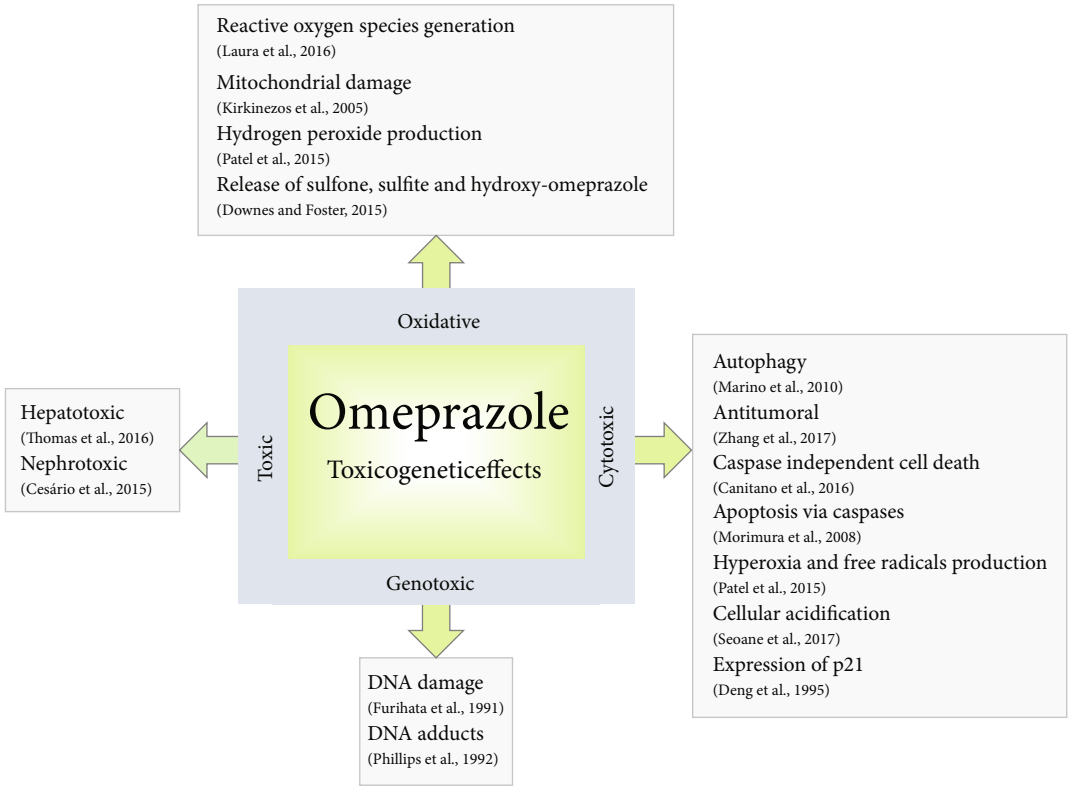

Figure 3: Toxicogenetic effects of omeprazole reported in clinical and nonclinical studies.

There are reports that OME can amplify oxidative stress as a result of gastritis, damaging the gastric mucosa rather than accelerate its healing [4]. Excess ROS can result in inhibition of the gastric acid pump in parietal cells that leads to the release of sulfone, sulfite, and hydroxy-OME [141]. Effects of hyperoxia, inflammation, oxidative stress, and vascular lesions are amplified with OME administration of 25 mg/kg in rats along with the lung and alveolar vascular simplification promoted by AhR [142].

ROS are responsible for modifications in mitochondrial permeability [143], causing mutations and damage to the mitochondrial DNA and the respiratory chain [144, 145]. OME can impart cytotoxicity of hyperoxia and induce ROS in lung microvascular endothelial cells, by producing hydrogen peroxide rather than acute hyperoxic lesions (*in vitro*) [146].

6.2. Genotoxic Effects. Genomic instability caused by drugs can be associated with genotoxicity induction [6, 7, 134]. *In vivo* studies suggest that OME can promote DNA damage [147] through the formation of covalent adduct with DNA in experimental animals [148]. Assessment of genotoxicity of chemicals, including the identification of their mechanisms of action, is important to establish distinctions among carcinogens, especially in the pharmaceutical industry [134]. Drugs that are potentially inductors of genetic instability must have to be monitored before consumption [133].

CYP1A1-inducible chemicals, such as benzo [a] pyrene and 2,3,7,8-tetra-chlorodibenzo-dioxins, usually have adverse effects related to genomic instability (mutagenic, carcinogenic, and teratogenic). However, studies indicate that OME does not induce carcinogenesis, but it may amplify the effects of environmental carcinogens [148]. Nevertheless, studies on DNA damage and chromosomes are necessary and relevant [149], since *in silico* studies showed that OME can cause genotoxicity and mutagenicity through the formation of chromosomal aberrations and micronuclei [150].

At the molecular level, hypo- or achlorhydria triggers the formation of *N*-nitrosamines, which may induce DNA damage and provoke nuclear abnormalities, such as micronuclei, pyknosis, and karyorrhexis [41]. OME does not have a direct mutagenic effect [151], but DNA breaks are a result of oxidative stress [81] in events originated from elevated ROS levels, which cause oxidative damage to cell proteins, membrane lipids, and genetic materials (e.g., DNA, RNA) [152].

6.3. Toxicity of Omeprazole. To understand the mechanisms of drug toxicity, it is necessary to verify drug-drug interactions, the formation of reactive metabolites, and individual susceptibility by genetic polymorphisms in drug-metabolizing enzymes [153]. Gastric lesions are characterized by increased production of $^{\cdot}OH$ and protein oxidation, especially in gastric ulcers [73], which are related to lesion severity [78], producing highly toxic lipid derivatives that may modify cell function and even cell death [79].

OME induces hepatotoxicity in pregnant women, as observed by the reduction of aspartate aminotransferase (AST) and alanine aminotransferase (ALT) enzymes [122]. Hepatotoxic and nephrotoxic effects, thrombocytopenia, acute interstitial nephritis, anaphylactic reactions, gynecomastia, and impotence have been seen in the long-term

OME use [154]. Several mechanisms are involved in drug hepatotoxicity; among those is the disassembly of actin fibrils that may result in cell lysis by changes in membrane transport pumps, as well as apoptosis by activation of the TNF-α [155]. Hepatic toxicity leads to hepatic lesions that disappear after discontinuation of the drug [156].

The PPIs can induce cytotoxicity through autophagic mechanisms, such as alterations in pH homeostasis [157]. OME presented cytotoxic effects in marine microalgae *Tetraselmis* sp. through hyperpolarization of cytoplasm and mitochondrial membranes, as well as by cell acidification and ROS generation [158]. Moreover, OME exerted toxic and cytotoxic effects in rabbit gastric gland cells that were attributed to oxidative processes [4].

More recent studies indicate that OME has antitumor activity against multiple myeloma as a single agent, and associated with chemotherapy, due to its cytotoxic activity as an apoptosis inductor, independently of caspases [159]. OME presented antitumor effects in association with chemotherapy in rectal cancer patients, including reducing the side effects of the treatment [160]. These effects were also observed in fibrosarcoma and colon cancer cells, suggesting that its use associated with anticancer drugs can be a promising therapy against malignant tumors [161].

Studies report that OME presents synergistic effects in rectal cancer chemotherapies [161]. Several mechanisms are proposed for the antitumor effect of Na^+/K^+ pump inhibitors [162], such as cell death stimulators *via* caspases, apoptosis inductors [163–166], an inhibitor of the V-ATPase activity, and turn tumors chemosensitive [167].

Antitumoral effects of OME were also described in studies with several cancer cell lines, including Heya8-MDR, SKOV3-TR, ES-2, and RMG-1; colon carcinoma cells (320WT and 320MUT) [168], neuroblastoma cells (SH-SY5Y), human microglia (THP), myeloma RPMI8226, U266, human gastric cancer (HGC-27), glioblastoma (U-87), human colon cancer (HCT-116 and HCA-7) cells, and *Jurkat T* lymphocytes at concentrations between 10 and 10^6 μM [169, 170].

In xenographic model of colon carcinoma and colon cells, antitumoral effects were also observed through increase expression of immediate early response gene X-1 (IEX-1), a stress-sensitive gene [171–173]. Other mechanisms have been suggested for the OME antitumor effect, such as reduction of Bcl-2 [174–176], Bcl-xL, and survivin [176], as well as reduction of other antiapoptotic proteins [177, 178].

In human gastric cancer cells (HGC-27) and polymorphonuclear neutrophils, OME exerted an antitumoral effect through increase in caspase 3 [123], apoptotic proteins [90], and cleavage of poly [ADP-ribose] polymerase 1 (PARP-1) [124, 169, 170]; OME was cytotoxic in colon cells through increased gastrin secretion and increasing expression of IEX-1. Moreover, OME showed antitumor effects in different carcinomas [172, 173] through mechanisms associated with reduction of Bcl-2 and Bcl-xL expression [176] and in chemoresistant cells (HeyA8-MDR, SKOV3-TR) in association with the anticancer drug paclitaxel [168].

In relation to genotoxicity in clinical studies, it has been reported for clastogenic effects and oxidative stress mechanisms [179] and hydroxylation induction and sulfoxidation in OME doses of 20 to 40 mg/kg [180]. Sulfonamide metabolites have also been reported as mechanisms for genotoxicity in *in vivo* studies [181]. Additionally, there are other mechanisms associated with DNA damage, including ornithine decarboxylase induction as a marker of cell proliferation [182], micronuclei induction [147], transcriptional changes [97], hyperplasia, hypertrophy, and other cellular alterations (Narimar et al., 2009).

OME antitumor effects in clinical studies are rare, but some have shown synergistic effects with antitumor drugs on modulating tumor acidity and apoptosis [160]. In *in vitro* studies, antitumor mechanisms have been related to expression of V-ATPase [168], inhibition of miR203-3p [183], and downregulation of metastatic CXCR4 proteins [184] and miRNAs [185]. In summary, other mechanisms indicative of genotoxicity, toxicity, and cytotoxicity of OME are shown in Table 7.

7. Carcinogenic Effects of Omeprazole

Severe pathological alterations on the stomach mucosa can lead to peptic ulcer and gastric cancer [20], especially due to complications with *H. pylori* infection and exposure to acid and pepsin [46, 107]. Gastric cancer is the 15th leading cause of death by cancer, more frequent in men and mostly influenced by age, diet, and stomach diseases, including *H. pylori* infection [193].

Studies are still controversial, but *H. pylori* can be associated with gastric carcinoma by mechanisms related to increased ROS/RNS and oncoprotein formation [194]. Gastric pathologies are commonly related to increased levels of gastrin [195, 196]. Atrophic gastritis, resulting from monotherapy with OME in the context of *H. pylori* infection, has been associated with an increased risk of mucosa dysplasia and gastric cancer [114].

Carcinogenicity studies are preliminary to the approval and commercialization of pharmaceutical products, including cytogenetic *in vivo* and *in vitro* assays [197–199]. Brambilla and his colleagues report that, out of 535 medications, 279 showed positive results for carcinogenicity in animal tests. Thus, the indication of drugs should consider the risk/benefit in relation to the carcinogenicity and should prioritize new therapeutic intervention strategies [6–11, 200].

Studies have shown that after chronic gastritis, atrophy, intestinal metaplasia, and dysplasia, there are increased risks for gastric cancer [27, 57], especially with *H. pylori* infection [201]. Esomeprazole can induce acid suppression, leading to indigestion and amplifying risks of bacterial infections that generate atrophic gastritis [108, 202].

Long-term use of OME may relate to the cell proliferation and carcinoid tumors [203]. Menegasse et al. [204] concluded that proliferative changes of the oxyntic mucosa occur in individuals with chronic use of PPIs, with statistical significance in association with age and proliferative cell alterations [205]. Several studies reported that acid-suppressing drugs increase risks of polyp formation and/or gastric cancer due to nitrosamine production and

Table 7: Mechanisms indicative of genotoxicity, toxicity, and cytotoxicity of OME and their implications for prevention and/or risk of genomic instability.

Activities	Dose/ concentration	Study	Study model	Mechanism of action	Prevention/risk for genetic material	References
Genotoxicity	20 and 40 mg/kg	Clinical	Endoscopy biopsy	DNA damage, clastogenic effects, oxidative stress	Genomic instability, genetic risks	[179]
Genotoxicity	20 and 600 mg	Clinical	Human ($n = 57$)	Interaction between genetic variations, CYP2C19 hydroxylation, and sulfoxidation	Oxidative stress	[180]
Genotoxicity	20 mg/kg	Clinical	Human ($n = 33$)	Cytogenetic change: micronuclei formation	Genomic instability	[186]
Genotoxicity	20 mg/kg	*In vivo*	Rats	Cytogenetic alterations, breaks of sister chromatids, micronucleus formation, chromosomal alterations	Genetic instability, cytogenetic damage	[186]
Genotoxicity	—	*In vivo*	Rodents	Sulfonamide metabolites	Reactivity with DNA	[150]
Genotoxicity	1-100 μM	*In vivo*	Rats	Activates sulfonamide groups, inhibition of DNA synthesis	DNA damage	[181]
Genotoxicity	30 and 100 mg/kg (p.o.)	*In vivo*	Rats	DNA synthesis, oxytocin decarboxylase induction	Cell proliferation	[182]
Genotoxicity	30 mg/kg	*In vivo*	Rats	Micronuclei formation, cellular alteration, cell proliferation	Chromosomal instability, genomic instability	[147]
Genotoxicity	10 and 100 mg/kg	*In vivo*	Rats	Cell proliferation and replication	Genomic instability	[187]
Genotoxicity	—	*In vivo*	Rats	Transcriptional changes in the gastric mucosa	Changes in inflammatory regulation genes and immune response	[97]
Genotoxicity	20 ml/kg	*In vitro*	Rats	Hyperplasia	Genomic instability	[188]
Toxicity	40 mg/kg	Clinical	Case study	Increased ALT and AST levels	Induction of apoptosis	[122]
Toxicity	—	Clinical	Human	Inflammatory, CYP2CI9 enzyme variation, acute nephritis	Genomic instability	[189]
Toxicity	30 and 60 mg/kg	Clinical	—	Microsomal hepatic inhibition, oxidase function, blocking of H^+/K^+-ATPase system	Oxidative damages	[190]
Toxicity	—	Clinical	Human ($n = 2{,}634$)	Interaction between anti-inflammatory and proton pump inhibitors	Apoptosis	[191]
Toxicity	40 mg/kg	Clinical	Human	Neutropenia	Nontoxic effect	[191]
Toxicity	100 μM	*In vivo*	Rats	Oxidation and toxicity, thiol oxidation, conversion of OME to thiolytic sulfonamides, binding to cysteine residues of H^+/K^+-ATPase system	Oxidative damages	[192]
Toxicity	0.0001 and 50 mM	*In vitro*	Polymorphonuclear neutrophils	Apoptosis, sulfhydryl groups	Apoptosis	[4]
Toxicity	0.0001 mM	*In vitro*	Jurkat cells, lymphomas	Cleavage caspase 3 and PARP	Apoptosis	[123]

Table 7: Continued.

Activities	Dose/ concentration	Study	Study model	Mechanism of action	Prevention/risk for genetic material	References
Antitumoral neoadjuvant	20 and 40 mg/kg (i.v.)	Clinical	Human ($n = 127$)	Modulation of tumor acidity, apoptotic cell death	Inhibition of cell proliferation	[124]
Antitumoral	80 mg/kg	Clinical	Human ($n = 94$)	Synergistic effects with antineoplastic drug	Apoptosis	[160]
Antitumoral	50, 100, and 200 μM	*In vitro*	Human melanoma cells	Cytotoxic effect	Apoptosis	[87]
Antitumoral	10-40 mg/kg	*In vitro*, *in vivo*	Ovary cancer ($n = 44$) patients	Expression of V-ATPase, inhibition of V-ATPase mRNA protein	Apoptosis and cytotoxicity	[159]
Antitumoral	100 μg/ml	*In vitro*	CP-A (ATCC CRL-4027) CP-B (ATCC-CRL4028) cells	Inhibits cell cycle growth (arrest cell cycle at G0/G1) by inhibiting miR203a-3p	Induction of apoptosis	[168]
Antitumoral	200 and 300 μM	*In vitro*	Breast cancer (MCF, $SKBR_3$ MDA–MB-468) cell lines	Decreases MDA-MB, decreases expression of prometastatic proteins and the expression of C-X-C chemokine receptor 4 (CXCR4)	Prevention of metastasis and inhibition of cell proliferation	[183]
Antitumoral	10 mg/kg	*In vivo*	Rats	Decreases NO levels, decreases the expression of TNF-α and B catechins	Apoptosis	[184]
Antitumoral	10 and 30 mg/kg	*In vitro*	HeLa cervical cancer line	Expression of ATPase *via* SiRNA	Cell proliferation	[70]
Antitumoral	50 and 200 μg/ml	*In vitro*	Pancreatic cancer cell lines	Interaction with ATPase function regulators, modulation of liposomal transport	Apoptosis	[22]
Antitumoral	100, 200, and 300 μM/l	*In vitro*	Esophageal adenocarcinoma (KYSE410)	Control intra and extracellular pH, expression of miRNAs	Antiproliferative effect	[165]
Antitumoral	160 μM	*In vitro*	Melanoma cells	Acidification and alkalinization of tumors, NADPH oxidase dysfunction	Autophagy, oxidative stress	[185]

hypergastrinemia. Decreased gastric acidity, due to gastric atrophy or to hypochloridria, may favor bacterial colonization, increasing the cancer risk [206]. OME (20 mg) induces gastric hyperplasia and polyps that increase with therapy and regress with discontinuation, independently of *H. pylori* infection [129].

Also, studies report that OME reacts with DNA and induces cancer in rodents [150]. OME, at high dose (30 mg/kg), was shown to induce carcinogenesis in the anterior stomach by influencing the levels of acid phosphatase (ACP) and *N*-acetyl-β-D-glucosaminidase (NAG) in the serum and spleen [207]. Other evidence showed that OME can induce hypergastrinemia and colorectal tumors [208].

PPIs are associated with *H. pylori*-induced chronic atrophic gastritis, metaplasia, and carcinoma [209]. Atrophic gastritis usually happens during monotherapies with OME, possibly resulting in dysplasia and gastric cancer [210].

In summary, other mechanisms of OME activity may also include carcinogenic risks due to its effects of hypergastrinemia and metaplasia [211]. Other mechanisms are also pointed out in *in vivo* studies such as ROS induction, oxidation of 8-DHD6 [212, 213], premalignant lesions [214], cell cycle alterations, genotoxicity, hyperplasia, and inhibition of liposomal hydrolases [215]. Several studies indicative of OME-mediated carcinogenicity are summarized in Table 8.

8. Conclusion

Studies on the mechanisms of action of OME are still controversial. As a gastroprotectant agent, it blocks proton pump, activates HSP70 proteins and TGF-β, exerts antioxidant activity, reduces lipid peroxidation, and activates expression of antioxidant defenses, without differentiation of doses and/or concentrations. Additionally, in *in vitro* and *in vivo* studies, anti-inflammatory effects of OME have been related to increased gastric flow, increased anti-inflammatory markers (COX-2, IL-10A, and IL-6), and antiapoptotic

Table 8: Mechanisms of action of omeprazole implicated in genomic instability, which are associated with cancer risks.

Dose/concentration	Study	Study model	Mechanism of action	Prevention/risk for genetic material	References
100 mg/kg	*In vivo*	Rats	Hypergastrinemia and pancreatic metaplasia	Genomic instability	[216]
20 mg/kg	Clinical	Case study	Hyperplasia, gastric carcinoma, hypoacidity	Cell proliferation	[211]
Not reported	Clinical	Human ($n = 230$) patients with *H. pylori*	Metaplasias, gastric atrophy	Gastric cancer	[217]
276 mg/kg	*In vivo*	Rats	Induction of ROS. 8-0Hd6	Apoptosis Tumors	[212, 213]
—	Several	Several	Premalignant lesions	Genetic alterations	[214]
30 mg/kg	*In vivo*	Rats	Inhibition of lysosomal hydrolase activity decreases P21 and mammalian target of rapamycin (mTOR) in the stomach	Changes in apoptosis and cell cycle	[215]
—	*In silico*	Artificial system	Formation of metabolites	Genomic instability	[218]

activity by reducing caspase 3, Bcl-2, mitochondrial calcium, and expression of *NTRK2* and *GGR1* genes. However, OME adverse effects, especially *in vivo*, such as changes in bacterial flora, enteric infections, gastric gland destruction, polyp formation, hypomagnesia, hypocalcemia, hyperplasia, intestinal metaplasia, electrolyte deficiency, and immunological component changes, may relate to the consequences of genomic instability. In summary, besides the gastroprotective effects, the adverse effects of OME may be due to its DNA damage capacity by inducing oxidative stress, apoptosis and necrosis, immunological alterations, cell proliferation, autophagy, and tumors.

Conflicts of Interest

The authors declare that they have no conflicts of interest.

Acknowledgments

We are thankful to the Federal University of Piauí and PPSUS/FAPEPI for the financial support.

References

[1] A. D. Asatryan and N. L. Komarova, "Evolution of genetic instability in heterogeneous tumors," *Journal of Theoretical Biology*, vol. 396, pp. 1–12, 2016.

[2] R. A. Burrell and C. Swanton, "Tumour heterogeneity and the evolution of polyclonal drug resistance," *Molecular Oncology*, vol. 8, no. 6, pp. 1095–1111, 2014.

[3] L. R. Ferguson, H. Chen, A. R. Collins et al., "Genomic instability in human cancer: Molecular insights and opportunities for therapeutic attack and prevention through diet and nutrition," *Seminars in Cancer Biology*, vol. 35, pp. S5–S24, 2015.

[4] J. E. Kohler, A. L. Blass, J. Liu, K. Tai, and D. I. Soybel, "Antioxidant pre-treatment prevents omeprazole-induced toxicity in an *in vitro* model of infectious gastritis," *Free Radical Biology and Medicine*, vol. 49, no. 5, pp. 786–791, 2010.

[5] R. Wadhwa, S. Song, J. S. Lee, Y. Yao, Q. Wei, and J. A. Ajani, "Gastric cancer—molecular and clinical dimensions," *Nature Reviews Clinical Oncology*, vol. 10, no. 11, pp. 643–655, 2013.

[6] N. Downes and J. Foster, "Regulatory forum opinion piece: carcinogen risk assessment: the move from screens to science," *Toxicologic Pathology*, vol. 43, no. 8, pp. 1064–1073, 2015.

[7] H. G. Neumann, "Risk assessment of chemical carcinogens and thresholds," *Critical Reviews in Toxicology*, vol. 39, no. 6, pp. 449–461, 2009.

[8] G. Brambilla, F. Mattioli, and A. Martelli, "Genotoxic and carcinogenic effects of gastrointestinal drugs," *Mutagenesis*, vol. 25, no. 4, pp. 315–326, 2010.

[9] G. Brambilla, F. Mattioli, L. Robbiano, and A. Martelli, "Genotoxicity and carcinogenicity testing of pharmaceuticals: correlations between induction of DNA lesions and carcinogenic activity," *Mutation Research/Reviews in Mutation Research*, vol. 705, no. 1, pp. 20–39, 2010.

[10] G. Brambilla, F. Mattioli, L. Robbiano, and A. Martelli, "Update of carcinogenicity studies in animals and humans of 535 marketed pharmaceuticals," *Mutation Research/Reviews in Mutation Research*, vol. 750, no. 1, pp. 1–51, 2012.

[11] G. Brambilla, F. Mattioli, L. Robbiano, and A. Martelli, "Studies on genotoxicity and carcinogenicity of antibacterial, antiviral, antimalarial and antifungal drugs," *Mutagenesis*, vol. 27, no. 4, pp. 387–413, 2012.

[12] J. Feher, *Quantitative human physiology: an introduction*, Academic Press, 2012.

[13] K. S. Jain, A. K. Shah, J. Bariwal et al., "Recent advances in proton pump inhibitors and management of acid-peptic disorders," *Bioorganic and Medicinal Chemistry*, vol. 15, no. 3, pp. 1181–1205, 2007.

[14] M. J. Ferrua and R. P. Singh, "Modeling the fluid dynamics in a human stomach to gain insight of food digestion," *Journal of Food Science*, vol. 75, no. 7, pp. R151–R162, 2010.

[15] R. Kenneth and M. D. Mcquaid, "Fármacos usados no tratamento de doenças gastrintesti-nais," in *Farmacologia básica e clínica*, B. G. Katzung, S. B. Masters, and A. J. Trevor, Eds., pp. 1081–1092, AMGH, Porto Alegre, 12 edition, 2014.

[16] J. L. Wallace and K. A. Sharkey, "Farmacoterapia da acidez gástrica, úlcera pépticas e doença do refluxo gastroesofágico," in *As bases farmacológicas da terapêutica de Goodman & Gil-man*, L. L. Brunton, B. A. Chabner, and B. C. Knolmann, Eds., pp. 1309–1321, AMGH, Porto Alegre, 12 edition, 2012.

[17] M. L. Schubert, "Gastric secretion," *Current Opinion in Gastroenterology*, vol. 30, no. 6, pp. 578–582, 2014.

[18] X. Yao and J. G. Forte, "Cell biology of acid secretion by the parietal cell," *Annual Review of Physiology*, vol. 65, no. 1, pp. 103–131, 2003.

[19] C. Y. Hong, S. Y. Lee, S. H. Ryu, S. S. Lee, and M. Kim, "Whole-Genome *De Novo* Sequencing of the lignin-degrading wood rot Fungus *Phanerochaete chrysosporium* (ATCC 20696)," *Genome Announcements*, vol. 5, no. 32, 2017.

[20] N. Dias, P. Santos, M. Pinto et al., "Análise de prontuários de pacientes com gastrite em um hospital na região oeste ii do estado de Goiás," *Revista Eletrônica Faculdade Montes Belos*, vol. 8, no. 1, pp. 1–9, 2015.

[21] V. K. Bansal and R. K. Goel, "Gastroprotective effect of *Acacia nilotica* young seedless pod extract: Role of polyphenolic constituents," *Asian Pacific Journal of Tropical Medicine*, vol. 5, no. 7, pp. 523–528, 2012.

[22] K. H. Song, S. R. Woo, J. Y. Chung et al., "REP1 inhibits FOXO3-mediated apoptosis to promote cancer cell survival," *Cell Death & Disease*, vol. 8, no. 1, article e2536, 2017.

[23] T. Brzozowski, A. Ptak-Belowska, S. Kwiecien et al., "Novel concept in the mechanism of injury and protection of gastric mucosa: role of renin-angiotensin system and active metabolites of angiotensin," *Current Medicinal Chemistry*, vol. 19, no. 1, pp. 55–62, 2012.

[24] R. Ballweg, F. Schozer, K. Elliott et al., "Multiscale positive feedbacks contribute to unidirectional gastric disease progression induced by Helicobacter pylori infection," *BMC Systems Biology*, vol. 11, no. 1, 2017.

[25] A. H. Willemijntje and J. P. Pankaj, "Agents used for control of gastric acidity and treatment of peptic ulcers and gastroesophageal reflux disease," in *The Pharmacological Basis of Therapeutics*, G. H. Joel and E. L. Lee, Eds., pp. 1010-1011, McGraw-Hill Medical Publishing Division, Britain, 2001.

[26] P. Malfertheiner, F. K. L. Chan, and K. E. L. Mccoll, "Peptic ulcer disease," *The Lancet*, vol. 374, no. 9699, pp. 1449–1461, 2009.

[27] D. Y. Graham, "History of *Helicobacter pylori*, duodenal ulcer, gastric ulcer and gastric cancer," *World Journal of Gastroenterology: WJG*, vol. 20, no. 18, pp. 5191–5204, 2014.

[28] V. D.'. A. Cartágenes, L. C. Martins, L. M. Carneiro, K. A. d. S. Barile, and T. C. Corvelo, "*Helicobacter pylori* em crianças e associação de cepas CagA na transmissão mãe-filho na Amazônia brasileira," *Revista da Sociedade Brasileira de Medicina Tropical*, vol. 42, no. 3, pp. 298–302, 2009.

[29] K. C. Machado, G. L. S. Oliveira, É. B. V. de Sousa et al., "Spectroscopic studies on the *in vitro* antioxidant capacity of isopentyl ferulate," *Chemico-Biological Interactions*, vol. 225, pp. 47–53, 2015.

[30] S. J. Konturek, P. C. Konturek, T. Brzozowski, J. W. Konturek, and W. W. Pawlik, "From nerves and hormones to bacteria in the stomach; Nobel prize for achievements in gastrology during last century," *Journal of Physiology and Pharmacology*, vol. 56, no. 4, pp. 507–530, 2005.

[31] R. Fiocca, L. Mastracci, S. E. Attwood et al., "Gastric exocrine and endocrine cell morphology under prolonged acid inhibition therapy: results of a 5-year follow-up in the LOTUS trial," *Alimentary Pharmacology & Therapeutics*, vol. 36, no. 10, pp. 959–971, 2012.

[32] I. Polanco Allué, "Microbiota y enfermedades gastrointestinales," *Anales de Pediatría (English Edition)*, vol. 83, no. 6, pp. 443.e1–443.e5, 2015.

[33] M. Kalayci, M. A. Kocdor, T. Kuloglu et al., "Comparison of the therapeutic effects of sildenafil citrate, heparin and neuropeptides in a rat model of acetic acid-induced gastric ulcer," *Life Sciences*, vol. 186, pp. 102–110, 2017.

[34] A. Lanas and F. K. L. Chan, "Peptic ulcer disease," *The Lancet*, vol. 390, no. 10094, pp. 613–624, 2017.

[35] E. Mnich, M. Kowalewicz-Kulbat, P. Sicińska et al., "Impact of Helicobacter pylori on the healing process of the gastric barrier," *World Journal of Gastroenterology*, vol. 22, no. 33, pp. 7536–7558, 2016.

[36] H. B. Pandya, H. H. Agravat, and J. S. Patel, "Prevalence of specific Helicobacter Pylori CagA, vacA, iceA, ureC genotypes and its clinical relevance in the patients with acid-peptic diseases," *Journal of Clinical and Diagnostic Research*, vol. 11, no. 8, pp. 23–26, 2017.

[37] G. Numico, V. Fusco, P. Franco, and F. Roila, "Proton pump inhibitors in cancer patients: how useful they are? A review of the most common indications for their use," *Critical Reviews In Oncology/hematology*, vol. 111, pp. 144–151, 2017.

[38] V. Savarino, P. Dulbecco, N. de Bortoli, A. Ottonello, and E. Savarino, "The appropriate use of proton pump inhibitors (PPIs): need for a reappraisal," *European Journal Of Internal Medicine*, vol. 37, pp. 19–24, 2017.

[39] A. Minalyan, J. N. Benhammou, A. Artashesyan, M. S. Lewis, and J. R. Pise-Gna, "Autoimmune atrophic gastritis: current perspectives," *Clinical and Experimental Gastroenterology*, vol. 10, pp. 19–27, 2017.

[40] M. L. Schubert and D. A. Peura, "Control of gastric acid secretion in health and disease," *Gastroenterology*, vol. 134, no. 7, pp. 1842–1860, 2008.

[41] A. Novotna, A. Srovnalova, M. Svecarova, M. Korhonova, I. Bartonkova, and Z. Dvorak, "Differential effects of omeprazole and lansoprazole enantiomers on aryl hydrocarbon receptor in human hepatocytes and cell lines," *PLoS One*, vol. 9, no. 6, article e98711, 2014.

[42] S. Park, Y. J. Hyun, Y. R. Kim et al., "Effects of CYP2C19 genetic polymorphisms on PK/PD responses of omeprazole in Korean healthy volunteers," *Journal of Korean Medical Science*, vol. 32, no. 5, pp. 729–736, 2017.

[43] Y. M. Hu, J. M. Xu, Q. Mei, X. H. Xu, and S. Y. Xu, "Pharmacodynamic effects and kinetic disposition of rabeprazole in relation to CYP2C19 genotype in healthy Chinese subjects," *Acta Pharmacologica Sinica*, vol. 26, no. 3, pp. 384–388, 2005.

[44] W. A. Hoogerwerf and P. J. Pasricha, "Pharmacotherapy of gastric acidity, peptic ulcers and gastroesophageal reflux disease," in *The Pharmacological Basis of Therapeutics*, A. G. Goodman, Ed., pp. 967–981, Mc Graw Hill, 2006.

[45] X. Wang and S. Li, "Protein mislocalization: mechanisms, functions and clinical applications in cancer," *Biochimica et Biophysica Acta (BBA) - Reviews on Cancer*, vol. 1846, no. 1, pp. 13–25, 2014.

[46] A. Novotna, M. Korhonova, I. Bartonkova et al., "Enantiospecific effects of ketoconazole on aryl hydrocarbon receptor," *PLoS One*, vol. 9, no. 7, article e101832, 2014.

[47] H. Holguín, M. Ceballos, and P. Amariles, "Clinical relevance of clopidogrel and omeprazole interaction: systematic review," *Revista Colombiana de Cardiología*, vol. 19, no. 1, pp. 25–32, 2012.

[48] E. Lahner, G. Galli, G. Esposito, E. Pilozzi, V. D. Corleto, and B. Annibale, "Updated features associated with type 1 gastric carcinoids patients: a single-center study," *Scandinavian Journal of Gastroenterology*, vol. 49, no. 12, pp. 1447–1455, 2014.

[49] A. Muthuraman and S. Sood, "Antisecretory, antioxidative and antiapoptotic effects of montelukast on pyloric ligation and water immersion stress induced peptic ulcer in rat," *Pros-taglandins, Leukotrienes and Essential Fatty Acids*, vol. 83, no. 1, pp. 55–60, 2010.

[50] N. E. El-Ashmawy, E. G. Khedr, H. A. El-Bahrawy, and H. M. Selim, "Nebivolol prevents indomethacin-induced gastric ulcer in rats," *Journal of Immunotoxicology*, vol. 13, no. 4, pp. 580–589, 2016.

[51] S. B. Almasaudi, N. A. el-Shitany, A. T. Abbas et al., "Antioxidant, anti-inflammatory, and antiulcer potential of manuka honey against gastric ulcer in rats," *Oxidative Medicine and Cellular Longevity*, vol. 2016, Article ID 3643824, 10 pages, 2016.

[52] C. Blandizzi, G. Gherardi, C. Marveggio, G. Natale, D. Carignani, and M. del Tacca, "Mechanisms of protection by omeprazole against experimental gastric mucosal damage in rats," *Digestion*, vol. 56, no. 3, pp. 220–229, 1995.

[53] R. N. El-Naga, "Apocynin protects against ethanol-induced gastric ulcer in rats by attenuating the upregulation of NADPH oxidases 1 and 4," *Chemico-Biological Interactions*, vol. 242, pp. 317–326, 2015.

[54] R. Al Batran, F. Al-Bayaty, M. M. Jamil Al-Obaidi et al., "In vivo antioxidant and antiulcer activity of *Parkia speciosa* ethanolic leaf extract against ethanol-induced gastric ulcer in rats," *PLoS One*, vol. 8, no. 5, article e64751, 2013.

[55] S. F. A. Albaayit, Y. Abba, R. Abdullah, and N. Abdullah, "Prophylactic effects of *Clausena excavata* Burum. f. leaf extract in ethanol-induced gastric ulcers," *Drug Design, Development and Therapy*, vol. 10, pp. 1973–1986, 2016.

[56] M. Mahmoud-Awny, A. S. Attia, M. F. Abd-Ellah, and H. S. El-Abhar, "Mangiferin mitigates gastric ulcer in ischemia/reperfused rats: involvement of PPAR-γ, NF-κB and Nrf 2/HO-1 signaling pathways," *PLoS One*, vol. 10, no. 7, article e0132497, 2015.

[57] J. S. Ahn, C. S. Eom, C. Y. Jeon, and S. M. Park, "Acid suppressive drugs and gastric cancer: a meta-analysis of observational studies," *World Journal of Gastroenterology*, vol. 19, no. 16, pp. 2560–2568, 2013.

[58] W. Asghar, E. Pittman, and F. Jamali, "Comparative efficacy of esomeprazole and omeprazole: racemate to single enantiomer switch," *DARU Journal of Pharmaceutical Sciences*, vol. 23, no. 1, p. 50, 2015.

[59] S. Kajiura, A. Hosokawa, A. Ueda et al., "Effective healing of endoscopic submucosal dissection-induced ulcers by a single week of proton pump inhibitor treatment: a retrospective study," *BMC Research Notes*, vol. 8, no. 1, p. 150, 2015.

[60] C. Blandizzi, G. Natale, G. Gherardi et al., "Gastroprotective effects of pantoprazole against experimental mucosal damage," *Fundamental & Clinical Pharmacology*, vol. 14, no. 2, pp. 89–99, 2000.

[61] F. Zhang, L. Wang, J. J. Wang, P. F. Luo, X. T. Wang, and Z. F. Xia, "The caspase-1 inhibitor AC-YVAD-CMK attenuates acute gastric injury in mice: involvement of silencing NLRP3 inflammasome activities," *Scientific Reports*, vol. 6, no. 1, article 24166, 2016.

[62] T. Kuramoto, E. Umegaki, S. Nouda et al., "Preventive effect of irsogladine or omeprazole on non-steroidal anti-inflammatory drug-induced esophagitis, peptic ulcers, and small intestinal lesions in humans, a prospective randomized controlled study," *BMC Gastroenterology*, vol. 13, no. 1, p. 85, 2013.

[63] D. N. Bateman, D. Colin-Jones, S. Hartz et al., "Mortality study of 18 000 patients treated with omeprazole," *Gut*, vol. 52, no. 7, pp. 942–946, 2003.

[64] Y. Choi, H. Han, D. Shin, K. S. Lim, and K. S. Yu, "Comparison of the pharmacokinetics and tolerability of HCP1004 (a fixed-dose combination of naproxen and esomeprazole strontium) and VIMOVO® (a marketed fixed-dose combination of naproxen and esomeprazole magnesium) in healthy volunteers," *Drug Design, Development and Therapy*, vol. 9, pp. 4127–4135, 2015.

[65] A. Nagahara, T. Suzuki, N. Nagata et al., "A multicentre randomised trial to compare the efficacy of omeprazole versus rabeprazole in early symptom relief in patients with reflux esophagitis," *Journal of Gastroenterology*, vol. 49, no. 12, pp. 1536–1547, 2014.

[66] T. Nishida, M. Tsujii, H. Tanimura et al., "Comparative study of esomeprazole and lansoprazole in triple therapy for eradication of Helicobacter pylori in Japan," *World Journal of Gastroenterology: WJG*, vol. 20, no. 15, pp. 4362–4369, 2014.

[67] K. Birkmann, H. K. Junge, E. Maischberger, M. Wehrli Eser, and C. C. Schwarzwald, "Efficacy of omeprazole powder paste or enteric-coated formulation in healing of gastric ulcers in horses," *Journal of Veterinary Internal Medicine*, vol. 28, no. 3, pp. 925–933, 2014.

[68] M. Y. Ibrahim, N. M. Hashim, S. M. Dhiyaaldeen et al., "Acute toxicity and gastroprotection studies of a new Schiff base derived manganese (II) complex against HCl/ethanol-induced gastric ulcerations in rats," *Scientific Reports*, vol. 6, no. 1, article 26819, 2016.

[69] W. Gao, H.-Y. Li, L.-X. Wang et al., "Protective effect of omeprazole on gastric mucosal of cirrhotic portal hypertension rats," *Asian Pacific Journal of Tropical Medicine*, vol. 7, no. 5, pp. 402–406, 2014.

[70] Y. J. Kim, J. S. Lee, K. S. Hong, J. W. Chung, J. H. Kim, and K. B. Hahm, "Novel application of proton pump inhibitor for the prevention of colitis-induced colorectal carcinogenesis beyond acid suppression," *Cancer Prevention Research*, vol. 3, no. 8, pp. 963–974, 2010.

[71] S. Puiac, X. Sem, A. Negrea, and M. Rhen, "Small-molecular virulence inhibitors show divergent and immunomodulatory effects in infection models of *Salmonella enterica* serovar Typhimurium," *International Journal of Antimicrobial Agents*, vol. 38, no. 5, pp. 409–416, 2011.

[72] S. K. Chanchal, U. B. Mahajan, S. Siddharth et al., "*In vivo* and *in vitro* protective effects of omeprazole against neuropathic pain," *Scientific Reports*, vol. 6, no. 1, pp. 1–10, 2016.

[73] K. Biswas, U. Bandyopadhyay, I. Chattopadhyay, A. Varadaraj, E. Ali, and R. K. Banerjee, "A novel antioxidant and antiapoptotic role of omeprazole to block gastric ulcer

through scavenging of hydroxyl radical," *Journal of Biological Chemistry*, vol. 278, no. 13, pp. 10993–11001, 2003.

[74] A. Patel, S. Zhang, A. K. Shrestha, P. Maturu, B. Moorthy, and B. Shivanna, "Omeprazole induces heme oxygenase-1 in fetal human pulmonary microvascular endothelial cells via hydrogen peroxide-independent Nrf2 signaling pathway," *Toxicology and Applied Pharmacology*, vol. 311, pp. 26–33, 2016.

[75] E. Balza, P. Piccioli, S. Carta et al., "Proton pump inhibitors protect mice from acute systemic inflammation and induce long-term cross-tolerance," *Cell Death & Disease*, vol. 7, no. 7, article e2304, 2016.

[76] S. Hashioka, A. Klegeris, and P. L. Mcgeer, "Proton pump inhibitors exert anti-inflammatory effects and decrease human microglial and monocytic THP-1 cell neurotoxicity," *Experimental Neurology*, vol. 217, no. 1, pp. 177–183, 2009.

[77] J.-W. Song, C.-S. Seo, T.-I. Kim et al., "Protective effects of manassantin A against ethanol-induced gastric injury in rats," *Biological and Pharmaceutical Bulletin*, vol. 39, no. 2, pp. 221–229, 2016.

[78] H. Zheng, Y. Chen, J. Zhang et al., "Evaluation of protective effects of costunolide and dehydrocostuslactone on ethanol-induced gastric ulcer in mice based on multi-pathway regulation," *Chemico-Biological Interactions*, vol. 250, pp. 68–77, 2016.

[79] A. T. Shimoyama, J. R. Santin, I. D. Machado et al., "Antiulcerogenic activity of chlorogenic acid in different models of gastric ulcer," *Naunyn-Schmiedeberg's Archives of Pharmacology*, vol. 386, no. 1, pp. 5–14, 2013.

[80] K. Kengkoom, N. Tirawanchai, W. Angkhasirisap, and S. Ampawong, "Omeprazole preserves the RER in chief cells and enhances re-epithelialization of parietal cells with SOD and AQP-4 up-regulation in ethanol-induced gastritis rats," *Experimental and Therapeutic Medicine*, vol. 14, no. 6, pp. 5871–5880, 2017.

[81] Z. Fang, J. Tang, Y. Bai et al., "Plasma levels of microRNA-24, microRNA-320a, and microRNA-423-5p are potential biomarkers for colorectal carcinoma," *Journal of Experimental & Clinical Cancer Research*, vol. 34, no. 1, p. 86, 2015.

[82] D. I. Hamdan, M. F. Mahmoud, M. Wink, and A. M. El-Shazly, "Effect of hesperidin and neohesperidin from bitter-sweet orange (*Citrus aurantium* var. *bigaradia*) peel on indomethacin-induced peptic ulcers in rats," *Environmental Toxicology and Pharmacology*, vol. 37, no. 3, pp. 907–915, 2014.

[83] C. Nassenstein, S. Kerzel, and A. Braun, "Neurotrophins and neurotrophin receptors in allergic asthma," *Progress in Brain Research*, vol. 146, pp. 347–367, 2004.

[84] S. Mao, G. Yang, W. Li et al., "Gastroprotective effects of astragaloside IV against acute gastric lesion in rats," *PLoS One*, vol. 11, no. 2, p. e0148146, 2016.

[85] R. Sabat, G. Grütz, K. Warszawska et al., "Biology of interleukin-10," *Cytokine & Growth Factor Reviews*, vol. 21, no. 5, pp. 331–344, 2010.

[86] T. Lawrence, "The nuclear factor NF-κB pathway in inflammation," *Cold Spring Harbor perspectives in biology*, vol. 1, no. 6, 2009.

[87] J. Wang, T. Zhang, L. Zhu, C. Ma, and S. Wang, "Anti-ulcerogenic effect of Zuojin Pill against ethanol-induced acute gastric lesion in animal models," *Journal of Ethnopharmacology*, vol. 173, pp. 459–467, 2015.

[88] B. K. Choo and S. S. Roh, "Berberine protects against esophageal mucosal damage in reflux esophagitis by suppressing proinflammatory cytokines," *Experimental and Therapeutic Medicine*, vol. 6, no. 3, pp. 663–670, 2013.

[89] Y. T. Ghebremariam, J. P. Cooke, W. Gerhart et al., "Pleiotropic effect of the proton pump inhibitor esomeprazole leading to suppression of lung inflammation and fibrosis.," *Journal of Translational Medicine*, vol. 13, no. 1, pp. 1–20, 2015.

[90] Z. Liu, Y. Luo, Y. Cheng et al., "Gastrin attenuates ischemia-reperfusion-induced intestinal injury in rats," *Experimental Biology and Medicine*, vol. 241, no. 8, pp. 873–881, 2016.

[91] R. P. Laura, D. Dong, W. F. Reynolds, and R. A. Maki, "T47D cells expressing myeloperoxidase are able to process, traffic and store the mature protein in lysosomes: studies in T47D cells reveal a role for Cys319 in MPO biosynthesis that precedes its known role in intermolecular disulfide bond formation," *PLoS One*, vol. 11, no. 2, article e0149391, 2016.

[92] J. Richter, J. Jimenez, T. Nagatomo et al., "Proton-pump inhibitor omeprazole attenuates hyperoxia induced lung injury," *Journal of Translational Medicine*, vol. 14, no. 1, p. 247, 2016.

[93] K. L. Niece, N. K. Boyd, and K. S. Akers, "In vitro study of the variable effects of proton pump inhibitors on voriconazole," *Antimicrobial Agents and Chemotherapy*, vol. 59, no. 9, pp. 5548–5554, 2015.

[94] E. Botelho-Nevers, S. Singh, L. Chiche, and D. Raoult, "Effect of omeprazole on vacuole size in *Coxiella burnetii* -infected cells," *Journal of Infection*, vol. 66, no. 3, pp. 288-289, 2013.

[95] D. I. Lou, J. A. Hussmann, R. M. Mcbee et al., "High-throughput DNA sequencing errors are reduced by orders of magnitude using circle sequencing," *Proceedings of the National Academy of Sciences of the United States of the America*, vol. 110, no. 49, pp. 19872–19877, 2013.

[96] A. Muthuraman, M. Ramesh, and A. Chauhan, "Mitochondrial dependent apoptosis: ameliorative effect of flunarizine on ischemia–reperfusion of celiac artery-induced gastric lesions in the rat," *Digestive Diseases and Sciences*, vol. 56, no. 8, pp. 2244–2251, 2011.

[97] K. G. Nørsett, A. Laegreid, M. Langaas et al., "Molecular characterization of rat gastric mucosal response to potent acid inhibition," *Physiological Genomics*, vol. 22, no. 1, pp. 24–32, 2005.

[98] S. M. Reed and D. E. Quelle, "p53 acetylation: regulation and consequences," *Cancers*, vol. 7, no. 1, pp. 30–69, 2014.

[99] H. Jiang, C. Hou, S. Zhang et al., "Matrine upregulates the cell cycle protein E2F-1 and triggers apoptosis via the mitochondrial pathway in K562 cells," *European Journal of Pharmacology*, vol. 559, no. 2-3, pp. 98–108, 2007.

[100] S. A. El-Maraghy, S. M. Rizk, and N. N. Shahin, "Gastroprotective effect of crocin in ethanol-induced gastric injury in rats," *Chemico-Biological Interactions*, vol. 229, pp. 26–35, 2015.

[101] S. G. Kinsey, D. K. Nomura, S. T. O'Neal et al., "Inhibition of monoacylglycerol lipase attenuates non-steroidal anti-inflammatory drug-induced gastric hemorrhages in mice," *Journal of Pharmacology and Experimental Therapeutics*, vol. 338, no. 3, pp. 795–802, 2011.

[102] G. Morini, D. Grandi, M. L. Arcari, and G. Bertaccini, "Gastroprotective activity of the novel proton pump inhibitor

lansoprazole in the rat," *General Pharmacology: The Vascular System*, vol. 26, no. 5, pp. 1021–1025, 1995.

[103] G. Morini, D. Grandi, M. L. Arcari, and G. Bertaccini, "Indomethacin-induced morphological changes in the rat gastric mucosa, with or without prior treatment with two proton pump inhibitors," *Alimentary Pharmacology and Therapeutics*, vol. 9, no. 6, pp. 615–623, 1995.

[104] B. Maity, S. K. Yadav, B. S. Patro, M. Tyagi, S. K. Bandyopadhyay, and S. Chattopadhyay, "Molecular mechanism of the anti-inflammatory activity of a natural diarylnonanoid, malabaricone C," *Free Radical Biology and Medicine*, vol. 52, no. 9, pp. 1680–1691, 2012.

[105] H. Sen, M. Oruç, V. M. Işik et al., "The effect of omeprazole usage on the viability of random pattern skin flaps in rats," *Annals of Plastic Surgery*, vol. 78, no. 6, pp. e5–e9, 2017.

[106] L. Wannmacher, "Inibidores da bomba de prótons: indicações racionais," *Brasília*, vol. 2, no. 1, 2004.

[107] G. R. Yanagihara, A. G. de Paiva, M. P. Neto et al., "Effects of long-term administration of omeprazole on bone mineral density and the mechanical properties of the bone," *Revista Brasileira de Ortopedia*, vol. 50, no. 2, pp. 232–238, 2015.

[108] S. Chubineh and J. Birk, "Proton pump inhibitors: the good, the bad, and the unwanted," *Southern Medical Journal*, vol. 105, no. 11, pp. 613–618, 2012.

[109] E. Gould, C. Clements, A. Reed et al., "A prospective, placebo-controlled pilot evaluation of the effect of omeprazole on serum calcium, magnesium, cobalamin, gastrin concentrations, and bone in cats," *Journal of Veterinary Internal Medicine*, vol. 30, no. 3, pp. 779–786, 2016.

[110] K. R. Kumar, R. Iqbal, E. Coss, C. Park, B. Cryer, and R. M. Genta, "*Helicobacter* gastritis induces changes in the oxyntic mucosa indistinguishable from the effects of proton pump inhibitors," *Human Pathology*, vol. 44, no. 12, pp. 2706–2710, 2013.

[111] A. J. Schoenfeld and D. Grady, "Adverse effects associated with proton pump inhibitors," *JAMA Internal Medicine*, vol. 176, no. 2, pp. 172–174, 2016.

[112] D. A. Corley, A. Kubo, W. Zhao, and C. Quesenberry, "Proton pump inhibitors and histamine-2 receptor antagonists are associated with hip fractures among at-risk patients," *Gastroenterology*, vol. 139, no. 1, pp. 93–101, 2010.

[113] J. Leonard, J. K. Marshall, and P. Moayyedi, "Systematic review of the risk of enteric infection in patients taking acid suppression," *The American Journal of Gastroenterology*, vol. 102, no. 9, pp. 2047–2056, 2007.

[114] A. E. Arai and S. M. C. Gallerani, *Uso Crônico de Fármacos Inibidores da Bomba de Prótons: Eficácia Clínica e Efeitos Adversos*, Monografia (Especialização em Farma-cologia) – Centro Universitário Filadélfia–Londrina, 2011.

[115] W. Liu, S. S. Baker, J. Trinidad et al., "Inhibition of lysosomal enzyme activities by proton pump inhibitors.," *Journal of Gastroenterology*, vol. 48, no. 12, pp. 1343–1352, 2013.

[116] W. M. Wong, K. C. Lai, K. F. Lam et al., "Prevalence, clinical spectrum and health care utilization of gastro-oesophageal reflux disease in a Chinese population: a population-based study," *Alimentary Pharmacology & Therapeutics*, vol. 18, no. 6, pp. 595–604, 2003.

[117] T. Tamura, T. Sakaeda, K. Kadoyama, and Y. Okuno, "Omeprazole- and esomeprazole-associated hypomagnesaemia: data mining of the public version of the FDA Adverse Event Reporting System," *International Journal of Medical Sciences*, vol. 9, no. 5, pp. 322–326, 2012.

[118] J. D. Mackay and P. T. Bladon, "Hypomagnesaemia due to proton-pump inhibitor therapy: a clinical case series," *QJM*, vol. 103, no. 6, pp. 387–395, 2010.

[119] M. Abbas, L. Cumella, Y. Zhang et al., "Outcomes of laparoscopic sleeve gastrectomy and Roux-en-Y gastric bypass in patients older than 60," *Obesity Surgery*, vol. 25, no. 12, pp. 2251–2256, 2015.

[120] J. J. Heidelbaugh, K. L. Goldberg, and J. M. Inadomi, "Adverse risks associated with proton pump inhibitors: a systematic review," *Gastroenterology & Hepatology*, vol. 5, no. 10, p. 725, 2009.

[121] J. G. Dekoven and A. M. Yu, "Occupational airborne contact dermatitis from proton pump inhibitors," *Dermatitis*, vol. 26, no. 6, pp. 287–290, 2015.

[122] B. Thomas, M. Mohamed, M. al Hail et al., "A case of probable esomeprazole-induced transient liver injury in a pregnant woman with hyperemesis," *Clinical Pharmacology: Advances and Applications*, vol. 8, pp. 199–202, 2016.

[123] E. Capodicasa, P. Cornacchione, B. Natalini et al., "Omeprazole induces apoptosis in normal human polymorphonuclear leucocytes," *International Journal of Immunopathology and Pharmacology*, vol. 21, no. 1, pp. 73–85, 2008.

[124] L. Scaringi, P. Cornacchione, E. Ayroldi et al., "Omeprazole induces apoptosis in Jurkat cells," *International journal of immunopathology and pharmacology*, vol. 17, no. 3, pp. 331–342, 2004.

[125] S. Cardile and C. Romano, "Clinical utility of esomeprazole for treatment of gastroesophageal reflux disease in pediatric and adolescent patients," *Adolescent Health, Medicine and Therapeutics*, vol. 3, pp. 27–31, 2012.

[126] A. El-Shenawy, M. Diab, M. Shemis et al., "Detection of *Helicobacter pylori vacA*, *cagA* and *iceA1* virulence genes associated with gastric diseases in Egyptian patients," *Egyptian Journal of Medical Human Genetics*, vol. 18, no. 4, pp. 365–371, 2017.

[127] S. Cohen, M. Bueno de Mesquita, and F. B. Mimouni, "Adverse effects reported in the use of gastroesophageal reflux disease treatments in children: a 10 years literature review," *British Journal of Clinical Pharmacology*, vol. 80, no. 2, pp. 200–208, 2015.

[128] R. Imai, T. Higuchi, M. Morimoto, R. Koyamada, and S. Okada, "Iron deficiency anemia due to the long-term use of a proton pump inhibitor," *Internal Medicine*, vol. 57, no. 6, pp. 899–901, 2018.

[129] S. Miyamoto, M. Kato, K. Matsuda et al., "Gastric hyperplastic polyps associated with proton pump inhibitor use in a case without a history of *Helicobacter pylori* infection," *Internal Medicine*, vol. 56, no. 14, pp. 1825–1829, 2017.

[130] A. B. R. Thomson, M. D. Sauve, N. Kassam, and H. Kamitakahara, "Safety of the long-term use of proton pump inhibitors," *World Journal of Gastroenterology*, vol. 16, no. 19, pp. 2323–2330, 2010.

[131] S. E. Attwood, C. Ell, J. P. Galmiche et al., "Long-term safety of proton pump inhibitor therapy assessed under controlled, randomised clinical trial conditions: data from the SOPRAN and LOTUS studies," *Alimentary Pharmacology & Therapeutics*, vol. 41, no. 11, pp. 1162–1174, 2015.

[132] D. M. Fitzgerald, P. J. Hastings, and S. M. Rosenberg, "Stress-induced mutagenesis: implications in cancer and drug

resistance," *Annual Review of Cancer Biology*, vol. 1, no. 1, pp. 119–140, 2017.

[133] E. Zeiger, "Illusions of safety: antimutagens can be mutagens, and anticarcinogens can be carcinogens," *Mutation Research/Reviews in Mutation Research*, vol. 543, no. 3, pp. 191–194, 2003.

[134] P. Lee, K. H. Vousden, and E. C. Cheung, "TIGAR, TIGAR, burning bright," *Cancer & Metabolism*, vol. 2, no. 1, p. 1, 2014.

[135] G. O. Adeoye, C. G. Alimba, and O. B. Oyeleke, "The genotoxicity and systemic toxicity of a pharmaceutical effluent in Wistar rats may involve oxidative stress induction," *Toxicology Reports*, vol. 2, pp. 1265–1272, 2015.

[136] T. Tsuchiya, A. Kijima, Y. Ishii et al., "Mechanisms of oxidative stress-induced *in vivo* mutagenicity by potassium bromate and nitrofurantoin," *Journal of Toxicologic Pathology*, vol. 31, no. 3, pp. 179–188, 2018.

[137] G. H. Danaei and M. Karami, "Protective effect of thymoquinone against diazinon-induced hematotoxicity, genotoxicity and immunotoxicity in rats," *Environmental Toxicology and Pharmacology*, vol. 55, pp. 217–222, 2017.

[138] L. M. Laskoski, R. L. Dittrich, C. A. A. Valadão et al., "Oxidative stress in hoof laminar tissue of horses with lethal gastrointestinal diseases," *Veterinary Immunology And Immunopathology*, vol. 171, pp. 66–72, 2016.

[139] A. Woźniak, M. Walawender, D. Tempka et al., "*In vitro* genotoxicity and cytotoxicity of polydopamine-coated magnetic nanostructures," *Toxicology In Vitro*, vol. 44, pp. 256–265, 2017.

[140] J. N. Moloney and T. G. Cotter, "ROS signalling in the biology of cancer," *Seminars in Cell & Developmental Biology*, vol. 80, pp. 50–64, 2018.

[141] G. Brambilla and A. Martelli, "Genotoxicity and carcinogenicity studies of analgesics, anti-inflammatory drugs and antipyretics," *Pharmacological Research*, vol. 60, no. 1, pp. 1–17, 2009.

[142] B. Shivanna, S. Zhang, A. Patel et al., "Omeprazole attenuates pulmonary aryl hydrocarbon receptor activation and potentiates hyperoxia-induced developmental lung injury in newborn mice," *Toxicological Sciences*, vol. 148, no. 1, pp. 276–287, 2015.

[143] I. G. Kirkinezos, S. R. Bacman, D. Hernandez et al., "Cytochrome c association with the inner mitochondrial membrane is impaired in the CNS of G93A-SOD1 mice," *Journal of Neuroscience*, vol. 25, no. 1, pp. 164–172, 2005.

[144] A. Pey, T. Zamoum, R. Christen, P. L. Merle, and P. Furla, "Characterization of glutathione peroxidase diversity in the symbiotic sea anemone *Anemonia viridis*," *Biochimie*, vol. 132, pp. 94–101, 2017.

[145] H. Sies, "Hydrogen peroxide as a central redox signaling molecule in physiological oxidative stress: oxidative eustress," *Redox Biology*, vol. 11, no. 1, pp. 613–619, 2017.

[146] A. Patel, S. Zhang, B. Moorthy, and B. Shivanna, "Omeprazole does not potentiate acute oxygen toxicity in fetal human pulmonary microvascular endothelial cells exposed to hyperoxia," *Pharmaceutica Analytica Acta*, vol. 6, no. 10, 2015.

[147] B. Burlinson, S. H. Morriss, D. G. Gatehouse et al., "Genotoxicity studies of gastric acid inhibiting drugs," *The Lancet*, vol. 335, no. 8686, pp. 419-420, 1990.

[148] D. H. Phillips, A. Hewer, and M. R. Osborne, "Interaction of omeprazole with DNA in rat tissues," *Mutagenesis*, vol. 7, no. 4, pp. 277–283, 1992.

[149] S. Sharma and R. Bhonde, "Influence of nuclear blebs and micronuclei status on the growth kinetics of human mesenchymal stem cells," *Journal of Cellular Physiology*, vol. 230, no. 3, pp. 657–666, 2015.

[150] H. S. Rosenkranz and G. Klopman, "Omeprazole: an exploration of its reported genotoxicity," *Mutagenesis*, vol. 6, no. 5, pp. 381–384, 1991.

[151] D. Scott, M. Reuben, G. Zampighi, and G. Sachs, "Cell isolation and genotoxicity assessment in gastric mucosa," *Digestive Diseases and Sciences*, vol. 35, no. 10, pp. 1217–1225, 1990.

[152] M. Pittaluga, A. Sgadari, I. Dimauro, B. Tavazzi, P. Parisi, and D. Caporossi, "Physical exercise and redox balance in type 2 diabetics: effects of moderate training on biomarkers of oxidative stress and DNA damage evaluated through comet assay," *Oxidative Medicine and Cellular Longevity*, vol. 2015, Article ID 981242, 7 pages, 2015.

[153] T. A. Baillie and A. E. Rettie, "Role of Biotransformation in Drug-Induced Toxicity: Influence of Intra- and Inter-Species Differences in Drug Metabolism," *Drug Metabolism and Pharmacokinetics*, vol. 26, no. 1, pp. 15–29, 2011.

[154] M. R. Cesário, B. S. Barros, C. Courson, D. M. A. Melo, and A. Kiennemann, "Catalytic performances of Ni-CaO-mayenite in CO_2 sorption enhanced steam methane reforming," *Fuel Processing Technology*, vol. 131, pp. 247–253, 2015.

[155] R. J. Fontana, P. H. Hayashi, J. Gu et al., "Idiosyncratic drug-induced liver injury is associated with substantial morbidity and mortality within 6 months from onset," *Gastroenterology*, vol. 147, no. 1, pp. 96–108.e4, 2014.

[156] N. Kaplowitz, "Drug-induced liver disorders," *Drug Safety*, vol. 24, no. 7, pp. 483–490, 2001.

[157] M. L. Marino, S. Fais, M. Djavaheri-Mergny et al., "Proton pump inhibition induces autophagy as a survival mechanism following oxidative stress in human melanoma cells," *Cell Death & Disease*, vol. 1, no. 10, article e87, 2010.

[158] M. Seoane, M. Esperanza, and A. Cid, "Cytotoxic effects of the proton pump inhibitor omeprazole on the non-target marine microalga *Tetraselmis suecica*," *Aquatic Toxicology*, vol. 191, pp. 62–72, 2017.

[159] A. Canitano, E. Iessi, E. P. Spugnini, C. Federici, and S. Fais, "Proton pump inhibitors induce a caspase-independent antitumor effect against human multiple myeloma," *Cancer Letters*, vol. 376, no. 2, pp. 278–283, 2016.

[160] J. L. Zhang, M. Liu, Q. Yang et al., "Effects of omeprazole in improving concurrent chemoradiotherapy efficacy in rectal cancer," *World Journal of Gastroenterology*, vol. 23, no. 14, pp. 2575–2584, 2017.

[161] T. Ishiguro, R. Ishiguro, M. Ishiguro, and S. Iwai, "Co-treatment of dichloroacetate, omeprazole and tamoxifen exhibited synergistically antiproliferative effect on malignant tumors: in vivo experiments and a case report," *Hepatogastroenterology*, vol. 59, no. 116, pp. 994–996, 2012.

[162] A. de Milito, R. Canese, M. L. Marino et al., "pH-dependent antitumor activity of proton pump inhibitors against human melanoma is mediated by inhibition of tumor acidity," *International Journal of Cancer*, vol. 127, no. 1, pp. 207–219, 2010.

[163] A. de Milito, E. Iessi, M. Logozzi et al., "Proton pump inhibitors induce apoptosis of human B-cell tumors through a caspase-independent mechanism involving reactive oxygen species," *Cancer Research*, vol. 67, no. 11, pp. 5408–5417, 2007.

[164] T. Morimura, K. Fujita, M. Akita, M. Nagashima, and A. Satomi, "The proton pump inhibitor inhibits cell growth and induces apoptosis in human hepatoblastoma," *Pediatric Surgery International*, vol. 24, no. 10, pp. 1087–1094, 2008.

[165] A. Udelnow, A. Kreyes, S. Ellinger et al., "Omeprazole inhibits proliferation and modulates autophagy in pancreatic cancer cells," *PLoS One*, vol. 6, no. 5, article e20143, 2011.

[166] M. Yeo, D. K. Kim, Y. B. Kim et al., "Selective induction of apoptosis with proton pump inhibitor in gastric cancer cells," *Clinical Cancer Research*, vol. 10, no. 24, pp. 8687–8696, 2004.

[167] M. Bellone, A. Calcinotto, P. Filipazzi, A. de Milito, S. Fais, and L. Rivoltini, "The acidity of the tumor microenvironment is a mechanism of immune escape that can be overcome by proton pump inhibitors," *OncoImmunology*, vol. 2, no. 1, article e22058, 2014.

[168] Y. Y. Lee, H. K. Jeon, J. E. Hong et al., "Proton pump inhibitors enhance the effects of cytotoxic agents in chemoresistant epithelial ovarian carcinoma," *Oncotarget*, vol. 6, no. 33, pp. 35040–35050, 2015.

[169] Q. Zhang, N. Huang, J. Wang et al., "The H^+/K^+-ATPase inhibitory activities of Trametenolic acid B from *Trametes lactinea* (Berk.) Pat, and its effects on gastric cancer cells," *Fitoterapia*, vol. 89, pp. 210–217, 2013.

[170] X. Zhang, H. Wang, L. He et al., "Using biochar for remediation of soils contaminated with heavy metals and organic pollutants," *Environmental Science and Pollution Research*, vol. 20, no. 12, pp. 8472–8483, 2013.

[171] A. D. Kondratyev, K. N. Chung, and M. O. Jung, "Identification and characterization of a radiation-inducible glycosylated human early-response gene," *Cancer Research*, vol. 56, no. 7, pp. 1498–1502, 1996.

[172] S. Müerköster, A. Isberner, A. Arlt et al., "Gastrin suppresses growth of CCK2 receptor expressing colon cancer cells by inducing apoptosis in vitro and in vivo," *Gastroenterology*, vol. 129, no. 3, pp. 952–968, 2005.

[173] S. S. Müerköster, A. V. Rausch, A. Isberner et al., "The apoptosis-inducing effect of gastrin on colorectal cancer cells relates to an increased IEX-1 expression mediating NF-κB inhibition," *Oncogene*, vol. 27, no. 8, pp. 1122–1134, 2008.

[174] T. Brzozowski, P. C. Konturek, M. Mierzwa et al., "Effect of probiotics and triple eradication therapy on the cyclooxygenase (COX)-2 expression, apoptosis, and functional gastric mucosal impairment in *Helicobacter pylori*-infected Mongolian gerbils," *Helicobacter*, vol. 11, no. 1, pp. 10–20, 2006.

[175] B. Brzozowski, A. Mazur-Bialy, R. Pajdo et al., "Mechanisms by which stress affects the experimental and clinical inflammatory bowel disease (IBD): role of brain-gut axis," *Current Neuropharmacology*, vol. 14, no. 8, pp. 892–900, 2016.

[176] J. M. Patlolla, Y. Zhang, Q. Li, V. E. Steele, and C. V. Rao, "Anti-carcinogenic properties of omeprazole against human colon cancer cells and azoxymethane-induced colonic aberrant crypt foci formation in rats," *International Journal of Oncology*, vol. 40, no. 1, pp. 170–175, 2012.

[177] C. Deng, P. Zhang, J. Wade Harper, S. J. Elledge, and P. Leder, "Mice Lacking p21 $^{CIP1/WAF1}$ undergo normal development, but are defective in G1 checkpoint control," *Cell*, vol. 82, no. 4, pp. 675–684, 1995.

[178] M. S. Pavlyukov, N. V. Antipova, M. V. Balashova, T. V. Vinogradova, E. P. Kopantzev, and M. I. Shakhparonov, "Survivin monomer plays an essential role in apoptosis regulation," *Journal of Biological Chemistry*, vol. 286, no. 26, pp. 23296–23307, 2011.

[179] P. Hrelia, C. Fimognari, F. Maffei, G. Brandi, G. Biasco, and G. Cantelli-Forti, "Mutagenic and clastogenic activity of gastric juice in human gastric diseases," *Mutation Research/Genetic Toxicology and Environmental Mutagenesis*, vol. 514, no. 1-2, pp. 125–132, 2002.

[180] V. Michaud, Y. Kreutz, T. Skaar et al., "Efavirenz-mediated induction of omeprazole metabolism is CYP2C19 genotype dependent," *The Pharmacogenomics Journal*, vol. 14, no. 2, pp. 151–159, 2014.

[181] J. Fryklund, A. K. Falknas, and H. F. Helander, "Omeprazole does not cause un-scheduled DNA synthesis in rabbit parietal cells in vitro," *Scandinavian Journal of Gastroenterology*, vol. 27, no. 6, pp. 521–528, 1992.

[182] C. Furihata, K. Hirose, and T. Matsushima, "Genotoxicity and cell proliferative activity of omeprazole in rat stomach mucosa," *Mutation Research Letters*, vol. 262, no. 1, pp. 73–76, 1991.

[183] Y. Hou, Q. Hu, J. Huang, and H. Xiong, "Omeprazole inhibits cell proliferation and induces G0/G1 cell cycle arrest through up-regulating miR-203a-3p expression in Barrett's esophagus cells," *Frontiers in Pharmacology*, vol. 8, p. 968, 2018.

[184] U. H. Jin, S. O. Lee, C. Pfent, and S. Safe, "The aryl hydrocarbon receptor ligand omeprazole inhibits breast cancer cell invasion and metastasis," *BMC Cancer*, vol. 14, no. 1, p. 498, 2014.

[185] K. Lindner, C. Borchardt, M. Schöpp et al., "Proton pump inhibitors (PPIs) impact on tumour cell survival, metastatic potential and chemotherapy resistance, and affect expression of resistance-relevant miRNAs in esophageal cancer," *Journal of Experimental & Clinical Cancer Research*, vol. 33, no. 1, p. 73, 2014.

[186] S. K. Goswami, D. Wan, J. Yang et al., "Anti-ulcer efficacy of soluble epoxide hydrolase inhibitor TPPU on diclofenac-induced intestinal ulcers," *Journal of Pharmacology and Experimental Therapeutics*, vol. 357, no. 3, pp. 529–536, 2016.

[187] J. M. Gutiérrez, S. Villar, and A. A. Plavan, "Micronucleus test in fishes as indicators of environmental quality in subestuaries of the Río de la Plata (Uruguay)," *Marine Pollution Bulletin*, vol. 91, no. 2, pp. 518–523, 2015.

[188] J. R. Graham, "Gastric polyposis: onset during long-term therapy with omeprazole," *The Medical Journal of Australia*, vol. 157, no. 4, pp. 287-288, 1992.

[189] P. F. Haastrup, M. S. Paulsen, R. D. Christensen, J. Søndergaard, J. M. Hansen, and D. E. Jarbøl, "Medical and non-medical predictors of initiating long-term use of proton pump inhibitors: a nationwide cohort study of first-time users during a 10-year period," *Alimentary Pharmacology & Therapeutics*, vol. 44, no. 1, pp. 78–87, 2016.

[190] T. Hagiwara, K. Mukaisho, T. Nakayama, H. Sugihara, and T. Hattori, "Long-term proton pump inhibitor administration worsens atrophic corpus gastritis and promotes adenocarcinoma development in Mongolian gerbils infected with *Helicobacter pylori*," *Gut*, vol. 60, no. 5, pp. 624–630, 2011.

[191] M. Bakhriansyah, P. C. Souverein, A. de Boer, and O. H. Klungel, "Gastrointestinal toxicity among patients taking selective COX-2 inhibitors or conventional NSAIDs, alone or combined with proton pump inhibitors: a case-control

study," *Pharmacoepidemiology and Drug Safety*, vol. 26, no. 10, pp. 1141–1148, 2017.

[192] D. Hanahan and R. A. Weinberg, "Hallmarks of cancer: the next generation," *Cell*, vol. 144, no. 5, pp. 646–674, 2011.

[193] Y. Hu, Z. Ma, Y. He, W. Liu, Y. Su, and Z. Tang, "LNCRNA-SNHG1 contributes to gastric cancer cell proliferation by regulating DNMT1," *Biochemical and Biophysical Research Communications*, vol. 491, no. 4, pp. 926–931, 2017.

[194] H. Suzuki and H. Mori, "World trends for *H. pylori* eradication therapy and gastric cancer prevention strategy by *H. pylori* test-and-treat," *Journal of Gastroenterology*, vol. 53, no. 3, pp. 354–361, 2018.

[195] M. D. Burkitt, A. Varro, and D. M. Pritchard, "Importance of gastrin in the pathogenesis and treatment of gastric tumors," *World Journal of Gastroenterology*, vol. 15, no. 1, pp. 1–16, 2009.

[196] L. Lundell, M. Vieth, F. Gibson, P. Nagy, and P. J. Kahrilas, "Systematic review: the effects of long-term proton pump inhibitor use on serum gastrin levels and gastric histology," *Alimentary Pharmacology & Therapeutics*, vol. 42, no. 6, pp. 649–663, 2015.

[197] CDER, *Guidelines for industry. S1A. The need for long-term rodent carcinogenicity studies of pharmaceuticals*, Center for Drug Evaluation and Research, Food and Drug Administration, USA, 1996.

[198] CDER US Department of Health and Human Services, Food and Drug Administration, Center for Drug Evaluation and Research, *Guidance for Industry. S1B. Testing for Carcinogenicity of Pharmaceuticals*, Center for Drug Evaluation and Research, Food and Drug Administration, USA, 1997.

[199] Iarc Working Group on the Evaluation of Carcinogenic Risks to Humans, "IARC monographs on the evaluation of carcinogenic risks to humans. Ingested nitrate and nitrite, and cyanobacterial peptide toxins," *IARC monographs on the evaluation of carcinogenic risks to humans*, vol. 94, 2010.

[200] Y. Li, X. Wen, L. Wang et al., "LncRNA ZEB1-AS1 predicts unfavorable prognosis in gastric cancer," *Surgical Oncology*, vol. 26, no. 4, pp. 527–534, 2017.

[201] M. Kodama, K. Murakami, T. Okimoto et al., "Helicobacter pylori eradication improves gastric atrophy and intestinal metaplasia in long-term observation," *Digestion*, vol. 85, no. 2, pp. 126–130, 2012.

[202] N. Kangwan, J. M. Park, E. H. Kim, and K. B. Hahm, "Quality of healing of gastric ulcers: natural products beyond acid suppression," *World Journal of Gastrointestinal Pathophysiology*, vol. 5, no. 1, pp. 40–47, 2014.

[203] M. P. Braga, C. D. B. d. Silva, and A. I. H. Adams, "Inibidores da bomba de prótons: Revisão e análise farmacoeconômica," *Saúde (Santa Maria)*, vol. 37, no. 2, p. 19, 2011.

[204] V. de Souza Menegassi, L. E. A. Czeczko, L. S. G. Czeczko, S. O. Ioshii, J. C. Pisani, and O. R. Junior, "Prevalência de alterações proliferativas gástricas em pacientes com uso crônico de inibidores de bomba de prótons," *Arquivos Brasileiros de Cirurgia Digestiva*, vol. 23, no. 3, pp. 145–149, 2010.

[205] Melbourne, Austrália Publicado em Global Family Doctor 2011, *Inibidores da bomba de prótons-efeitos adversos incomuns*, Disponível em, 2013, http://www.sbmfc.org.br/default.asp?siteAcao=mostraPagina&paginaId=748.

[206] L. Eslami and S. Nasseri-Moghaddam, "Meta-analyses: does long-term PPI use increase the risk of gastric premalignant lesions?," *Archives of Iranian Medicine*, vol. 16, no. 8, pp. 449–458, 2013.

[207] L. Huang, D. J. Qi, W. He, and A. Xu, "Omeprazole promotes carcinogenesis of fore-stomach in mice with co-stimulation of nitrosamine," *Oncotarget*, vol. 8, no. 41, pp. 70332–70344, 2017.

[208] J. W. Freston, M. Hisada, D. A. Peura et al., "The clinical safety of long-term lansoprazole for the maintenance of healed erosive oesophagitis," *Alimentary Pharmacology & Therapeutics*, vol. 29, no. 12, pp. 1249–1260, 2009.

[209] B. G. Schneider, M. B. Piazuelo, L. A. Sicinschi et al., "Virulence of infecting *Helicobacter pylori* strains and intensity of mononuclear cell infiltration are associated with levels of DNA hypermethylation in gastric mucosae," *Epigenetics*, vol. 8, no. 11, pp. 1153–1161, 2014.

[210] M. Tsuda, M. Asaka, M. Kato et al., "Effect on *Helicobacter pylori* eradication therapy against gastric cancer in Japan," *Helicobacter*, vol. 22, no. 5, p. e12415, 2017.

[211] N. Nandy, J. A. Hanson, R. G. Strickland, and D. M. McCarthy, "Solitary gastric carcinoid tumor associated with long-term use of omeprazole: a case report and review of the literature," *Digestive Diseases and Sciences*, vol. 61, no. 3, pp. 708–712, 2016.

[212] H. Hayashi, K. Shimamoto, E. Taniai et al., "Liver tumor promoting effect of omeprazole in rats and its possible mechanism of action," *The Journal of Toxicological Sciences*, vol. 37, no. 3, pp. 491–501, 2012.

[213] H. Hayashi, E. Taniai, R. Morita et al., "Enhanced liver tumor promotion but not liver initiation activity in rats subjected to combined administration of omeprazole and β-naphthoflavone," *The Journal of Toxicological Sciences*, vol. 37, no. 5, pp. 969–985, 2012.

[214] H. Song, J. Zhu, and D. Lu, "Long-term proton pump inhibitor (PPI) use and the development of gastric pre-malignant lesions," *Cochrane Database of Systematic Reviews*, no. 12, article CD010623, 2014.

[215] P. Ekström, L. Carling, P. Unge, O. Anker-Hansen, S. Sjöstedt, and H. Sellström, "Lansoprazole versus omeprazole in active duodenal ulcer:a double-blind, randomized, comparative study," *Scandinavian Journal of Gastroenterology*, vol. 30, no. 3, pp. 210–215, 1995.

[216] T. Hagiwara, K.-i. Mukaisho, Z.-Q. Ling, H. Sugihara, and T. Hattori, "Development of pancreatic acinar cell metaplasia after successful administration of omeprazole for 6 months in rats," *Digestive Diseases and Sciences*, vol. 52, no. 5, pp. 1219–1224, 2007.

[217] N. Vakil, "Rationale for a *Helicobacter pylori* test and treatment strategy in gastroesophageal reflux disease," *Gastroenterology Clinics of North America*, vol. 44, no. 3, pp. 661–666, 2015.

[218] J. Ashby, "Consideration of CASE predictions of genotoxic carcinogenesis for omeprazole, methapyrilene and azathioprine," *Mutation Research/Environmental Mutagenesis and Related Subjects*, vol. 272, no. 1, pp. 1–7, 1992.

Hindawi
Oxidative Medicine and Cellular Longevity
Volume 2020, Article ID 2930347, 13 pages
https://doi.org/10.1155/2020/2930347

Review Article

Metabolic Biomarkers of Squamous Cell Carcinoma of the Aerodigestive Tract: A Systematic Review and Quality Assessment

Yan Mei Goh, Stefan S. Antonowicz, Piers Boshier, and George B. Hanna

Department of Surgery & Cancer, Imperial College London, London W2 1NY, UK

Correspondence should be addressed to George B. Hanna; g.hanna@imperial.ac.uk

Received 5 September 2019; Revised 22 December 2019; Accepted 21 January 2020; Published 21 February 2020

Guest Editor: Kanhaiya Singh

Introduction. Aerodigestive squamous cell carcinomas (ASCC) constitute a major source of global cancer deaths. Patients typically present with advanced, incurable disease, so new means of detecting early disease are a research priority. Metabolite quantitation is amenable to point-of-care analysis and can be performed in ASCC surrogates such as breath and saliva. The purpose of this systematic review is to summarise progress of ASCC metabolomic studies, with an emphasis on the critical appraisal of methodological quality and reporting. *Method.* A systematic online literature search was performed to identify studies reporting metabolic biomarkers of ASCC. This review was conducted in accordance with the recommendations of the Cochrane Library and MOOSE guidelines. *Results.* Thirty studies comprising 2117 patients were included in the review. All publications represented phase-I biomarker discovery studies, and none validated their findings in an independent cohort. There was heterogeneity in study design and methodological and reporting quality. Sensitivities and specificities were higher in oesophageal and head and neck squamous cell carcinomas compared to those in lung squamous cell carcinoma. The metabolic phenotypes of these cancers were similar, as was the kinetics of metabolite groups when comparing blood, tissue, and breath/saliva concentrations. Deregulation of amino acid metabolism was the most frequently reported theme. *Conclusion.* Metabolite analysis has shown promising diagnostic performance, especially for oesophageal and head and neck ASCC subtypes, which are phenotypically similar. However, shortcomings in study design have led to inconsistencies between studies. To support future studies and ultimately clinical adoption, these limitations are discussed.

1. Introduction

Squamous cell carcinomas of the aerodigestive tract (ASCC) constitute a major health burden globally, with an estimated 4.3 million new cases and 2.6 million deaths annually [1]. Poor survival that is associated with ASCC reflects their often delayed presentation to medical professionals, such that many patients are not suitable for curative therapy [2–5]. Whilst the ability to diagnose ASCC at an early stage is associated with improved long-term survival, current strategies have inadequate diagnostic performance and are not recommended in national guidelines. There remains an unmet clinical need to develop reliable noninvasive and cost-effective methods for the early detection of ASCC.

ASCC arise from nonkeratinising stratified squamous epithelium lining the upper digestive tract (lips to lower oesophagus) and respiratory tract. This convenient location renders ASCC suitable for noninvasive testing using breath and saliva. The use of proteomics and genomics has historically been at the forefront of diagnostic studies. However, these techniques provide monothematic information and are less suited to point-of-care technologies needed for large-scale application [6]. Metabolites may be more appealing as they are amenable to noninvasive sampling and translatable to point-of-care analytical tools [7]. For example, in upper gastrointestinal adenocarcinoma (the other major ASCC subtype), exhaled metabolites have demonstrated promise for detecting treatable disease stages [8–10]. However, progress in this field has been hampered by inadequate standardisation, inconsistent quality assurance, and evolving analytical technology [11–14].

The purpose of this systematic review is to summarise progress of ASCC metabolomic studies. The specific objectives are (i) to assess methodological quality, (ii) to summarise the

discriminatory performance of the proposed metabolic biomarkers, and (iii) to describe emerging metabolic themes for these cancers.

2. Materials and Methods

2.1. Literature Search. This review set out to identify all studies that measured differences in metabolites between patients with ASCC and relevant controls. A systematic literature search was conducted in accordance with the recommendations of the Cochrane Library and MOOSE guidelines [15]. The following databases were searched: Medline (1946–present) via OvidSP, Ovid Embase (1947–18th January 2019), and Cochrane Library. Three strings using the following search terms were used: biomarkers; metabonomics; metabolic profiling; volatile organic compounds; magnetic resonance spectroscopy; mass spectrometry; and squamous cell carcinoma. All variations in spelling including a truncated search term using wild card characters and "related articles" function were used in combination with the Boolean operators AND OR. Full details of the search strategy were provided as a supplementary file. The reference lists of identified articles were also searched to identify other potentially relevant studies.

Two independent reviewers (YMG, PB) screened the titles and abstracts of all studies identified by the primary electronic search. The full texts of potentially relevant articles were retrieved to assess eligibility for inclusion. Included studies were those where metabolomic techniques to identify biomarkers of ASCC were performed in treatment-naïve human subjects. Studies were excluded if they reported on mixed cancer subtypes where results for ASCC could not be separately determined. Studies that did not report named biomarkers of ASCC, animal and in vitro studies, studies not published in the English language, and review articles and conference abstracts were also excluded. A third reviewer (SA) was consulted in the case of a disagreement.

2.2. Definitions. Metabolomics is defined as "the global and unbiased definition of the complement of small molecules in biofluids, tissues, organs, or organisms" [16]. Biomarkers were defined as a naturally occurring molecule, which were significantly different in a disease state. ASCC included tumours affecting squamous mucosa of the oral cavity, oropharynx, lung, and oesophagus.

2.3. Outcome Measures. The following data items were extracted from included publications: year of publication, country of origin, study design, recruitment time, total number of participants, tumour of origin, biomarker phase, tumour stage, analytical platform used, sample type, number of compounds identified, compounds noted to be increased/-decreased in cancer, statistical analysis performed, prediction model used, sensitivity and specificity, and area under the receiver operating characteristic (ROC) curve derived from diagnostic models.

2.4. Statistical Analysis. Statistical analysis was performed using R (version 3.2.1, The R Project for Statistical Computing, http://www.r-project.org). Using the sensitivity, specificity, and area under the ROC curves derived from individual published models, bivariate meta-analyses were performed to create pooled point estimates of the hierarchal summary ROC curve of VOC analysis in accordance with previously validated methods [17].

2.5. Metabolite Analysis. All metabolites identified were classed in accordance to the Kyoto Encyclopedia of Genes and Genomes (KEGG) pathway, and statistical analysis was performed using the pathway analysis module in MetaboAnalyst version 4.0. Metabolites determined to be significantly increased or decreased in each study were selected. Data preprocessing included name check against the Human Metabolome Database (HMDB), data checks, and missing values. Parameters used to analyse this data were the hypergeometric test for overrepresentation analysis and the relative-betweenness centrality test for pathway topology analysis based on the KEGG pathway library [18–20]. Normalisation was performed using the weighted means of identified metabolite that were increased/decreased in squamous cell carcinoma (SCC) in each sample type. The mean proportion of each compound identified was analysed as the proportion of the total number of compounds identified per metabolite class per study, divided by the total number of compounds identified in total in each SCC site subtype, multiplied by the total number of studies; this compound was identified in Figure 1.

2.6. Quality Assessment. Study quality was assessed with three tools: first, Quality Assessment of Diagnostic Accuracy Studies-2 (QUADAS-2) checklist [21] to assess methodological bias. Second, the Standards for Reporting of Diagnostic Accuracy Studies (STARD) checklist [22, 23] was used to assess general reporting quality of a clinical diagnostic tool. Third, the Chemical Analysis Working Group- (CAWG-) Metabolomics Standard Initiative (MSI) criteria was used as this focused on the reporting quality of metadata of metabolomic studies [14]. The CAWG-MSI Metabolite Identification Levels were used to summarise studies' identification rigour: level 1 (most confident, at least two orthogonal analytical data types, e.g., retention time, isotope labelling), level 2 (one data type, spectral similarity to commercial library), level 3 (one data type related to a spectral or chemical property).

3. Results

A systematic literature search identified a total of 30 studies comprising of a total of 2117 subjects of which 1144 had a diagnosis of ASCC (Figure 2). Details of included studies were provided in Table 1. All studies were Phase I biomarker discovery studies. Of the 30 included studies, 18 were from Asia and the Far East [8, 9, 11–26], seven from Europe [27–33], three from North America [34–36], and two from the Middle East [37, 38]. ASCC tumour sites identified were the head and neck ($n = 17$), oesophageal ($n = 8$), and lung ($n = 5$). The majority of studies compared patients with cancer to normal controls and or benign conditions [16, 25, 26, 28, 29, 34, 38–43].

Liquid chromatography mass spectrometry (LC-MS) was the most commonly used analytical platform ($n = 14$)

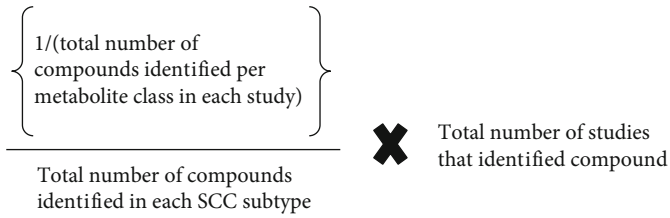

Figure 1: Equation for weighted means of each identified metabolite. Key: SCC: squamous cell carcinoma.

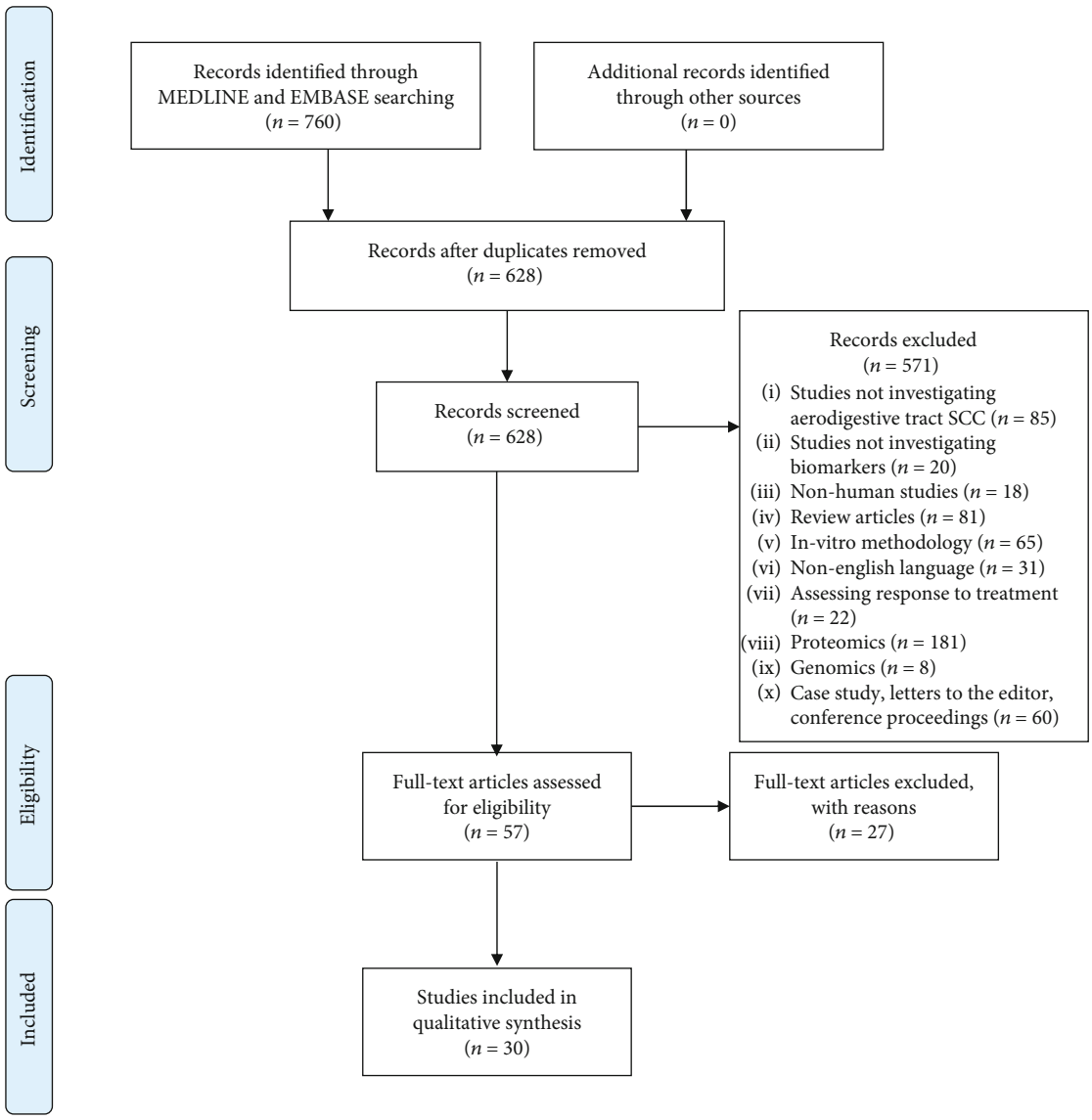

Figure 2: PRISMA chart.

followed by gas chromatography mass spectrometry (GC-MS, $n = 12$). Sample types used in these studies were tissue ($n = 10$), saliva ($n = 13$), plasma ($n = 13$), urine ($n = 5$), and breath ($n = 6$). Several studies used more than one analytical platform [34, 35, 38, 40] and/or sample types for analysis [34, 35] (Table 1). Eight studies used targeted methods, and 22 studies untargeted methods. All studies that used untargeted methods covered a large range of commonly identified metabolites, ranging from small fatty acids to larger glycolipid and carbohydrate metabolites. Only five studies identified volatile compounds [26, 30, 36–38].

3.1. Quality. Assessment of bias and applicability of outcomes were analysed with QUADAS-2 (Table 1). The QUADAS-2 was divided into risk of bias of the following: patient selection, diagnostic test, reference standard, and patient flow and timing. Additionally, this test investigated applicability of patient selection, diagnostic test, and

Table 1: Study characteristics, statistical analysis, and prediction model performed.

Author	Country	Sample type	SCC stage	Targeted/ untargeted method	Analytical platform	Statistical analysis/prediction model	STARD score	QUADAS		CAWG-MSI metabolite ID level	CAWG-MSI score	Sn (%)	Sp (%)	AUC
								Risk of bias	Applicability					
Studies of oesophageal squamous cell carcinoma														
Liu 2013	China	Plasma	Late: 17 Control: 53	Untargeted	UPLC-ESI-TOF-MS	PCA, hierarchical cluster analysis	37	Low	Low	2	13	—	—	—
Wang L 2013	China	Tissue	Early: 28 Late: 71 Control: 30	Untargeted	1H-NMR	OPLS-DA	35	Low	High	2	7	—	—	—
Jin 2014	China	Plasma	Early: 49 Late: 31 Control: 30	Untargeted	GC-MS	Model of 3 compounds based on OPLS-DA model	33	Low	Low	2	16	90	96.67	0.964
Ma 2014	China	Plasma	Early: 51 Control: 60	Targeted	HPLC	Student *t*-test, PLS-DA	32	Low	Low	2	10	—	—	—
Wang J 2016	China	Plasma	Early: 28 Late: 30 Control: 105	Untargeted	UHPLC-QTOF/MS	Model of 16 compounds based on random forest model	37	Low	Low	1	19	85	90.5	0.929
Xu 2016	China	Urine	Late: 40 Control: 62	Untargeted	LC-MS/MS	Model of 7 compounds based on binary logistic regression and ROC curve	25	Unclear	Low	2	19	90.2	96.0	0.961
Cheng 2017	China	Plasma	Patient: 40 Control: 27	Targeted	LC-MS/MS	Model of 4 compounds based on fivefold cross-validation test	32	Low	Low	2	15	77.5	85.33	0.798
Zhang 2017	China	Plasma	Early: 17 Late: 23 Control: 40	Untargeted	1H-NMR, UHPLC	Model of 9 compounds based on binary logistic regression and ROC curves	33	Low	Low	2	14	97.4	95	0.988
Studies of lung squamous cell carcinoma														
Song 2010	China	Breath	Early: 20 Late: 33 Control: 41	Untargeted	SPME GC-MS	Wilcoxon rank sum test, ROC	29	Low	Low	2	11	—	—	—
De Castro 2014	Spain	Plasma	Patient: 30 Control: 35	Targeted	GC-MS	Model of 1 compound	30	Unclear	Low	1	13	77	66	0.7

Table 1: Continued.

Author	Country	Sample type	SCC stage	Targeted/ untargeted method	Analytical platform	Statistical analysis/prediction model	STARD score	QUADAS		CAWG-MSI metabolite ID level	CAWG-MSI score	Sn (%)	Sp (%)	AUC
								Risk of bias	Applicability					
						based on ROC curves								
Handa 2014	Germany	Breath	Early: 19 late: 31 Normal: 39	Untargeted	IMS	Model of 11 compounds based on decision tree algorithm	27	Unclear	Low	3	6	97.4	60	—
Rocha 2015	Portugal	Tissue	Patient: 19 Control: 37	Untargeted	1H-NMR	PLS-DA, Wilcoxon rank sum test	25	Unclear	Low	2	7	—	—	—
Sanchez-Rodriguez 2015	Spain	Plasma	Late: 18 Control: 50	Targeted	GC-MS	Model of 1 compound based on ROC curves	31	Low	Low	1	17	69	68	0.68
Studies of head and neck squamous cell carcinoma														
Mizukawa 1998	Japan	Saliva	Patient: 18 Control: 18	Targeted	HPLC	Nil–peak detection only	21	Low	High	1	7	—	—	—
Somashekar 2011	USA	Tissue	Patient: 22 Control: 22	Untargeted	HR-magic angle spinning proton NMR spectroscopy	PCA	23	Low	Low	1	8	—	—	—
Wei 2011	China	Saliva	Early: 21 Late: 16 Control: 66	Untargeted	UPLC-QTOF-MS	Model of 5 compounds based on ROC curves	31	Low	Low	3	13	86.5	82.4	0.89
Yonezawa 2013	Japan	Tissue, plasma	Early: 7 Late: 10 Control: 22	Untargeted	GC-MS	Student's *t*-test, Bartlett's test, Wilcoxon rank sum test	27	Low	Low	2	17	—	—	—
Gruber 2014	Israel	Breath	Early: 9 Late: 11 Control: 40	Untargeted	GC-MS, sensors	Model of 3 compounds based on discriminant factor analysis	30	Low	Low	3	10	77	90	0.83
Wang Q (Clinica Chimica Acta) 2014	China	Saliva	Early: 13 Late: 17 Control: 0	Targeted	UPLC-MS	Model of 4 compounds based on ROC curves	30	Unclear	Low	1	24	92.3	91.7	—
Wang Q (Scientific Reports) 2014	China	Saliva	Early: 13 Late: 17 Control: 30	Untargeted	RPLC-MS, HILIC-MS	Model of 5 compounds based on ROC curve	24	Unclear	Low	1	16	100	96.7	0.997

Table 1: Continued.

Author	Country	Sample type	SCC stage	Targeted/ untargeted method	Analytical platform	Statistical analysis/prediction model	STARD score	QUADAS		CAWG-MSI metabolite ID level	CAWG-MSI score	Sn (%)	Sp (%)	AUC
								Risk of bias	Applicability					
Wang Q (Talanta) 2014	China	Saliva	Early: 13 Late: 17 Control: 60	Targeted	UPLC-ESI-MS	Model of 2 compounds based on logistic regression model	25	Low	Unclear	1	25	92.3	91.7	0.871
Gupta 2015	India	Plasma	Early: 28 Late: 72 Control: 175	Untargeted	H-NMR	Model of 2 compounds based on OPLS-DA	33	Unclear	Low	2	10	90	94	0.979
Szabo 2015	Hungary	Breath	Cancer: 14 Control: 11	Targeted	OralChroma and GC-MS	Nil–peak detection only	22	Unclear	Low	1	8	—	—	—
Kekatpure 2016	India	Urine	Early: 14 Late: 64 Control: 94	Untargeted	LC-triple quadrupole-MS/MS	Kruskal-Wallis, Fisher exact test, Cox proportional hazards model	23	Low	High	2	13	—	—	—
Mukherjee 2016	USA	Tissue, saliva	Early: 2 Late: 5 Control: 7	Untargeted	LC-MS, LC-MS/MS, GC-MS	Kruskal-Wallis with adjustment for multiple testing	36	Low	Low	3	15	—	—	—
Shoffel-Havakuk 2016	Israel	Saliva	Cancer: 6 Control: 4	Untargeted	GC-MS	Mann–Whitney *U*, Fisher exact test	24	Low	Low	2	11	—	—	—
Bouza 2017	Spain	Breath	Early: 11 Late: 15 Control: 26	Untargeted	SPME, GC-MS	Kruskal-Wallis, Mann–Whitney, PLS-DA, SIMCA prediction	25	Unclear	Low	2	10	—	—	—
Hartwig 2017	Germany	Breath	Early: 5 Late: 5 Control: 4	Untargeted	GC-MS	Jackknife/leave-one-out cross-validation	34	Unclear	Low	3	6	—	—	—
Kamarajan 2017	USA	Tissue, saliva, plasma	Early: 17 Late: 30 Control: 19	Untargeted	UPLC-MS/MS, GC-MS	Anova, *t*-test, random forest classification, PCA	31	Low	Low	2	20	—	—	—
Ohshima 2017	Japan	Saliva	Early: 14 Late: 8 Control: 21	Untargeted	CE-TOF-MS	Hierarchical cluster analysis, Wilcoxon rank sum test	37	Low	Low	3	9	—	—	—

Key: LC: liquid chromatography; GC: gas chromatography; UPLC: ultra-performance liquid chromatography; HPLC: high-performance liquid chromatography; QTOF: quad-time-of-flight; 1H-NMR: proton nuclear magnetic resonance; UHPLC: ultra-high performance liquid chromatography; IMS: ion mobility spectroscopy; ESI: electrospray ionisation; SPME: solid-phase microextraction; CE: capillary electrophoresis; RPLC: reverse-phase liquid chromatography; HILIC: hydrophilic interaction chromatography; MS: mass spectrometry; PCA: principal component analysis; PLS-DA: partial least squares discriminant analysis; MCCV: Monte Carlo cross-validation; OPLS-DA: orthogonal partial least squares discriminant analysis; ROC: receiver operating curve.

reference standard to the systematic review. There was an overall low risk of bias of these diagnostic tests and high applicability of these studies to the review question. In this QUADAS-2 analysis, the nature of patient flow and timing of sample analysis was least reported in studies in this review ($n = 11$) [16, 28–30, 33, 36, 39, 40, 44].

General reporting quality of a clinical diagnostic tool was assessed by the STARD checklist (Table 1). The STARD score for reported studies ranged from 21 to 37 with a mean of 29.4 (±4.76 S.D) where the maximum score is 41. More than 75% of studies reported inclusion and exclusion criteria, described the reference test and standards, and reported potential bias and analysis of diagnostic accuracy well. However, more than two thirds of studies failed to clearly demonstrate patient recruitment protocol, specifically, how patients were identified and recruited, the nature of recruitment, e.g., consecutive or random series and [22, 37, 40, 41, 45–47] sample size estimation [35, 42, 48], participant flow [24, 31, 35, 39, 49, 50], and adverse effects as a consequence of the diagnostic tool.

Reporting of clinical demographics was not consistent in each study. Of the 30 studies, only 10 fully reported all clinical demographics [28, 30, 34, 35, 38, 41, 43, 47, 49, 51], 13 reported at least patient age, gender, and clinical stage [16, 25, 26, 31, 36, 39, 40, 42, 45, 46, 48, 52, 53]. Seven studies did not report differences in metabolite profile at different tumour stages [24, 27, 29, 32, 36, 37, 46]. In these seven studies, four compared differences in metabolic profile between cancer and noncancer cohorts [24, 27, 32, 37].

Definitions of normal control differed most in tissue sample analysis, where Zhang et al. specified normal adjacent control tissue samples a minimum of 5 cm from the tumour site [54] in contrast to the other five tissue studies that used adjacent normal controls [26, 29, 45, 46, 53] without demonstrating adequacy of tissue clearance. Of all 30 studies in this review, only Shoffel-Havakuk et al. used patients with benign histology as controls [37]. No tissue study used normal samples from patients with no endoluminal pathology, which is pertinent as metabolic field effects exist in endolumens [55]. Various exclusion criteria were given to control donors' characteristics, including use of nonsteroidal anti-inflammatory drugs within the past week, antibiotic treatment and consumption of specific food, history of mucosal disorder, chronic and/or systemic disease such as diabetes, autoimmune disorders, heart disease, infection, and liver disease. Twenty-six studies involving biofluids or breath used healthy volunteer controls, one additionally used patients with benign diseases [24, 25, 27, 28, 30–43, 46–49, 51, 52, 56, 57]. The definition for healthy volunteers was based on history (six studies) or endoluminal study (18 studies).

Reporting of metadata in metabolomics datasets was assessed using CAWG-MSI [14] (Supplementary Table 2). A summary of the minimum reported metadata is summarised in Table 1. Twenty of the 30 studies included in this systematic review used relative quantification of compounds [16, 24, 25, 28, 29, 31, 33–38, 40–43, 45, 48, 49, 52], whilst 10 included studies provided absolute quantification of compounds [27, 30, 32, 39, 46, 47, 51–53, 56]. Despite the availability of reporting guidelines for metabolomics analysis, only three studies reported greater than 50% of the CAWG-MSI criteria [34, 39, 52]. Overall, studies reported sample preparation, experimental analysis, and instrumental performance well. However, the majority (80%) did not provide method validation data [16, 24, 25, 27, 28, 30–38, 40–42, 45–49, 51, 52, 54, 56]. Thirteen studies that analysed relative quantification of metabolites identified used either internal standards or normalised the results to allow for instrument variation [16, 24, 25, 29, 33–36, 40–42, 45, 49]. Six of the 10 studies that used absolute quantification did not report accuracy or precision validation data for their method on the instrument [30, 44, 46, 47, 51, 56] whilst two of 10 studies reported the limits of quantification and detection of their method [39, 52]. Out of 30 studies, only 12 declared evidence of data preprocessing [25, 29, 33, 34, 36, 37, 40, 41, 43, 45, 48, 49]. Levels one, two, and three metabolite identification were reported in nine [25, 27, 30, 32, 36, 39, 40, 46, 52], 15 [16, 24, 26, 29, 33, 34, 37, 42, 43, 45, 47, 49, 51, 56, 58], and six [28, 31, 35, 38, 41, 48] studies, respectively. Only two of the 30 studies reported all of the statistical aspects suggested by the CAWG-MSI guidelines [59].

3.2. Discriminatory Features. The highest sensitivity of oesophageal squamous cell cancer (OSCC) diagnosis was reported by Zhang et al. at 97.4% with a specificity of 95% and AUC of 0.988 [44]. Jin et al. reported the highest specificity at 96.67% with a sensitivity of 90% and AUC of 0.964 [42]. The highest sensitivities and specificities of lung squamous cell cancer (LSCC) were poorer with Handa et al. reporting the highest sensitivity of 97.4% [28] and Sanchez-Rodriguez et al. reporting the highest specificity of 68% and AUC of 0.7 [30]. The highest sensitivity, specificity, and AUC were reported for head and neck squamous cell cancer (HNSCC): 100%, 96.7%, and 0.997, respectively (Table 1). However, no groups subsequently validated their initial findings in independent cohorts. Of the 6 studies which reported AUC > 0.90, a high risk of bias was not present and CAWG-MSI metabolite identification was level 1 or 2.

3.3. Metabolic Themes. A total of 181 metabolites identified were associated with an increase or decrease in concentration in patients with ASCC compared to their normal controls (Supplementary Table 3). These compounds were identified in a range of sample types including tissue, plasma, urine, saliva, and breath. The majority were amino acids, carboxylic acids, or fatty acids, and these were more commonly identified in tissue, saliva, and plasma samples. The least common metabolites identified were vitamins, nitrogen, and sulphur containing compounds (Supplementary Figure 1). Sixty-eight compounds that changed in ASCC were reported in more than one study. These metabolites were selected based on metabolites that were identified to be increased or decreased in cancer in different studies. Of these, 27 compounds were noted to be involved in amino acid and lipid metabolism (Supplementary Table 4). All biomarkers showed a consistent increase or decrease in the sample types across different studies (see Supplementary Tables 3 and 4).

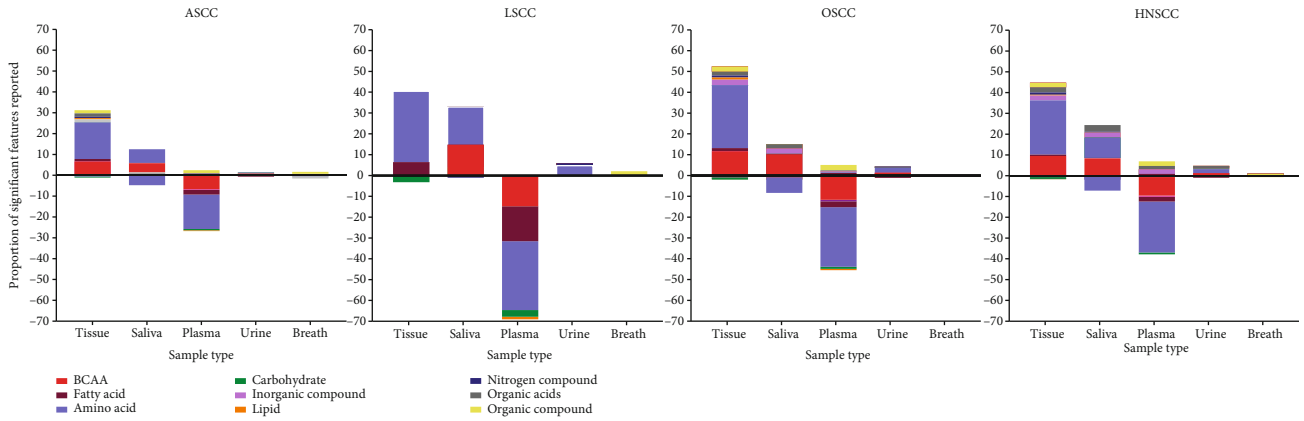

Figure 3: Proportion of identified compounds in each ASCC, LSCC, OSCC, and HNSCC in different sample types. Key: ASCC: aerodigestive squamous cell carcinoma; OSCC: oesophageal squamous cell carcinoma; LSCC: lung squamous cell carcinoma; HNSCC: head and neck squamous cell carcinoma; BCAA: branched chain amino acid.

A particularly deregulated pathway was branched chain amino acid metabolism (BCAAs, see Figures 3 and 4 and Supplementary Table 3). There were 36 significant differences in BCAA concentrations, or their downstream metabolites, across 12 studies [25, 28, 34–36, 39–41, 43, 45, 46, 49]. The QUADAS-2 risk of bias was low for nine of these studies [34–36, 40, 41, 45–47, 49]. Five of these studies were of good quality and five of fair quality as assessed by the STARD checklist. One study reported the minimum metadata required from the CAWG-MSI checklist [39]. Of these 12 studies, two reported level 1 metabolite identification [35, 39], seven reported level 2 [25, 28, 36, 41, 43, 45, 60], and three reported level 3 metabolite identification [34, 40, 46].

3.4. Influence of Anatomical Location on Metabolic Themes. LSCC ($n = 9$) had the lowest number of metabolite classes compared to OSCC ($n = 20$) or HNSCC ($n = 18$) (Figure 3). Common metabolites that were identified in all ASCC sites were amino acids, fatty acids, carbohydrate, nitrogen compounds, and organic acids. OSCC and HNSCC appear to demonstrate similar metabolic profiles compared to LSCC (see Figures 3 and 4). Metabolic pathways commonly deregulated in both OSCC and HNSCC mainly concerned amino acid mobilisation, uptake, and polymerisation; lipid synthesis; and alternative energy. All twelve studies demonstrating BCAA deregulation were either OSCC or HNSCC. These compounds were increased in tissue and saliva but decreased in cancer patients' plasma. Breakdown products of BCAA, alpha-ketoisocaproic acid (KIC), alpha-ketoisovaleric acid (KIV), and alpha-ketomethylvaleric acid (KMV) were reported in three metabolomic studies [35, 42, 48] related to OSCC and HNSCC. However, the design and reporting heterogeneity meant these site-specific results should be approached with caution, and further detailed analyses were not performed.

3.5. Influence of Biosample Type on Metabolic Themes. There was an overall positive deflection in the proportion of metabolites present in the tissue, saliva, urine, and breath of ASCC patients and a negative deflection in plasma (Figure 3). This was particularly evident for amino acids. Metabolites in ASCC saliva samples were more similar to tissue than plasma. In particular, increased BCAAs were identified in tissue and saliva of patients with ASCC. In contrast, plasma BCAAs were decreased in ASCC plasma and not identified in urine or breath. This trend was also noted in other amino acids. BCKAs were decreased in the plasma of ASCC patients, but the proportions of fatty acids increase and decrease were similar in tissue samples. However, the design and reporting heterogeneity meant these sample-specific results should be approached with caution, and further detailed analyses were not performed.

4. Discussion

This systematic review provides an overview of progress in ASCC metabolic biomarker studies. The principal findings of this review were (i) favourable diagnostic performance of metabolic biomarkers for the detection of OSCC and HNSCC but not LSCC in pooled analysis, (ii) shared metabolic features of OSCC and HNSCC, and (iii) suggestion of a consistent role of the KEGG amino acid metabolic pathway in ASCC. Additionally, comparing sample types suggests metabolites are often depleted in the circulation and enriched in both tumour tissue and luminal surrogates, suggesting a model for ASCC biomarker kinetics. From the design perspective, clinical methodology and reporting quality was of a reasonable standard, but analytical methodology and reporting quality were often of a poor standard, and no studies performed exceptionally in both aspects.

ASCCs all have high mortality due to late disease detection. Currently, there are no screening strategies for any subtype of sufficient accuracy and quality to support political endorsement. Pooled analysis of identified studies regarding the detection of ASCC gave an area under the curve (AUC) of 0.927 with sensitivity of 85.7% (95% CI 78.9–92%), respectively. This diagnostic performance compares favourably to existing screening programmes such as faecal occult blood testing for colorectal cancer and cytological cervical screening test that currently are associated with lower sensitivity and specificity [61, 62]. Although the studies were generally

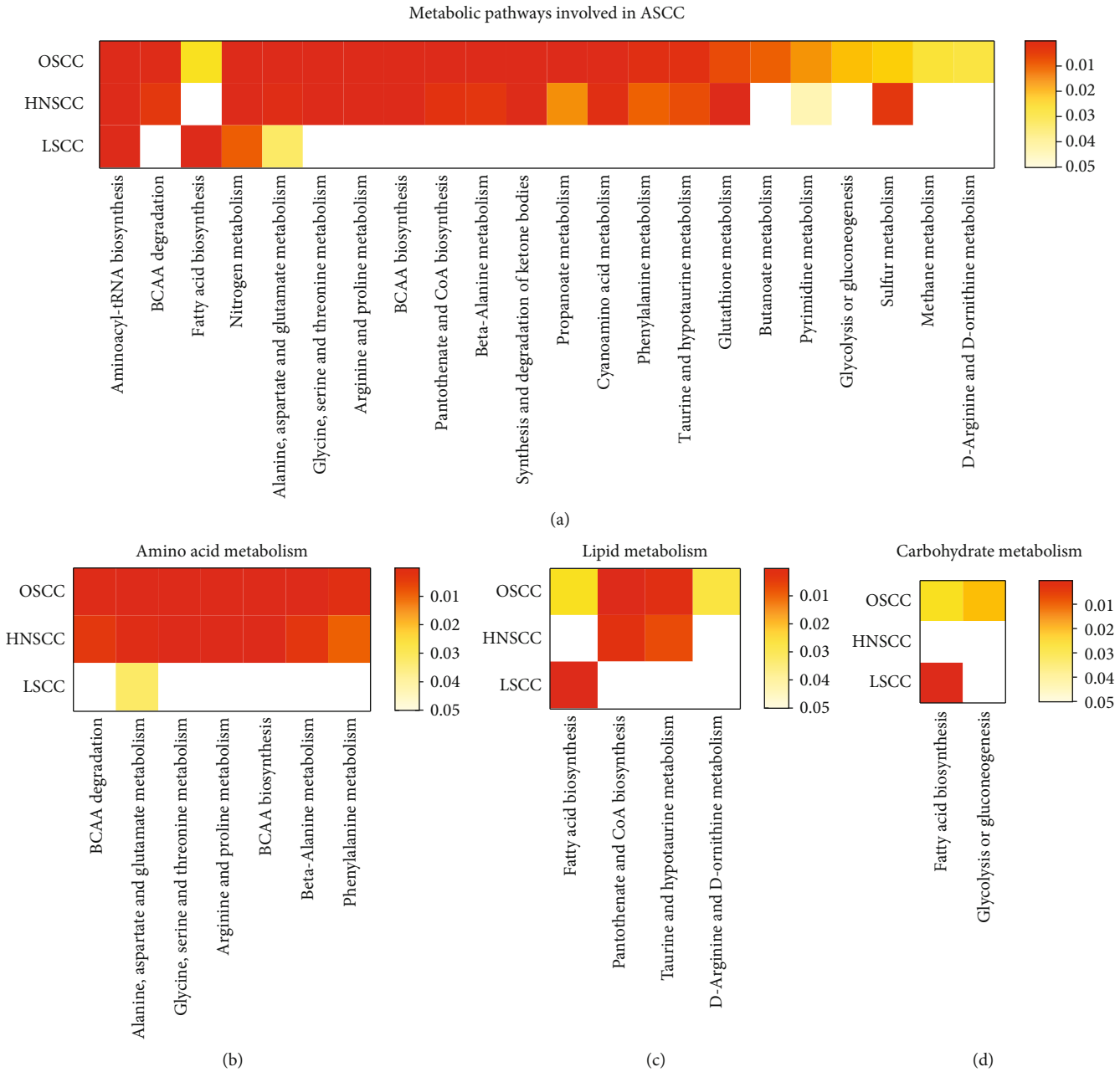

Figure 4: Metabolic pathways involved in all ASCC: (a) all metabolic pathways, (b) amino acid metabolism, (c) lipid metabolism, and (d) carbohydrate metabolism.

of an exploratory nature without extensive validation, these results are encouraging and suggest metabolic biomarkers of ASCC may provide novel screening tools to identify high-risk populations, provided these efforts can progress to high-quality validation studies with appropriate power. The finding that the six studies reporting the highest AUC values had good clinical design and used targeted metabolomic methods suggests methodological rigour and hypothesis-driven metabolomics generate the best results.

In both discriminatory performance and metabolic themes, HNSCC and OSCC clustered away from LSCC, suggesting the underlying biology of those cancers is better suited to metabolic biomarker studies. Both HNSCC and OSCC arise from normally resident squamous cells, whereas LSCC arise from metaplastic squamous cells, perhaps explaining LSCCs' relative metabolic heterogeneity. Moreover, genomic studies suggest LSCC to be distinct from HNSCC and OSCC [63–65]. Nonetheless, the relatively lower number of quantified metabolites for LSCC suggests this cancer warrants further study, perhaps using the similar analytical approaches from the best OSCC/HNSCC studies.

Despite using weighting to account for multiplicity from untargeted approaches, the heterogeneity in study design and quality, and the lack of independent validation, made comprehensive biological interpretation of the observed metabolic difference speculative. An exception to this was BCAA

metabolism, which was a consistent theme in across the ASCC subtypes. There were 36 significant differences in BCAA concentrations or their downstream metabolites, across 12 studies [25, 26, 28, 34–36, 41–43, 46, 56, 66]. This was far more than any other metabolite group. Increased BCAAs were observed in ASCC tissue samples from four studies [26, 36, 45, 53], and decreased BCAA levels in cancer-blood samples were observed in two studies [42, 56]. These differences were often stark. This suggests uptake of BCAAs into ASCCs against the concentration gradient. BCAAs constitute 35-40% of human protein and are thus essential amino acids necessary for protein synthesis in rapidly dividing cells [67]. They also have additional proproliferative effects. For example, leucine potently activates the mammalian target of rapamycin complex 1 [60, 68–70] and BCAA deamination is a major source of glutamine for alternative energy [68, 71]. Thus, BCAA metabolism is emerging as critical mediators of transformation and treatment escape in a number of malignancies including other squamous cancers [72, 73] and the present finding of consistent BCAA reprogramming in ASCC warrants further targeted study.

Metabolomic biomarker analytics has evolved considerably in the last 15 years, and that progress is reflected in the design heterogeneity of the included studies. Critical appraisal of analytical design using CAWG-MSI generally revealed a low standard. In contrast, only six of the studies included in this review demonstrated poor STARD/QUADAS-2 scores (score of less than 25), indicating a reasonable quality of clinical design and reporting (Supplementary Table 1). A key issue with metabolomic studies is the compromise between metabolomic coverage and unambiguous compound identification. Several studies used untargeted methodologies [16, 25, 26, 28, 29, 31, 33–38, 40–43, 45, 47–49, 51, 53] or more than one platform [3, 8, 9, 12] to increase their metabolomic coverage, although none used ultra-high coverage techniques such as Fourier-transform ion cyclotron resonance mass spectrometry (FT-ICR). No studies did not meet their objectives, or overstated their conclusions; however, this suggests that significant aspects of the ASCC metabolome have not been explored. Six studies that performed targeted methodology achieved level 1 identification of compounds of interest [27, 30, 32, 39, 46, 52], and two further studies used only commercially available spectral libraries for confirmation of their compound of interest [24, 56].

Additionally, our critical review has highlighted the following recurrent shortcomings in the current ASCC metabolomic literature: (i) lack of a clear sample size calculation; (ii) poor description of patient recruitment and inadequate description of clinical metadata; (iii) poor description of method validation; (iv) inconsistent quality assurance, especially replicate analysis; (v) biomarker performance frequently reported as multivariable models rather than clinical metrics; and (vi) lack of model validation data, either using internal cross-validation, or independent validation cohorts or studies. Using the CAWG-MSI checklist during study design would help to mitigate these issues [14].

A potential limitation was that more patients included in this review had late-stage disease ($n = 548$) rather than early-stage disease ($n = 331$), and that the case mix was usually just reported rather than subject to subgroup analysis. Typically, the clinical motivation for the work was early cancer detection, which seems at odds with test populations enriched for late-stage disease, without subgroup analysis. However, the majority of these studies were performed in tertiary centre settings, which meant that patients would typically have been on a curative pathway. Thus, the observed metabolic differences can detect treatable disease, which provides a platform for further studies powered to detect truly early disease. It should also be noted that more than half of the articles in this review were performed in China and Japan and may not be applicable to Western populations.

5. Conclusion

This review summarised progress in using metabolites to identify patients with ASCC. There was significant heterogeneity in methodology and quality; however, especially for OSCC and HNSCC, metabolites showed promise for minimally invasive diagnosis. These two ASCC subtypes had similar metabolic phenotypes, with deregulation of amino acid metabolism particularly pronounced. Comparative analysis of different sample types suggested a kinetics model for amino acids across the endolumen. To aid the development of future studies and ultimately clinical translation, the summarised recurrent methodological weaknesses must be addressed, especially with respect to analytical design.

Conflicts of Interest

The authors declare that there is no conflict of interest regarding the publication of this paper.

Acknowledgments

This project is funded by the Medical Research Council, UK. The funding reference number is MR/S022112/1.

Supplementary Materials

Supplementary Information Supplementary Figure 1: proportion of identified compound classes in different biosamples. Supplementary Table 1: summary of quality assessments. Supplementary Table 2: quality assessment of metabolic metadata based on CAWG-MSI guidelines. Supplementary Table 3: list of all metabolites, chemical class, and studies that identified them to be increased or decreased in biosamples. Supplementary Table 4: summary of significantly different metabolites listed in Supplementary Table 3. *(Supplementary Materials)*

References

[1] F. Bray, J. Ferlay, I. Soerjomataram, R. L. Siegel, L. A. Torre, and A. Jemal, "Global cancer statistics 2018: GLOBOCAN estimates of incidence and mortality worldwide for 36 cancers in 185 countries," *CA: A Cancer Journal for Clinicians*, vol. 68, no. 6, pp. 394–424, 2018.

[2] A. C. O. V. CampionLe, C. M. B. Ribeiro, R. R. Luiz et al., "Low survival rates of oral and oropharyngeal squamous cell

carcinoma," *International Journal of Dentistry*, vol. 2017, Article ID 5815493, 7 pages, 2017.

[3] R. L. Siegel, K. D. Miller, and A. Jemal, "Colorectal cancer mortality rates in adults aged 20 to 54 years in the United States, 1970-2014," *JAMA*, vol. 318, no. 6, pp. 572–574, 2017.

[4] S. A. Narod, J. Iqbal, and A. B. Miller, "Why have breast cancer mortality rates declined?," *Journal of Cancer Policy*, vol. 5, pp. 8–17, 2015.

[5] K. A. Burton, K. A. Ashack, and A. Khachemoune, "Cutaneous squamous cell carcinoma: a review of high-risk and metastatic disease," *American Journal of Clinical Dermatology*, vol. 17, no. 5, pp. 491–508, 2016.

[6] C. Manzoni, D. A. Kia, J. Vandrovcova et al., "Genome, transcriptome and proteome: the rise of omics data and their integration in biomedical sciences," *Briefings in Bioinformatics*, vol. 19, no. 2, pp. 286–302, 2018.

[7] A. Zhang, H. Sun, G. Yan, P. Wang, and X. Wang, "Metabolomics for biomarker discovery: moving to the clinic," *BioMed Research International*, vol. 2015, Article ID 354671, 6 pages, 2015.

[8] S. Kumar, J. Huang, N. Abbassi-Ghadi, P. Španěl, D. Smith, and G. B. Hanna, "Selected ion flow tube mass spectrometry analysis of exhaled breath for volatile organic compound profiling of esophago-gastric cancer," *Analytical Chemistry*, vol. 85, no. 12, pp. 6121–6128, 2013.

[9] S. R. Markar, T. Wiggins, S. Antonowicz et al., "Assessment of a noninvasive exhaled breath test for the diagnosis of oesophagogastric cancer," *JAMA Oncology*, vol. 4, no. 7, pp. 970–976, 2018.

[10] H. Haick, Y. Y. Broza, P. Mochalski, V. Ruzsanyi, and A. Amann, "Assessment, origin, and implementation of breath volatile cancer markers," *Chemical Society Reviews*, vol. 43, no. 5, pp. 1423–1449, 2014.

[11] G. B. Hanna, P. R. Boshier, S. R. Markar, and A. Romano, "Accuracy and methodologic challenges of volatile organic compound–based exhaled breath tests for cancer diagnosis: a systematic review and meta-analysis," *JAMA Oncology*, vol. 5, no. 1, article e182815, 2019.

[12] P. Masson, K. Spagou, J. K. Nicholson, and E. J. Want, "Technical and biological variation in UPLC-MS-based untargeted metabolic profiling of liver extracts: application in an experimental toxicity study on galactosamine," *Analytical Chemistry*, vol. 83, no. 3, pp. 1116–1123, 2011.

[13] H. P. Benton, E. J. Want, and T. M. D. Ebbels, "Correction of mass calibration gaps in liquid chromatography-mass spectrometry metabolomics data," *Bioinformatics*, vol. 26, no. 19, pp. 2488-2489, 2010.

[14] L. W. Sumner, A. Amberg, D. Barrett et al., "Proposed minimum reporting standards for chemical analysis: chemical analysis working group (CAWG) metabolomics standards initiative (MSI)," *Metabolomics*, vol. 3, no. 3, pp. 211–221, 2007.

[15] D. F. Stroup, J. A. Berlin, S. C. Morton et al., "Meta-analysis of observational studies in epidemiology: a proposal for reporting. Meta-analysis Of Observational Studies in Epidemiology (MOOSE) group," *Journal of the American Medical Association*, vol. 283, no. 15, pp. 2008–2012, 2000.

[16] J. Xu, Y. Chen, R. Zhang et al., "Global metabolomics reveals potential urinary biomarkers of esophageal squamous cell carcinoma for diagnosis and staging," *Scientific Reports*, vol. 6, no. 1, article 35010, 2016.

[17] R. M. Harbord, P. Whiting, J. A. C. Sterne et al., "An empirical comparison of methods for meta-analysis of diagnostic accuracy showed hierarchical models are necessary," *Journal of Clinical Epidemiology*, vol. 61, no. 11, pp. 1095–1103, 2008.

[18] J. Chong and J. Xia, "MetaboAnalystR: an R package for flexible and reproducible analysis of metabolomics data," *Bioinformatics*, vol. 34, no. 24, pp. 4313-4314, 2018.

[19] J. Chong, M. Yamamoto, and J. Xia, "MetaboAnalystR 2.0: from raw spectra to biological insights," *Metabolites*, vol. 9, no. 3, p. 57, 2019.

[20] J. Ma, A. Shojaie, and G. Michailidis, "A comparative study of topology-based pathway enrichment analysis methods," *BMC Bioinformatics*, vol. 20, no. 1, article 546, 2019.

[21] P. F. Whiting, A. W. S. Rutjes, M. E. Westwood et al., "Quadas-2: a revised tool for the quality assessment of diagnostic accuracy studies," *Annals of Internal Medicine*, vol. 155, no. 8, pp. 529–536, 2011.

[22] J. F. Cohen, D. A. Korevaar, D. G. Altman et al., "STARD 2015 guidelines for reporting diagnostic accuracy studies: explanation and elaboration," *BMJ Open*, vol. 6, no. 11, article e012799, 2016.

[23] P. M. Bossuyt, J. B. Reitsma, D. E. Bruns et al., "STARD 2015: an updated list of essential items for reporting diagnostic accuracy studies," *BMJ*, vol. 351, article h5527, 2015.

[24] J. Cheng, G. Zheng, H. Jin, and X. Gao, "Towards tyrosine metabolism in esophageal squamous cell carcinoma," *Combinatorial Chemistry & High Throughput Screening*, vol. 20, no. 2, pp. 133–139, 2017.

[25] J. Wang, T. Zhang, X. Shen et al., "Serum metabolomics for early diagnosis of esophageal squamous cell carcinoma by UHPLC-QTOF/MS," *Metabolomics*, vol. 12, no. 7, p. 116, 2016.

[26] L. Wang, J. Chen, L. Chen et al., "^{1}H-NMR based metabonomic profiling of human esophageal cancer tissue," *Molecular Cancer*, vol. 12, no. 1, p. 25, 2013.

[27] J. De Castro, M. C. Rodríguez, V. S. Martínez-Zorzano, P. Sánchez-Rodríguez, and J. Sánchez-Yagüe, "Erythrocyte fatty acids as potential biomarkers in the diagnosis of advanced lung adenocarcinoma, lung squamous cell carcinoma, and small cell lung cancer," *American Journal of Clinical Pathology*, vol. 142, no. 1, pp. 111–120, 2014.

[28] H. Handa, A. Usuba, S. Maddula, J. I. Baumbach, M. Mineshita, and T. Miyazawa, "Exhaled breath analysis for lung cancer detection using ion mobility spectrometry," *PLoS One*, vol. 9, no. 12, article e114555, 2014.

[29] C. M. Rocha, A. S. Barros, B. J. Goodfellow et al., "NMR metabolomics of human lung tumours reveals distinct metabolic signatures for adenocarcinoma and squamous cell carcinoma," *Carcinogenesis*, vol. 36, no. 1, pp. 68–75, 2015.

[30] P. Sánchez-Rodríguez, M. C. Rodríguez, and J. Sánchez-Yagüe, "Identification of potential erythrocyte phospholipid fatty acid biomarkers of advanced lung adenocarcinoma, squamous cell lung carcinoma, and small cell lung cancer," *Tumor Biology*, vol. 36, no. 7, pp. 5687–5698, 2015.

[31] S. Hartwig, J. D. Raguse, D. Pfitzner, R. Preissner, S. Paris, and S. Preissner, "Volatile organic compounds in the breath of oral squamous cell carcinoma patients: a pilot study," *Otolaryngology–Head and Neck Surgery*, vol. 157, no. 6, pp. 981–987, 2017.

[32] A. Szabó, Z. Tarnai, C. Berkovits et al., "Volatile sulphur compound measurement with OralChroma™: a methodological

improvement," *Journal of Breath Research*, vol. 9, no. 1, article 016001, 2015.

[33] M. Bouza, J. Gonzalez-Soto, R. Pereiro, J. C. de Vicente, and A. Sanz-Medel, "Exhaled breath and oral cavity VOCs as potential biomarkers in oral cancer patients," *Journal of Breath Research*, vol. 11, no. 1, article 016015, 2017.

[34] P. Kamarajan, T. M. Rajendiran, J. Kinchen, M. Bermúdez, T. Danciu, and Y. L. Kapila, "Head and neck squamous cell carcinoma metabolism draws on glutaminolysis, and stemness is specifically regulated by glutaminolysis via aldehyde dehydrogenase," *Journal of Proteome Research*, vol. 16, no. 3, pp. 1315–1326, 2017.

[35] P. K. Mukherjee, P. Funchain, M. Retuerto et al., "Metabolomic analysis identifies differentially produced oral metabolites, including the oncometabolite 2-hydroxyglutarate, in patients with head and neck squamous cell carcinoma," *BBA Clinical*, vol. 7, pp. 8–15, 2017.

[36] B. S. Somashekar, P. Kamarajan, T. Danciu et al., "Magic angle spinning NMR-based metabolic profiling of head and neck squamous cell carcinoma tissues," *Journal of Proteome Research*, vol. 10, no. 11, pp. 5232–5241, 2011.

[37] H. Shoffel-Havakuk, I. Frumin, Y. Lahav, L. Haviv, N. Sobel, and D. Halperin, "Increased number of volatile organic compounds over malignant glottic lesions," *The Laryngoscope*, vol. 126, no. 7, pp. 1606–1611, 2016.

[38] M. Gruber, U. Tisch, R. Jeries et al., "Analysis of exhaled breath for diagnosing head and neck squamous cell carcinoma: a feasibility study," *British Journal of Cancer*, vol. 111, no. 4, pp. 790–798, 2014.

[39] Q. Wang, P. Gao, X. Wang, and Y. Duan, "Investigation and identification of potential biomarkers in human saliva for the early diagnosis of oral squamous cell carcinoma," *Clinica Chimica Acta*, vol. 427, pp. 79–85, 2014.

[40] Q. Wang, P. Gao, X. Wang, and Y. Duan, "The early diagnosis and monitoring of squamous cell carcinoma via saliva metabolomics," *Scientific Reports*, vol. 4, no. 1, article 6802, 2015.

[41] J. Wei, G. Xie, Z. Zhou et al., "Salivary metabolite signatures of oral cancer and leukoplakia," *International Journal of Cancer*, vol. 129, no. 9, pp. 2207–2217, 2011.

[42] H. Jin, F. Qiao, L. Chen, C. Lu, L. Xu, and X. Gao, "Serum metabolomic signatures of lymph node metastasis of esophageal squamous cell carcinoma," *Journal of Proteome Research*, vol. 13, no. 9, pp. 4091–4103, 2014.

[43] A. Gupta, S. Gupta, and A. A. Mahdi, "^{1}H NMR-derived serum metabolomics of leukoplakia and squamous cell carcinoma," *Clinica Chimica Acta*, vol. 441, pp. 47–55, 2015.

[44] H. Zhang, L. Wang, Z. Hou et al., "Metabolomic profiling reveals potential biomarkers in esophageal cancer progression using liquid chromatography-mass spectrometry platform," *Biochemical and Biophysical Research Communications*, vol. 491, no. 1, pp. 119–125, 2017.

[45] K. Yonezawa, S. Nishiumi, J. Kitamoto-Matsuda et al., "Serum and tissue metabolomics of head and neck cancer," *Cancer Genomics Proteomics*, vol. 10, no. 5, pp. 233–238, 2013.

[46] N. Mizukawa, K. Sugiyama, J. Fukunaga et al., "Defensin-1, a peptide detected in the saliva of oral squamous cell carcinoma patients," *Anticancer Research*, vol. 18, no. 6B, pp. 4645–4649, 1998.

[47] V. D. Kekatpure, N. Bs, H. Wang et al., "Elevated levels of urinary PGE-M are found in tobacco users and indicate a poor prognosis for oral squamous cell carcinoma patients," *Cancer Prevention Research*, vol. 9, no. 6, pp. 428–436, 2016.

[48] M. Ohshima, K. Sugahara, K. Kasahara, and A. Katakura, "Metabolomic analysis of the saliva of Japanese patients with oral squamous cell carcinoma," *Oncology Reports*, vol. 37, no. 5, pp. 2727–2734, 2017.

[49] R. Liu, Y. Peng, X. Li et al., "Identification of plasma metabolomic profiling for diagnosis of esophageal squamous-cell carcinoma using an UPLC/TOF/MS platform," *International Journal of Molecular Sciences*, vol. 14, no. 5, pp. 8899–8911, 2013.

[50] K. Jia, W. Li, F. Wang et al., "Novel circulating peptide biomarkers for esophageal squamous cell carcinoma revealed by a magnetic bead-based MALDI-TOFMS assay," *Oncotarget*, vol. 7, no. 17, pp. 23569–23580, 2016.

[51] G. Song, T. Qin, H. Liu et al., "Quantitative breath analysis of volatile organic compounds of lung cancer patients," *Lung Cancer*, vol. 67, no. 2, pp. 227–231, 2010.

[52] Q. Wang, P. Gao, F. Cheng, X. Wang, and Y. Duan, "Measurement of salivary metabolite biomarkers for early monitoring of oral cancer with ultra performance liquid chromatography-mass spectrometry," *Talanta*, vol. 119, pp. 299–305, 2014.

[53] X. Zhang, L. Xu, J. Shen et al., "Metabolic signatures of esophageal cancer: NMR-based metabolomics and UHPLC- based focused metabolomics of blood serum," *Biochimica et Biophysica Acta (BBA) - Molecular Basis of Disease*, vol. 1832, no. 8, pp. 1207–1216, 2013.

[54] L. Zhang, J. Jiang, M. Arellano et al., "Quantification of serum proteins of metastatic oral cancer patients using LC-MS/MS and iTRAQ labeling," *The Open Proteomics Journal*, vol. 1, no. 1, pp. 72–78, 2008.

[55] D. Yakoub, H. C. Keun, R. Goldin, and G. B. Hanna, "Metabolic profiling detects field effects in nondysplastic tissue from esophageal cancer patients," *Cancer Research*, vol. 70, no. 22, pp. 9129–9136, 2010.

[56] H. Ma, A. Hasim, B. Mamtimin, B. Kong, H. P. Zhang, and I. Sheyhidin, "Plasma free amino acid profiling of esophageal cancer using high-performance liquid chromatography spectroscopy," *World Journal of Gastroenterology*, vol. 20, no. 26, pp. 8653–8659, 2014.

[57] J. Xu, Y. Chen, R. Zhang et al., "Global and targeted metabolomics of esophageal squamous cell carcinoma discovers potential diagnostic and therapeutic biomarkers," *Molecular & Cellular Proteomics*, vol. 12, no. 5, pp. 1306–1318, 2013.

[58] F. Zhang, Y. Zhang, W. Zhao et al., "Metabolomics for biomarker discovery in the diagnosis, prognosis, survival and recurrence of colorectal cancer: a systematic review," *Oncotarget*, vol. 8, no. 21, pp. 35460–35472, 2017.

[59] R. A. Spicer, R. Salek, and C. Steinbeck, "Compliance with minimum information guidelines in public metabolomics repositories," *Scientific Data*, vol. 4, no. 1, article 170137, 2017.

[60] H. Zhen, Y. Kitaura, Y. Kadota et al., "mTORC1 is involved in the regulation of branched-chain amino acid catabolism in mouse heart," *FEBS Open Bio*, vol. 6, no. 1, pp. 43–49, 2016.

[61] Y. Niv and A. D. Sperber, "Sensitivity, specificity, and predictive value of fecal occult blood testing (Hemoccult II) for colorectal neoplasia in symptomatic patients: a prospective study with total colonoscopy," *The American Journal of Gastroenterology*, vol. 90, no. 11, pp. 1974–1977, 1995.

[62] J. Cuzick, C. Clavel, K. U. Petry et al., "Overview of the European and North American studies on HPV testing in primary

cervical cancer screening," *International Journal of Cancer*, vol. 119, no. 5, pp. 1095–1101, 2006.

[63] The Cancer Genome Atlas Research Network, "Comprehensive genomic characterization of squamous cell lung cancers," *Nature*, vol. 489, no. 7417, pp. 519–525, 2012.

[64] The Cancer Genome Atlas Network, "Comprehensive genomic characterization of head and neck squamous cell carcinomas," *Nature*, vol. 517, no. 7536, pp. 576–582, 2015.

[65] The Cancer Genome Atlas Research Network, "Integrated genomic characterization of oesophageal carcinoma," *Nature*, vol. 541, no. 7636, pp. 169–175, 2017.

[66] Q. Wang, Q. Yu, Q. Lin, and Y. Duan, "Emerging salivary biomarkers by mass spectrometry," *Clinica Chimica Acta*, vol. 438, pp. 214–221, 2015.

[67] Y. Shimomura, T. Murakami, N. Nakai, M. Nagasaki, and R. A. Harris, "Exercise promotes BCAA catabolism: effects of BCAA supplementation on skeletal muscle during exercise," *The Journal of Nutrition*, vol. 134, no. 6, pp. 1583S–1587S, 2004.

[68] E. A. Ananieva and A. C. Wilkinson, "Branched-chain amino acid metabolism in cancer," *Current Opinion in Clinical Nutrition and Metabolic Care*, vol. 21, no. 1, pp. 64–70, 2018.

[69] M. Moberg, W. Apró, B. Ekblom, G. Van Hall, H. C. Holmberg, and E. Blomstrand, "Activation of mTORC1 by leucine is potentiated by branched-chain amino acids and even more so by essential amino acids following resistance exercise," *American Journal of Physiology-Cell Physiology*, vol. 310, no. 11, pp. C874–C884, 2016.

[70] K. M. Dodd and A. R. Tee, "Leucine and mTORC1: a complex relationship," *American Journal of Physiology. Endocrinology and Metabolism*, vol. 302, no. 11, pp. E1329–E1342, 2012.

[71] S. Zhang, X. Zeng, M. Ren, X. Mao, and S. Qiao, "Novel metabolic and physiological functions of branched chain amino acids: a review," *Journal of Animal Science and Biotechnology*, vol. 8, no. 1, p. 10, 2017.

[72] H.-J. Lu, C. C. Hsieh, C. C. Yeh et al., "Clinical, pathophysiologic, and genomic analysis of the outcomes of primary head and neck malignancy after pulmonary metastasectomy," *Scientific Reports*, vol. 9, no. 1, article 12913, 2019.

[73] Y. Wang, J. Zhang, S. Ren et al., "Branched-chain amino acid metabolic reprogramming orchestrates drug resistance to EGFR tyrosine kinase inhibitors," *Cell Reports*, vol. 28, no. 2, pp. 512–525.e6, 2019.

Hindawi
Oxidative Medicine and Cellular Longevity
Volume 2019, Article ID 5381692, 12 pages
https://doi.org/10.1155/2019/5381692

Review Article

Understanding of ROS-Inducing Strategy in Anticancer Therapy

Su Ji Kim,[1,2] **Hyun Soo Kim**,[1,2] **and Young Rok Seo**[1,2]

[1]*Institute of Environmental Medicine for Green Chemistry, Dongguk University Biomedi Campus, 32 Dongguk-ro, Ilsandong-gu, Goyang-si, Gyeonggi-do 10326, Republic of Korea*
[2]*Department of Life Science, Dongguk University Biomedi Campus, 32 Dongguk-ro, Ilsandong-gu, Goyang-si, Gyeonggi-do 10326, Republic of Korea*

Correspondence should be addressed to Young Rok Seo; seoyr@dongguk.edu

Received 19 April 2019; Revised 19 November 2019; Accepted 23 November 2019; Published 20 December 2019

Guest Editor: Adil Mardinoglu

Redox homeostasis is essential for the maintenance of diverse cellular processes. Cancer cells have higher levels of reactive oxygen species (ROS) than normal cells as a result of hypermetabolism, but the redox balance is maintained in cancer cells due to their marked antioxidant capacity. Recently, anticancer therapies that induce oxidative stress by increasing ROS and/or inhibiting antioxidant processes have received significant attention. The acceleration of accumulative ROS disrupts redox homeostasis and causes severe damage in cancer cells. In this review, we describe ROS-inducing cancer therapy and the anticancer mechanism employed by prooxidative agents. To understand the comprehensive biological response to certain prooxidative anticancer drugs such as 2-methoxyestradiol, buthionine sulfoximine, cisplatin, doxorubicin, imexon, and motexafin gadolinium, we propose and visualize the drug-gene, drug-cell process, and drug-disease interactions involved in oxidative stress induction and antioxidant process inhibition as well as specific side effects of these drugs using pathway analysis with a big data-based text-mining approach. Our review will be helpful to improve the therapeutic effects of anticancer drugs by providing information about biological changes that occur in response to prooxidants. For future directions, there is still a need for pharmacogenomic studies on prooxidative agents as well as the molecular mechanisms underlying the effects of the prooxidants and/or antioxidant-inhibitor agents for effective anticancer therapy through selective killing of cancer cells.

1. Introduction

Reactive oxygen species (ROS) are generally defined as chemically reactive molecules containing oxygen, produced as a result of cellular metabolism [1]. A moderate level of ROS plays an essential role in the cellular signaling that regulates cell proliferation and cell survival [2]. However, an increase in ROS levels can damage cellular components such as lipids, proteins, and DNA, causing an imbalance between cellular reduction-oxidation (redox) conditions and resulting in the disruption of homeostasis [3]. Chronically increased ROS cause severe cellular damage and lead to carcinogenesis by modulating cell signaling in biological processes including cell proliferation and survival, angiogenesis, and metastasis [4, 5].

Anticancer therapies based on oxidative damage through the acceleration of accumulative ROS or the defective antioxidant system in cancer cells have been developed [2, 6]. Due to uncontrolled metabolic processes during hyperproliferation, cancer cells have a higher basal ROS level than normal cells [7]. Adaptation to excessive ROS conditions in cancer cells has been reported, suggesting they have a higher level of antioxidative capacity and ROS than normal cells [2]. ROS-inducing approaches rely on the fact that increasing the ROS level over the cytotoxic threshold can selectively kill cancer cells. The elevated ROS level breaks the redox homeostasis and consequently causes cancer cell death. If exogenous ROS-generating agents are triggered, the redox-imbalanced cancer cells become more vulnerable than normal cells, thereby leading to cell death [8] (Figure 1). Accordingly,

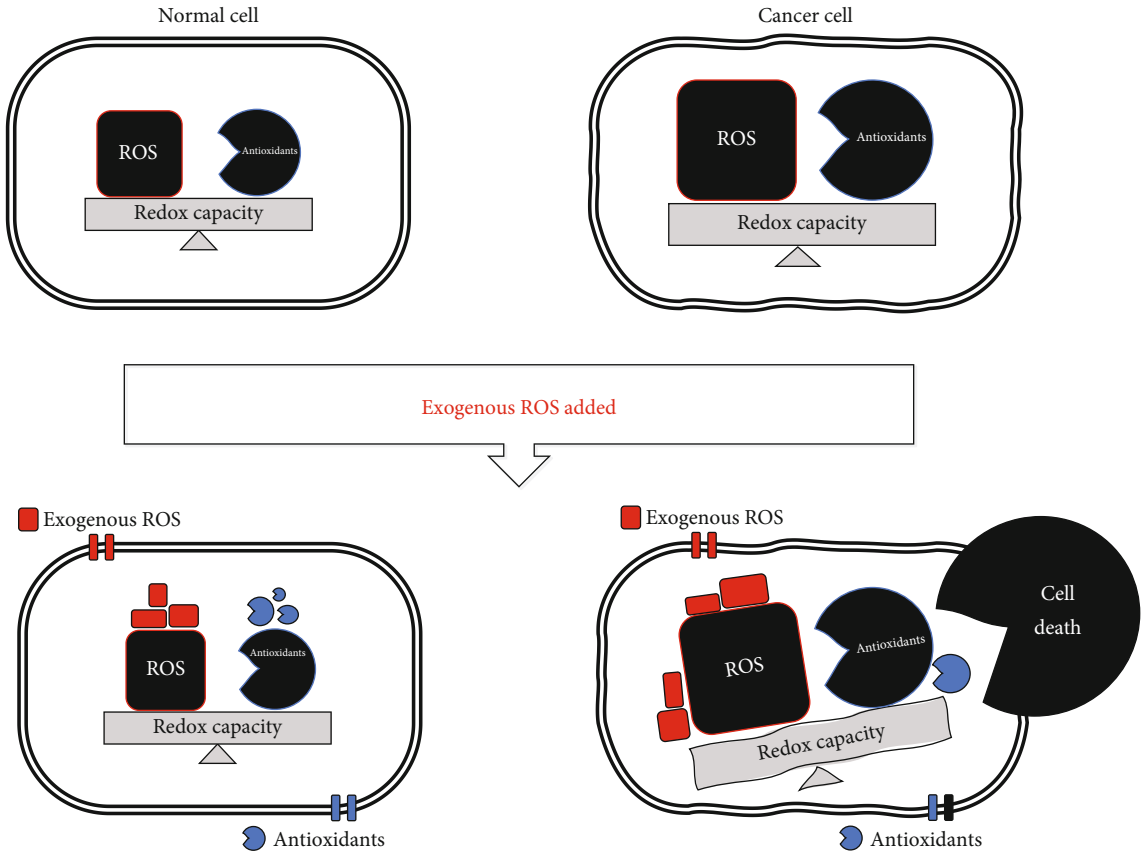

Figure 1: Differential ROS levels in normal and cancer cells. Normal cells have a lower basal ROS level than cancer cells. In normal cells, a moderate ROS level is essential to promote cell proliferation and survival whereas an excessive ROS level has detrimental effects such as tumor progression and angiogenesis. The redox balance in cancer cells is readily regulated by increasing antioxidant processes. Once the ROS level exceeds the redox capacity in cancer cells, severe oxidative stress occurs, resulting in cancer cell death via the activation of apoptosis, autophagic cell death, and necroptosis.

prooxidative agents have been investigated as anticancer drugs that interrupt redox adaptation and eventually induce cytotoxicity in ROS-dependent cancer cells [9].

In this review, we summarize the mechanisms underlying the effects of anticancer drugs utilized in oxidative stress-inducing chemotherapy for direct or indirect ROS generation. To grasp the biological alterations mediated by prooxidative drugs, the drug-focused pathways were analyzed and visualized using big data-based network analysis software. We also suggest crucial therapeutic strategies for anticancer drugs and provide information regarding potential side effects and drug resistance based on the results of the pathway analysis.

2. Basic Concepts of ROS: Generation and Elimination

Oxygen is an essential molecule for maintaining metabolism and life in organisms. However, the metabolism of oxygen produces highly reactive molecules called ROS, a major source of oxidative stress. There are many types of ROS, including superoxide ($O_2^{\cdot-}$), hydroxyl radicals ($OH^{\cdot}$), hydrogen peroxide (H_2O_2), and singlet oxygen ($^1O_2$) [10]. The cellular redox state refers to the balance between the oxidized and reduced states in cells. In living organisms, redox equilibrium is important for cellular homeostasis [11]. As previously demonstrated, the impairment of redox homeostasis mediated by an excess of oxidized biological molecules is associated with cellular toxic effects [12]. Accordingly, proper regulation of the redox status through ROS generation and elimination is crucial.

Most endogenous ROS are mainly generated in the mitochondrial electron transport chain (ETC) and NADPH oxidase complex (NOX) [13, 14]. During oxidative phosphorylation, the leakage of electrons by ETC complexes I and III occurs in the inner mitochondrial membrane, leading to the reduction of oxygen into superoxide. Subsequently, superoxide dismutase (SOD) converts superoxide into hydrogen peroxide in the intermembrane space or the matrix of mitochondria [8, 14]. Hydrogen peroxide can be converted into hydroxyl radicals in the presence of Fe^{2+} [15]. Likewise, NOX, a transmembrane enzyme complex consisting of seven subunits, catalyzes the oxidation of NADPH by transferring electrons to molecular oxygen, leading to the production of superoxide [16].

To avoid endogenous ROS overproduction, cells have diverse defense systems to eliminate ROS using antioxidant molecules and enzymes such as glutathione (GSH),

peroxiredoxin (Prx), thioredoxin (Trx), SOD, and catalase [17]. GSH protects cellular components against oxidative damage through interactions with a cofactor of GSH peroxidase (GPx) and/or participation in other antioxidant components [18, 19]. In the presence of NADPH, GSH reductase catalyzes the reduction of GSH. Two reduced GSH molecules are oxidized into GSH disulfide (GSSG) via a reaction with GPx, which catalyzes the reduction of hydrogen peroxide to water and oxygen molecules through the redox cycle [20, 21]. GSH deficiency has been shown to reduce tissue ascorbate levels and increase oxidative stress, ultimately resulting in diverse disorders such as mitochondrial disease, hepatic injuries, and HIV [19, 22, 23]. Several anticancer drugs and xenobiotics have been developed for GSH-targeted chemotherapies or detoxifying agent-based chemoprevention [24]. Both Prx and Trx, which contain cysteine residues with redox-reactive thiol groups, can scavenge hydrogen peroxide via thiol/disulfide exchange [25]. Hydrogen peroxide is reduced by Prx, which is simultaneously oxidized to form a disulfide bond, and Prx is subsequently reduced by transferring the disulfide bond to Trx [26]. In the presence of NADPH, Trx is reduced by a reaction with Trx reductase [27, 28]. SOD catalyzes the breakdown of superoxide to molecular oxygen and hydrogen peroxide using metal ion cofactors including copper, zinc, and manganese [29, 30]. Catalases reduce hydrogen peroxide to water and oxygen with a manganese ion cofactor [31].

Although cellular antioxidant systems have a vital role in balancing endogenous ROS levels and the redox status for cell protection against oxidative stress [32, 33], exogenously prooxidants-induced ROS levels and an ineffective cellular defense system result in significant imbalance between prooxidants and antioxidants [34], possibly enabling cellular damage and cell death.

3. Application of ROS Induction for Anticancer Strategies

A lot of anticancer therapies have employed antioxidant supplements as a strategy to prevent or treat cancer cells. *tert*-Butylhydroquinone (tBHQ) mediates the dissociation of Nrf2 via oxidative modification of the Keap1 cysteine residues by ROS generated during the metabolic process [35]. Nrf2 activation promotes the regulation of downstream cytoprotective genes, which play important roles in cancer prevention [36]. Selenocompounds exhibit anticancer effects through potentiating the antioxidative defense system from ROS-induced cellular damage [37, 38] and through redox modification of redox-active, cysteine-rich regions of protein kinase C (PKC), a receptor for tumor promoters [39, 40].

However, controversial issues remain regarding the chemotherapeutic activities of antioxidants. Indeed, it has been widely reported that Nrf2 activation contributes to chemoresistance in cancer cells [41–44]. Additionally, a high concentration of tBHQ has been reported to increase carcinogenic risk [45, 46]. The efficacy and safety of selenium are also actively discussed due to its toxicity and side effects [47, 48]. Thus, chemotherapies involving antioxidants may not be sufficient to kill cancer cells and further studies are needed to determine whether they have unexpected adverse effects.

ROS has double-edged sword characteristics in terms of its low-dose cell signaling and high-dose cytotoxicity [49]. A mild level of ROS regulates cell development and homeostasis, whereas a high level inflicts severe cellular damage [50, 51]. Cancer cells are more sensitive to the presence of prooxidants and the inhibition of antioxidants due to their excessive ROS levels [52–54]. The ROS-inducing approach for killing cancer cells relies on oxidative stress-dependent cytotoxic effects through apoptosis, necroptosis, and autophagic cell death [55].

In the early stages, cancer cells exhibit uncontrolled cell growth and proliferation via the modulation of transcription factors and are vulnerable to DNA damage [56, 57] through therapeutic strategies focused on inducing genetic damage using radiation or oxidative stress [58–60] (Figure 2). In the late stages, metastatic cancers undergo metabolic changes such as increased endogenous antioxidant levels to buffer oxidative stress conditions [61]. Indeed, the GSH/GSSG ratio tends to be lower in circulating melanoma or metastatic cancers, suggesting that late-stage cancers have better antioxidant processes than early-stage cancers [62, 63]. Although NADPH-independent catalase activity has been reported to decrease with cancer progression [64], the remarkable antioxidant capacity is one of the reasons for chemoresistance in advanced cancer cells [65, 66]. ROS-inducing and/or antioxidant-suppressing approaches can be applied appropriately for the treatment of malignant cancer cells. Oxidative stress-modulated therapeutics for attacking cancer cells are being actively researched in the anticancer field [67, 68]. The cell-killing potential of ROS has been harnessed for anticancer therapies with two major approaches: direct ROS generation and antioxidant process inhibition [6].

3.1. Direct ROS Generation. Electrons derived from metabolism and respiratory processes are representative ROS sources in cells [69]. Impairing the respiratory cycles with the alteration of radical intermediates produces superoxide by which motexafin gadolinium and anthracyclines function [69–71]. Motexafin gadolinium, an avid electron acceptor, enhances the therapeutic index of radiotherapy, since it can inhibit the repair activities of cancer cells after irradiation [72, 73]. It is effective in patients with brain tumors, brain metastases, and pediatric gliomas [72]. Indeed, anthracycline-based anticancer drugs such as doxorubicin can induce the chelation of intracellular iron, leading to the accumulation of hydroxyl radicals and ultimately to cell death [74]. These drugs are effective for malignant lymphomas, acute leukemia, and diverse solid tumors [75]. Cisplatin, a well-known anticancer agent with cross-linking activity, directly damages mitochondrial DNA (mtDNA), which leads to ETC impairment [76]. It can also interfere with DNA replication and consequently induce oxidative stress to target cancer cells [77]. The drug is effective for diverse cancer types, especially ovarian cancer [78, 79]. 2-Methoxyestradiol is known to inhibit ETC complex I [80], inducing mitochondrial production of hydrogen peroxide [81]. Subsequently, it rapidly activates c-Jun N-terminal

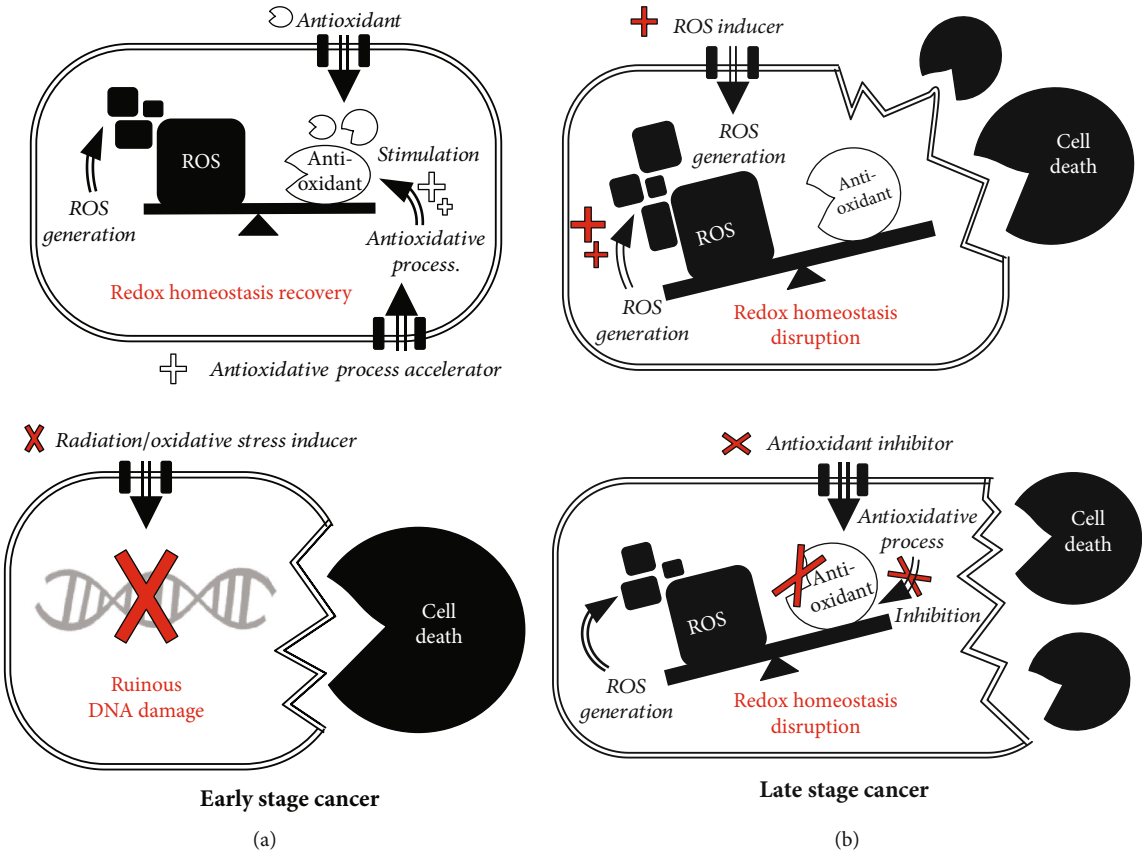

Figure 2: Anticancer therapeutic strategies attacking early-stage and late-stage cancer cells. (a) Early-stage cancer cells simply enable recovery of the disrupted redox status using antioxidants/antioxidative process accelerators. Briefly, chemotherapy with radiation or oxidative stress inducers is used to remove these cancer cells, in which significant DNA damage occurs. (b) Late-stage cancer cells have higher basal ROS levels and antioxidative activities than normal or early-stage cancer cells. In this case, cancer cells can be killed by redox homeostasis disruption following severe cytotoxic effects mediated by direct ROS inducers and/or antioxidant inhibitors. Prooxidative agents hold promise for potent cancer chemotherapy. The double-lined arrows and double-lined squares indicate the direction of anticancer molecules for movement and in cancer cells, respectively.

kinase (JNK), resulting in cytochrome c release and caspase-9 activation to initiate apoptosis [82, 83]. The drug can promote the therapeutic capability of other anticancer agents [84–86]. *In vitro* and *in vivo* studies have demonstrated that 2-methoxyestradiol-mediated chemotherapy can inhibit malignant cell proliferation as its own activity or in combination with synergistic drugs [87–90]. The ROS-accelerating anticancer agents described above are listed in Table 1.

Although anticancer drugs with direct ROS-accumulating activity have been shown to be effective for treating different types of cancer, the effects on normal cells are still controversial as they damage not only cancer cells but also normal cells. For instance, the radiosensitizer motexafin gadolinium interrupts the DNA repair process and causes injuries to surrounding normal cells [91]. Additionally, anthracyclines induce cardiotoxicity since their metabolites (e.g., oxygen-centered free radicals) can cause heart failure or cardiomyopathy, with a higher risk for younger patients [92–94]. Cisplatin-induced ototoxicity has been reported, attributed to its direct binding to DNA and consequent activation of the inflammatory cascade [95]. Additionally, liver function

Table 1: Mechanism of action of ROS-inducing anticancer drugs.

Name	Mechanism of action	Reference
Direct ROS generation		
Motexafin gadolinium	Accepts electrons to form superoxide	[69]
Doxorubicin	Induces chelation of iron to generate hydroxyl radical	[74]
Cisplatin	Damages mtDNA and ETC	[76]
2-Methoxyestradiol	Inhibits ETC complex I	[80]
Antioxidant process inhibition		
Buthionine sulfoximine	Binds to enzyme related to GSH synthesis	[101]
Imexon	Binds to thiol to GSH activity disruption	[102, 103]

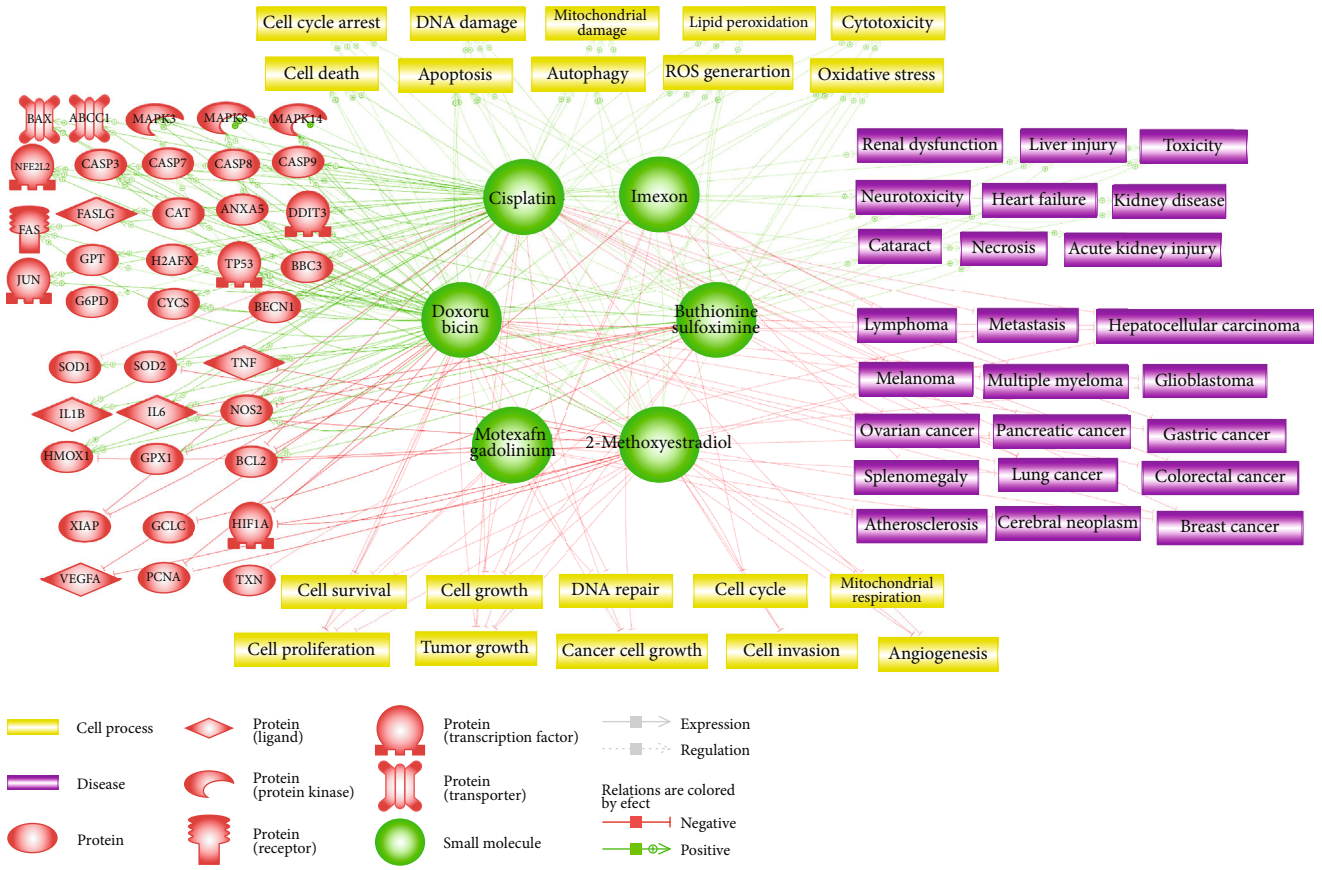

FIGURE 3: Proposed biological pathways related to prooxidative anticancer drugs. Comprehensive illustration of the drug-gene, drug-cell process, and drug-disease relationships for certain anticancer drugs with prooxidative activity (buthionine sulfoximine, cisplatin, doxorubicin, imexon, 2-methoxyestradiol, and motexafin gadolinium). Green and red lines denote the positive and negative effects of each drug, respectively. The legend for the diagrams is located at the bottom part of the figure. Target proteins (red), drug molecules (green), cell processes (yellow), and diseases (purple) are symbolized and organized in a complex biological network.

abnormalities, fatigue, and diarrhea have been reported in patients treated with 2-methoxyestradiol [85, 96, 97].

3.2. Antioxidant Process Inhibition. Although direct ROS induction is one of the effective strategies for treating malignant cancer cells [98], its combination with the disruption of antioxidative processes leads to the best results for overcoming the resistance characteristics of cancer cells. Depletion of GSH activity is regarded as an indirect method of generating oxidative stress. Cells can synthesize GSH via an ATP-dependent process catalyzed by glutamate-cysteine ligase (GCL) and GSH synthetase [99, 100]. For instance, buthionine sulfoximine, a typical GSH synthesis inhibitor, can bind to the GCL site that normally binds to the acceptor amino acid [101]. Imexon, a small-molecule chemotherapeutic agent, is widely used to treat advanced cancers of the breast, lung, and prostate. It can disrupt GSH activity by binding to the thiol functional group of reduced GSH [102, 103] and subsequently deplete the GSH pool for antioxidative activity. Due to a decrease in the GSH level by imexon treatment, loss of the mitochondrial membrane potential and the accumulation of oxidative stress occur in cancer cells.

Although anticancer therapy needs to disrupt, both directly and indirectly, the redox adaptation status of cancer cells, the inhibition of antioxidative enzyme has deleterious side effects on normal cells in tissues and organs. For instance, buthionine sulfoximine is known to be associated with cardiac hypertrophy and heart failure by inducing soluble epoxide hydrolase [104]. Imexon has potential side effects in normal cells due to its cytotoxicity [105–107]. For the future direction of oxidative stress-accelerating anticancer therapy, further study is needed to identify ways to not only reduce the side effects but also increase cancer cell-specific killing efficiency. For instance, cotreatment with antioxidant supplements that attenuate cisplatin-mediated nephrotoxicity through Nrf2 signaling has been investigated [108]. Moreover, plant-derived phytochemicals such as flavonoids and carotenoids that act as both antioxidants and prooxidants to improve the therapeutic effects and to reduce the cytotoxic effect have been reported [109–111].

4. Pathway Analysis to Understand the Process of Prooxidative Cancer Therapy

Identifying biological changes in cancer cells caused by anticancer drugs is meaningful to improve their therapeutic effect. Although several mechanism studies have been actively conducted to determine the mode of action of

Table 2: List of proteins, cell processes, and diseases targeted by anticancer drugs.

Drugs	Target type	Relation	Relation effect	Target
2-Methoxyestradiol	Protein	Expression	Positive	BAX, TP53
			Negative	HIF1A, IL6, PCNA, TNF, VEGFA
		Regulation	Positive	CASP9, MAPK8
			Negative	BCL2, HIF1A, SOD2
	Cell process	Regulation	Positive	Apoptosis, autophagy, cell cycle arrest, cell death, DNA damage, mitochondrial damage, oxidative stress, ROS generation
			Negative	Angiogenesis, cell cycle, cell growth, cell invasion, cell proliferation, cell survival, mitochondrial respiration, tumor growth
	Disease	Regulation	Negative	Atherosclerosis, breast cancer, hepatocellular carcinoma, melanoma, pancreatic cancer
Buthionine sulfoximine	Protein	Expression	Positive	BCL2, HMOX1, JUN, NFE2L2, SOD2, TNF
			Negative	GPX1, IL6, NOS2
		Regulation	Positive	BCL2, CASP3, MAPK14
			Negative	GCLC
	Cell process	Regulation	Positive	Apoptosis, autophagy, cell death, cytotoxicity, DNA damage, lipid peroxidation, oxidative stress, ROS generation
			Negative	Cell growth, cell proliferation, tumor growth
	Disease	Regulation	Positive	Cataract, liver injury, necrosis, neurotoxicity, toxicity
			Negative	Hepatocellular carcinoma, lung cancer
Cisplatin	Protein	Expression	Positive	ABCC1, BAX, BBC3, BECN1, CASP3, CASP8, CASP9, CYCS, DDIT3, FAS, FASLG, GPT, H2AFX, HMOX1, IL1B, IL6, JUN, NFE2L2, NOS2, TNF, TP53
			Negative	BCL2, SOD2, XIAP
		Regulation	Positive	CASP3, CASP7, CYCS, G6PD, MAPK14, MAPK3, MAPK8, TP53
			Negative	SOD1
	Cell process	Regulation	Positive	Apoptosis, autophagy, cell cycle arrest, cell death, cytotoxicity, DNA damage, lipid peroxidation, mitochondrial damage, oxidative stress, ROS generation
			Negative	Angiogenesis, cancer cell growth, cell growth, cell invasion, cell proliferation, cell survival, tumor growth
	Disease	Regulation	Positive	Acute kidney injury, kidney disease, liver injury, necrosis, neurotoxicity, renal dysfunction, toxicity
			Negative	Breast cancer, colorectal cancer, gastric cancer, hepatocellular carcinoma, lung cancer, lymphoma, melanoma, metastasis, ovarian cancer, pancreatic cancer
Doxorubicin	Protein	Expression	Positive	ABCC1, BAX, BBC3, BECN1, CASP3, CASP7, CASP8, CASP9, CAT, CYCS, DDIT3, FAS, FASLG, GPX1, H2AFX, HMOX1, IL1B, IL6, MAPK3, MAPK8, NFE2L2, NOS2, SOD1, TNF, TP53
			Negative	BCL2, PCNA, VEGFA, XIAP
		Regulation	Positive	ANXA5, CASP3, CASP7, CASP8, FAS, GPT, IL6, MAPK14, MAPK3, MAPK8, NOS2, TP53
			Negative	HIF1A
	Cell process	Regulation	Positive	Apoptosis, autophagy, cell cycle arrest, cell death, cytotoxicity, DNA damage, lipid peroxidation, mitochondrial damage, oxidative stress, ROS generation
			Negative	Angiogenesis, cancer cell growth, cell growth, cell proliferation, cell survival, DNA repair, mitochondrial respiration, tumor growth
	Disease	Regulation	Positive	Acute kidney injury, kidney disease, liver injury, necrosis, neurotoxicity, renal dysfunction, toxicity
			Negative	Breast cancer, colorectal cancer, gastric cancer, hepatocellular carcinoma, lung cancer, lymphoma, melanoma, metastasis, ovarian cancer, pancreatic cancer

Table 2: Continued.

Drugs	Target type	Relation	Relation effect	Target
Imexon	Protein	Expression	Negative	HIF1A
		Regulation	Positive	CASP3, CASP9
	Cell process	Regulation	Positive	Apoptosis, cell cycle arrest, oxidative stress
			Negative	Cancer cell growth, cell cycle, cell growth, tumor growth
	Disease	Regulation	Negative	Lymphoma, melanoma, multiple myeloma, splenomegaly
Motexafin gadolinium	Protein	Regulation	Negative	HMOX1, TXN
	Cell process	Regulation	Positive	Apoptosis, cell death, cytotoxicity, oxidative stress, ROS generation
			Negative	Cell proliferation, cell survival, DNA repair, tumor growth
	Disease	Regulation	Negative	Atherosclerosis, cerebral neoplasm, glioblastoma, lung cancer, metastasis

anticancer drugs for cancer treatment, the efficacy and toxicity of anti- and prooxidants remain controversial. In this regard, pathway analysis has the advantage of comprehensively elucidating the molecular network involved in the response to certain drugs. However, very few studies have been performed to explore biological modulation during treatment with prooxidant anticancer agents. In this review, we explore and visualize key information on drug-gene, drug-cell process, and drug-disease relationships for six anticancer drugs abovementioned with prooxidative activity (2-methoxyestradiol, buthionine sulfoximine, cisplatin, doxorubicin, imexon, and motexafin gadolinium) using a text mining-based biological network analysis tool, Pathway Studio ver. 12.2 (Elsevier, USA). This database provides information describing the relationships between the entities including the drugs, genes, cell processes, and diseases through a curated resource based on text mining from biology articles.

Each drug molecule was first inputted to build a network, and then the genes, cell processes, and diseases associated with the drugs were analyzed based on data provided in five or more references (Figure 3). Cisplatin and doxorubicin had the largest networks, implying that these two drugs have been extensively studied compared to the others, while imexon and motexafin gadolinium had the fewest connections. Figure 3 comprehensively illustrates the biological pathways including the target genes, key cellular processes, and target types of cancer that can be positively or negatively affected by these anticancer drugs. There were two types of relationships in the identified networks: Expression and Regulation. In Expression relationship, the drug alters the protein abundance by affecting the levels of transcript or protein stability. In Regulation relationships, the drug directly or indirectly changes the activity of the genes, cell processes, and diseases. In addition, we evaluated the possible side effects related to the prooxidant anticancer drugs such as neurotoxicity and cardiovascular diseases. Table 2 summarizes the detailed information obtained from pathway analysis regarding the relationship of each drug with the targeted genes, cell processes, and diseases. We also explored the association of drug resistance with each drug through network analysis.

Based on the high number of references in the pathway analysis, we found that 2-methoxyestradiol is not only a potent inhibitor of HIF1A and VEGFA, which play important roles in angiogenesis [112], it also activates MAPK8, which triggers apoptosis [113]. Consistent with these results, 2-methoxyestradiol has been shown to be closely associated with cellular processes such as apoptosis, cell proliferation, and angiogenesis. Breast cancer, melanoma, and pancreatic cancer were predicted to be major targets for this drug, and atherosclerosis can also be attenuated due to its antiangiogenetic effects. Moreover, 2-methoxyestradiol-mediated autophagy promoting cancer cell survival could lead to drug resistance [114].

Buthionine sulfoximine was shown to effectively inhibit GCLC, blocking GSH synthesis [115]. The expression of GPX1 was also found to decrease while that of NFE2L2, HMOX1, and SOD2 increased in direct response to GSH depletion [116]. Oxidative stress, apoptosis, and cell death were identified as the main cell processes induced by buthionine sulfoximine-mediated GSH inhibition. Hepatocellular carcinoma and lung cancer were predicted to be the main target diseases, and cataract can be evoked by increased lipid peroxidation in the lens [117]. The increased NFE2L2 can upregulate ABCC1, which is a cell membrane transporter protein [118]. Accordingly, increased drug efflux through the transporter leads to drug resistance [119]. Buthionine sulfoximine-mediated autophagy can also negatively affect drug sensitivity.

Cisplatin was shown to significantly induce expression of the well-known tumor suppressor TP53 as well as proapoptotic genes such as TNF, BAX, CASP3, and FAS, while decreasing antiapoptotic BCL2 and XIAP expression. Consistently, cell processes including apoptosis, ROS generation, DNA damage, and mitochondrial damage were found to be significantly induced by cisplatin treatment. Diseases effectively targeted by cisplatin were predicted to be ovarian, lung, gastric, and breast cancer. However, cisplatin-induced proinflammatory cytokines IL1B, IL6, and TNF are at risk of causing side effects such as acute kidney injury and renal dysfunction. Cisplatin also plays important roles in drug resistance by inducing autophagy and activating NFE2L2 and ABCC1, which elevate drug efflux.

Doxorubicin was shown to have similar effects to cisplatin on targeted genes and cell processes. It also significantly increases TP53, BAX, TNF, CASP3, and FAS expression and decreases BCL2 and XIAP expression, promoting apoptosis. Oxidative stress, DNA damage, and lipid peroxidation

were suggested to be doxorubicin-mediated cell processes. Doxorubicin is mainly used to treat breast, ovarian, and lung cancer as well as lymphoma, but there is a risk of heart failure and neurotoxicity. Drug resistance in doxorubicin was predicted to be attributable to increased autophagy and the upregulation of NFE2L2 and ABCC1.

Imexon was found to positively regulate the activity of CASP3 and CASP9 which have critical roles in apoptosis. Oxidative stress and cell cycle arrest can be stimulated by imexon, which was predicted to have therapeutic effects on multiple myeloma and splenomegaly.

Motexafin gadolinium was shown to inhibit the activity of TXN and HMOX1, leading to apoptosis. It was suggested to exhibit anticancer effects by promoting ROS generation and oxidative stress and by disrupting the DNA repair process. Motexafin gadolinium was expected to target diseases including lung cancer and cerebral neoplasm.

5. Conclusions

Redox homeostasis plays an essential role in maintaining diverse cellular processes [120]. The disruption of redox homeostasis is being actively investigated in the field of chemotherapy since cancer cells can be effectively killed by accelerating their oxidative stress state. In this review, we presented an overview of ROS-inducing anticancer therapy and the anticancer strategy using prooxidative agents in terms of direct and indirect ROS accumulation. For a comprehensive understanding of biological network of prooxidant drugs and molecular targets, our pathway analysis highlighted the crucial effects of each anticancer drug on genes, cell processes, and diseases related to ROS generation and antioxidant inhibition. Our explanation of changes in biological processes relevant to specific drugs and potential side effects would be meaningful for better understanding of the toxicological aspects as well as for predicting the efficacy of chemotherapies using prooxidative anticancer drugs with undetectable side effects. Although several previous studies have investigated the modes of action for prooxidant drugs, pharmacogenomic studies evaluating the drug treatments are still required to elucidate the exact anticancer mechanisms and potential molecular targets. Our review will help researchers better understand the current gene-targeting anticancer strategies involving prooxidative drugs in order to overcome their controversial side effects.

Conflicts of Interest

The authors declare no conflict of interest.

Acknowledgments

This work was supported by grants (2017001970001 and 2018001350006) from the Korean Ministry of Environment. Also, this work was supported by the Dongguk University Research Fund of 2019.

References

[1] K. Brieger, S. Schiavone, J. Miller, and K. H. Krause, "Reactive oxygen species: from health to disease," *Swiss Medical Weekly*, vol. 142, article w13659, 2012.

[2] D. Trachootham, J. Alexandre, and P. Huang, "Targeting cancer cells by ROS-mediated mechanisms: a radical therapeutic approach?," *Nature Reviews Drug Discovery*, vol. 8, no. 7, pp. 579–591, 2009.

[3] C. E. Cross, B. Halliwell, E. T. Borish et al., "Oxygen radicals and human disease," *Annals of Internal Medicine*, vol. 107, no. 4, pp. 526–545, 1987.

[4] A. Glasauer and N. S. Chandel, "Targeting antioxidants for cancer therapy," *Biochemical Pharmacology*, vol. 92, no. 1, pp. 90–101, 2014.

[5] S. C. Gupta, J. H. Kim, S. Prasad, and B. B. Aggarwal, "Regulation of survival, proliferation, invasion, angiogenesis, and metastasis of tumor cells through modulation of inflammatory pathways by nutraceuticals," *Cancer Metastasis Reviews*, vol. 29, no. 3, pp. 405–434, 2010.

[6] J. Wang and J. Yi, "Cancer cell killing via ROS: to increase or decrease, that is the question," *Cancer Biology & Therapy*, vol. 7, no. 12, pp. 1875–1884, 2008.

[7] P. Storz, "KRas, ROS and the initiation of pancreatic cancer," *Small GTPases*, vol. 8, no. 1, pp. 38–42, 2017.

[8] M. H. Raza, S. Siraj, A. Arshad et al., "ROS-modulated therapeutic approaches in cancer treatment," *Journal of Cancer Research and Clinical Oncology*, vol. 143, no. 9, pp. 1789–1809, 2017.

[9] C. Martin-Cordero, A. J. Leon-Gonzalez, J. M. Calderon-Montano, E. Burgos-Moron, and M. Lopez-Lazaro, "Pro-oxidant natural products as anticancer agents," *Current Drug Targets*, vol. 13, no. 8, pp. 1006–1028, 2012.

[10] K. J. Davies, "Oxidative stress: the paradox of aerobic life," *Biochemical Society Symposium*, vol. 61, pp. 1–31, 1995.

[11] H. Sies, "Oxidative stress: a concept in redox biology and medicine," *Redox Biology*, vol. 4, pp. 180–183, 2015.

[12] M. Valko, H. Morris, and M. T. Cronin, "Metals, toxicity and oxidative stress," *Current Medicinal Chemistry*, vol. 12, no. 10, pp. 1161–1208, 2005.

[13] Y. Liu, G. Fiskum, and D. Schubert, "Generation of reactive oxygen species by the mitochondrial electron transport chain," *Journal of Neurochemistry*, vol. 80, no. 5, pp. 780–787, 2002.

[14] J. L. Meitzler, S. Antony, Y. Wu et al., "NADPH oxidases: a perspective on reactive oxygen species production in tumor biology," *Antioxidants & Redox Signaling*, vol. 20, no. 17, pp. 2873–2889, 2014.

[15] S. Chen, X. F. Meng, and C. Zhang, "Role of NADPH oxidase-mediated reactive oxygen species in podocyte injury," *BioMed Research International*, vol. 2013, Article ID 839761, 7 pages, 2013.

[16] G. Minotti and S. D. Aust, "The requirement for iron (III) in the initiation of lipid peroxidation by iron (II) and hydrogen peroxide," *The Journal of Biological Chemistry*, vol. 262, no. 3, pp. 1098–1104, 1987.

[17] C. Nicco and F. Batteux, "ROS modulator molecules with therapeutic potential in cancers treatments," *Molecules*, vol. 23, no. 1, p. 84, 2017.

[18] R. Bigley, M. Riddle, D. Layman, and L. Stankova, "Human cell dehydroascorbate reductase. Kinetic and functional

properties," *Biochimica et Biophysica Acta (BBA) - Enzymology*, vol. 659, no. 1, pp. 15–22, 1981.

[19] J. Martensson and A. Meister, "Glutathione deficiency decreases tissue ascorbate levels in newborn rats: ascorbate spares glutathione and protects," *Proceedings of the National Academy of Sciences*, vol. 88, no. 11, pp. 4656–4660, 1991.

[20] F. J. Giblin, "Glutathione: a vital lens antioxidant," *Journal of Ocular Pharmacology and Therapeutics*, vol. 16, no. 2, pp. 121–135, 2000.

[21] D. P. Jones, "Redox potential of GSH/GSSG couple: assay and biological significance," *Methods in Enzymology*, vol. 348, pp. 93–112, 2002.

[22] G. M. Enns, T. Moore, A. le et al., "Degree of glutathione deficiency and redox imbalance depend on subtype of mitochondrial disease and clinical status," *PLoS One*, vol. 9, no. 6, article e100001, 2014.

[23] A. Pompella, A. Visvikis, A. Paolicchi, V. D. Tata, and A. F. Casini, "The changing faces of glutathione, a cellular protagonist," *Biochemical Pharmacology*, vol. 66, no. 8, pp. 1499–1503, 2003.

[24] Y. Chen, H. Dong, D. C. Thompson, H. G. Shertzer, D. W. Nebert, and V. Vasiliou, "Glutathione defense mechanism in liver injury: insights from animal models," *Food and Chemical Toxicology*, vol. 60, pp. 38–44, 2013.

[25] R. Xiao, J. Lundström-Ljung, A. Holmgren, and H. F. Gilbert, "Catalysis of thiol/disulfide exchange. Glutaredoxin 1 and protein-disulfide isomerase use different mechanisms to enhance oxidase and reductase activities," *The Journal of Biological Chemistry*, vol. 280, no. 22, pp. 21099–21106, 2005.

[26] R. Benfeitas, M. Uhlen, J. Nielsen, and A. Mardinoglu, "New challenges to study heterogeneity in cancer redox metabolism," *Frontiers in Cell and Development Biology*, vol. 5, p. 65, 2017.

[27] K. Aoyama and T. Nakaki, "Glutathione in cellular redox homeostasis: association with the excitatory amino acid carrier 1 (EAAC1)," *Molecules*, vol. 20, no. 5, pp. 8742–8758, 2015.

[28] H. Miki and Y. Funato, "Regulation of intracellular signalling through cysteine oxidation by reactive oxygen species," *Journal of Biochemistry*, vol. 151, no. 3, pp. 255–261, 2012.

[29] J. V. Bannister, W. H. Bannister, and G. Rotilio, "Aspects of the structure, function, and applications of superoxide Dismutas," *Critical Reviews in Biochemistry*, vol. 22, no. 2, pp. 111–180, 1987.

[30] I. N. Zelko, T. J. Mariani, and R. J. Folz, "Superoxide dismutase multigene family: a comparison of the CuZn-SOD (SOD1), Mn-SOD (SOD2), and EC-SOD (SOD3) gene structures, evolution, and expression," *Free Radical Biology & Medicine*, vol. 33, no. 3, pp. 337–349, 2002.

[31] P. Chelikani, I. Fita, and P. C. Loewen, "Diversity of structures and properties among catalases," *Cellular and Molecular Life Sciences*, vol. 61, no. 2, pp. 192–208, 2004.

[32] C. Nathan and A. Cunningham-Bussel, "Beyond oxidative stress: an immunologist's guide to reactive oxygen species," *Nature Reviews Immunology*, vol. 13, no. 5, pp. 349–361, 2013.

[33] X. Zhao and K. Drlica, "Reactive oxygen species and the bacterial response to lethal stress," *Current Opinion in Microbiology*, vol. 21, pp. 1–6, 2014.

[34] H. Sies, "Oxidative stress: oxidants and antioxidants," *Experimental Physiology*, vol. 82, no. 2, pp. 291–295, 1997.

[35] Y. Abiko, T. Miura, B. H. Phuc, Y. Shinkai, and Y. Kumagai, "Participation of covalent modification of Keap1 in the activation of Nrf2 by tert-butylbenzoquinone, an electrophilic metabolite of butylated hydroxyanisole," *Toxicology and Applied Pharmacology*, vol. 255, no. 1, pp. 32–39, 2011.

[36] A. Giudice and M. Montella, "Activation of the Nrf2-ARE signaling pathway: a promising strategy in cancer prevention," *BioEssays*, vol. 28, no. 2, pp. 169–181, 2006.

[37] M. Kieliszek and S. Blazejak, "Current knowledge on the importance of selenium in food for living organisms: a review," *Molecules*, vol. 21, no. 5, p. 609, 2016.

[38] H. W. Tan, H.-Y. Mo, A. Lau, and Y.-M. Xu, "Selenium species: current status and potentials in cancer prevention and therapy," *International Journal of Molecular Sciences*, vol. 20, no. 1, p. 75, 2018.

[39] R. Gopalakrishna, Z. H. Chen, and U. Gundimeda, "Selenocompounds induce a redox modulation of protein kinase C in the cell, compartmentally independent from cytosolic glutathione: its role in inhibition of tumor promotion," *Archives of Biochemistry and Biophysics*, vol. 348, no. 1, pp. 37–48, 1997.

[40] R. Gopalakrishna and S. Jaken, "Protein kinase C signaling and oxidative stress," *Free Radical Biology & Medicine*, vol. 28, no. 9, pp. 1349–1361, 2000.

[41] X. Bai, Y. Chen, X. Hou, M. Huang, and J. Jin, "Emerging role of NRF2 in chemoresistance by regulating drug-metabolizing enzymes and efflux transporters," *Drug Metabolism Reviews*, vol. 48, no. 4, pp. 541–567, 2016.

[42] J. H. No, Y. B. Kim, and Y. S. Song, "Targeting nrf2 signaling to combat chemoresistance," *Journal of Cancer Prevention*, vol. 19, no. 2, pp. 111–117, 2014.

[43] P. Telkoparan-Akillilar, S. Suzen, and L. Saso, "Pharmacological applications of Nrf2 inhibitors as potential antineoplastic drugs," *International Journal of Molecular Sciences*, vol. 20, no. 8, p. 2025, 2019.

[44] X. J. Wang, Z. Sun, N. F. Villeneuve et al., "Nrf2 enhances resistance of cancer cells to chemotherapeutic drugs, the dark side of Nrf2," *Carcinogenesis*, vol. 29, no. 6, pp. 1235–1243, 2008.

[45] N. Gharavi, S. Haggarty, and A. O. El-Kadi, "Chemoprotective and carcinogenic effects of tert-butylhydroquinone and its metabolites," *Current Drug Metabolism*, vol. 8, no. 1, pp. 1–7, 2007.

[46] Y. Li, A. Seacat, P. Kuppusamy, J. L. Zweier, J. D. Yager, and M. A. Trush, "Copper redox-dependent activation of 2-tert-butyl(1,4)hydroquinone: formation of reactive oxygen species and induction of oxidative DNA damage in isolated DNA and cultured rat hepatocytes," *Mutation Research*, vol. 518, no. 2, pp. 123–133, 2002.

[47] J. Brozmanova, D. Mániková, V. Vlčková, and M. Chovanec, "Selenium: a double-edged sword for defense and offence in cancer," *Archives of Toxicology*, vol. 84, no. 12, pp. 919–938, 2010.

[48] R. Muecke, L. Schomburg, J. Buentzel, K. Kisters, O. Micke, and German Working Group Trace Elements and Electrolytes in Oncology, "Selenium or no selenium-that is the question in tumor patients: a new controversy," *Integrative Cancer Therapies*, vol. 9, no. 2, pp. 136–141, 2010.

[49] K. R. Martin and J. C. Barrett, "Reactive oxygen species as double-edged swords in cellular processes: low-dose cell signaling versus high-dose toxicity," *Human & Experimental Toxicology*, vol. 21, no. 2, pp. 71–75, 2002.

[50] M. Schieber and N. S. Chandel, "ROS function in redox signaling and oxidative stress," *Current Biology*, vol. 24, no. 10, pp. R453–R462, 2014.

[51] E. L. Yarosz and C. H. Chang, "The role of reactive oxygen species in regulating T cell-mediated immunity and disease," *Immune Network*, vol. 18, no. 1, article e14, 2018.

[52] N. Aykin-Burns, I. M. Ahmad, Y. Zhu, L. W. Oberley, and D. R. Spitz, "Increased levels of superoxide and H2O2 mediate the differential susceptibility of cancer cells versus normal cells to glucose deprivation," *The Biochemical Journal*, vol. 418, no. 1, pp. 29–37, 2009.

[53] A. Singh, V. Misra, R. K. Thimmulappa et al., "Dysfunctional KEAP1-NRF2 interaction in non-small-cell lung cancer," *PLoS Medicine*, vol. 3, no. 10, article e420, 2006.

[54] J. Wang, B. Luo, X. Li et al., "Inhibition of cancer growth in vitro and in vivo by a novel ROS-modulating agent with ability to eliminate stem-like cancer cells," *Cell Death & Disease*, vol. 8, no. 6, article e2887, 2017.

[55] C. A. Neumann and Q. Fang, "Are peroxiredoxins tumor suppressors?," *Current Opinion in Pharmacology*, vol. 7, no. 4, pp. 375–380, 2007.

[56] P. Birner, M. Schindl, A. Obermair, C. Plank, G. Breitenecker, and G. Oberhuber, "Overexpression of hypoxia-inducible factor 1alpha is a marker for an unfavorable prognosis in early-stage invasive cervical cancer," *Cancer Research*, vol. 60, no. 17, pp. 4693–4696, 2000.

[57] J. C. Soria, S. J. Jang, F. R. Khuri et al., "Overexpression of cyclin B1 in early-stage non-small cell lung cancer and its clinical implication," *Cancer Research*, vol. 60, no. 15, pp. 4000–4004, 2000.

[58] K. J. Davies, "The broad spectrum of responses to oxidants in proliferating cells: a new paradigm for oxidative stress," *IUBMB Life*, vol. 48, no. 1, pp. 41–47, 1999.

[59] L. R. Prosnitz, I. S. Goldenberg, R. A. Packard et al., "Radiation therapy as initial treatment for early stage cancer of the breast without mastectomy," *Cancer*, vol. 39, 2 Suppl, pp. 917–923, 1977.

[60] R. Timmerman, R. Paulus, J. Galvin et al., "Stereotactic body radiation therapy for inoperable early stage lung cancer," *JAMA*, vol. 303, no. 11, pp. 1070–1076, 2010.

[61] M. Peiris-Pages, U. E. Martinez-Outschoorn, F. Sotgia, and M. P. Lisanti, "Metastasis and oxidative stress: are antioxidants a metabolic driver of progression?," *Cell Metabolism*, vol. 22, no. 6, pp. 956–958, 2015.

[62] E. Piskounova, M. Agathocleous, M. M. Murphy et al., "Oxidative stress inhibits distant metastasis by human melanoma cells," *Nature*, vol. 527, no. 7577, pp. 186–191, 2015.

[63] K. Le Gal, M. X. Ibrahim, C. Wiel et al., "Antioxidants can increase melanoma metastasis in mice," *Science Translational Medicine*, vol. 7, no. 308, article 308re8, 2015.

[64] R. Benfeitas, G. Bidkhori, B. Mukhopadhyay et al., "Characterization of heterogeneous redox responses in hepatocellular carcinoma patients using network analysis," *eBioMedicine*, vol. 40, pp. 471–487, 2019.

[65] Q. Kong and K. O. Lillehei, "Antioxidant inhibitors for cancer therapy," *Medical Hypotheses*, vol. 51, no. 5, pp. 405–409, 1998.

[66] T. Ozben, "Oxidative stress and apoptosis: impact on cancer therapy," *Journal of Pharmaceutical Sciences*, vol. 96, no. 9, pp. 2181–2196, 2007.

[67] C. Gorrini, I. S. Harris, and T. W. Mak, "Modulation of oxidative stress as an anticancer strategy," *Nature Reviews Drug Discovery*, vol. 12, no. 12, pp. 931–947, 2013.

[68] Z. Zou, H. Chang, H. Li, and S. Wang, "Induction of reactive oxygen species: an emerging approach for cancer therapy," *Apoptosis*, vol. 22, no. 11, pp. 1321–1335, 2017.

[69] D. Magda and R. A. Miller, "Motexafin gadolinium: a novel redox active drug for cancer therapy," *Seminars in Cancer Biology*, vol. 16, no. 6, pp. 466–476, 2006.

[70] O. Tacar, P. Sriamornsak, and C. R. Dass, "Doxorubicin: an update on anticancer molecular action, toxicity and novel drug delivery systems," *The Journal of Pharmacy and Pharmacology*, vol. 65, no. 2, pp. 157–170, 2013.

[71] G. T. Wondrak, "NQO1-activated phenothiazinium redox cyclers for the targeted bioreductive induction of cancer cell apoptosis," *Free Radical Biology & Medicine*, vol. 43, no. 2, pp. 178–190, 2007.

[72] D. Khuntia and M. Mehta, "Motexafin gadolinium: a clinical review of a novel radioenhancer for brain tumors," *Expert Review of Anticancer Therapy*, vol. 4, no. 6, pp. 981–989, 2004.

[73] M. P. Mehta, P. Rodrigus, C. H. Terhaard et al., "Survival and neurologic outcomes in a randomized trial of motexafin gadolinium and whole-brain radiation therapy in brain metastases," *Journal of Clinical Oncology*, vol. 21, no. 13, pp. 2529–2536, 2003.

[74] S. Kotamraju, C. R. Chitambar, S. V. Kalivendi, J. Joseph, and B. Kalyanaraman, "Transferrin receptor-dependent iron uptake is responsible for doxorubicin-mediated apoptosis in endothelial cells: role of oxidant-induced iron signaling in apoptosis," *The Journal of Biological Chemistry*, vol. 277, no. 19, pp. 17179–17187, 2002.

[75] Y. J. Kang, Y. Chen, and P. N. Epstein, "Suppression of doxorubicin cardiotoxicity by overexpression of catalase in the heart of transgenic mice," *The Journal of Biological Chemistry*, vol. 271, no. 21, pp. 12610–12616, 1996.

[76] R. Marullo, E. Werner, N. Degtyareva et al., "Cisplatin induces a mitochondrial-ROS response that contributes to cytotoxicity depending on mitochondrial redox status and bioenergetic functions," *PLoS One*, vol. 8, no. 11, article e81162, 2013.

[77] G. A. Omura and G. Gynecologic Oncology, "Progress in gynecologic cancer research: the Gynecologic Oncology Group experience," *Seminars in Oncology*, vol. 35, no. 5, pp. 507–521, 2008.

[78] S. Dasari and P. B. Tchounwou, "Cisplatin in cancer therapy: molecular mechanisms of action," *European Journal of Pharmacology*, vol. 740, pp. 364–378, 2014.

[79] C. W. Helm and J. C. States, "Enhancing the efficacy of cisplatin in ovarian cancer treatment - could arsenic have a role," *Journal of ovarian research*, vol. 2, no. 1, p. 2, 2009.

[80] T. Hagen, G. D'Amico, M. Quintero et al., "Inhibition of mitochondrial respiration by the anticancer agent 2-methoxyestradiol," *Biochemical and Biophysical Research Communications*, vol. 322, no. 3, pp. 923–929, 2004.

[81] S. L. Mooberry, "Mechanism of action of 2-methoxyestradiol: new developments," *Drug Resistance Updates*, vol. 6, no. 6, pp. 355–361, 2003.

[82] M. Djavaheri-Mergny, J. Wietzerbin, and F. Besancon, "2-Methoxyestradiol induces apoptosis in Ewing sarcoma cells through mitochondrial hydrogen peroxide production," *Oncogene*, vol. 22, no. 17, pp. 2558–2567, 2003.

[83] R. Kachadourian, S. I. Liochev, D. E. Cabelli, M. N. Patel, I. Fridovich, and B. J. Day, "2-methoxyestradiol does not inhibit superoxide dismutase," *Archives of Biochemistry and Biophysics*, vol. 392, no. 2, pp. 349–353, 2001.

[84] P. Huang, L. Feng, E. A. Oldham, M. J. Keating, and W. Plunkett, "Superoxide dismutase as a target for the selective killing of cancer cells," *Nature*, vol. 407, no. 6802, pp. 390–395, 2000.

[85] N. J. Lakhani, M. A. Sarkar, J. Venitz, and W. D. Figg, "2-Methoxyestradiol, a promising anticancer agent," *Pharmacotherapy*, vol. 23, no. 2, pp. 165–172, 2003.

[86] T. Mukhopadhyay and J. A. Roth, "Superinduction of wild-type p 53 protein after 2-methoxyestradiol treatment of Ad5p53-transduced cells induces tumor cell apoptosis," *Oncogene*, vol. 17, no. 2, pp. 241–246, 1998.

[87] M. Cushman, H. M. He, J. A. Katzenellenbogen, C. M. Lin, and E. Hamel, "Synthesis, antitubulin and antimitotic activity, and cytotoxicity of analogs of 2-methoxyestradiol, an endogenous mammalian metabolite of estradiol that inhibits tubulin polymerization by binding to the colchicine binding site," *Journal of Medicinal Chemistry*, vol. 38, no. 12, pp. 2041–2049, 1995.

[88] M. Kataoka, G. Schumacher, R. J. Cristiano, E. N. Atkinson, J. A. Roth, and T. Mukhopadhyay, "An agent that increases tumor suppressor transgene product coupled with systemic transgene delivery inhibits growth of metastatic lung cancer in vivo," *Cancer Research*, vol. 58, no. 21, pp. 4761–4765, 1998.

[89] T. H. Lippert, H. Adlercreutz, M. R. Berger, H. Seeger, W. Elger, and A. O. Mueck, "Effect of 2-methoxyestradiol on the growth of methyl-nitroso-urea (MNU)-induced rat mammary carcinoma," *The Journal of Steroid Biochemistry and Molecular Biology*, vol. 84, no. 1, pp. 51–56, 2003.

[90] A. O. Mueck and H. Seeger, "2-Methoxyestradiol—biology and mechanism of action," *Steroids*, vol. 75, no. 10, pp. 625–631, 2010.

[91] D. Francis, G. M. Richards, A. Forouzannia, M. P. Mehta, and D. Khuntia, "Motexafin gadolinium: a novel radiosensitizer for brain tumors," *Expert Opinion on Pharmacotherapy*, vol. 10, no. 13, pp. 2171–2180, 2009.

[92] J. G. Blanco, C. L. Sun, W. Landier et al., "Anthracycline-related cardiomyopathy after childhood cancer: role of polymorphisms in carbonyl reductase genes—a report from the Children's Oncology Group," *Journal of Clinical Oncology*, vol. 30, no. 13, pp. 1415–1421, 2012.

[93] E. J. Bowles, R. Wellman, H. S. Feigelson et al., "Risk of heart failure in breast cancer patients after anthracycline and trastuzumab treatment: a retrospective cohort study," *Journal of the National Cancer Institute*, vol. 104, no. 17, pp. 1293–1305, 2012.

[94] D. Cardinale, A. Colombo, G. Bacchiani et al., "Early detection of anthracycline cardiotoxicity and improvement with heart failure therapy," *Circulation*, vol. 131, no. 22, pp. 1981–1988, 2015.

[95] S. Waissbluth and S. J. Daniel, "Cisplatin-induced ototoxicity: transporters playing a role in cisplatin toxicity," *Hearing Research*, vol. 299, pp. 37–45, 2013.

[96] I. Ben Mosbah, Y. Mouchel, J. Pajaud et al., "Pretreatment with mangafodipir improves liver graft tolerance to ischemia/reperfusion injury in rat," *PLoS One*, vol. 7, no. 11, article e50235, 2012.

[97] S. Kono, G. R. Merriam, D. D. Brandon, D. L. Loriaux, and M. B. Lipsett, "Radioimmunoassay and metabolism of the catechol estrogen 2-hydroxyestradiol," *The Journal of Clinical Endocrinology and Metabolism*, vol. 54, no. 1, pp. 150–154, 1982.

[98] S. Kumari, A. K. Badana, M. M. G, S. G, and R. R. Malla, "Reactive oxygen species: a key constituent in cancer survival," *Biomarker Insights*, vol. 13, article 1177271918755391, 2018.

[99] Y. Chen, Y. Yang, M. L. Miller et al., "Hepatocyte-specific Gclc deletion leads to rapid onset of steatosis with mitochondrial injury and liver failure," *Hepatology*, vol. 45, no. 5, pp. 1118–1128, 2007.

[100] C. C. White, H. Viernes, C. M. Krejsa, D. Botta, and T. J. Kavanagh, "Fluorescence-based microtiter plate assay for glutamate-cysteine ligase activity," *Analytical Biochemistry*, vol. 318, no. 2, pp. 175–180, 2003.

[101] O. W. Griffith and A. Meister, "Potent and specific inhibition of glutathione synthesis by buthionine sulfoximine (S-n-butyl homocysteine sulfoximine)," *The Journal of Biological Chemistry*, vol. 254, no. 16, pp. 7558–7560, 1979.

[102] S. Moulder, N. Dhillon, C. Ng et al., "A phase I trial of imexon, a pro-oxidant, in combination with docetaxel for the treatment of patients with advanced breast, non-small cell lung and prostate cancer," *Investigational New Drugs*, vol. 28, no. 5, pp. 634–640, 2010.

[103] E. V. Sheveleva, T. H. Landowski, B. K. Samulitis, G. Bartholomeusz, G. Powis, and R. T. Dorr, "Imexon induces an oxidative endoplasmic reticulum stress response in pancreatic cancer cells," *Molecular Cancer Research*, vol. 10, no. 3, pp. 392–400, 2012.

[104] G. Abdelhamid and A. O. El-Kadi, "Buthionine sulfoximine, an inhibitor of glutathione biosynthesis, induces expression of soluble epoxide hydrolase and markers of cellular hypertrophy in a rat cardiomyoblast cell line: roles of the NF-κB and MAPK signaling pathways," *Free Radical Biology & Medicine*, vol. 82, pp. 1–12, 2015.

[105] K. Dvorakova, C. M. Payne, T. H. Landowski, M. E. Tome, D. S. Halperin, and R. T. Dorr, "Imexon activates an intrinsic apoptosis pathway in RPMI8226 myeloma cells," *Anti-Cancer Drugs*, vol. 13, no. 10, pp. 1031–1042, 2002.

[106] K. Dvorakova, C. M. Payne, M. E. Tome, M. M. Briehl, T. McClure, and R. T. Dorr, "Induction of oxidative stress and apoptosis in myeloma cells by the aziridine- containing agent imexon," *Biochemical Pharmacology*, vol. 60, no. 6, pp. 749–758, 2000.

[107] K. Dvorakova, C. N. Waltmire, C. M. Payne, M. E. Tome, M. M. Briehl, and R. T. Dorr, "Induction of mitochondrial changes in myeloma cells by imexon," *Blood*, vol. 97, no. 11, pp. 3544–3551, 2001.

[108] U. Kilic, E. Kilic, Z. Tuzcu et al., "Melatonin suppresses cisplatin-induced nephrotoxicity via activation of Nrf-2/HO-1 pathway," *Nutrition & Metabolism*, vol. 10, no. 1, p. 7, 2013.

[109] J. Fiedor and K. Burda, "Potential role of carotenoids as antioxidants in human health and disease," *Nutrients*, vol. 6, no. 2, pp. 466–488, 2014.

[110] K. Sak, "Cytotoxicity of dietary flavonoids on different human cancer types," *Pharmacognosy Reviews*, vol. 8, no. 16, pp. 122–146, 2014.

[111] Z. Tavsan and H. A. Kayali, "Flavonoids showed anticancer effects on the ovarian cancer cells: involvement of reactive oxygen species, apoptosis, cell cycle and invasion," *Biomedicine & Pharmacotherapy*, vol. 116, article 109004, 2019.

[112] J. L. Ricker, Z. Chen, X. P. Yang, V. S. Pribluda, G. M. Swartz, and C. van Waes, "2-Methoxyestradiol inhibits hypoxia-inducible factor 1alpha, tumor growth, and angiogenesis

and augments paclitaxel efficacy in head and neck squamous cell carcinoma," *Clinical Cancer Research*, vol. 10, no. 24, pp. 8665–8673, 2004.

[113] T. L. Yue, X. Wang, C. S. Louden et al., "2-Methoxyestradiol, an endogenous estrogen metabolite, induces apoptosis in endothelial cells and inhibits angiogenesis: possible role for stress-activated protein kinase signaling pathway and Fas expression," *Molecular Pharmacology*, vol. 51, no. 6, pp. 951–962, 1997.

[114] Y. J. Li, Y. H. Lei, N. Yao et al., "Autophagy and multidrug resistance in cancer," *Chinese Journal of Cancer*, vol. 36, no. 1, p. 52, 2017.

[115] J. J. Haddad, "L-Buthionine-(S,R)-sulfoximine, an irreversible inhibitor of gamma-glutamylcysteine synthetase, augments LPS-mediated pro-inflammatory cytokine biosynthesis: evidence for the implication of an IkappaB-alpha/NF-kappaB insensitive pathway," *European Cytokine Network*, vol. 12, no. 4, pp. 614–624, 2001.

[116] J. F. Ewing and M. D. Maines, "Glutathione depletion induces heme oxygenase-1 (HSP32) mRNA and protein in rat brain," *Journal of Neurochemistry*, vol. 60, no. 4, pp. 1512–1519, 1993.

[117] M. Khorsand, M. Akmali, S. Sharzad, and M. Beheshtitabar, "Melatonin reduces cataract formation and aldose reductase activity in lenses of streptozotocin-induced diabetic rat," *Iranian Journal of Medical Sciences*, vol. 41, no. 4, pp. 305–313, 2016.

[118] Y. Liu, Q. Li, L. Zhou et al., "Cancer drug resistance: redox resetting renders a way," *Oncotarget*, vol. 7, no. 27, pp. 42740–42761, 2016.

[119] C. Holohan, S. van Schaeybroeck, D. B. Longley, and P. G. Johnston, "Cancer drug resistance: an evolving paradigm," *Nature Reviews Cancer*, vol. 13, no. 10, pp. 714–726, 2013.

[120] A. Ayer, C. W. Gourlay, and I. W. Dawes, "Cellular redox homeostasis, reactive oxygen species and replicative ageing in Saccharomyces cerevisiae," *FEMS Yeast Research*, vol. 14, no. 1, pp. 60–72, 2014.

Hindawi
Oxidative Medicine and Cellular Longevity
Volume 2019, Article ID 3643715, 10 pages
https://doi.org/10.1155/2019/3643715

Research Article

The Antioxidant Alpha-Lipoic Acid Inhibits Proliferation and Invasion of Human Gastric Cancer Cells via Suppression of STAT3-Mediated MUC4 Gene Expression

Yu Yang,[1] Erhu Fang,[2] Jiajun Luo,[1] Hongxue Wu,[1] Yue Jiang,[1] Ying Liu,[1] Shilun Tong,[1] Zhihua Wang,[3] Rui Zhou,[4] and Qiang Tong[1]

[1]*Department of Gastrointestinal Surgery I Section, Renmin Hospital of Wuhan University, Wuhan 430060, China*
[2]*Department of Pediatric Surgery, Tongji Hospital, Tongji Medical College, Huazhong University of Science and Technology, Wuhan 430030, China*
[3]*Central Laboratory, Renmin Hospital of Wuhan University, Wuhan 430060, China*
[4]*Hubei Province Key Laboratory of Allergy and Immunology, School of Basic Medical Sciences, Wuhan University, Wuhan 430071, China*

Correspondence should be addressed to Qiang Tong; qiangtong@whu.edu.cn

Received 26 August 2019; Revised 6 November 2019; Accepted 26 November 2019; Published 13 December 2019

Guest Editor: Kanhaiya Singh

Background. Metastasis and invasion are the main causes of mortality in gastric cancer. To improve the treatment of gastric cancer, the development of effective and innovative antitumor agents toward invasion and proliferation is needed. Alpha-lipoic acid (ALA), a naturally occurring thiol antioxidant, showed antiproliferative and cytotoxic effects on several cancers. So it is feasible to explore whether ALA can be used to inhibit proliferation and invasion in human gastric cancer. *Methods*. The expression of MUC4 in human gastric cancer tissues was assayed by immunohistochemistry. Then, we performed *in vitro* cell proliferation and invasion analysis to explore the antitumor effect of ALA using AGS, BGC-823, and MKN-28 cells. To further explore the mechanism of ALA-mediated downregulation of MUC4, we cotransfected human gastric cancer cells with STAT3 siRNA and STAT3 overexpression construct. ChIP assays were carried out to find the relationship between MUC4 and STAT3. *Results*. We found that the MUC4 gene was strongly expressed in human gastric cancer tissues. Meanwhile, ALA reduced proliferation and invasion of human gastric cancer cells by suppressing MUC4 expression. We also found that STAT3 was involved in the inhibition of MUC4 by ALA. Mechanistically, ALA suppressed MUC4 expression by inhibiting STAT3 binding to the MUC4 promoter region. *Conclusion*. ALA inhibits both proliferation and invasion of gastric cancer cells by suppression of STAT3-mediated MUC4 gene expression.

1. Introduction

Gastric cancer is the fifth most common cancer throughout the world, and it is the third leading cause of mortality related to cancer [1]. Most gastric cancer patients have had adjacent organs or distant metastasis, which is the main cause of death in gastric cancer patients. Although there has been great progress in gastric cancer treatment in the clinic, the outcomes of gastric cancer patients are still not satisfied [2]. Thus, it is necessary to find effective and innovative antitumor agents which can inhibit proliferation and invasion of gastric cancer.

The stability of redox plays a vital role in the normal growth of cells. However, there is continuous and abundant production of reactive oxygen species (ROS) in tumor cells, which promote tumor growth by causing DNA damage and reprogramming cell metabolism [3]. The overproduction of ROS without proper management is called oxidative stress. Alpha-lipoic acid (ALA) is a coenzyme of pyruvate dehydrogenase and glycine decarboxylase synthesized in mitochondria

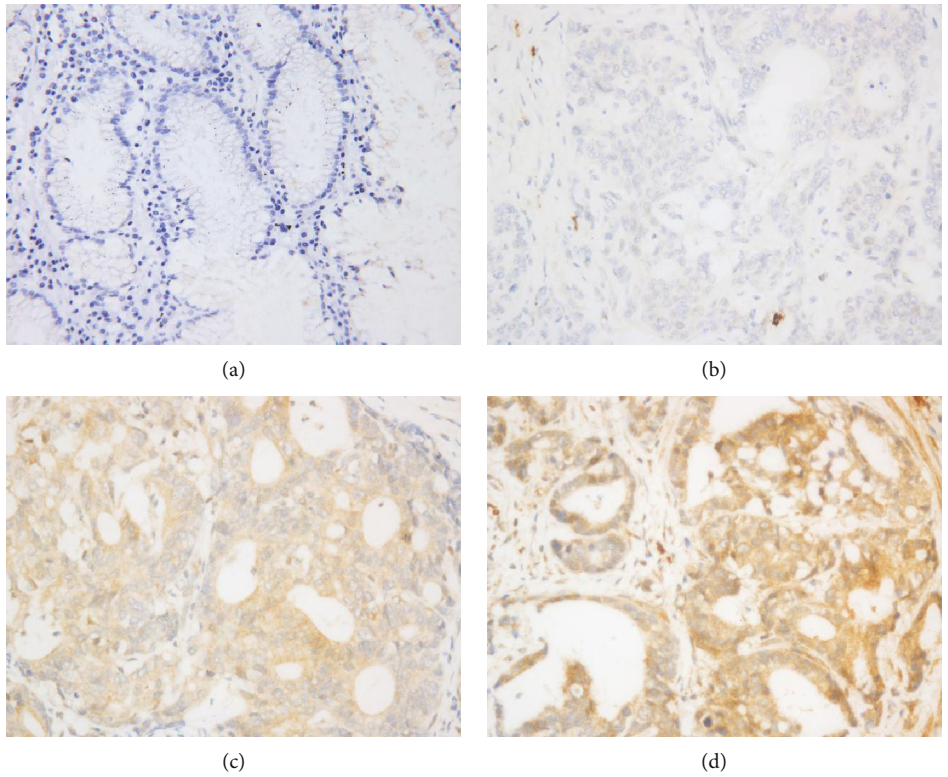

Figure 1: Expression of MUC4 in human gastric tissues. (a) Negative expression of MUC4 in normal gastric samples located away from cancer (400x). (b–d) Low, modest, and high expression of MUC4 in gastric cancer cells, respectively (400x).

[4]. As a powerful antioxidant, ALA can not only clear the excessive ROS directly but also regenerate endogenous antioxidants such as vitamin C, vitamin E, coenzyme Q10, glutathione, and ALA itself [5]. ALA affects the process of free radical scavenging in cells, such as increasing glutathione synthesis and regulating activity of transcription factors [6]. Nowadays, ALA is widely used in the clinical treatment of diseases associated with excessive oxidative stress, such as diabetic peripheral neuropathy [7]. In recent years, ALA has been used as an anticancer agent in experimental studies of different cancers and achieved satisfying results [8, 9]. However, the underlying molecular mechanism is still unclear.

Mucins are high-molecular-weight glycoproteins, which can maintain integrity and lubricate and protect surfaces of epithelia [10]. To date, at least eighteen different mucin genes have been identified [11]. Mucin 4 (MUC4) is membrane-bound mucin, which is expressed in normal gastric mucosa and gastric cancer [12]. Recent research demonstrated that MUC4 is involved in the oncogenesis, differentiation, proliferation, invasion, and migration of tumors and can be used as a reference indicator for the evaluation of some tumor conditions. It has been reported that activator protein- (AP-) 2α inhibits MUC4 expression which in turn suppresses proliferation and invasion of pancreatic cancer cells [13]. Besides, the expression of MUC4 is mediated through upregulation of signal transducer and activator of transcription (STAT) in pancreatic cancer and gastric cancer [10, 14].

Table 1: The expression of MUC4 in the gastric cancer tissues and normal gastric tissues.

Groups	n	MUC4 expression		p
		Negative	Positive	
Gastric cancer tissues	240	56	184	<0.001
Normal gastric tissues	240	160	80	

The current study was carried out to identify the effects of ALA on human gastric cancer progression. We found that MUC4 was upregulated in gastric cancer compared to normal tissues. ALA decreased STAT3 binding to MUC4 promoter region, repressed MUC4 expression, and consequently inhibited proliferation and invasion of human gastric cancer cells. Our data provide an in-depth mechanism by which ALA inhibits proliferation and invasion of gastric cancer cells, which validates the clinical use of ALA as a potential agent to enhance treatment outcomes in gastric cancer patients.

2. Materials and Methods

2.1. Patients and Samples. A total of 240 patients were diagnosed with gastric adenocarcinoma and underwent radical gastrectomy at Renmin Hospital of Wuhan University from June 2014 to July 2015. None of them received either preoperative chemotherapy or radiotherapy. Preoperative written consent was obtained from each patient. Primary lesion and

corresponding noncancerous tissues were kept during operation and then were embedded in paraffin for immunohistochemistry. The depth of invasion was observed by the surgeon during the operation. Lymph node metastasis was observed by pathological examination. Distant metastasis was confirmed according to imageology such as computed tomography and positron emission tomography. All patients were followed up until August 2018, with a total of 12 cases (5% patients) lost in follow-up period. This study was approved by the Ethics Committee of Renmin Hospital of Wuhan University.

2.2. Cell Culture and Reagents. Human gastric cancer cell lines are as follows: AGS, BGC-823, and MKN-28 cells. AGS cell line was purchased from American Type Culture Collection (ATCC, Manassas, USA); BGC-823 and MKN-28 cell lines were gifts from Tongji Medical College, Huazhong University of Science and Technology (Wuhan, China). The cells were cultured in Roswell Park Memorial Institute- (RPMI-) 1640 medium supplemented with 10% fetal bovine serum (FBS). Cells were maintained in a 37°C incubator with 5% CO_2. All cell lines tested negative for mycoplasma. Alpha-lipoic acid and TNF-α were purchased from Solarbio (Beijing, China). Anti-MUC4 antibody, anti-STAT3 antibody, and specific primary antibody were purchased from Sigma-Aldrich.

2.3. Immunohistochemistry. Paraffin-embedded tissue samples were cut into 4 μm thick sections and mounted on poly-L-lysine-coated slides. Samples were dewaxed in xylene and rehydrated using a graded series of ethanol solutions. After deparaffinization, endogenous peroxidase activity was blocked by incubation in a 3% peroxide-methanol solution at room temperature (RT) for 10 min, and then, antigen retrieval was performed at 100°C in an autoclave for 7 min. Samples were then incubated at RT for 30 min. Afterward, sections were washed with phosphate-buffered saline (PBS) 3 times, 5 min each time. They were then incubated with rabbit anti-MUC4 antibody (Sigma-Aldrich, USA). Thoroughly washing with PBS was then performed, and primary antibody binding was visualized under a microscope.

2.4. Cell Transfection. Cells were plated in 6-well plates with RPMI-1640 medium supplemented with 10% medium FBS for 24 h before transfection. Transfections were performed using siRNAs and Lipofectamine RNAiMAX (Thermo Fisher) transfection reagent diluted in RPMI-1640 medium. Indicated plasmids were transfected using Lipofectamine 2000 (Thermo Fisher) according to the manufacturer's instruction.

2.5. Quantitative Real-Time PCR (qRT-PCR). The total RNA was extracted from tissues using TRIzol Reagent (Thermo Fisher, USA) according to the manufacturer's instructions. Then, RNA was reverse transcribed to cDNA with 1 μg total RNA, using reverse transcriptase and Oligo dT primers (Takara, Japan). The cDNA was then amplified with specific primers by PCR. The primers used for PCR were listed below. The conditions for qRT-PCR were as follows: 95°C for 3 min, followed by 40 cycles of 10 s at 95°C,10 s at 60°C, and 15 s at 70°C, followed by heating from 65°C to 95°C. Primers for qRT-PCR are listed as follows: MUC4 forward primer 5′-CTTCAGATGCGATGGCTACA-3′ and reverse primer 5′-GTTTCATGCTCAGGTGCTCA-3′, STAT3 forward primer 5′-GGCCATCTTGAGCACTAAGC-3′ and reverse primer 5′-CGGACTGGATCTGGGTCTTA-3′, 18S rRNA forward primer 5′-CGGCTACATCCAAGGAA-3′ and reverse primer 5′-GCTGGAATTACCGCGGCT-3′.

Table 2: Correlations between MUC4 expression and clinicpathologic factors.

Characteristics	n	MUC4 expression		p
		Negative	Positive	
Age				
≥65	112	9	103	<0.001
<65	128	47	81	
Gender				
Male	159	42	117	0.114
Female	81	14	67	
Tumor size				
≥5 cm	144	28	116	0.081
<5 cm	96	28	68	
Tumor location				
Upper	25	10	15	†0.103
Middle	87	29	58	‡0.144
Lower	128	31	97	††0.071
Depth of invasion				
T1+T2	102	36	66	<0.001
T3+T4	138	20	118	
TNM stage				
I+II	110	40	70	<0.001
III+IV	130	16	114	
Lymph node metastasis				
Present	134	20	114	0.001
Absent	106	36	70	
Distant metastasis				
Present	34	25	9	<0.001
Absent	206	31	175	

Note: †upper *vs.* lower; ‡middle *vs.* lower; ††upper and middle *vs.* lower.

2.6. Western Blotting. Total protein was extracted from cells and its concentration was measured by BCA Protein Assay Kit (Solarbio, China). The protein samples were separated by SDS-PAGE and transferred to polyvinylidene fluoride (PVDF) membranes. After blocking, the membranes were incubated with specific primary antibodies overnight at 4°C and secondary antibody for 1 h at room temperature. Protein expression levels were normalized to β-actin. Densitometric scanning (Bio-Rad) was used to determine relative protein band intensity.

2.7. MTT. Cells were digested into a single cell suspension and were seeded into a 96-well plate at 5000 cells per well

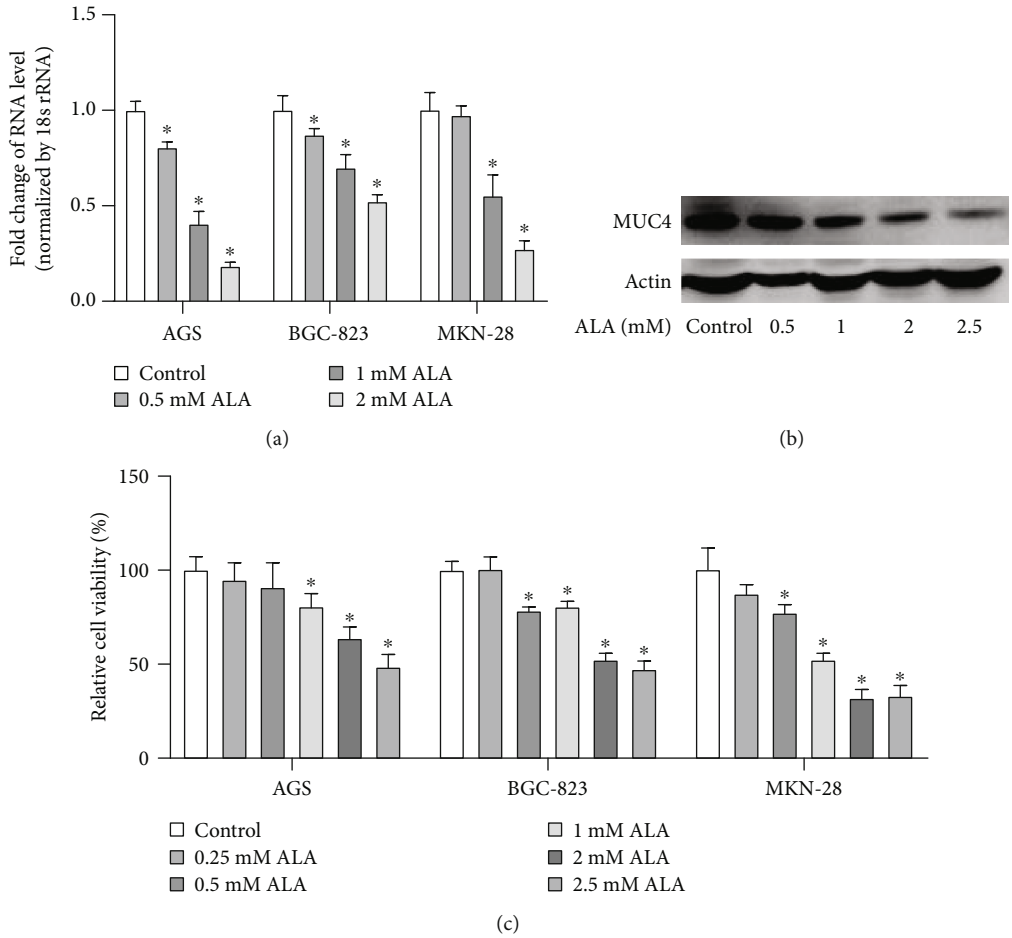

Figure 2: Alpha-lipoic acid inhibits the expression of endogenous MUC4 in human gastric cancer cells. (a) When cell confluence was 60%, AGS, BGC-823, and MKN-28 cells were incubated with 0, 0.5, 1, or 2 mM ALA for 24 h in RPMI with 10% FBS. After incubation, MUC4 mRNA in the cell lysates was examined by RT-PCR. (b) AGS cells were incubated with 0, 0.5, 1, 2, or 2.5 mM ALA for 24 h in RPMI with 10% FBS. Then, MUC4 protein was tested by western blotting. (c) AGS, BGC-823, and MKN-28 cells were incubated with 0, 0.25, 0.5, 1, 2, or 2.5 mM ALA for 24 h, and then, the viability was tested by the MTT method. Data represent mean ± SD from 3 independent experiments. $^*p < 0.05$ compared to the control group.

in 200 μL. After coincubating with indicated concentration of ALA for 24 h, MTT solution (5 mg/mL, prepared with PBS, pH = 7.4, Solarbio, China) was added into the medium at 10 μL per well. Cells were incubated for another 4 h, then the culture was terminated, and the supernatant was carefully absorbed and discarded. 100 μL DMSO was added to each well and oscillated for 10 min to fully melt the crystallites. The wavelength of 490 nm was selected to determine the absorbance of each well.

2.8. Matrigel Invasion Assay. The cell invasion assay was performed using the BioCoat™ Matrigel apparatus (Corning Inc., USA), with RPMI-1640 medium supplemented with 10% medium FBS as the chemoattractant in the lower chamber. AGS cells (10^5) in 300 μL were added to the upper chamber, with or without addition of ALA or anti-MUC4, to invade the Matrigel for 24 h. Noninvading cells on the upper surface were removed, and invading cells on the lower surface were stained with the Diff-Quick stain kit (Solarbio, China). The number of invasion cells was counted by a phase contrast microscope.

2.9. Chromatin Immunoprecipitation. The chromatin immunoprecipitation assay (ChIP) kit was purchased from Abcam, United Kingdom. Briefly, AGS (6.0×10^6) cells were fixed with 1% of formaldehyde. Genomic DNA was sheared to lengths ranging from 200 to 1000 bp with a Sonic Dismembrator (Fisher Scientific): Ampl 80%, 3 seconds on, 10 seconds off, for 10 cycles. One percent of the cell extract was taken as "input," and the rest of the extract was incubated with anti-STAT3 or control IgG overnight at 4°C, followed by precipitation with protein A agarose beads. The immunoprecipitates were sequentially washed with a low salt buffer, a high salt buffer, a LiCl buffer, and with TE buffer. The DNA-protein complex was eluted and proteins were then digested with proteinase K. The DNA was detected by qRT-PCR analysis, and the data obtained by qRT-PCR for specific antibody were normalized to IgG

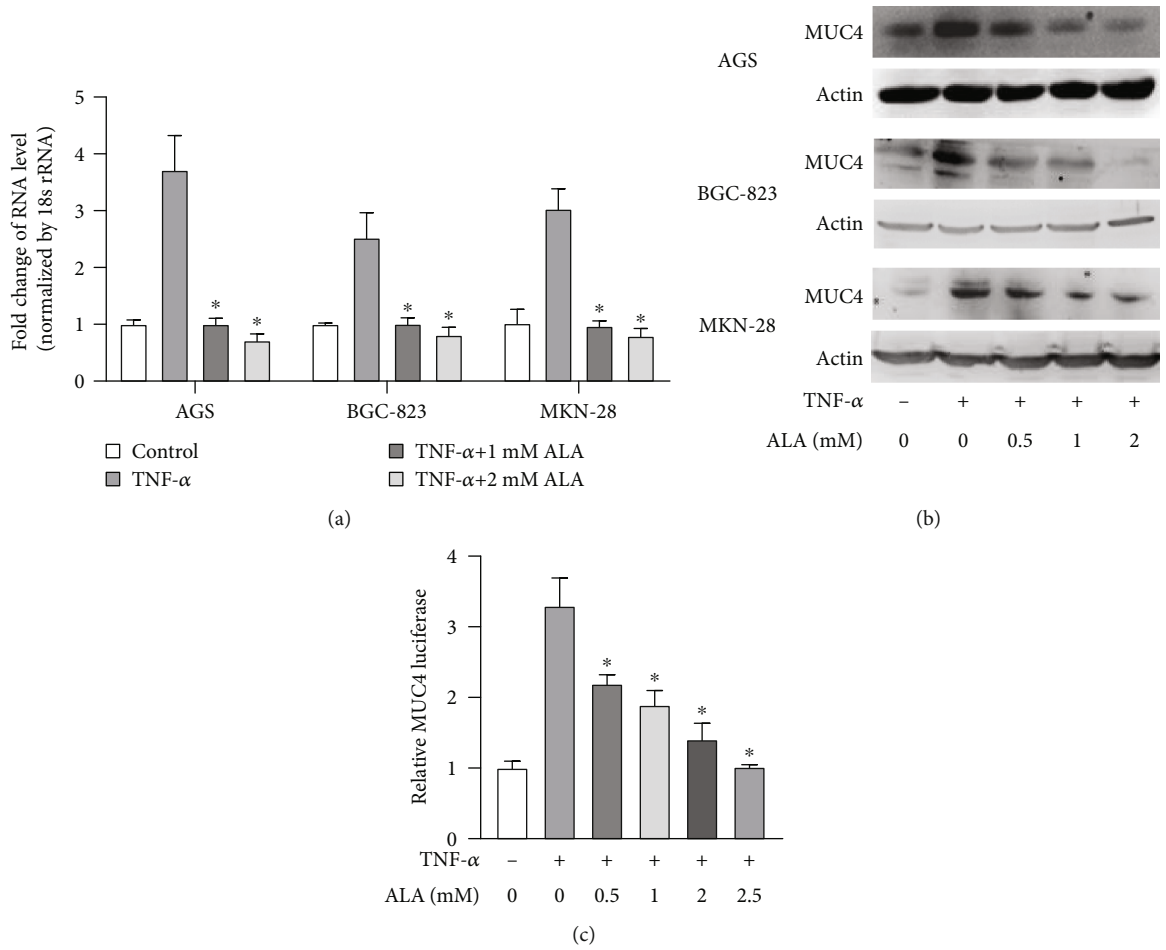

Figure 3: Alpha-lipoic acid inhibits TNF-α-induced MUC4 in gastric cancer cell lines. (a) AGS, BGC-823, and MKN-28 cells pretreated with the indicated concentrations of ALA for 24 h were treated with 20 ng/mL TNF-α for 4 h. After TNF-α treatment, RT-PCR was performed to analyze the MUC4 mRNA. (b) AGS, BGC-823, and MKN-28 cells pretreated with 0, 0.5, 1, or 2 mM ALA for 24 h in RPMI with 10% FBS were treated with or without 20 ng/mL TNF-α. And then, western blotting was performed to analyze the expression of MUC4 at protein levels. (c) The pGL3-MUC4 promoter construct-transfected AGS cells were pretreated with the indicated concentrations of ALA for 24 h, then incubated with 20 ng/mL TNF-α for 4 h and luciferase activity was determined using a luminometer. Data represent mean ± SD from 3 independent experiments. $^*p < 0.05$ compared to only TNF-α treatment group.

control and plotted as percent input. qRT-PCR was performed using two different sets of primers: Primer set 1: 5′-TCATAC AGCCCCAAGGTCGC-3′ (sense) and 5′-TAGCCGGGTTC CTGGGTCC-3′ (antisense), corresponding to the MUC4 promoter region 3251–3373 (NCBI sequence, accession number AF241535), and Primer set 2: 5′-GAAAAGGGTGATTA GCGTGG-3′ (sense) and 5′-TCCCCTCAGGCGGCTG GCC-3′ (antisense), corresponding to the 3528–3632 region of MUC4 promoter.

2.10. Statistical Analysis. Statistical differences were determined by two-tailed t-test in two-group comparisons. The correlation between MUC4 and tumor clinicopathologic characteristics was analyzed by the chi-square test. $p < 0.05$ was considered statistically significant. IBM SPSS Statistics version 21.0 and GraphPad Prism version 7.0 were used to analyze data.

3. Results

3.1. MUC4 Gene Was Strongly Expressed in Human Gastric Cancer Tissues. To identify the expression of MUC4 in human gastric cancer and normal gastric tissues, we performed immunohistochemistry staining on normal gastric samples located away from cancer ($n = 240$) and gastric cancer ($n = 240$), respectively. As shown in Figure 1, the expression of MUC4 in normal gastric samples was negative (Figure 1(a)), and the expression of MUC4 in gastric cancer was positive by contrast (Figures 1(b)–1(d)). As shown in Table 1, the expression of MUC4 showed positive in 184 out of 240 gastric cancer tissues, while the expression of MUC4 showed positive in 80 out of 240 normal gastric tissues. These results thus demonstrated that MUC4 is significantly upregulated in human gastric cancer tissues compared with normal gastric tissues (Table 1, $p < 0.001$). Additionally, chi-squared tests demonstrated significant

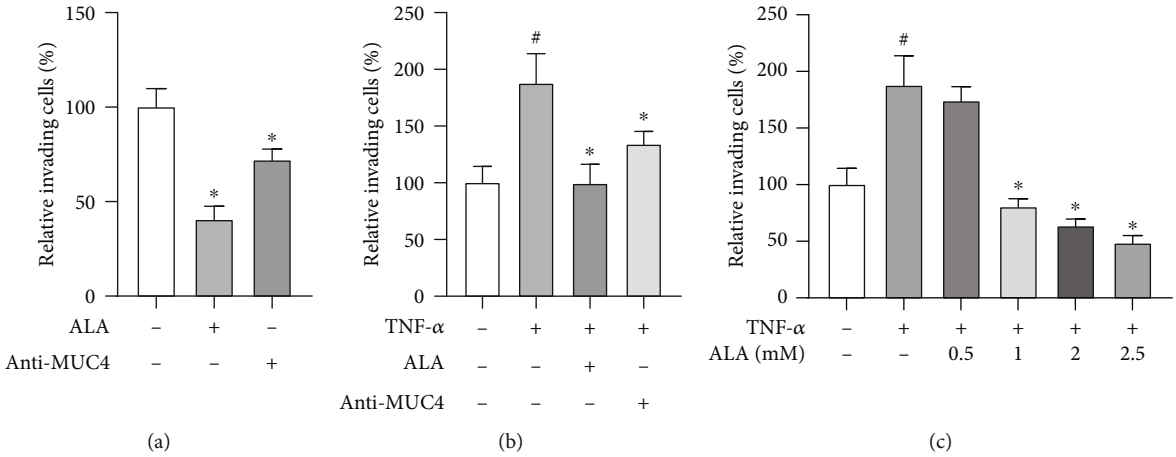

Figure 4: Alpha-lipoic acid inhibits invasion of AGS cells by suppressing MUC4 expression. (a) AGS cells were incubated with either 2 mM ALA or 200 ng/mL MUC4 antibody in a BioCoat™ Matrigel apparatus with 8 μM pore membrane for 24 h. (b) AGS cells were incubated with 20 ng/mL TNF-α in the presence or absence of 2 mM ALA or 200 ng/mL MUC4 antibody in a BioCoat™ Matrigel apparatus for 24 h. (c) AGS cells were incubated with 20 ng/mL TNF-α in the presence of 0-2.5 mM alpha-lipoic acid or 200 ng/mL MUC4 antibody. After incubation, the cells that invaded the lower surface of the chambers were counted using a phase contrast light microscope after staining with a Diff-Quick Stain kit. Data represent the mean ± SD from 3 independent experiments. $^{\#}p < 0.05$ versus control; $^{*}p < 0.05$ versus TNF-α only.

correlations between the expression of MUC4 and age, depth of invasion, TNM stage, lymph node metastasis, and distant metastasis (Table 2).

3.2. Alpha-Lipoic Acid Significantly Inhibits Endogenous MUC4 Expression in Human Gastric Cancer Cells. To identify the effect of ALA on the endogenous expression of MUC4 in human gastric cancer cells, we incubated AGS, BGC-823, and MKN-28 cells with 0, 0.5, 1, or 2 mM ALA for 24 h in RPMI with 10% FBS when cell confluence was 60%. MUC4 mRNA in the cell lysates was examined by RT-PCR. As shown in Figure 2(a), ALA significantly inhibited the endogenous MUC4 expression in gastric cancer cells in a dose-dependent manner. Complementarily, AGS cells were incubated with 0, 0.5, 1, 2, or 2.5 mM ALA for 24 h in RPMI with 10% FBS, then MUC4 protein was measured by western blotting. As shown in Figure 2(b), ALA significantly inhibited the expression of endogenous MUC4 in AGS cells. We next sought to examine the effect of ALA on the viability of human gastric cancer cells; for this, AGS, BGC-823, and MKN-28 cells were incubated with 0, 0.25, 0.5, 1, 2, or 2.5 mM ALA for 24 h followed by MTT assay. As shown in Figure 2(c), significant decreases of cancer cell viability were detected in cells treated with 1, 2, and 2.5 mM ALA.

3.3. Alpha-Lipoic Acid Inhibits TNF-α-Induced MUC4 in Gastric Cancer Cells. We sought to determine whether ALA can suppress TNF-α-induced MUC4 in human gastric cancer; to this end, we pretreated AGS, BGC-823, and MKN-28 cells with the indicated concentrations of ALA for 24 h followed by exposure of the cells with 20 ng/mL TNF-α for 4 h. After TNF-α treatment, RT-PCR was performed to analyze the MUC4 mRNA. As shown in Figure 3(a), TNF-α significantly induced MUC4 expression, and pretreatment of ALA significantly inhibited TNF-α-induced expression of MUC4 in gastric cancer cells. Complementarily, AGS, BGC-823, and MKN-28 cells pretreated with 0, 0.5, 1, or 2 mM ALA for 24 h in RPMI with 10% FBS were treated with or without 20 ng/mL TNF-α. And then, western blotting showed that the expression of MUC4 was significantly decreased in the presence of ALA (Figure 3(b)). In addition, the pGL3-MUC4 promoter construct-transfected AGS cells were pretreated with the indicated concentrations of ALA for 24 h, then incubated with 20 ng/mL TNF-α for 4 h. Luciferase activity was determined using a luminometer. As shown in Figure 3(c), the relative MUC4 luciferase activity was significantly decreased in cells treated with ALA at higher concentrations. Taken together, ALA inhibits TNF-α-induced MUC4 in gastric cancer cells.

3.4. Alpha-Lipoic Acid Inhibits AGS Cell Invasion by Suppressing MUC4 Expression. We then tested whether ALA suppressed invasion of the gastric cancer cells. Matrigel invasion assay showed that the number of relative invading cells was significantly decreased in the ALA-treated group compared with the control group and anti-MUC4 showed a similar effect (Figure 4(a)). Interestingly, the effect can also be observed after TNF-α treatment (Figure 4(b)). In addition, the higher the concentration of ALA, the fewer number of relative invading cells was observed (Figure 4(c)).

3.5. STAT3 Is Involved in the Inhibition of MUC4 by Alpha-Lipoic Acid. It has been reported that STAT3 plays a role in human gastric cancer development. To identify whether STAT3 is involved in inhibition of MUC4 by ALA in gastric cancer cells, the STAT3 siRNA was cotransfected with pGL3-MUC4 promoter construct into AGS cells pretreated with 2 mM ALA. After incubation with 20 ng/mL TNF-α for 4 h, the luciferase was determined using a luminometer. The relative MUC4 luciferase activity was significantly decreased in STAT3-transfected AGS cells compared to the control group (Figure 5(a)). Complementarily, STAT3 overexpression construct was cotransfected with a pGL3-MUC4 promoter construct into AGS cells. The transfected cells pretreated

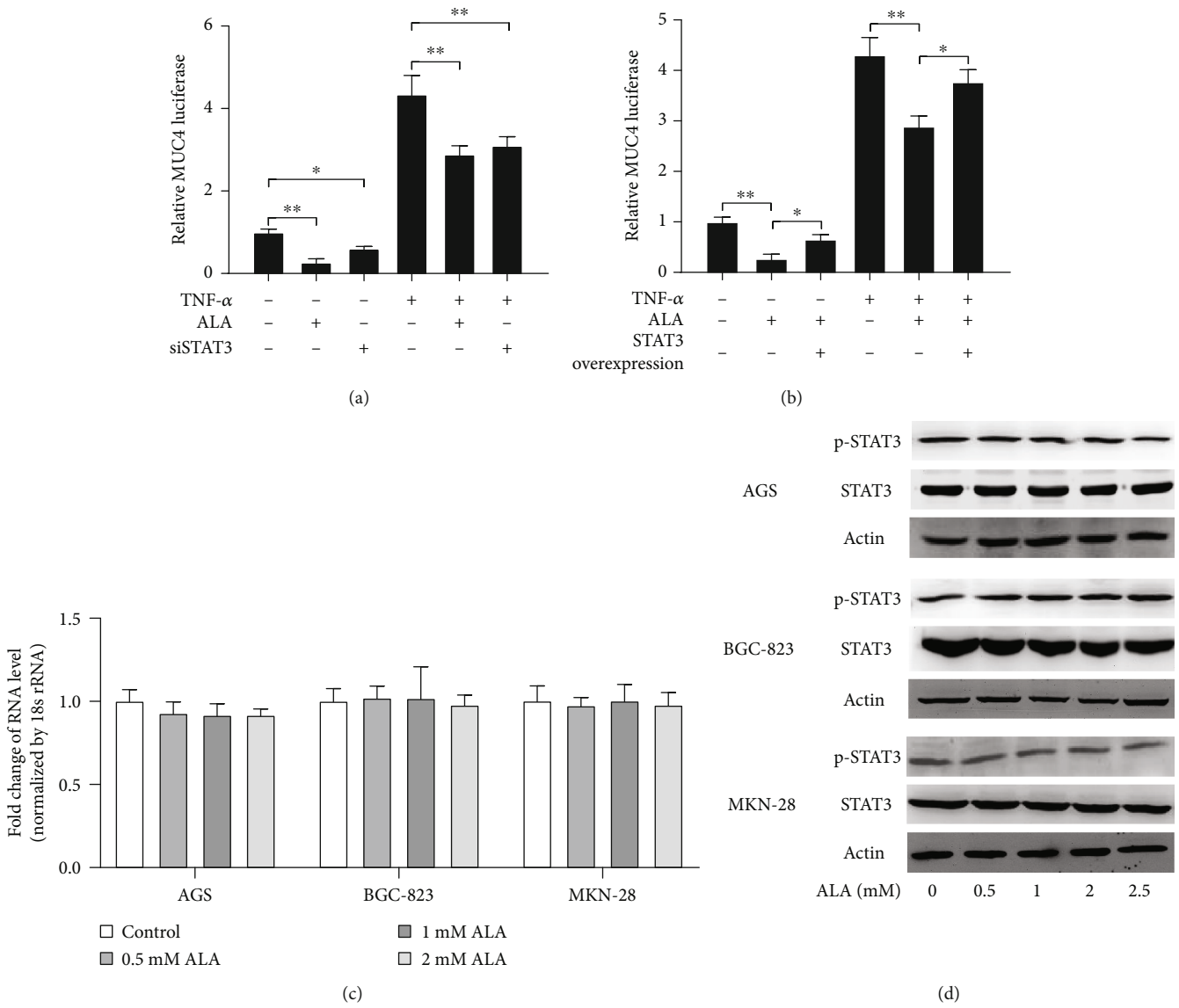

Figure 5: The role of STAT3 in the inhibition of MUC4 by alpha-lipoic acid in gastric cancer cells. (a) The STAT3 siRNA was cotransfected with pGL3-MUC4 promoter construct into AGS cells pretreated with 2 mM ALA. After incubation with 20 ng/mL TNF-α for 4 h, luciferase activity was determined using a luminometer. (b) STAT3 overexpression construct was cotransfected with a pGL3-MUC4 promoter construct into AGS cells. The transfected cells pretreated with or without 2 mM ALA were incubated with 20 ng/mL TNF-α for 4 h, and then, MUC4 luciferase activity was determined using a luminometer. (c) When cell confluence was 60%, AGS, BGC-823, and MKN-28 cells were incubated with 0, 0.5, 1, or 2 mM ALA for 24 h in RPMI with 10% FBS. After incubation, STAT3 mRNA in the cell lysates was examined by RT-PCR. (d) AGS, BGC-823, and MKN-28 cells pretreated with 0, 0.5, 1, 2, or 2.5 mM ALA for 24 h in RPMI with 10% FBS were treated with or without 20 ng/mL TNF-α. And then, western blotting was performed to analyze p-STAT3 and STAT3 protein level. Data represent the mean ± SD from 3 independent experiments.

with or without 2 mM ALA were incubated with 20 ng/mL TNF-α for 4 h, and then, the MUC4 luciferase activity was determined using a luminometer. As shown in Figure 5(b), the relative MUC4 luciferase activity was significantly higher in STAT3 overexpression cells than in cells only incubated with ALA. These two assays indicated that the expression of MUC4 gene is regulated by STAT3. Furthermore, to explore the role of STAT3 in the inhibition of MUC4 by ALA in gastric cancer cells, AGS, BGC-823, and MKN-28 cells were incubated with 0, 0.5, 1, or 2 mM ALA for 24 h in RPMI with 10% FBS when cell confluence was 60%. After incubation, STAT3 mRNA in the cell lysates was examined by RT-PCR. There was no significant difference between the STAT3 mRNA levels in cells incubated with indicated concentrations of ALA (Figure 5(c)). In addition, AGS, BGC-823, and MKN-28 cells pretreated with 0, 0.5, 1, 2, or 2.5 mM ALA for 24 h in RPMI with 10% FBS were treated with or without 20 ng/mL TNF-α. And then, western blotting was performed to analyze p-STAT3 and STAT3 protein levels. There was no significant difference between the p-STAT3 and STAT3 protein levels of cells incubated with indicated concentrations of alpha-lipoic acid. Taken together, STAT3

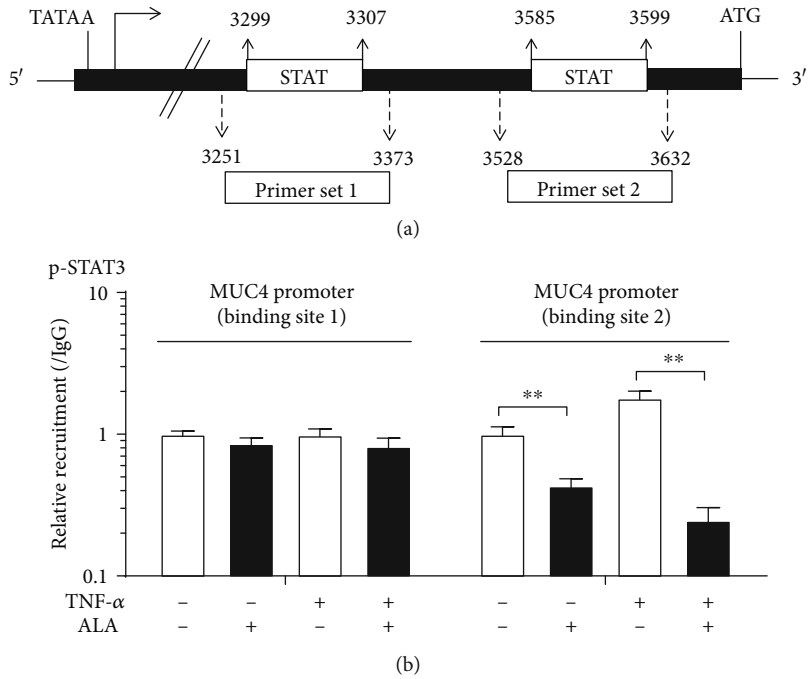

Figure 6: Alpha-lipoic acid inhibits STAT3 binding to the MUC4 promoter region. (a) Schematic representation of MUC4 promoter. The two putative STAT-binding sites as well as the primers used for chromatin immunoprecipitation experiments (Primer set 1 and Primer set 2) are shown. (b) Binding of p-STAT3 to MUC4 promoter by ALA with or without TNF-α treatment. AGS cells were treated with 2 mM ALA overnight and then exposed to 20 ng/mL TNF-α for 4 h, followed by ChIP assay using anti-p-STAT3 and PCR primers covering 2 different regions of the MUC4 promoter. Data represent the mean ± SD from 3 independent experiments. $^{**}p < 0.05$.

was involved in the inhibition of MUC4 by ALA, but its expression level was not affected.

3.6. Alpha-Lipoic Acid Inhibits STAT3 Binding to the MUC4 Promoter Region. Figure 6(a) shows the schematic representation of MUC4 promoter. The two putative STAT-binding sites as well as the primers used for chromatin immunoprecipitation experiments (Primer set 1 and Primer set 2) are shown. AGS cells were treated with 2 mM ALA overnight and then exposed to 20 ng/mL TNF-α for 4 h or without TNF-α treatment, followed by ChIP assay using anti-p-STAT3 and PCR primers covering 2 different regions of the MUC4 promoter. As shown in Figure 6(b), ALA inhibits STAT3 binding to site 2 in the MUC4 promoter region.

4. Discussion

In the present study, we demonstrated the inhibitory effect of ALA on human gastric cancer cell proliferation and invasion. The possible mechanism of this inhibitory effect was through suppression of MUC4. ALA inhibited STAT3 binding to the MUC4 promoter region, reduced the expression of MUC4, which in turn inhibited the proliferation and invasion of gastric cancer cells. To our knowledge, this is the first study showing the effect of ALA on resistance to cell proliferation and invasion in gastric cancer.

MUC4 protects cancer cells during hematological transmission and promotes the invasion and colonization of cancer cells to metastatic sites [15]. Many studies have shown that high MUC4 expression in the gastric cancer is related to the poor prognosis, such as lymph node metastasis and vascular invasion, which is the main cause of death in patients with gastric cancer [16]. We performed immunohistochemistry staining, the results showed positive MUC4 expression in gastric cancer tissues compared with normal tissues (Figure 1 and Table 1, $p < 0.001$), which is in accordance with known study results. Immunohistochemistry of prognostic factors showed that there were significant differences in MUC4 expression under different conditions such as ages, depth of invasion, TNM stage, lymph node metastasis, and distant metastasis (Table. 2, $p < 0.05$). MUC4 has been further studied as a target for treating various types of cancer, such as breast cancer [17] and colorectal cancer [18]. Since MUC4 was closely related to gastric cancer, it may be possible to suppress gastric cancer by regulating MUC4 expression.

It has been reported that ALA has a protective effect on gastric ulcer in rats because of its antioxidant and anti-inflammatory properties [19]. In view of the inhibitory effect of ALA on the proliferation and metastasis in various cancer cells [6], we treated gastric cancer cells with ALA and found that 1 mM ALA can reduce the viability of gastric cancer cells (Figure 2(c)). Its inhibitory effect on gastric cancer cells may be related to the inhibition of MUC4 expression (Figures 2(a) and 2(b)).

TNF-α and IL-6 can both induce MUC4 gene expression. To explore the mechanism, we found that the effect of ALA on gastric cancer cells might be related to STAT3. Therefore, we hope that the drugs or factors can induce exogenous MUC4 without affecting the expression level of STAT3.

However, it has been reported that IL-6 may activate STAT3, leading to transcriptional upregulation of downstream growth-related genes [20]. On the contrary, TNF-α induces MUC4 through independent STAT3 pathway (such as NF-κB pathway). Therefore, we use TNF-α to increase exogenous MUC4 in our study [17]. TNF-α-induced MUC4 was significantly decreased in both mRNA and protein level after being treated with ALA, and the effect was positively correlated with ALA concentration (Figure 3). In addition, we also proved that ALA inhibited gastric cancer cell invasion much strongly than anti-MUC4, which suggested that the inhibitory effect of ALA on gastric cancer was partly by suppression of MUC4 (Figure 4). These experiments demonstrated that ALA inhibited both endogenous MUC4 and MUC4 induced by TNF-α in gastric cancer cells, which may contribute to its inhibition on gastric cancer.

MUC4 is a downstream target gene of STAT3, and its expression is regulated by STAT3 [21]. In our study, both knockdown of STAT3 and treatment of ALA reduced MUC4 levels (Figure 5(a)), while overexpression of STAT3 reduced the effect of ALA on MUC4 (Figure 5(b)), and treatment of ALA did not change the level of STAT3 (Figure 5(c)). Therefore, we speculated that the mechanism of ALA inhibiting MUC4 was not to change the levels of upstream target gene STAT3, but to affect the function of STAT3.

STAT3 can be activated by various cytokines, including the interleukin 6 (IL-6) family of cytokines, granulocyte colony-stimulating factor, leptin, and epidermal growth factor [22]. STAT3 has redox-sensitive cysteines within its structure, and STAT3 is susceptible to redox regulation [23]. The cysteine thiol is very unstable and is readily oxidized to form disulfide bonds, which results in intermediate conformational changes within proteins [24]. Therefore, the change of redox state in the extracellular environment would affect the spatial conformation of STAT3 protein and further affect its function [25]. ALA can scavenge excessive ROS and regenerate endogenous antioxidants, which may influence the state of oxidative stress in cancer cells. Changes of redox in the cell are very likely to interfere STAT3 protein structure stability and affect its function. Consistent with our hypothesis, we proved that ALA blocked the binding of STAT3 to the MUC4 promoter (Figure 6). However, the mechanism by which ALA inhibits STAT3 binding to the promoter of MUC4 requires further extensive investigation.

5. Conclusion

In summary, ALA inhibits proliferation and invasion of gastric cancer cells through downregulation of MUC4. Specifically, ALA suppresses STAT3 binding to the promoter of MUC4. Our findings suggest that ALA could be used in the treatment of gastric cancer and even in the early stage of gastric cancer to inhibit the progress of gastric cancer.

Abbreviations

ALA: Alpha-lipoic acid
ROS: Reactive oxygen species
SOD: Superoxide dismutase
MUC4: Mucin 4
STAT3: Signal transducer and activator of transcription 3
FBS: Fetal bovine serum
qRT-PCR: Quantitative real-time PCR
ChIP: Chromatin immunoprecipitation.

Data Availability

The datasets used and analyzed during the current study are available from the corresponding author on reasonable request.

Conflicts of Interest

There are no conflicts of interest for all the authors.

Authors' Contributions

Qiang Tong designed the study, interpreted the results, and wrote the manuscript. Yu Yang, Erhu Fang, Jiajun Luo, Hongxue Wu, Yue Jiang, Ying Liu, and Shilun Tong performed the experiments. Zhihua Wang and Rui Zhou participated in the design and coordination of this study. Yu Yang and Erhu Fang contributed equally to this work.

Acknowledgments

This work was supported by the National Natural Science Foundation of China (No. 81172186) (QT), by the Natural Science Foundation of Hubei Province (No. 2018CFB504) (QT), by the Guidance Foundation of Renmin Hospital of Wuhan University (No. RMYD2018M67) (QT), and by the National Science Fund for Excellent Young Scholars (No. 81722007) (ZHW).

References

[1] F. Bray, J. Ferlay, I. Soerjomataram, R. L. Siegel, L. A. Torre, and A. Jemal, "Global cancer statistics 2018: GLOBOCAN estimates of incidence and mortality worldwide for 36 cancers in 185 countries," *CA: A Cancer Journal for Clinicians*, vol. 68, no. 6, pp. 394–424, 2018.

[2] G. Y. Ku and D. H. Ilson, "Management of gastric cancer," *Current Opinion in Gastroenterology*, vol. 30, no. 6, pp. 596–602, 2014.

[3] P. L. de Sá Junior, D. A. D. Câmara, A. S. Porcacchia et al., "The roles of ROS in cancer heterogeneity and therapy," *Oxidative Medicine and Cellular Longevity*, vol. 2017, Article ID 2467940, 12 pages, 2017.

[4] M. Badran, B. Abuyassin, S. Golbidi, N. Ayas, and I. Laher, "Alpha lipoic acid improves endothelial function and oxidative stress in mice exposed to chronic intermittent hypoxia," *Oxidative Medicine and Cellular Longevity*, vol. 2019, Article ID 4093018, 13 pages, 2019.

[5] A. Solmonson and R. J. DeBerardinis, "Lipoic acid metabolism and mitochondrial redox regulation," *Journal of Biological Chemistry*, vol. 293, no. 20, pp. 7522–7530, 2018.

[6] D. Tibullo, G. Li Volti, C. Giallongo et al., "Biochemical and clinical relevance of alpha lipoic acid: antioxidant and anti-inflammatory activity, molecular pathways and therapeutic

potential," *Inflammation Research*, vol. 66, no. 11, pp. 947–959, 2017.

[7] V. M. Mendoza-Núñez, B. I. García-Martínez, J. Rosado-Pérez, E. Santiago-Osorio, J. Pedraza-Chaverri, and V. J. Hernández-Abad, "The effect of 600 mg alpha-lipoic acid supplementation on oxidative stress, inflammation, and RAGE in older adults with type 2 diabetes mellitus," *Oxidative Medicine and Cellular Longevity*, vol. 2019, Article ID 3276958, 12 pages, 2019.

[8] M. J. Jeon, W. G. Kim, S. Lim et al., "Alpha lipoic acid inhibits proliferation and epithelial mesenchymal transition of thyroid cancer cells," *Molecular and Cellular Endocrinology*, vol. 419, pp. 113–123, 2016.

[9] H. S. Moon, "Chemopreventive effects of alpha lipoic acid on obesity-related cancers," *Annals of Nutrition & Metabolism*, vol. 68, no. 2, pp. 137–144, 2016.

[10] R. Mejías-Luque, S. K. Lindén, M. Garrido et al., "Inflammation modulates the expression of the intestinal mucins MUC2 and MUC4 in gastric tumors," *Oncogene*, vol. 29, no. 12, pp. 1753–1762, 2010.

[11] H. Jono, H. Xu, H. Kai et al., "Transforming growth factor-β-Smad signaling pathway negatively regulates nontypeable *Haemophilus influenzae*-induced *MUC5AC* mucin transcription via mitogen-activated protein kinase (MAPK) phosphatase-1-dependent inhibition of p38 MAPK," *The Journal of Biological Chemistry*, vol. 278, no. 30, pp. 27811–27819, 2003.

[12] M. P. Buisine, L. Devisme, T. C. Savidge et al., "Mucin gene expression in human embryonic and fetal intestine," *Gut*, vol. 43, no. 4, pp. 519–524, 1998.

[13] V. Fauquette, S. Aubert, S. Groux-Degroote et al., "Transcription factor AP-2α represses both the mucin MUC4 expression and pancreatic cancer cell proliferation," *Carcinogenesis*, vol. 28, no. 11, pp. 2305–2312, 2007.

[14] C. Kossow, D. Jose, R. Jaster, O. Wolkenhauer, and K. Rateitschak, "Mathematical modelling unravels regulatory mechanisms of interferon–induced STAT1 serine-phosphorylation and MUC4 expression in pancreatic cancer cells," *IET Systems Biology*, vol. 6, no. 3, pp. 73–85, 2012.

[15] R. Bhatia, S. K. Gautam, A. Cannon et al., "Cancer-associated mucins: role in immune modulation and metastasis," *Cancer Metastasis Reviews*, vol. 38, no. 1-2, pp. 223–236, 2019.

[16] Y. Tamura, M. Higashi, S. Kitamoto et al., "MUC4 and MUC1 expression in adenocarcinoma of the stomach correlates with vessel invasion and lymph node metastasis: an immunohistochemical study of early gastric cancer," *PLoS One*, vol. 7, no. 11, article e49251, 2012.

[17] M. F. Mercogliano, M. de Martino, L. Venturutti et al., "TNFα-induced mucin 4 expression elicits trastuzumab resistance in HER2-positive breast cancer," *Clinical Cancer Research*, vol. 23, no. 3, pp. 636–648, 2017.

[18] S. Das, S. Rachagani, Y. Sheinin et al., "Mice deficient in Muc4 are resistant to experimental colitis and colitis-associated colorectal cancer," *Oncogene*, vol. 35, no. 20, pp. 2645–2654, 2016.

[19] A. M. S. Gomaa, N. A. Abd El-Mottaleb, and H. A. Aamer, "Antioxidant and anti-inflammatory activities of alpha lipoic acid protect against indomethacin-induced gastric ulcer in rats," *Biomedicine & Pharmacotherapy*, vol. 101, pp. 188–194, 2018.

[20] K. Chen, W. Sun, Y. Jiang et al., "Ginkgolide B suppresses TLR4-mediated inflammatory response by inhibiting the phosphorylation of JAK2/STAT3 and p38 MAPK in high glucose-treated HUVECs," *Oxidative Medicine and Cellular Longevity*, vol. 2017, Article ID 9371602, 12 pages, 2017.

[21] R. Mejías-Luque, S. Peiró, A. Vincent, I. van Seuningen, and C. de Bolós, "IL-6 induces MUC4 expression through gp130/STAT3 pathway in gastric cancer cell lines," *Biochimica et Biophysica Acta (BBA) - Molecular Cell Research*, vol. 1783, no. 10, pp. 1728–1736, 2008.

[22] K. Takeda, K. Noguchi, W. Shi et al., "Targeted disruption of the mouse *Stat3* gene leads to early embryonic lethality," *Proceedings of the National Academy of Sciences of the United States of America*, vol. 94, no. 8, pp. 3801–3804, 1997.

[23] W. Cai, X. Yang, S. Han et al., "Notch1 pathway protects against burn-induced myocardial injury by repressing reactive oxygen species production through JAK2/STAT3 signaling," *Oxidative Medicine and Cellular Longevity*, vol. 2016, Article ID 5638943, 14 pages, 2016.

[24] Q. Tong, Y. Zhu, J. W. Galaske et al., "MnTE-2-PyP modulates thiol oxidation in a hydrogen peroxide-mediated manner in a human prostate cancer cell," *Free Radical Biology & Medicine*, vol. 101, pp. 32–43, 2016.

[25] E. Butturini, E. Darra, G. Chiavegato et al., "S-Glutathionylation at Cys328 and Cys542 impairs STAT3 phosphorylation," *ACS Chemical Biology*, vol. 9, no. 8, pp. 1885–1893, 2014.

Hindawi
Oxidative Medicine and Cellular Longevity
Volume 2019, Article ID 9290728, 18 pages
https://doi.org/10.1155/2019/9290728

Research Article

Metformin Suppresses Self-Renewal Ability and Tumorigenicity of Osteosarcoma Stem Cells via Reactive Oxygen Species-Mediated Apoptosis and Autophagy

Bin Zhao,[1,2] Jie Luo,[1,2] Ye Wang,[1,2] Liangfu Zhou,[1,2] Jingmin Che,[1,2] Fang Wang,[1,2] Songlin Peng,[3] Ge Zhang,[4] and Peng Shang[1,5]

[1]*Research & Development Institute of Northwestern Polytechnical University in Shenzhen, Shenzhen 518057, China*
[2]*School of Life Science, Northwestern Polytechnical University, Xi'an, Shaanxi 710072, China*
[3]*Department of Spine Surgery, Shenzhen People' Hospital, Shenzhen 518000, China*
[4]*Institute of Integrated Bioinfomedicine and Translational Science, School of Chinese Medicine, Hong Kong Baptist University, Hong Kong 999077, China*
[5]*Key Laboratory for Space Bioscience and Biotechnology, Institute of Special Environmental Biophysics, Northwestern Polytechnical University, Xi'an, Shaanxi 710072, China*

Correspondence should be addressed to Peng Shang; shangpeng@nwpu.edu.cn

Received 12 August 2019; Revised 5 October 2019; Accepted 11 October 2019; Published 18 November 2019

Academic Editor: Mithun Sinha

Osteosarcoma is the most frequently diagnosed primary malignant bone sarcoma in children and adolescents. Recent studies have shown that cancer stem cells (CSCs), a cluster of tumor cells with the ability to self-renew, play an essential role in tumor recurrence and metastasis. Thus, it is necessary to develop therapeutic strategies specifically targeting CSCs. Metformin, the first-line drug for type 2 diabetes, exhibits antineoplastic activities in various kinds of tumors. New evidence has suggested that metformin may target CSCs and prevent their recurrence. However, the underlying specific mechanisms remain unclear. In this study, we found that metformin significantly suppressed the self-renewal ability of osteosarcoma stem cells (OSCs) and induced G0/G1 phase arrest by blocking the activity of cyclin-dependent kinases. Furthermore, metformin induced apoptosis through a mitochondria-dependent pathway, leading to the collapse of the mitochondrial transmembrane potential and the production of reactive oxygen species (ROS). Importantly, metformin acted directly on the mitochondria, which resulted in decreased ATP synthesis. This change allowed access to the downstream AMPK kinase, and the activation of AMPK led to the reversal of the mTOR pathway, triggering autophagy. Particularly, metformin-mediated autophagy disturbed the homeostasis of stemness and pluripotency in the OSCs. Additionally, our mouse xenograft model confirmed the potential therapeutic use of metformin in targeting OSCs. In conclusion, our findings suggest that metformin suppresses the self-renewal ability and tumorigenicity of OSCs via ROS-mediated apoptosis and autophagy.

1. Introduction

Osteosarcoma, the most frequently diagnosed primary malignant tumor in children and adolescents, is characterized by a high risk of developing lung metastasis and poor prognosis [1]. Despite steady progress in the research and development of cancer therapeutics, the 5-year survival rates of osteosarcoma remain the same as they were in the 1970s [2]. Cancer stem cells (CSCs), a subgroup of cancer cells with the ability to self-renew, play an essential role in tumor recurrence and metastasis [3]. Study has showed that the key challenge of cancer was the late occurrence of distant metastases, in which CSCs played a dominant role [4]. Therefore, targeting CSCs may be a promising strategy for the future of cancer treatment.

Metformin, the most widely used drug in the treatment of type 2 diabetes, exerted antineoplastic activities on a vast majority of cancers [5–7]. Moreover, numerous studies have

indicated that metformin is a promising therapy against CSCs [8–10]. Autophagy, an essential homeostatic process for protein degradation, was recently identified as a crucial regulator in tumorigenesis [11]. Further research suggested that autophagy may regulate drug sensitivity and the pluripotency of CSCs [12]. However, the roles that autophagy plays in CSCs are largely unknown. Understanding these roles, as well as the molecular mechanisms underlying the maintenance of CSCs, may be critical for oncotherapy.

In this study, osteosarcoma stem cells (OSCs) from K7M2 and MG63 osteosarcoma cell lines were isolated by methods of both side population (SP) analysis and serum-free suspension culture. Both K7M2 and MG63 OSCs expressed high levels of stem cell markers including Sox2, Oct4, Nanog, CD44, CD133, and ALDH1. Also, both K7M2 and MG63 OSCs had the ability to differentiate into osteogenic and chondrogenic lineages. Notably, metformin treatment induced cell cycle arrest and decreased the viability of both the K7M2 and MG63 OSCs. In addition, metformin triggered apoptosis in both K7M2 and MG63 OSCs via a caspase-dependent mitochondrial apoptotic pathway, which was associated with alterations in the morphology of the mitochondrial structure and the balance of mitochondrial Bcl-2 and Bax. Most importantly, we found that autophagic flux was higher in these OSCs than it was in their parental cells. Treatment with metformin abrogated the pluripotency in the K7M2 and MG63 OSCs associated with the upregulation of autophagy through the AMPK/mTOR pathway. When the OSCs were treated with 3-methyladenine (3MA), an inhibitor of autophagy, there was a decrease in their stemness properties. Likewise, treatment with the autophagy inducer rapamycin also impaired the pluripotency of both OSCs, abolishing their stemness. Additionally, the therapeutic efficacy of metformin was further confirmed in mice bearing K7M2 osteosarcoma xenografts. This study suggests that metformin has promising anticancer activity in OSCs through regulation of autophagy.

2. Material and Methods

2.1. Drugs, Reagents, and Antibodies. Metformin (D150959), Hoechst 33342 (14533), verapamil (V4629), 3MA (189490), and rapamycin (553210) were purchased from Sigma-Aldrich (Saint Louis, USA). The cell mitochondria isolation kit (C3601), Reactive Oxygen Species Assay Kit (S0033), FITC-Annexin V/PI apoptosis detection kit (C1062L), ATP assay kit (S0026), and anti-p21 (AP021), anti-Cyclin D1 (AC853), anti-Cyclin D3 (AC856), anti-ATG5 (AF2269), anti-ATG7 (AA820), and anti-Nanog (AF1912) antibodies were purchased from Beyotime (Haimen, China). The anti-Bcl-2 (ab182858), anti-Bax (ab182733), anti-active Caspase9 (ab2324), anti-active Caspase3 (ab2302), anti-cytochrome c (ab133504), anti-LC3 (ab48394), anti-Oct4 (ab181557), anti-Sox2 (ab97959), anti-Ki67 (ab15580), anti-AMPK (ab80039), anti-phospho AMPK (ab133448), anti-mTOR (ab134903), anti-phospho mTOR (ab109268), CD105 (ab135528), and Stro-1 (ab106531) antibodies were obtained from Abcam (USA). The anti-β-actin (4967S and E4D9Z) was purchased from Cell Signaling Technology (Danvers, USA). Mito Tracker® Red CMXRos (M7512) and Lyso Tracker Red DND-99 (L7528) were obtained from Thermo Fisher Scientific (Waltham, USA). Alexa Fluor® 488 mouse/human anti-Sox2 antibody (656109), PE anti-mouse/human Oct4 antibody (653703), APC anti-mouse/-human CD44 antibody (103011), APC anti-mouse CD133 antibody (141207), and PE/Cy7 anti-human CD133 antibody (372809) were obtained from Biolegend (San Diego, USA). Acridine orange/ethidium bromide (AO/EB) was from Solarbio (Beijing, China). DAPI (BD5010) was obtained from Bioworld Technology, Inc. DMEM (12800082), DMEM/F12 (12400024), Fetal Bovine Serum (FBS, 10099-141), B27 Supplement (17504044), epidermal growth factor (EGF, PHG0311), and basic fibroblast growth factor (bFGF, 13256029) were purchased from Gibco (USA).

2.2. Animals. Four-week-old male Balb/c mice were obtained from the Fourth Military Medical University. All experimental procedures were conducted under the protocol reviewed and approved by the Ethics Committee of the Northwestern Polytechnical University.

2.3. Cell Viability Assay. The viability of the K7M2 and MG63 OSCs was evaluated by CCK-8 assay. Briefly, cultured K7M2 and MG63 OSCs were seeded into 96-well microtiter plates at a density of 1×10^4 cells/well and treated with different concentrations of metformin (0, 6.4, 12.8, 25.6, and 51.2 mM) for 24-72 h. The cells were then treated with CCK-8 solution, and the absorbances were measured by multiscan spectrum (Bio-Rad, USA) at 570 nm. The cell death of the K7M2 and MG63 OSCs was also determined by staining with AO/PI for 10 min. Images were taken using a ZEISS inversion fluorescence microscope (Zeiss, Germany).

2.4. Cell Cycle Analysis. The cell cycle distribution of the K7M2 and MG63 OSCs was assessed by flow cytometry. Briefly, after 48 h of metformin (0, 6.4, 12.8, 25.6, and 51.2 mM) treatment, the K7M2 and MG63 OSCs were harvested and made into single cell suspensions by mechanical blow method. The cells were then fixed, centrifuged, resuspended, stained with 50 mg/mL of PI and 0.5 mg/mL of RNase A for 30 min in the dark, and then analyzed by flow cytometry (BD FACS Calibur, USA).

2.5. Apoptosis Assay. The K7M2 and MG63 OSCs were seeded into 90 mm culture plates at a density of 1×10^6 cells/well and treated with metformin (0, 6.4, 12.8, 25.6, and 51.2 mM) for 48 h. The cells were harvested and labeled with FITC-Annexin V/PI at room temperature for 20 min according to the instructions. The samples were then analyzed using flow cytometry (BD FACS Calibur, USA).

2.6. Side Population (SP) Assay. Flow cytometry was used to identify the SP fractions as described by Steiniger et al. [13]. In brief, cultured cells were trypsinized and resuspended in prewarmed DMEM prior to incubation with 5 μg/mL Hoechst 33342 either alone or in the presence of 50 μg/mL of the ABC transporter inhibitor verapamil for 90 min at 37°C. The cells were then passed through a 100 μm mesh filter (BD, USA) and sorted by a FACS Aria III flow cytometer

(BD, USA) equipped with Hoechst Blue with a 375 broad pass filter and Hoechst Red with a 675 broad pass filter laser. The sorted SP cells were collected and fluorescent-labeled with Sox2, Oct4, CD44, CD133, CD105, and Stro-1 to detect their stemness by a flow cytometer.

2.7. Aldehyde Dehydrogenase (ALDH1) Assay. K7M2 and MG63 OSCs were treated with 6.4 mM metformin, 0.5 mM 3MA, 6.4 mM metformin, and 0.5 mM 3MA together, or 5 μM rapamycin for 48 h. The ALDH1-positive subpopulation was analyzed using an ALDEFLUOR assay kit (Stem Cell Technologies, Canada). Approximately 1×10^6 K7M2 and MG63 OSCs were collected and incubated in the ALDEFLUOR assay buffer for 40 min at 37°C. Negative control samples were treated with 50 μM of diethylaminobenzaldehyde (DEAB), an inhibitor of ALDH1. Following that, the cells were harvested and resuspended in ALDEFLUOR buffer and subjected to the FACS Aria III flow cytometer.

2.8. Mitochondrial Membrane Depolarization. Mitochondrial membrane potential was monitored by Mito flow fluorescent dye (Cell Technology Inc., USA). Briefly, approximately 5×10^5 K7M2 and MG63 OSCs were incubated with the indicated concentrations of metformin (0, 6.4, 12.8, 25.6, and 51.2 mM) for 48 h. The cells were then stained with fluorescent dye for 30 min and detected by a BD FACS Calibur flow cytometer.

2.9. Reactive Oxygen Species (ROS) Detection. ROS were detected by measuring the oxidation of dichloro-dihydro-fluorescein diacetate (DCFH-DA) using Reactive Oxygen Species Assay Kit. Cells at 50%-60% confluency were incubated with metformin (0, 6.4, 12.8, 25.6, and 51.2 mM) for 48 h and then treated with 10 μM of DCFH-DA for 30 min at 37°C in the dark. The cells were then washed and harvested prior to analysis using the FACS Aria III flow cytometer.

2.10. Measurement of Intracellular ATP. Intracellular ATP content was determined using an ATP assay kit according to the manufacturer's instructions. In brief, K7M2 and MG63 OSCs were planted on 96-well plates and treated with metformin (0, 6.4, 12.8, 25.6, and 51.2 mM) for 48 h. The cells were lysed with an ATP extraction buffer and centrifuged to collect the supernatant. The supernatant was then mixed with the dilution buffer containing luciferase and measured by multiscan spectrum (Bio-Rad, USA).

2.11. Real-Time PCR. Total RNA was extracted from the metformin-treated OSCs by TRIzol reagent (Invitrogen, USA). The isolated RNA was reverse transcribed into cDNA using the Prime Script RT Reagent kit (Takara Biotechnology, China). Primers were obtained from Sangon Biotech (Shanghai, China). Quantitative PCR was performed using an IQ5 real-time PCR system (Bio-Rad, USA) in a 20 μL reaction volume. The sequences of primers are listed as follows: human *P21*: 5′-AGCAGCGGAACAAGGAGT-3′ (sense) and 5′-CGTTAGTGCCAGGAAAGACA-3′ (antisense); mouse *P21*: 5′-GACAAGAGGCCCAGTACTTC-3′ (sense) and 5′-TAGAAATCTGTCAGGCTGGT-3′ (antisense); human *Cyclin D1*: 5′-TCTCCAAAATGCCAGAGGCG-3′ (sense) and 5′-AGGAAGTTGTTGGGGCTCCT-3′ (antisense); mouse *Cyclin D1*: 5′-CGGATGAGAACAAGCAGACC-3′ (sense) and 5′-GCAGGAGAGGAAGTTGTTGG-3′ (antisense); human *Cyclin D3*: 5′-AGGGATCACTGGCACTGAAG-3′ (sense) and 5′-ACAGGTGTATGGCTGTGACAT-3′ (antisense); mouse *Cyclin D3*: 5′-CTATGAACTACCTGGATCGCTACCT-3′ (sense) and 5′-CAGACGGTACCTAGAAGCTGCAA-3′ (antisense); human *SOX2*: 5′-AACCCCAAGATGCACAACTC-3′ (sense) and 5′-CGGGGCCGGTATTTATAATC-3′ (antisense); mouse *SOX2*: 5′-GCGGAGTGGAAACTTTTGTCC-3′ (sense) and 5′-GGGAAGCGTGTACTTATCCTTCT-3′ (antisense); human *OCT4*: 5′-GCTCGAGAAGGATGTGGTCC-3′ (sense) and 5′-CGTTGTGCATAGTCGCTGCT-3′ (antisense); mouse *OCT4*: 5′-CGGAAGAGAAAGCGAACTAGC-3′ (sense) and 5′-ATTGGCGATGTGAGTGATCTG-3′ (antisense); human *NANOG*: 5′-CAAAGGCAAACAACCCACTT-3′ (sense) and 5′-TCTGCTGGAGGCTGAGGTAT-3′ (antisense); mouse *NANOG*: 5′-TGACCTCAACTACATGGTCTACA-3′ (sense) and 5′-CTTCCCATTCTCGGCCTTG-3′ (antisense); human *ATG5*: 5′-CACA AGCAACTCTGGATGGGATT-3′ (sense) and 5′-CCATCTTCAG GATCAATAGCAGAAG-3′ (antisense); mouse *ATG5*: 5′-GTGCTTCGAGATGTGTGGTTTGGA-3′ (sense) and 5′-CGTCAAATAGCTGACTCTTGGCAA-3′ (antisense); human *ATG7*: 5′-GGTCAAAGGACGAAGATAACA-3′ (sense) and 5′-GGTCACGGAAGCAAACAACT-3′ (antisense); mouse *ATG7*: 5′-GCTAATGGACACCAGGGAGA-3′ (sense) and 5′-AAAAAGTGAGGAGCCCAGGT-3′ (antisense); human *GAPDH*: 5′-TTGATGGCAACAATCTCCAC-3′ (sense) and 5′-CGTCCCGTAGACAAAATGGT-3′ (antisense); and mouse *GAPDH*: 5′-CAACAGCAACTCCCACTCTTC-3′ (sense) and 5′-GGTCCAGGGTTTCTTACTCCTT-3′ (antisense).

2.12. Western Blot. Mitochondria were extracted by the mitochondria isolation kit according to the manufacturer's instructions. The isolated mitochondria or cells were lysed with RIPA buffer containing protease inhibitor or phosphatase inhibitor (Beyotime, China) and determined by bicinchoninic acid assay (Beyotime, China). Thirty micrograms of protein was loaded onto SDS-PAGE, separated by electrophoresis, and transferred to polyvinylidene difluoride membrane (PVDF). The membranes were blocked with 1% bovine serum albumin (BSA), incubated with primary antibodies, washed with TBST buffer, and then incubated with HRP-conjugated secondary antibodies (Boster, China). Immunoblot images were taken and quantified using ImageJ software (National Institutes of Health, USA). The intensities of the bands were determined and normalized to β-actin.

2.13. Tumor Sphere Assay. K7M2 and MG63 OSCs were treated with 6.4 mM metformin, 0.5 mM 3MA, 6.4 mM metformin, and 0.5 mM 3MA together, or 5 μM rapamycin for

48 h. Tumor spheres were induced by 6-well ultralow adherent culture plates (Corning, USA). K7M2 and MG63 cells were seeded at a density of 5×10^3 cells/well in a serum-free DMEM/F12 medium supplemented with 1× B27, 10 ng/mL EGF, and 10 ng/mL bFGF. Tumor sphere formation was quantified 7 days after initial seeding by staining with 0.1% crystal violet (Sigma-Aldrich, USA) and imaged with an inverted microscope (Olympus, Japan).

2.14. Immunohistochemistry (IHC) and Immunofluorescence (IF). For IHC, tumor tissues were harvested, fixed, dehydrated, embedded in paraffin, and sliced into 4 μm sections. The slices were then stained with hematoxylin-eosin (H&E) and IHC against LC3, ATG5, Ki67, Sox2, and Oct4. For IF, the cells were fixed with 4% paraformaldehyde, blocked with 1% BSA, and then incubated in primary antibodies overnight at 4°C. The cells were then washed with phosphate-buffered saline (PBS) and incubated with fluorescence-labeled secondary antibodies at room temperature in the dark. Images were taken using an FSX100 microscope (Olympus, Japan) or an FV10i Confocal Laser Scanning Microscope (Olympus, Japan).

2.15. Differentiation Potential of OSCs. The K7M2 and MG63 OSCs treated with/without metformin were cultured in a commercial osteogenic and chondrogenic differentiation medium (Cyagen, China) in 6-well cell culture plates for three weeks. The cells were then fixed with 4% paraformaldehyde and stained with Alizarin Red (Cyagen, China) for detection of osteogenic differentiation and Alcian Blue (Cyagen, China) for chondrogenic differentiation. Images were taken using an FSX100 microscope (Olympus, Japan).

2.16. Transmission Electron Microscope (TEM). For TEM detection, cells with different treatments were fixed with 2% phosphotungstic acid, dropped onto formvar/carbon-coated copper mesh grids, and then left to dry at room temperature. Images were taken with a Hitachi HT7700 transmission electron microscope (Hitachi, Japan).

2.17. Scanning Electron Microscope (SEM). OSCs were fixed with 2.5% glutaraldehyde, dehydrated in ethanol, dried at the critical point, and then placed on copper grids. The specimens were then imaged using a Hitachi SU8010 scanning electron microscope (Hitachi, Japan).

2.18. Orthotopic Intratibial Mouse Model of Osteosarcoma. After pretreatment of 6.4 mM metformin for 48 h, approximately 1×10^5, 1×10^4, or 1×10^3 of the K7M2 OSCs were suspended in 30 μL PBS and implanted into the tibia of male Balb/c mice by intratibial injection. Mice were anesthetized, the left leg was held with the knee, and the needle was inserted into the tibial tuberosity using a drilling motion. After 2 weeks, the mice were euthanized, and the tumor volumes and weights were measured (tumor volume = (length × width × height)/2). To further assess the effect of metformin-mediated autophagy on tumorigenesis, approximately 1×10^5 of K7M2 OSCs suspended in 30 μL PBS were injected into the tibia of male Balb/c mice. When tumor volumes reached about 100 mm^3, the mice were then randomly divided into five groups, receiving intraperitoneal injection of (1) PBS, (2) 250 mg/kg/day metformin diluted with PBS [14], (3) 15 mg/kg/day 3MA diluted with PBS [15], (4) 250 mg/kg metformin + 15 mg/kg/day 3MA, and (5) 1 mg/kg/day rapamycin diluted with PBS [16]. The mice were killed after 21 days, and the tumors were removed, weighed, and subjected to IHC staining for LC3, ATG5, Ki67, Sox2, and Oct4.

2.19. Statistical Analysis. Data analysis was performed using GraphPad Prism (GraphPad Software Inc., USA). Statistical analysis was performed by independent samples t-test for comparison between two groups or one-way ANOVA among the groups. $P < 0.05$ was considered statistically significant.

3. Results

3.1. Autophagic Flux Was Enhanced in OSCs. We isolated OSCs from K7M2 and MG63 osteosarcoma cell lines of which side population (SP) phenotype revealed as a characteristic tail separated from the complete population in Figure 1(a). The median percentage of K7M2 and MG63 SP cells was 1.25% and 1.07%, respectively, and the SP cells decreased to 0.2% and 0.2% upon treatment with verapamil, the inhibitor of the ABC transporter. To determine whether the basal level of autophagic flux was different between general osteosarcoma cells and their OSCs, we first observed the autophagosomes by TEM. As shown in Figure 1(b), the numbers of autophagosomes were significantly increased in SP cells than in non-SP cells, indicating that K7M2 and MG63 OSCs have a higher basal autophagic flux. Moreover, OSCs from K7M2 and MG63 osteosarcoma cells were successfully isolated via serum-free suspension culture for 7 days, and the tumor spheres were formed as showed in Figure 1(c). To further characterize the spheres and their parental cells, the stemness and autophagic properties were studied. As shown in Figure 1(d), the sphere cells from both K7M2 and MG63 had higher protein expression levels of the pluripotent transcription factors including Sox2, Oct4, and Nanog, as well as the high levels of autophagy-associated proteins LC3-II, ATG5, and ATG7. Real-time PCR (Figure 1(e)) also revealed that the sphere cells of both K7M2 and MG63 had higher mRNA levels of the pluripotent genes *SOX2*, *OCT4*, and *NANOG* and the autophagy-related genes *ATG5* and *ATG7*. Immunofluorescent staining assay (Figure 1(f)) confirmed that both K7M2 and MG63 SP cells have stronger fluorescent punctate structures of LC3-II than their non-SP cells, indicating higher levels of autophagy in OSCs. To determine the differentiation ability of the SP cells, they were cultured in an adhesive culture system in an osteogenic and chondrogenic differentiation medium for 3 weeks. SP cells cultured in a DMEM/F12 medium served as a control. As shown in Figure 1(g), both K7M2 and MG63 OSCs were found to have more calcium nodular and proteoglycan depositions than the non-SP cells, suggesting that the OSCs had undergone osteogenesis and chondrogenesis. These results indicated that the OSCs had the ability to differentiate into

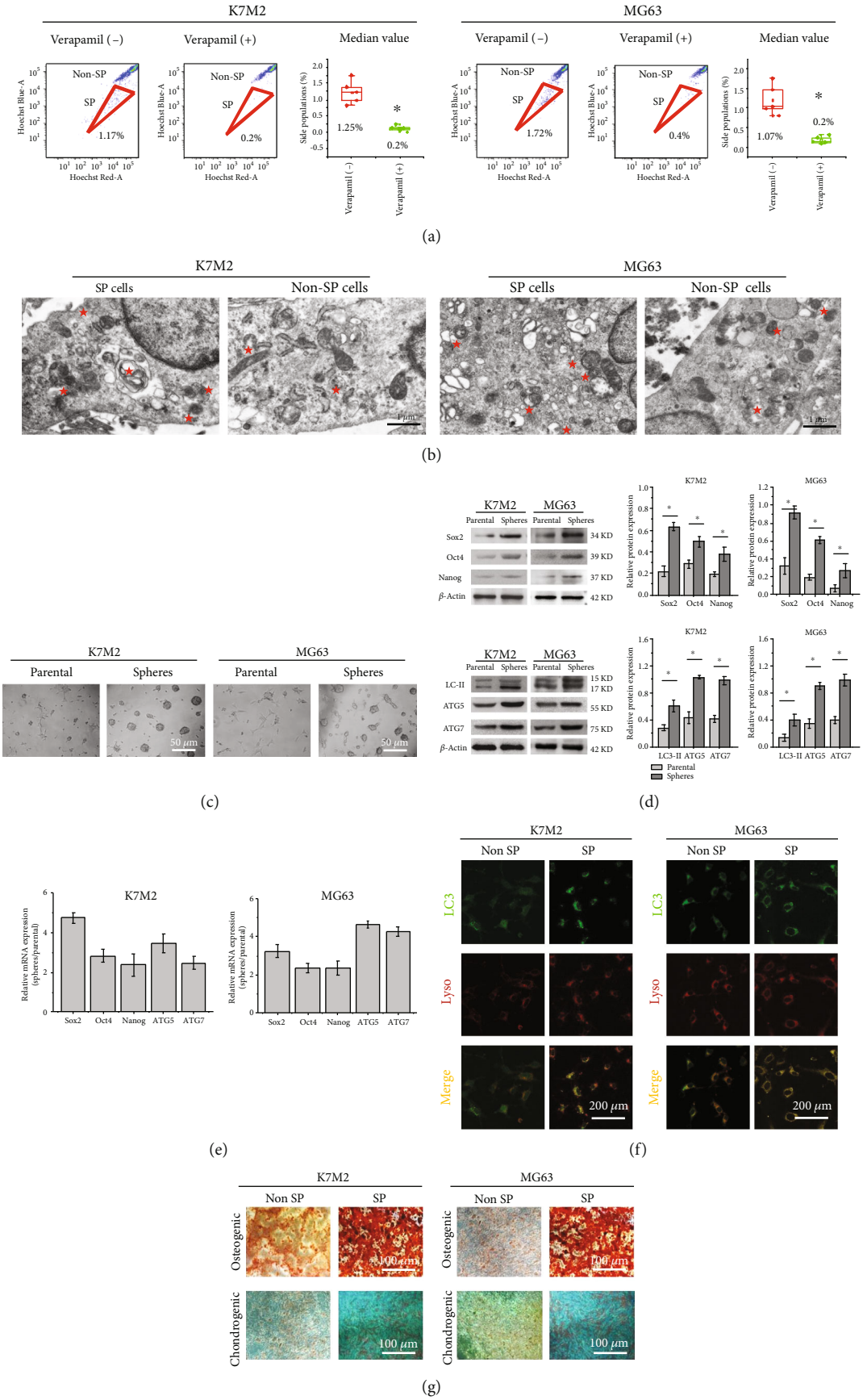

Figure 1: Continued.

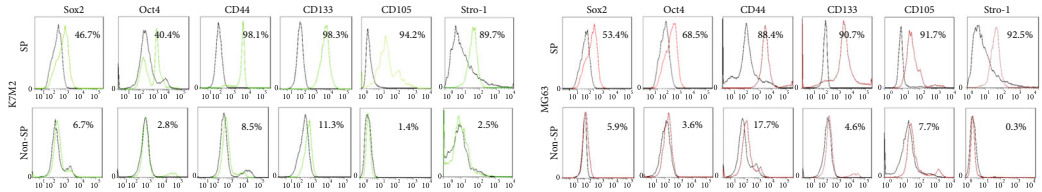

(h)

Figure 1: Characteristics of OSCs. (a) The representative images of SP cells from K7M2 and MG63 osteosarcoma cell lines. The median value of K7M2 and MG63 SP cells was 1.25% and 1.07%, respectively. $n = 5$. (b) The representative TEM images of autophagosomes in K7M2 and MG63 SP cells. The pentagrams stand for autophagosomes. Scale bars = 1 μm. (c) Tumor spheres of K7M2 and MG63 osteosarcoma cells after culturing in the serum-free medium DMEM/F12-bFGF-EGF-B27 for 7 days. The parental K7M2 and MG63 cells cultured in DMEM/F12 supplemented with 1% FBS served as a control. Scale bars = 50 μm. $n = 5$. (d) Western blot analysis of the pluripotent transcription factors Sox2, Oct4, and Nanog and the autophagy markers LC3, ATG5, and ATG7 in K7M2 and MG63 OSCs. Data are shown as mean ± SD, $n = 3$. (e) The mRNA expression levels of the pluripotency-associated genes *SOX2*, *OCT4*, and *NANOG* and the autophagy-related genes *ATG5* and *ATG7*. $n = 3$. (f) Immunofluorescence analysis of autophagy in K7M2 and MG63 SP cells. The colocalization (orange) staining of LC3 (green) with lysosome (red) indicates autophagy. Scale bars = 200 μm. $n = 3$. (g) Osteogenic and chondrogenic differentiation of K7M2 and MG63 SP cells. Cells differentiated into osteoblasts and chondroblasts were detected by staining with Alizarin Red and Alcian Blue. Scale bars = 100 μm. $n = 3$. (h) Flow cytometry-based assay for the pluripotent transcription factors Sox2 and Oct4 and the CSC surface markers CD44, CD105, CD133, and Stro-1 in K7M2 and MG63 SP cells. $n = 3$. $^*P < 0.05$ was considered statistically significant.

osteoblasts and chondrocytes. Furthermore, the pluripotent transcription factors Sox2 and Oct4 and CSC markers CD44, CD105, CD133, and Stro-1 were more highly expressed in both K7M2 and MG63 SP cells than in non-SP cells (Figure 1(h)), indicating that the SP cells have the characteristics of CSCs. Furthermore, we found that there is no difference in biomarkers in CD44, CD133, CD105, and Stro-1 between sphere-forming cells and SP cells from the K7M2 and MG63 (Figure S1). Therefore, in the following experiment, we used sphere-forming cells.

3.2. Metformin Induces Cell Cycle Arrest in K7M2 and MG63 OSCs. A dose- and time-dependent decrease in cell viability following metformin treatment was observed in Figure 2(a). The half-maximal inhibitory concentration (IC50) of metformin at 48 h was 11.8 ± 0.8 mM for the K7M2 OSCs and 7.9 ± 1.1 mM for the MG63 OSCs (Figure 2(b)). Flow cytometric analysis was used to examine the effect of metformin on the cell cycle. Treatment with increasing concentrations of metformin for 48 h resulted in the accumulation of cells in the G0/G1 phase and a decrease in the number of cells in the S phase (Figures 2(c) and 2(d)). Real-time PCR (Figure 2(e)) and western blot analysis (Figures 2(f) and 2(g)) clearly showed that the expression levels of cell cycle regulatory genes and proteins Cyclin D1 and Cyclin D3 were downregulated in both K7M2 and MG63 OSCs following metformin treatment, while P21 was upregulated. These results suggested that metformin induced cell cycle arrest in OSCs *in vitro* by blocking the G0 to G1 transition.

3.3. Metformin Activates a ROS-Mediated Mitochondrial Pathway to Induce Apoptosis. As apoptosis is often associated with mitochondrial function, we first assessed the effect of metformin on the mitochondrial morphology of the OSCs. Treatment with metformin for 48 h resulted in a change from the tubular network morphology to the disintegration of the mitochondrial network and reduced mitochondrial branching (Figure 3(a)). To evaluate the changes in the mitochondrial membrane potential as a result of metformin treatment, cells were subjected to Mito flow fluorescent dye. As shown in Figure 3(b), the metformin-treated cells decreased mitochondrial membrane polarization in a dose-dependent manner. Also, the intracellular ATP concentrations were declined dramatically following metformin treatment for 48 h (Figure 3(c)). We next explored whether the metformin-mediated apoptotic effect was a function of ROS modulation within the OSCs. As illustrated in Figure 3(d), immunofluorescence assay showed that OSCs treated with metformin for 48 h had higher fluorescent intensity compared to the controls, indicating an elevated ROS level upon metformin treatment. In addition, flow cytometric analysis in Figure 3(e) also indicated that metformin treatment for 48 h markedly increased ROS production in a dose-dependent manner. However, N-acetyl-L-cysteine (NAC) partly reversed the metformin-induced increase in ROS levels. Furthermore, the proapoptotic effects of metformin were evaluated by the FITC-Annexin V/PI apoptosis detection kit. As shown in Figures 3(f) and 3(g), metformin induced apoptosis in both K7M2 and MG63 OSCs in a dose-dependent manner. Western blot analysis (Figures 3(h) and 3(i)) showed that treatment with metformin decreased antiapoptotic Bcl-2 and increased proapoptotic Bax in both K7M2 and MG63 OSCs, confirming that metformin induced apoptosis in the OSCs. In addition, metformin was found to stimulate the translocation of cytochrome c from the mitochondria to the cytosol and upregulate both activated Caspase9 and activated Caspase3. Taken together, these results suggested that metformin induced apoptosis in OSCs mainly through a ROS-mediated mitochondrial dysfunction pathway.

3.4. Metformin Impairs Stemness and Pluripotency of OSCs. Sphere formation assays were conducted to evaluate the stemness characteristics of the K7M2 and MG63 OSCs. The numbers of spheres significantly decreased in a dose-

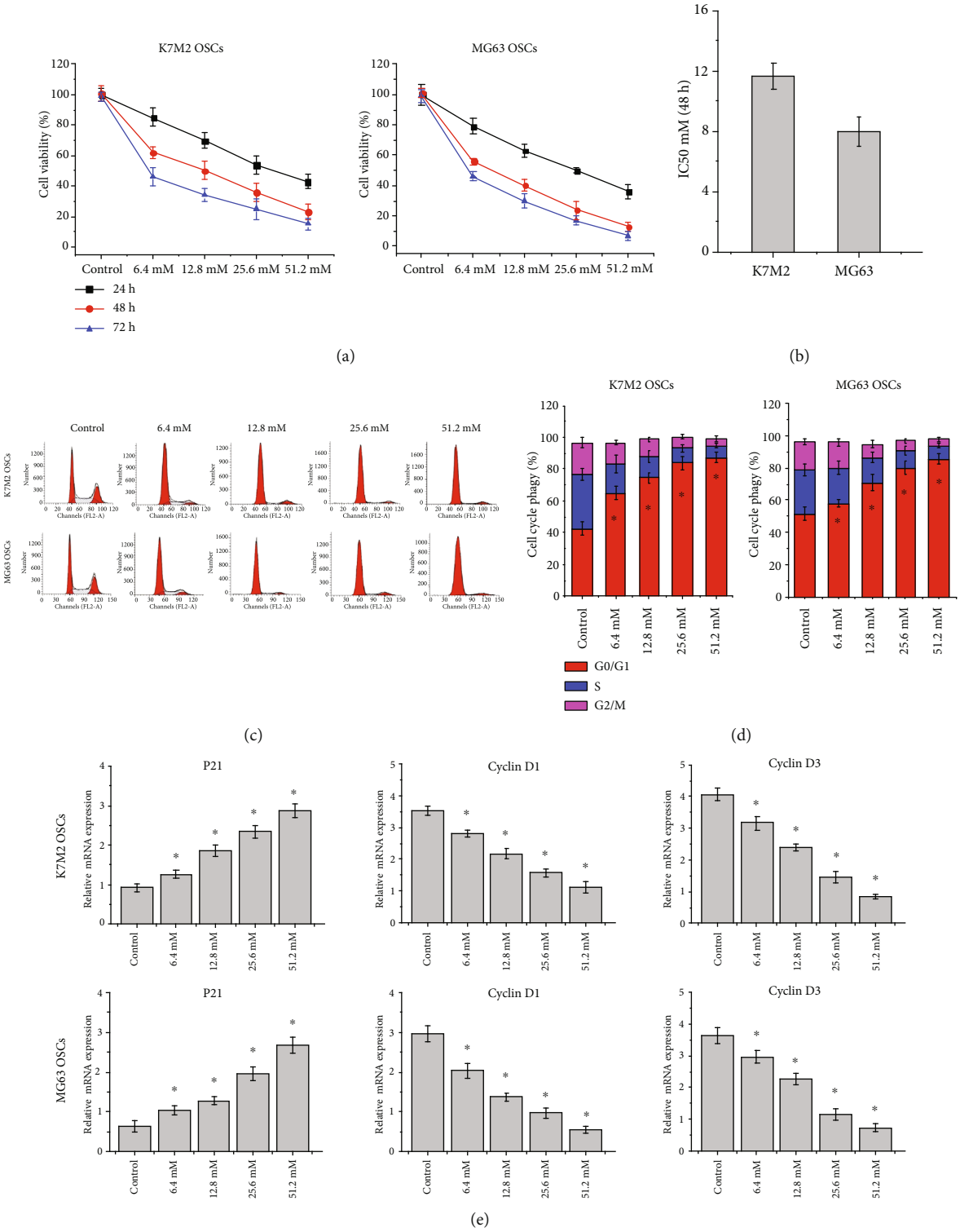

FIGURE 2: Continued.

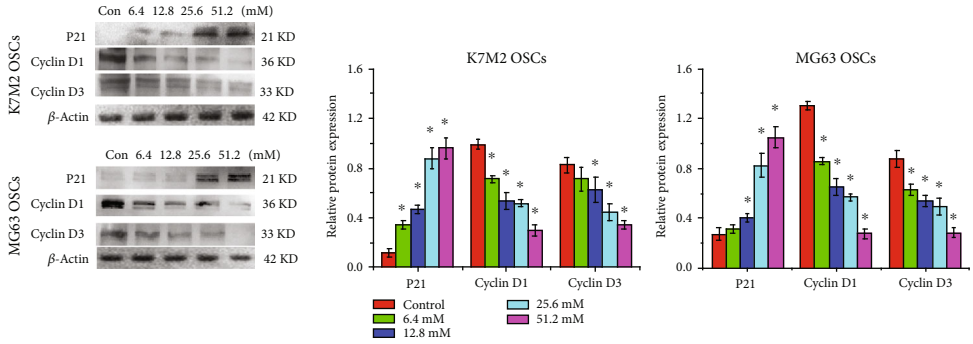

(f) (g)

Figure 2: Metformin inhibits cell proliferation and induces G0/G1 arrest in OSCs. (a) The effect of metformin on the viability of K7M2 and MG63 OSCs by CCK-8. Cells were treated with 0, 6.4, 12.8, 25.6, or 51.2 mM of metformin for 24, 48, and 72 h. $n = 3$. (b) The IC50 of metformin in K7M2 and MG63 OSCs at 48 h. $n = 3$. (c) Cell cycle progression of K7M2 and MG63 OSCs treated with metformin. $n = 3$. (d) The percentage of cell cycle distribution in metformin-treated K7M2 and MG63 OSCs. (e) The mRNA expression levels of the cell cycle regulation genes *P21*, *Cyclin D1*, and *Cyclin D3* in K7M2 and MG63 OSCs. $n = 3$. (f) Western blot analysis of the cell cycle-related proteins p21, Cyclin D1, and Cyclin D3 in K7M2 and MG63 OSCs. $n = 3$. (g) Densitometric analyses of the cell cycle-related proteins. $^*P < 0.05$ was considered statistically significant.

dependent manner following metformin treatment compared to the controls (Figures 4(a) and 4(b)). To investigate the effect of metformin on the pluripotency on the OSCs, the sphere-forming cells of K7M2 and MG63 were cultured in an osteogenic and chondrogenic induction differentiation medium with or without metformin. Osteogenesis (Figures 4(c) and 4(d)) and chondrogenesis (Figures 4(e) and 4(f)) were confirmed by the deposition of calcium and proteoglycans. The results showed that metformin reduced the pluripotency ability of the OSCs to differentiate into osteoblasts and chondrocytes in a dose-dependent manner. To further evaluate the effect of metformin on the stemness properties of the OSCs, the CSC markers CD44, CD105, CD133, and Stro-1 were also measured by flow cytometry (Figure 4(g)). As expected, the expression of CD44, CD105, CD133, and Stro-1 was downregulated in OSCs following metformin treatment in a dose-dependent manner, demonstrating that metformin may inhibit the stemness of OSCs.

3.5. Metformin Regulates Autophagy via the AMPK/mTOR Pathway. Metformin treatment resulted in a dose-dependent activation of AMPK phosphorylation (p-AMPK) in both the K7M2 OSCs (Figure 5(a)) and the MG63 OSCs (Figure 5(b)). Further investigation showed that metformin repressed the phosphorylation of mTOR (p-mTOR) and that this prolonged inactivation of mTOR and eventually induced autophagy. These results indicated that the AMPK signaling pathway might be involved in metformin-induced autophagy in K7M2 and MG63 OSCs. To further determine whether the AMPK signaling pathway is required for the induction of autophagy in response to metformin, K7M2 and MG63 OSCs were treated with an AMPK inhibitor, compound C. After treatment with 10 μM compound C for 48 h, the metformin-induced autophagy of the K7M2 OSCs (Figure 5(c)) and MG63 OSCs (Figure 5(d)) was partially attenuated. In contrast to the effects of metformin, inhibition of AMPK activated the protein expression of p-mTOR and reduced the expression of LC3. TEM images (Figure 5(e)) and immunofluorescence assay (Figure 5(f)) further illustrated that inhibition of the AMPK signaling pathway by compound C attenuated the metformin-induced autophagy of both K7M2 OSCs and MG63 OSCs. Thus, our results indicated that metformin regulated the autophagy of OSCs via the AMPK/mTOR signaling pathway.

3.6. Autophagy Regulates Homeostasis of Pluripotency in OSCs. To verify whether the metformin-mediated autophagy is associated with the pluripotency and stemness of the OSCs, K7M2 and MG63 OSCs were treated with metformin, autophagy inhibitor 3MA, and metformin together with 3MA. The autophagy inhibitor 3MA alone served as a negative control, and the autophagy inducer rapamycin served as a positive control. Following treatment, markers of autophagy, stemness, and pluripotency were detected. Our results revealed that metformin induced autophagy, while metformin+3MA significantly alleviated the metformin-induced autophagy. Treatment with 3MA, the autophagy inhibitor, decreased the number of autophagosomes while autophagy inducer rapamycin promoted the occurrence of autophagy (Figure 6(a)). In addition, immunofluorescence expression levels of LC3 were elevated in OSCs treated with metformin or rapamycin, while treatment with 3MA inhibited the expression of LC3 as shown in Figure 6(b). In addition, the expression of ALDH1 of OSCs was decreased in the OSCs in all cases, no matter if the autophagy was enhanced (rapamycin or metformin) or impaired (3MA) as shown in Figures 6(c) and 6(d). The clone formation of OSCs was also assessed by crystal violet staining (Figure 6(e)) and SEM observations (Figure 6(f)). In agreement with the above results, both inhibition and induction of autophagy blocked the clone formation of the K7M2 and MG63 OSCs. These data indicated that autophagy might play a critical role in the maintenance of pluripotency of OSCs, since the pluripotency of stem cells was mainly maintained by the networks of pluripotency-associated transcription factors such as Oct4, Sox2, and Nanog. When autophagy was enhanced, the

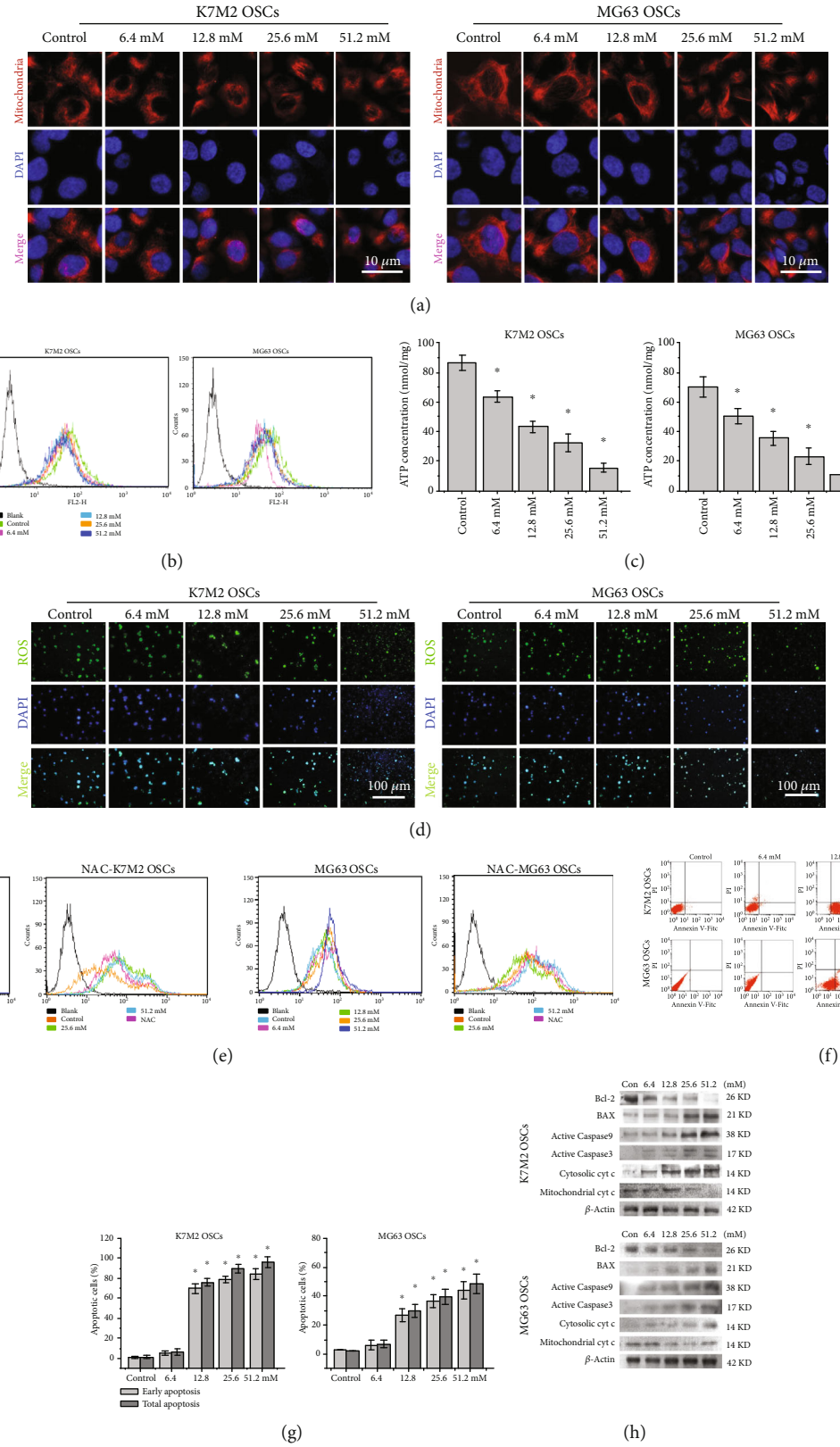

FIGURE 3: Continued.

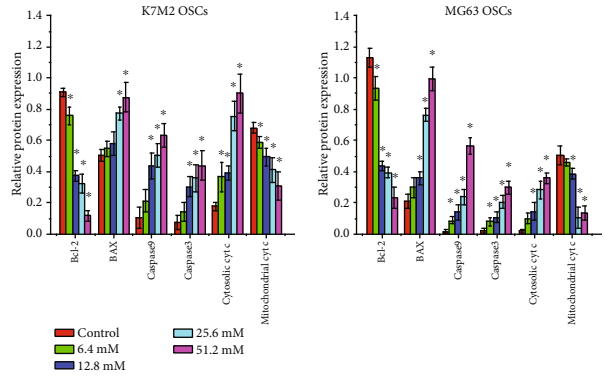

(i)

Figure 3: Metformin activates the mitochondrial pathway to induce apoptosis. (a) Confocal laser scanning microscope of the mitochondrial morphology in K7M2 and MG63 OSCs by Mito Tracker. Nuclei were counterstained with DAPI. Scale bars = 10 μm. $n = 3$. (b) Flow cytometry analysis of mitochondrial membrane potential in K7M2 and MG63 OSCs exposed to metformin. $n = 3$. (c) ATP concentrations in K7M2 and MG63 OSCs after metformin treatment for 48 h. $n = 3$. (d) Immunofluorescence analysis of ROS in K7M2 and MG63 OSCs using the DCFH-DA probe. Nuclei were counterstained with DAPI. Scale bars = 100 μm. $n = 3$. (e) Measurement of intracellular ROS in K7M2 and MG63 OSCs labeled with DCFH-DA by flow cytometry. Cells were pretreated with 10 mM of the ROS scavenger NAC to eliminate ROS. $n = 3$. (f) Annexin V-FITC/PI staining of apoptosis in metformin-mediated K7M2 and MG63 OSCs by flow cytometry. $n = 3$. (g) The percentage of OSCs in early apoptosis and total apoptosis upon treatment of metformin. (h) Western blot analysis of mitochondrial apoptotic pathway-related proteins in metformin-treated K7M2 and MG63 OSCs. $n = 3$. (i) Densitometric analyses of mitochondrial apoptotic pathway-related proteins. $^*P < 0.05$ was considered statistically significant.

degradation of pluripotency-associated transcription factors was also enhanced, whereas autophagy inhibition caused an increase of pluripotency-associated transcription factors as shown in Figures 6(g) and 6(h). Although markers of pluripotency such as Sox2 and Oct4 were enhanced in OSCs when autophagy was inhibited, the tumor sphere formation and stemness were significantly attenuated (Figures 6(c)–6(f)). Given these results, we speculated that autophagy may regulate homeostasis of pluripotency in OSCs.

3.7. Metformin Inhibits Tumor Growth and OSC Capacities in a Mouse Xenograft Model. Since 6.4 mM metformin could induce autophagy (Figure 5(a)) without causing apoptosis (Figure 3(f)) or death (Figure S2) of K7M2 OSCs, so we pretreated K7M2 OSCs with 6.4 mM metformin for 48 h to evaluate the tumorigenicity *in vivo*. As shown in Figures 7(a) and 7(b), K7M2 OSCs implanted at a cell density of 1×10^5 formed tumors in 100% of control mice, whereas the tumor formation rate was reduced to 57.14% in metformin treatment. The tumor formation rate after implantation of 1×10^4 OSCs were 85.71% in the control group and again 57.14% in the metformin-treated group. Implantation with 1000 cells resulted in a tumor formation rate of 85.71% in the control group; however, implantation at this density resulted in a sharp decrease in the tumor formation rate in the metformin-treated group to 28.57%. Moreover, metformin treatment significantly decreased the tumor volumes (Figure 7(c)) and weights (Figure 7(d)).

In order to determine whether metformin affected tumor growth *in vivo*, 1×10^5 K7M2 OSCs were introduced into mice via intratibial injection. When the tumors reached approximately 100 mm^3, the mice were randomly divided into the 5 groups described above (Figure 7(e)). After 3 weeks of treatment, the mice were executed, and the tumor tissues were stripped and weighed. Strikingly, the tumor volumes (Figure 7(f)) and tumor weights (Figure 7(g)) in all groups were significantly reduced compared with the control group. Lung metastases of the mice were also observed by visible metastatic nodules. There were significantly fewer mice with lung metastases in the metformin group than in the control group (Figure 7(h)). Metastatic nodules in the lungs were markedly decreased in the metformin-treated group (only 2 out of 6 mice) compared to the control group (4/6), indicating that metformin reduced the progression of osteosarcoma metastasis. This effect was also observed in mice treated with 3MA (1/6) and rapamycin (2/6). H&E staining of lung tissues (Figure 7(i)) further confirmed these findings that metformin- and rapamycin-induced autophagy suppressed the tumorigenicity of K7M2 OSCs *in vivo*. IHC staining (Figure 7(j)) revealed that both LC3 and ATG5 were upregulated, indicating that autophagy was induced in the tumors of mice treated with metformin compared to the control, whereas the expression of Ki67 was downregulated. Interestingly, Sox2 and Oct4 accumulated when autophagy was inhibited by 3MA and decreased when autophagy was induced by either metformin or rapamycin, which was consistent with the results *in vitro*.

4. Discussion

CSCs, also known as tumor-initiating cells, contribute to tumor initiation, progression, and metastasis [17]. The sphere formation assay is a classically widely used method to isolate and characterize CSCs [18]. Accumulating evidence has demonstrated that SP cells, which exhibit the characteristics of CSCs and are responsible for tumor metastasis and chemoradiotherapy resistance, are able to effectively exclude Hoechst 33342 dye [19]. Some pluripotent transcription

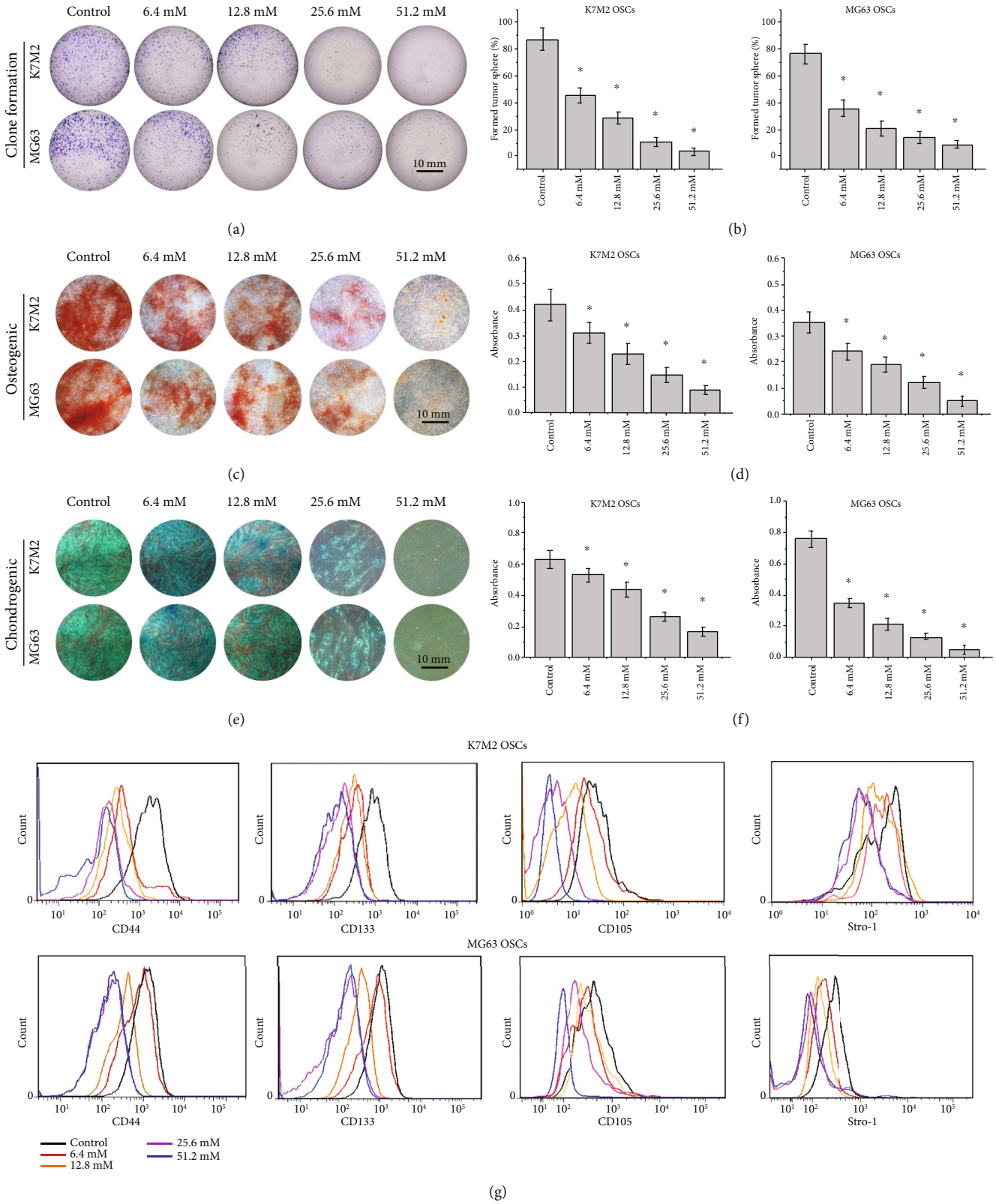

Figure 4: Metformin impairs stemness of OSCs. (a) Colony formation images of K7M2 and MG63 OSCs treated with metformin. Scale bars = 10 mm. $n = 5$. (b) Quantification of tumor spheres formed at day 7. (c) Osteogenic differentiation of K7M2 and MG63 OSCs treated with metformin. Scale bars = 10 mm. $n = 3$. (d) Semiquantification of the osteogenic differentiation capacity of K7M2 and MG63 OSCs by a spectrophotometer. (e) Chondrogenic differentiation of K7M2 and MG63 OSCs. Scale bars = 10 mm. $n = 3$. (f) Semiquantification of the chondrogenic differentiation capacity of K7M2 and MG63 OSCs by a spectrophotometer. (g) Flow cytometry of CSC surface markers CD44, CD105, CD133, and Stro-1 in K7M2 and MG63 OSCs. $n = 3$. $^*P < 0.05$ was considered statistically significant.

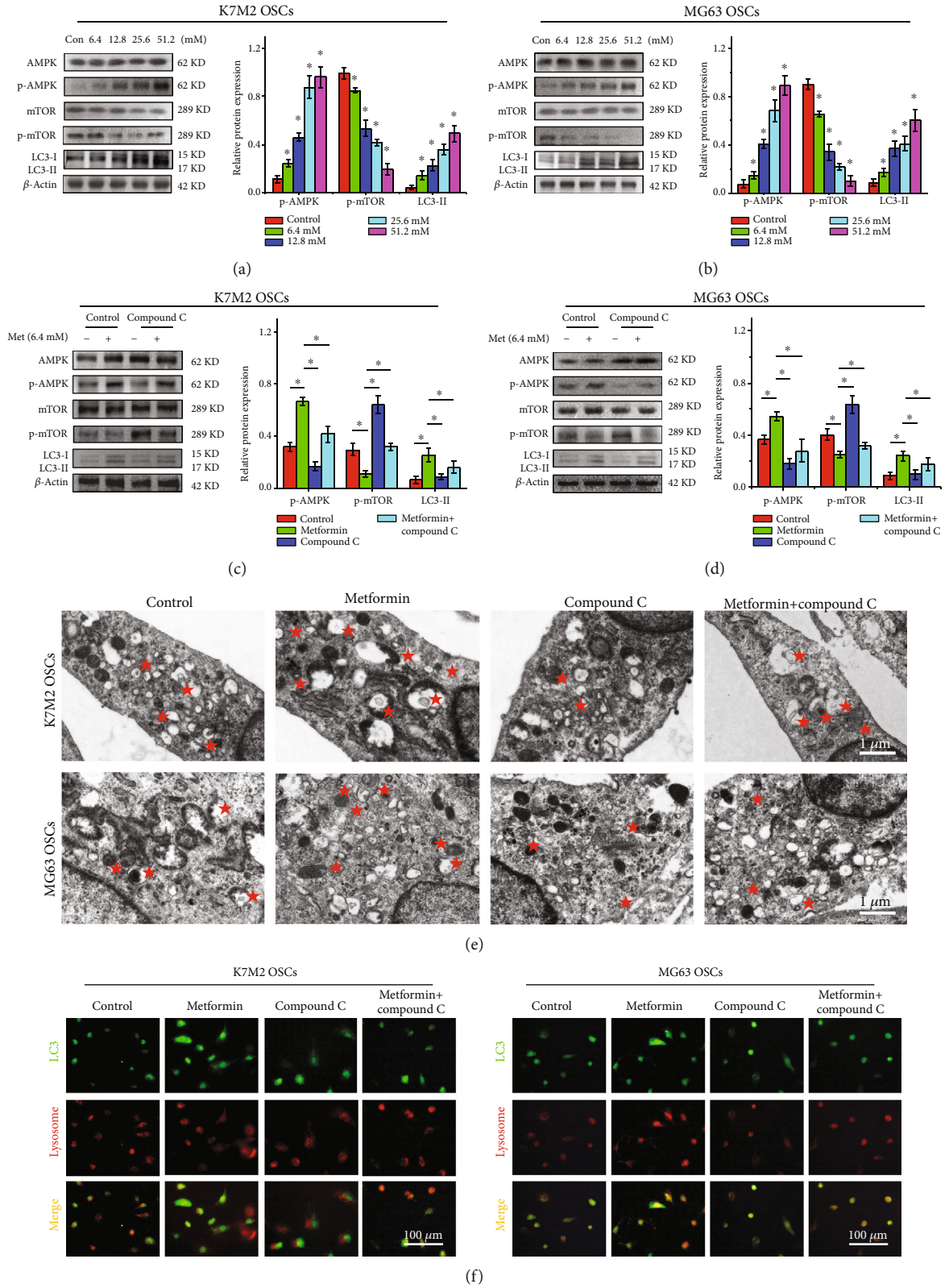

Figure 5: Metformin regulates autophagy via the AMPK/mTOR pathway. (a) Western blot analysis and (b) densitometric analyses of metformin on the AMPK pathway in K7M2 OSCs and MG63 OSCs. (c) Western blot and (d) densitometric analyses of compound C on metformin-mediated autophagy in K7M2 and MG63 OSCs. (e) TEM images of autophagosomes in the compound C-treated K7M2 and MG63 OSCs. The pentagrams stand for autophagosomes. Scale bars = 1 μm. (f) Immunofluorescence assay of autophagy in the compound C-treated K7M2 and MG63 OSCs. Scale bars = 100 μm. Each experiment was performed in triplicate. $^*P < 0.05$ was considered statistically significant.

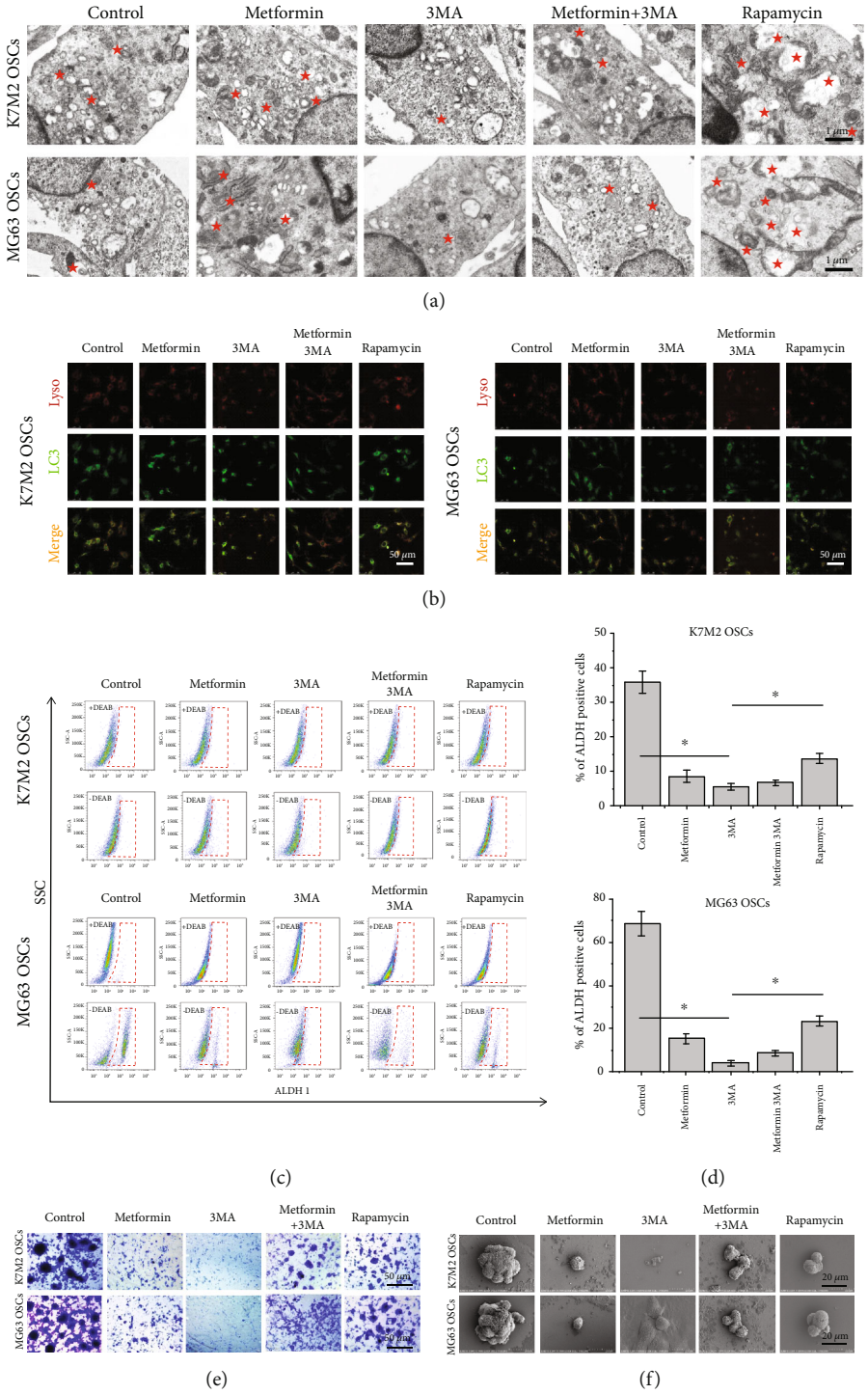

Figure 6: Continued.

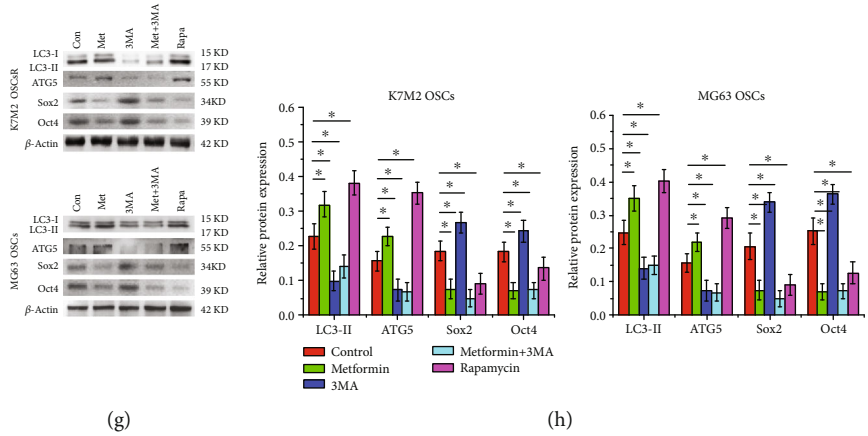

(g) (h)

Figure 6: Autophagy regulates the homeostasis of pluripotency in OSCs. (a) TEM images of autophagosomes in metformin-treated K7M2 and MG63 OSCs. The pentagrams stand for autophagosomes. Scale bars = 1 μm. (b) Immunofluorescence analysis of autophagy in K7M2 and MG63 OSCs. The colocalization (orange) staining of LC3 (green) with lysosome (red) indicates autophagy. Scale bars = 50 μm. $n = 3$. (c) Flow cytometry analysis of the effect of autophagy on ALDH1 activity. The upper panel shows that OSCs were incubated with DEAB, a specific ALDH inhibitor. The lower panel shows ALDH1-positive OSCs. $n = 3$. (d) The percentage of ALDH1-positive OSCs. (e) Clone formation of K7M2 and MG63 OSCs. Scale bars = 50 μm. $n = 5$. (f) SEM images of sphere forming of K7M2 and MG63 OSCs. Scale bars = 20 μm. $n = 3$. (g) Western blot analysis of the autophagy markers ATG5 and ATG7 and the pluripotency-associated proteins Sox2 and Oct4 in K7M2 and MG63 OSCs. $n = 3$. (h) Densitometric analyses of autophagy markers and pluripotency-associated proteins. Each experiment was conducted at least three occasions. $^*P < 0.05$ was considered statistically significant.

factors such as Oct4, Sox2, and Nanog are essential to maintain the pluripotency and self-renewal of CSCs [20]. Furthermore, similar to pluripotent transcription factors, CD44 and CD133 are other established and ubiquitous CSC surface markers [21]. ALDH1, an enzyme located in the cytoplasm and mitochondria, has been identified as a predictive marker of OSC in cancer [22]. In this study, we used both tumor sphere culture and SP analysis to evaluate the characteristic of CSCs in K7M2 and MG63 osteosarcoma cell lines. We observed that the proportion of SP cells in K7M2 and MG63 was about 1%-2%, and this was reduced to about 0% after suppression by treatment with verapamil. Furthermore, both K7M2 and MG63 could form tumor spheres when cultured in a serum-free medium. Interestingly, we found that tumor spheres derived from K7M2 and MG63 osteosarcoma cells have higher indications of stemness, and the basal autophagy flux level was higher in tumor spheres than in their parental adherent cells, which is consistent with other studies that showed that autophagy regulated the stemness of CSCs [23]. When cultured in osteogenic and chondrogenic differentiation induction media, the OSCs differentiated into osteoblast-like and chondroblast-like cells. In correlation with the above research, the isolated OSCs were also positive for Sox2, Oct4, CD133, CD105, Stro-1, and ALDH1, whereas their parental cells were not.

Metformin, the first-line pharmacotherapy for type 2 diabetes [24], has recently emerged as a potential anticancer drug [25–27]. Since anticancer effect is usually concurrent with cell growth inhibition and cell cycle arrest, cell cycle deregulation is considered to be one of the hallmarks of tumor cells [28]. The vast majority of tumor cells have been found to have alterations in the cell cycle transition from G1 to S phase, which is mediated by cyclin-dependent kinase (CDK). p21, an inhibitor of CDK2, plays a critical role in G1/S transition [29]. This study demonstrated that metformin treatment activated the expression of *P21* gene and suppressed the expression of CDK genes such as *Cyclin D1* and *Cyclin D3*, resulting in the accumulation of OSCs halted in the G0/G1 phase. This observation is in agreement with the findings of Wang et al. [30], who showed that metformin blocked cell cycle progression in myeloma cells. More recently, Bao et al. [31] found that metformin weakens the migratory and invasive capacities of osteosarcoma cells *in vitro* and *in vivo*. In correlation with these results, mice treated with metformin had a significant decrease in tumor volumes compared to control mice in our study, confirming the antitumor effect of metformin.

Apoptosis, a programmed cell death apart from necrosis, plays a pivotal role in cancer therapy [32]. It is well known that apoptosis is usually driven by mitochondrial dysfunction, which results in the loss of the mitochondrial transmembrane potential and the accumulation of intercellular endogenous ROS [33], and excess ROS can oxidize DNA, proteins, and lipids and subsequently activate caspase-mediated apoptosis [34]. We confirmed that metformin treatment triggered excessive ROS production, while pretreatment with NAC partly reversed the metformin-induced accumulation of ROS in OSCs. Particularly, the loss of the mitochondrial transmembrane potential induced an imbalance between Bcl-2 and Bax. Bax, a proapoptotic protein, translocated to mitochondria and thereby resulted in the release of cytochrome c [35]. In correlation with these results, metformin treatment induced mitochondrial dysfunction accompanied by the loss of mitochondrial transmembrane potential, as well as decreased the expression of antiapoptotic protein Bcl-2 and increased the activities of Caspase9 and Caspase3.

There is accumulating evidence demonstrating that AMPK signaling could suppress the proliferation of cancer cells and enhance their CSC properties [36]. In addition,

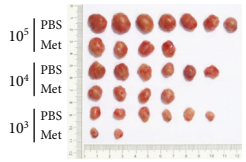

(a)

Cell numbers	PBS	Metformin
1×10^5	7/7 (100%)	4/7 (57.14%)
1×10^4	6/7 (85.71%)	4/7 (57.14%)
1×10^3	6/7 (85.71%)	2/7 (28.57%)

(b)

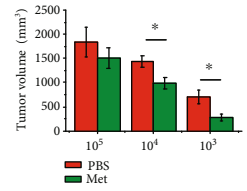

(c)

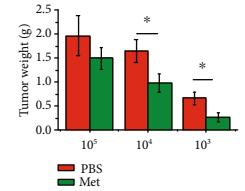

(d)

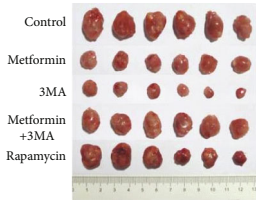

(e)

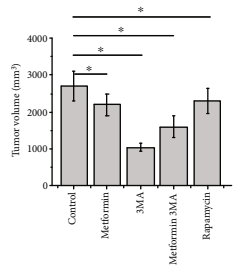

(f)

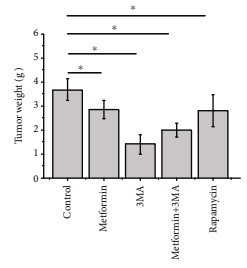

(g)

	Lung metastasis
Control	$n = 4/6$
Metformin	$n = 2/6$
3MA	$n = 1/6$
Metformin+3MA	$n = 3/6$
Rapamycin	$n = 2/6$

(h)

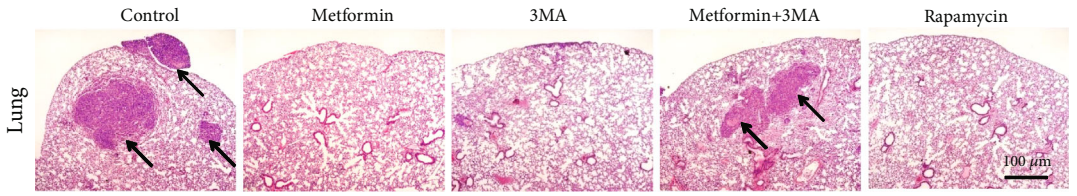

(i)

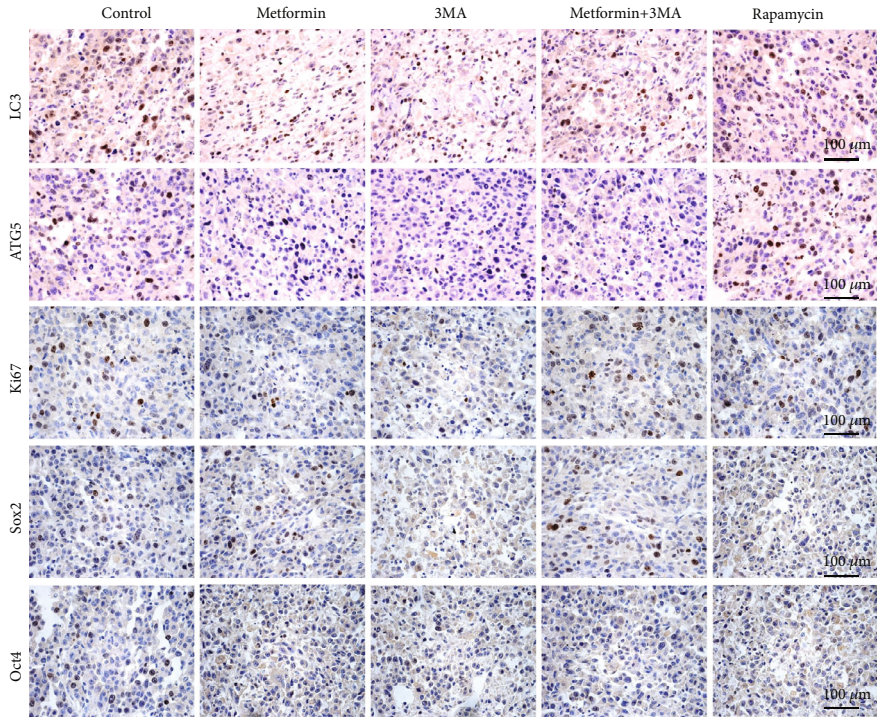

(j)

FIGURE 7: Metformin decreases K7M2 xenograft tumor growth and inhibits lung metastasis *in vivo*. (a) Metformin suppressed tumorigenicity of K7M2 OSCs *in vivo* by limited dilution assay. $n = 7$. (b) The tumor formation rate of K7M2 OSCs treated with metformin. (c) The tumor volumes and (d) tumor weights at the end of the experiments. (e) Images of resected tumor xenografts on day 21. $n = 6$. (f) The tumor volumes and (g) the tumor weights at the end of the experiments. (h) Numbers of mice with lung metastasis. (i) H&E staining of lung tissues for metastatic nodules. The arrows represent smaller tumor nodules in the lung. Scale bars = 100 μm. (j) Immunohistochemical staining of LC3, ATG5, Ki67, Sox2, and Oct4 of three different tumors from each group. Scale bars = 100 μm. $^*P < 0.05$ was considered statistically significant.

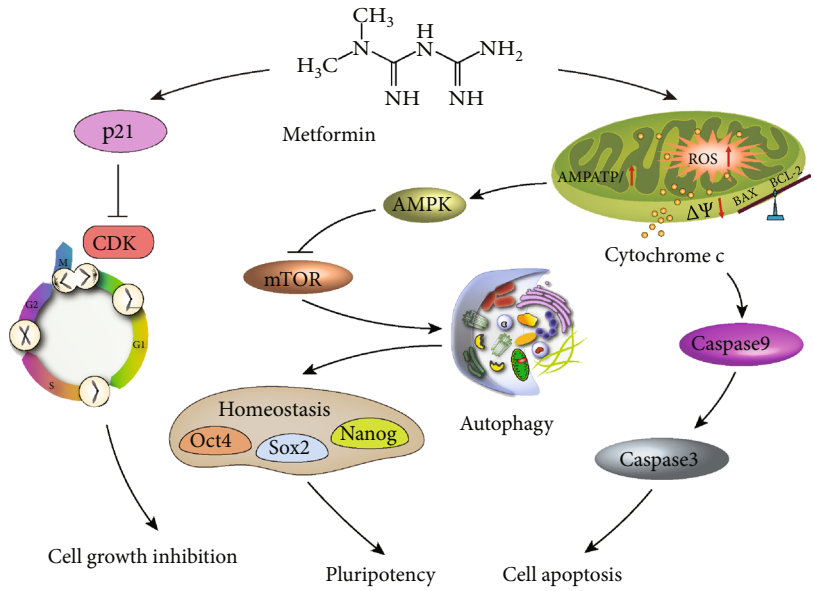

Figure 8: Proposed mechanisms of metformin on osteosarcoma. Metformin significantly induced G0/G1 phase arrest by blocking the activity of cyclin-dependent kinases. Metformin also resulted in apoptosis via a ROS-dependent mitochondrial pathway. Moreover, metformin induced autophagy via the AMPK/mTOR pathway and then disrupted the homeostasis of stemness and pluripotency of OSCs.

metformin has been known to suppress the self-renewal ability of CSCs in colorectal cancer, dependent on the relative regulation of glutamine metabolism [37]. Consistent with these findings, we showed that metformin substantially reduced the pluripotency of K7M2 and MG63 OSCs through the inhibition of ATP synthesis in mitochondria and the activation of AMPK. This is also in line with the finding that autophagy is regulated by the AMPK/mTOR pathway [38]. Moreover, the AMPK inhibitor, compound C, and the autophagy inhibitor, 3MA, were applied to study the roles of the AMPK/mTOR pathway in autophagy [39]. Our results showed that activation of AMPK inhibited the mTOR pathway, in which the autophagy seemed to be enhanced.

Autophagy, a lysosomal degradation pathway involved in the maintenance of cellular homeostasis is emerging as an attractive therapeutic target in certain types of tumors [40]. Several methods exist to induce autophagy in cells, including starvation and treatment with rapamycin [41]. In this study, we found that the autophagy markers LC3, ATG5, and ATG7 were notably increased in OSCs treated with metformin, indicating that metformin can stimulate autophagy, which is consistent with the results of Wang et al.'s study [30] in myeloma cells. Using this model, we first examined the viability of OSCs and found that it decreased upon treatment with metformin. Moreover, the expression of stem cell markers Oct4 and Sox2 was decreased when autophagy was induced by metformin or rapamycin, indicating that autophagy might help to maintain the pluripotency of OSC. Finally, we confirmed the direct influence of autophagy on the capacity of the OSCs to self-renew by suppressing autophagy with 3MA. Although the potential stem cell markers Oct4 and Sox2 were more highly expressed in cells treated with 3MA, however, the cloning capacity of OSCs was weakened. Furthermore, the metformin-mediated reduction in the number of spheres observed could be partially reversed by 3MA treatment, suggesting that autophagy is essential for the maintenance of pluripotency in OSCs. Similarly, it has been demonstrated that autophagy regulates the homeostasis of pluripotency-associated proteins in human embryonic stem cells [42], and imbalances in these proteins may lead to the loss of pluripotency in embryonic stem cells [43]. In the present study, we demonstrated for the first time that metformin suppresses self-renewal ability and tumorigenicity of OSCs by targeting autophagy, and autophagy regulates homeostasis of pluripotency of OSCs.

5. Conclusions

In conclusion, we found that treatment with metformin inhibited the proliferation of K7M2 and MG63 OSCs by inducing G0/G1 phase cell cycle arrest. In addition, metformin simultaneously triggered apoptosis in OSCs, which promoted cell death via a ROS-dependent mitochondria-mediated pathway. Strikingly, metformin significantly suppressed the self-renewal ability and tumorigenicity of OSCs by regulating autophagy, which was modulated by the AMPK/mTOR pathway (Figure 8). Taken together, these data indicated that metformin exerted antitumor effects against OSCs and that autophagy may be a promising therapeutic target for osteosarcoma.

Data Availability

The data used to support the findings of this study are available from the corresponding author upon request.

Conflicts of Interest

The authors declare that they have no conflict of interest.

Authors' Contributions

Bin Zhao, Jie Luo, and Ye Wang contributed equally to this work.

Acknowledgments

We thank LetPub (https://www.letpub.com) for its linguistic assistance during the preparation of this manuscript. We also thank Xijing Hospital of the Fourth Military Medical University for providing the BD FACS Aria III flow cytometer. This work was supported by the Science and Technology Planning Project of Shenzhen of China (JCYJ20170412140904406) and the Innovation Foundation for Doctoral Dissertation of Northwestern Polytechnical University (CX201969).

Supplementary Materials

Supplementary 1. Figure S1: flow-cytometric analysis of biomarkers in CD44, CD133, CD105, and Stro-1 between sphere-forming cells and SP cells. Both the K7M2 and MG63 OSCs were positive for CSC markers CD44, CD133, CD105, and Stro-1. Proper isotype antibodies were used as a control (black lines).

Supplementary 2. Figure S2: AO/PI staining of K7M2 OSCs. Living cells are stained with AO (green), while dead cells are with PI (red). There is no significant difference in death after metformin incubation. AO: acridine orange; PI: propidium iodide. Scale bar = 100 μm.

References

[1] X. Xiao, W. Wang, Y. Li et al., "HSP90AA1-mediated autophagy promotes drug resistance in osteosarcoma," *Journal of Experimental & Clinical Cancer Research*, vol. 37, no. 1, p. 201, 2018.

[2] D. J. Harrison, D. S. Geller, J. D. Gill, V. O. Lewis, and R. Gorlick, "Current and future therapeutic approaches for osteosarcoma," *Expert Review of Anticancer Therapy*, vol. 18, no. 1, pp. 39–50, 2018.

[3] E. Vlashi and F. Pajonk, "Cancer stem cells, cancer cell plasticity and radiation therapy," *Seminars in Cancer Biology*, vol. 31, pp. 28–35, 2015.

[4] L. Shi, X. Tang, M. Qian et al., "A SIRT1-centered circuitry regulates breast cancer stemness and metastasis," *Oncogene*, vol. 37, no. 49, pp. 6299–6315, 2018.

[5] A. Vancura, P. Bu, M. Bhagwat, J. Zeng, and I. Vancurova, "Metformin as an anticancer agent," *Trends in Pharmacological Sciences*, vol. 39, no. 10, pp. 867–878, 2018.

[6] C. Garofalo, M. Capristo, M. C. Manara et al., "Metformin as an adjuvant drug against pediatric sarcomas: hypoxia limits therapeutic effects of the drug," *PLoS One*, vol. 8, no. 12, article e83832, 2013.

[7] I. Quattrini, A. Conti, L. Pazzaglia et al., "Metformin inhibits growth and sensitizes osteosarcoma cell lines to cisplatin through cell cycle modulation," *Oncology Reports*, vol. 31, no. 1, pp. 370–375, 2014.

[8] N. Saini and X. Yang, "Metformin as an anti-cancer agent: actions and mechanisms targeting cancer stem cells," *Acta Biochimica et Biophysica Sinica*, vol. 50, no. 2, pp. 133–143, 2018.

[9] H. Y. Xu, W. Fang, Z. W. Huang et al., "Metformin reduces SATB2-mediated osteosarcoma stem cell-like phenotype and tumor growth via inhibition of N-cadherin/NF-kB signaling," *European Review for Medical and Pharmacological Sciences*, vol. 21, no. 20, pp. 4516–4528, 2017.

[10] D. Shang, J. Wu, L. Guo, Y. Xu, L. Liu, and J. Lu, "Metformin increases sensitivity of osteosarcoma stem cells to cisplatin by inhibiting expression of PKM2," *International Journal of Oncology*, vol. 50, no. 5, pp. 1848–1856, 2017.

[11] J. S. Muhammad, S. Nanjo, T. Ando et al., "Autophagy impairment by *Helicobacter pylori*-induced methylation silencing of *MAP1LC3Av1* promotes gastric carcinogenesis," *International Journal of Cancer*, vol. 140, no. 10, pp. 2272–2283, 2017.

[12] M.-F. Wei, M.-W. Chen, K.-C. Chen et al., "Autophagy promotes resistance to photodynamic therapy-induced apoptosis selectively in colorectal cancer stem-like cells," *Autophagy*, vol. 10, no. 7, pp. 1179–1192, 2014.

[13] S. C. J. Steiniger, J. A. Coppinger, J. A. Krüger, J. Yates III, and K. D. Janda, "Quantitative mass spectrometry identifies drug targets in cancer stem cell-containing side population," *Stem Cells*, vol. 26, no. 12, pp. 3037–3046, 2008.

[14] M. T. Kelleni, E. F. Amin, and A. M. Abdelrahman, "Effect of metformin and sitagliptin on doxorubicin-induced cardiotoxicity in rats: impact of oxidative stress, inflammation, and apoptosis," *Journal of Toxicology*, vol. 2015, Article ID 424813, 8 pages, 2015.

[15] X. Wu, L. He, F. Chen et al., "Impaired autophagy contributes to adverse cardiac remodeling in acute myocardial infarction," *PLoS One*, vol. 9, no. 11, article e112891, 2014.

[16] W. Wang, W. D. Jia, G. L. Xu et al., "Antitumoral activity of rapamycin mediated through inhibition of HIF-1alpha and VEGF in hepatocellular carcinoma," *Digestive Diseases and Sciences*, vol. 54, no. 10, pp. 2128–2136, 2009.

[17] F. Marcucci, P. Ghezzi, and C. Rumio, "The role of autophagy in the cross-talk between epithelial-mesenchymal transitioned tumor cells and cancer stem-like cells," *Molecular Cancer*, vol. 16, no. 1, p. 3, 2017.

[18] H. F. Bahmad, K. Cheaito, R. M. Chalhoub et al., "Sphere-formation assay: three-dimensional in vitro culturing of prostate cancer stem/progenitor sphere-forming cells," *Frontiers in Oncology*, vol. 8, p. 347, 2018.

[19] J. Liao, P. P. Liu, G. Hou et al., "Regulation of stem-like cancer cells by glutamine through β-catenin pathway mediated by redox signaling," *Molecular Cancer*, vol. 16, no. 1, p. 51, 2017.

[20] R. Baillie, S. T. Tan, and T. Itinteang, "Cancer stem cells in oral cavity squamous cell carcinoma: a review," *Frontiers in Oncology*, vol. 7, p. 112, 2017.

[21] H. Jing, C. Weidensteiner, W. Reichardt et al., "Imaging and selective elimination of glioblastoma stem cells with theranostic near-infrared-labeled CD133-specific antibodies," *Theranostics*, vol. 6, no. 6, pp. 862–874, 2016.

[22] L. Mele, D. Liccardo, and V. Tirino, "Evaluation and isolation of cancer stem cells using ALDH activity assay," *Cancer Stem Cells*, vol. 1692, pp. 43–48, 2018.

[23] Y. Yang, L. Yu, J. Li et al., "Autophagy regulates the stemness of cervical cancer stem cells," *Biologics: Targets and Therapy*, vol. 11, pp. 71–79, 2017.

[24] S. C. Palmer and G. F. M. Strippoli, "Metformin as first-line treatment for type 2 diabetes," *The Lancet*, vol. 392, no. 10142, p. 120, 2018.

[25] D. Jin, J. Guo, D. Wang et al., "The antineoplastic drug metformin downregulates YAP by interfering with IRF-1 binding to the *YAP* promoter in NSCLC," *EBioMedicine*, vol. 37, pp. 188–204, 2018.

[26] T. Uehara, S. Eikawa, M. Nishida et al., "Metformin induces $CD11b^+$-cell-mediated growth inhibition of an osteosarcoma: implications for metabolic reprogramming of myeloid cells and anti-tumor effects," *International Immunology*, vol. 31, no. 4, pp. 187–198, 2019.

[27] Z. Li, L. Wang, N. Luo et al., "Metformin inhibits the proliferation and metastasis of osteosarcoma cells by suppressing the phosphorylation of Akt," *Oncology Letters*, vol. 15, no. 5, pp. 7948–7954, 2018.

[28] J. Yu, D. Liu, X. Sun et al., "CDX2 inhibits the proliferation and tumor formation of colon cancer cells by suppressing Wnt/β-catenin signaling via transactivation of GSK-3β and Axin2 expression," *Cell Death & Disease*, vol. 10, no. 1, p. 26, 2019.

[29] A. Deshpande, P. Sicinski, and P. W. Hinds, "Cyclins and cdks in development and cancer: a perspective," *Oncogene*, vol. 24, no. 17, pp. 2909–2915, 2005.

[30] Y. Wang, W. Xu, Z. Yan et al., "Metformin induces autophagy and G0/G1 phase cell cycle arrest in myeloma by targeting the AMPK/mTORC1 and mTORC2 pathways," *Journal of Experimental & Clinical Cancer Research*, vol. 37, no. 1, p. 63, 2018.

[31] X. Bao, L. Zhao, H. Guan, and F. Li, "Inhibition of LCMR1 and ATG12 by demethylation-activated miR-570-3p is involved in the anti-metastasis effects of metformin on human osteosarcoma," *Cell Death & Disease*, vol. 9, no. 6, p. 611, 2018.

[32] M. Hassan, H. Watari, A. AbuAlmaaty, Y. Ohba, and N. Sakuragi, "Apoptosis and molecular targeting therapy in cancer," *BioMed Research International*, vol. 2014, Article ID 150845, 23 pages, 2014.

[33] Y. Li, L. Zhang, T. Qu, X. Tang, L. Li, and G. Zhang, "Conservation and divergence of mitochondrial apoptosis pathway in the Pacific oyster, *Crassostrea gigas*," *Cell Death & Disease*, vol. 8, no. 7, article e2915, 2017.

[34] Y. F. Chen, H. Liu, X. J. Luo et al., "The roles of reactive oxygen species (ROS) and autophagy in the survival and death of leukemia cells," *Critical Reviews in Oncology/Hematology*, vol. 112, pp. 21–30, 2017.

[35] A. Pena-Blanco and A. J. Garcia-Saez, "Bax, Bak and beyond — mitochondrial performance in apoptosis," *The FEBS Journal*, vol. 285, no. 3, pp. 416–431, 2018.

[36] K. de Veirman, E. Menu, K. Maes et al., "Myeloid-derived suppressor cells induce multiple myeloma cell survival by activating the AMPK pathway," *Cancer Letters*, vol. 442, pp. 233–241, 2019.

[37] J. H. Kim, K. J. Lee, Y. Seo et al., "Effects of metformin on colorectal cancer stem cells depend on alterations in glutamine metabolism," *Scientific Reports*, vol. 8, no. 1, p. 409, 2018.

[38] S. Jiang, T. Li, T. Ji et al., "AMPK: potential therapeutic target for ischemic stroke," *Theranostics*, vol. 8, no. 16, pp. 4535–4551, 2018.

[39] X. Li, D. Roife, Y. Kang, B. Dai, M. Pratt, and J. B. Fleming, "Extracellular lumican augments cytotoxicity of chemotherapy in pancreatic ductal adenocarcinoma cells via autophagy inhibition," *Oncogene*, vol. 35, no. 37, pp. 4881–4890, 2016.

[40] Q. Meng, J. Xu, C. Liang et al., "GPx1 is involved in the induction of protective autophagy in pancreatic cancer cells in response to glucose deprivation," *Cell Death & Disease*, vol. 9, no. 12, p. 1187, 2018.

[41] C. Liu, E. P. DeRoo, C. Stecyk, M. Wolsey, M. Szuchnicki, and E. G. Hagos, "Impaired autophagy in mouse embryonic fibroblasts null for Krüppel-like factor 4 promotes DNA damage and increases apoptosis upon serum starvation," *Molecular Cancer*, vol. 14, no. 1, p. 101, 2015.

[42] Y. H. Cho, K. M. Han, D. Kim et al., "Autophagy regulates homeostasis of pluripotency-associated proteins in hESCs," *Stem Cells*, vol. 32, no. 2, pp. 424–435, 2014.

[43] Z. Wang, E. Oron, B. Nelson, S. Razis, and N. Ivanova, "Distinct lineage specification roles for NANOG, OCT4, and SOX2 in human embryonic stem cells," *Cell Stem Cell*, vol. 10, no. 4, pp. 440–454, 2012.

Hindawi
Oxidative Medicine and Cellular Longevity
Volume 2019, Article ID 8201079, 14 pages
https://doi.org/10.1155/2019/8201079

Review Article

Dichloroacetate (DCA) and Cancer: An Overview towards Clinical Applications

Tiziana Tataranni[1] **and Claudia Piccoli**[1,2]

[1]*Laboratory of Pre-Clinical and Translational Research, IRCCS-CROB, Referral Cancer Center of Basilicata, Rionero in Vulture (Pz), 85028, Italy*
[2]*Department of Clinical and Experimental Medicine, University of Foggia, Foggia 71121, Italy*

Correspondence should be addressed to Tiziana Tataranni; tiziana.tataranni@crob.it

Received 24 July 2019; Revised 12 September 2019; Accepted 11 October 2019; Published 14 November 2019

Guest Editor: Kanhaiya Singh

An extensive body of literature describes anticancer property of dichloroacetate (DCA), but its effective clinical administration in cancer therapy is still limited to clinical trials. The occurrence of side effects such as neurotoxicity as well as the suspicion of DCA carcinogenicity still restricts the clinical use of DCA. However, in the last years, the number of reports supporting DCA employment against cancer increased also because of the great interest in targeting metabolism of tumour cells. Dissecting DCA mechanism of action helped to understand the bases of its selective efficacy against cancer cells. A successful coadministration of DCA with conventional chemotherapy, radiotherapy, other drugs, or natural compounds has been tested in several cancer models. New drug delivery systems and multiaction compounds containing DCA and other drugs seem to ameliorate bioavailability and appear more efficient thanks to a synergistic action of multiple agents. The spread of reports supporting the efficiency of DCA in cancer therapy has prompted additional studies that let to find other potential molecular targets of DCA. Interestingly, DCA could significantly affect cancer stem cell fraction and contribute to cancer eradication. Collectively, these findings provide a strong rationale towards novel clinical translational studies of DCA in cancer therapy.

1. Introduction

Cancer is one of the leading causes of death worldwide. Despite the significant progression in diagnostic and therapeutic approaches, its eradication still represents a challenge. Too many factors are responsible for therapy failure or relapse, so there is an urgent need to find new approaches to treat it. Apart from the typical well-known properties featuring malignant cells, including abnormal proliferation, deregulation of apoptosis, and cell cycle [1, 2], cancer cells also display a peculiar metabolic machine that offers a further promising approach for cancer therapy [3–5]. Our group had already suggested the importance of a metabolic characterization of cancer cells to predict the efficacy of a metabolic treatment [6]. Drugs able to affect cancer metabolism are already under consideration, showing encouraging results in terms of efficacy and tolerability [7]. In the last decade, the small molecule DCA, already used to treat acute and chronic lactic acidosis, inborn errors of mitochondrial metabolism, and diabetes [8], has been largely purposed as an anticancer drug. DCA is a 150 Da water-soluble acid molecule, analog of acetic acid in which two of the three hydrogen atoms of the methyl group have been replaced by chlorine atoms (Figure 1(a)) [9]. DCA administration in doses ranging from 50 to 200 mg/Kg/die is associated to a decrease of tumour mass volume, proliferation rate, and metastasis dissemination in several preclinical models [10]. Our group had already observed an inverse correlation between DCA ability to kill cancer cells and their mitochondrial respiratory capacity in oral cell carcinomas [11]. Moreover, we recently described DCA ability to affect mitochondrial function and retarding cancer progression in a pancreatic cancer model [12]. To date, consistent data from clinical trials and case reports describing DCA administration in cancer patients are available [13–16], but, despite the growing body of literature sustaining the efficacy of

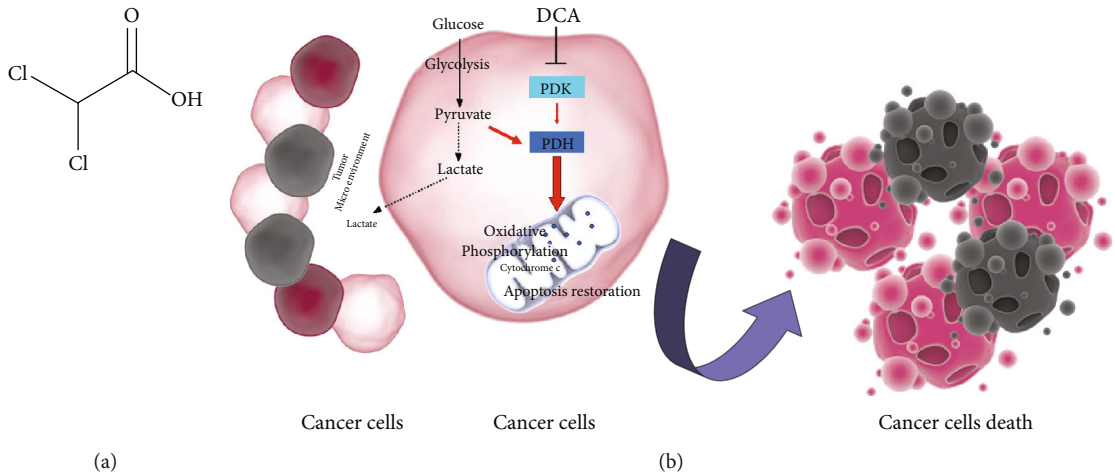

Figure 1: (a) Chemical structure of DCA. (b) Mechanism of action of DCA: PDK: pyruvate dehydrogenase kinase; PDH: pyruvate dehydrogenase. Black dotted lines, biochemical processes inhibited by DCA; Red arrows, metabolic pathways activated by DCA.

DCA against cancer, it is not under clinical use yet. This review is aimed at summarizing the very recent reports suggesting the employment of DCA in cancer therapy, in combination with chemotherapy agents, radiotherapy, and other chemical or natural compounds showing anticancer properties. Moreover, we described data about new purposed pharmacological formulations of DCA able to avoid side effects and ameliorate drug bioavailability and efficacy, further encouraging its possible clinical employment. Finally, we reviewed latest findings suggesting other potential mechanisms of action of DCA, including new data about its aptitude to affect cancer stem cell fraction.

2. DCA and Cancer: Mechanism of Action

The potential efficacy of DCA in cancer therapy comes from metabolic properties of cancer cells, typically characterized by increased glycolytic activity and reduced mitochondrial oxidation, regardless of oxygen availability, the well-known Warburg effect [17]. The excessive glycolysis and the resulting lactate overproduction provoke a state of metabolic acidosis in tumour microenvironment [18]. Glycolysis-derived lactate is taken up by surrounding cells to support tumour growth and inhibits apoptotic cell death mechanisms [19, 20]. Several enzymes involved in glycolysis regulate apoptosis, and their overexpression in cancer cells contributes to apoptosis suppression [21]. In this setting, salts of DCA selectively target cancer cells shifting their metabolism from glycolysis to oxidative phosphorylation by inhibition of pyruvate dehydrogenase kinase (PDK), the inhibitor of pyruvate dehydrogenase (PDH) [10]. PDH activation fosters mitochondrial oxidation of pyruvate and disrupts the metabolic advantage of cancer cells. Mitochondrial DNA mutations, often occurring in tumorigenesis and resulting in respiratory chain dysfunction [22, 23], make malignant cells unable to sustain cellular energy demand. Furthermore, reducing lactate production, DCA counteracts the acidosis state of tumour microenvironment, contributing to the inhibition of tumour growth and dissemination [24]. The delivery of pyruvate into mitochondria causes organelles remodelling resulting in an increased efflux of cytochrome c and other apoptotic-inducing factors and upregulation of ROS levels with a consequent reduction of cancer cell viability [9] (Figure 1(b)).

3. Side Effects and Limitations to DCA Employment

Clinical employment of DCA is available in both oral and parenteral formulations, and doses range from 10 to 50 mg/Kg/die [25]. No evidence of severe hematologic, hepatic, renal, or cardiac toxicity confirms DCA safety [26]. Common gastrointestinal side effects often occur in a percentage of patients treated with DCA [15]. The best-known limitation to DCA administration, observed both in preclinical and in clinical studies, is peripheral neuropathy [27]. The selectivity of DCA-induced damage for the nervous system may be due to the lack of well-equipped machinery able to handle a more sustained oxidative phosphorylation in cells producing ATP mostly via glycolysis [28]. The resulting mitochondrial overload compromises the antioxidant systems' efficiency, unable to face the excessive amount of ROS. In this setting, the contemporary administration of antioxidants should represent a further strategy to minimize DCA-induced neuropathy [27]. The expression and the activity of glutathione transferase zeta1 (GSTZ1), the first enzyme responsible for DCA clearance, may influence the entity of damage. Nonsynonymous functional single-nucleotide polymorphisms (SNPs) in human GSTZ1 gene give rise to different haplotypes that are responsible for a different DCA kinetic and dynamics. A clear association between GSTZ1 haplotype and DCA clearance has been demonstrated. On this basis, a personalized DCA dosage, not only based on body weight, may minimize or prevent adverse effects in patients chronically treated with this drug [29]. The occurrence of neuropathy is associated to DCA chronic oral administration and is a reversible effect, limited to the time of treatment [30]. The intravenous route reduces,

therefore, the potential for neurotoxicity and let the achievement of higher drug concentrations bypass the digestive system [13].

Since DCA is among water disinfection by-products found in low concentrations in drinking water, its potential carcinogenicity is under evaluation. Studies performed in mouse models associate DCA early-life exposure to an increased incidence of hepatocellular tumours [31]. It is conceivable that persistent changes in cell metabolism induced by DCA may produce epigenetic effects. Long-term induction of PDH and other oxidative pathways related to glucose metabolism could contribute to increase reactive oxygen species and mitochondrial stress [27]. However, no evidence of carcinogenetic effect is reported in clinical studies, when DCA is administered in cancer therapy.

4. Synergistic Effect of DCA and Chemotherapeutic Agents

Combining different drugs is a well-accepted strategy to produce a synergistic beneficial effect in cancer therapy, reducing drug dosage, minimizing toxicity risks, and overcoming drug resistance. Coadministration of DCA and traditional chemotherapeutic agents has been purposed and tested in several cancer models (Table 1). DCA treatment seems to improve the efficacy of chemotherapy by inducing biochemical and metabolic alterations, resulting in significant changes of cancer cells' energetic balance. A study performed in non-small-cell lung cancer (NSCLC) showed both *in vitro* and *in vivo* that coadministration of DCA with paclitaxel increased the efficiency of cell death through autophagy inhibition [32]. An effective combination of DCA and doxorubicin (DOX) was tested in HepG2 cells, demonstrating the ability of DCA to disrupt cellular antioxidant defences, thus favouring oxidative damage in turn triggered by DOX treatment [33]. There is a strong association between PDK overexpression and chemoresistance; thus, it is conceivable that PDK inhibition might help to resensitize cancer cells to drugs. PDK2 isoform overexpression was associated to paclitaxel resistance in NSCLC. Interestingly, DCA combination with paclitaxel was more effective in killing resistant cells than either paclitaxel or DCA treatment alone [34]. Similarly to NSCLC, an interesting *in vivo* study performed in advanced bladder cancer showed an increased expression of PDK4 isoform in high grade compared to lower-grade cancers and cotreatment of DCA and cisplatin dramatically reduced tumour volumes as compared to either DCA or cisplatin alone [35]. A recent study confirmed the ability of DCA to revert PDK4-related chemoresistance also in human hepatocellular carcinoma (HCC) [36].

5. Synergistic Effect of DCA and Other Potential Anticancer Drugs

A consistent body of literature suggests positive effects of DCA coadministration with compounds currently employed to treat other diseases but showing anticancer properties in several cancer models (Table 2). Contemporary administration of DCA and the antibiotic salinomycin, recently rediscovered for its cytotoxic properties as a potential anticancer drug, has been tested in colorectal cancer cell lines. Their treatment seems to exert a synergistic cytotoxic effect by inhibiting the expression of proteins related to multidrug resistance [37]. Cancer cells lacking metabolic enzymes involved in arginine metabolism may result to sensitivity to arginase treatment. Interestingly, a combined administration of recombinant arginase and DCA produces antiproliferative effects in triple-negative breast cancer, due to the activation of p53 and the induction of cell cycle arrest [38]. COX2 inhibitors, primarily used as anti-inflammatory drugs, have been recently suggested as antitumor drugs because of their antiproliferative activity. An intriguing study performed in cervical cancer cells showed the inability of DCA to kill cervical cancer cells overexpressing COX2 and demonstrated that COX2 inhibition by celecoxib makes cervical cancer cells more sensitive to DCA both *in vitro* and *in vivo* experiments [39]. Since DCA fosters oxidative phosphorylation by decreasing glycolytic activity, the combination of DCA with other drugs enhancing a state of glucose dependence may be a promising strategy. Such an approach has been tested in head and neck cancer in which the administration of propranolol, a nonselective beta-blocker able to affect tumour cells' mitochondrial metabolism, produced glycolytic dependence and energetic stress, making cells more vulnerable to DCA treatment [40]. Similar results were obtained in melanoma cells in which the administration of retinoic acid receptor β (RARβ) inhibitors confer sensitization to DCA [41]. A positive effect of DCA coadministration with metformin, a hypoglycaemic drug widely used to treat diabetes was demonstrated in a preclinical model of glioma [42] as well as in a low metastatic variant of Lewis lung carcinoma (LLC) [43]. Jiang and colleagues investigated the effects of phenformin, a metformin analog, and DCA in glioblastoma, demonstrating that contemporary inhibition of complex I and PDK by phenformin and DCA, respectively, decreased self-renewal and viability of glioma stem cells (GSCs), thus suggesting their possible employment to affect cancer stem cell fraction [44].

6. Combined Use of DCA and Natural Compounds

The clinical employment of natural compounds represents a promising novel approach to treat several diseases [45]. An increasing body of literature supports the detection, among natural compounds, of biologically active substances isolated by plants, mushrooms, and bacteria or marine organism that show beneficial effects for human health [46–48]. The assumption of natural compounds or their derivatives seems to represent an encouraging approach to prevent cancer initiation or recurrence, and it is generally called chemoprevention [49]. Moreover, natural substances produce beneficial effects in cancer therapy when coadministered with other drugs, showing their ability to overcome drug resistance, to increase anticancer potential, and to reduce drug doses and toxicity [50, 51]. Interestingly, the coadministration of DCA and natural compounds has been recently purposed. A study investigated the combined

Table 1: List of reports suggesting beneficial effect of DCA and chemotherapy coadministration in several types of cancers.

Tumour entity	Model system	Chemotherapy drug coadministered with DCA	Mechanism of action	Outcome	References
Lung cancer	A549-H1975 cell lines/ xenograft model	Paclitaxel	Autophagy inhibition	Efficacious cancer chemotherapy sensitization	[32]
Hepatocarcinoma	HepG2 cell line	Doxorubicin	Antioxidant defence disruption	Increased cellular damage by oxidative stress induction	[33]
Lung cancer	A549 cell line	Paclitaxel	Increased chemosensitivity through PDK2 inhibition	Paclitaxel resistance overcome	[34]
Bladder cancer	HTB-9, HT-1376, HTB-5, HTB-4 cell lines/xenograft model	Cisplatin	Increased chemosensitivity through PDK4 inhibition	Increased cell death of cancer cells and potential therapeutic advantage	[35]
Hepatocarcinoma	Sphere cultures from HepaRG and BC2 cell lines	Cisplatin, sorafenib	Increased chemosensitivity through PDK4 inhibition	Improved therapeutic effect of chemotherapy by mitochondrial activity restoration	[36]

Table 2: List of drugs with their main function tested in combination with DCA in several cancer models.

Drug	Main function	Tumour entity	Model system	Outcome	References
Salinomycin	Antibiotic	Colorectal cancer	DLD-1 and HCT116 cell lines	Inhibition of multidrug resistance-related proteins	[37]
Arginase	Arginine metabolism	Breast cancer	MDA-MB231 and MCF-7/ xenograft model	Antiproliferative effect due to p53 activation and cell cycle arrest	[38]
COX2 inhibitors	Inflammation	Cervical cancer	HeLa and SiHa cell lines/ xenograft model	Cancer cell growth suppression	[39]
Propranolol	Beta-blocker	Head and neck cancer	mEERL and MLM3 cell lines/C57Bl/6 mice	Glucose dependence promotion and enhancement of chemoradiation effects	[40]
RARβ inhibitors	Vitamin A metabolism	Melanoma	ED-007, ED-027, ED-117, and ED196 cell lines	Glucose dependence promotion and sensitization to DCA	[41]
Metformin	Diabetes	Glioma, Lewis lung carcinoma	Xenograft model; LLC/R9 cells	Prolonged lifespan of mice with glioma; severe glucose dependency in tumour microenvironment	[42, 43]
Phenformin	Diabetes	Glioblastoma	Glioma stem cells/xenograft model	Self-renewal inhibition of cancer stem cells	[44]

effect of DCA with essential oil-blended curcumin, a compound with beneficial properties both in prevention and treatment of cancer [52], demonstrating an anticancer potential against HCC [53]. In particular, the combination of both compounds synergistically reduced cell survival, promoting cell apoptosis and inducing intracellular ROS generation. Betulin, a natural compound isolated from birch bark, is already known for its antiproliferative and cytotoxic effects against several cancer cell lines [54–56]. An *in vitro* investigation of the antitumor activity of betulin derivatives in NSCLC confirmed its ability to inhibit *in vivo* and *in vitro* growth of lung cancer cells, blocking G2/M phase of the cell cycle and inducing caspase activation and DNA fragmentation. Interestingly, betulin derivative Bi-L-RhamBet was able to perturb mitochondrial electron transport chain (ETC), inducing ROS production. Given the property of DCA to increase the total oxidation of glucose in mitochondria via the Krebs cycle and ETC, the authors combined Bi-L-RhamBet with DCA, demonstrating its significant potentiated cytotoxicity [57].

7. DCA and Radiosensitization

Radiotherapy represents a further strategy to treat cancer and provides a local approach by the administration of high-energy rays [58]. The main effect of radiation is the induction of ROS with a consequent DNA damage, chromosomal instability, and cell death by apoptosis [59]. However, several tumours show or develop radioresistance that is responsible for radiotherapy failure and high risk of tumour recurrence or metastasis [60]. Several factors may be responsible of radioresistance [61]. Among these, hypoxia, a common condition of tumour microenvironment characterized by low oxygen levels and reduced ROS species generation, can block the efficacy of ionizing radiations [62]. Increasing tumour oxygenation so to favour a considerable amount of ROS [63] or directly induce ROS production may therefore represent a strategy to increase radiosensitization [64, 65]. In this setting, DCA administration, known to induce ROS production [11, 66], could represent a strategy to overcome tumour radioresistance. Moreover, metabolic alterations featuring cancer development are known to affect radiosensitivity [67, 68]. Therefore, targeting cancer metabolic intermediates may represent a strategy to improve a selective cancer response to irradiation [69]. The efficacy of DCA to increase radiation sensitivity has been already demonstrated both in glioblastoma cells [70] and in oesophageal squamous cell carcinoma [71]. More recently, it was demonstrated that DCA increases radiosensitivity in a cellular model of medulloblastoma, a fatal brain tumour in children, inducing alterations of ROS metabolism and mitochondrial function and suppressing DNA repair capacity [72]. Since the role of immunotherapy in the restoration of the immune defences against tumour progression and metastasis is arousing great attention in the last years [73], Gupta and Dwarakanath provided a state of the art of the possible effects of glycolytic inhibitors, including DCA, on tumour radiosensitization, focusing their attention on the interplay between metabolic modifiers and immune modulation in the radiosensitization processes [74]. Interestingly, they reported the ability of DCA to promote immune stimulation through the inhibition of lactate accumulation, further sustaining its utilization as adjuvant of radiotherapy.

8. DCA and New Drug Formulations

There is a growing interest in designing new drug formulations so to improve drug delivery, increasing the efficacy and reducing the doses and consequently undesirable effects. In this setting, drug delivery systems (DDSs) represent a new frontier in the modern medicine [75]. DDSs offer the possibility to create a hybrid of metal-organic frameworks (MOFs), combining the biocompatibility of organic system to the high loadings of inorganic fraction [76]. Several lines of evidence suggest an efficient functionalization of nanoparticles with DCA. Lazaro and colleagues [77] explored different protocols for DCA functionalization of the zirconium (Zr) terephthalate (UiO-66) nanoparticles. They demonstrated the cytotoxicity and selectivity of the same DDSs against different cancer cell lines. Moreover, they excluded a possible response of the immune system to DCA-MOF *in vitro*. The same group later showed the possibility to load Zr MOFs with a second anticancer drug, such as 5-fluorouracil (5-FU), so to reproduce the synergistic effect of the two drugs [78]. Zirconium-based MOF loaded with DCA was also purposed as an attractive alternative to UiO-66, showing selective *in vitro* cytotoxicity towards several cancer cell lines and a good toleration by the immune system of several species [79]. Recently, Štarha et al. [80] synthesized and characterized, for the first time, half-sandwich complexes containing ruthenium or osmium and DCA (Figure 2(a)). Both Ru-dca and Os-DCA complexes were screened in ovarian carcinoma cell lines, demonstrating to be more cytotoxic than cisplatin alone. Both complexes were able to induce cytochrome c (Cytc) release from mitochondria, an indirect index of apoptosome activation and seemed to be less toxic towards healthy primary human hepatocytes, thus indicating selectivity for cancer over noncancerous cells. Promising results were also obtained in triple-negative breast cancer cells [81]. Rhenium (I)-DCA conjugate has demonstrated an efficient penetration into cancer cells and a selective accumulation into mitochondria, inducing mitochondrial dysfunction and metabolic disorders [82]. In the recent years, several multiactive drugs have been designed to contemporary target different intracellular pathways using a single formulation. A safe, simple, reproducible nanoformulation of the complex doxorubicin-DCA (Figure 2(b)) was successfully tested in a murine melanoma model, showing an increase in drug-loading capability, lower side effects, and enhanced therapeutic effect [83]. Dual-acting antitumor Pt (IV) prodrugs of kiteplatin with DCA axial ligands have been synthesized (Figure 2(c)), characterized, and tested in different tumour cell lines and *in vivo* [84]. To overcome cancer resistance, triple action Pt (IV) derivatives of cisplatin have been proposed as new potent anticancer agents, able to conjugate the action of cisplatin, cyclooxygenase inhibitors, and DCA (Figure 2(d)) [85]. A

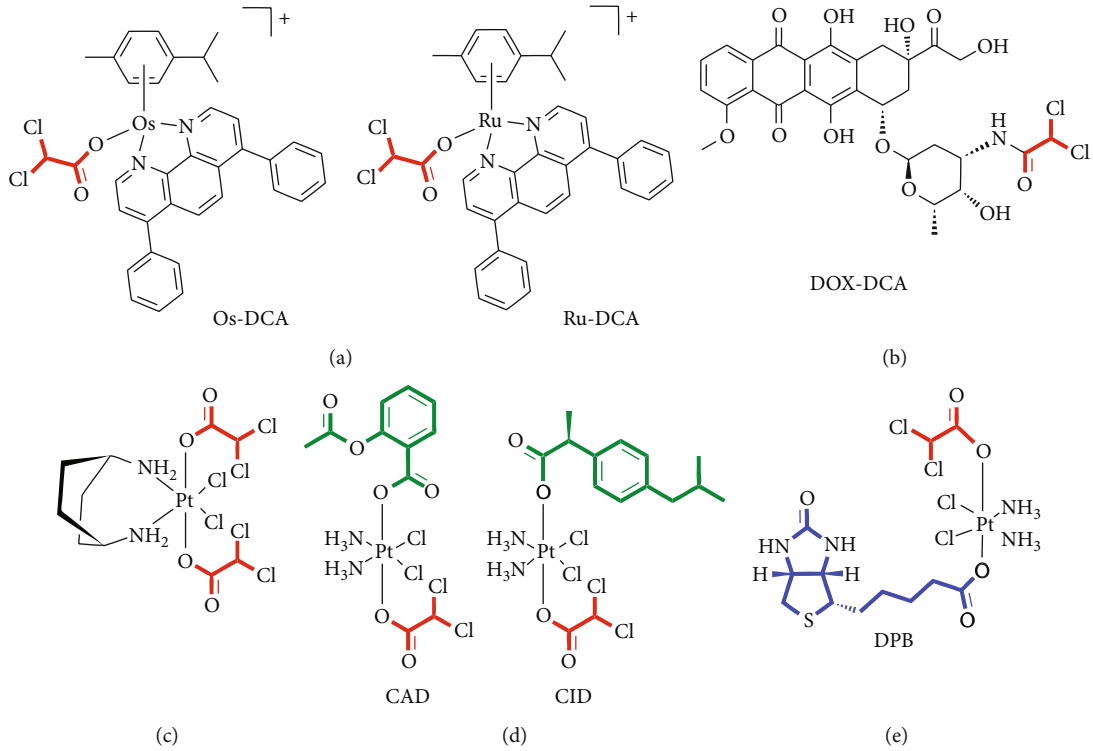

Figure 2: New drug formulations containing DCA. (a) Schematic representation of Os-DCA and Ru-DCA complexes [81]. (b) Doxorubicin (DOX)-DCA complex [83]. (c) Dual action Pt prodrugs of kiteplatin and DCA [84]. (d) Examples of triple action Pt($_{IV}$) derivatives of cisplatin containing DCA (red), derivatives of cisplatin (black), and COX inhibitors (green) [85]. (e) Chemical structure of DPB containing DCA (red), biotin (blue), and Platinum (Pt) complex (black) [86].

novel complex containing DCA, Platinum, and Biotin (DPB) has been successfully tested, exhibiting multifacet antitumor properties (Figure 2(e)). Authors demonstrated the ability of such a prodrug to affect energy metabolism, to promote apoptosis, and to interact with DNA. The high selectivity of biotin for cancer cells minimizes the detrimental effects on normal cells and improves the curative effect on tumours [86]. Features and experimental evidence of the main classes of compounds are summarized in Table 3.

9. Other Proposed Mechanisms of Action of DCA

The metabolic shift from glycolysis to glucose oxidation due to the inhibition of PDK and the consequent activation of PDH is the best-known and well-accepted molecular effect of DCA administration. The consequent biochemical alterations, including ROS increase and mitochondrial membrane potential variation, may be responsible for proliferation arrest and cancer cell death, thus explaining DCA beneficial potential in cancer treatment [9]. However, the molecular intermediates activated after DCA administration are still unknown. It is conceivable that such a small molecule might directly or indirectly affect other cellular and molecular targets (Figure 3), displaying other mechanisms of action, so to explain its efficacy also in cellular models where it does not produce the expected metabolic shift [12]. A proteomic approach applied to cells of lung cancer demonstrated the ability of DCA to increase the concentration of every TCA intermediate while it did not affect glucose uptake or the glycolytic process from glucose to pyruvate [87]. In the attempt to shed light to DCA mode of action, Dubuis and colleagues used a metabolomics-based approach on several ovarian cancer cell lines treated with DCA and found a common marked depletion of intracellular pantothenate, a CoA precursor, as well as a concomitant increase of CoA, thus suggesting DCA ability to increase CoA de novo biosynthesis. Since high concentrations of CoA resulted to be toxic for cells, this metabolic effect could be responsible of cancer cell toxicity mediated by DCA [88]. A very recent work by El Sayed et al. introduced a novel evidence-based hypothesis, suggesting that DCA efficiency against cancer may derive from its ability to antagonize acetate [89], known to be an energetic substrate for glioblastoma and brain metastases, able to enhance DNA, RNA, and protein synthesis and posttranslational modifications, thus favouring cell proliferation and cancer progression. Moreover, high acetate levels are associated to anticancer drug resistance [90]. It has been shown that DCA is able to revert metabolic alterations induced by acetate by restoring physiological serum levels of lactate and free fatty acid and potassium and phosphorus concentration. According to the authors, thanks to a structural similarity to acetate, DCA could inhibit metabolic effects driven by acetate, responsible for cancer cell growth and chemoresistance [89]. Another possible additional effect of DCA could be pH modulation. pH level modulation is known to affect proliferation and apoptosis processes [91] as well as chemotherapy sensitivity [92]. DCA treatment may both increase and

Table 3: Properties of the main classes of DCA drug formulations tested in cancer cell lines and *in vivo* models with experimental evidence related.

Class of drug formulation	Features	*In vitro* tests	*In vivo* tests	Experimental evidence	References
Metal-DCA frameworks (no platinum)	Metal ions linked to organic ligands into porous scaffolds	MCF-7/MDA-MB-231 (breast) HeLa/LO2 (cervix) A2780 (ovary) A549/NCl-H1229 (lung)	Breast mouse models	Biocompatibility selective cytotoxicity Immune system compatibility Low mutagenicity	[77–82]
Doxorubicin-DCA conjugate	Complexes of DCA and chemotherapy drugs	B16F10 (melanoma)	Sarcoma and melanoma mouse models	Selective cytotoxicity safety In vivo antitumour efficiency	[83]
Platinum prodrugs with DCA	Platinum core associated to DCA and others drugs	MCF-7 (breast) LoVo/HCT-15/HCT116 (colon) A549 (lung) BxPC3/PSN-1 (pancreas) A375 (melanoma) BCPAP (thyroid) HeLa (cervix) HepG2 (hepatocarcinoma)	Lung carcinoma mouse models	Selective cytotoxicity multiple action Increased cellular uptake	[84–86]

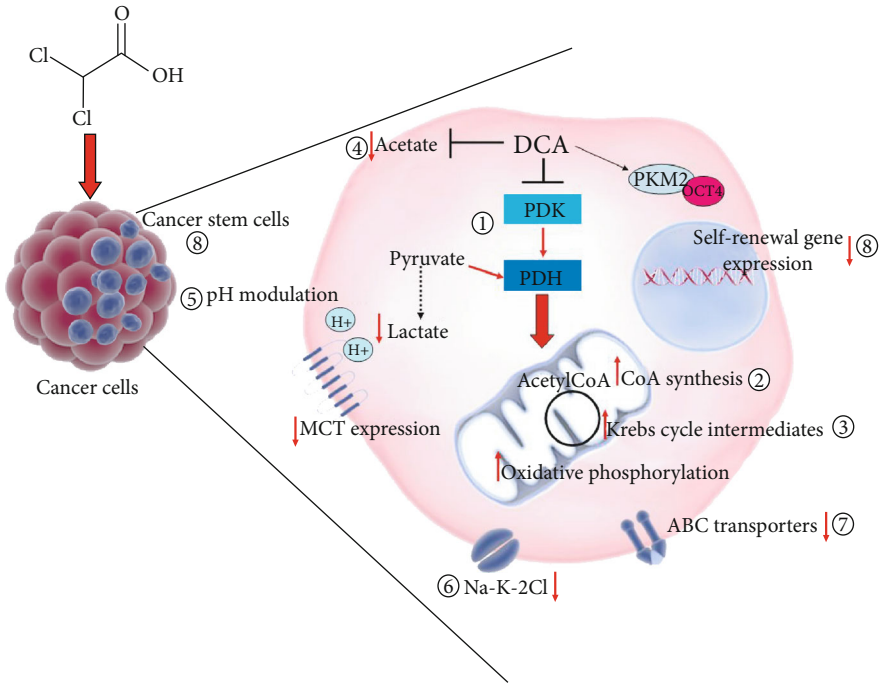

Figure 3: Other proposed mechanisms of action of DCA. DCA's main mechanism is to inhibit pyruvate dehydrogenase kinase (PDK), leading to pyruvate dehydrogenase (PDH) activation and fostering oxidative phosphorylation (1). DCA also increases each Krebs cycle intermediate concentration (2) [87]. DCA induces cell toxicity via de novo synthesis of CoA (3) [88]. DCA may antagonize acetate (4) [90]. DCA modulates intracellular acidification (5) [93, 94]. DCA inhibits Na-K-2Cl cotransporter (6) [96]. DCA downregulates gene and protein expression of ABC transporters (7) [97]. DCA reduces the expression of self-renewal-related genes and affects cancer stem cell fraction (8) [99].

reduce intracellular pH. A secondary effect of pyruvate redirecting into the mitochondria by DCA would be lactate reduction and a consequent increase in intracellular pH. On the other side, DCA is able to decrease the expression of monocarboxilate transporters and V-ATPase with a consequent reduction of pH, and this especially occurs in tumour cells, expressing higher amount of these carriers, compared to normal counterparts [93]. Given the ability to induce rapid tumour intracellular acidification, Albatany et al. [94] speculated about a possible employment of DCA as a tracker in *in vivo* imaging of a glioblastoma murine model and supported a therapeutic use of DCA since intracellular acidification is known to induce caspase activation and DNA fragmentation of cancer cells [95]. Animal models allow to identify a possible further molecular target of DCA. Experiments performed in rats highlighted the ability of DCA to inhibit the expression of the renal cotransporter Na-K-2Cl (NKCC) in the kidney of rats [96]. As NKCC is an important biomarker of extracellular and intracellular ion homeostasis regulation and participates in cell cycle progression, it plays an important role in cancer cell proliferation, apoptosis, and invasion. Belkahla et al. [97] investigated the interplay between metabolism targeting and the expression of ABC transporters, responsible for drug export from cells and a consequent multidrug resistance, and found that DCA treatment is able to reduce gene and protein expression of ABC transporters in several tumour cells expressing wild type p53, both *in vitro* and *in vivo* [98]. It has been already demonstrated the ability of DCA to induce differentiation through the modulation of PKM2/Oct4 interaction in glioma cells [99]. The resulting reduction of Oct4 transcription levels was associated to a reduction of stemness phenotype and a significant increased sensitivity to cell stress. This observation lets to hypothesize a potential role of DCA against cancer stem cells (CSCs).

10. DCA and Cancer Stem Cells

There is a growing interest in targeting cancer stem cells (CSCs) which seem to be the main responsible for tumour relapse [100]. CSCs share the ability of self-renewal with normal stem cells and can give rise to differentiating cells, responsible for tumour initiation as well as malignant progression [101]. A low proliferation rate and specific metabolic profile contribute to make CSCs resistant to conventional chemotherapy [102]. An urgent need emerged in the developing of new therapeutic agents able to affect cancer stem cell viability [103] in order to completely eradicate the tumour mass. An extensive body of literature is focusing the attention on the metabolic phenotype of CSCs, which seem to differ from differentiated cancer cells and could represent a therapeutic target [104–108]. In this setting, the possible sensitivity of CSC fraction to DCA has been hypothesized and tested in different cancer models. Embryonal carcinoma stem cells represent one of the more appropriate models for the study of CSC maintenance and differentiation and the identification of drugs and molecules able to modulate these processes [109]. Studies performed on embryonic

stem cells (ESCs) constitute preliminary important proofs supporting a possible efficacy of DCA [110]. Interestingly, DCA treatment of ESCs promotes loss of pluripotency and shifts towards a more active oxidative metabolism, accompanied by a significant decrease in HIF1a and p53 expression [111]. Vega-Naredo et al. [112] described the importance of mitochondrial metabolism in directing stemness and differentiation in such a model. They characterized the metabolic profile of stem cell fraction and guessed the less susceptibility of stem phenotype to mitochondrial-directed therapies. Forcing CSCs towards an oxidative metabolism by DCA treatment enabled departure from stemness to differentiation. Several reports support the existence of CSCs in glioma [113, 114], and the efficiency of DCA to hit CSCs has been extensively evaluated in such a cancer type, so difficult to treat with conventional therapies and characterized by low rates of survival. Already in 2010, Michelakis and colleagues had suggested, both *in vitro* and *in vivo*, DCA ability to induce apoptosis of cancer stem cell fraction [26]. A rat model of glioma, recapitulating several features of human glioblastoma, confirmed the efficacy of DCA to potentiate apoptosis of glioma CSCs, characterized by a significant glycolytic pathway overstimulation, compared to normal stem cells [115]. Also, Jiang et al. investigated the effect of DCA on the small population of glioma stem cells (GSCs) isolated from glioblastoma, demonstrating a reduction of self-renewal properties and an increase in cell death percentage [44]. Moreover, an *in vivo* test on mice bearing DCA-treated GSC-derived xenografts showed a significant increase in overall survival. DCA treatment was also tested in melanoma stem cell fraction, and the derived bioenergetics modulation was able to counteract protumorigenic action of a c-Met inhibitor [116]. A very recent work performed on human hepatocellular carcinoma identified PDK4 overexpression in spheres originated from cancer cells, featuring a defined stem-like phenotype. Interestingly, DCA treatment was able to reduce cell viability both of cancer-differentiated cells and cancer stem cells and reversed chemoresistance to conventional therapy [36]. Our group has recently experienced the ability of DCA to reduce the expression of cancer stem cell markers CD24/CD44/EPCAM in a pancreatic cancer cell line as well as to compromise spheroid formation and viability [12], further corroborating data obtained in other cancer models. Together with chemoresistance, also radioresistance represents a limit to an efficient cancer treatment, and CSCs seem to be responsible for such refractoriness [117]. Sun et al. demonstrated the ability of DCA to increase radiosensitivity of medulloblastoma cells by affecting stem-like clones, reducing the expression percentage of CD133-positive cells and reducing sphere formation [72]. Moreover, in the same cellular model, they showed an altered mechanism of DNA repair induced by DCA able to explain the increased effectiveness of radiotherapy.

11. Conclusions

Targeting cancer cell metabolism represents a new pharmacological approach to treat cancer. DCA ability to shift metabolism from glycolysis to oxidative phosphorylation has increased the interest towards this drug already known for its anticancer properties. The evidence accumulated in the last years confirms the capability of DCA to overcome chemo, radioresistance in several cancer types and lets to hypothesize additional cellular targets able to explain its skill to kill cancer cells. There is a need to design further clinical studies now limited to poor-prognosis patients with advanced, recurrent neoplasms, already refractory to other conventional therapies. Its potential efficacy against cancer stem cells as well as the development of new drug formulations takes us closer to reach an effective clinical employment of DCA.

Conflicts of Interest

The authors declare no conflict of interest.

Acknowledgments

This work was supported by Current Research Funds, Italian Ministry of Health, to IRCCS-CROB, Rionero in Vulture, Potenza, Italy.

References

[1] T. G. Lee, E. H. Jeong, I. J. Min, S. Y. Kim, H. R. Kim, and C. H. Kim, "Altered expression of cellular proliferation, apoptosis and the cell cycle-related genes in lung cancer cells with acquired resistance to Egfr tyrosine kinase inhibitors," *Oncology Letters*, vol. 14, no. 2, pp. 2191–2197, 2017.

[2] J. Chen, "The cell-cycle arrest and apoptotic functions of P53 in tumor initiation and progression," *Cold Spring Harbor Perspectives in Medicine*, vol. 6, no. 3, p. a026104, 2016.

[3] C. Thakur and F. Chen, "Connections between metabolism and epigenetics in cancers," *Seminars in Cancer Biology*, vol. 57, pp. 52–58, 2019.

[4] S. Subramaniam, V. Jeet, J. A. Clements, J. H. Gunter, and J. Batra, "Emergence of micrornas as key players in cancer cell metabolism," *Clinical Chemistry*, vol. 65, no. 9, pp. 1090–1101, 2019.

[5] D. Williams and B. Fingleton, "Non-canonical roles for metabolic enzymes and intermediates in malignant progression and metastasis," *Clinical & Experimental Metastasis*, vol. 36, no. 3, pp. 211–224, 2019.

[6] T. Tataranni, F. Agriesti, V. Ruggieri et al., "Rewiring carbohydrate catabolism differentially affects survival of pancreatic cancer cell lines with diverse metabolic profiles," *Oncotarget*, vol. 8, no. 25, pp. 41265–41281, 2017.

[7] A. Luengo, D. Y. Gui, and M. G. Vander Heiden, "Targeting metabolism for cancer therapy," *Cell Chemical Biology*, vol. 24, no. 9, pp. 1161–1180, 2017.

[8] M. O. James, S. C. Jahn, G. Zhong, M. G. Smeltz, Z. Hu, and P. W. Stacpoole, "Therapeutic applications of dichloroacetate and the role of glutathione transferase zeta-1," *Pharmacology & Therapeutics*, vol. 170, pp. 166–180, 2017.

[9] E. D. Michelakis, L. Webster, and J. R. Mackey, "Dichloroacetate (Dca) as a potential metabolic-targeting therapy for cancer," *British Journal of Cancer*, vol. 99, no. 7, pp. 989–994, 2008.

[10] S. Kankotia and P. W. Stacpoole, "Dichloroacetate and cancer: new home for an orphan drug?," *Biochimica et Biophysica Acta*, vol. 1846, no. 2, pp. 617–629, 2014.

[11] V. Ruggieri, F. Agriesti, R. Scrima et al., "Dichloroacetate, a selective mitochondria-targeting drug for oral squamous cell carcinoma: a metabolic perspective of treatment," *Oncotarget*, vol. 6, no. 2, pp. 1217–1230, 2015.

[12] T. Tataranni, F. Agriesti, C. Pacelli et al., "Dichloroacetate affects mitochondrial function and stemness-associated properties in pancreatic cancer cell lines," *Cells*, vol. 8, no. 5, p. 478, 2019.

[13] A. Khan, D. Marier, E. Marsden, D. Andrews, and I. Eliaz, "A novel form of dichloroacetate therapy for patients with advanced cancer: a report of 3 cases," *Alternative Therapies in Health and Medicine*, vol. 20, Supplement 2, pp. 21–28, 2014.

[14] E. M. Dunbar, B. S. Coats, A. L. Shroads et al., "Phase 1 trial of dichloroacetate (Dca) in adults with recurrent malignant brain tumors," *Investigational New Drugs*, vol. 32, no. 3, pp. 452–464, 2014.

[15] Q. S.-C. Chu, R. Sangha, J. Spratlin et al., "A phase I open-labeled, single-arm, dose-escalation, study of dichloroacetate (DCA) in patients with advanced solid tumors," *Investigational New Drugs*, vol. 33, no. 3, pp. 603–610, 2015.

[16] A. Khan, D. Andrews, and A. C. Blackburn, "Long-term stabilization of stage 4 colon cancer using sodium dichloroacetate therapy," *World Journal of Clinical Cases*, vol. 4, no. 10, pp. 336–343, 2016.

[17] G. Sutendra and E. D. Michelakis, "Pyruvate dehydrogenase kinase as a novel therapeutic target in oncology," *Frontiers in Oncology*, vol. 3, p. 38, 2013.

[18] S. R. Pillai, M. Damaghi, Y. Marunaka, E. P. Spugnini, S. Fais, and R. J. Gillies, "Causes, consequences, and therapy of tumors acidosis," *Cancer Metastasis Reviews*, vol. 38, no. 1-2, pp. 205–222, 2019.

[19] R. J. DeBerardinis, J. J. Lum, G. Hatzivassiliou, and C. B. Thompson, "The biology of cancer: metabolic reprogramming fuels cell growth and proliferation," *Cell Metabolism*, vol. 7, no. 1, pp. 11–20, 2008.

[20] N. Zamzami and G. Kroemer, "The mitochondrion in apoptosis: how Pandora's box opens," *Nature Reviews Molecular Cell Biology*, vol. 2, no. 1, pp. 67–71, 2001.

[21] J. W. Kim and C. V. Dang, "Multifaceted roles of glycolytic enzymes," *Trends in Biochemical Sciences*, vol. 30, no. 3, pp. 142–150, 2005.

[22] P. A. Gammage and C. Frezza, "Mitochondrial DNA: the overlooked oncogenome?," *BMC Biology*, vol. 17, no. 1, p. 53, 2019.

[23] L. H. Stockwin, S. X. Yu, S. Borgel et al., "Sodium dichloroacetate selectively targets cells with defects in the mitochondrial ETC," *International Journal of Cancer*, vol. 127, no. 11, pp. 2510–2519, 2010.

[24] P. W. Stacpoole, N. V. Nagaraja, and A. D. Hutson, "Efficacy of dichloroacetate as a lactate-lowering drug," *Journal of Clinical Pharmacology*, vol. 43, no. 7, pp. 683–691, 2003.

[25] P. W. Stacpoole, "Therapeutic targeting of the pyruvate dehydrogenase complex/pyruvate dehydrogenase kinase (PDC/PDK) axis in cancer," *JNCI: Journal of the National Cancer Institute*, vol. 109, no. 11, 2017.

[26] E. D. Michelakis, G. Sutendra, P. Dromparis et al., "Metabolic modulation of glioblastoma with dichloroacetate," *Science Translational Medicine*, vol. 2, no. 31, article 31ra34, 2010.

[27] P. W. Stacpoole, C. J. Martyniuk, M. O. James, and N. A. Calcutt, "Dichloroacetate-induced peripheral neuropathy," *International Review of Neurobiology*, vol. 145, pp. 211–238, 2019.

[28] N. Felitsyn, P. W. Stacpoole, and L. Notterpek, "Dichloroacetate causes reversible demyelination in vitro: potential mechanism for its neuropathic effect," *Journal of Neurochemistry*, vol. 100, no. 2, pp. 429–436, 2007.

[29] T. Langaee, R. Wagner, L. P. Horne et al., "Personalized dosing of dichloroacetate using Gstz1 clinical genotyping assay," *Genetic Testing and Molecular Biomarkers*, vol. 22, no. 4, pp. 266–269, 2018.

[30] D. Brandsma, T. P. Dorlo, J. H. Haanen, J. H. Beijnen, and W. Boogerd, "Severe encephalopathy and polyneuropathy induced by dichloroacetate," *Journal of Neurology*, vol. 257, no. 12, pp. 2099-2100, 2010.

[31] United States Environmental Protection Agency, EPA, *Toxicological Review of Dichloroacetic Acid, CAS 79-43-6*, 2003.

[32] X. Lu, D. Zhou, B. Hou et al., "Dichloroacetate enhances the antitumor efficacy of chemotherapeutic agents via inhibiting autophagy in non-small-cell lung cancer," *Cancer Management and Research*, vol. 10, pp. 1231–1241, 2018.

[33] A. Korga, M. Ostrowska, M. Iwan, M. Herbet, and J. Dudka, "Inhibition of glycolysis disrupts cellular antioxidant defense and sensitizes Hepg2 cells to doxorubicin treatment," *FEBS Open Bio*, vol. 9, no. 5, pp. 959–972, 2019.

[34] H. Sun, A. Zhu, X. Zhou, and F. Wang, "Suppression of pyruvate dehydrogenase kinase-2 re-sensitizes paclitaxel-resistant human lung cancer cells to paclitaxel," *Oncotarget*, vol. 8, no. 32, pp. 52642–52650, 2017.

[35] B. L. Woolbright, D. Choudhary, A. Mikhalyuk et al., "The role of pyruvate dehydrogenase kinase-4 (PDK4) in bladder cancer and chemoresistance," *Molecular Cancer Therapeutics*, vol. 17, no. 9, pp. 2004–2012, 2018.

[36] K. Fekir, H. Dubois-Pot-Schneider, R. Désert et al., "Retrodifferentiation of human tumor hepatocytes to stem cells leads to metabolic reprogramming and chemoresistance," *Cancer Research*, vol. 79, no. 8, pp. 1869–1883, 2019.

[37] A. Skeberdytė, I. Sarapinienė, J. Aleksander-Krasko, V. Stankevičius, K. Sužiedėlis, and S. Jarmalaitė, "Dichloroacetate and salinomycin exert a synergistic cytotoxic effect in colorectal cancer cell lines," *Scientific Reports*, vol. 8, no. 1, p. 17744, 2018.

[38] A. Verma, Y. M. Lam, Y. C. Leung et al., "Combined use of arginase and dichloroacetate exhibits anti-proliferative effects in triple negative breast cancer cells," *The Journal of Pharmacy and Pharmacology*, vol. 71, no. 3, pp. 306–315, 2019.

[39] B. Li, X. Li, H. Xiong et al., "Inhibition of COX2 enhances the chemosensitivity of dichloroacetate in cervical cancer cells," *Oncotarget*, vol. 8, no. 31, pp. 51748–51757, 2017.

[40] C. Lucido, W. Miskimins, and P. Vermeer, "Propranolol promotes glucose dependence and synergizes with dichloroacetate for anti-cancer activity in HNSCC," *Cancers*, vol. 10, no. 12, p. 476, 2018.

[41] C. Abildgaard, C. Dahl, A. Abdul-Al, A. Christensen, and P. Guldberg, "Inhibition of retinoic acid receptor B signaling confers glycolytic dependence and sensitization to dichloroacetate in melanoma cells," *Oncotarget*, vol. 8, no. 48, pp. 84210–84223, 2017.

[42] I. V. Prokhorova, O. N. Pyaskovskaya, D. L. Kolesnik, and G. I. Solyanik, "Influence of metformin, sodium

dichloroacetate and their combination on the hematological and biochemical blood parameters of rats with gliomas C6," *Experimental Oncology*, vol. 40, no. 3, pp. 205–210, 2018.

[43] D. L. Kolesnik, O. N. Pyaskovskaya, Y. R. Yakshibaeva, and G. I. Solyanik, "Time-dependent cytotoxicity of dichloroacetate and metformin against Lewis lung carcinoma," *Experimental Oncology*, vol. 41, no. 1, pp. 14–19, 2019.

[44] W. Jiang, S. Finniss, S. Cazacu et al., "Repurposing phenformin for the targeting of glioma stem cells and the treatment of glioblastoma," *Oncotarget*, vol. 7, no. 35, pp. 56456–56470, 2016.

[45] B. Waltenberger, A. Mocan, K. Šmejkal, E. Heiss, A. Atanasov, and A. G. Atanasov, "Natural products to counteract the epidemic of cardiovascular and metabolic disorders," *Molecules*, vol. 21, no. 6, p. 807, 2016.

[46] M. Zadorozhna, T. Tataranni, and D. Mangieri, "Piperine: role in prevention and progression of cancer," *Molecular Biology Reports*, vol. 46, no. 5, pp. 5617–5629, 2019.

[47] G. Della Sala, F. Agriesti, C. Mazzoccoli, T. Tataranni, V. Costantino, and C. Piccoli, "Clogging the ubiquitin-proteasome machinery with marine natural products: last decade update," *Marine Drugs*, vol. 16, no. 12, p. 467, 2018.

[48] A. G. Atanasov, B. Waltenberger, E. M. Pferschy-Wenzig et al., "Discovery and resupply of pharmacologically active plant-derived natural products: a review," *Biotechnology Advances*, vol. 33, no. 8, pp. 1582–1614, 2015.

[49] M. B. Sporn and N. Suh, "Chemoprevention: an essential approach to controlling cancer," *Nature Reviews Cancer*, vol. 2, no. 7, pp. 537–543, 2002.

[50] C. K. Singh, J. George, and N. Ahmad, "Resveratrol-based combinatorial strategies for cancer management," *Annals of the New York Academy of Sciences*, vol. 1290, pp. 113–121, 2013.

[51] S. Redondo-Blanco, J. Fernández, I. Gutiérrez-del-Río, C. J. Villar, and F. Lombó, "New insights toward colorectal cancer chemotherapy using natural bioactive compounds," *Frontiers in Pharmacology*, vol. 8, p. 109, 2017.

[52] B. B. Aggarwal, A. Kumar, and A. C. Bharti, "Anticancer potential of curcumin: preclinical and clinical studies," *Anticancer Research*, vol. 23, no. 1A, pp. 363–398, 2003.

[53] P. C. Kan, Y. J. Chang, C. S. Chien, C. Y. Su, and H. W. Fang, "Coupling dichloroacetate treatment with curcumin significantly enhances anticancer potential," *Anticancer Research*, vol. 38, no. 11, pp. 6253–6261, 2018.

[54] K. Hata, K. Hori, H. Ogasawara, and S. Takahashi, "Anti-leukemia activities of Lup-28-Al-20(29)-En-3-one, a lupane triterpene," *Toxicology Letters*, vol. 143, no. 1, pp. 1–7, 2003.

[55] C. A. Dehelean, S. Feflea, J. Molnár, I. Zupko, and C. Soica, "Betulin as an antitumor agent tested in vitro on A431, Hela and MCF7, and as an angiogenic inhibitor in vivo in the cam assay," *Natural Product Communications*, vol. 7, no. 8, pp. 981–985, 2012.

[56] M. Drag, P. Surowiak, M. Drag-Zalesinska, M. Dietel, H. Lage, and J. Oleksyszyn, "Comparision of the cytotoxic effects of birch bark extract, betulin and betulinic acid towards human gastric carcinoma and pancreatic carcinoma drug-sensitive and drug-resistant cell lines," *Molecules*, vol. 14, no. 4, pp. 1639–1651, 2009.

[57] M. Mihoub, A. Pichette, B. Sylla, C. Gauthier, and J. Legault, "Bidesmosidic betulin saponin bearing L-rhamnopyranoside moieties induces apoptosis and inhibition of lung cancer cells growth in vitro and in vivo," *PLoS One*, vol. 13, no. 3, article e0193386, 2018.

[58] H. Wang, H. Jiang, M. Van De Gucht, and M. De Ridder, "Hypoxic radioresistance: can ROS be the key to overcome it?," *Cancers*, vol. 11, no. 1, p. 112, 2019.

[59] J. P. Pouget, S. Frelon, J. L. Ravanat, I. Testard, F. Odin, and J. Cadet, "Formation of modified DNA bases in cells exposed either to gamma radiation or to high-let particles," *Radiation Research*, vol. 157, no. 5, pp. 589–595, 2002.

[60] K. Rycaj and D. G. Tang, "Cancer stem cells and radioresistance," *International Journal of Radiation Biology*, vol. 90, no. 8, pp. 615–621, 2014.

[61] L. Tang, F. Wei, Y. Wu et al., "Role of metabolism in cancer cell radioresistance and radiosensitization methods," *Journal of Experimental & Clinical Cancer Research*, vol. 37, no. 1, p. 87, 2018.

[62] G. Xie, Y. Liu, Q. Yao et al., "Hypoxia-induced angiotensin II by the lactate-chymase-dependent mechanism mediates radioresistance of hypoxic tumor cells," *Scientific Reports*, vol. 7, no. 1, article 42396, 2017.

[63] J. Overgaard, "Hypoxic radiosensitization: adored and ignored," *Journal of Clinical Oncology*, vol. 25, no. 26, pp. 4066–4074, 2007.

[64] Y. Zhang and S. G. Martin, "Redox proteins and radiotherapy," *Clinical Oncology*, vol. 26, no. 5, pp. 289–300, 2014.

[65] H. Jiang, H. Wang, and M. De Ridder, "Targeting antioxidant enzymes as a radiosensitizing strategy," *Cancer Letters*, vol. 438, pp. 154–164, 2018.

[66] M. R. Niewisch, Z. Kuçi, H. Wolburg et al., "Influence of dichloroacetate (DCA) on lactate production and oxygen consumption in neuroblastoma cells: is DCA a suitable drug for neuroblastoma therapy?," *Cellular Physiology and Biochemistry*, vol. 29, no. 3-4, pp. 373–380, 2012.

[67] S. P. Pitroda, B. T. Wakim, R. F. Sood et al., "Stat1-dependent expression of energy metabolic pathways links tumour growth and radioresistance to the Warburg effect," *BMC Medicine*, vol. 7, no. 1, p. 68, 2009.

[68] T. Shimura, N. Noma, Y. Sano et al., "Akt-mediated enhanced aerobic glycolysis causes acquired radioresistance by human tumor cells," *Radiotherapy and Oncology*, vol. 112, no. 2, pp. 302–307, 2014.

[69] V. Bol, A. Bol, C. Bouzin et al., "Reprogramming of tumor metabolism by targeting mitochondria improves tumor response to irradiation," *Acta Oncologica*, vol. 54, no. 2, pp. 266–274, 2015.

[70] H. Shen, E. Hau, S. Joshi, P. J. Dilda, and K. L. McDonald, "Sensitization of glioblastoma cells to irradiation by modulating the glucose metabolism," *Molecular Cancer Therapeutics*, vol. 14, no. 8, pp. 1794–1804, 2015.

[71] G. Dong, Q. Chen, F. Jiang et al., "Diisopropylamine dichloroacetate enhances radiosensitization in esophageal squamous cell carcinoma by increasing mitochondria-derived reactive oxygen species levels," *Oncotarget*, vol. 7, no. 42, pp. 68170–68178, 2016.

[72] L. Sun, T. Moritake, K. Ito et al., "Metabolic analysis of radioresistant medulloblastoma stem-like clones and potential therapeutic targets," *PLoS One*, vol. 12, no. 4, article e0176162, 2017.

[73] L. Zitvogel, L. Apetoh, F. Ghiringhelli, F. André, A. Tesniere, and G. Kroemer, "The anticancer immune response:

indispensable for therapeutic success?," *The Journal of Clinical Investigation*, vol. 118, no. 6, pp. 1991–2001, 2008.

[74] S. Gupta and B. Dwarakanath, "Modulation of Immunobiome during radio-sensitization of tumors by glycolytic inhibitors," *Current Medicinal Chemistry*, vol. 25, 2018.

[75] D. Peer, J. M. Karp, S. Hong, O. C. Farokhzad, R. Margalit, and R. Langer, "Nanocarriers as an emerging platform for cancer therapy," *Nature Nanotechnology*, vol. 2, no. 12, pp. 751–760, 2007.

[76] R. C. Huxford, J. Della Rocca, and W. Lin, "Metal-organic frameworks as potential drug carriers," *Current Opinion in Chemical Biology*, vol. 14, no. 2, pp. 262–268, 2010.

[77] I. A. Lázaro, S. A. Lázaro, and R. S. Forgan, "Enhancing anticancer cytotoxicity through bimodal drug delivery from ultrasmall Zr MOF nanoparticles," *Chemical Communications*, vol. 54, no. 22, pp. 2792–2795, 2018.

[78] I. Abánades Lázaro, S. Haddad, J. M. Rodrigo-Muñoz et al., "Surface-functionalization of Zr-fumarate MOF for selective cytotoxicity and immune system compatibility in nanoscale drug delivery," *ACS Applied Materials & Interfaces*, vol. 10, no. 37, pp. 31146–31157, 2018.

[79] I. Abánades Lázaro, S. Haddad, J. M. Rodrigo-Muñoz et al., "Mechanistic investigation into the selective anticancer cytotoxicity and immune system response of surface-functionalized, dichloroacetate-loaded, UiO-66 nanoparticles," *ACS Applied Materials & Interfaces*, vol. 10, no. 6, pp. 5255–5268, 2018.

[80] P. Štarha, Z. Trávníček, J. Vančo, and Z. Dvořák, "Half-sandwich Ru(II) and Os(II) bathophenanthroline complexes containing a releasable dichloroacetato ligand," *Molecules*, vol. 23, no. 2, p. 420, 2018.

[81] J. Pracharova, V. Novohradsky, H. Kostrhunova et al., "Half-sandwich Os(ii) and Ru(ii) bathophenanthroline complexes: anticancer drug candidates with unusual potency and a cellular activity profile in highly invasive triple-negative breast cancer cells," *Dalton Transactions*, vol. 47, no. 35, pp. 12197–12208, 2018.

[82] J. Yang, Q. Cao, H. Zhang et al., "Targeted reversal and phosphorescence lifetime imaging of cancer cell metabolism _via_ a theranostic rhenium(I)-DCA conjugate," *Biomaterials*, vol. 176, pp. 94–105, 2018.

[83] C. Yang, T. Wu, Y. Qin et al., "A facile doxorubicin-dichloroacetate conjugate nanomedicine with high drug loading for safe drug delivery," *International Journal of Nanomedicine*, vol. 13, pp. 1281–1293, 2018.

[84] S. Savino, V. Gandin, J. D. Hoeschele, C. Marzano, G. Natile, and N. Margiotta, "Dual-acting antitumor Pt(IV) prodrugs of kiteplatin with dichloroacetate axial ligands," *Dalton Transactions*, vol. 47, no. 21, pp. 7144–7158, 2018.

[85] E. Petruzzella, R. Sirota, I. Solazzo, V. Gandin, and D. Gibson, "Triple action Pt(iv) derivatives of cisplatin: a new class of potent anticancer agents that overcome resistance," *Chemical Science*, vol. 9, no. 18, pp. 4299–4307, 2018.

[86] S. Jin, Y. Guo, D. Song et al., "Targeting energy metabolism by a platinum(IV) prodrug as an alternative pathway for cancer suppression," *Inorganic Chemistry*, vol. 58, no. 9, pp. 6507–6516, 2019.

[87] W. Zhang, X. Hu, W. Zhou, and K. Y. Tam, "liquid chromatography-tandem mass spectrometry method revealed that lung cancer cells exhibited distinct metabolite profiles upon the treatment with different pyruvate dehydrogenase kinase inhibitors," *Journal of Proteome Research*, vol. 17, no. 9, pp. 3012–3021, 2018.

[88] S. Dubuis, K. Ortmayr, and M. Zampieri, "A framework for large-scale metabolome drug profiling links coenzyme a metabolism to the toxicity of anti-cancer drug dichloroacetate," *Communications Biology*, vol. 1, no. 1, p. 101, 2018.

[89] S. M. El Sayed, H. Baghdadi, N. S. Ahmed et al., "Dichloroacetate is an antimetabolite that antagonizes acetate and deprives cancer cells from its benefits: a novel evidence-based medical hypothesis," *Medical Hypotheses*, vol. 122, pp. 206–209, 2019.

[90] D. M. Jaworski, A. M. Namboodiri, and J. R. Moffett, "Acetate as a metabolic and epigenetic modifier of cancer therapy," *Journal of Cellular Biochemistry*, vol. 117, no. 3, pp. 574–588, 2016.

[91] B. A. Webb, M. Chimenti, M. P. Jacobson, and D. L. Barber, "Dysregulated pH: a perfect storm for cancer progression," *Nature Reviews Cancer*, vol. 11, no. 9, pp. 671–677, 2011.

[92] D. Neri and C. T. Supuran, "Interfering with pH regulation in tumours as a therapeutic strategy," *Nature Reviews Drug Discovery*, vol. 10, no. 10, pp. 767–777, 2011.

[93] A. Kumar, S. Kant, and S. M. Singh, "Antitumor and chemosensitizing action of dichloroacetate implicates modulation of tumor microenvironment: a role of reorganized glucose metabolism, cell survival regulation and macrophage differentiation," *Toxicology and Applied Pharmacology*, vol. 273, no. 1, pp. 196–208, 2013.

[94] M. Albatany, A. Li, S. Meakin, and R. Bartha, "Dichloroacetate induced intracellular acidification in glioblastoma: in vivo detection using AACID-CEST MRI at 9.4 Tesla," *Journal of Neuro-Oncology*, vol. 136, no. 2, pp. 255–262, 2018.

[95] H. J. Park, J. C. Lyons, T. Ohtsubo, and C. W. Song, "Acidic environment causes apoptosis by increasing caspase activity," *British Journal of Cancer*, vol. 80, no. 12, pp. 1892–1897, 1999.

[96] J. Stanevičiūtė, M. Juknevičienė, J. Palubinskienė et al., "Sodium dichloroacetate pharmacological effect as related to Na-K-2Cl cotransporter inhibition in rats," *Dose Response*, vol. 16, no. 4, article 155932581881152, 2018.

[97] S. Belkahla, A. U. Haq Khan, D. Gitenay et al., "Changes in metabolism affect expression of ABC transporters through ERK5 and depending on p53 status," *Oncotarget*, vol. 9, no. 1, pp. 1114–1129, 2018.

[98] J. A. Bush and G. Li, "Cancer chemoresistance: the relationship between P53 and multidrug transporters," *International Journal of Cancer*, vol. 98, no. 3, pp. 323–330, 2002.

[99] M. Morfouace, L. Lalier, L. Oliver et al., "Control of glioma cell death and differentiation by PKM2-Oct4 interaction," *Cell Death & Disease*, vol. 5, no. 1, pp. e1036–e1036, 2014.

[100] A. Turdo, V. Veschi, M. Gaggianesi et al., "Meeting the challenge of targeting cancer stem cells," *Frontiers in Cell and Development Biology*, vol. 7, p. 16, 2019.

[101] P. Zhu and Z. Fan, "Cancer stem cells and tumorigenesis," *Biophysics Reports*, vol. 4, no. 4, pp. 178–188, 2018.

[102] S. Prasad, S. Ramachandran, N. Gupta, I. Kaushik, and S. K. Srivastava, "Cancer cells stemness: a doorstep to targeted therapy," *Biochimica et Biophysica Acta - Molecular Basis of Disease*, p. 165424, 2019.

[103] M. Yang, P. Liu, and P. Huang, "Cancer stem cells, metabolism, and therapeutic significance," *Tumour Biology*, vol. 37, no. 5, pp. 5735–5742, 2016.

[104] P. Sancho, D. Barneda, and C. Heeschen, "Hallmarks of cancer stem cell metabolism," *British Journal of Cancer*, vol. 114, no. 12, pp. 1305–1312, 2016.

[105] F. Sotgia, M. Fiorillo, and M. P. Lisanti, "Hallmarks of the cancer cell of origin: comparisons with "energetic" cancer stem cells (e-CSCs)," *Aging*, vol. 11, no. 3, pp. 1065–1068, 2019.

[106] S. Skvortsov, I. I. Skvortsova, D. G. Tang, and A. Dubrovska, "Concise review: prostate cancer stem cells: current understanding," *Stem Cells*, vol. 36, no. 10, pp. 1457–1474, 2018.

[107] S. Bordel, "Constraint based modeling of metabolism allows finding metabolic cancer hallmarks and identifying personalized therapeutic windows," *Oncotarget*, vol. 9, no. 28, pp. 19716–19729, 2018.

[108] Y. Y. Wang, J. Chen, X. M. Liu, R. Zhao, and H. Zhe, "Nrf2-mediated metabolic reprogramming in cancer," *Oxidative Medicine and Cellular Longevity*, vol. 2018, Article ID 9304091, 7 pages, 2018.

[109] M. W. McBurney, "P19 embryonal carcinoma cells," *The International Journal of Developmental Biology*, vol. 37, no. 1, pp. 135–140, 1993.

[110] R. Loureiro, S. Magalhães-Novais, K. A. Mesquita et al., "Melatonin antiproliferative effects require active mitochondrial function in embryonal carcinoma cells," *Oncotarget*, vol. 6, no. 19, pp. 17081–17096, 2015.

[111] A. S. Rodrigues, M. Correia, A. Gomes et al., "Dichloroacetate, the pyruvate dehydrogenase complex and the modulation of mESC pluripotency," *PLoS One*, vol. 10, no. 7, article e0131663, 2015.

[112] I. Vega-Naredo, R. Loureiro, K. A. Mesquita et al., "Mitochondrial metabolism directs stemness and differentiation in P19 embryonal carcinoma stem cells," *Cell Death and Differentiation*, vol. 21, no. 10, pp. 1560–1574, 2014.

[113] S. K. Singh, C. Hawkins, I. D. Clarke et al., "Identification of human brain tumour initiating cells," *Nature*, vol. 432, no. 7015, pp. 396–401, 2004.

[114] X. Yuan, J. Curtin, Y. Xiong et al., "Isolation of cancer stem cells from adult glioblastoma multiforme," *Oncogene*, vol. 23, no. 58, pp. 9392–9400, 2004.

[115] M. Morfouace, L. Lalier, M. Bahut et al., "Comparison of spheroids formed by rat glioma stem cells and neural stem cells reveals differences in glucose metabolism and promising therapeutic applications," *The Journal of Biological Chemistry*, vol. 287, no. 40, pp. 33664–33674, 2012.

[116] L. Kucerova, L. Demkova, S. Skolekova, R. Bohovic, and M. Matuskova, "Tyrosine kinase inhibitor SU11274 increased tumorigenicity and enriched for melanoma-initiating cells by bioenergetic modulation," *BMC Cancer*, vol. 16, no. 1, p. 308, 2016.

[117] Z. Zhao, K. Zhang, Z. Wang et al., "A comprehensive review of available omics data resources and molecular profiling for precision glioma studies," *Biomedical Reports*, vol. 10, no. 1, pp. 3–9, 2019.

Hindawi
Oxidative Medicine and Cellular Longevity
Volume 2019, Article ID 2360945, 10 pages
https://doi.org/10.1155/2019/2360945

Review Article

Hydrogen Sulfide: Emerging Role in Bladder, Kidney, and Prostate Malignancies

Masoud Akbari,[1,2] **Emrullah Sogutdelen**,[2,3] **Smriti Juriasingani**,[1,2] **and Alp Sener**[1,2,3,4]

[1]*Department of Microbiology & Immunology, Schulich School of Medicine & Dentistry, University of Western Ontario, Dental Sciences Building, Rm 3014, London, Ontario, Canada N6A 5C1*
[2]*Matthew Mailing Center for Translational Transplant Studies, University Hospital, London Health Sciences Center, 339 Windemere Road, London, Ontario, Canada N6A 5A5*
[3]*Department of Surgery, Schulich School of Medicine & Dentistry, St. Joseph's Health Care London, PO BOX 5777, STN B, London, Ontario, Canada N6A 4V2*
[4]*Multi-Organ Transplant Program, University Hospital, London Health Sciences Centre, 339 Windemere Road, London, Ontario, Canada N6A 5A5*

Correspondence should be addressed to Alp Sener; alp.sener@lhsc.on.ca

Received 18 April 2019; Revised 22 July 2019; Accepted 30 September 2019; Published 3 November 2019

Guest Editor: Jayeeta Ghose

Hydrogen sulfide (H_2S) is the latest member of the gasotransmitter family and known to play essential roles in cancer pathophysiology. H_2S is produced endogenously and can be administered exogenously. Recent studies showed that H_2S in cancers has both pro- and antitumor roles. Understanding the difference in the expression and localization of tissue-specific H_2S-producing enzymes in healthy and cancer tissues allows us to develop tools for cancer diagnosis and treatment. Urological malignancies are some of the most common cancers in both men and women, and their early detection is vital since advanced cancers are recurrent, metastatic, and often resistant to treatment. This review summarizes the roles of H_2S in cancer and looks at current studies investigating H_2S activity and expression of H_2S-producing enzymes in urinary cancers. We specifically focused on urothelial carcinoma, renal cell carcinoma, and prostate cancer, as they form the majority of newly diagnosed urinary cancers. Recent studies show that besides the physiological activity of H_2S in cancer cells, there are patterns between the development and prognosis of urinary cancers and the expression of H_2S-producing enzymes and indirectly the H_2S levels. Though controversial and not completely understood, studying the expression of H_2S-producing enzymes in cancer tissue may represent an avenue for novel diagnostic and therapeutic strategies for addressing urological malignancies.

1. Hydrogen Sulfide

For several centuries, hydrogen sulfide (H_2S) was known as a pollutant, but now its physiological and pathophysiological processes are well known. H_2S is widely recognized as the third endogenous gasotransmitter after carbon monoxide (CO) and nitric oxide (NO) in mammals and some other species, with similar pathophysiological characteristics [1, 2]. H_2S is synthesized endogenously by reverse transsulfidation and oxidation of cysteine [3–6], by three tissue-specific enzymes: cystathionine β-synthase (CBS), cystathionine γ-lyase (CSE), and 3-mercaptopyruvate sulfurtransferase (3-MPST) [3, 4, 7–11]. All of them are cytosolic [12–14], but 3-MPST is also localized in the mitochondria [3, 12, 15]. Upon synthesis in different cell compartments such as in the mitochondria, a free form of H_2S can be released into the cytoplasm or be stored inside the cell as bound sulfane sulfur for subsequent release of H_2S (Figure 1) [16, 17].

Endogenous H_2S is a key signaling molecule in humans and other mammals. It has been detected in many organs, and it is involved in the various physiological and

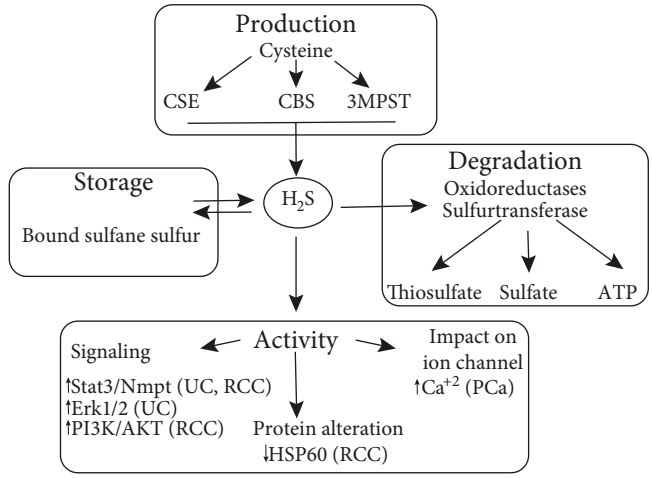

FIGURE 1: Synthesis, storage, degradation, and activity of H_2S, especially in urinary cancers. H_2S has roles in different pathways of urinary cancers such as signaling or ion channel. Abbreviations: CBS: cystathionine β-synthase, CSE: cystathionine γ-lyase, 3-MPST: 3-mercaptopyruvate sulfurtransferase, Stat3/Nmpt: signal transducer and activator of transcription 3/nicotinamide phosphoribosyltransferase, HSP60: heat shock protein 60, PI3K/AKT: phosphatidylinositol 3-kinase, UC: urothelial carcinoma, RCC: renal cell cancer, PCa: prostate cancer.

pathophysiological processes [12, 18–20]. H_2S is known to play a role in redox homeostasis and antioxidant responses [21–23], angiogenesis [24–30], vasodilation [31], regulation of synaptic transmission [32], inflammatory responses [33], glucose metabolism [34, 35], ATP production [36], and apoptosis and cell proliferation [23, 31, 37–42]. The role that H_2S plays in these processes appears to be concentration dependent. The concentration of free H_2S in plasma could not be measured in a proper way because it is affected by environmental factors such as pH [43], but an initial study utilizing the methylene blue method reported to be between 50 and160 μM in human and rat serum [44]. However, the recent studies are suggesting that the endogenous concentration of H_2S is much less and is between 10 nM and 3 μM [45, 46]. As H_2S has a dual effect, at lower concentrations, it has a physiological function in different tissues, whereas at higher concentrations, H_2S exerts its toxic effects by reversibly blocking of cytochrome C oxidase and inhibiting the electron transport chain in the mitochondria [47–49]. The catabolism of H_2S occurs mainly in the mitochondria by enzymatic pathways such as oxidoreductases and sulfurtransferase that break it into thiosulfate and sulfate. Moreover, oxidation of H_2S reduces the FAD prosthetic group, which uses ubiquinone (Q) as an electron acceptor, in electron transport chain which has a role in ATP production (Figure 1) [15, 36, 50–52]. However, under hypoxic conditions, oxidation of H_2S in the mitochondria reduces, allowing H_2S to accumulate and function as an oxygen sensor [53, 54]. H_2S accumulation during hypoxia helps to maintain cell function by upregulating anaerobic metabolic pathways like glycolysis [55] and other cytoprotective pathways [56]. H_2S also promotes restoration of the tissue oxygen supply by relaxation of vascular smooth muscles (vasodilation) and also stimulation of endothelial cell proliferation and migration (angiogenesis) [24, 57]. Beside the mitochondrial sulfide oxidation [58], H_2S can be oxidized and catabolized by two other minor pathways [9, 59]. The first pathway is the methylation of H_2S by thiol S-methyltransferase in the cytosol [60], and the second pathway is an interaction between H_2S and methemoglobin that leads to the production of sulfhemoglobin and polysulfides, which can be used as a biomarker for plasma H_2S levels [61, 62].

2. H_2S in Cancer

Several studies have shown that H_2S and its synthases are associated with the pathophysiology of tumors [20, 49, 63–66]. It has been shown that H_2S can modulate oxidative stress, interact with free radicals, and activate tumorigenic pathways [39, 61]. Several studies investigated the role and presence of H_2S in tumors. The expression of H_2S-producing enzymes (CBS, CSE, and 3-MPST) has been studied in various cancers including liver, colon, ovarian, breast, gastric, lung, oral squamous cell carcinoma, and melanoma [42, 49, 67–74]. However, the role and effect of H_2S on tumor biology, development, and progression are controversial [75–78]. Previous reviews have adequately summarized that H_2S can have pro- or anticancerous effects based on the type of tumor and the involved organ [23, 67]. It is reported that endogenous H_2S can have procancerous effects and help the survival of tumors by stimulating angiogenesis along with promoting cell proliferation, metastasis, and drug resistance [32, 49, 67, 79–81]. The anticancerous effects of exogenous H_2S administration have been reported for several human cancers [82, 83]. Endogenous H_2S can be employed as a biomarker for cancer imaging in mice and for differentiating cancer cells [84, 85]. Several pathways, such as inhibition of proliferation, induction of apoptosis, reduction of NF-κB levels, DNA damage, and modification of the cell cycle, are involved in the anticancer activity of H_2S [27, 29, 82, 86].

Similar to endogenous H_2S, the effect of exogenous H_2S treatment also shows a biphasic dose-dependent response on cancer cells as it does in healthy tissues whereby low concentrations of H_2S exhibit a procancerous effect and high concentrations exert an anticancerous effect [65, 67, 82, 83, 87]. The hypoxic environment of solid tumors [88] leads to

a higher level of endogenous H_2S synthesis [89, 90] and reduces the sulfide detoxification ability of the mitochondria [54, 91], which makes tumors more susceptible to H_2S toxicity. However, Malagrinò et al. showed that in hypoxic conditions, the activity of the mitochondrial sulfide-oxidizing pathway of quinone oxidoreductase (SQR) adaptively increased and improved the H_2S detoxification of mitochondria [92].

The direct quantification of H_2S in tissue samples is a challenge since it has a very short half-life [93]; one study used live fluorescent imaging techniques to visualize the H_2S in live cells directly [90]. However, in general, the expression level of H_2S-producing enzymes can be used to indirectly show the correlation between H_2S and its effects on healthy tissues and tumors [49, 80]. Increased levels of H_2S and the upregulation of one or more H_2S-synthesizing enzymes in comparison to healthy tissues have been reported in several tumors [49, 71, 72, 80, 94, 95]. It is also quite interesting that these three enzymes are expressed differently according to the type of cancer [67] and hence lend themselves as potential new targets for therapy.

3. H_2S in Urinary Cancers

Urinary cancers specifically kidney, urothelial, and prostate are relatively common in developed countries. Prostate cancer [96] is the second most commonly diagnosed cancer in men, and urothelial carcinomas (UCs) [97] are the fourth most common tumors both in men and in women. Kidney cancers are highly lethal, and their incidence is increasing incidentally by the common use of diagnostic tools. It is estimated that more than 300,000 new cases of urinary cancers and 33,429 deaths (excluding prostate cancer) will occur in 2019 in the United States [97]. As such, the role of H_2S and the differential expression of H_2S-producing enzymes in urinary cancers are of interest, and this review is aimed at summarizing recent evidence on this subject in the context of three common urinary cancers: urothelial cancer, renal cell carcinoma, and prostate cancer.

3.1. Urothelial Cancer. Urothelial carcinoma can be located in the lower (bladder and urethra) or the upper (pyelocaliceal cavities and ureter) urinary tract. Bladder tumors account for 90-95% of UCs and are the most common urinary tract malignancy. Sixty percent of upper tract urothelial cancers are invasive at diagnosis compared with 15-25% of bladder tumors [98]. The high recurrence rate and potential of metastasis are two critical characteristics of bladder cancer [99, 100]. Environmental (smoking and exposure to chemical-occupational toxins) and genetic factors all play a role in the etiology of bladder cancer, as does gender since it is more frequent in men older than 65 years of age [101].

Several studies have highlighted the importance of abnormal redox and cellular signaling in the incidence of bladder cancer [102]. Various reports suggest that alterations in H_2S synthesis pathways may increase the risk of bladder cancer [103, 104], suggesting that the modification of these pathways may lead to the development of novel diagnostic and therapeutic approaches for urological cancers [4].

H_2S has been detected in bladder homogenates of trout, mice, pigs, rats, and humans [105–109]. In humans, H_2S is involved in the control of bladder tone homeostasis [110], as it has previously been shown that exogenous H_2S or its substrate, L-cysteine, could decrease the tone of human and rat bladder strips in a dose-dependent manner [107, 108]. All of the H_2S-producing enzymes are also found in rat and human bladders, whereas in the mouse, only CSE could be detected [107–109]. The expression of these enzymes in human bladder cancer tissues and cell lines has been investigated. A recent study examined the expression of H_2S-producing enzymes in human bladder cancer tissues and compared them to healthy ones. They compared 94 human bladder cancer at different stages/grades and 20 human healthy bladder tissues in term of H_2S content as well as the H_2S synthases while attempting to find a correlation between the expression of H_2S-producing enzymes and the malignant progression of bladder cancer. They showed that H_2S content, as well as the expression of CBS, CSE, and 3-MPST, was higher in bladder cancer than in healthy samples. More interestingly, the enzyme expression of all three enzymes was correlated to different stages of bladder cancer. They suggested that this correlation between the malignancy and the expression of H_2S enzymes could lead to novel diagnosis and treatment applications [111]. Another recent study also showed, both *in vitro* and *in vivo* models, that apoptosis of bladder cancer cell lines or tissues with cisplatin was enhanced after the inhibition of H_2S production by propargylglycine (PAG) [23] and was inhibited upon adding the exogenous H_2S. These authors suggested the activation of the Erk1/2 signaling pathway and the blockage of mitochondrial apoptosis as the possible mechanisms behind their results [112].

Exogenous H_2S administration has also been shown to affect bladder cancer cell lines. The *in vitro* treatment of the bladder cancer cell line EJ with NaHS enhances cell proliferation and the invasion ability of the cells [113]. Interestingly, these authors also found that the expression of matrix metalloproteinases (MMP) 2 and 9, which are essential for the digestion of collagen IV, was increased in a dose-dependent manner upon the treatment of bladder cancer cells with NaHS. These two enzymes are essential in hydrolyzing the extracellular matrix during the invasion; therefore, H_2S might be necessary for the invasion of bladder cancer [113]. In addition, nicotinamide phosphoribosyltransferase (Nampt) is the rate-limiting step of nicotinamide adenine dinucleotide synthesis also increased in some cancers [114]. The signal transducer and activator of transcription 3 (Stat3) is one of the cell signaling molecules of the H_2S, and its activation induces Nampt protein expression via a positive feedback loop. A recent study showed that UC is immunoreactive for the enzymatically active phosphor-Stat3 signal transduction pathway and increased the Nampt and CBS protein expression [115]. Overall, bladder cancer appears to present with higher H_2S levels in cancer tissue homogenates and increased the expression of H_2S-producing enzymes, which suggests that H_2S may be essential for bladder cancer progression and growth, especially in the context of the induction of cell proliferation,

inhibition of apoptosis, and facilitation of tissue invasion. Further research is needed to establish consistent expression patterns and other cellular mechanisms for potential diagnostic and therapeutic approaches.

3.2. Renal Cell Carcinoma. Renal cell carcinoma (RCC) represents 2-3% of all cancers with the highest incidence in Western countries. The incidence varies globally, with the highest rates in developed countries such as North America and Europe and the lowest rates in Asia and Africa [116]. Over 300,000 men and women are diagnosed with kidney cancer around the world each year, and approximately 150,000 patients will die of the disease [96].

Clear cell renal cell carcinoma (ccRCC), papillary carcinoma, and chromophobe are the common subtypes of RCC [117], although ccRCC accounts for 80% of all RCCs [118]. Because of the lack of early warning signs and the absence of screening tests for people with a higher risk of kidney cancer, more than 30% of patients are at the metastatic stage at the time of diagnosis [119]. Metastatic RCC is highly resistant to systemic chemotherapy and radiation therapy [120, 121].

Inactivation of the Von Hippel-Lindau (VHL) tumor suppressor, which is responsible for the degradation of hypoxia-inducible factor alpha subunits (HIF-1/2α) during normoxia, occurs in 90% of ccRCC cases [122, 123]. As a result, HIF-1/2α subunits are not degraded under normoxic conditions in RCC cells, and the cells become pseudohypoxic [118]. The Warburg effect, which refers to a shift from mitochondrial respiration to glycolysis and production of lactate [124], enhances tumor growth and metastasis in RCC [125]. Using live cell imaging, Sonke et al. have previously shown that VHL-deficient ccRCC cell lines (769-P and 786-O) have significantly higher H_2S levels in comparison to ccRCC cells with wild-type VHL (Caki-1). They also showed that the inhibition of H_2S-producing enzymes by hydroxylamine (HA), which is an inhibitor of CBS and CSE, and PAG, an inhibitor of CSE, significantly decreases the H_2S levels in VHL-deficient ccRCC cell lines and subsequently inhibits their proliferation and metabolic activity. Moreover, this inhibition of H_2S synthesis in VHL-deficient ccRCC cell lines results in a two-fold reduction in cell survival rate in comparison to untreated cells. Another key finding from this work was that systemic inhibition of H_2S enzymes by HA administration in xenografted ccRCC in chicken embryos inhibited their vascularization and the subsequent growth of xenografts, which supports the known angiogenic activity of H_2S [79].

Two more recent studies have also evaluated the expression of H_2S enzymes in ccRCC. Shackelford et al. compared the expression of CBS in between human benign and Fuhrman grade I-IV ccRCC tissues by using tissue microarray and immunohistochemistry. They showed that CBS expressed weakly in benign tissues and even weaker in Fuhrman grade I ccRCC; however, its expression increased with increasing Fuhrman grades, and CBS expression was the highest in Fuhrman grade IV ccRCC samples [95]. Moreover, the Nmpt expression was correlated with CBS in increasing grade of tumors. Therefore, H_2S may play a contributory role in the progression of RCC [95]. Breza et al. also investigated the expression of H_2S-producing enzymes in 21 human ccRCC tissues and compared it to the normal/healthy portion of the same kidney sample using microarray and immunohistochemistry. They found that 66% of ccRCC tissue samples exhibited stable expression of CBS, and the remaining samples showed downregulation. CSE was downregulated in all samples except in three where it was unchanged. The expression of 3-MPST was decreased by 70% of ccRCC samples and remained unchanged in 30% of ccRCC samples [121]. These data suggest that the expression of H_2S enzymes is heterogeneously regulated in ccRCC. The contradiction between results might be attributed to Shackelford et al. not comparing benign/malignant tissues from the same patient. Breza et al. also showed that, upon induction of apoptosis, the expression of these enzymes was upregulated in the RCC4 cell line (human RCC cell line) and silencing of CBS and CSE expression made the cells resistant to apoptosis [121]. It is possible that endogenous H_2S induces apoptosis in ccRCC as it was previously reported with exogenous administration [126–130]. The mechanisms behind RCC progression are not well understood, but it is suggested that knocking down of heat shock protein 60 (HSP60) increases the epithelial to mesenchymal transition and enhances invasion and also disturbs the respiratory complex 1 and triggers reactive oxygen molecules and then DNA methylation for further tumorigenesis [131–133]. Tang et al. results supported that suggestion and showed that HSP60 expression is lower in ccRCC tissues compared to pericancerous tissues [134]. The PI3K/AKT pathway is another important pathway in RCC progression, and it is reported that exogenous H_2S inhibits this pathway, and therefore, exogenous H_2S could be a novel targeted therapy of RCC [135, 136]. Overall, the expression of H_2S enzymes could one day become a new tool for establishing prognosis in patients with RCC. However, further studies are necessary to elucidate the exact role of H_2S in RCC and to explain the contradictions between different studies.

3.3. Prostate Cancer. Prostate cancer (PCa) is the second most common cancer in men, with an estimated 1.1 million new cases worldwide in 2012, accounting for 15% of all cancers diagnosed. The incidence of PCa varies widely between different geographical areas, highest in developed countries, mainly due to the use of prostate-specific antigen (PSA) testing and the aging of the population [96]. Surgery, radiotherapy, and androgen deprivation therapies are the primary treatment modalities that are effective, especially in the early stages of the disease [137]. Although a physical exam and the serum PSA test are commonly used to screen and detect for prostate cancer; their utility is ineffective in diagnosing early stages of prostate cancer.

The relationship between H_2S activity and prostate cancer has been reviewed previously [138]. The expression of H_2S-producing enzymes was compared between cancerous and healthy prostate tissues [108, 139]. Endogenous H_2S and all three enzymes (CBS, CSE, and 3-MPST) have been demonstrated in healthy and prostate cancer. CSE has been

Table 1: Summary of H_2S and its producing enzymes in three common urinary cancers.

	H_2S highlights
Urothelial carcinoma	(i) Expressions of H_2S and its synthases are higher in cancer tissue [111]. (ii) H_2S protects the bladder cancer against apoptosis [112]. (iii) H_2S increases the cell proliferation, invasion, and metastasis of bladder cancer [113].
Renal cell carcinoma	(i) Enhanced expression of H_2S in ccRCC due to VHL deficiency improves the survival, growth, and metastasis [79]. (ii) Controversial reports about the comparative expression of H_2S enzymes [95, 121]. (iii) H_2S contributes to the induction of apoptosis in RCC [121].
Prostate cancer	(i) H_2S enzymes are expressed in the prostate [107]. (ii) CSE is the main H_2S-producing enzyme in the prostate [107, 139, 142]. (iii) CSE is downregulated in prostate cancer [140].

shown to have a higher expression in the smooth muscle layer of the prostate cancer samples [94]. However, in another study, they could not detect the expression of 3-MPST in both normal and cancerous prostate tissues, but they showed that CSE was significantly downregulated in prostate cancer, whereas CBS was not changed in each sample. This study also showed that antiandrogen-resistant prostate cancer cells express less CSE and have lower H_2S content in comparison to the parental cell line [140].

Moreover, new evidence suggests that H_2S-releasing molecules could be effective in the treatment of chemotherapy-resistant prostate cancers [141]. The stromal part of the prostate tissue and the stromal cell line showed average to high CSE expression [139]. In addition, both CBS and CSE are present in mouse prostate cancers, unrelated to androgen dependency, and *in vitro* work showed that CSE is the main contributor to H_2S production in prostate cancer cell lines (PC-3). The critical role of CSE was confirmed upon finding that aged CSE knockout mice have higher cell proliferation and significantly less H_2S production in the prostate [142]. Interestingly, the androgen-dependent prostate cell line showed the highest expression of CBS and CSE, and their expression was downregulated upon dihydrotestosterone treatment [139]. These data suggest that CSE may be a potential therapeutic target and diagnostic tool for prostate cancer.

As mentioned earlier, thiosulfate is the stable breakdown product of H_2S in the mitochondria that can be tracked in the urine. Therefore, the thiosulfate level in urine can be an indicator of exposure to H_2S or disruption in the breakdown process. Chwatko et al. investigated urinary thiosulfate levels amongst the malignant in comparison to benign prostate hyperplasia (BPH) patients and healthy volunteers. They also found that the urine level of thiosulfate in malignant prostate cancer patients was 50 times higher than the healthy volunteers and five times higher than the BPH patients, and also, there was a positive correlation between the size of the prostate and the urine level of thiosulfate in comparison between the BPH and the control group [143]. In the nude mouse model of human prostate cancer, the plasma concentration of cysteine was significantly decreased after advanced tumor growth [144]. Contrary to these results, five years after prostatectomy, cysteine, homocysteine, and cystathionine were found to be higher in the urine of recurrent prostate cancer patients in comparison to recurrence-free patients [145]. Recent studies showed that methionine catabolism [146], and increased level of cystathionine [147] and sarcosine (N-methylglycine), a by-product of methionine catabolism [148], in urine correlated with prostate cancer stage. In addition, recent data suggest that neuroendocrine-like differentiation of prostate cancer (LNCaP) cells contributes to the androgen-independent growth [149, 150]. The expression and activity of CSE and CBS, in LNCaP cell, are much more than those in healthy prostatic epithelial cells [139]. The H_2S donors, NaHS and Na_2S, further enhance the upregulated calcium channels in the LNCaP cells [151]. Overall, it appears that cysteine, homocysteine, cystathionine, and sarcosine could all potentially be biomarkers for prostate cancer.

4. Conclusion

Despite significant research efforts in recent years, the role of H_2S in the context of cancer pathophysiology remains controversial (Table 1). Several studies have partially elucidated the vital role of H_2S activity, which plays a different role in urological malignancies (Figure 1). Interestingly, the expression patterns of H_2S-producing enzymes appear to be contradictory, depending upon the subtype of cancer, which was evaluated and in fact, may be tissue dependent. However, these studies, as mentioned earlier, lay the groundwork for future work that may lead to the development of new diagnostic tools for detecting urinary cancers in earlier stages. Moreover, pharmacological modulation of H_2S synthetic pathways and exogenous administration of donor molecules may one day provide us with additional therapeutic avenues in treating patients with urological malignancies.

Conflicts of Interest

The authors declare that there is no conflict of interest regarding the publication of this paper.

References

[1] P. Fagone, E. Mazzon, P. Bramanti, K. Bendtzen, and F. Nicoletti, "Gasotransmitters and the immune system: mode of action and novel therapeutic targets," *European Journal of Pharmacology*, vol. 834, pp. 92–102, 2018.

[2] R. Wang, "Gasotransmitters: growing pains and joys," *Trends in Biochemical Sciences*, vol. 39, no. 5, pp. 227–232, 2014.

[3] H. Kimura, "Hydrogen sulfide: its production, release and functions," *Amino Acids*, vol. 41, no. 1, pp. 113–121, 2011.

[4] L. Li, P. Rose, and P. K. Moore, "Hydrogen sulfide and cell signaling," *Annual Review of Pharmacology and Toxicology*, vol. 51, no. 1, pp. 169–187, 2011.

[5] T. Ida, T. Sawa, H. Ihara et al., "Reactive cysteine persulfides and S-polythiolation regulate oxidative stress and redox signaling," *Proceedings of the National Academy of Sciences of the United States of America*, vol. 111, no. 21, pp. 7606–7611, 2014.

[6] P. K. Yadav, M. Martinov, V. Vitvitsky et al., "Biosynthesis and reactivity of cysteine persulfides in signaling," *Journal of the American Chemical Society*, vol. 138, no. 1, pp. 289–299, 2016.

[7] O. Kabil and R. Banerjee, "Enzymology of H_2S biogenesis, decay and signaling," *Antioxidants & Redox Signaling*, vol. 20, no. 5, pp. 770–782, 2014.

[8] K. R. Olson, "H_2S and polysulfide metabolism: conventional and unconventional pathways," *Biochemical Pharmacology*, vol. 149, pp. 77–90, 2018.

[9] A. Giuffrè and J. B. Vicente, "Hydrogen sulfide biochemistry and interplay with other gaseous mediators in mammalian physiology," *Oxidative Medicine and Cellular Longevity*, vol. 2018, Article ID 6290931, 31 pages, 2018.

[10] S. Pandey, "Hydrogen sulfide: a new node in the abscisic acid-dependent guard cell signaling network?," *Plant Physiology*, vol. 166, no. 4, pp. 1680-1681, 2014.

[11] J. T. Hancock and M. Whiteman, "Hydrogen sulfide and cell signaling: team player or referee?," *Plant Physiology and Biochemistry*, vol. 78, pp. 37–42, 2014.

[12] R. Wang, "Physiological implications of hydrogen sulfide: a whiff exploration that blossomed," *Physiological Reviews*, vol. 92, no. 2, pp. 791–896, 2012.

[13] B. D. Paul and S. H. Snyder, "H_2S signalling through protein sulfhydration and beyond," *Nature Reviews Molecular Cell Biology*, vol. 13, no. 8, pp. 499–507, 2012.

[14] Y. Liu, R. Yang, X. Liu et al., "Hydrogen sulfide maintains mesenchymal stem cell function and bone homeostasis via regulation of Ca^{2+} channel sulfhydration," *Cell Stem Cell*, vol. 15, no. 1, pp. 66–78, 2014.

[15] O. Kabil and R. Banerjee, "Redox biochemistry of hydrogen sulfide," *The Journal of Biological Chemistry*, vol. 285, no. 29, pp. 21903–21907, 2010.

[16] X. Shen, M. Carlstrom, S. Borniquel, C. Jadert, C. G. Kevil, and J. O. Lundberg, "Microbial regulation of host hydrogen sulfide bioavailability and metabolism," *Free Radical Biology & Medicine*, vol. 60, pp. 195–200, 2013.

[17] M. Whiteman, S. Le Trionnaire, M. Chopra, B. Fox, and J. Whatmore, "Emerging role of hydrogen sulfide in health and disease: critical appraisal of biomarkers and pharmacological tools," *Clinical Science*, vol. 121, no. 11, pp. 459–488, 2011.

[18] M. M. Kuo, D. H. Kim, S. Jandu et al., "MPST but not CSE is the primary regulator of hydrogen sulfide production and function in the coronary artery," *American Journal of Physiology-Heart and Circulatory Physiology*, vol. 310, no. 1, pp. H71–H79, 2016.

[19] K. Kashfi, R. Kodela, N. Nath, M. Chattopadhyay, D. E. Nesbitt, and C. A. Velázquez-Martínez, "Hydrogen sulfide-releasing naproxen suppresses colon cancer cell growth and inhibits NF-κB signaling," *Drug Design, Development and Therapy*, vol. 9, article 4873, 2015.

[20] M. R. Hellmich and C. Szabo, "Hydrogen sulfide and cancer," *Handbook of Experimental Pharmacology*, vol. 230, pp. 233–241, 2015.

[21] H. Ahn, E. Lee, K. Kim, and C. Lee, "Effect of glutathione and its related enzymes on chemosensitivity of renal cell carcinoma and bladder carcinoma cell lines," *The Journal of Urology*, vol. 151, no. 1, pp. 263–267, 1994.

[22] T. Simic, A. Savic-Radojevic, M. Pljesa-Ercegovac, M. Matic, and J. Mimic-Oka, "Glutathione S-transferases in kidney and urinary bladder tumors," *Nature Reviews Urology*, vol. 6, no. 5, pp. 281–289, 2009.

[23] A. Ianaro and G. Cirino, "Hydrogen sulfide pathway and cancer," *Brain Metastases from Primary Tumors, Volume 3*, vol. 3, pp. 133–144, 2016.

[24] C. Coletta, A. Papapetropoulos, K. Erdelyi et al., "Hydrogen sulfide and nitric oxide are mutually dependent in the regulation of angiogenesis and endothelium-dependent vasorelaxation," *Proceedings of the National Academy of Sciences of the United States of America*, vol. 109, no. 23, pp. 9161–9166, 2012.

[25] E. Pupo, A. Fiorio Pla, D. Avanzato et al., "Hydrogen sulfide promotes calcium signals and migration in tumor-derived endothelial cells," *Free Radical Biology and Medicine*, vol. 51, no. 9, pp. 1765–1773, 2011.

[26] S. L. Davis, P. J. Fadel, J. Cui, G. D. Thomas, and C. G. Crandall, "Skin blood flow influences near-infrared spectroscopy-derived measurements of tissue oxygenation during heat stress," *Journal of Applied Physiology*, vol. 100, no. 1, pp. 221–224, 2006.

[27] W.-J. Cai, M.-J. Wang, L.-H. Ju, C. Wang, and Y.-C. Zhu, "Hydrogen sulfide induces human colon cancer cell proliferation: role of Akt, ERK and p21," *Cell Biology International*, vol. 34, no. 6, pp. 565–572, 2010.

[28] G. A. Bellingham, R. S. Smith, P. Morley-Forster, and J. M. Murkin, "Use of near infrared spectroscopy to detect impaired tissue oxygen saturation in patients with complex regional pain syndrome type 1," *Canadian Journal of Anaesthesia*, vol. 61, no. 6, pp. 563–570, 2014.

[29] Q. Cao, L. Zhang, G. Yang, C. Xu, and R. Wang, "Butyrate-stimulated H_2S production in colon cancer cells," *Antioxidants & Redox Signaling*, vol. 12, no. 9, pp. 1101–1109, 2010.

[30] Y. Kimura, Y.-I. Goto, and H. Kimura, "Hydrogen sulfide increases glutathione production and suppresses oxidative stress in mitochondria," *Antioxidants & Redox Signaling*, vol. 12, no. 1, pp. 1–13, 2010.

[31] G. Yang, L. Wu, B. Jiang et al., "H_2S as a physiologic vasorelaxant: hypertension in mice with deletion of Cystathionine γ-Lyase," *Science*, vol. 322, no. 5901, pp. 587–590, 2008.

[32] D. K. Ma, R. Vozdek, N. Bhatla, and H. R. Horvitz, "CYSL-1 Interacts with the O_2-Sensing Hydroxylase EGL-9 to Promote H_2S-Modulated Hypoxia-Induced Behavioral Plasticity in *C. elegans*," *Neuron*, vol. 73, no. 5, pp. 925–940, 2012.

[33] M. Bhatia, "Hydrogen sulfide and substance P in inflammation," *Antioxidants & Redox Signaling*, vol. 12, no. 10, pp. 1191–1202, 2010.

[34] R. Xue, D.-D. Hao, J.-P. Sun et al., "Hydrogen sulfide treatment promotes glucose uptake by increasing insulin receptor sensitivity and ameliorates kidney lesions in type 2 diabetes," *Antioxidants & Redox Signaling*, vol. 19, no. 1, pp. 5–23, 2013.

[35] C. T. Yang, L. Chen, S. Xu, J. J. Day, X. Li, and M. Xian, "Recent development of hydrogen sulfide releasing/stimulating reagents and their potential applications in cancer and glycometabolic disorders," *Frontiers in Pharmacology*, vol. 8, 2017.

[36] M. Fu, W. Zhang, L. Wu, G. Yang, H. Li, and R. Wang, "Hydrogen sulfide (H_2S) metabolism in mitochondria and its regulatory role in energy production," *Proceedings of the National Academy of Sciences of the United States of America*, vol. 109, no. 8, pp. 2943–2948, 2012.

[37] I. Lobb, M. Davison, D. Carter et al., "Hydrogen sulfide treatment mitigates renal allograft ischemia-reperfusion injury during cold storage and improves early transplant kidney function and survival following allogeneic renal transplantation," *The Journal of Urology*, vol. 194, no. 6, pp. 1806–1815, 2015.

[38] G.-D. Yang and R. Wang, "H(2)S and cellular proliferation and apoptosis," *Sheng Li Xue Bao*, vol. 59, no. 2, pp. 133–140, 2007.

[39] C. Szabó, "Hydrogen sulphide and its therapeutic potential," *Nature Reviews Drug Discovery*, vol. 6, no. 11, pp. 917–935, 2007.

[40] R. Guo, J. Lin, W. Xu et al., "Hydrogen sulfide attenuates doxorubicin-induced cardiotoxicity by inhibition of the p38 MAPK pathway in H9c2 cells," *International Journal of Molecular Medicine*, vol. 31, no. 3, pp. 644–650, 2013.

[41] J. Du, Y. Huang, H. Yan et al., "Hydrogen sulfide suppresses oxidized low-density lipoprotein (Ox-LDL)-stimulated monocyte chemoattractant protein 1 generation from macrophages via the nuclear factor κB (NF-κB) pathway," *The Journal of Biological Chemistry*, vol. 289, no. 14, pp. 9741–9753, 2014.

[42] E. Panza, P. de Cicco, C. Armogida et al., "Role of the cystathionine γ lyase/hydrogen sulfide pathway in human melanoma progression," *Pigment Cell & Melanoma Research*, vol. 28, no. 1, pp. 61–72, 2015.

[43] N. L. Whitfield, E. L. Kreimier, F. C. Verdial, N. Skovgaard, and K. R. Olson, "Reappraisal of H_2S/sulfide concentration in vertebrate blood and its potential significance in ischemic preconditioning and vascular signaling," *American Journal of Physiology-Regulatory, Integrative and Comparative Physiology*, vol. 294, no. 6, pp. R1930–R1937, 2008.

[44] M. Whiteman and P. K. Moore, "Hydrogen sulfide and the vasculature: a novel vasculoprotective entity and regulator of nitric oxide bioavailability?," *Journal of Cellular and Molecular Medicine*, vol. 13, no. 3, pp. 488–507, 2009.

[45] M. Ishigami, K. Hiraki, K. Umemura, Y. Ogasawara, K. Ishii, and H. Kimura, "A source of hydrogen sulfide and a mechanism of its release in the brain," *Antioxidants & Redox Signaling*, vol. 11, no. 2, pp. 205–214, 2009.

[46] M. D. Levitt, M. S. Abdel-Rehim, and J. Furne, "Free and acid-labile hydrogen sulfide concentrations in mouse tissues: anomalously high free hydrogen sulfide in aortic tissue," *Antioxidants & Redox Signaling*, vol. 15, no. 2, pp. 373–378, 2011.

[47] C. E. Cooper and G. C. Brown, "The inhibition of mitochondrial cytochrome oxidase by the gases carbon monoxide, nitric oxide, hydrogen cyanide and hydrogen sulfide: chemical mechanism and physiological significance," *Journal of Bioenergetics and Biomembranes*, vol. 40, no. 5, pp. 533–539, 2008.

[48] R. Baskar and J. Bian, "Hydrogen sulfide gas has cell growth regulatory role," *European Journal of Pharmacology*, vol. 656, no. 1–3, pp. 5–9, 2011.

[49] C. Szabo, C. Coletta, C. Chao et al., "Tumor-derived hydrogen sulfide, produced by cystathionine-β-synthase, stimulates bioenergetics, cell proliferation, and angiogenesis in colon cancer," *Proceedings of the National Academy of Sciences of the United States of America*, vol. 110, no. 30, pp. 12474–12479, 2013.

[50] T. M. Hildebrandt and M. K. Grieshaber, "Three enzymatic activities catalyze the oxidation of sulfide to thiosulfate in mammalian and invertebrate mitochondria," *The FEBS Journal*, vol. 275, no. 13, pp. 3352–3361, 2008.

[51] K. Kashfi and K. R. Olson, "Biology and therapeutic potential of hydrogen sulfide and hydrogen sulfide-releasing chimeras," *Biochemical Pharmacology*, vol. 85, no. 5, pp. 689–703, 2013.

[52] M. R. Jackson, S. L. Melideo, and M. S. Jorns, "Human sulfide:quinone oxidoreductase catalyzes the first step in hydrogen sulfide metabolism and produces a sulfane sulfur metabolite," *Biochemistry*, vol. 51, no. 34, pp. 6804–6815, 2012.

[53] E. Lagoutte, S. Mimoun, M. Andriamihaja, C. Chaumontet, F. Blachier, and F. Bouillaud, "Oxidation of hydrogen sulfide remains a priority in mammalian cells and causes reverse electron transfer in colonocytes," *Biochimica et Biophysica Acta (BBA) - Bioenergetics*, vol. 1797, no. 8, pp. 1500–1511, 2010.

[54] K. R. Olson, "Hydrogen sulfide as an oxygen sensor," *Antioxidants & Redox Signaling*, vol. 22, no. 5, pp. 377–397, 2015.

[55] A. K. Mustafa, M. M. Gadalla, N. Sen et al., "H_2S signals through protein S-sulfhydration," *Science Signaling*, vol. 2, no. 96, article ra72, 2009.

[56] N. Sen, B. D. Paul, M. M. Gadalla et al., "Hydrogen sulfide-linked sulfhydration of NF-κB mediates its antiapoptotic actions," *Molecular Cell*, vol. 45, no. 1, pp. 13–24, 2012.

[57] C. Szabó and A. Papapetropoulos, "Hydrogen sulphide and angiogenesis: mechanisms and applications," *British Journal of Pharmacology*, vol. 164, no. 3, pp. 853–865, 2011.

[58] M. D. Levitt, J. Furne, J. Springfield, F. Suarez, and E. DeMaster, "Detoxification of hydrogen sulfide and methanethiol in the cecal mucosa," *The Journal of Clinical Investigation*, vol. 104, no. 8, pp. 1107–1114, 1999.

[59] R. A. Weisiger, L. M. Pinkus, and W. B. Jakoby, "Thiol *S*-methyltransferase: suggested role in detoxication of intestinal hydrogen sulfide," *Biochemical Pharmacology*, vol. 29, no. 20, pp. 2885–2887, 1980.

[60] D. J. Polhemus and D. J. Lefer, "Emergence of hydrogen sulfide as an endogenous gaseous signaling molecule in cardiovascular disease," *Circulation Research*, vol. 114, no. 4, pp. 730–737, 2014.

[61] M. Kajimura, R. Fukuda, R. M. Bateman, T. Yamamoto, and M. Suematsu, "Interactions of multiple gas-transducing systems: hallmarks and uncertainties of CO, NO, and H_2S gas biology," *Antioxidants & Redox Signaling*, vol. 13, no. 2, pp. 157–192, 2010.

[62] V. Vitvitsky, P. K. Yadav, S. An, J. Seravalli, U.-S. Cho, and R. Banerjee, "Structural and mechanistic insights into hemoglobin-catalyzed hydrogen sulfide oxidation and the fate of polysulfide products," *The Journal of Biological Chemistry*, vol. 292, no. 13, pp. 5584–5592, 2017.

[63] L. Zhang, Q. Qi, J. Yang et al., "An anticancer role of hydrogen sulfide in human gastric cancer cells," *Oxidative Medicine and Cellular Longevity*, vol. 2015, Article ID 636410, 8 pages, 2015.

[64] M. Lv, Y. Li, M.-H. Ji, M. Zhuang, and J.-H. Tang, "Inhibition of invasion and epithelial-mesenchymal transition of human breast cancer cells by hydrogen sulfide through decreased phospho-p38 expression," *Molecular Medicine Reports*, vol. 10, no. 1, pp. 341–346, 2014.

[65] M. R. Hellmich, C. Coletta, C. Chao, and C. Szabo, "The therapeutic potential of cystathionine β-synthetase/hydrogen sulfide inhibition in cancer," *Antioxidants & Redox Signaling*, vol. 22, no. 5, pp. 424–448, 2015.

[66] X. Cao, L. Ding, Z. Xie et al., "A review of hydrogen sulfide synthesis, metabolism, and measurement: is modulation of hydrogen sulfide a novel therapeutic for cancer?," *Antioxidants & Redox Signaling*, vol. 31, no. 1, pp. 1–38, 2019.

[67] D. Wu, W. Si, M. Wang, S. Lv, A. Ji, and Y. Li, "Hydrogen sulfide in cancer: friend or foe?," *Nitric Oxide*, vol. 50, pp. 38–45, 2015.

[68] M. A. Kaium, Y. Liu, Q. Zhu et al., "H_2S donor, S-propargyl-cysteine, increases CSE in SGC-7901 and cancer-induced mice: evidence for a novel anti-cancer effect of endogenous H_2S?," *PLoS One*, vol. 6, no. 6, article e20525, 2011.

[69] S. Ramasamy, S. Singh, P. Taniere, M. J. S. Langman, and M. C. Eggo, "Sulfide-detoxifying enzymes in the human colon are decreased in cancer and upregulated in differentiation," *American Journal of Physiology-Gastrointestinal and Liver Physiology*, vol. 291, no. 2, pp. G288–G296, 2006.

[70] M. Chattopadhyay, R. Kodela, N. Nath, A. Barsegian, D. Boring, and K. Kashfi, "Hydrogen sulfide-releasing aspirin suppresses NF-κB signaling in estrogen receptor negative breast cancer cells in vitro and in vivo," *Biochemical Pharmacology*, vol. 83, no. 6, pp. 723–732, 2012.

[71] S. Bhattacharyya, S. Saha, K. Giri et al., "Cystathionine beta-synthase (CBS) contributes to advanced ovarian cancer progression and drug resistance," *PLoS One*, vol. 8, no. 11, article e79167, 2013.

[72] K. Módis, C. Coletta, A. Asimakopoulou et al., "Effect of S-adenosyl-l-methionine (SAM), an allosteric activator of cystathionine-β-synthase (CBS) on colorectal cancer cell proliferation and bioenergetics *in vitro*," *Nitric Oxide*, vol. 41, pp. 146–156, 2014.

[73] B. Szczesny, M. Marcatti, J. R. Zatarain et al., "Inhibition of hydrogen sulfide biosynthesis sensitizes lung adenocarcinoma to chemotherapeutic drugs by inhibiting mitochondrial DNA repair and suppressing cellular bioenergetics," *Scientific Reports*, vol. 6, no. 1, 2016.

[74] A. T. Meram, J. Chen, S. Patel et al., "Hydrogen sulfide is increased in oral squamous cell carcinoma compared to adjacent benign oral mucosae," *Anticancer Research*, vol. 38, no. 7, pp. 3843–3852, 2018.

[75] Z.-W. Lee, X.-Y. Teo, E. Y.-W. Tay et al., "Utilizing hydrogen sulfide as a novel anti-cancer agent by targeting cancer glycolysis and pH imbalance," *British Journal of Pharmacology*, vol. 171, no. 18, pp. 4322–4336, 2014.

[76] Z. Ma, Q. Bi, and Y. Wang, "Hydrogen sulfide accelerates cell cycle progression in oral squamous cell carcinoma cell lines," *Oral Diseases*, vol. 21, no. 2, pp. 156–162, 2015.

[77] C. Szabo and M. R. Hellmich, "Endogenously produced hydrogen sulfide supports tumor cell growth and proliferation," *Cell Cycle*, vol. 12, no. 18, pp. 2915-2916, 2014.

[78] B. Renga, "Hydrogen sulfide generation in mammals: the molecular biology of cystathionine-β-synthase (CBS) and cystathionine-γ-lyase (CSE)," *Inflammation & Allergy - Drug Targets*, vol. 10, no. 2, pp. 85–91, 2011.

[79] E. Sonke, M. Verrydt, C. O. Postenka et al., "Inhibition of endogenous hydrogen sulfide production in clear-cell renal cell carcinoma cell lines and xenografts restricts their growth, survival and angiogenic potential," *Nitric Oxide*, vol. 49, pp. 26–39, 2015.

[80] H. Jurkowska, W. Placha, N. Nagahara, and M. Wróbel, "The expression and activity of cystathionine-γ-lyase and 3-mercaptopyruvate sulfurtransferase in human neoplastic cell lines," *Amino Acids*, vol. 41, no. 1, pp. 151–158, 2011.

[81] A. A. Untereiner, A. Pavlidou, N. Druzhyna, A. Papapetropoulos, M. R. Hellmich, and C. Szabo, "Drug resistance induces the upregulation of H_2S-producing enzymes in HCT116 colon cancer cells," *Biochemical Pharmacology*, vol. 149, pp. 174–185, 2018.

[82] M. Chattopadhyay, N. Nath, R. Kodela et al., "Hydrogen sulfide-releasing aspirin inhibits the growth of leukemic Jurkat cells and modulates β-catenin expression," *Leukemia Research*, vol. 37, no. 10, pp. 1302–1308, 2013.

[83] M. Chattopadhyay, R. Kodela, N. Nath et al., "Hydrogen sulfide-releasing NSAIDs inhibit the growth of human cancer cells: a general property and evidence of a tissue type-independent effect," *Biochemical Pharmacology*, vol. 83, no. 6, pp. 715–722, 2012.

[84] C. Zhang, Q.-Z. Zhang, K. Zhang et al., "Dual-biomarker-triggered fluorescence probes for differentiating cancer cells and revealing synergistic antioxidant effects under oxidative stress," *Chemical Science*, vol. 10, no. 7, pp. 1945–1952, 2019.

[85] K. Zhang, J. Zhang, Z. Xi et al., "A new H2S-specific near-infrared fluorescence-enhanced probe that can visualize the H_2S level in colorectal cancer cells in mice," *Chemical Science*, vol. 8, no. 4, pp. 2776–2781, 2017.

[86] P. Rose, "Hydrogen sulfide protects colon cancer cells from chemopreventative agent β-phenylethyl isothiocyanate induced apoptosis," *World Journal of Gastroenterology*, vol. 11, no. 26, pp. 3990–3997, 2005.

[87] D. Wu, M. Li, W. Tian et al., "Hydrogen sulfide acts as a double-edged sword in human hepatocellular carcinoma cells through EGFR/ERK/MMP-2 and PTEN/AKT signaling pathways," *Scientific Reports*, vol. 7, 2017.

[88] B. Muz, P. de la Puente, F. Azab, and A. K. Azab, "The role of hypoxia in cancer progression, angiogenesis, metastasis, and resistance to therapy," *Hypoxia*, vol. 3, pp. 83–92, 2015.

[89] N. Takano, Y.-J. Peng, G. K. Kumar et al., "Hypoxia-inducible factors regulate human and rat cystathionine β-synthase gene expression," *The Biochemical Journal*, vol. 458, no. 2, pp. 203–211, 2014.

[90] M. Wang, Z. Guo, and S. Wang, "Regulation of cystathionine γ-lyase in mammalian cells by hypoxia," *Biochemical Genetics*, vol. 52, no. 1–2, pp. 29–37, 2014.

[91] B. Wu, H. Teng, L. Zhang et al., "Interaction of hydrogen sulfide with oxygen sensing under hypoxia," *Oxidative Medicine*

and Cellular Longevity, vol. 2015, Article ID 758678, 9 pages, 2015.

[92] F. Malagrinò, K. Zuhra, L. Mascolo et al., "Hydrogen sulfide oxidation: adaptive changes in mitochondria of SW480 colorectal cancer cells upon exposure to hypoxia," *Oxidative Medicine and Cellular Longevity*, vol. 2019, Article ID 8102936, 11 pages, 2019.

[93] V. Vitvitsky, O. Kabil, and R. Banerjee, "High turnover rates for hydrogen sulfide allow for rapid regulation of its tissue concentrations," *Antioxidants & Redox Signaling*, vol. 17, no. 1, pp. 22–31, 2012.

[94] S. Sen, B. Kawahara, D. Gupta et al., "Role of cystathionine β-synthase in human breast cancer," *Free Radical Biology and Medicine*, vol. 86, pp. 228–238, 2015.

[95] R. E. Shackelford, J. Abdulsattar, E. X. Wei, J. Cotelingam, D. Coppola, and G. A. Herrera, "Increased nicotinamide phosphoribosyltransferase and Cystathionine-β-Synthase in renal oncocytomas, renal urothelial carcinoma, and renal clear cell carcinoma," *Anticancer Research*, vol. 37, no. 7, pp. 3423–3427, 2017.

[96] J. Ferlay, I. Soerjomataram, R. Dikshit et al., "Cancer incidence and mortality worldwide: sources, methods and major patterns in GLOBOCAN 2012," *International Journal of Cancer*, vol. 136, no. 5, pp. E359–E386, 2015.

[97] R. L. Siegel, K. D. Miller, and A. Jemal, "Cancer statistics, 2019," *CA: A Cancer Journal for Clinicians*, vol. 69, no. 1, pp. 7–34, 2018.

[98] V. Margulis, S. F. Shariat, S. F. Matin et al., "Outcomes of radical nephroureterectomy: a series from the Upper Tract Urothelial Carcinoma Collaboration," *Cancer*, vol. 115, no. 6, pp. 1224–1233, 2009.

[99] S. R. Krishna and B. R. Konety, "Current concepts in the management of muscle invasive bladder cancer," *Indian Journal of Surgical Oncology*, vol. 8, no. 1, pp. 74–81, 2017.

[100] X. Zhang, C. Han, and J. He, "Recent advances in the diagnosis and management of bladder cancer," *Cell Biochemistry and Biophysics*, vol. 73, no. 1, pp. 11–15, 2015.

[101] A. Althunayan and W. Kassouf, "Asymptomatic microscopic hematuria: clinical significance and evaluation," *Current Medical Literature*, vol. 17, 2011.

[102] H. Wallerand, R. R. Reiter, and A. Ravaud, "Molecular targeting in the treatment of either advanced or metastatic bladder cancer or both according to the signalling pathways," *Current Opinion in Urology*, vol. 18, no. 5, pp. 524–532, 2008.

[103] C.-J. Chung, Y.-S. Pu, C.-T. Su et al., "Polymorphisms in one-carbon metabolism pathway genes, urinary arsenic profile, and urothelial carcinoma," *Cancer Causes & Control*, vol. 21, no. 10, pp. 1605–1613, 2010.

[104] L. E. Moore, N. Malats, N. Rothman et al., "Polymorphisms in one-carbon metabolism and trans-sulfuration pathway genes and susceptibility to bladder cancer," *International Journal of Cancer*, vol. 120, no. 11, pp. 2452–2458, 2007.

[105] R. A. Dombkowski, "Hydrogen sulfide mediates hypoxia-induced relaxation of trout urinary bladder smooth muscle," *The Journal of Experimental Biology*, vol. 209, no. 16, pp. 3234–3240, 2006.

[106] V. S. Fernandes, A. S. F. Ribeiro, M. V. Barahona et al., "Hydrogen sulfide mediated inhibitory neurotransmission to the pig bladder neck: role of K_{ATP} channels, sensory nerves and calcium signaling," *The Journal of Urology*, vol. 190, no. 2, pp. 746–756, 2013.

[107] F. Fusco, R. d'Emmanuele di Villa Bianca, E. Mitidieri, G. Cirino, R. Sorrentino, and V. Mirone, "Sildenafil Effect on the human bladder involves the L-cysteine/hydrogen sulfide pathway: a novel mechanism of action of phosphodiesterase type 5 inhibitors," *European Urology*, vol. 62, no. 6, pp. 1174–1180, 2012.

[108] J.-W. Gai, W. Wahafu, H. Guo et al., "Further evidence of endogenous hydrogen sulphide as a mediator of relaxation in human and rat bladder," *Asian Journal of Andrology*, vol. 15, no. 5, pp. 692–696, 2013.

[109] M. Matsunami, T. Miki, K. Nishiura et al., "Involvement of the endogenous hydrogen sulfide/$Ca_v3.2$ T-type Ca^{2+} channel pathway in cystitis-related bladder pain in mice," *British Journal of Pharmacology*, vol. 167, no. 4, pp. 917–928, 2012.

[110] W. C. de Groat and N. Yoshimura, "Pharmacology of the lower urinary tract," *Annual Review of Pharmacology and Toxicology*, vol. 41, no. 1, pp. 691–721, 2001.

[111] J.-W. Gai, W. Qin, M. Liu et al., "Expression profile of hydrogen sulfide and its synthases correlates with tumor stage and grade in urothelial cell carcinoma of bladder," *Urologic Oncology: Seminars and Original Investigations*, vol. 34, no. 4, pp. 166.e15–166.e20, 2016.

[112] W. Wahafu, J. Gai, L. Song et al., "Increased H2S and its synthases in urothelial cell carcinoma of the bladder, and enhanced cisplatin-induced apoptosis following H2S inhibition in EJ cells," *Oncology Letters*, vol. 15, 2018.

[113] H. Liu, J. Chang, Z. Zhao, Y. Li, and J. Hou, "Effects of exogenous hydrogen sulfide on the proliferation and invasion of human bladder cancer cells," *Journal of Cancer Research and Therapeutics*, vol. 13, no. 5, pp. 829–832, 2017.

[114] R. E. Shackelford, K. Mayhall, N. M. Maxwell, E. Kandil, and D. Coppola, "Nicotinamide phosphoribosyltransferase in malignancy: a review," *Genes & Cancer*, vol. 4, no. 11–12, pp. 447–456, 2013.

[115] R. Sanokawa-Akakura, E. A. Ostrakhovitch, S. Akakura, S. Goodwin, and S. Tabibzadeh, "A H_2S-Nampt dependent energetic circuit is critical to survival and cytoprotection from damage in cancer cells," *PLoS One*, vol. 9, no. 9, article e108537, 2014.

[116] U. Capitanio, K. Bensalah, A. Bex et al., "Epidemiology of renal cell carcinoma," *European Urology*, vol. 75, no. 1, pp. 74–84, 2019.

[117] G. Kovacs, M. Akhtar, B. J. Beckwith et al., "The Heidelberg classification of renal cell tumours," *The Journal of Pathology*, vol. 183, no. 2, pp. 131–133, 1997.

[118] K. P. van Houwelingen, B. A. C. van Dijk, C. A. Hulsbergen-van de Kaa et al., "Prevalence of *von Hippel-Lindau* gene mutations in sporadic renal cell carcinoma: results from the Netherlands cohort study," *BMC Cancer*, vol. 5, no. 1, 2005.

[119] B. I. Rini, S. C. Campbell, and B. Escudier, "Renal cell carcinoma," *The Lancet*, vol. 373, no. 9669, pp. 1119–1132, 2009.

[120] R. J. Motzer and P. Russo, "Systemic therapy for renal cell carcinoma," *The Journal of Urology*, vol. 163, no. 2, pp. 408–417, 2000.

[121] J. Breza, A. Soltysova, S. Hudecova et al., "Endogenous H_2S producing enzymes are involved in apoptosis induction in clear cell renal cell carcinoma," *BMC Cancer*, vol. 18, 2018.

[122] F. Audenet, D. R. Yates, G. Cancel-Tassin, O. Cussenot, and M. Rouprêt, "Genetic pathways involved in carcinogenesis

of clear cell renal cell carcinoma: genomics towards personalized medicine," *BJU International*, vol. 109, no. 12, pp. 1864–1870, 2012.

[123] P. H. Maxwell, M. S. Wiesener, G.-W. Chang et al., "The tumour suppressor protein VHL targets hypoxia-inducible factors for oxygen-dependent proteolysis," *Nature*, vol. 399, no. 6733, pp. 271–275, 1999.

[124] A. Schulze and A. L. Harris, "How cancer metabolism is tuned for proliferation and vulnerable to disruption," *Nature*, vol. 491, no. 7424, pp. 364–373, 2012.

[125] X. Chen, Y. Qian, and S. Wu, "The Warburg effect: evolving interpretations of an established concept," *Free Radical Biology & Medicine*, vol. 79, pp. 253–263, 2015.

[126] P. De Cicco, E. Panza, G. Ercolano et al., "ATB-346, a novel hydrogen sulfide-releasing anti-inflammatory drug, induces apoptosis of human melanoma cells and inhibits melanoma development in vivo," *Pharmacological Research*, vol. 114, pp. 67–73, 2016.

[127] L. Lencesova, M. Vlcek, O. Krizanova, and S. Hudecova, "Hypoxic conditions increases H_2S-induced ER stress in A2870 cells," *Molecular and Cellular Biochemistry*, vol. 414, no. 1–2, pp. 67–76, 2016.

[128] S. Lu, L. Chen, Q. Huang et al., "Decomposition of ammonia and hydrogen sulfide in simulated sludge drying waste gas by a novel non-thermal plasma," *Chemosphere*, vol. 117, pp. 781–785, 2014.

[129] J. Markova, S. Hudecova, A. Soltysova et al., "Sodium/calcium exchanger is upregulated by sulfide signaling, forms complex with the β1 and β3 but not β2 adrenergic receptors, and induces apoptosis," *Pflügers Archiv - European Journal of Physiology*, vol. 466, no. 7, pp. 1329–1342, 2014.

[130] A. Misak, M. Grman, Z. Bacova et al., "Polysulfides and products of H_2S/S-nitrosoglutathione in comparison to H_2S, glutathione and antioxidant Trolox are potent scavengers of superoxide anion radical and produce hydroxyl radical by decomposition of H_2O_2," *Nitric Oxide*, vol. 76, pp. 136–151, 2018.

[131] F. Cappello, E. Conway de Macario, L. Marasà, G. Zummo, and A. J. L. Macario, "Hsp60 expression, new locations, functions, and perspectives for cancer diagnosis and therapy," *Cancer Biology & Therapy*, vol. 7, no. 6, pp. 801–809, 2008.

[132] J. C. Ghosh, T. Dohi, B. H. Kang, and D. C. Altieri, "Hsp60 regulation of tumor cell apoptosis," *The Journal of Biological Chemistry*, vol. 283, no. 8, pp. 5188–5194, 2008.

[133] Y.-P. Tsai, M.-H. Yang, C.-H. Huang et al., "Interaction between HSP60 and β-catenin promotes metastasis," *Carcinogenesis*, vol. 30, no. 6, pp. 1049–1057, 2009.

[134] H. Tang, Y. Chen, X. Liu et al., "Downregulation of HSP60 disrupts mitochondrial proteostasis to promote tumorigenesis and progression in clear cell renal cell carcinoma," *Oncotarget*, vol. 7, no. 25, 2016.

[135] Q. Dong, B. Yang, J.-G. Han et al., "A novel hydrogen sulfide-releasing donor, HA-ADT, suppresses the growth of human breast cancer cells through inhibiting the PI3K/AKT/mTOR and Ras/Raf/MEK/ERK signaling pathways," *Cancer Letters*, vol. 455, pp. 60–72, 2019.

[136] H. Guo, P. German, S. Bai et al., "The PI3K/AKT pathway and renal cell carcinoma," *Journal of Genetics and Genomics*, vol. 42, no. 7, pp. 343–353, 2015.

[137] L. B. Valenca, C. J. Sweeney, and M. M. Pomerantz, "Sequencing current therapies in the treatment of metastatic prostate cancer," *Cancer Treatment Reviews*, vol. 41, no. 4, pp. 332–340, 2015.

[138] M. Liu, L. Wu, S. Montaut, and G. Yang, "Hydrogen sulfide signaling axis as a target for prostate cancer therapeutics," *Prostate Cancer*, vol. 2016, Article ID 8108549, 9 pages, 2016.

[139] H. Guo, J.-W. Gai, Y. Wang, H.-F. Jin, J.-B. Du, and J. Jin, "Characterization of hydrogen sulfide and its synthases, cystathionine β-synthase and cystathionine γ-lyase, in human prostatic tissue and cells," *Urology*, vol. 79, no. 2, pp. 483.e1–483.e5, 2012.

[140] K. Zhao, S. Li, L. Wu, C. Lai, and G. Yang, "Hydrogen sulfide represses androgen receptor transactivation by targeting at the second zinc finger module," *The Journal of Biological Chemistry*, vol. 289, no. 30, pp. 20824–20835, 2014.

[141] E. Bigagli, C. Luceri, M. de Angioletti et al., "New NO- and H_2S-releasing doxorubicins as targeted therapy against chemoresistance in castration-resistant prostate cancer: in vitro and in vivo evaluations," *Investigational New Drugs*, vol. 36, no. 6, pp. 985–998, 2018.

[142] Y. Pei, B. Wu, Q. Cao, L. Wu, and G. Yang, "Hydrogen sulfide mediates the anti-survival effect of sulforaphane on human prostate cancer cells," *Toxicology and Applied Pharmacology*, vol. 257, no. 3, pp. 420–428, 2011.

[143] G. Chwatko, E. Forma, J. Wilkosz et al., "Thiosulfate in urine as a facilitator in the diagnosis of prostate cancer for patients with prostate-specific antigen less or equal 10 ng/mL," *Clinical Chemistry and Laboratory Medicine*, vol. 51, no. 9, pp. 1825–1831, 2013.

[144] F. Al-Awadi, M. Yang, Y. Tan, Q. Han, S. Li, and R. M. Hoffman, "Human tumor growth in nude mice is associated with decreased plasma cysteine and homocysteine," *Anticancer Research*, vol. 28, no. 5A, pp. 2541–2544, 2008.

[145] W. Zhang, A. Braun, Z. Bauman, H. Olteanu, P. Madzelan, and R. Banerjee, "Expression profiling of homocysteine junction enzymes in the NCI60 panel of human cancer cell lines," *Cancer Research*, vol. 65, no. 4, pp. 1554–1560, 2005.

[146] F. Kimura, K. H. Franke, C. Steinhoff et al., "Methyl group metabolism gene polymorphisms and susceptibility to prostatic carcinoma," *The Prostate*, vol. 45, no. 3, pp. 225–231, 2000.

[147] S. Stabler, T. Koyama, Z. Zhao et al., "Serum methionine metabolites are risk factors for metastatic prostate cancer progression," *PLoS One*, vol. 6, no. 8, article e22486, 2011.

[148] C. Stephan, K. Jung, K. Miller, and B. Ralla, "New biomarkers in serum and urine for detection of prostate cancer," *Aktuelle Urologie*, vol. 46, no. 2, pp. 129–143, 2015.

[149] P. D. Deeble, M. E. Cox, H. F. Frierson Jr. et al., "Androgen-independent growth and tumorigenesis of prostate cancer cells are enhanced by the presence of PKA-differentiated neuroendocrine cells," *Cancer Research*, vol. 67, no. 8, pp. 3663–3672, 2007.

[150] A. Komiya, H. Suzuki, T. Imamoto et al., "Neuroendocrine differentiation in the progression of prostate cancer," *International Journal of Urology*, vol. 16, no. 1, pp. 37–44, 2009.

[151] J. H. Heo, H. N. Seo, Y. J. Choe et al., "T-type Ca^{2+} channel blockers suppress the growth of human cancer cells," *Bioorganic & Medicinal Chemistry Letters*, vol. 18, no. 14, pp. 3899–3901, 2008.

Hindawi
Oxidative Medicine and Cellular Longevity
Volume 2019, Article ID 3461251, 13 pages
https://doi.org/10.1155/2019/3461251

Research Article

H-Ferritin Affects Cisplatin-Induced Cytotoxicity in Ovarian Cancer Cells through the Modulation of ROS

Alessandro Salatino,[1] Ilenia Aversa,[1] Anna Martina Battaglia,[1] Alessandro Sacco,[1] Anna Di Vito,[1] Gianluca Santamaria,[2] Roberta Chirillo,[1] Pierangelo Veltri,[3] Giuseppe Tradigo,[3] Annalisa Di Cello,[4] Roberta Venturella,[4] Flavia Biamonte,[1] and Francesco Costanzo[1,5]

[1]*Research Center of Biochemistry and Advanced Molecular Biology, Department of Experimental and Clinical Medicine, "Magna Græcia" University of Catanzaro, Campus Salvatore Venuta-Viale Europa, 88100 Catanzaro, Italy*
[2]*Klinikumrechts der Isar, Department of Regenerative Medicine in Cardiovascular Disease, Ismaningerstr., 22 Munich, Germany*
[3]*The Department of Medical and Surgical Sciences, University of Catanzaro, Italy*
[4]*Unit of Obstetrics and Gynaecology, "Magna Graecia" University of Catanzaro, Catanzaro, Italy*
[5]*Interdepartmental Center of Services (CIS), University "Magna Graecia" of Catanzaro, Campus Salvatore Venuta-Viale Europa, 88100 Catanzaro, Italy*

Correspondence should be addressed to Flavia Biamonte; flavia.biamonte.fb@gmail.com

Received 20 April 2019; Revised 29 July 2019; Accepted 9 September 2019; Published 31 October 2019

Academic Editor: Mithun Sinha

Reactive oxygen species (ROS) mediates cisplatin-induced cytotoxicity in tumor cells. However, when cisplatin-induced ROS do not reach cytotoxic levels, cancer cells may develop chemoresistance. This phenomenon can be attributed to the inherited high expression of antioxidant protein network. H-Ferritin is an important member of the antioxidant system due to its ability to store iron in a nontoxic form. Altered expression of H-Ferritin has been described in ovarian cancers; however, its functional role in cisplatin-based chemoresistance of this cancer type has never been explored. Here, we investigated whether the modulation of H-Ferritin might affect cisplatin-induced cytotoxicity in ovarian cancer cells. First, we characterized OVCAR3 and OVCAR8 cells for their relative ROS and H-Ferritin baseline amounts. OVCAR3 exhibited lower ROS levels compared to OVCAR8 and greater expression of H-Ferritin. In addition, OVCAR3 showed pronounced growth potential and survival accompanied by the strong activation of pERK/pAKT and overexpression of c-Myc and cyclin E1. When exposed to different concentrations of cisplatin, OVCAR3 were less sensitive than OVCAR8. At the lowest concentration of cisplatin (6 μM), OVCAR8 underwent a consistent apoptosis along with a downregulation of H-Ferritin and a consistent increase of ROS levels; on the other hand, OVCAR3 cells were totally unresponsive, H-Ferritin was almost unaffected, and ROS amounts met a slight increase. Thus, we assessed whether the modulation of H-Ferritin levels was able to affect the cisplatin-mediated cytotoxicity in both the cell lines. H-Ferritin knockdown strengthened cisplatin-mediated ROS increase and significantly restored sensitivity to 6 μM cisplatin in resistant OVCAR3 cells. Conversely, forced overexpression of H-Ferritin significantly suppressed the cisplatin-mediated elevation of intracellular ROS subsequently leading to a reduced responsiveness in OVCAR8 cells. Overall, our findings suggest that H-Ferritin might be a key protein in cisplatin-based chemoresistance and that its inhibition may represent a potential approach for enhancing cisplatin sensitivity of resistant ovarian cancer cells.

1. Introduction

The oxygen-containing reactive species (ROS) are unstable by-products of cellular metabolism that are essential for several biological processes including mitochondrial and plasma membrane functioning, cell signalling and immune response [1]. The rate and magnitude of ROS production are tightly controlled by an antioxidant defense system

(catalases, superoxide dismutase (SOD), glutathione peroxidase (GPx), thioredoxin (Trx), and ferritin heavy subunit (FHC)) that eliminates them over time [2, 3]. The imbalance in the circuitries of ROS production and removal leads to impairment of cell signalling, oxidative damage of cell components, and cytotoxicity [1–4]. On the other hand, recent evidences indicate that ROS are characterized by a dualistic property in determining cell fate [4, 5]. A persistent ROS overproduction may induce cellular adaptation as it occurs in many diseases, especially in cancer. Otherwise, an excessive ROS production may give rise to fatal lesions that cause cell deaths [4, 5]. Thus, many of the current chemotherapy strategies are aimed at raising ROS over the cytotoxic threshold levels in malignant cells [6–10]. To keep ROS in the prooncogenic zone, cancer cells are provided by an extensive supply of antioxidant molecules that reduce the efficacy of prooxidant drugs and enable tumor cells to acquire chemoresistance [11, 12].

Cisplatin is a prooxidant chemotherapeutic agent widely used for the treatment of ovarian cancer [13–16]. Nevertheless, ovarian cancer cells often develop cisplatin resistance by increasing the expression of the antioxidant systems [14–17]. Consequently, the final concentration of ROS evoked by cisplatin exposure is crucial for the effectiveness of this prooxidant cancer therapy [17]. For this reason, there is a strong need to develop new therapeutic strategies able to overcome platinum resistance in recurrent and metastatic ovarian cancer.

In the antioxidant enzyme family, the heavy subunit of human ferritin (H-Ferritin, FHC) acts by sequestering iron in a bioavailable and catalytically inactive form thus preventing its accumulation in the intracellular labile pool (LIP) and its participation in ROS-generating Fenton reactions [18]. The role of FHC as an antioxidant protein is underscored by the variety of mechanisms leading to its transcriptional and post-transcriptional upregulation in response to oxidative stimuli [19]. FHC expression is usually altered in cancer cells as reported in lung [20], breast [21, 22], melanoma [23], and ovarian cancer cells [24]. However, the possible relationship between FHC amounts and the aptitude of cancer cells to develop chemoresistance to cisplatin is still poorly characterized.

In the current study, we investigated whether and to which extent the modulation of H-Ferritin amounts might affect the cisplatin sensitivity in OVCAR3, a well-established *in vitro* experimental model of chemoresistant ovarian cancer cells [25], in comparison to OVCAR8 cells. Through a series of assays including FHC knockdown and forced overexpression, we demonstrate for the first time that ferritin heavy subunit, through its ability to modulate ROS amounts, is a key element in determining the response of ovarian cancer cells to cisplatin exposure.

2. Materials and Methods

2.1. Cell Lines and Cell Culture. We selected as *in vitro* experimental models two human ovarian cancer lines OVCAR3 and OVCAR8 representative of epithelial ovarian adenocarcinoma. Cells obtained from the American Type Culture Collection (ATCC, Rockville, MD, USA). According to ATCC, OVCAR3 cells derive from an ascitic metastatic site and are an appropriate model system to study cisplatin resistance in ovarian cancer. Both the cell lines are characterized by mutations in p53 gene. OVCAR3 and OVCAR8 cells were maintained in RPMI 1640 media (Sigma-Aldrich, St. Louis, MO, USA). Both culture media were supplemented with 10% fetal bovine serum at 37°C in a humidified atmosphere containing 5% CO_2. Each cell line has been examined for mycoplasma contamination through LookOut® Mycoplasma PCR Detection Kit (Sigma-Aldrich, St. Louis, Missouri, USA).

Table 1: Clinical, pathological, and surgical characteristics of patients with High-Grade Serous Ovarian Cancer (HGSC).

	HGSC ($n = 28$)
Age (years)	59.5 ± 19.0
FIGO stage (n, %)	
Stage II	7 (25.0)
Stage III	15 (53.6)
Stage IV	6 (21.4)
Primary debulking surgery (n, %)	17 (100)
Chemotherapy (n, %)	
Platinum+Taxol+Beva	28 (100)
Response to chemotherapy	
Resistant	13 (46.4)
Sensitive	15 (53.6)
Major comorbidities (n, %)	5 (17.8)
Follow-up (months)	26.2 ± 18.2

2.2. Patients and Specimens. We selected a group of 28 patients with High-Grade Serous Ovarian Cancer (HGSC) who were treated at the Unit of Gynaecologic Oncology, Magna Graecia University, Germaneto, and Pugliese-Ciaccio Hospital, Catanzaro, Italy, between April 2013 and March 2016. Tissue and serum samples of patients were retrieved from our biobank to perform analysis of FHC mRNA expression. Inclusion criteria were as follows: availability of clinical data and biological samples; stage II-III-IV HGSC surgically staged. Patients with previous or concurrent cancer located in other sites, known genetic susceptibility to gynecologic or nongynecologic cancers (BRCA1-2 carriers, associated polyposis conditions (APC), Fanconi syndrome) [14], or positive family anamnesis for ovarian and/or breast cancer were excluded. Patients' clinical data are reported in Table 1.

Procedures carried out in this study were in accordance with the guidelines of the Helsinki Declaration on human experimentation and good clinical practice (GCP). Approval by the "Pugliese-Ciaccio" institutional review board (IRB number: AOPC12404) was obtained before starting patient's enrolment. Furthermore, an informed consent was obtained from all patients before processing their data from the time of hospitalization, even if data did not include any personal identifying information. Biological samples consist in

surgical tissue specimens fixed in 4% paraformaldehyde and subsequently embedded in paraffin.

2.3. Reagents. Cisplatin was obtained from the outpatient pharmacy at Unit of Gynaecologic Oncology, Magna Graecia University, Germaneto. OVCAR3 and OVCAR8 cells were seeded in a 24-well plate in antibiotic-free medium. Cisplatin was added into the medium at various concentrations (6 μM, 12 μM, 24 μM and 48 μM). Treatments were performed at least three times on independent biological replicates. EC_{50} was calculated by using GraphPad Prism® version 5.01. N-Acetyl cysteine (NAC) was purchased from Sigma-Aldrich (Sigma-Aldrich, St. Louis, MO, USA) and used at 10 mM for 2 h.

2.4. ROS Detection. Intracellular ROS amounts were detected using three different methods. CellROX® Green Reagent (Thermo Fisher Scientific, Waltham, Massachusetts, USA) detects total ROS intracellular content while MitoSOX™ Red Indicator (Thermo Fisher Scientific, Waltham, Massachusetts, USA) specifically probes superoxide radicals. Detection was performed by immunofluorescence analysis. For immunofluorescence analysis, OVCAR3 and OVCAR8 cells were cultured on a cover slip, and upon 24 h, cells were incubated with CellROX® Green Reagent for 30 min. Both cell lines were incubated with MitoSOX™ Red Indicator for 10 min at 37°C. Cells were then gently washed. Cover slips were mounted on microscope slides using a mounting solution ProLong Gold antifade reagent (Thermo Fisher Scientific, Waltham, Massachusetts, USA). Images were collected using a Leica DM-IRB/TC-SP2 confocal microscopy system (63x). ROS were also determined by incubating cells with the redox-sensitive probe 2′-7′-DCF (CM-H2CFDA; Molecular Probes, Eugene, OR, USA). Analysis was performed as described in Aversa et al. [26]. Fluorescence was revealed using the Victor3 Multilabel Counter (PerkinElmer, Turku, Finland) at 485 nm and 535 nm for excitation and emission, respectively. Results were normalized on protein concentration.

2.5. MTT Assay. For the MTT assays, 3-[4,5-dimethylthiaoly]-2,5-diphenyltetrazolium bromide (MTT) (Sigma-Aldrich, St. Louis, MO, USA) was used. Briefly, OVCAR3 and OVCAR8 cells (50×10^3 cells/well) were seeded into a 24-well plate. Upon specific treatments, fresh MTT 2 mg/mL (Sigma-Aldrich, St. Louis, MO, USA), resuspended in PBS, was added to each well containing both the cell lines; fresh MTT 2 mg/mL (Sigma-Aldrich, St. Louis, MO, USA). After 2 h incubation, culture medium was discarded and replaced with 200 μL of isopropanol. Optical density was measured at 595 nm in a spectrophotometer. Analysis of OVCAR3 and OVCAR8 cell growth was performed at 0 h, 12 h, 24 h, 48 h and 72 h. For each sample, MTT assay was performed in triplicate.

2.6. Cell Cycle Analysis. A total of 2×10^5 cells were fixed with 100% ethanol and stored at 4°C overnight. Cells were rehydrated with PBS for 10 min at RT, and then cells were stained with propidium iodide (PI) staining solution containing 50 μg/mL PI (Sigma-Aldrich, St. Louis, MO, USA), 100 μg/mL DNase-free RNase A (Calbiochem, La Jolla, CA), and 0.01 % NP-40 (USB, Cleveland, OH) in PBS for 60 min at room temperature. Stained cells were analyzed for cell cycle analysis in BD LSRFortessa™ X-20 (BD Biosciences, San Jose, CA) and FlowJo software.

2.7. Apoptosis Analysis. Apoptosis analysis was performed through the Alexa Fluor®488 Annexin V/Dead Cell Apoptosis Kit (Thermo Fisher Scientific, Waltham, Massachusetts, USA) according to the manufacturer's instructions. After staining, cells were incubated at room temperature for 15 min in the dark. Each tube was diluted with 400 μL of Annexin Binding Buffer, and then, cells were analyzed by flow cytometry using the BD LSRFortessa™ X-20 (BD Biosciences, San Jose, CA) and FACSDiva7.0 program (BD Biosciences, San Jose, CA).

2.8. Western Blotting. Total cell lysates were prepared using RIPA buffer, as described by Aversa et al. [27]. Each protein sample (40–60 μg) was separated by 10–15% SDS–PAGE and then transferred to nitrocellulose membranes. Membranes were incubated with primary antibodies at 4°C overnight. Primary antibodies against FHC (1 : 200, sc-376594), SOD1 (1 : 500, G-11, sc-17767), GPx 1/2 (1 : 500, B-6, sc-133160), c-Myc (1 : 500, C33, sc-42), CCNE1 (1 : 500, E-4, sc-377100) were purchased from Santa Cruz Biotechnology (Santa Cruz Biotechnology, Dallas, Texas). Primary antibodies against caspase 3 (1 : 1000, #9662S), AKT/pAKT (1 : 1000, 9772S/4058S), ERK/pERK (1 : 1000, 9772S/4058S), Phospho-Chk2 (Thr68) (1 : 1000, C13C1), and Chk2 (D9C6, 1 : 1000) were purchased from Cell Signalling Technology (Leiden, Netherlands). Membranes were then washed and incubated, for 2 h, with secondary antibodies HRP-conjugated goat anti-mouse IgG (1 : 2000, sc-2005) and HRP-conjugated goat anti-rabbit IgG (1 : 2000, sc-2357) (Santa Cruz Biotechnology, Dallas, Texas), and immunoreactive bands were visualized with the ECL western blotting detection system (Santa Cruz Biotechnology, Dallas, Texas). To ensure equal loading of proteins, we used goat polyclonal anti-γ-tubulin antibody (C-20) (1 : 2000, sc-7396, Santa Cruz Biotechnology). Experiments were performed three times and representative images are reported. Western blot densitometry was performed using ImageJ software.

2.9. FHC Transient Knockdown and Overexpression. OVCAR3 and OVCAR8 cells were plated into six-well plates at 5×10^5 cells/well and starved overnight prior to transfection. FHC transient knockdown was performed by using a specific FHC siRNA (s5385, Thermo Fisher Scientific, Waltham, Massachusetts, USA) ($OVCAR3^{siFHC}$ and $OVCAR8^{siFHC}$). To ensure an optimal control, OVCAR3 and OVCAR8 cells were further transfected with *Silencer*™ Select Negative Control siRNA (Thermo Fisher Scientific, Waltham, Massachusetts, USA) ($OVCAR3^{Neg\ Control}$ and $OVCAR8^{Neg\ Control}$). FHC transient overexpression was performed by using a specific pc3FHC expression vector ($OVCAR3^{pc3FHC}$ and $OVCAR8^{pc3FHC}$) as previously reported in Zolea et al. [28]. Cells were further transiently transfected with an empty pc3DNA expression vector as

negative control (OVCAR3^{pc3DNA} and OVCAR8^{pc3DNA}). All transfections were performed three times using the Lipofectamine 2000 reagents according to the manufacturer's recommendations (Thermo Fisher Scientific, Waltham, Massachusetts, USA). After 48 h, FHC-specific overexpression and silencing were checked at protein levels through western blot.

2.10. RNA Isolation and Absolute qRT-PCR Analysis. Total RNA isolation and single-stranded complementary DNA (cDNA) generation were performed as previously reported in Di Sanzo et al. [29]. RNA from paraffin-embedded tissue specimens were obtained by a series of incubation with xylene and subsequent ethanol washes. Absolute qPCR analysis was also used to determine the expression of FHC mRNA in the 28 tumor tissue specimens. FHC expression analysis was performed by using SYBR Green qPCR Master Mix (Thermo Fisher Scientific, Waltham, Massachusetts, USA). Primers used to detect FHC were as follows: FW: 5′-CATCAACCGCCAGATCAAC-3′ and REV: 5′-GATGGC TTTCACCTGCTCAT-3′. Analysis was performed on QuantStudio 3 Applied Biosystems by Thermo Fisher Scientific. Starting from a sample of known template concentration, a 5-point 10-fold serial standard curve was prepared, and the concentration of all other samples was calculated by simple interpolation of each threshold cycle (Ct) into this standard curve. FHC mRNA expression data are reported as log (quantity, ng) and represent the mean of three independent technical replicates.

2.11. Statistical Analysis. Results are expressed as mean ± SD and analyzed using the unpaired Student's *t*-test or two-way ANOVA as indicated in the figure legends. GraphPad Prism® version 5.01 was used to calculate EC_{50}; Sidak test was used to identify statistical significance in the EC_{50} values. FHC tumor tissue levels in chemoresistant *vs*. chemosensitive HGSC patients were compared using the nonparametric Kruskal–Wallis test to identify statistical differences between groups. The Kruskal-Wallis test has been chosen as a nonparametric alternative to one-way ANOVA and an extension of the Mann-Whitney *U* test to allow the comparison of more than two independent groups. $p \leq 0.05$ was considered to be significant.

3. Results

3.1. OVCAR3 Cells Exhibit Lower Endogenous ROS and Higher Endogenous FHC Levels Than OVCAR8 Cells. We selected as *in vitro* experimental models OVCAR3 and OVCAR8 cell lines representative of epithelial ovarian adenocarcinoma. OVCAR3 has been chosen as experimental model for studying cisplatin chemoresistance [25]. First, we performed ROS analysis in OVCAR3 and OVCAR8 cells by using two fluorogenic probes: CellROX® Green Reagent able to detect total intracellular ROS content and MitoSOX™ Red Indicator able to selectively detect superoxide radicals. As shown in Figures 1(a) and 1(b), fluorescence microscopy highlights that CellROX® Green fluorescence intensity was significantly higher in OVCAR8 cells compared to OVCAR3 cells. Conversely, MitoSOX staining showed only a slightly different intensity between the two cell lines. These results suggest that OVCAR8 cells are characterized by higher levels of total ROS content compared to OVCAR3 cells. The superoxide radical contribution to this different levels appeared inconsistent. Differences in baseline ROS amounts might reflect, in principle, diverse expression of antioxidant enzymes. Thus, we analyzed the expression of FHC protein, belonging to the antioxidant system, in both OVCAR3 and OVCAR8 cells. Representative western blot analyses and relative densitometry reported in Figure 1(c) highlight that the antioxidant protein FHC was consistently more expressed in OVCAR3 compared to OVCAR8 cells. This behaviour was mirrored by the expression of the other two antioxidant enzymes SOD1 and GPx (Figure S1).

3.2. OVCAR3 Cells Show Enhanced Cell Cycle S-Phase and Cell Growth. We next assessed whether the differences in intracellular baseline ROS amount and FHC protein levels were paralleled by different cancer cell growth. Figure 2(a) shows a representative plot and histograms indicating the mean ± SD of three cell cycle cytofluorimetric analyses, performed by staining cells with PI solution. Results highlight that a significant higher percentage of OVCAR3 cells were in S-phase compared to OVCAR8 cells (S%: 73.9 ± 0.3 *vs*. 53.9 ± 0.7, $p < 0.05$). Accordingly, results from the MTT analysis show that OVCAR3 exhibited an enhanced cell growth potential at 24 h, 48 h, and 72 h (Figure 2(b)). As reported in Figure 2(c), OVCAR3 cells were also characterized by consistent overexpression of the specific S-phase cyclin E1 (CCNE1) along with increased expression of the proto-oncogene c-Myc and enhanced phosphorylation of ERK1/2 and AKT compared to OVCAR8 cells. On the contrary, no phosphorylation of the S-phase cyclin-dependent kinase Chk2 (Thr68) was observed in OVCAR3 and OVCAR8 cells. Optical densitometry of each WB analysis is reported in Figure S1.

3.3. Cisplatin Treatment Induces Significant FHC Downregulation and ROS Increase Exclusively in Chemosensitive OVCAR8 Cells. The sensitivity of OVCAR3 and OVCAR8 cells to cisplatin was determined by treating both cell lines with increasing concentrations of the drug (6 μM, 12 μM, 24 μM and 48 μM). After 24 h, we performed the MTT assay to monitor cell viability following treatment. As shown in Figure 3(a), we found that OVCAR3 cells were, overall, more resistant to treatment than OVCAR8 cells (log EC_{50} OVCAR3 *vs*. log EC_{50} OVCAR8: 1.46 ± 0.06 vs. 0.85 ± 0.05, $p < 0.0001$). In particular, at the lowest cisplatin concentration (6 μM) OVCAR8 cell viability was almost halved while OVCAR3 cells were totally unresponsive. DCFDA luminometric analysis highlighted that the extent of ROS accumulation induced by cisplatin treatments in OVCAR8 cells was significantly higher than that induced in OVCAR3 cells at each concentration apart from 48 μM (Figure 3(b)). Next, we observed that the exposure to 6 μM cisplatin induced a clear cleavage of caspase 3 in OVCAR8 cells and not in OVCAR3 cells (Figure 3(c)). Furthermore, FHC protein levels showed a completely different behaviour between

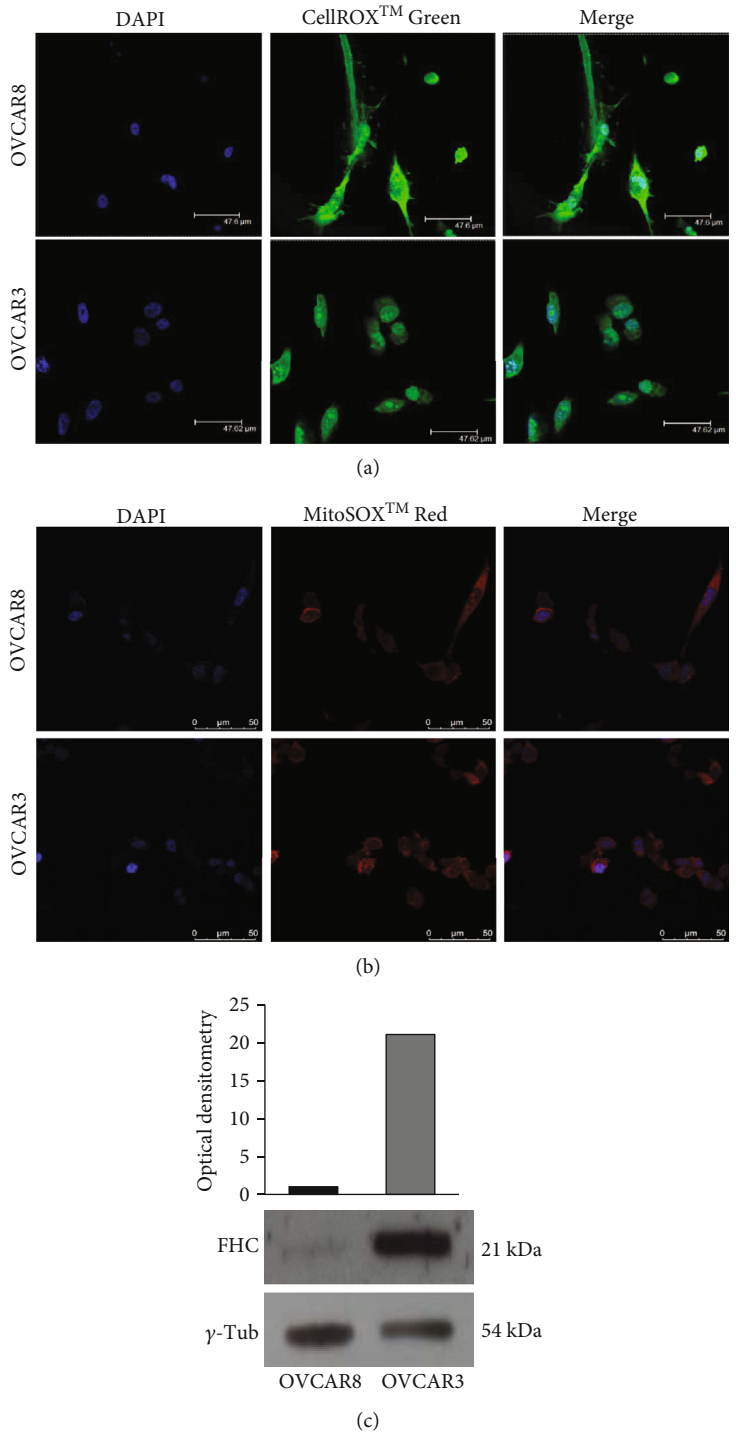

Figure 1: Analysis of ROS intracellular amounts and FHC antioxidant protein levels in OVCAR3 and OVCAR8 cells. (a) Immunofluorescence analysis of ROS levels in OVCAR3 and OVCAR8 cells by staining with CellROX® Green Reagent (green). Nuclei were stained with DAPI (blue). Analysis was performed in duplicate and representative images are reported. (b) Immunofluorescence analysis of superoxide radical levels in OVCAR3 and OVCAR8 cells by staining with MitoSOX™ Red Indicator (red). Nuclei were stained with DAPI (blue). Analysis was performed in duplicate and representative images are reported. (c) Representative western blot of antioxidant protein FHC in OVCAR3 and OVCAR8 cells. γ-Tubulin was used as internal control. WB has been quantified by using ImageJ software and optical densitometry is reported. WB analysis was performed three times and results were reproducible.

the two cell lines; at 6 μM cisplatin, FHC was consistently downregulated in OVCAR8 cells whereas it was almost unaffected in OVCAR3 cells (Figure 3(c)). Optical densitometries of WB are reported in Fig. S2. The analysis of SOD1 and GPx protein levels upon 6 μM cisplatin showed, instead, a slight increase in both the cell lines

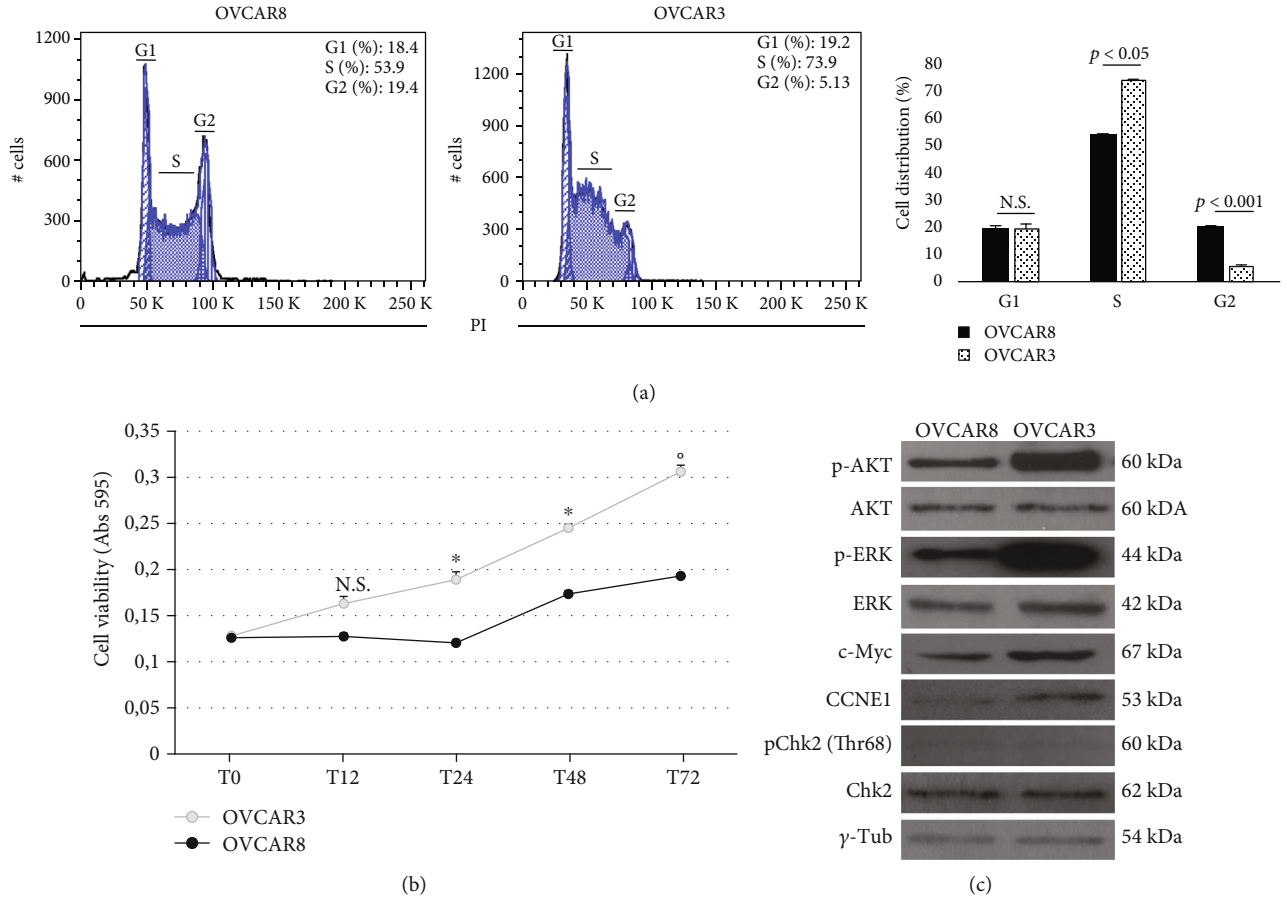

Figure 2: OVCAR3 cells exhibit increased growth potential compared to OVCAR8 cells. (a) Cell cycle FACS analysis of OVCAR3 and OVCAR8 cells stained with PI. The experiments were performed in triplicate. Representative plots of a single experiment (left); histograms showing the mean ± SD of three independent experiments (right). $^*p$ value < 0.05, OVCAR3 *vs.* OVCAR8. (b) MTT analysis of OVCAR3 and OVCAR8 cell growth at 12 h, 24 h, 48 h, and 72 h. Data are reported as absorbance measured at 595 nm and shown as mean ± SD of three independent replicates ($^*p < 0.05$, OVCAR3 *vs.* OVCAR8); ($^\circ p < 0.01$, OVCAR3 *vs.* OVCAR8); N.S.: not significant. (c) Representative WB of c-Myc, cyclin E1 (CCNE1), pChk2 (Thr68), pERK1/2, and pAKT in OVCAR3 and OVCAR8 cells. γ-Tubulin was used as internal control. WB analysis was performed three times and results were reproducible.

(Figure S2). Furthermore, immunofluorescence analysis highlighted that 6 μM cisplatin induced a significant increase in both total ROS and superoxide radical levels in the drug-responsive OVCAR8 cells compared to OVCAR3 resistant cells (Figures 3(d) and 3(e)).

3.4. Modulation of Intracellular FHC Levels Affects Sensitivity to Cisplatin in OVCAR3 and OVCAR8 Cells. Here, we asked whether a change in FHC levels might affect the EOC cell response to cisplatin. To this, we first transiently transfected OVCAR3 cells with a specific FHC siRNA (OVCAR3^{siFHC}) or negative control (OVCAR3$^{Neg\ Control}$) for 48 h. Annexin V/7-AAD cytofluorimetric analysis showed that 6 μM cisplatin was unable to induce a consistent apoptosis in OVCAR3$^{Neg\ Control}$ (early apoptosis: 9.70% ± 0.57; late apoptosis: 6.80% ± 0.99). On the contrary, the same drug concentration promoted a significant increase of apoptotic cell death in OVCAR3^{siFHC} cells (early apoptosis: 45.65% ± 0.78; late apoptosis: 9.80% ± 1.13) compared to either untreated OVCAR3$^{Neg\ Control}$ ($p < 0.05$) or OVCAR3-$^{Neg\ Control}$ treated with 6 μM cisplatin alone ($p < 0.05$). Apoptosis assays performed in OVCAR3$^{Neg\ Control}$ cells treated with (i) 10 mM N-acetyl-cysteine (NAC) alone and (ii) 10 mM N-acetyl-cysteine (NAC) in combination with 6 μM cisplatin and in untreated OVCAR3^{siFHC} revealed no considerable changes. Results of three independent biological replicates are reported as mean ± SD in Table 2 as well as in Figure 4(a).

Accordingly, detection with CellROX® Green Reagent revealed that the ROS amounts evoked by 6 μM cisplatin treatment in combination with FHC knockdown in OVCAR3 cells (OVCAR3^{siFHC} cisplatin 6 μM) were consistently higher than those induced by either cisplatin treatment alone (OVCAR3$^{Neg\ Control}$ cisplatin 6 μM) or FHC silencing alone (OVCAR3^{siFHC}) (Figure 4(b)). No considerable changes have been observed in OVCAR3 cells treated with 10 mM NAC (OVCAR3$^{Neg\ Control}$ NAC 10 mM) in comparison with OVCAR3$^{Neg\ Control}$ untreated cells. As expected, NAC treatment reduced ROS accumulation in OVCAR3 cells treated with 6 μM of cisplatin (OVCAR3$^{Neg\ Control}$

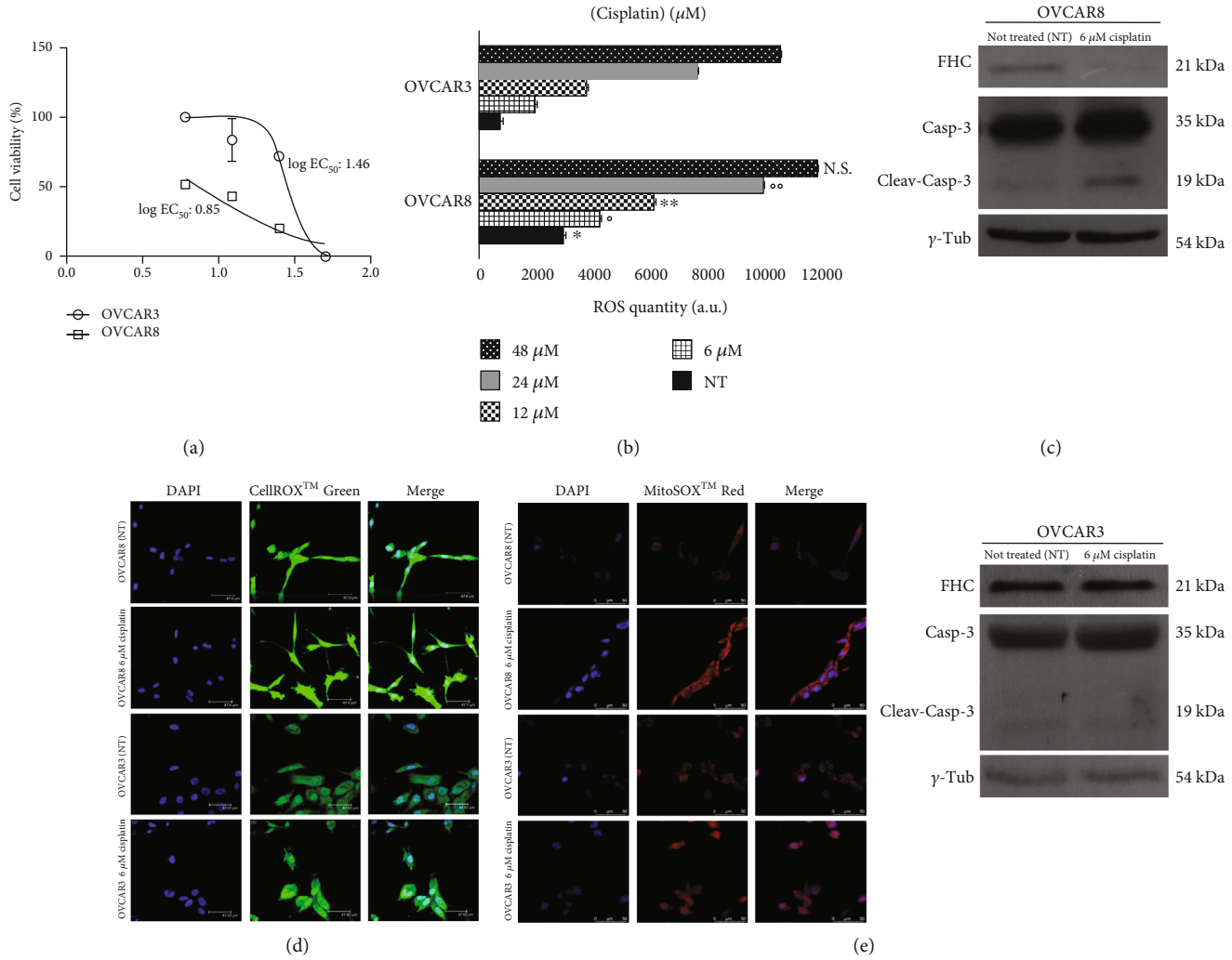

FIGURE 3: OVCAR8 cells are characterized by ROS accumulation and FHC downregulation upon 6 μM cisplatin treatment. (a) Cell viability assay performed by MTT analysis in OVCAR3 and OVCAR8 cells treated with 6 μM, 12 μM, 24 μM and 48 μM of cisplatin for 24 h. Cisplatin concentrations are reported as log [cisplatin (μM)]. Cell viability is expressed as percentage (%). Treatments were performed at least three times on independent biological replicates and the mean concentration of the drug that gives half-maximal response (log EC_{50}) was used to compare cytotoxicity. (b) Quantification of ROS amounts through DCFDA staining in OVCAR3 and OVCAR8 untreated (NT) and upon treatment with 6 μM, 12 μM, 24 μM and 48 μM cisplatin for 24 h. Data represent the mean ± SD of three biological replicates. $^{*}p$ value < 0.01 OVCAR3 NT *vs.* OVCAR8 NT; $^{\circ}p$ value < 0.01 OVCAR3 6 μM cisplatin *vs.* OVCAR8 6 μM cisplatin; $^{**}p$ value < 0.05 OVCAR3 12 μM cisplatin *vs.* OVCAR8 12 μM cisplatin; $^{\circ\circ}p$ value < 0.05 OVCAR3 24 μM cisplatin *vs.* OVCAR8 24 μM cisplatin; N.S.: not significant: OVCAR3 48 μM cisplatin *vs.* OVCAR8 48 μM cisplatin. (c) Representative western blot of FHC, cleaved caspase 3, and caspase 3 in OVCAR3 and OVCAR8 untreated (NT) and upon treatment with 6 μM cisplatin for 24h. γ-Tub was used as internal control. WB analysis was performed three times and results were reproducible. (d) Immunofluorescence analysis of ROS levels in untreated (NT) and treated with 6 μM cisplatin OVCAR3 and OVCAR8 cells by staining with CellROX® Green Reagent (green). Nuclei were stained with DAPI (blue). Analysis was performed in duplicate and representative images are reported. (e) Immunofluorescence analysis of superoxide radical levels untreated (NT) and treated with 6 μM cisplatin OVCAR3 and OVCAR8 cells by staining with MitoSOX™ Red Indicator (red). Nuclei were stained with DAPI (blue). Analysis was performed in duplicate and representative images are reported.

cisplatin 6 μM/NAC 10 mM). In addition, western blot analysis revealed that 6 μM of cisplatin exposure led to a further downregulation of FHC protein levels in $OVCAR3^{siFHC}$ cells; conversely, cisplatin left FHC levels unaltered in $OVCAR3^{Neg\ Control}$ cells (Figure 4(c)).

Next, we performed FHC overexpression in OVCAR8 cells. As shown in Figures 5(a) and 5(c), the forced FHC overexpression significantly protected OVCAR8 cells from 6 μM cisplatin-induced cytotoxicity ($OVCAR3^{pc3FHC}$ cisplatin (6 μM) *vs.* $OVCAR8^{pc3DNA}$ cisplatin (6 μM), $p < 0.05$). Similar results were obtained when OVCAR8 cells were treated with 6 μM cisplatin for 24 h in combination with 10 mM of ROS scavenger NAC for 2 h ($OVCAR8^{pc3DNA}$ cisplatin (6 μM)/NAC (10 mM) *vs.* $OVCAR8^{pc3DNA}$ cisplatin (6 μM), $p < 0.05$). Results of three independent biological replicates are reported as mean ± SD in Table 3. Accordingly, detection with CellROX® Green Reagent further revealed that FHC overexpression, as well as NAC treatment, consistently

Table 2: Data analysis of Annexin/7-AAD cytofluorimetric apoptosis assays in OVCAR3 cells.

Samples	Early apoptosis (% ± SD)	Late apoptosis (% ± SD)	Live cells (% ± SD)
$OVCAR3^{Neg\ Control}$ NT*	1.85 ± 0.64	6.55 ± 0.78	90.45 ± 1.77
$OVCAR3^{Neg\ Control}$ cisplatin (6 μM)**	9.70 ± 0.57	6.80 ± 0.99	83.85 ± 1.20
$OVCAR3^{Neg\ Control}$ NAC (10 mM)	0.85 ± 0.79	6.35 ± 0.92	92.18 ± 1.77
$OVCAR3^{Neg\ Control}$ cisplatin (6 μM)/NAC (10 mM)	6.80 ± 0.42	4.15 ± 0.35	89.45 ± 0.92
$OVCAR3^{siFHC}$	4.70 ± 0.14	12.15 ± 0.49	76.65 ± 1.06
$OVCAR3^{siFHC}$ cisplatin (6 μM)	45.65 ± 0.78	9.80 ± 1.13	43.85 ± 0.49

*$OVCAR3^{siFHC}$ cisplatin (6 μM) vs. $OVCAR3^{Neg\ Control}$ NT, p value < 0.05 (two-way ANOVA test). **$OVCAR3^{siFHC}$ cisplatin (6 μM) vs. $OVCAR3^{Neg\ Control}$ cisplatin (6 μM), p value < 0.05 (two-way ANOVA test).

reduced ROS amounts evoked by 6 μM cisplatin treatment alone in OVCAR8 cells (Figures 5(b)).

3.5. FHC Tissue Levels Are Higher in Chemoresistant High-Grade Serous Ovarian Cancer (HGSC) Patients Compared to Chemosensitive Ones. In light of the *in vitro* findings, we performed absolute qPCR analysis of *FHC* mRNA tissue levels in a small cohort of 28 patients with High-Grade Serous Ovarian Cancer (HSGC, stages II, III, and IV) treated with platinum-based chemotherapy, among which 13 were chemoresistant and 15 were chemosensitive. As shown in the box plot in Figure S3, statistical Kruskal–Wallis test suggests that patients with resistance to chemotherapy may be characterized by higher FHC levels compared to the chemosensitive ones. However, data do not reach the statistical significance.

4. Discussion

Despite considerable efforts for developing novel and more efficient therapeutic strategies, ovarian cancer patients often suffer from aggressive and therapy-resistant disease characterized by poor prognosis and high mortality [14, 30, 31]. Cisplatin is a prooxidant chemotherapeutic agent largely used as first-line therapy in ovarian cancer; however, its efficacy is quite limited since most patients ultimately die with platinum-resistant disease [30, 31]. Numerous evidences indicate that altered redox balance, which is now widely considered as one of the main cancer hallmarks, can be pivotal in the resistance to antitumor agents including cisplatin [1, 2, 4].

As a consequence of genetic, metabolic, and microenvironment-related aberrations, cancer cells are subjected to persistent prooxidant stimuli that ultimately increase baseline ROS levels and promote tumor growth by inducing genomic instability and metabolism reprogramming [32]. However, tumor cells have developed an efficient ROS detoxification system through which they gain advantage when subjected to further prooxidant conditions. This dependency from the antioxidant systems represents a specific vulnerability so as the current used prooxidant chemotherapeutic agents act by increasing oxidative stress above the toxicity threshold [1–5].

In this study, by analyzing changes of intracellular ROS levels, we explored the role of FHC, an important antioxidant enzyme, in the development of resistance to cisplatin-based therapy in ovarian cancer cells.

FHC, the heavy subunit of the human ferritin, has a ferroxidase activity through which it safely stores iron in catalytically inactive Fe^{3+} form thus tightly controlling the homeostasis of the labile prooxidant iron pool [33]. We and others have previously demonstrated that FHC is a downstream effector of NFkB-mediated inhibition of the oxidative stress-induced apoptosis [26, 34]. In addition, FHC is transcriptionally upregulated by the antioxidant transcription factor Nrf2 to maintain iron and redox homeostasis [35, 36].

As an *in vitro* experimental model, we selected OVCAR3 and OVCAR8 cell lines as representative of ovarian cancer cells. In particular, OVCAR3 cells have been selected as cisplatin refractory cell line established from metastatic ascites of a patient with ovarian adenocarcinoma [25].

Overall, our results strongly suggest that the antioxidant properties of FHC play a key role in determining the response of ovarian cancer cells to cisplatin treatment. First, we observed that the chemoresistant OVCAR3 cells are characterized by higher constitutive FHC levels and by lower endogenous ROS content in comparison to OVCAR8 cells. Moreover, prooxidant cisplatin treatment affects FHC levels in OVCAR8 cells by inducing its downregulation while it leaves unchanged FHC amounts in OVCAR3 cells. These effects appear to be selective for FHC since other two antioxidant enzymes, namely SOD1 and GPx, were not consistently modified upon cisplatin exposure. Recent evidences indicate that H-Ferritin may undergo degradation in cells exposed to anticancer compound and this is accompanied by intracellular iron accumulation and increase in iron-dependent ROS production [37]. Indeed, we noticed that in OVCAR8 cells the downregulation of FHC mediated by cisplatin exposure was accompanied by an enormous increase in ROS accumulation that likely exceed the cytotoxic threshold levels. Conversely, in OVCAR3 cells the cisplatin hit was insufficient to push ROS production over the cytotoxic levels.

In the past decades, three main approaches have been proposed to exploit the cancer cell killing potential of ROS: (i) enhancing the generation of ROS in tumor cells by increasing the dose of a single prooxidant chemotherapeutic drug, (ii) combination of conventional anticancer agents with natural

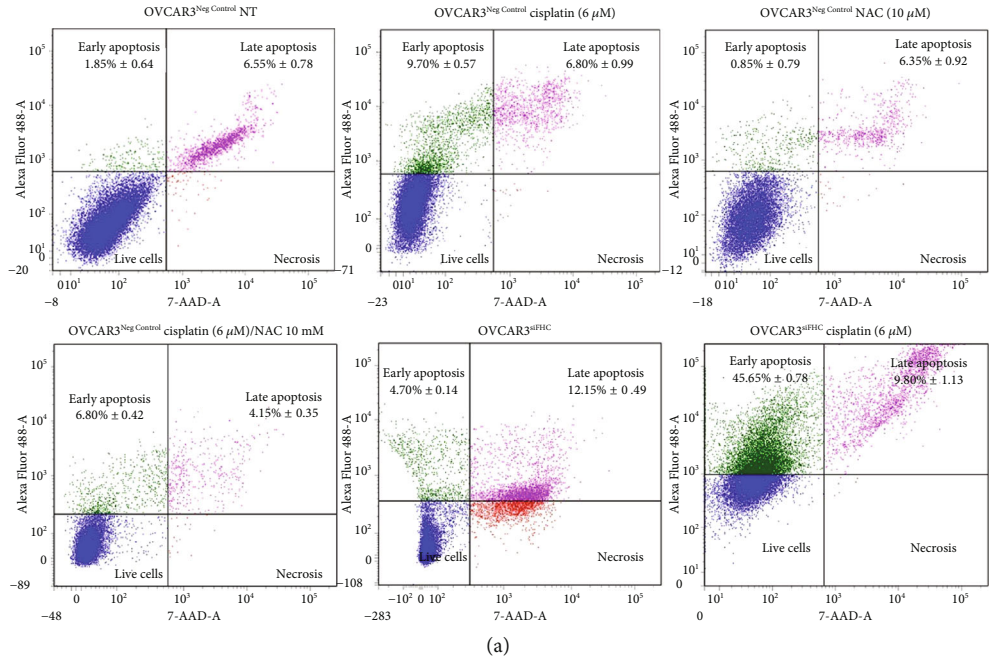

(a)

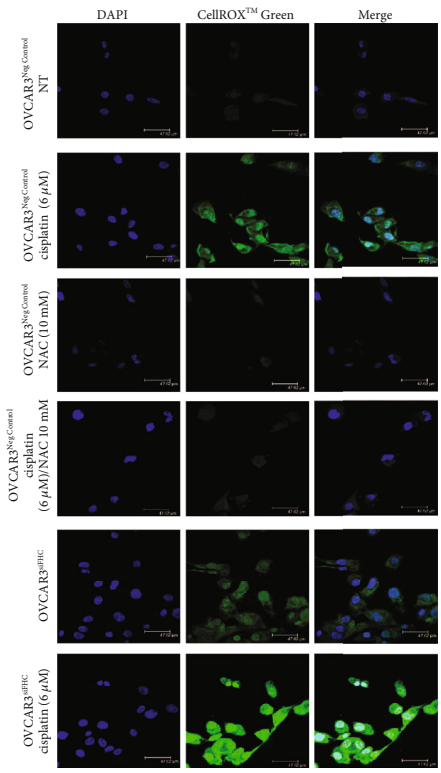

(b)

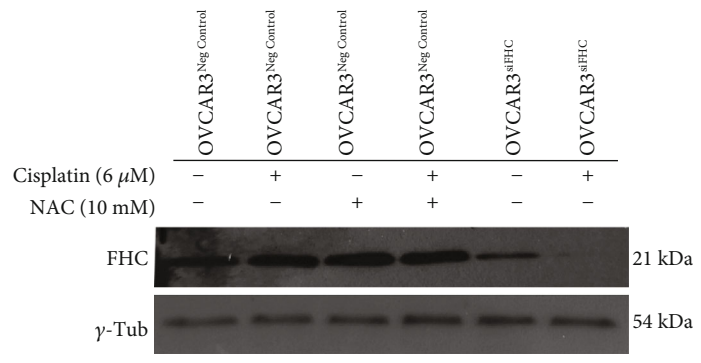

(c)

Figure 4: FHC knockdown improves OVCAR3 response to 6 μM cisplatin by increasing ROS production. (a) Representative plots of Annexin V/7-AAD apoptosis assays in OVCAR3$^{\text{Neg Control}}$, OVCAR3$^{\text{Neg Control}}$ (6 μM) cisplatin, OVCAR3$^{\text{Neg Control}}$ 10 mM NAC, OVCAR3$^{\text{Neg Control}}$ (6 μM) cisplatin/10 mM NAC, OVCAR3$^{\text{siFHC}}$, and OVCAR3$^{\text{siFHC}}$ (6 μM) cisplatin. Cisplatin treatment was performed for 24 h while NAC treatment was performed for 2 h. FACS plots are representative of single experiments. Values are expressed as mean ± SD of three biological replicates. (b) Immunofluorescence analysis of ROS levels in OVCAR3$^{\text{Neg Control}}$, OVCAR3$^{\text{Neg Control}}$ (6 μM) cisplatin, OVCAR3$^{\text{Neg Control}}$ 10 mM NAC OVCAR3$^{\text{Neg Control}}$ (6 μM) cisplatin/10 mM NAC, OVCAR3$^{\text{siFHC}}$, and OVCAR3$^{\text{siFHC}}$ (6 μM) cisplatin, by staining with CellROX® Green Reagent (green). Nuclei were stained with DAPI (blue). (c) Representative western blot of FHC in OVCAR3$^{\text{Neg Control}}$, OVCAR3$^{\text{Neg Control}}$ (6 μM) cisplatin, OVCAR3$^{\text{Neg Control}}$ 10 mM NAC, OVCAR3$^{\text{Neg Control}}$ (6 μM) cisplatin/10 mM NAC, OVCAR3$^{\text{siFHC}}$, and OVCAR3$^{\text{siFHC}}$ (6 μM) cisplatin. γ-Tubulin was used as internal control. WB analysis was performed three times and results were reproducible.

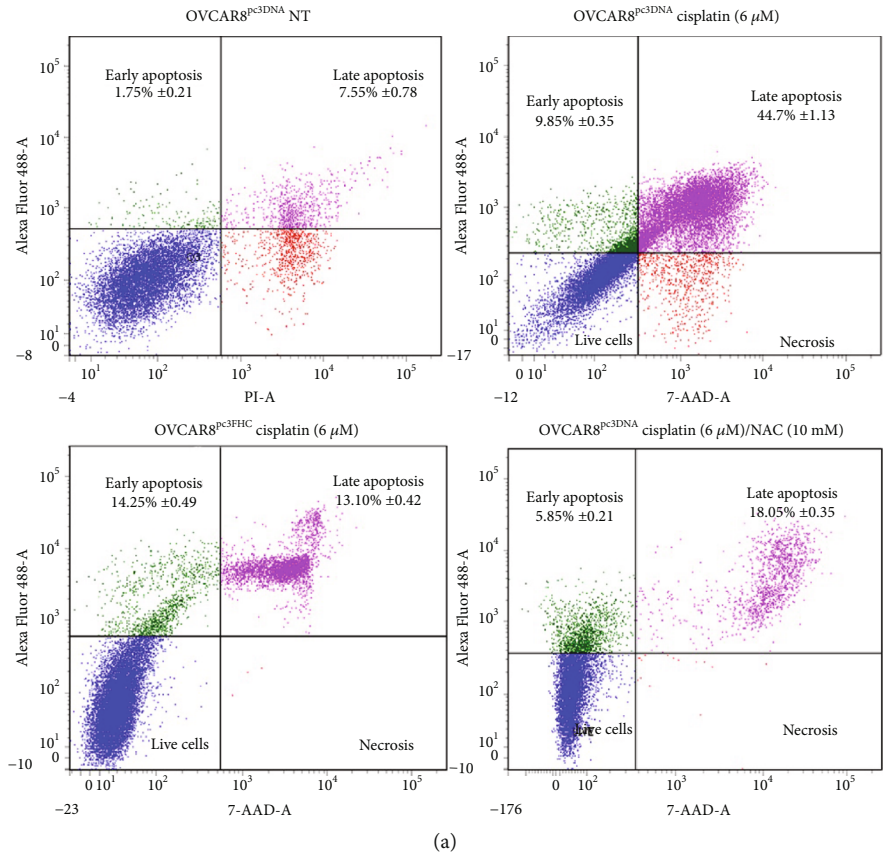

(a)

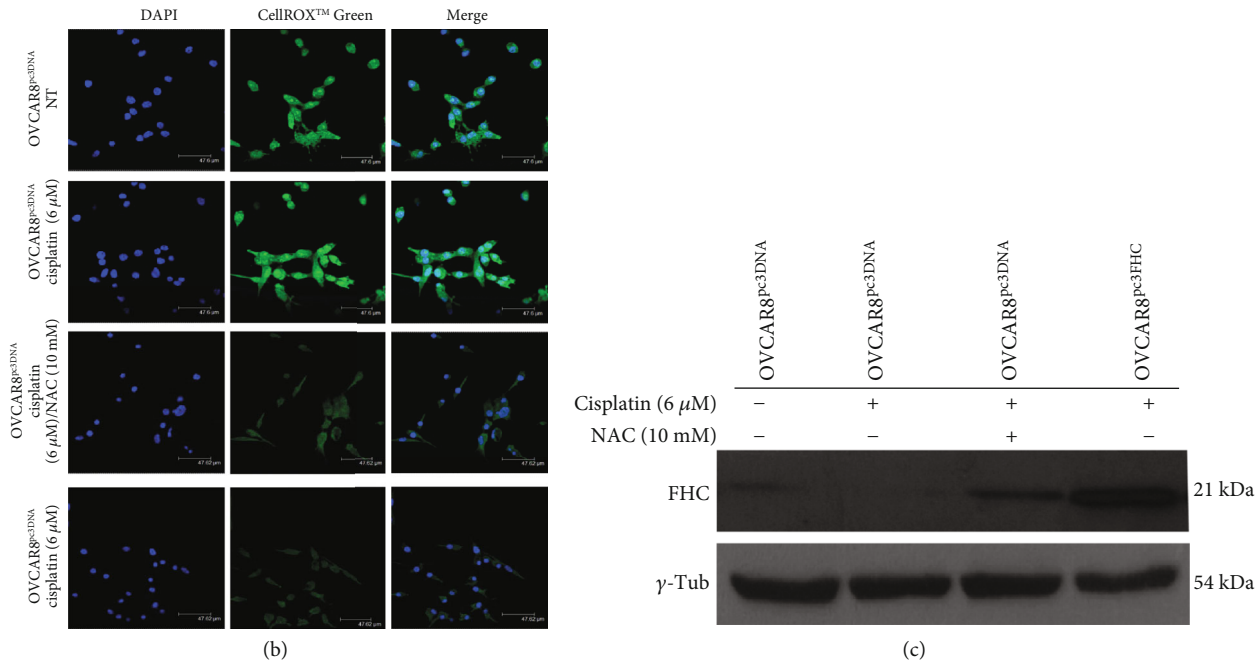

(b) (c)

Figure 5: FHC overexpression or NAC treatment reduces OVCAR8 response to cisplatin. (a) Representative plots of Annexin V/7-AAD apoptosis assays in OVCAR8^{pc3DNA}, OVCAR8^{pc3DNA} (6 μM) cisplatin, OVCAR8^{pc3DNA} (6 μM) cisplatin/10 mM NAC, and OVCAR8^{pc3FHC} (6 μM) cisplatin. Cisplatin treatment was performed for 24 h while NAC treatment was performed for 2 h. FACS plots are representative of single experiments. Values are expressed as mean ± SD of three biological replicates. (b) Immunofluorescence analysis of ROS levels in OVCAR8^{pc3DNA}, OVCAR8^{pc3DNA} (6 μM) cisplatin, OVCAR8^{pc3DNA} (6 μM) cisplatin/10 mM NAC, and OVCAR8^{pc3FHC} (6 μM) cisplatin, by staining with CellROX® Green Reagent (green). Nuclei were stained with DAPI (blue). (c) Representative western blot of FHC in OVCAR8^{pc3DNA}, OVCAR8^{pc3DNA} (6 μM) cisplatin, OVCAR8^{pc3DNA} (6 μM) cisplatin/10 mM NAC, and OVCAR8^{pc3FHC} (6 μM) cisplatin. γ-Tubulin was used as internal control. WB analysis was performed three times and results were reproducible.

Table 3: Data analysis of Annexin/7-AAD cytofluorimetric apoptosis assays in OVCAR8 cells.

Samples	Early apoptosis (% ± SD)	Late apoptosis (% ± SD)	Live cells (% ± SD)
$OVCAR8^{pc3DNA}$ NT	1.75 ± 0.21	7.55 ± 0.78	82.75 ± 1.20
$OVCAR8^{pc3DNA}$ cisplatin (6 μM)	9.85 ± 0.35	44.70 ± 1.13	42.35 ± 1.20
$OVCAR8^{pc3DNA}$ cisplatin (6 μM)/NAC (10 mM)*	5.85 ± 0.21	18.05 ± 0.35	71.70 ± 0.99
$OVCAR3^{pc3FHC}$ cisplatin (6 μM)**	14.25 ± 0.49	13.10 ± 0.42	71.25 ± 1.63

*$OVCAR8^{pc3DNA}$ cisplatin (6 μM)/NAC (10 mM) vs. $OVCAR8^{pc3DNA}$ cisplatin (6 μM), p value < 0.05 (two-way ANOVA test). **$OVCAR3^{pc3FHC}$ cisplatin (6 μM) vs. $OVCAR8^{pc3DNA}$ cisplatin (6 μM), p value < 0.05 (two-way ANOVA test).

compounds that increase ROS production, the so-called "ROS+ROS concept," and (iii) inhibition of the antioxidant defense system of tumor cells. Remarkably, the first two approaches are very challenging to translate from *in vitro* models to *in vivo* conditions because of significant side effects [10, 38, 39]. On the contrary, disabling key antioxidant systems in the presence of ROS inducers represents the most promising new anticancer strategy in resistant tumor cells. Indeed, impairing antioxidant capacity, such as Nrf2, SOD, and GPx, has emerged as a good strategy to target many cancer types [40]. Here, we proved, for the first time, that modulation of intracellular H-Ferritin (FHC) protein is able to condition ovarian cancer cell response to cisplatin thus adding this molecule to the targetable antioxidant protein panel. The relevance of FHC/ROS axis in modulating ovarian cancer cell response to cisplatin has been demonstrated by FHC knockdown or forced overexpression in our *in vitro* system. The knockdown of FHC, by using a specific siRNA, is accompanied by a significant augment in the cytotoxic effects of cisplatin in the drug-resistant OVCAR3 cells. Accordingly, an overexpression of FHC in the drug-sensitive OVCAR8 cells suppresses the cytototoxic effects of the drug at a level comparable to that obtained by scavenging ROS through NAC treatment. The fundamental mechanism through which FHC knockdown is able to restore OVCAR3 sensitivity to cisplatin appears to be strictly related to its antioxidant properties and to its capacity to lead the effective final amounts of ROS over those evoked by the cisplatin treatment alone.

At last, we also analyzed FHC cancer tissue levels in 28 patients with HGSC receiving a platinum-based chemotherapy. Although suggestive of a possible association between high levels of FHC and chemoresistance, the collected data do not reach the statistical significance. This trend prompted us to increase, in future studies, the analyzed cohort of patients to provide additional arguments in favor of the importance of estimating ROS amounts and FHC status to improve the therapeutic outcomes in treatment of ovarian cancer.

5. Conclusions

In conclusion, our data demonstrate for the first time the association of FHC/ROS axis with cisplatin resistance in ovarian cancer cells. Furthermore, we propose that inhibition of FHC might be a potential approach for restoring cisplatin sensitivity of resistant ovarian cancer cells. The conjugation of siRNA carrier system with ligands that exhibit high affinity to specific receptors overexpressed in ovarian cancer cells could make feasible this approach also *in vivo*.

Data Availability

The data used to support the findings of this study are included within the article.

Conflicts of Interest

The authors declare no conflicts of interest.

Authors' Contributions

Alessandro Salatino and Ilenia Aversa equally contributed to this work.

Acknowledgments

We thank Caterina Alessi for the editorial assessment.

Supplementary Materials

Fig.S1: WB analysis of SOD1, GPx, CCNE1, c-Myc, ERK/-pERK, AKT/pAKT, and Chk2/pChk2 in OVCAR3 and OVCAR8 cells. Representative western blot of antioxidant proteins SOD1 and GPx, CCNE1, and c-Myc together with ERK/AKT/Chk2 phosphorylation in OVCAR3 and OVCAR8 cells. γ-Tubulin was used as internal control. Each plot has been quantified by using ImageJ software and optical densitometry is reported. WB analysis was performed three times and results were reproducible. Fig. S2: WB analysis of FHC, caspase 3/cleaved caspase 3, SOD1, and GPx in OVCAR3 and OVCAR8 cells untreated or treated with 6 μM cisplatin. Representative western blot of FHC, caspase 3/cleaved caspase 3, SOD1, and GPx in OVCAR3 and OVCAR8 cells untreated (NT) or treated with 6 μM cisplatin. γ-Tubulin was used as internal control. Each plot has been quantified by using ImageJ software and optical densitometry is reported. WB analysis was performed three times and results were reproducible. Fig. S3: WB analysis of FHC, caspase 3/cleaved caspase 3, SOD1, and GPx in OVCAR3 and OVCAR8 cells upon several treatments. Representative western blot of FHC in $OVCAR3^{Neg\ Control}$, $OVCAR3^{Neg\ Control}$ (6 μM) cisplatin, $OVCAR3^{Neg\ Control}$ 10 mM NAC, $OVCAR3^{Neg\ Control}$ (6 μM) cisplatin/10 mM NAC (6 μM) cisplatin, $OVCAR3^{siFHC}$, $OVCAR3^{siFHC}$ (6 μM) cisplatin, $OVCAR8^{pc3DNA}$, $OVCAR8^{pc3DNA}$ (6 μM) cisplatin, $OVCAR8^{pc3DNA}$ (6 μM) cisplatin/10 mM NAC, and $OVCAR8^{pc3FHC}$ (6 μM) cisplatin. γ-Tubulin was used as internal control. Each plot has been quantified by using ImageJ software and optical densitometry is reported.

WB analysis was performed three times and results were reproducible. Fig. S4: analysis of FHC tumor tissue levels in 28 HGSC patients. Representative images of ovarian cancer tissue specimens (left). Box plot depicting FHC mRNA levels, expressed as log (ng), as assessed by absolute qPCR analysis in cancer tissue specimens of chemoresistant HGSC patients ($n = 13$) and chemosensitive HGSC patients ($n = 15$) (right). Data are not statistically significant (N.S.). *(Supplementary Materials)*

References

[1] H. Yang, R. M. Villani, H. Wang et al., "The role of cellular reactive oxygen species in cancer chemotherapy," *Journal of Experimental & Clinical Cancer Research*, vol. 37, no. 1, p. 266, 2018.

[2] C. Espinosa-Diez, V. Miguel, D. Mennerich et al., "Antioxidant responses and cellular adjustments to oxidative stress," *Redox Biology*, vol. 6, pp. 183–197, 2015.

[3] F. Biamonte, A. M. Battaglia, F. Zolea et al., "Ferritin heavy subunit enhances apoptosis of non-small cell lung cancer cells through modulation of miR-125b/p53 axis," *Cell Death & Disease*, vol. 9, no. 12, article 1174, 2018.

[4] E. Panieri and M. M. Santoro, "ROS homeostasis and metabolism: a dangerous liason in cancer cells," *Cell Death & Disease*, vol. 7, no. 6, article e2253, 2016.

[5] A. Acharya, I. Das, D. Chandhok, and T. Saha, "Redox regulation in cancer: a double-edged sword with therapeutic potential," *Oxidative Medicine and Cellular Longevity*, vol. 3, no. 1, 34 pages, 2010.

[6] S. Kumari, A. K. Badana, M. M. G, S. G, and R. R. Malla, "Reactive oxygen species: a key constituent in cancer survival," *Biomark Insights*, vol. 13, 2018.

[7] N. Durand and P. Storz, "Targeting reactive oxygen species in development and progression of pancreatic cancer," *Expert Review of Anticancer Therapy*, vol. 17, no. 1, pp. 19–31, 2016.

[8] M. Ogrunc, R. di Micco, M. Liontos et al., "Oncogene-induced reactive oxygen species fuel hyperproliferation and DNA damage response activation," *Cell Death & Differentiation*, vol. 21, no. 6, pp. 998–1012, 2014.

[9] J. Wang, B. Luo, X. Li et al., "Inhibition of cancer growth in vitro and in vivo by a novel ROS-modulating agent with ability to eliminate stem-like cancer cells," *Cell Death & Disease*, vol. 8, no. 6, article e2887, 2017.

[10] J. Wang and J. Yi, "Cancer cell killing via ROS: to increase or decrease, that is the question," *Cancer Biology & Therapy*, vol. 7, no. 12, pp. 1875–1884, 2008.

[11] L. Norouzi-Barough, M. R. Sarookhani, M. Sharifi, S. Moghbelinejad, S. Jangjoo, and R. Salehi, "Molecular mechanisms of drug resistance in ovarian cancer," *Journal of Cellular Physiology*, vol. 233, no. 6, pp. 4546–4562, 2018.

[12] M. Landriscina, F. Maddalena, G. Laudiero, and F. Esposito, "Adaptation to oxidative stress, chemoresistance, and cell survival," *Antioxidants & Redox Signaling*, vol. 11, no. 11, pp. 2701–2716, 2009.

[13] S. Dasari and P. B. Tchounwou, "Cisplatin in cancer therapy: molecular mechanisms of action," *European Journal of Pharmacology*, vol. 740, pp. 364–378, 2014.

[14] F. Biamonte, G. Santamaria, A. Sacco et al., "MicroRNA let-7g acts as tumor suppressor and predictive biomarker for chemoresistance in human epithelial ovarian cancer," *Scientific Reports*, vol. 9, no. 1, article 5668, 2019.

[15] P. Davalli, G. Marverti, A. Lauriola, and D. D'Arca, "Targeting oxidatively induced DNA damage response in cancer: opportunities for novel cancer therapies," *Oxidative Medicine and Cellular Longevity*, vol. 2018, Article ID 2389523, 21 pages, 2018.

[16] A. K. Godwin, A. Meister, P. J. O'Dwyer, C. S. Huang, T. C. Hamilton, and M. E. Anderson, "High resistance to cisplatin in human ovarian cancer cell lines is associated with marked increase of glutathione synthesis," *Proceedings of the National Academy of Sciences of the United States of America*, vol. 89, no. 7, pp. 3070–3074, 1992.

[17] A. Leone, M. S. Roca, C. Ciardiello, S. Costantini, and A. Budillon, "Oxidative stress gene expression profile correlates with cancer patient poor prognosis: identification of crucial pathways might select novel therapeutic approaches," *Oxidative Medicine and Cellular Longevity*, vol. 2017, Article ID 2597581, 18 pages, 2017.

[18] P. Arosio and S. Levi, "Ferritin, iron homeostasis, and oxidative damage," *Free Radical Biology & Medicine*, vol. 33, no. 4, pp. 457–463, 2002.

[19] F. M. Torti and S. V. Torti, "Regulation of ferritin genes and protein," *Blood*, vol. 99, no. 10, pp. 3505–3516, 2002.

[20] A. V. Kudriavtseva, E. A. Anedchenko, N. Y. Oparina et al., "Expression of *FTL* and *FTH* genes encoding ferritin subunits in lung and renal carcinomas," *Molecular Biology*, vol. 43, no. 6, article 6095, pp. 972–981, 2009.

[21] N. Q. Liu, T. de Marchi, A. M. Timmermans et al., "Ferritin heavy chain in triple negative breast cancer: a favorable prognostic marker that relates to a cluster of differentiation 8 positive (CD8+) effector T-cell response," *Molecular & Cellular Proteomics*, vol. 13, no. 7, pp. 1814–1827, 2014.

[22] S. V. Chekhun, N. Y. Lukyanova, Y. V. Shvets, A. P. Burlaka, and L. G. Buchinska, "Significance of ferritin expression in formation of malignant phenotype of human breast cancer cells," *Experimental Oncology*, vol. 36, no. 3, pp. 179–183, 2014.

[23] C. P. Gray, P. Arosio, and P. Hersey, "Association of increased levels of heavy-chain ferritin with increased $CD4^+$ $CD25^+$ regulatory T-cell levels in patients with melanoma," *Clinical Cancer Research*, vol. 9, no. 7, pp. 2551–2559, 2003.

[24] J. Jiang, S. Wang, L. Zhang, J. Lu, and C. Yi, "Characteristics of the distribution of ferritin in epithelial ovarian tumor patients: results of a retrospective, observational study," *Yangtze Medicine*, vol. 2, no. 2, pp. 51–61, 2018.

[25] S. S. Sakhare, G. G. Rao, S. N. Mandape, and S. Pratap, "Transcriptome profile of OVCAR3 cisplatin-resistant ovarian cancer cell line," *BMC Bioinformatics*, vol. 15, Supplement 10, p. 21, 2014.

[26] I. Aversa, R. Chirillo, E. Chiarella et al., "Chemoresistance in H-ferritin silenced cells: the role of NF-κB," *International Journal of Molecular Sciences*, vol. 19, no. 10, p. 2969, 2018.

[27] I. Aversa, F. Zolea, C. Ieranò et al., "Epithelial-to-mesenchymal transition in FHC-silenced cells: the role of CXCR4/CXCL12 axis," *Journal of Experimental & Clinical Cancer Research*, vol. 36, no. 1, p. 104, 2017.

[28] F. Zolea, F. Biamonte, A. M. Battaglia, M. C. Faniello, G. Cuda, and F. Costanzo, "Caffeine positively modulates ferritin heavy chain expression in H460 cells: effects on cell proliferation," *PLoS One*, vol. 11, no. 9, article e0163078, 2016.

[29] M. di Sanzo, R. Chirillo, I. Aversa et al., "shRNA targeting of ferritin heavy chain activates H19/miR-675 axis in K562 cells," *Gene*, vol. 657, pp. 92–99, 2018.

[30] A. J. Cortez, P. Tudrej, K. A. Kujawa, and K. M. Lisowska, "Advances in ovarian cancer therapy," *Cancer Chemotherapy and Pharmacology*, vol. 81, no. 1, article 3501, pp. 17–38, 2018.

[31] S. Kim, Y. Han, S. I. Kim, H. S. Kim, S. J. Kim, and Y. S. Song, "Tumor evolution and chemoresistance in ovarian cancer," *npj Precision Oncology*, vol. 2, no. 1, p. 20, 2018.

[32] F. Zolea, F. Biamonte, P. Candeloro et al., "H ferritin silencing induces protein misfolding in K562 cells: a Raman analysis," *Free Radical Biology & Medicine*, vol. 89, pp. 614–623, 2015.

[33] P. Arosio, L. Elia, and M. Poli, "Ferritin, cellular iron storage and regulation," *IUBMB Life*, vol. 69, no. 6, pp. 414–422, 2017.

[34] C. G. Pham, C. Bubici, F. Zazzeroni et al., "Ferritin Heavy Chain Upregulation by NF-κB Inhibits TNFα-Induced Apoptosis by Suppressing Reactive Oxygen Species," *Cell*, vol. 119, no. 4, pp. 529–542, 2004.

[35] M. J. Kerins and A. Ooi, "The roles of NRF2 in modulating cellular iron homeostasis," *Antioxidants & Redox Signaling*, vol. 29, no. 17, pp. 1756–1773, 2018.

[36] E. C. Pietsch, J. Y. Chan, F. M. Torti, and S. V. Torti, "Nrf2 mediates the induction of ferritin H in response to xenobiotics and cancer chemopreventive dithiolethiones," *Journal of Biological Chemistry*, vol. 278, no. 4, pp. 2361–2369, 2003.

[37] A. Borkowska, A. Sielicka-Dudzin, A. Herman-Antosiewicz, M. Halon, M. Wozniak, and J. Antosiewicz, "P66Shc mediated ferritin degradation—A novel mechanism of ROS formation," *Free Radical Biology & Medicine*, vol. 51, no. 3, pp. 658–663, 2011.

[38] C. Gorrini, I. S. Harris, and T. W. Mak, "Modulation of oxidative stress as an anticancer strategy," *Nature Reviews Drug Discovery*, vol. 12, no. 12, pp. 931–947, 2013.

[39] B. Ramanathan, K. Y. Jan, C. H. Chen, T. C. Hour, H. J. Yu, and Y. S. Pu, "Resistance to paclitaxel is proportional to cellular total antioxidant capacity," *Cancer Research*, vol. 65, no. 18, pp. 8455–8460, 2005.

[40] A. Sznarkowska, A. Kostecka, K. Meller, and K. P. Bielawski, "Inhibition of cancer antioxidant defense by natural compounds," *Oncotarget*, vol. 8, no. 9, pp. 15996–16016, 2017.

Hindawi
Oxidative Medicine and Cellular Longevity
Volume 2019, Article ID 4568964, 16 pages
https://doi.org/10.1155/2019/4568964

Review Article

Natural Sesquiterpene Lactones Enhance Chemosensitivity of Tumor Cells through Redox Regulation of STAT3 Signaling

Elena Butturini, Alessandra Carcereri de Prati, Diana Boriero, and Sofia Mariotto

Department of Neuroscience, Biomedicine and Movement Sciences, Section of Biological Chemistry, University of Verona, Strada Le Grazie, 8, 37134 Verona, Italy

Correspondence should be addressed to Sofia Mariotto; sofia.mariotto@univr.it

Received 16 April 2019; Revised 7 August 2019; Accepted 5 September 2019; Published 28 October 2019

Guest Editor: Adil Mardinoglu

STAT3 is a nuclear transcription factor that regulates genes involved in cell cycle, cell survival, and immune response. Although STAT3 activation drives cells to physiological response, its deregulation is often associated with the development and progression of many solid and hematological tumors as well as with drug resistance. STAT3 is a redox-sensitive protein, and its activation state is related to intracellular GSH levels. Under oxidative conditions, STAT3 activity is regulated by S-glutathionylation, a reversible posttranslational modification of cysteine residues. Compounds able to suppress STAT3 activation and, on the other hand, to modulate intracellular redox homeostasis may potentially improve cancer treatment outcome. Nowadays, about 35% of commercial drugs are natural compounds that derive from plant extracts used in phytotherapy and traditional medicine. Sesquiterpene lactones are an interesting chemical group of plant-derived compounds often employed in traditional medicine against inflammation and cancer. This review focuses on sesquiterpene lactones able to downmodulate STAT3 signaling leading to an antitumor effect and correlates the anti-STAT3 activity with their ability to decrease GSH levels in cancer cells. These properties make them lead compounds for the development of a new therapeutic strategy for cancer treatment.

1. Introduction

Cancer is the main single cause of death in both men and women, claiming over 6 million lives each year worldwide. The hallmarks of cancer include tumor cell proliferation and survival, tumor angiogenesis, and metastasis. Tumor cells exhibit an altered metabolism that allows them to sustain high proliferative rates and resist to some cell death signals, particularly those mediated by increased oxidative stress. Several studies have identified a critical role of aberrant activation of STAT3 signaling in oncogenesis. Therefore, any treatment counteracting the STAT3 hyperactivation has been considered as a new strategy to treat different tumors.

Over the last 20 years, a lot of literature evidence indicates that many derived plant substances are potentially interesting in cancer therapy or can be considered as lead compounds to develop new possible anticancer drugs.

2. Signal Transducer and Activator of Transcription 3

2.1. STAT3 Structure. Signal transducer and activator of transcription 3 (STAT3) is a member of a family of seven proteins (STAT 1, 2, 3, 4, 5a, 5b, and 6) activated by growth factors and cytokines that participate in physiological cellular responses [1, 2]. The transcript of STAT3 undergoes alternative splicing, resulting in the full length STAT3α (92 kDa) and in the truncated isoform STAT3β (83 kDa) that lacks the C-terminal domain including Ser727 [3].

Two crystal structures of STAT3 are deposited in the Protein Data Bank (PDB): the phosphorylated STAT3β-DNA complex (1BG1) [4] and the unphosphorylated STAT3 core fragment (3CWG) [5]. Sequence comparisons, biochemical assays, and mutagenesis have identified six functional conserved domains within the STAT3 molecule, each of them contributing to various aspects of signal transduction

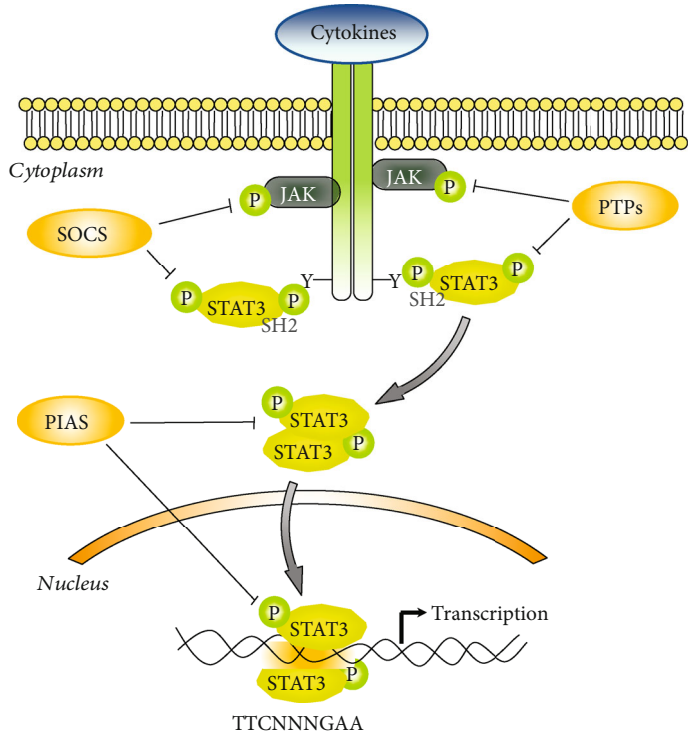

Figure 1: STAT3 signaling pathway. p-STAT3: phosphorylated STAT3; p-JAKs: phosphorylated JAKs; SOCS: suppressor of cytokine signaling proteins; PIAS: protein inhibitors of activated STATs; PTPs: protein tyrosine phosphatases.

pathway. The domains are arranged in the protein structure as follows: an N-terminal domain (NTD) (1-137), a coiled-coil domain (CCD) (138-320) formed by a four-helix bundle, a DNA-binding domain (DBD) (321-494) comprising an eight-stranded β-barrel, a α-helical linker domain (LD) (495-583), a Src homology 2 (SH2) domain (584-688), and a C-terminal transcriptional activation domain (TAD) (723-770). The NTD is a conserved sequence that mediates tetramerization of two phosphorylated dimers which cooperatively bind specific STAT3 sites in a gene promoter [6, 7]. The CCD is critical for recruitment of STAT3 to the receptor, subsequent phosphorylation and dimerization, and its translocation into the nucleus [8]. Moreover, the CCD is involved in protein-protein interactions leading to multiple types of dimer complexes, and it also contains a lysine residue (Lys140) subject to methylation by histone methyl transferase SET9, which is a negative regulatory event [9]. The DBD allows the recognition and the binding to a specific consensus sequence defining the DNA-binding specificity. The SH2 domain is required for the recruitment of signal transduction proteins to activated receptors and contains a key binding pocket where the phosphotyrosine residue of other STAT proteins can bind to form homo- or heterodimers [10]. Other than SH2 domain interaction, we have recently detected two interchain disulfides between cysteine 367 and cysteine 542 and between cysteine 418 and cysteine 426 (Cys367-Cys542 and Cys418-Cys426) responsible for STAT3 dimer stabilization [11]. Finally, the TAD is involved in transcriptional activation and promotes the full STAT3 activation through the phosphorylation of the serine residue 727 (Ser727). In the C-terminal domain, between SH2 and TAD, there is a tail segment with the phosphorylation site tyrosine 705 (Tyr705) that controls dimerization and yields the DNA-binding activity of STAT3 [12].

2.2. STAT3 Signaling Cascade. Multiple distinct steps are involved within the STAT3 signaling pathway. According to the classical model, STAT3 is activated through the binding of growth factors and cytokines to their cell-surface receptors. Cytokines, like IL-6, IL-10, and IL-11, as well as growth factors, like endothelial growth factor (EGF), vascular endothelial growth factor (VEGF), and fibroblast growth factor (FGF), can activate the phosphorylation cascade. This event allows rapid transphosphorylation and activation of Janus tyrosine kinases (JAKs, JAK1, JAK2, JAK3, and Tyk2) that phosphorylate tyrosine residues on the cytoplasmic tail of the receptors. The SH2 domain of STAT3 recognizes and binds to these docking sites, placing STAT3 within close proximity of active JAKs, which subsequently phosphorylate STAT3 at Tyr705. The phosphorylated form of STAT3 homo- or heterodimerizes via reciprocal SH2 domain interaction and translocates from the cytoplasm to the nucleus, where it regulates the transcription of target genes (Figure 1) [13, 14]. In addition to JAKs, STAT3 can be activated by nonreceptor tyrosine kinases such as Src and ABL [15–17]. Furthermore, various serine kinases, like protein kinase C (PKC), mitogen-activated protein kinases (MAPK), and CDK5, phosphorylate the OH residue of Ser727. Although serine phosphorylation occurs in several cells, its biologic role is still controversial. Some authors report that

Table 1: STAT3-regulated genes.

Tumor-supporting functions of STAT3			
Biological functions	Genes		References
Apoptosis	Bcl-2	↑	[44]
	Mcl-1	↑	[24, 30]
	Bcl-xL	↑	[25, 30]
	Survivin	↑	[26, 30]
	Skp2	↑	[27]
	Fas	↓	[28]
Proliferation	c-Myc	↑	[30]
	Pim-1	↑	[30]
	Cyclin-D1	↑	[23]
Angiogenesis	VEGF	↑	[29, 31]
	bFGF	↑	[32]
Immune suppression	IL-10	↑	[33]
	IL-12	↓	[34]
Invasion and metastasis	MMP-1	↑	[30, 36]
	MMP-2	↑	[30, 35]
	MMP-3	↑	[36]
	MMP-9	↑	[36, 37]
	Vimentin	↑	[38]
	TWIST-1	↑	[39]
	p53	↓	[45]
Cancer stem cell	CPT1B	↑	[40]
Self-renewal	ALDH1A1	↑	[41]
Chemoresistance	SOX2	↑	[42]

serine phosphorylation allows to achieve maximal transcriptional activity [18], whereas others demonstrate that serine phosphorylation inhibits STAT3 activity [19, 20].

The binding of STAT3 to a specific DNA domain promotes the expression of numerous genes involved in cell cycle progression, apoptosis, tumor angiogenesis, invasion, metastasis, chemoresistance, immunosuppression, and cancer stem cell renewal (Table 1) [21–40]. Intriguingly, many downstream target genes of STAT3 encode cytokines and growth factors that trigger the same STAT3 signaling pathway, thereby providing a mechanism of autocrine and paracrine STAT3 activation.

Under physiological conditions, the activation of STAT3 signaling is a transient and tightly regulated process that can last from half an hour to several hours. After this period, the signal decays and STAT3 are exported back to the cytoplasm. This decay entails downregulation of both receptors and JAKs, as well as of STAT3 transcriptional activity, and involves several negative protein modulators, including the family of suppressor of cytokine signaling proteins (SOCS), the protein inhibitors of activated STATs (PIAS), and several protein tyrosine phosphatases (PTPs) [41, 42] (Figure 1).

The SOCS family is composed by eight inducible intracellular proteins, all characterized by the SH2 domain that interacts with phosphorylated JAKs and/or with the intracellular domains of the receptors to impede the recruitment of STATs to the docking sites as well as to inhibit JAK activity. Moreover, via their SOCS box domain, SOCS interact with E3 ubiquitin ligase and promote the ubiquitin-dependent degradation of targets [43]. Specifically, STAT3 stimulates SOCS3 gene transcription and the resulting protein binds phospho-JAKs and/or the receptors to turn off the cascade.

Other than SOCS, STAT3 transcriptional activity is controlled by PIAS3, a nuclear protein member of PIAS family proteins which prevents active STAT3 from binding DNA and inhibits STAT3-mediated gene activation [44].

Furthermore, STAT3 transcriptional activity is controlled by PTPs, a family of tyrosine phosphatases, that operate on various steps of signaling cascade. The best characterization of these proteins is SHP-1 and SHP-2 that contain SH2 domain and ensure that tyrosine phosphorylation of JAKs does not persist after the removal of the cytokine [2, 12]. Inactivation of STAT3 in the nucleus occurs through the dephosphorylation of Tyr705 by TC-PTP and TC45 [45].

There is a growing body of evidence demonstrating that STAT3 signaling is also regulated via a complex interplay with cellular miRNAs. Both direct and indirect regulatory mechanisms mediate several positive and negative feedback loops between miRNAs and the STAT3 signaling pathway. Approximately, 50 miRNAs are predicted to bind the 3′-UTR of STAT3; among them, let-7, miR-20a, and miR-93 were directly validated using STAT3-3′-UTR-Reporter constructs. Several miRNAs directly induce STAT3 upregulation (miR-551b 3p) or act to reduce the expression of negative regulators of STAT3 (miR-18a, miR-221, and miR-222), and others are activated by STAT3 (miR-21) through binding within the promoters of these oncomiRs. A more thorough review can be found in the manuscript by [46].

2.3. STAT3 and Oncogenesis. Growing evidence over the last years suggests a critical role of STAT3 as a point of convergence of various signaling pathways that are deregulated in cancer. In healthy cells, STAT3 is closely regulated to maintain a transient active state. Conversely, STAT3 is improperly and persistently activated in numerous hematopoietic and solid malignancies [47, 48]. Constitutively active STAT3 induces deregulation of growth and survival, promotion of angiogenesis, and suppression of host's immune surveillance against tumor. Moreover, it promotes epithelial-mesenchymal transition, invasion, and metastasis thereby contributing to tumor progression. In the last years, increasing evidence indicates that STAT3 also promotes resistance to conventional chemo- and radiation therapy as well as to pharmacological inhibition of several pathways of oncogene-driven malignancies [49, 50].

Although recent studies have revealed activating STAT3 mutations in some malignancies (hepatocellular adenoma, 40% of large granular lymphocytic leukemia, and 30% of chronic lymphoproliferative disease of NK cells), these mutations are too rare to account for the high prevalence of STAT3 activation in solid tumors.

The constitutive activation of STAT3 in cancer is caused mostly by the higher secretion of cytokines and growth factors in tumor microenvironment. Furthermore, in this

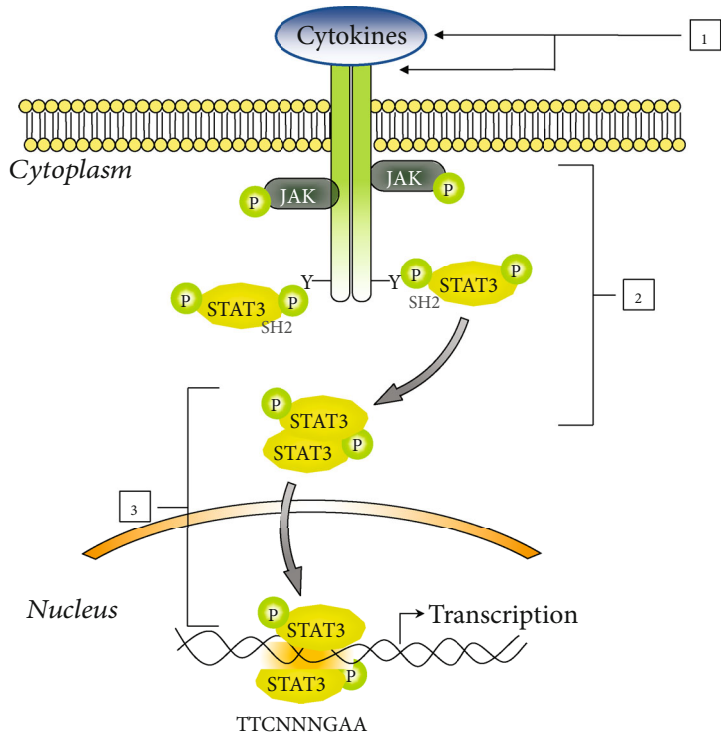

Figure 2: Strategies for inhibition of the STAT3 signaling pathway. Several agents targeting various nodes of STAT3 cascade have been developed. Agents that act on nodes 1 and 2 indirectly switch off STAT3 signaling. Compounds at node 3 directly target STAT3 protein or its DNA-binding downmodulating STAT3 activation. p-STAT3: phosphorylated STAT3; p-JAKs: phosphorylated JAKs.

context, it has been recognized a critical role to the deregulation of receptors with intrinsic tyrosine kinase activity (e.g., EGFR or HER-2/neu) or of nonreceptor tyrosine kinases (e.g., Src or Abl), as well as to the epigenetic modulation of negative regulators of STAT3. High levels of IL-6 have been reported in a lot of cancer patients and are also described as a potent negative regulator of dendritic cell maturation *in vivo*, contributing to control T cell-mediated immune responses [51].

Studies of myeloma, hepatocellular carcinomas, and non-small-cell lung cancer report the loss of proteins that negatively regulate STAT3, such as PIAS [52] or SOCS [53].

On the other hand, JAK mutations and their relevance in the pathogenesis of hematological disorders are well described, with JAK2 V617F being the most well-known mutation, which is found in >95% of patients with polycythaemia vera, primary myelofibrosis, and essential thrombocytosis [54]. Mutations in the genes encoding JAK enzymes seem to be much less common in solid tumors.

Abnormal STAT3 signaling is also associated with defects in activation of JAKs due to a chromosomal translocation resulting in a fusion protein that contains the kinase domain of JAK2 fused to the oligomerization domain of the Ets transcription factor (Tel-JAK2) and possesses constitutive tyrosine kinase activity [55].

It has been reported that also noncanonical pathways of STAT3 signaling play a significant role in malignant transformation, causing alternative posttranslational modifications like phosphorylation of Ser727 and acetylation of Lys685 [56–59].

In the last years, miRNAs are emerging as important regulators of the JAK-STAT3 pathway in the pathogenesis of cancer, causing up- or downmodulation of STAT3 signaling, as well as in the development of chemoresistance in several types of cancer. Further insights on the subject are by [46].

2.4. Treatment Strategies Targeting STAT3 Protein. The understanding that STAT3 signaling promotes tumorigenesis and chemoresistance while severely hinders antitumor immunity has stimulated the search for clinical agents that can effectively inhibit this pathway. Over the last 15 years, many direct or indirect inhibitors targeting various members of the STAT3 pathway have been employed to disrupt STAT3 activity (Figure 2) and some of them entered in clinical trials for treatment of solid or hematological tumor.

Two principal approaches that indirectly inhibit STAT3 activation have been developed. First of all, antibodies that target IL-6 or its receptor are extensively evaluated preclinically and clinically (Figure 2, node 1). Siltuximab and tocilizumab are two antibodies approved by the FDA for the treatment of arthritis or Castleman disease that have been testing in phase I/II clinical trials in different hematological as well as solid tumor [60–65]. Another indirect but efficient mechanism is the use of JAK or Src inhibitors (Figure 2, node 2) [66]. A number of small JAK and Src inhibitors are now in various stages of clinical trials, and some of them result in approved drugs, specifically ruxolitinib and tofacitinib [67]. Other JAK and Src inhibitors such as AZD1480, WP-1066, desatinib, and saracatinib demonstrate the reduction of STAT3 phosphorylation as well as

downstream implications like increased apoptosis and decreased tumor growth [68–71]. Unfortunately, the JAK and IL-6 inhibitors determine an increased rate of infection and off-target neurotoxicity. Moreover, the inhibition of these kinases may influence different signaling cascades and give rise to additional off-target effects. For example, the crucial role of STAT1 in inflammatory response and in disrupting cell proliferation is well known, as well as in antitumor and immune surveillance [72–75]. Therefore, STAT1 should not be downregulated, while attempting to inhibit the actions of STAT3. It is clear that further investigation of all these inhibitors is necessary to understand how to optimize STAT3 inhibition.

For all these reasons, a better strategy for STAT3 inhibition is through the direct targeting of functional phosphorylated STAT3. A lot of peptides and small molecules that impair dimerization, nuclear translocation, and DNA binding of STAT3 have been developed (Figure 2, node 3).

The small peptides designed on STAT3 SH2 domain sequence that contain a tyrosine-phosphorylation site (PY*LKTK) bind to the SH2 domain of STAT3 preventing its dimerization and translocation into the nucleus [76, 77]. Although these compounds have proapoptotic and antitumor activity in cancer cells, they have primarily been used as research tools due to their limited cellular uptake and stability.

Nonpeptidic small molecules able to permeate cells represent a more attractive approach to inhibit aberrant STAT3 activity in cancer cells [78]. Compounds, such as STATTIC, STA-21, LLL-3, LLL-12, WP1066, S3I-201, BP-1-102, STX-0119, and HJC0123, inhibit the growth of tumor cells with hyperactivated STAT3 [79–82]. Although many SH2 domain inhibitors have proved to be promising in laboratory studies, only a few have been evaluated in clinical trials.

An alternative approach useful to inhibit STAT3 function involves competitive inhibition of the interactions between DBD domain of STAT3 and promoter elements in target genes. Platinum (IV) complex, such as CPA-1, CPA-7, and IS3-295, inhibits the STAT3 DNA-binding activity leading to apoptosis in human cancer cell lines [83]. A 15 bp double-stranded decoy oligonucleotide that correspond to the STAT3 response element in the c*FOS* promoter competitively inhibits STAT3 DNA binding and suppresses the tumor growth of preclinical models of ovarian, breast, head-and-neck, lung, brain, and skin cancers as well as acute myeloid leukemia [84–87].

Although many of these anti-STAT3 compounds have antitumor effects *in vitro* and *in vivo*, there are no currently approved drug directly targeting STAT3 and the research of STAT3 inhibitors is still evolving.

3. Redox Homeostasis in Cancer Cells

3.1. Intracellular Redox Homeostasis. In contrast to normal tissue, most of solid tumors are characterized by regions of low oxygen (hypoxia), low pH, and low levels of glucose which result from an architecturally abnormal microcirculation, rapid growth of tumor cells, and high interstitial pressure. Hypoxia and the high energetic metabolism induced by tumor microenvironment contribute to upregulation of reactive oxygen species (ROS) production in mitochondria, peroxisomes, and endoplasmic reticulum [88–91]. Excessive levels of ROS cause oxidative damage to DNA, proteins, and lipids, compromising their structures and function. To prevent oxidative damage, cancer cells activate various enzymatic and nonenzymatic antioxidant systems. The first ones include superoxide dismutase, catalase, glutathione peroxidase, and glutathione reductase whereas α-tocopherol (vitamin E), β-carotene (vitamin A), ascorbic acid (vitamin C), and uric acid represent the ROS scavenging molecules. Furthermore, multiple and interrelated redox couples, such as NADPH/$NADP^+$, GSH/GSSG, Trx/TrxSS, and cysteine/cystine, contribute to the intracellular redox homeostasis [92–99].

A number of human cancer tissues, including breast, brain, colon, pancreas, lungs, and leukemia, produce high concentrations of glutathione (GSH) that contribute to cancer initiation, progression, and metastasis formation and to chemoresistance [100–103]. In accordance with the elevated level of GSH in cancer cells, several drugs known to reduce GSH concentration are currently being used in clinical trials to improve efficacy of targeted therapy. In this regard, the use of disulfiram, alone or combined with arsenic trioxide, has been approved as therapy for metastatic melanoma and nonacute promyelocytic leukemia [101, 104]. Buthionine sulfoximine (BSO), a synthetic inhibitor of GSH production, confers increased sensitivity to chemotherapy in myeloma and neck cancers [105] and has been clinically used in various types of cancers [106]. Similarly, phenylethyl isothiocyanate (PEITC), which conjugates with GSH, inhibits the oncogenic transformation of ovarian epithelial cells and hematopoietic cells [107].

Collectively, modulation of the GSH level is an alternative way to increase the sensitivity of tumor cells to conventional chemotherapy and provides a viable option for patients suffering from therapy-resistant tumors.

3.2. [GSH]/[GSSG] Redox Couple. The tripeptide glutathione (Glu-Gly-Cys) is the most abundant intracellular nonenzymatic ROS scavenger reaching millimolar concentrations in the cells. Intracellular glutathione can exist as a monomer in its reduced form (GSH) or as a disulfide dimer (GSSG) after its oxidation which usually accounts for less than 1% of the total intracellular glutathione content.

As antioxidant and intracellular redox buffer, GSH has essential roles in ROS scavenging and in detoxification of electrophiles, xenobiotics, and heavy metals. Two oxidized GSH molecules dimerize by a SS bond to form GSSG. Glutathione reductase, a NADPH-dependent enzyme, reverts this reaction to reconstitute GSH pool. GSH reduces peroxides and generates GSSG via glutathione peroxidase (GPx) or it reacts with many electrophiles to generate glutathione *S*-conjugates (GS-R). Although these reactions can occur spontaneously, they are often catalyzed by the glutathione *S*-transferase (GST) [108, 109] (Figure 3).

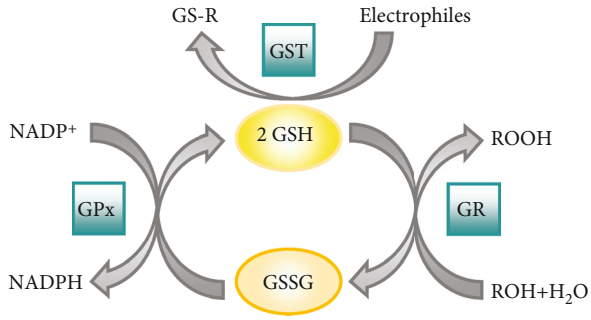

Figure 3: Antioxidant function of glutathione. GST: glutathione transferase; GS-R: electrophile-GSH adduct; GPx: glutathione peroxidase; GR: glutathione reductase.

The cellular redox status can be evaluated measuring the GSH/GSSG ratio by the Nernst equation [110]. At 25°C and pH 7, E° of the GSH/GSSG redox couple is

$$\mathrm{GSSG} + 2e^{-} + 2H^{+} \leftrightarrows 2\mathrm{GSH} \quad E^{\circ}_{\mathrm{GSH/GSSG}} = -240\,\mathrm{mV}. \tag{1}$$

Since two GSH molecules are needed to form one GSSG molecule, the reaction is second order with respect to GSH. Thus, any changes in the absolute concentration of GSH will change the redox potential, even without changes in the GSH/GSSG ratio. This suggests that cells with much higher GSH level have a greater reducing capacity than cells with lower GSH concentration.

The cellular redox state is one of the master regulators of different cellular processes, and physiological cellular function is maintained by a fine balance between reducing and oxidizing conditions. It has been reported that the etiology and/or progression of many human diseases, including cancer, are related to GSH/GSSG homeostasis. Generally, elevated levels of GSH that determine a more reducing cellular environment stimulate cell proliferation whereas a mild oxidizing environment results in cell differentiation. A further shift toward a more oxidant cellular environment leads to apoptosis or necrosis [108, 110, 111].

3.3. Redox Regulation of STAT3. Under oxidative stress, many proteins undergo reversible and irreversible *oxidative* modifications, which may lead to changes in the structure and/or function of the oxidized protein. These redox-sensitive proteins exhibit a striking differential susceptibility to oxidative stress; while a protein may contain numerous residues, only a minority of them will have the chemical properties to function as a possible target site for oxidant. This is largely due to the reactivity of anionic sulfur of various oxidizing agents.

Mild oxidative stress induces selective modifications of proteins at critical cysteine thiols including reversible oxidation to sulfenic acids, intra- and intermolecular disulfides, S-glutathionylation, and S-nitrosylation [112]. S-Glutathionylation, the reversible formation of protein-mixed disulfides with GSH, represents the most common steady-state derivative due to cellular abundance of GSH and ready conversion of cysteine-sulfenic acid and S-nitrosocysteine precursors to S-glutathionylcysteine disulfides. This reaction may protect proteins from irreversible damage or modulate protein function. Conversely, excessive oxidative stress is associated with permanent loss of function, misfolding, and aggregation due to irreversible modification of SH groups of protein [113–115].

Several studies demonstrate that intracellular redox environment influences STAT3 activation cascade although it is still not clear if ROS up- or down-regulate STAT3 activation. Some authors report that ROS trigger Tyr705 STAT3 phosphorylation and upregulate its DNA-binding activity [116, 117]. On the other hand, other authors indicate that ROS oxidize conserved cysteines in STAT3 DNA-binding domain impairing its transcriptional activity [118, 119]. Moreover, there is evidence from the literature which prove that ROS scavengers and inhibitors of NADPH oxidase enzymes (NOX) generally inhibit STAT3 activity [120, 121]. In addition, it has been shown that nitrosocyclohexyl acetate, a nitroxyl donor, inhibits STAT3 phosphorylation through the formation of sulfenic acid at the cysteine residues in endothelial cells [122].

S-Glutathionylation and S-nitrosylation inhibit STAT3 phosphorylation as well as its DNA-binding activity in different cell lines and in *in vitro* studies. Although the 3D model of nitrosylated/glutathionylated STAT3 is not available, it can be speculated that the small conformational changes induced by NO or GSH addition could in turn induce a conformational change in the phosphorylation site of protein inhibiting accessibility to JAKs [119, 123–125].

Our group has been studying STAT3 redox regulation for the past ten years. Particularly, we identified three sesquiterpene lactones, costunolide, dehydrocostuslactone, and cynaropicrin, able to inhibit IL-6-induced as well as constitutive activation of STAT3 in different cancer cell lines. These compounds disrupt intracellular redox homeostasis, induce reversible S-glutathionylation of STAT3, and decrease its Tyr705 phosphorylation [126, 127]. Deepening inside the redox regulation of STAT3 signaling, we reported that Cys328 and Cys542 in the DNA-binding domain and in the linker domain, respectively, are a target of S-glutathionylation [123, 128].

Since STAT3 is validated as a therapeutic target in different solid and hematologic tumor, the modulation of oxidative stress could be a new strategy to inhibit STAT3 hyperactivation. On the other end, the consequent decrease in GSH levels could sensitize tumor cells to conventional chemotherapy.

4. Sesquiterpene Lactones

4.1. Sesquiterpene Lactone Structure. Sesquiterpene lactones (SLs) are colorless, bitter, and stable compounds of terpenoids, a class of lipophilic plant secondary metabolites. More than 5000 SLs have been characterized in species of the plant kingdom, in particular in the family Asteraceae, and plant extracts rich in SLs have long been employed in traditional medicine against inflammatory-related diseases. SLs possess a broad spectrum of biological activities, including anti-inflammatory, antibacterial, and immunomodulatory effects. These compounds also inhibit cell cycle and proliferation and

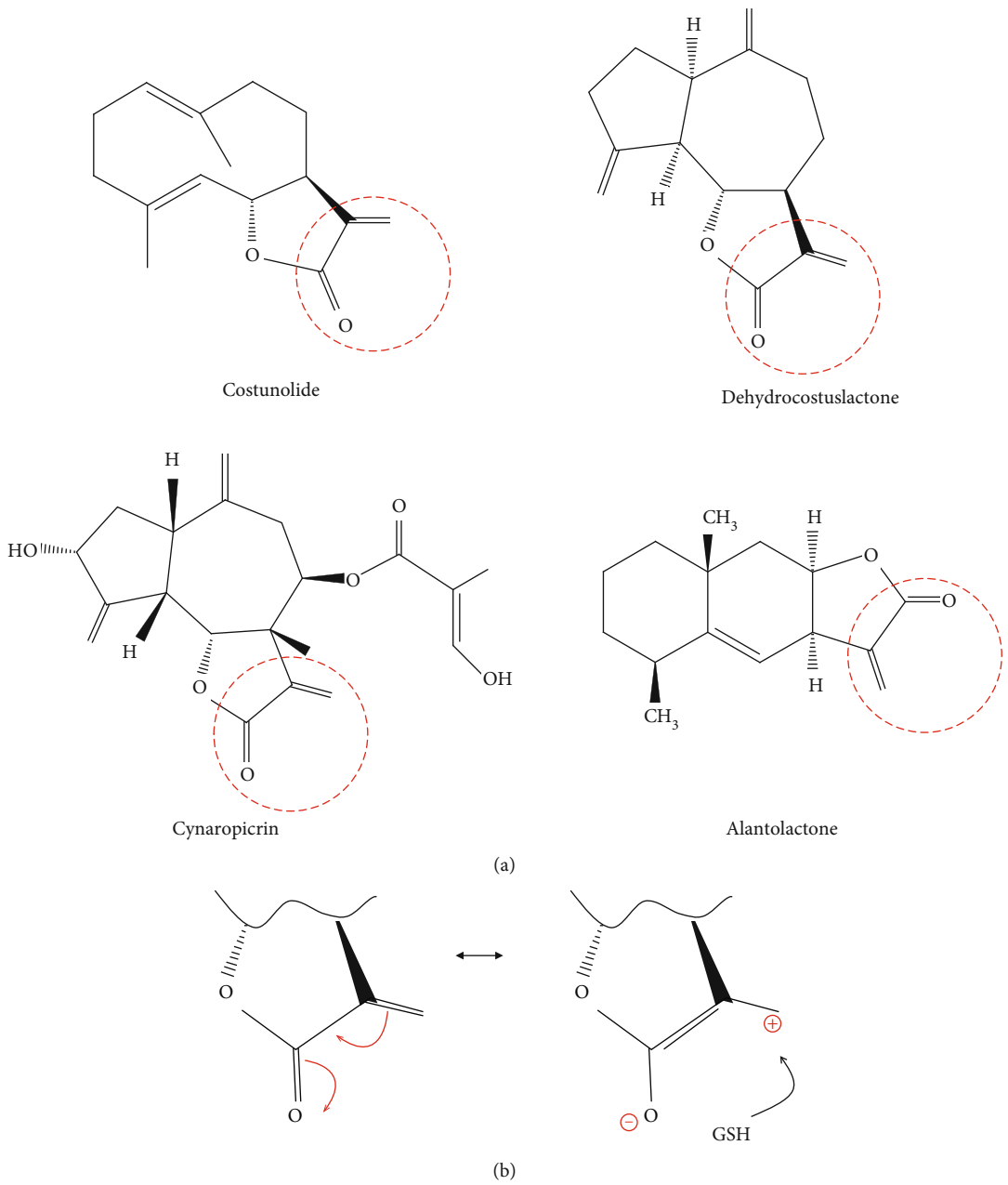

Figure 4: (a) Chemical structure of SLs that induce STAT3 S-glutathionylation and impair STAT3 phosphorylation. The reactive centre of SLs is evidenced with a red circle. (b) Schematic representation of Michael reaction.

induce apoptosis, in different cancer cell lines and in many *in vivo* studies [129–131]. Although the exact mechanisms of action are not well elucidated, emerging data suggest that the biological effect of SLs is associated with depletion of GSH and ROS generation [126, 127, 132, 133].

SLs are 15 carbon compounds consisting of three isoprene (5-C) units arranged in several characteristic ring systems, including one or more lactone rings. The α-β-unsaturated carbonyl group present in most of these compounds is the major responsible for their biological effects [134]. The α-β-unsaturated carbonyl group is a strong alkylating agent that may react by Michael-type addition with intracellular nucleophiles, such as cysteine sulfhydryl residues in proteins, leading to disruption of their biological function. The α-β-unsaturated carbonyl moiety may also react with the sulfhydryl group of cysteine residue in GSH leading to redox homeostasis disruption and oxidative stress in cells (Figure 4(b)) [134–136].

Further chemical features, such as lipophilicity and molecular geometry of compounds as well as the chemical environment of the target nucleophiles, also influence the bioavailability and biological activity of SLs [137, 138].

4.2. Sesquiterpene Lactones and STAT3. In the last years, many natural SLs able to induce apoptosis through the inhibition of STAT3 signaling have been recognized in

Table 2: Anti-STAT3 SLs.

Compound	Cell lines/murine model	STAT3 signaling	Molecular mechanism of STAT3 inhibition	Oxidative stress	Biological effect
Alantolactone	A549, NCI-H1650 [139]	p^{Tyr705}STAT3 ↓ STAT3 DNA binding ↓	STAT3 glutathionylation	ROS ↑ GSH/GSSG ↓	Apoptosis Enhanced chemosensitivity
	HepG2 [140]	p^{Tyr705}STAT3 ↓	STAT3 glutathionylation?	ROS ↑ [GSH] ↓	Apoptosis
	MDA-MB231, MCF-7 [141]	p^{Tyr705}STAT3 ↓	STAT3 glutathionylation?	ROS ↑ [GSH] ↓	Apoptosis
	BxPC-3, AsPC-1, PANC-1 Athymic BALB/cA [142]	p^{Tyr705}STAT3 ↓	Binding to STAT3 SH2 domain	No evaluated	Cytotoxicity Inhibited cell migration Enhanced chemosensitivity
Santamarine	HepG2 [143]	p^{Tyr705}STAT3 ↓ pSrc ↓	STAT3 glutathionylation?	ROS ↑ GSH/GSSG ↓	Apoptosis
Parthenolide	SGC-7901/DDP [144]	p^{Tyr705}STAT3 ↓	?	No evaluated	Apoptosis Inhibited cell migration and invasion Enhanced chemosensitivity
	HepG2, HT-29, Lovo, MDA-MB-231, MDA-MB-468, HCT116, H460, NCI-H1299, Colo205, BGC [145]	p^{Tyr705}STAT3 ↓ $p^{Tyr1007/1008}$ JAK2 ↓	Binding to JAK2	ROS ↑	Cytotoxicity
Costunolide	THP1 [126]	p^{Tyr705}STAT3 ↓ $p^{Tyr1007/1008}$ JAK2 ↓ $p^{Tyr1022/1023}$ JAK1 ↓ $p^{Tyr1054/1055}$TyK2 ↓	STAT3 glutathionylation?	ROS ↑ GSH/GSSG ↓	
1β-hydroxyl-5α-chloro-8-epi-xanthatin	SK-Hep-1, HepG2, SMMC-7721 [146]	p^{Tyr705}STAT3 ↓ $p^{Tyr1007/1008}$ JAK2 ↓	STAT3 glutathionylation?	ROS ↑ GSH/GSSG ↓	Cytostatic Apoptosis
Bigelovin	HCT 116 HT-29 26-M01 BALB/c nude mice [147, 148]	p^{Tyr705}STAT3 ↓ STAT3 ↓	STAT3 glutathionylation?	ROS ↑	Inhibited cell migration and invasion Apoptosis
Dehydrocostuslactone	THP1 [126]	p^{Tyr705}STAT3 ↓ $p^{Tyr1007/1008}$ JAK2 ↓ $p^{Tyr1022/1023}$ JAK1 ↓ $p^{Tyr1054/1055}$TyK2 ↓	STAT3 glutathionylation?	ROS ↑ GSH/GSSG ↓	
	MCF-7, MDA-MB-231 BALB/cA-nu [149]	$p^{Tyr1007/1008}$ JAK2 ↓ $p^{Tyr1022/1023}$ JAK1 ↓ p^{Tyr705}STAT3 ↓	SOCS-1 ↑ SOCS-3 ↑	No evaluated	Cell cycle arrest Apoptosis
	K562 [150]	$p^{Tyr1007/1008}$ JAK2 ↓ p^{Tyr705}STAT3 ↓	?	ROS ↑	Apoptosis

Table 2: Continued.

Compound	Cell lines/murine model	STAT3 signaling	Molecular mechanism of STAT3 inhibition	Oxidative stress	Biological effect
Cynaropicrin	THP-1 DU-145 [127]	p^{Tyr705}STAT3 ↓ STAT3 DNA binding ↓	STAT3 glutathionylation?	ROS ↑ [GSH] ↓	Apoptosis Enhanced chemosensitivity
Deoxyelephantopin	HCT 116, K562, KB, T47D [151]	p^{Tyr705}STAT3 ↓	STAT3 glutathionylation?	ROS ↑	Cytotoxicity Apoptosis Autophagy
	B16-F10, MeWo A375, A2058, SK-MEL-2 NOD/SCID mice [152]	p^{Tyr705}STAT3 ↓	STAT3 glutathionylation?	ROS ↑	Cytotoxicity Apoptosis Enhanced chemosensitivity
6-O-angeloylplenolin	NCI-H1975, L78, NCI-292, HCC827, A549, 16HBE, BEAS-2B SCID mice [153]	p^{Tyr705}STAT3 ↓	Binding to STAT3 SH2 domain	Not evaluated	Apoptosis
	MM.1S, MM.1R, U266 BALB/c nude mice [154]	p^{Tyr705}STAT3 ↓ $p^{Tyr1007/1008}$ JAK2 ↓	?	Not evaluated	Apoptosis Enhanced chemosensitivity
Antrocin	A549, H1975, H441, PC9, BEAS-2B Mice [155]	p^{Tyr705}STAT3 ↓ $p^{Tyr1007/1008}$ JAK2 ↓ $p^{Tyr1022/1023}$ JAK1 ↓ $p^{Tyr1054/1055}$TyK2 ↓ STAT3 DNA binding ↓	?		Apoptosis

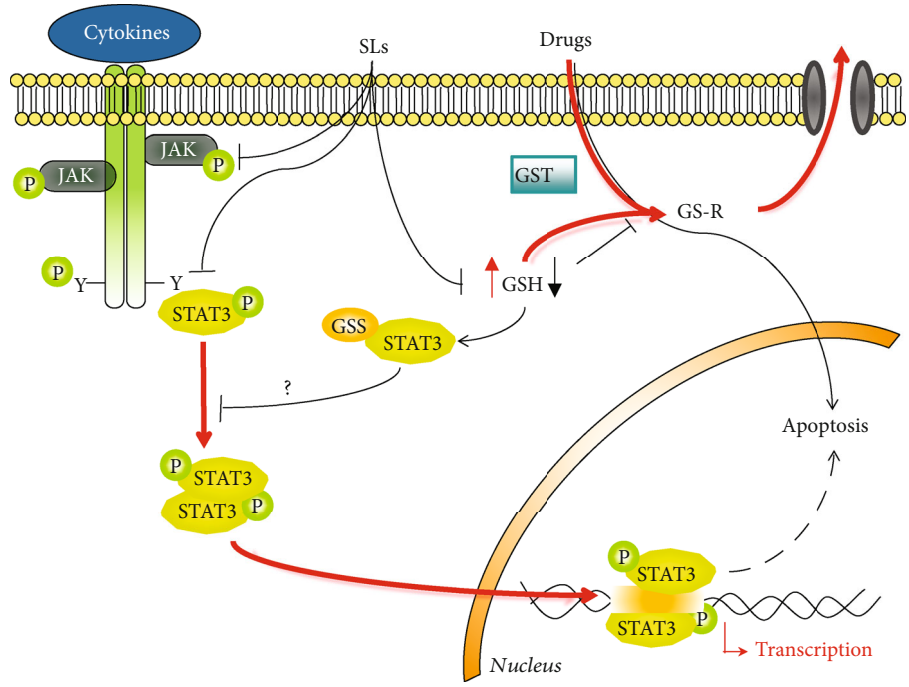

Figure 5: Cancer cells are characterized by elevated levels of GSH that confer resistance to several chemotherapeutic drugs and by constitutive activation of STAT3 signaling that contributes to tumorigenesis and tumor growth, promotes angiogenesis and metastasis, suppresses immune response, and induces chemoresistance (red line). SLs inhibit STAT3 signaling targeting different steps in the signaling cascade (black line). The mild oxidative stress, derived by the direct binding of SLs to GSH, induced S-glutathionylation of STAT3 switching off STAT3 signaling (black line). Moreover, the reduced GSH levels contribute to overcome chemoresistance. GST: glutathione transferase; GS-R: drug-GSH adduct; GSS-STAT3: glutathionylated STAT3; p-STAT3: phosphorylated STAT3; pJAKs: phosphorylated JAKs.

different cancer cellular and animal models (Table 2) [126, 127, 139–155]. Induction of apoptosis was found to be linked with increased ROS production, GSH depletion, and modulation of GSH/GSSG ratio. Although the final biological outcome of all SLs is well described, the molecular mechanism of anti-STAT3 activity is not reported for all of them. Cheng et al. demonstrate that 6-O-angeloylplenolin directly interacts with the SH2 domain of STAT3 and inhibits the constitutive and IL-6-induced STAT3 activity in lung cancer cells [153]. A direct interaction with STAT3 SH2 domain is also reported for alantolactone [142]. Furthermore, Liu et al. describe that parthenolide covalently binds to Cys residues of JAKs suppressing its kinase activity and downmodulating the STAT3 pathway [145].

Other studies show that SLs inhibit STAT3 signaling through S-glutathionylation of Cys residues in STAT3 protein. Dehydrocostuslactone, costunolide, cynaropicrin, and alantolactone that contain an α-β-unsaturated carbonyl group directly interact with GSH by Micheal addition and induce a rapid drop in GSH concentration, thereby triggering S-glutathionylation of STAT3. This event impairs STAT3 phosphorylation switching off the signaling cascade (Figure 4(b)) [126, 127, 139]. It is possible to speculate that S-glutathionylation is the common molecular mechanism of anti-STAT3 activity of other SLs able to disrupt GSH/GSSG homeostasis [140, 141, 143, 146–148, 150–152]. The exact molecular mechanism by which S-glutathionylation inhibits STAT3 phosphorylation is not completely clarified. We reported that S-glutathionylation of STAT3 slightly modulates the secondary and tertiary structure of STAT3 affecting the phosphorylation site thus hampering the recognition of Tyr705 site by JAKs [123].

Various *in vitro* and *in vivo* studies reveal that suppression of STAT3 activation by SLs overcomes drug resistance [127, 139, 142, 144, 152, 154, 155]. Since the central role of STAT3 in carcinogenesis and chemoresistance, SLs able to switch off STAT3 signaling have gained considerable attention from the researchers for the development of a new therapeutic strategy for cancer treatment.

5. Concluding Remarks

Very often, the rational development of drugs that kill cancer cells interacting with one signaling has a sporadic success due to the activation of other pathways as well as to the development of chemoresistance. It is known that oxidative stress is closely related to carcinogenesis and to resistance toward classical drug treatment. Therefore, the use of molecules able to reduce STAT3 activation and, on the other hand, to induce a mild oxidative stress in a high-reduced cellular environment may potentially improve cancer treatment outcome. In this context, SLs are promising compounds in cancer drug discovery and their anti-STAT3 activity as well as their ability to disrupt redox homeostasis place them as lead compounds in the development of innovative therapies (Figure 5).

Conflicts of Interest

The authors declare no conflict of interest.

Acknowledgments

The authors' research was supported by the Joint Project 2017 (University of Verona, Italy, and Aboca, Sansepolcro (AR) Italy) and by funds from the Italian Ministry for Research and Education (FUR2018MS).

References

[1] Y. Nagata and K. Todokoro, "Interleukin 3 activates not only JAK2 and STAT5, but also Tyk2, STAT1, and STAT3," *Biochemical and Biophysical Research Communications*, vol. 221, no. 3, pp. 785–789, 1996.

[2] P. C. Heinrich, I. Behrmann, G. Müller-Newen, F. Schaper, and L. Graeve, "Interleukin-6-type cytokine signalling through the gp130/Jak/STAT pathway," *Biochemical Journal*, vol. 334, no. 2, pp. 297–314, 1998.

[3] E. Caldenhoven, T. B. van Dijk, R. Solari et al., "STAT3β, a splice variant of transcription factor STAT3, is a dominant negative regulator of transcription," *Journal of Biological Chemistry*, vol. 271, no. 22, pp. 13221–13227, 1996.

[4] S. Becker, G. L. Corthals, R. Aebersold, B. Groner, and C. W. Müller, "Expression of a tyrosine phosphorylated, DNA binding Stat3β dimer in bacteria," *FEBS Letters*, vol. 441, no. 1, pp. 141–147, 1998.

[5] Z. Ren, X. Mao, C. Mertens et al., "Crystal structure of unphosphorylated STAT3 core fragment," *Biochemical and Biophysical Research Communications*, vol. 374, no. 1, pp. 1–5, 2008.

[6] X. Zhang and J. E. Darnell Jr., "Functional importance of Stat3 tetramerization in activation of the α2-macroglobulin gene," *Journal of Biological Chemistry*, vol. 276, no. 36, pp. 33576–33581, 2001.

[7] J. X. Lin, P. Li, D. Liu et al., "Critical role of STAT5 transcription factor tetramerization for cytokine responses and normal immune function," *Immunity*, vol. 36, no. 4, pp. 586–599, 2012.

[8] J. Ma, T. Zhang, V. Novotny-Diermayr, A. L. C. Tan, and X. Cao, "A novel sequence in the coiled-coil domain of Stat3 essential for its nuclear translocation," *Journal of Biological Chemistry*, vol. 278, no. 31, pp. 29252–29260, 2003.

[9] J. Yang, J. Huang, M. Dasgupta et al., "Reversible methylation of promoter-bound STAT3 by histone-modifying enzymes," *Proceedings of the National Academy of Sciences of the United States of America*, vol. 107, no. 50, pp. 21499–21504, 2010.

[10] S. Haan, U. Hemmann, U. Hassiepen et al., "Characterization and binding specificity of the monomeric STAT3-SH2 domain," *Journal of Biological Chemistry*, vol. 274, no. 3, pp. 1342–1348, 1999.

[11] E. Butturini, G. Gotte, D. Dell'Orco et al., "Intermolecular disulfide bond influences unphosphorylated STAT3 dimerization and function," *Biochemical Journal*, vol. 473, no. 19, pp. 3205–3219, 2016.

[12] M. Benekli, H. Baumann, and M. Wetzler, "Targeting signal transducer and activator of transcription signaling pathway in leukemias," *Journal of Clinical Oncology*, vol. 27, no. 26, pp. 4422–4432, 2009.

[13] J. E. Darnell Jr., "STATs and gene regulation," *Science*, vol. 277, no. 5332, pp. 1630–1635, 1997.

[14] Z. Zhong, Z. Wen, and J. Darnell, "Stat3: a STAT family member activated by tyrosine phosphorylation in response to epidermal growth factor and interleukin-6," *Science*, vol. 264, no. 5155, pp. 95–98, 1994.

[15] C. Yu, D. Meyer, G. Campbell et al., "Enhanced DNA-binding activity of a Stat3-related protein in cells transformed by the Src oncoprotein," *Science*, vol. 269, no. 5220, pp. 81–83, 1995.

[16] J. Turkson, T. Bowman, R. Garcia, E. Caldenhoven, R. P. de Groot, and R. Jove, "Stat3 activation by Src induces specific gene regulation and is required for cell transformation," *Molecular and Cellular Biology*, vol. 18, no. 5, pp. 2545–2552, 1998.

[17] J. F. Bromberg, C. M. Horvath, D. Besser, W. W. Lathem, and J. E. Darnell Jr., "Stat3 activation is required for cellular transformation by v-*src*," *Molecular and Cellular Biology*, vol. 18, no. 5, pp. 2553–2558, 1998.

[18] Z. Wen, Z. Zhong, and J. E. Darnell Jr., "Maximal activation of transcription by Statl and Stat3 requires both tyrosine and serine phosphorylation," *Cell*, vol. 82, no. 2, pp. 241–250, 1995.

[19] Z. Wen and Darnell JEJr., "Mapping of Stat3 serine phosphorylation to a single residue (727) and evidence that serine phosphorylation has no influence on DNA binding of Stat1 and Stat3," *Nucleic Acids Research*, vol. 25, no. 11, pp. 2062–2067, 1997.

[20] C. P. Lim and X. Cao, "Serine phosphorylation and negative regulation of Stat3 by JNK," *Journal of Biological Chemistry*, vol. 274, no. 43, pp. 31055–31061, 1999.

[21] H. Yu, D. Pardoll, and R. Jove, "STATs in cancer inflammation and immunity: a leading role for STAT3," *Nature Reviews Cancer*, vol. 9, no. 11, pp. 798–809, 2009.

[22] R. Catlett-Falcone, T. H. Landowski, M. M. Oshiro et al., "Constitutive activation of Stat3 signaling confers resistance to apoptosis in human U266 myeloma cells," *Immunity*, vol. 10, no. 1, pp. 105–115, 1999.

[23] W. Li, M. R. Lee, T. Kim, Y. W. Kim, and M. Y. Cho, "Activated STAT3 may participate in tumor progression through increasing CD133/survivin expression in early stage of colon cancer," *Biochemical and Biophysical Research Communications*, vol. 497, no. 1, pp. 354–361, 2018.

[24] H. Huang, W. Zhao, and D. Yang, "Stat3 induces oncogenic Skp2 expression in human cervical carcinoma cells," *Biochemical and Biophysical Research Communications*, vol. 418, no. 1, pp. 186–190, 2012.

[25] H. Y. Lin, S. C. Hou, S. C. Chen et al., "(−)-epigallocatechin gallate induces Fas/CD95-mediated apoptosis through Inhibiting constitutive and IL-6-induced JAK/STAT3 signaling in head and neck squamous cell carcinoma cells," *Journal of Agricultural and Food Chemistry*, vol. 60, no. 10, pp. 2480–2489, 2012.

[26] K. Liu, H. Gao, Q. Wang et al., "Hispidulin suppresses cell growth and metastasis by targeting *PIM1* through JAK2/STAT3 signaling in colorectal cancer," *Cancer Science*, vol. 109, no. 5, pp. 1369–1381, 2018.

[27] F. C. Hsieh, G. Cheng, and J. Lin, "Evaluation of potential Stat3-regulated genes in human breast cancer," *Biochemical and Biophysical Research Communications*, vol. 335, no. 2, pp. 292–299, 2005.

[28] G. Zhao, G. Zhu, Y. Huang et al., "IL-6 mediates the signal pathway of JAK-STAT3-VEGF-C promoting growth, invasion and lymphangiogenesis in gastric cancer," *Oncology Reports*, vol. 35, no. 3, pp. 1787–1795, 2016.

[29] M. Zhao, F. H. Gao, J. Y. Wang et al., "JAK2/STAT3 signaling pathway activation mediates tumor angiogenesis by upregulation of VEGF and bFGF in non-small-cell lung cancer," *Lung Cancer*, vol. 73, no. 3, pp. 366–374, 2011.

[30] M. Kortylewski, H. Xin, M. Kujawski et al., "Regulation of the IL-23 and IL-12 balance by Stat3 signaling in the tumor microenvironment," *Cancer Cell*, vol. 15, no. 2, pp. 114–123, 2009.

[31] X. Xuan, S. Li, X. Lou et al., "Stat3 promotes invasion of esophageal squamous cell carcinoma through up-regulation of MMP2," *Molecular Biology Reports*, vol. 42, no. 5, pp. 907–915, 2015.

[32] S. A. Tsareva, R. Moriggl, F. M. Corvinus et al., "Signal transducer and activator of transcription 3 activation promotes invasive growth of colon carcinomas through matrix metal loproteinase induction," *Neoplasia*, vol. 9, no. 4, pp. 279–291, 2007.

[33] Z. H. Jia, Y. Jia, F. J. Guo, J. Chen, X. W. Zhang, and M. H. Cui, "Phosphorylation of STAT3 at Tyr705 regulates MMP-9 production in epithelial ovarian cancer," *PLoS One*, vol. 12, no. 8, article e0183622, 2017.

[34] D. Sun, W. Shen, F. Zhang et al., "α-Hederin inhibits interleukin 6-induced epithelial-to-mesenchymal transition associated with disruption of JAK2/STAT3 signaling in colon cancer cells," *Biomedicine & Pharmacotherapy*, vol. 101, pp. 107–114, 2018.

[35] Y. Li, M. Bai, Y. Xu, W. Zhao, N. Liu, and J. Yu, "TPPP3 promotes cell proliferation, invasion and tumor metastasis via STAT3/ twist1 pathway in non-small-cell lung carcinoma," *Cellular Physiology and Biochemistry*, vol. 50, no. 5, pp. 2004–2016, 2018.

[36] T. Wang, J. F. Fahrmann, H. Lee et al., "JAK/STAT3-regulated fatty acid β-oxidation is critical for breast cancer stem cell self-renewal and chemoresistance," *Cell Metabolism*, vol. 27, no. 1, pp. 136–150.e5, 2018.

[37] L. Lin, B. Hutzen, H. F. Lee et al., "Evaluation of STAT3 signaling in ALDH+ and ALDH+/CD44+/CD24– subpopulations of breast cancer cells," *PLoS One*, vol. 8, no. 12, article e82821, 2013.

[38] L. Hüser, S. Sachindra, K. Granados et al., "SOX2-mediated upregulation of CD24 promotes adaptive resistance toward targeted therapy in melanoma," *International Journal of Cancer*, vol. 143, no. 12, pp. 3131–3142, 2018.

[39] R. Montone, M. G. Romanelli, A. Baruzzi, F. Ferrarini, E. Liboi, and P. M. J. Lievens, "Mutant FGFR3 associated with SADDAN disease causes cytoskeleton disorganization through PLCγ1/Src-mediated paxillin hyperphosphorylation," *The International Journal of Biochemistry & Cell Biology*, vol. 95, pp. 17–26, 2018.

[40] Y. Tsujita, A. Horiguchi, S. Tasaki et al., "STAT3 inhibition by WP1066 suppresses the growth and invasiveness of bladder cancer cells," *Oncology Reports*, vol. 38, no. 4, pp. 2197–2204, 2017.

[41] K. Shuai and B. Liu, "Regulation of JAK–STAT signalling in the immune system," *Nature Reviews Immunology*, vol. 3, no. 11, pp. 900–911, 2003.

[42] B. B. Aggarwal, A. B. Kunnumakkara, K. B. Harikumar et al., "Signal transducer and activator of transcription-3, inflammation, and cancer," *Annals of the New York Academy of Sciences*, vol. 1171, no. 1, pp. 59–76, 2009.

[43] E. M. Linossi and S. E. Nicholson, "The SOCS box—adapting proteins for ubiquitination and proteasomal degradation," *IUBMB Life*, vol. 64, no. 4, pp. 316–323, 2012.

[44] C. D. Chung, J. Liao, B. Liu et al., "Specific inhibition of Stat3 signal transduction by PIAS3," *Science*, vol. 278, no. 5344, pp. 1803–1805, 1997.

[45] T. Yamamoto, Y. Sekine, K. Kashima et al., "The nuclear isoform of protein-tyrosine phosphatase TC-PTP regulates interleukin-6-mediated signaling pathway through STAT3 dephosphorylation," *Biochemical and Biophysical Research Communications*, vol. 297, no. 4, pp. 811–817, 2002.

[46] Q. Cao, Y. Y. Li, W. F. He et al., "Interplay between microRNAs and the STAT3 signaling pathway in human cancers," *Physiological Genomics*, vol. 45, no. 24, pp. 1206–1214, 2013.

[47] J. Turkson and R. Jove, "STAT proteins: novel molecular targets for cancer drug discovery," *Oncogene*, vol. 19, no. 56, pp. 6613–6626, 2000.

[48] R. Buettner, L. B. Mora, and R. Jove, "Activated STAT signaling in human tumors provides novel molecular targets for therapeutic intervention," *Clinical Cancer Research*, vol. 8, no. 4, pp. 945–954, 2002.

[49] A. A. Zulkifli, F. H. Tan, T. L. Putoczki, S. S. Stylli, and R. B. Luwor, "STAT3 signaling mediates tumour resistance to EGFR targeted therapeutics," *Molecular and Cellular Endocrinology*, vol. 451, pp. 15–23, 2017.

[50] L. Wang, Q. Wang, M. Gao et al., "STAT3 activation confers trastuzumab-emtansine (T-DM1) resistance in HER2-positive breast cancer," *Cancer Science*, vol. 109, no. 10, pp. 3305–3315, 2018.

[51] S. J. Park, T. Nakagawa, H. Kitamura et al., "IL-6 regulates in vivo dendritic cell differentiation through STAT3 activation," *The Journal of Immunology*, vol. 173, no. 6, pp. 3844–3854, 2004.

[52] L. Wang and S. Banerjee, "Differential PIAS3 expression in human malignancy," *Oncology Reports*, vol. 11, no. 6, pp. 1319–1324, 2004.

[53] B. He, L. You, K. Uematsu et al., "SOCS-3 is frequently silenced by hypermethylation and suppresses cell growth in human lung cancer," *Proceedings of the National Academy of Sciences of the United States of America*, vol. 100, no. 24, pp. 14133–14138, 2003.

[54] C. James, V. Ugo, J. P. le Couédic et al., "A unique clonal JAK2 mutation leading to constitutive signalling causes polycythaemia vera," *Nature*, vol. 434, no. 7037, pp. 1144–1148, 2005.

[55] V. Lacronique, A. Boureux, V. D. Valle et al., "A TEL-JAK2 fusion protein with constitutive kinase activity in human leukemia," *Science*, vol. 278, no. 5341, pp. 1309–1312, 1997.

[56] T. Decker and P. Kovarik, "Serine phosphorylation of STATs," *Oncogene*, vol. 19, no. 21, pp. 2628–2637, 2000.

[57] R. Wang, P. Cherukuri, and J. Luo, "Activation of Stat3 sequence-specific DNA binding and transcription by p300/CREB-binding protein-mediated acetylation," *Journal of Biological Chemistry*, vol. 280, no. 12, pp. 11528–11534, 2005.

[58] Z.-l. Yuan, Y.-j. Guan, D. Chatterjee, and Y. E. Chin, "Stat3 dimerization regulated by reversible acetylation of

a single lysine residue," *Science*, vol. 307, no. 5707, pp. 269–273, 2005.

[59] H. J. Kang, Y. W. Yi, S.-J. Hou et al., "Disruption of STAT3-DNMT1 interaction by SH-I-14 induces re-expression of tumor suppressor genes and inhibits growth of triple-negative breast tumor," *Oncotarget*, vol. 8, no. 48, pp. 83457–83468, 2017.

[60] K. Suzuki, M. Ogura, Y. Abe et al., "Phase 1 study in Japan of siltuximab, an anti-IL-6 monoclonal antibody, in relapsed/refractory multiple myeloma," *International Journal of Hematology*, vol. 101, no. 3, pp. 286–294, 2015.

[61] R. Z. Orlowski, L. Gercheva, C. Williams et al., "A phase 2, randomized, double-blind, placebo-controlled study of siltuximab (anti-IL-6 mAb) and bortezomib versus bortezomib alone in patients with relapsed or refractory multiple myeloma," *American Journal of Hematology*, vol. 90, no. 1, pp. 42–49, 2015.

[62] P. M. Voorhees, R. F. Manges, P. Sonneveld et al., "A phase 2 multicentre study of siltuximab, an anti-interleukin-6 monoclonal antibody, in patients with relapsed or refractory multiple myeloma," *British Journal of Haematology*, vol. 161, no. 3, pp. 357–366, 2013.

[63] E. M. Dijkgraaf, S. J. A. M. Santegoets, A. K. L. Reyners et al., "A phase I trial combining carboplatin/doxorubicin with tocilizumab, an anti-IL-6R monoclonal antibody, and interferon-α2b in patients with recurrent epithelial ovarian cancer," *Annals of Oncology*, vol. 26, no. 10, pp. 2141–2149, 2015.

[64] J. Karkera, H. Steiner, W. Li et al., "The anti-interleukin-6 antibody siltuximab down-regulates genes implicated in tumorigenesis in prostate cancer patients from a phase I study," *The Prostate*, vol. 71, no. 13, pp. 1455–1465, 2011.

[65] K. Fizazi, J. S. de Bono, A. Flechon et al., "Randomised phase II study of siltuximab (CNTO 328), an anti-IL-6 monoclonal antibody, in combination with mitoxantrone/prednisone versus mitoxantrone/prednisone alone in metastatic castration-resistant prostate cancer," *European Journal of Cancer*, vol. 48, no. 1, pp. 85–93, 2012.

[66] M. Buchert, C. J. Burns, and M. Ernst, "Targeting JAK kinase in solid tumors: emerging opportunities and challenges," *Oncogene*, vol. 35, no. 8, pp. 939–951, 2016.

[67] R. K. Rampal, J. O. Mascarenhas, H. E. Kosiorek et al., "Safety and efficacy of combined ruxolitinib and decitabine in accelerated and blast-phase myeloproliferative neoplasms," *Blood Advances*, vol. 2, no. 24, pp. 3572–3580, 2018.

[68] E. R. Plimack, P. M. LoRusso, P. McCoon et al., "AZD1480: a phase I study of a novel JAK2 inhibitor in solid tumors," *The Oncologist*, vol. 18, no. 7, pp. 819-820, 2013.

[69] T. Murakami, N. Takigawa, T. Ninomiya et al., "Effect of AZD1480 in an epidermal growth factor receptor-driven lung cancer model," *Lung Cancer*, vol. 83, no. 1, pp. 30–36, 2014.

[70] H. D. Brooks, B. S. Glisson, B. N. Bekele et al., "Phase 2 study of dasatinib in the treatment of head and neck squamous cell carcinoma," *Cancer*, vol. 117, no. 10, pp. 2112–2119, 2011.

[71] A. Ferrajoli, S. Faderl, Q. van et al., "WP1066 disrupts Janus kinase-2 and induces caspase-dependent apoptosis in acute myelogenous leukemia cells," *Cancer Research*, vol. 67, no. 23, pp. 11291–11299, 2007.

[72] R. M. Zemek, E. de Jong, W. L. Chin et al., "Sensitization to immune checkpoint blockade through activation of a STAT1/NK axis in the tumor microenvironment," *Science Translational Medicine*, vol. 11, no. 501, article eaav7816, 2019.

[73] L. Jiang, J. Y. Liu, Y. Shi et al., "MTMR2 promotes invasion and metastasis of gastric cancer via inactivating IFNγ/STAT1 signaling," *Journal of Experimental & Clinical Cancer Research*, vol. 38, no. 1, p. 206, 2019.

[74] E. Butturini, D. Boriero, A. Carcereri de Prati, and S. Mariotto, "STAT1 drives M1 microglia activation and neuroinflammation under hypoxia," *Archives of Biochemistry and Biophysics*, vol. 669, pp. 22–30, 2019.

[75] A. E. Koromilas and V. Sexl, "The tumor suppressor function of STAT1 in breast cancer," *JAK-STAT*, vol. 2, no. 2, article e23353, 2013.

[76] J. Turkson, D. Ryan, J. S. Kim et al., "Phosphotyrosyl peptides block Stat3-mediated DNA binding activity, gene regulation, and cell transformation," *Journal of Biological Chemistry*, vol. 276, no. 48, pp. 45443–45455, 2001.

[77] P. K. Mandal, F. Gao, Z. Lu et al., "Phosphotyrosyl peptides block Stat3-mediated DNA binding activity, gene regulation, and cell transformation," *Journal of Medicinal Chemistry*, vol. 54, no. 10, pp. 3549–3563, 2011.

[78] S. Fletcher, J. Singh, X. Zhang et al., "Disruption of transcriptionally active Stat3 dimers with non-phosphorylated, salicylic acid-based small molecules: potent in vitro and tumor cell activities," *ChemBioChem*, vol. 10, no. 12, pp. 1959–1964, 2009.

[79] J. Schust, B. Sperl, A. Hollis, T. U. Mayer, and T. Berg, "Stattic: a small-molecule inhibitor of STAT3 activation and dimerization," *Chemistry & Biology*, vol. 13, no. 11, pp. 1235–1242, 2006.

[80] K. Siddiquee, S. Zhang, W. C. Guida et al., "Selective chemical probe inhibitor of Stat3, identified through structure-based virtual screening, induces antitumor activity," *Proceedings of the National Academy of Sciences of the United States of America*, vol. 104, no. 18, pp. 7391–7396, 2007.

[81] H. Song, R. Wang, S. Wang, and J. Lin, "A low-molecular-weight compound discovered through virtual database screening inhibits Stat3 function in breast cancer cells," *Proceedings of the National Academy of Sciences of the United States of America*, vol. 102, no. 13, pp. 4700–4705, 2005.

[82] B. Fuh, M. Sobo, L. Cen et al., "LLL-3 inhibits STAT3 activity, suppresses glioblastoma cell growth and prolongs survival in a mouse glioblastoma model," *British Journal of Cancer*, vol. 100, no. 1, pp. 106–112, 2009.

[83] J. Turkson, S. Zhang, J. Palmer et al., "Inhibition of constitutive signal transducer and activator of transcription 3 activation by novel platinum complexes with potent antitumor activity," *Molecular Cancer Therapeutics*, vol. 3, no. 12, pp. 1533–1542, 2004.

[84] P. L. Leong, G. A. Andrews, D. E. Johnson et al., "Targeted inhibition of Stat3 with a decoy oligonucleotide abrogates head and neck cancer cell growth," *Proceedings of the National Academy of Sciences of the United States of America*, vol. 100, no. 7, pp. 4138–4143, 2003.

[85] S. Xi, W. E. Gooding, and J. R. Grandis, "In vivo antitumor efficacy of STAT3 blockade using a transcription factor decoy approach: implications for cancer therapy," *Oncogene*, vol. 24, no. 6, pp. 970–979, 2005.

[86] J. Shen, R. Li, and G. Li, "Inhibitory effects of decoy-ODN targeting activated STAT3 on human glioma growth in vivo," *In vivo*, vol. 23, no. 2, pp. 237–243, 2009.

[87] X. Zhang, J. Zhang, L. Wang, H. Wei, and Z. Tian, "Therapeutic effects of STAT3 decoy oligodeoxynucleotide on human lung cancer in xenograft mice," *BMC Cancer*, vol. 7, no. 1, p. 149, 2007.

[88] K. Wang, J. Jiang, Y. Lei, S. Zhou, Y. Wei, and C. Huang, "Targeting metabolic–redox circuits for cancer therapy," *Trends in Biochemical Sciences*, vol. 44, no. 5, pp. 401–414, 2019.

[89] M. Schieber and N. S. Chandel, "ROS function in redox signaling and oxidative stress," *Current Biology*, vol. 24, no. 10, pp. R453–R462, 2014.

[90] R. A. Cairns, I. S. Harris, and T. W. Mak, "Regulation of cancer cell metabolism," *Nature Reviews Cancer*, vol. 11, no. 2, pp. 85–95, 2011.

[91] S. S. Sabharwal and P. T. Schumacker, "Mitochondrial ROS in cancer: initiators, amplifiers or an Achilles' heel?," *Nature Reviews Cancer*, vol. 14, no. 11, pp. 709–721, 2014.

[92] W. Xiao, R. S. Wang, D. E. Handy, and J. Loscalzo, "NAD(H) and NADP(H) redox couples and cellular energy metabolism," *Antioxidants & Redox Signaling*, vol. 28, no. 3, pp. 251–272, 2018.

[93] R. Moreno-Sánchez, J. C. Gallardo-Pérez, S. Rodríguez-Enríquez, E. Saavedra, and Á. Marín-Hernández, "Control of the NADPH supply for oxidative stress handling in cancer cells," *Free Radical Biology & Medicine*, vol. 112, pp. 149–161, 2017.

[94] H. Jurkowska and M. Wróbel, "Cystathionine promotes the proliferation of human astrocytoma U373 cells," *Anticancer Research*, vol. 38, no. 6, pp. 3501–3505, 2018.

[95] J. H. Lee, C. Kim, S. G. Lee, G. Sethi, and K. S. Ahn, "Ophiopogonin D, a steroidal glycoside abrogates STAT3 signaling cascade and exhibits anti-cancer activity by causing GSH/GSSG imbalance in lung carcinoma," *Cancers*, vol. 10, no. 11, p. 427, 2018.

[96] P. Zhang, J. Wu, F. Xiao, D. Zhao, and Y. Luan, "Disulfide bond based polymeric drug carriers for cancer chemotherapy and relevant redox environments in mammals," *Medicinal Research Reviews*, vol. 38, no. 5, pp. 1485–1510, 2018.

[97] M. L. Circu and T. Y. Aw, "Intestinal redox biology and oxidative stress," *Seminars in Cell & Developmental Biology*, vol. 23, no. 7, pp. 729–737, 2012.

[98] L. C. Flores, M. G. Roman, G. M. Cunningham et al., "Continuous overexpression of thioredoxin 1 enhances cancer development and does not extend maximum lifespan in male C57BL/6 mice," *Pathobiology of Aging & Age-Related Diseases*, vol. 8, no. 1, article 1533754, 2018.

[99] B. Haas, L. Schütte, M. Wos-Maganga, S. Weickhardt, M. Timmer, and N. Eckstein, "Thioredoxin confers intrinsic resistance to cytostatic drugs in human glioma cells," *International Journal of Molecular Sciences*, vol. 19, no. 10, p. 2874, 2018.

[100] A. Bansal and M. C. Simon, "Glutathione metabolism in cancer progression and treatment resistance," *Journal of Cell Biology*, vol. 217, no. 7, pp. 2291–2298, 2018.

[101] N. Traverso, R. Ricciarelli, M. Nitti et al., "Role of glutathione in cancer progression and chemoresistance," *Oxidative Medicine and Cellular Longevity*, vol. 2013, Article ID 972913, 10 pages, 2013.

[102] G. Wu, Y. Z. Fang, S. Yang, J. R. Lupton, and N. D. Turner, "Glutathione metabolism and its implications for health," *The Journal of Nutrition*, vol. 134, no. 3, pp. 489–492, 2004.

[103] S. C. Lu, "Regulation of glutathione synthesis," *Molecular Aspects of Medicine*, vol. 30, no. 1-2, pp. 42–59, 2009.

[104] C. Conticello, D. Martinetti, L. Adamo et al., "Disulfiram, an old drug with new potential therapeutic uses for human hematological malignancies," *International Journal of Cancer*, vol. 131, no. 9, pp. 2197–2203, 2012.

[105] A. Tagde, H. Singh, M. H. Kang, and C. P. Reynolds, "The glutathione synthesis inhibitor buthionine sulfoximine synergistically enhanced melphalan activity against preclinical models of multiple myeloma," *Blood Cancer Journal*, vol. 4, no. 7, article e229, 2014.

[106] O. W. Griffith, "Mechanism of action, metabolism, and toxicity of buthionine sulfoximine and its higher homologs, potent inhibitors of glutathione synthesis," *Journal of Biological Chemistry*, vol. 257, pp. 13704–13712, 1982.

[107] M. Lo, V. Ling, C. Low, Y. Z. Wang, and P. W. Gout, "Potential use of the anti-inflammatory drug, sulfasalazine, for targeted therapy of pancreatic cancer," *Current Oncology*, vol. 17, no. 3, pp. 9–16, 2010.

[108] I. Dalle-Donne, A. Milzani, N. Gagliano, R. Colombo, D. Giustarini, and R. Rossi, "Molecular mechanisms and potential clinical significance of *S*-glutathionylation," *Antioxidants & Redox Signaling*, vol. 10, no. 3, pp. 445–474, 2008.

[109] A. Pastore, G. Federici, E. Bertini, and F. Piemonte, "Analysis of glutathione: implication in redox and detoxification," *Clinica Chimica Acta*, vol. 333, no. 1, pp. 19–39, 2003.

[110] F. Q. Schafer and G. R. Buettner, "Redox environment of the cell as viewed through the redox state of the glutathione disulfide/glutathione couple," *Free Radical Biology & Medicine*, vol. 30, no. 11, pp. 1191–1212, 2001.

[111] D. P. Jones, "Redox sensing: orthogonal control in cell cycle and apoptosis signalling," *Journal of Internal Medicine*, vol. 268, no. 5, pp. 432–448, 2010.

[112] J. J. Mieyal, M. M. Gallogly, S. Qanungo, E. A. Sabens, and M. D. Shelton, "Molecular mechanisms and clinical implications of reversible protein *S*-glutathionylation," *Antioxidants & Redox Signaling*, vol. 10, no. 11, pp. 1941–1988, 2008.

[113] R. Sitia and S. N. Molteni, "Stress, protein (mis)folding, and signaling: the redox connection," *Science Signaling*, vol. 2004, no. 239, article pe27, 2004.

[114] J. M. Held and B. W. Gibson, "Regulatory control or oxidative damage? Proteomic approaches to interrogate the role of cysteine oxidation status in biological processes," *Molecular & Cellular Proteomics*, vol. 11, no. 4, 2012.

[115] C. C. Winterbourn and M. B. Hampton, "Thiol chemistry and specificity in redox signaling," *Free Radical Biology & Medicine*, vol. 45, no. 5, pp. 549–561, 2008.

[116] M. Carballo, M. Conde, R. el Bekay et al., "Oxidative stress triggers STAT3 tyrosine phosphorylation and nuclear translocation in human lymphocytes," *Journal of Biological Chemistry*, vol. 274, no. 25, pp. 17580–17586, 1999.

[117] Y. Qu, A. M. Oyan, R. Liu et al., "Generation of prostate tumor–initiating cells is associated with elevation of reactive oxygen species and IL-6/STAT3 signaling," *Cancer Research*, vol. 73, no. 23, pp. 7090–7100, 2013.

[118] L. Li, S. H. Cheung, E. L. Evans, and P. E. Shaw, "Modulation of gene expression and tumor cell growth by redox modification of STAT3," *Cancer Research*, vol. 70, no. 20, pp. 8222–8232, 2010.

[119] J. I. Kim, S. H. Choi, K. J. Jung, E. Lee, H. Y. Kim, and K. M. Park, "Protective role of methionine sulfoxide reductase A

against ischemia/reperfusion injury in mouse kidney and its involvement in the regulation of trans-sulfuration pathway," *Antioxidants & Redox Signaling*, vol. 18, no. 17, pp. 2241–2250, 2013.

[120] A. R. Simon, U. Rai, B. L. Fanburg, and B. H. Cochran, "Activation of the JAK-STAT pathway by reactive oxygen species," *American Journal of Physiology-Cell Physiology*, vol. 275, no. 6, pp. C1640–C1652, 1998.

[121] G. Waris, K. W. Huh, and A. Siddiqui, "Mitochondrially associated hepatitis B virus X protein constitutively activates transcription factors STAT-3 and NF-κB via oxidative stress," *Molecular and Cellular Biology*, vol. 21, no. 22, pp. 7721–7730, 2001.

[122] C. Zgheib, M. Kurdi, F. A. Zouein et al., "Acyloxy nitroso compounds inhibit LIF signaling in endothelial cells and cardiac myocytes: evidence that STAT3 signaling is redox-sensitive," *PLoS One*, vol. 7, no. 8, article e43313, 2012.

[123] E. Butturini, E. Darra, G. Chiavegato et al., "S-Glutathionylation at Cys328 and Cys542 impairs STAT3 phosphorylation," *ACS Chemical Biology*, vol. 9, no. 8, pp. 1885–1893, 2014.

[124] E. Butturini, F. Cozzolino, D. Boriero et al., "S-Glutathionylation exerts opposing roles in the regulation of STAT1 and STAT3 signaling in reactive microglia," *Free Radical Biology & Medicine*, vol. 117, pp. 191–201, 2018.

[125] Y. Xie, S. Kole, P. Precht, M. J. Pazin, and M. Bernier, "S-Glutathionylation impairs signal transducer and activator of transcription 3 activation and signaling," *Endocrinology*, vol. 150, no. 3, pp. 1122–1131, 2009.

[126] E. Butturini, E. Cavalieri, A. Carcereri de Prati et al., "Two naturally occurring terpenes, dehydrocostuslactone and costunolide, decrease intracellular GSH content and inhibit STAT3 activation," *PLoS One*, vol. 6, no. 5, article e20174, 2011.

[127] E. Butturini, A. Carcereri de Prati, G. Chiavegato et al., "Mild oxidative stress induces S-glutathionylation of STAT3 and enhances chemosensitivity of tumoural cells to chemotherapeutic drugs," *Free Radical Biology & Medicine*, vol. 65, pp. 1322–1330, 2013.

[128] E. Butturini and D. Boriero, "Carcereri de Prati A., Mariotto S., Immunoprecipitation methods to identify S-glutathionylation in target proteins," *MethosX*, vol. 6, pp. 1992–1998, 2019.

[129] J. Y. Cho, K. U. Baik, J. H. Jung, and M. H. Park, "In vitro anti-inflammatory effects of cynaropicrin, a sesquiterpene lactone, from *Saussurea lappa*," *European Journal of Pharmacology*, vol. 398, no. 3, pp. 399–407, 2000.

[130] A. Bachelier, R. Mayer, and C. D. Klein, "Sesquiterpene lactones are potent and irreversible inhibitors of the antibacterial target enzyme MurA," *Bioorganic & Medicinal Chemistry Letters*, vol. 16, no. 21, pp. 5605–5609, 2006.

[131] J. Y. Cho, A. R. Kim, H. G. Joo et al., "Cynaropicrin, a sesquiterpene lactone, as a new strong regulator of CD29 and CD98 functions," *Biochemical and Biophysical Research Communications*, vol. 313, no. 4, pp. 954–961, 2004.

[132] J. Wen, K. R. You, S. Y. Lee, C. H. Song, and D. G. Kim, "Oxidative stress-mediated apoptosis," *Journal of Biological Chemistry*, vol. 277, no. 41, pp. 38954–38964, 2002.

[133] M. Khan, C. Ding, A. Rasul et al., "Isoalantolactone induces reactive oxygen species mediated apoptosis in pancreatic carcinoma PANC-1 cells," *International Journal of Biological Sciences*, vol. 8, no. 4, pp. 533–547, 2012.

[134] S. Zhang, Y. K. Won, C. N. Ong, and H. M. Shen, "Anti-cancer potential of sesquiterpene lactones: bioactivity and molecular mechanisms," *Current Medicinal Chemistry-Anti-Cancer Agents*, vol. 5, no. 3, pp. 239–249, 2005.

[135] J. Heilmann, M. R. Wasescha, and T. J. Schmidt, "The influence of glutathione and cysteine levels on the cytotoxicity of helenanolide type sesquiterpene lactones against KB cells," *Bioorganic & Medicinal Chemistry*, vol. 9, no. 8, pp. 2189–2194, 2001.

[136] D. W. Knight, "Feverfew: chemistry and biological activity," *Natural Product Reports*, vol. 12, no. 3, pp. 271–276, 1995.

[137] A. Ghantous, H. Gali-Muhtasib, H. Vuorela, N. A. Saliba, and N. Darwiche, "What made sesquiterpene lactones reach cancer clinical trials?," *Drug Discovery Today*, vol. 15, no. 15-16, pp. 668–678, 2010.

[138] M. Chadwick, H. Trewin, F. Gawthrop, and C. Wagstaff, "Sesquiterpenoids lactones: benefits to plants and people," *International Journal of Molecular Sciences*, vol. 14, no. 6, pp. 12780–12805, 2013.

[139] A. Maryam, T. Mehmood, H. Zhang, Y. Li, M. Khan, and T. Ma, "Alantolactone induces apoptosis, promotes STAT3 glutathionylation and enhances chemosensitivity of A549 lung adenocarcinoma cells to doxorubicin via oxidative stress," *Scientific Reports*, vol. 7, no. 1, p. 6242, 2017.

[140] M. Khan, T. Li, M. K. Ahmad Khan et al., "Alantolactone induces apoptosis in HepG2 cells through GSH depletion, inhibition of STAT3 activation, and mitochondrial dysfunction," *BioMed Research International*, vol. 2013, Article ID 719858, 11 pages, 2013.

[141] L. Cui, W. Bu, J. Song et al., "Apoptosis induction by alantolactone in breast cancer MDA-MB-231 cells through reactive oxygen species-mediated mitochondrion-dependent pathway," *Archives of Pharmacal Research*, vol. 41, no. 3, pp. 299–313, 2018.

[142] H. Zheng, L. Yang, Y. Kang et al., "Alantolactone sensitizes human pancreatic cancer cells to EGFR inhibitors through the inhibition of STAT3 signaling," *Molecular Carcinogenesis*, vol. 58, no. 4, pp. 565–576, 2019.

[143] T. Mehmood, A. Maryam, X. Tian, M. Khan, and T. Ma, "Santamarine inhibits NF-κB and STAT3 activation and induces apoptosis in HepG2 liver cancer cells via oxidative stress," *Journal of Cancer*, vol. 8, no. 18, pp. 3707–3717, 2017.

[144] H. Li, H. Lu, M. Lv, Q. Wang, and Y. Sun, "Parthenolide facilitates apoptosis and reverses drug-resistance of human gastric carcinoma cells by inhibiting the STAT3 signaling pathway," *Oncology Letters*, vol. 15, no. 3, pp. 3572–3579, 2018.

[145] M. Liu, C. Xiao, M. Sun, M. Tan, L. Hu, and Q. Yu, "Parthenolide inhibits STAT3 signaling by covalently targeting Janus kinases," *Molecules*, vol. 23, no. 6, p. 1478, 2018.

[146] X. Y. Fang, H. Zhang, L. Zhao et al., "A new xanthatin analogue 1β-hydroxyl-5α-chloro-8-epi-xanthatin induces apoptosis through ROS-mediated ERK/p38 MAPK activation and JAK2/STAT3 inhibition in human hepatocellular carcinoma," *Biochimie*, vol. 152, pp. 43–52, 2018.

[147] M. Li, L. H. Song, G. G. L. Yue et al., "Bigelovin triggered apoptosis in colorectal cancer in vitro and in vivo via upregulating death receptor 5 and reactive oxidative species," *Scientific Reports*, vol. 7, no. 1, article 42176, 2017.

[148] M. Li, G. G. L. Yue, L. H. Song et al., "Natural small molecule bigelovin suppresses orthotopic colorectal tumor growth and

inhibits colorectal cancer metastasis via IL6/STAT3 pathway," *Biochemical Pharmacology*, vol. 150, pp. 191–201, 2018.

[149] P. L. Kuo, W. C. Ni, E. M. Tsai, and Y. L. Hsu, "Dehydrocostuslactone disrupts signal transducers and activators of transcription 3 through up-regulation of suppressor of cytokine signaling in breast cancer cells," *Molecular Cancer Therapeutics*, vol. 8, no. 5, pp. 1328–1339, 2009.

[150] H. Cai, X. Qin, and C. Yang, "Dehydrocostus lactone suppresses proliferation of human chronic myeloid leukemia cells through Bcr/Abl-JAK/STAT signaling pathways," *Journal of Cellular Biochemistry*, vol. 118, no. 10, pp. 3381–3390, 2017.

[151] F. A. Kabeer, D. S. Rajalekshmi, M. S. Nair, and R. Prathapan, "Molecular mechanisms of anticancer activity of deoxyelephantopin in cancer cells," *Integrative Medicine Research*, vol. 6, no. 2, pp. 190–206, 2017.

[152] J. H. Feng, K. Nakagawa-Goto, K. H. Lee, and L. F. Shyur, "A novel plant sesquiterpene lactone derivative, DETD-35, suppresses $BRAF^{V600E}$ mutant melanoma growth and overcomes acquired vemurafenib resistance in mice," *Molecular Cancer Therapeutics*, vol. 15, no. 6, pp. 1163–1176, 2016.

[153] X. Cheng, Y. Q. Liu, G. Z. Wang et al., "Proteomic identification of the oncoprotein STAT3 as a target of a novel Skp1 inhibitor," *Oncotarget*, vol. 8, no. 2, pp. 2681–2693, 2017.

[154] Y. Liu, X. Q. Chen, H. X. Liang et al., "Small compound 6-O-angeloylplenolin induces mitotic arrest and exhibits therapeutic potentials in multiple myeloma," *PLoS One*, vol. 6, no. 7, article e21930, 2011.

[155] C. T. Yeh, W. C. Huang, Y. K. Rao et al., "A sesquiterpene lactone antrocin from *Antrodia camphorata* negatively modulates JAK2/STAT3 signaling via microRNA let-7c and induces apoptosis in lung cancer cells," *Carcinogenesis*, vol. 34, no. 12, pp. 2918–2928, 2013.

Hindawi
Oxidative Medicine and Cellular Longevity
Volume 2019, Article ID 8127362, 11 pages
https://doi.org/10.1155/2019/8127362

Review Article

Emerging Perspective: Role of Increased ROS and Redox Imbalance in Skin Carcinogenesis

Dehai Xian,[1] Rui Lai,[2] Jing Song,[2] Xia Xiong,[2] and Jianqiao Zhong[2]

[1]*Department of Anatomy, Southwest Medical University, Luzhou 646000, China*
[2]*Department of Dermatology, The Affiliated Hospital of Southwest Medical University, Luzhou 646000, China*

Correspondence should be addressed to Jianqiao Zhong; zjq7632@hotmail.com

Received 18 April 2019; Revised 25 June 2019; Accepted 31 July 2019; Published 16 September 2019

Academic Editor: Mithun Sinha

Strategies to battle malignant tumors have always been a dynamic research endeavour. Although various vehicles (e.g., chemotherapeutic therapy, radiotherapy, surgical resection, etc.) are used for skin cancer management, they mostly remain unsatisfactory due to the complex mechanism of carcinogenesis. Increasing evidence indicates that redox imbalance and aberrant reactive oxygen species (ROS) are closely implicated in the oncogenesis of skin cancer. When ROS production goes beyond their clearance, excessive or accumulated ROS could disrupt redox balance, induce oxidative stress, and activate the altered ROS signals. These would damage cellular DNA, proteins, and lipids, further leading to gene mutation, cell hyperproliferation, and fatal lesions in cells that contribute to carcinogenesis in the skin. It has been known that ROS-mediated skin carcinogenesis involves multiple ways, including modulating related signaling pathways, changing cell metabolism, and causing the instability of the genome and epigenome. Nevertheless, the exact role of ROS in skin cancer has not been thoroughly elucidated. In spite of ROS inducing skin carcinogenesis, toxic-dose ROS could trigger cell death/apoptosis and, therefore, may be an efficient therapeutic tool to battle skin cancer. Considering the dual role of ROS in the carcinogenesis and treatment of skin cancer, it would be essential to clarify the relationship between ROS and skin cancer. Thus, in this review, we get the related data together to seek the connection between ROS and skin carcinogenesis. Besides, strategies basing on ROS to fight skin cancer are discussed.

1. Introduction

Skin cancer is the most common type of cancer, and its incidence has gradually increased in recent years [1]. It is characterized by aberrant cell growth with a potential to invade or spread elsewhere in the body, which involves the complex process of carcinogenesis [2]. At present, the main types of skin cancer are melanoma and nonmelanoma skin cancer (NMSC), while the latter includes basal cell carcinoma (BCC) and squamous cell carcinoma (SCC). Ultraviolet (UV) exposure is one of the main factors inducing skin cancer, and cutaneous cells may be damaged directly by UV radiation or indirectly by UV-mediated reactive oxygen species (ROS) overproduction [3]. Long-term UV radiation could cause photochemical reactions or/and oxidative DNA damage, induce DNA mutation and misexpression, and trigger skin carcinogenesis [4]. UV irradiation induces the skin to produce substantial ROS, which results in nuclear DNA damage via forming a large amount of cyclobutane pyrimidine dimers (CPDs), pyrimidine (6-4), pyrimidone photoproducts, and 8-oxodG [5]. 8-oxodG, a biomarker of oxidative damage to DNA, could be removed from the damaged DNA by the enzyme human 8-oxoguanine-DNA glycosylase 1 (hOGG1). In the study, it was shown that UVB-induced ROS triggered 8-oxoguanine (8-oxoG) production and hOGG1 reduction in the skin, further damaging the DNA repair pathway, and eventually initiating cutaneous carcinogenesis [6, 7].

ROS belong to oxygen-derived small molecules including oxygen-centered radical species (e.g., superoxide ($O_2^{\bullet-}$), hydroxyl ($^{\bullet}OH$), peroxyl ($R\text{-}O_2^{\bullet}$), and alkoxyl ($RO^{\bullet}$)) and nonradical compounds that are either oxidizing agents or

easily converted into radicals, such as hypochlorous acid (HOCl), ozone (O_3), singlet oxygen ($^1O_2$), and hydrogen peroxide (H_2O_2) [8]. ROS are one of the normal products of physiological metabolism and are mainly derived from endogenous and exogenous sources [9]. Endogenous sources are primarily produced by complex I and complex III in the oxidative respiratory electron transport chain (ETC) of mitochondria [10]. Some also originate from enzymes, including NADPH-oxidases (NOXs), lipoxygenases, xanthine oxidases, nitric oxide synthases, and cytochrome p450 enzymes [11]. Apart from the previously mentioned sources, environmental stress (e.g., chemical substances, drugs, UV radiation, ionizing radiation (IR), and hypoxia) could induce ROS production. Under physiological conditions, ROS production and scavenging are in a dynamic equilibrium and the body is in a redox homeostasis at the presence of the antioxidant defense system, which is vital to normal physiological response [12]. The antioxidant defense system mainly includes an enzymatic antioxidant system (e.g., superoxide dismutase (SOD), glutathione peroxidase (GSH-Px), catalase (CAT), thioredoxin (TRX), and peroxiredoxin) and a nonenzymatic one (e.g., tripeptide glutathione (GSH), vitamins (vitamins C and E), β-carotene, and uric acid) [13]. Through these two antioxidant systems, oxygen radicals and nonradicals ($O_2^{\bullet-}$, $^{\bullet}OH$, H_2O_2, etc.) could be converted into H_2O and eventually into O_2 [14, 15].

ROS importantly work in the physiology of the skin. As the first barrier of body, the skin protects the body against various harmful factors like pathogens, physical factors, and chemical drugs. At a low level, ROS are beneficial to maintain normal metabolism and cell growth through mediating a variety of signal transduction pathways as a second messenger [16]. They are quite essential for skin physiological processes such as cutaneous cell proliferation, dermal angiogenesis, wound healing, and skin repair [17]. Nevertheless, high-level ROS produced by various external factors (e.g., chemical toxicants, UV, IR, and pathogen infection) or internal factors (e.g., ischemia/reperfusion, inflammation, and hypoxia) would disrupt redox homeostasis in the skin, further trigger severe oxidative stress, and then cause cell membrane lipid peroxidation, eventually resulting in DNA/-cell damage or variation and even carcinogenesis [18]. These may encourage cutaneous lesion appearance and tumor growth in the skin, such as melanoma, BCC, and SCC [19]. It is confirmed that ROS participate in carcinogenesis in various ways like modulating related signaling pathways, changing cell metabolism, and causing the instability of the genome and epigenome [20, 21]. However, the role of ROS in skin cancer has not been completely clarified. In addition, it is reported that a super high dose of ROS could fight cancer basing on ROS inducing cell death/apoptosis, which indicates that ROS would be a potential target of anticancer therapy. The effects of different concentrations of ROS on cells are summarized in Figure 1. Herein, we review the recent data about ROS and skin cancer to elucidate the role of ROS in carcinogenesis and their correlation. Moreover, treatments based on ROS for skin cancer, including chemotherapy, phototherapy, radiotherapy, and dietary antioxidants, are also discussed.

2. Role of ROS in Carcinogenesis

There are two ways for ROS to work in carcinogenesis: genotoxicity and nongenotoxicity. The former is chiefly about genotoxic substance-induced direct DNA damage, which may cause protooncogene activation, tumor suppressor gene inactivation, genomic instability, and epigenetic modifications, further leading to mutations. The latter has an indirect effect on DNA through the activation of related signaling pathways. The following are the details that ROS mediate in cancer, skin cancer in particular, through these two ways.

2.1. ROS-Mediated Genotoxicity in Carcinogenesis

2.1.1. Genomic Instability. As one of the most potent DNA-damaging agents, ROS induce genomic instability in numerous ways. ROS, derived from mitochondrial respiratory chain complex III, greatly encourage DNA oxidative damage, not only destroying DNA bases to generate 7,8-dihydro-8-oxo-2′-deoxyguanosine (8-oxodG) but also producing spontaneous DNA double-strand breaks (DSBs), ultimately resulting in chromosomal aberrations and the accumulation of tyrosine kinase inhibitor-resistant BCR-ABL1 mutants [22]. Weyemi et al. in their reports showed that ROS-produced NOX4 played a critical role in oncogenic Ras-induced DNA damage. H-Ras continuously stimulated the overexpression of NOX4 and its functional partner $p22^{phox}$, and thereby produced a large amount of H_2O_2 which would induce DNA damage and initiate carcinogenesis [23]. By activating the expression of Ras and c-Myc oncogenes, ROS promote cancer progression and invasion; Ras in turn induces ROS overproduction [24]. Recent studies revealed that NOX-derived ROS were largely responsible for the development of melanoma; NOX1/NOX4-induced ROS could trigger the invasion of melanoma through enhancing Rac1 expression, participating in the epithelial-mesenchymal transition (EMT) process, and activating the downstream signals of the AKT pathway [25]. Aydin et al. meanwhile reported that NOX2-derived ROS encouraged metastasis of melanoma cells via diminishing the effects of NK cells and lymphocytes [26]. Similarly, NOX5-derived ROS elevated the proliferation of human UACC-257 melanoma cells via stimulating HIF-1α expression, further enhancing new blood vessel formation and accelerating the growth and invasion of tumors [27]. Moreover, endogenous estrogen metabolite-produced ROS could cause oxidative damage and DSB production, which induce antioncogene BRCA1 mutations and prevent DNA damage repair, eventually encouraging genomic instability and tumorigenesis [28]. Normally, the tumor suppressor gene p53 plays crucial roles in DNA damage repair, cell growth/apoptosis, and tumorigenesis inhibition; however, ROS-induced mutations in p53 may spoil these functions and promote carcinogenesis including skin cancer, lung cancer, gastric cancer, and colon cancer [29–31].

2.1.2. Epigenetic Changes. On the other hand, ROS-induced epigenetic instability/modification also plays an important part in carcinogenesis via the genotoxicity way. The ROS-induced epigenetic modification often manifests as a global hypomethylation of the genome and an abnormal

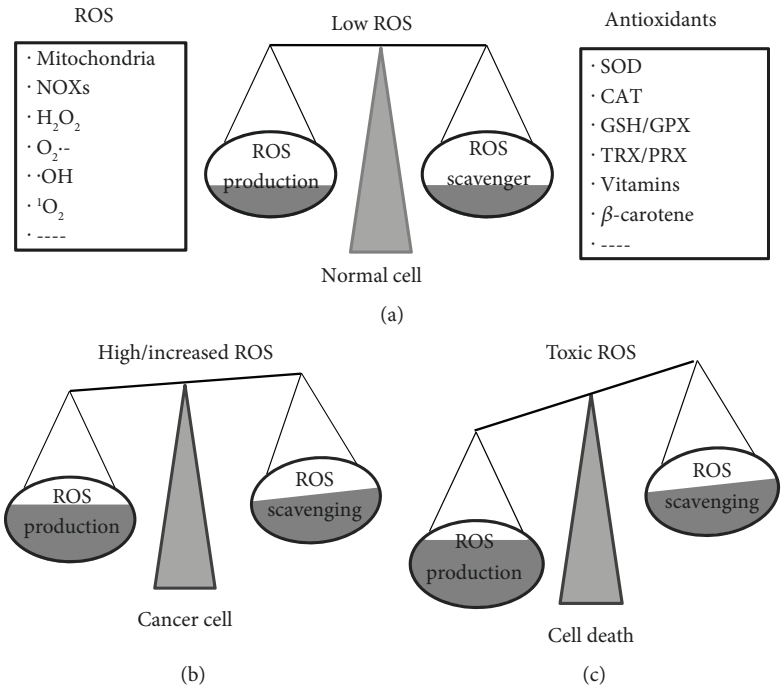

Figure 1: The effects of different concentrations of ROS on cells. (a) ROS, derived from mitochondria, NOXs, etc., mainly contain H_2O_2, $O_2^{\bullet-}$, $^{\bullet}OH$, and others. Scavenging involves the antioxidation system, such as SOD, CAT, TRX/PRX, and vitamins. Low doses of ROS production and scavenging are in a dynamic equilibrium, which is beneficial to the physiological function of normal cells. (b) High-level ROS encourage cell variation and conversion into malignant cells. The production of ROS and antioxidation ability in tumor cells are both increased in various degrees, but cancer cells tend to be in a higher oxidation environment. (c) Toxic-dose ROS cause cell death or apoptosis and is also the killer of cancer cells.

hypermethylation in the CpG island region of some genes. ROS could promote DNA methylation to result in the silence of the tumor suppressor gene and the activation of oncogene by upregulating the expression of DNA methyltransferases (DNMTs) or by forming a new DNMT-containing complex [32]. For example, H_2O_2 powerfully induced the hypermethylation of CDX1 or runt domain transcription factor 3 (RUNX3) promoter and silenced these genes in colorectal cancer, which indicated that ROS could promote cancer cell proliferation by inducing tumor inhibitor gene silence [33, 34]. As the main scavenger of ROS, glutathione peroxidase 3 (GPX3) is considered to be a potent tumor suppressor in many cancers; nevertheless, GPX3 promoter hypermethylation could stop its antioxidant function in clear cell renal cell carcinoma (ccRCC), which indicates that the failure of the antioxidant system in ccRCC cells may be related to renal carcinogenesis [35]. Furthermore, ROS could promote carcinogenesis through mediating histone modifications or interfering microRNA (miRNA) dysregulation. Gene activation or inhibition caused by ROS-mediated histone modification depends on the modified amino acid residues, and histone acetylation modification is mainly coordinated by histone acetyltransferase (HAT) and histone deacetylase (HDAC), while the level of histone acetylation is always low in cancer cells; especially, the hypomethylation of histone H3K9 leads to melanoma epigenetic instability [36]. Besides, ROS-induced miRNA (such as miR-125b) dysregulation is closely implicated in skin carcinogenesis via interfering with the normal activities of key genes [37].

2.2. ROS-Mediated Nongenotoxicity in Carcinogenesis: Abnormal Activation of Cellular Signaling Pathways. Moderate-dose ROS like $O_2^{\bullet-}$ and H_2O_2 facilitate the abnormal proliferation, metastasis, and infiltration of various tumor cells through activating multiple pathways including oxidative stress-related pathways and antioxidant stress pathways, such as the mitogen activated-protein kinase (MAPK) pathway, the phosphoinositide-3-kinase (PI3K)/protein kinase B (PKB or AKT)/mammalian target of rapamycin (mTOR) pathway, the nuclear factor-κB (NF-κB) pathway, and the nuclear factor erythroid 2-related factor 2 (Nrf2) pathway [38]. First, the MAPK signal pathway, consisting of the extracellular-regulated kinase (ERK), the c-Jun N-terminal kinase (JNK), and the p38 kinase isoenzyme, effectively works in mitosis, metabolism, cell proliferation, and growth, as well as apoptosis [39]. In many studies, it has been observed that elevated ROS could activate the MAPK/ERK signaling pathway and enhance the proliferation, invasion, and metastasis of tumor cells [40, 41]; most melanoma patients carried BRAF gene mutations, which might activate the MAPK/ERK signaling pathway, further promoting tumor cell proliferation through regulating the downstream signals, and ultimately leading to tumorigenesis and even tumor progression [42]. Second, the PI3K/AKT/mTOR pathway, as a classic signaling pathway, widely exists in cells to promote cell survival, inhibit apoptosis, and prevent autophagy; this pathway is overactivated in various tumor tissues and facilitates carcinogenesis and angiogenesis [43, 44]. ROS are able to activate the PI3K/AKT/mTOR pathway and mediate the

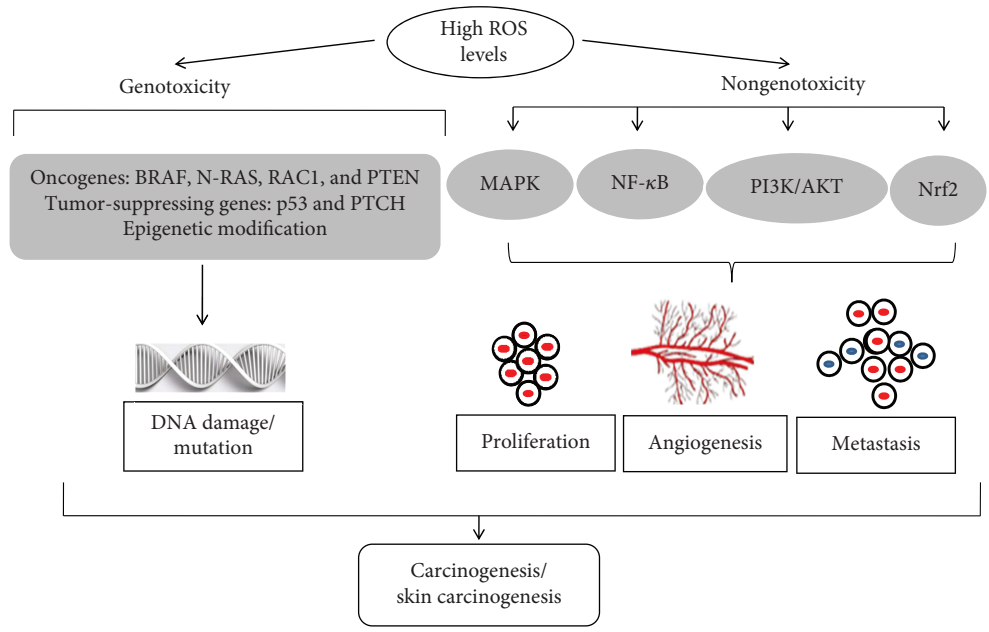

Figure 2: ROS crucially mediates in carcinogenesis/skin carcinogenesis. High/increased levels of ROS benefit carcinogenesis, especially the development and progression of skin cancer including melanoma, SCC, and BCC. On the one hand, they activate protooncogenes (BRAF, N-Ras, RAC1, PTEN, etc.), inactivate tumor suppressor genes (p53, PTCH, etc.), and cause epigenetic modification. These changes lead to DNA damage and mutation resulting in skin carcinogenesis in a genotoxic way. On the other hand, they trigger cancer in a nongenotoxic way, namely, through the activation of related signaling pathways, such as MAPK, NF-κB, PI3K/AKT/mTOR, and Nrf2. The activation of these signaling pathways leads to the proliferation, angiogenesis, and metastasis of skin cancer cells. Together, these processes cause the occurrence of carcinogenesis/skin carcinogenesis.

proliferation and migration of tumor cells [45]. Indeed, ROS enhance the proliferation of melanoma cells via stimulating the PI3K/AKT pathway that interacts with the MAPK pathway [46]. Third, the NF-κB signaling pathway is greatly activated by increased ROS in cancer cells and has a large influence on carcinogenesis [47]. Accumulating findings indicate that NF-κB target genes remarkably benefit cellular survival. It has been shown that ROS could activate the NF-κB signal pathway to promote the angiogenesis and progression of melanoma [48, 49]. On the contrary, the metastatic activity of malignant cells would significantly decrease when ROS-mediated NF-κB activation was suppressed [50]. Fourth, Nrf2 has a dual effect of antitumorigenesis and protumorigenesis in different stages [51]. In the early stage of UV-induced skin carcinogenesis, Nrf2 activation promotes the proliferation of normal cells which greatly outnumbers precancerous cells, and prevents precancerous cell expansion and mutant transformation. Inversely in the late stage, Nrf2 activation is quite beneficial to precancerous/cancerous cell survival, due to oncogene mutations providing higher proliferation and viability for these cells via upregulating Nrf2 expression [52]. On one hand, Nrf2 facilitates carcinogenesis and cancer cell growth/proliferation; numerous studies have demonstrated that Nrf2 highly expresses in a variety of cancer cells and promotes ROS detoxification and tumorigenesis [53–55]. Meanwhile, ROS-related Nrf2 activation of macrophages increased vascular endothelial growth factor (VEGF) expression and facilitated cancer cell EMT [56]. Another study showed that the activated Nrf2 positively worked in skin tumor by protecting the protumorigenic activity of keratinocytes from ROS-induced damage and apoptosis [57]. On the other hand, Nrf2 has an antitumorigenesis effect. The decreased Nrf2 spoils the impaired antioxidant defense system, which may increase the incidence of skin cancer including melanoma, SCC, and BCC [58]. Similarly, Nrf2 knockout mice were more susceptible to SCC than controls [59]. More importantly, it has been demonstrated that Nrf2 knockout mice could be subjected to persistent DNA damage, substantial extracellular matrix degradation, and serious inflammation; inversely, the activation of Nrf2 benefited the prevention of skin carcinogenesis in Nrf2 knockout mice [60]. Therefore, the activation of Nrf2 would be a promising strategy for the treatment and prevention of skin carcinogenesis by improving antioxidant capacity to protect cells from oxidative damage. Many Nrf2-activating compounds are beneficial to the prevention of skin cancer, and they contain curcumin, quercetin, and resveratrol [61]. Besides, other redox signaling pathways are implicated in carcinogenesis and tumor development, containing Wnt/β-catenin, TGF-β/Smad, etc. [62, 63]. Figure 2 sketches the role of ROS in carcinogenesis, especially in skin carcinogenesis.

3. Relationship between ROS and Skin Cancer

ROS could promote cutaneous carcinogenesis and cancer progression by mediating related pathways. But until now, the mechanism of ROS influencing skin cancer has not been completely clarified and only part of them have been explored. Herein, we endeavour to elucidate the relationship between ROS and skin cancer basing on the related data.

Melanoma, derived from melanocytes, is a highly invasive tumor with the incidence increasing yearly [64]. Excessive UV exposure is a crucial susceptibility factor, and UV-produced substantial ROS contribute to nuclear DNA damage. ROS not only trigger the occurrence and development of melanoma by way of genotoxicity and some specific signaling pathway activation but they also cause oncogene activation or tumor-suppressing gene inactivation in melanoma consisting of BRAF, c-Myc, p53, and Ras genes. N-Ras is upstream of the MAPK pathway, and its mutation commonly occurs in melanoma, which contributes to cancer cell proliferation [65]. Moreover, ROS also drive the stable expression of HIF-1α to activate the Met protooncogene, which facilitates the proliferation of the extracellular matrix, angiogenesis, and the proliferation and metastasis of melanoma cells [66]. Other oncogenes, RAC1 in particular, are associated with an increased risk of melanoma [67]. The activation of RAC1 depends on the levels of ROS and determines the ability of the migration and invasion of B16 melanoma cells which could be weakened by the suppression of ROS-mediated Rac-1 activation [68]. Apart from the abovementioned factors, other signaling pathways especially the PI3K/AKT pathway and NF-κB are implicated in the initiation and progression of melanoma [69]. Therefore, ROS are crucially responsible for the occurrence and development of melanoma through inducing related gene mutations and activating a serial of signaling pathways [70]. However, too much ROS generation would encourage apoptosis, which may become a useful vehicle to kill melanoma cells. Subsequently, these will be discussed in the follow-up part of treatments.

Originating from the basal cells near the epidermis-dermis junction, BCC primarily occurs in middle-aged and elderly people, and its lesions mostly appear in exposed areas such as the head, face, and neck. Many factors (e.g., UV, some harmful chemicals, and IR) may trigger BCC initiation, among which UV exposure is a particularly important one [71]. UV-induced ROS could promote the occurrence and development of BCC by generating 8-oxoG and reducing hOGG1 [6]. The imbalance of ROS would encourage skin inflammation, abnormal metabolism, and decreased immunity, which eventually leads to cell mutation and carcinogenesis. Compared with control individuals, there was a high level of MDA in BCC patients, with a reduction of antioxidant components, which enhanced the occurrence of BCC [72]. In the same way, the expression of oxidative DNA damage product 8-oxoG increased, while the levels of antioxidation defenses (e.g., hOGG1, CAT, GPx, and Nrf2) decreased in BCC tissues [73]. UV radiation and oxidative stress facilitate the membrane receptor PTCH gene mutations, which would result in abnormal activation of the hedgehog signaling pathway; in turn, PTCH gene activation and the abnormal activation of the hedgehog signaling pathway are closely involved in the pathogenesis of BCC [74].

As an extremely common type of skin cancer, SCC is derived from keratinocytes and attacks the upper layer of the skin. Excessive UV exposure is a main causative factor for SCC, and UV-induced ROS play a crucial role in carcinogenesis and in the promotion of SCC, while ROS-mediated oxidative stress exacerbates the oxidative damage of DNA, protein, and lipid, further magnifying the progression and invasion of SCC [75, 76]. UV-produced ROS in skin always act as an essential role in inducing p53 mutation. As a tumor suppressor protein, p53 conserves genome stability, maintains normal cell growth, and prevents cell malignant transformation. Once DNA is damaged, p53 would accelerate DNA replication and repair by activating DNA repair proteins, prevent cell growth from arresting the cell cycle, and initiate programmed cell death if DNA damage is irreparable [77]. In humans, *TP53* is the major gene encoding p53, and its mutational inactivation most frequently occurs in skin cancers, e.g., SCC and BCC, especially in SCC [78]. Liu et al. discovered that in the absence of p53 function, inhibition of p38α MAPK activity enhanced A431 SCC cell proliferation and drove UV-induced skin carcinogenesis in $p53^{-/-}$/SKH-1 mice, which was closely associated with increased ROS/NOX2 as well as aberrant p53 [79]. In addition, accumulative ROS could induce *PTEN* gene mutation and inactivation in oxidative damage-related skin cancers, SCC in particular. *PTEN*, a tumor suppressor gene, negatively regulates the PI3K/AKT pathway and often undergoes mutations, deletions, or silencing in many cancers [80]. Ming et al. showed that *PTEN* expression markedly decreased in SCC, suggesting a critical effect of *PTEN* in skin carcinogenesis and skin cancer procession [81].

4. Treatments for Skin Cancer Targeting ROS

There are many therapies for skin cancer, including surgery, chemotherapy, radiotherapy, photodynamic therapy (PDT), and molecular targeting therapy, etc., among which surgery is the most common and important one [82]. Nevertheless, numerous studies have shown that higher-level ROS and redox imbalance often emerge from cancer cells, which could cause multidrug resistance (MDR) and immunosuppression of cancer cells and thereby make it quite difficult to control tumors [83]. At the same time, when the skin cancer occurs at a special site, or the lesions are too large or many to operate, or the patient is too old to tolerate surgery, or distant metastasis of tumors occurs, other medical approaches such as radiotherapy, PDT, and/or chemotherapy may be better alternatives [84]. Given that ROS play an important role in promoting skin cancer, many ROS-targeted treatments would be well developed (shown in Figure 3).

4.1. Medical Treatments for Skin Cancer Basing on ROS. Skin cancer cells have a higher oxidative environment, and ROS have a double effect on cutaneous carcinoma. On the one hand, reducing ROS production contributes to inhibiting skin cancer; but on the other hand, diminishing antioxidant enzymes may enhance toxic-dose ROS production and weaken the body's antioxidant defense, eventually inducing cancer cell death. Thus, more and more ROS-targeted therapies/drugs have been discovered in recent years.

Related researches have shown that celecoxib combined with 5-fluorouracil (5-FU) could suppress the phosphorylation of AKT to reduce the proliferation of SCC cells via producing a large amount of ROS in a dose-dependent manner.

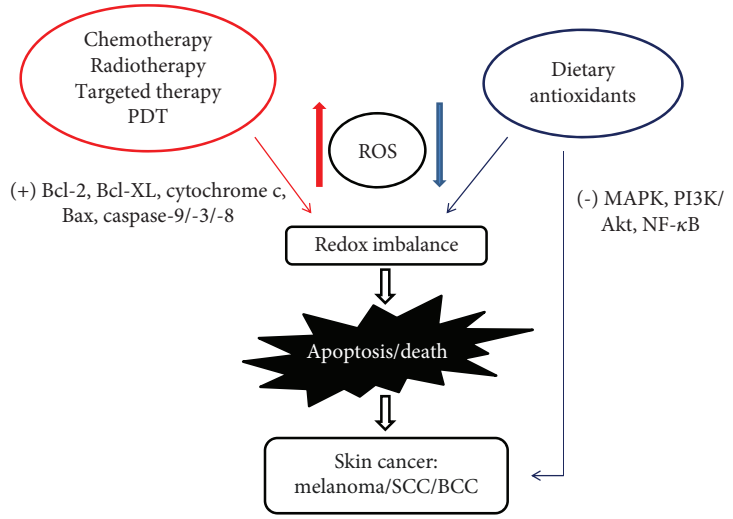

Figure 3: Therapies for skin cancer basing on ROS. There are many treatments for skin cancer in a ROS-targeted way, including chemotherapy, radiotherapy, targeted therapy, and PDT. These therapies cause toxic-dose ROS production and then lead to redox imbalance, further activating Bcl-2, Bax, and caspase-9 as well as other pathways to induce skin cancer cell death/apoptosis. On the other hand, dietary antioxidants reduce the production of ROS by inhibiting signal pathways such as MAPK, PI3K-Akt, and NF-κB to prevent and control skin cancer (melanoma, SCC, and BCC). In fact, the mechanism of the ROS-based treatment of skin cancer is often interactive. (+) indicates activation and (-) indicates inactivation.

Once FU is converted into FU deoxynucleotides in cells, it would block thymidine nucleotide synthetase and inhibit DNA synthesis. FU meanwhile interferes with the synthesis of RNA to resist tumors. Moreover, increased ROS cause oxidative damage and then result in the breakage of NMSC cell membrane lipids, proteins, and DNA strand chain [85, 86]. The targeted inhibitors dabrafenib and trametinib were used to treat melanoma and SCC mainly by involving ROS overproduction and caspase-activated apoptosis [87]. Daniel et al. also found that the combined therapy of vemurafenib and potassium channel inhibitor TRAM-34 decreased ERK phosphorylation and significantly increased intracellular ROS levels, which stimulated caspase-3 and other proapoptotic pathways and decreased the mitochondrial membrane potential, further leading to the apoptosis of melanoma cells [88]. For example, targeting BRAF gene drugs vemurafenib and dabrafenib could inhibit the growth and division of BRAF-mutated metastatic melanoma cells via blocking the MAPK signaling pathway and upregulating ROS [89]. Meanwhile, the MEK inhibitor trametinib combining with dabrafenib significantly enhanced the therapeutic effect on melanoma in the presence of high-level ROS [90]. Besides, chaetocin derived from the *Chaetomium* species has a powerful antitumor proliferative activity. It significantly inhibited melanoma cell proliferation and promoted its apoptosis via increasing cellular ROS, decreasing the mitochondrial membrane potential and activating the caspase-9/3 pathway [91]. Nevertheless, Yu et al. and Wang et al. discovered that the ROS-responsive gel scaffold that they created in their study could break immune tolerance and enhance immune response to melanoma through reducing the level of local ROS and inhibiting the programmed death-ligand 1 (PD-L1) [92, 93].

PDT is a phototherapy based on the accumulation of photosensitizers in the body and the irradiation of light with a specific wave length, which can generate substantial ROS to produce cytotoxicity and kill cancer cells. Currently, 5-methylaminolevulinic acid (MAL) and 5-aminolevulinic acid (ALA) are both extremely common photosensitizers in PDT, and PDT has been widely used to treat skin tumors, e.g., SCC, BCC, and Bowen's disease. The presence of either MAL or ALA in the body may be converted into protoporphyrin IX (PpIX) with strong photosensitivity, which produces substantial ROS to kill cancer cells after irradiation with adequate-wavelength light, while neighbouring normal cells are scarcely affected [94]. However, PDT has a large limitation in skin cancer due to the infiltration of photosensitizers into deep skin tissue. To overcome this deficiency, some improvements, including pretreatment with a laser or a microneedle and encapsulating the photosensitizer in nanoparticles and combining with drugs, are made to enhance PDT efficacy in skin cancer [95]. Others, like indoline-fused-triazole-mediated PDT can increase ROS production and enhance apoptosis-related protein expression, thereby inducing BBC cell death [96].

Furthermore, there are other ways for skin cancer treatment targeting ROS. Typically, radiotherapy is an effective vehicle in the management of skin cancer in recent decades [97]. Via locally producing and releasing a large quantity of ROS, radiotherapy can cause violent oxidative eruptions to kill tumor cells and make solid tumor smaller [98]. Recently, it has been demonstrated that some ROS-inducers are conducive to enhancing the sensitivity of skin cancer cells to IR through a ROS-mediated manner. Selenadiazole derivatives, for example, could increase the sensitivity of A375 human melanoma cells to X-ray by the induction of ROS-mediated DNA damage and AKT inactivation. Besides, IR benefits more ROS generation, G2/M phase arrest, and melanoma cell apoptosis [99].

4.2. Dietary Antioxidants for Skin Cancer Basing on ROS. Dietary antioxidants are widely distributed in fruits, vegetables, grain, herbs, spices, and other foods, which are rich in vitamins, minerals, polyphenols, and flavonoids. Dietary antioxidants possess various antineoplastic activities: antiproliferation, anti-inflammation, immune regulation, antiangiogenesis, and inhibition of metastasis [100, 101]. Dietary intake of vitamins, including vitamin C, vitamin E, selenium, and vitamin A, is inversely proportional to the risk of cancer and prevents skin carcinogenesis as antioxidant micronutrients [102]. When UV-induced ROS are beyond the antioxidant defense, oxidative stress occurs; nevertheless, these vitamins could effectively eliminate ROS and prevent oxidative stress through strengthening the antioxidant defense, ultimately protecting the skin against UV-induced cancer [103]. Moreover, polyphenols are a group of natural substances with excellent biological properties and have become potent dietary-preventive agents against cancer. The polypodium leucotomos extract (PL), a strong antioxidant with a high-content phenolic compound, is able to prevent and control skin cancer mainly by inhibiting UV-induced ROS production, suppressing NF-κB activation, and activating the p53 protein [104]. Heo et al. found that the decrease of Nrf2 expression and the antioxidant defense ability in resveratrol-treated melanoma cells encouraged the generation of a large amount of ROS and endoplasmic reticulum stress, then triggered the occurrence of oxidative stress; in turn, the increased ROS and oxidative stress further inhibited the growth and proliferation of melanoma cells by downregulating the Bcl-2 protein level and upregulating the Bcl-2-related X protein expression [105]. As a member of the flavonoid family, quercetin is excellent in strengthening the antioxidant defense via removing H_2O_2, $O_2^{\bullet-}$, and $^{\bullet}OH$ and has a powerful anticancer effect on skin cancer through regulating molecular mechanisms, e.g., inhibiting activation of the MAPK, PI3K-Akt/PKB, and NF-κB signal pathways [106]. Another natural flavonoid, caffeic acid n-butyl ester (CAE), stimulates the accumulation of toxic ROS and the decrease of MMP in A431 skin cancer cells to inhibit the PI3K/AKT/mTOR signaling pathway and thus induce cancer cell apoptosis [107]. Lee et al. meanwhile showed that the flavonoid Cudraflavone C was a novel natural drug for the treatment of melanoma; this drug could activate the phosphorylation of MAPKs (p38, ERK, and JNK) and increase the expression of apoptosis proteins (Bax, cytochrome c, caspase-9, and caspase-3/7) to induce the apoptosis of melanoma cells by increasing mitochondrial ROS production [108]. Proanthocyanidins, a group of flavonoids derived from grapes, apples, bilberry, cranberry, and other plants, have potent abilities of deducing the proliferation and invasion of tumor cells through the production of toxic-dose ROS and inhibition of MMP-2/9 expression, eventually preventing skin carcinogenesis, especially SCC [109]. Other studies also have demonstrated that proanthocyanidins, owing to their strong antineoplastic and antiangiogenic properties in cancers, could downregulate VEGF expression, suppress endothelial cell migration, and lessen vascularization via attenuating the phosphorylation of Akt, ERK, and p38 MAPK [110]. In addition, dietary antioxidants like some Thai plants have protective effects against UV-induced skin cancer [111]. Overall, dietary antioxidants have diverse beneficial properties and provide a protection against skin cancer through regulating some molecular mechanisms between ROS and cancer.

Figure 3 summarizes these ROS-targeted treatments on skin cancer.

5. Conclusion and Future Perspective

Taken together, there is convincing evidence to support the critical role of ROS in cutaneous carcinogenesis and skin cancer progression. Increased ROS contribute to DNA damage and epigenetic instability, metabolic adaptation, cancer cell proliferation and migration, and cell death in some cases. In recent years, it has become a research hot spot in the tumor therapy field whether to focus on antioxidation or promote oxidation. In this review, a series of mechanisms in ROS-mediated skin cancers have been discussed, including protooncogene activation, tumor suppressor gene inactivation, genomic instability/mutations, and epigenetic modifications, as well as multiple related signaling pathways; several therapeutic approaches targeting ROS, like PDT, radiotherapy, and dietary therapy, are also introduced. Although the relationship between ROS and skin carcinogenesis has been largely elucidated, how they specifically regulate each other needs further research. We look forward to finding the balance between ROS and skin carcinogenesis in the near future and searching a reliable and effective method for the treatment of skin cancer.

Conflicts of Interest

The authors declare that they have no conflicts of interest.

Authors' Contributions

Dehai Xian and Rui Lai are coauthors.

Acknowledgments

We thank Professor Yang Xu and Dr. Yongqiong Deng for helpful discussion on this paper.

References

[1] M. Hosseini, Z. Kasraian, and H. R. Rezvani, "Energy metabolism in skin cancers: a therapeutic perspective," *Biochimica et Biophysica Acta - Bioenergetics*, vol. 1858, no. 8, pp. 712–722, 2017.

[2] P. S. Roy and B. J. Saikia, "Cancer and cure: a critical analysis," *Indian Journal of Cancer*, vol. 53, no. 3, pp. 441-442, 2016.

[3] F. Liu-Smith, J. Jia, and Y. Zheng, "UV-induced molecular signaling differences in melanoma and non-melanoma skin cancer," *Advances in Experimental Medicine and Biology*, vol. 996, pp. 27–40, 2017.

[4] A. Kyrgidis, T. G. Tzellos, K. Vahtsevanos, and S. Triaridis, "New concepts for basal cell carcinoma. Demographic, clinical, histological risk factors, and biomarkers. A systematic

review of evidence regarding risk for tumor development, susceptibility for second primary and recurrence," *The Journal of Surgical Research*, vol. 159, no. 1, pp. 545–556, 2010.

[5] G. P. Pfeifer and A. Besaratinia, "UV wavelength-dependent DNA damage and human non-melanoma and melanoma skin cancer," *Photochemical & Photobiological Sciences*, vol. 11, no. 1, pp. 90–97, 2012.

[6] X. X. Huang, R. A. Scolyer, A. Abubakar, and G. M. Halliday, "Human 8-oxoguanine-DNA glycosylase-1 is downregulated in human basal cell carcinoma," *Molecular Genetics and Metabolism*, vol. 106, no. 1, pp. 127–130, 2012.

[7] M. Kunisada, F. Yogianti, K. Sakumi, R. Ono, Y. Nakabeppu, and C. Nishigori, "Increased expression of versican in the inflammatory response to UVB and reactive oxygen species-induced skin tumorigenesis," *The American Journal of Pathology*, vol. 179, no. 6, pp. 3056–3065, 2011.

[8] J. N. Moloney and T. G. Cotter, "ROS signalling in the biology of cancer," *Seminars in Cell & Developmental Biology*, vol. 80, pp. 50–64, 2018.

[9] S. I. Liochev, "Reactive oxygen species and the free radical theory of aging," *Free Radical Biology & Medicine*, vol. 60, pp. 1–4, 2013.

[10] L. A. Sena and N. S. Chandel, "Physiological roles of mitochondrial reactive oxygen species," *Molecular Cell*, vol. 48, no. 2, pp. 158–167, 2012.

[11] S. Di Meo, T. T. Reed, P. Venditti, and V. M. Victor, "Role of ROS and RNS sources in physiological and pathological conditions," *Oxidative Medicine and Cellular Longevity*, vol. 2016, Article ID 1245049, 44 pages, 2016.

[12] F. Ursini, M. Maiorino, and H. J. Forman, "Redox homeostasis: the golden mean of healthy living," *Redox Biology*, vol. 8, pp. 205–215, 2016.

[13] M. Vučetić, Y. Cormerais, S. K. Parks, and J. Pouysségur, "The central role of amino acids in cancer redox homeostasis: vulnerability points of the cancer redox code," *Frontiers in Oncology*, vol. 7, p. 319, 2017.

[14] M. del Pilar Sosa Idelchik, U. Begley, T. J. Begley, and J. Andrés Melendez, "Mitochondrial ROS control of cancer," *Seminars in Cancer Biology*, vol. 47, pp. 57–66, 2017.

[15] M. Valko, K. Jomova, C. J. Rhodes, K. Kuča, and K. Musílek, "Redox and non-redox-metal-induced formation of free radicals and their role in human disease," *Archives of Toxicology*, vol. 90, no. 1, pp. 1–37, 2016.

[16] U. Wölfle, G. Seelinger, G. Bauer, M. C. Meinke, J. Lademann, and C. M. Schempp, "Reactive molecule species and antioxidative mechanisms in normal skin and skin aging," *Skin Pharmacology and Physiology*, vol. 27, no. 6, pp. 316–332, 2014.

[17] J. Rudolf, H. Raad, A. Taieb, and H. R. Rezvani, "NADPH oxidases and their roles in skin homeostasis and carcinogenesis," *Antioxidants & Redox Signaling*, vol. 28, no. 13, pp. 1238–1261, 2018.

[18] A. G. Georgakilas, "Oxidative stress, DNA damage and repair in carcinogenesis: have we established a connection?," *Cancer Letters*, vol. 327, no. 1-2, pp. 3-4, 2012.

[19] E. Emanuele, J. M. Spencer, and M. Braun, "From DNA repair to proteome protection: new molecular insights for preventing non-melanoma skin cancers and skin aging," *Journal of Drugs in Dermatology*, vol. 13, no. 3, pp. 274–281, 2014.

[20] J. Kim, J. Kim, and J. S. Bae, "ROS homeostasis and metabolism: a critical liaison for cancer therapy," *Experimental & Molecular Medicine*, vol. 48, no. 11, article e269, 2016.

[21] S. Prasad, S. C. Gupta, and A. K. Tyagi, "Reactive oxygen species (ROS) and cancer: role of antioxidative nutraceuticals," *Cancer Letters*, vol. 387, pp. 95–105, 2017.

[22] M. Nieborowska-Skorska, P. K. Kopinski, R. Ray et al., "Rac2-MRC-cIII-generated ROS cause genomic instability in chronic myeloid leukemia stem cells and primitive progenitors," *Blood*, vol. 119, no. 18, pp. 4253–4263, 2012.

[23] U. Weyemi, O. Lagente-Chevallier, M. Boufraqech et al., "ROS-generating NADPH oxidase NOX4 is a critical mediator in oncogenic H-Ras-induced DNA damage and subsequent senescence," *Oncogene*, vol. 31, no. 9, pp. 1117–1129, 2012.

[24] M.-T. Park, M.-J. Kim, Y. Suh et al., "Novel signaling axis for ROS generation during K-Ras-induced cellular transformation," *Cell Death and Differentiation*, vol. 21, no. 8, pp. 1185–1197, 2014.

[25] F. Liu-Smith, R. Dellinger, and F. L. Meyskens Jr., "Updates of reactive oxygen species in melanoma etiology and progression," *Archives of Biochemistry and Biophysics*, vol. 563, pp. 51–55, 2014.

[26] E. Aydin, J. Johansson, F. H. Nazir, K. Hellstrand, and A. Martner, "Role of NOX2-derived reactive oxygen species in NK cell-mediated control of murine melanoma metastasis," *Cancer Immunology Research*, vol. 5, no. 9, pp. 804–811, 2017.

[27] S. Antony, G. Jiang, Y. Wu et al., "NADPH oxidase 5 (NOX5)—induced reactive oxygen signaling modulates normoxic HIF-1α and $p27^{Kip1}$ expression in malignant melanoma and other human tumors," *Molecular Carcinogenesis*, vol. 56, no. 12, pp. 2643–2662, 2017.

[28] M. Li, Q. Chen, and X. Yu, "Chemopreventive effects of ROS targeting in a murine model of BRCA1-deficient breast cancer," *Cancer Research*, vol. 77, no. 2, pp. 448–458, 2017.

[29] A. V. Budanov, "Stress-responsive sestrins link p53 with redox regulation and mammalian target of rapamycin signaling," *Antioxidants & Redox Signaling*, vol. 15, no. 6, pp. 1679–1690, 2011.

[30] F. Mantovani, L. Collavin, and G. Del Sal, "Mutant p53 as a guardian of the cancer cell," *Cell Death and Differentiation*, vol. 26, no. 2, pp. 199–212, 2019.

[31] M. Nakayama and M. Oshima, "Mutant p53 in colon cancer," *Journal of Molecular Cell Biology*, vol. 11, no. 4, pp. 267–276, 2019.

[32] Q. Wu and X. Ni, "ROS-mediated DNA methylation pattern alterations in carcinogenesis," *Current Drug Targets*, vol. 16, no. 1, pp. 13–19, 2015.

[33] R. Zhang, K. A. Kang, K. C. Kim et al., "Oxidative stress causes epigenetic alteration of CDX1 expression in colorectal cancer cells," *Gene*, vol. 524, no. 2, pp. 214–219, 2013.

[34] K. A. Kang, R. Zhang, G. Y. Kim, S. C. Bae, and J. W. Hyun, "Epigenetic changes induced by oxidative stress in colorectal cancer cells: methylation of tumor suppressor RUNX3," *Tumour Biology*, vol. 33, no. 2, pp. 403–412, 2012.

[35] Q. Liu, J. Jin, J. Ying et al., "Frequent epigenetic suppression of tumor suppressor gene glutathione peroxidase 3 by promoter hypermethylation and its clinical implication in clear cell renal cell carcinoma," *International Journal of Molecular Sciences*, vol. 16, no. 12, pp. 10636–10649, 2015.

[36] Y. Sang and Y. Deng, "Current insights into the epigenetic mechanisms of skin cancer," *Dermatologic Therapy*, vol. 32, no. 4, article e12964, 2019.

[37] J. He and B. H. Jiang, "Interplay between reactive oxygen species and microRNAs in cancer," *Current Pharmacology Reports*, vol. 2, no. 2, pp. 82–90, 2016.

[38] B. Farhood, M. Najafi, E. Salehi et al., "Disruption of the redox balance with either oxidative or anti-oxidative overloading as a promising target for cancer therapy," *Journal of Cellular Biochemistry*, vol. 120, no. 1, pp. 71–76, 2019.

[39] Y. Sun, W. Z. Liu, T. Liu, X. Feng, N. Yang, and H. F. Zhou, "Signaling pathway of MAPK/ERK in cell proliferation, differentiation, migration, senescence and apoptosis," *Journal of Receptor and Signal Transduction Research*, vol. 35, no. 6, pp. 600–604, 2015.

[40] C. Wang, P. Li, J. Xuan et al., "Cholesterol enhances colorectal cancer progression via ROS elevation and MAPK signaling pathway activation," *Cellular Physiology and Biochemistry*, vol. 42, no. 2, pp. 729–742, 2017.

[41] L. Cao, X. Chen, X. Xiao, Q. Ma, and W. Li, "Resveratrol inhibits hyperglycemia-driven ROS-induced invasion and migration of pancreatic cancer cells via suppression of the ERK and p38 MAPK signaling pathways," *International Journal of Oncology*, vol. 49, no. 2, pp. 735–743, 2016.

[42] G. T. Gibney, J. L. Messina, I. V. Fedorenko, V. K. Sondak, and K. S. M. Smalley, "Paradoxical oncogenesis—the long-term effects of BRAF inhibition in melanoma," *Nature Reviews Clinical Oncology*, vol. 10, no. 7, pp. 390–399, 2013.

[43] X. Liu, L. Zhang, Y. Liu et al., "Circ-8073 regulates CEP55 by sponging miR-449a to promote caprine endometrial epithelial cells proliferation *via* the PI3K/AKT/mTOR pathway," *Biochimica et Biophysica Acta (BBA) - Molecular Cell Research*, vol. 1865, no. 8, pp. 1130–1147, 2018.

[44] X. Tan, Z. Zhang, H. Yao, and L. Shen, "Tim-4 promotes the growth of colorectal cancer by activating angiogenesis and recruiting tumor-associated macrophages via the PI3K/AKT/mTOR signaling pathway," *Cancer Letters*, vol. 436, pp. 119–128, 2018.

[45] A. Silva, A. Gírio, I. Cebola, C. I. Santos, F. Antunes, and J. T. Barata, "Intracellular reactive oxygen species are essential for PI3K/Akt/mTOR-dependent IL-7-mediated viability of T-cell acute lymphoblastic leukemia cells," *Leukemia*, vol. 25, no. 6, pp. 960–967, 2011.

[46] S. Meierjohann, "Oxidative stress in melanocyte senescence and melanoma transformation," *European Journal of Cell Biology*, vol. 93, no. 1-2, pp. 36–41, 2014.

[47] M. J. Morgan and Z. G. Liu, "Crosstalk of reactive oxygen species and NF-κB signaling," *Cell Research*, vol. 21, no. 1, pp. 103–115, 2011.

[48] M. K. Schaafhausen, W. J. Yang, L. Centanin et al., "Tumor angiogenesis is caused by single melanoma cells in a manner dependent on reactive oxygen species and NF-κB," *Journal of Cell Science*, vol. 126, no. 17, pp. 3862–3872, 2013.

[49] I. M. W. Ruma, E. . W. Putranto, E. Kondo et al., "MCAM, as a novel receptor for S100A8/A9, mediates progression of malignant melanoma through prominent activation of NF-κB and ROS formation upon ligand binding," *Clinical & Experimental Metastasis*, vol. 33, no. 6, pp. 609–627, 2016.

[50] A. Kim, M. Im, N. H. Yim, Y. P. Jung, and J. Y. Ma, "Aqueous extract of Bambusae Caulis in Taeniam inhibits PMA-induced tumor cell invasion and pulmonary metastasis: suppression of NF-κB activation through ROS signaling," *PLoS One*, vol. 8, no. 10, article 78061, 2013.

[51] H. Satoh, T. Moriguchi, D. Saigusa et al., "NRF2 intensifies host defense systems to prevent lung carcinogenesis, but after tumor initiation accelerates malignant cell growth," *Cancer Research*, vol. 76, no. 10, pp. 3088–3096, 2016.

[52] H. Ikehata and M. Yamamoto, "Roles of the KEAP1-NRF2 system in mammalian skin exposed to UV radiation," *Toxicology and Applied Pharmacology*, vol. 360, pp. 69–77, 2018.

[53] G. M. DeNicola, F. A. Karreth, T. J. Humpton et al., "Oncogene-induced Nrf2 transcription promotes ROS detoxification and tumorigenesis," *Nature*, vol. 475, no. 7354, pp. 106–109, 2011.

[54] A. Cuadrado, A. I. Rojo, G. Wells et al., "Therapeutic targeting of the NRF2 and KEAP1 partnership in chronic diseases," *Nature Reviews Drug Discovery*, vol. 18, no. 4, pp. 295–317, 2019.

[55] Y. R. Kim, J. E. Oh, M. S. Kim et al., "Oncogenic NRF2 mutations in squamous cell carcinomas of oesophagus and skin," *The Journal of Pathology*, vol. 220, no. 4, pp. 446–451, 2010.

[56] R. Feng, Y. Morine, T. Ikemoto et al., "Nrf2 activation drive macrophages polarization and cancer cell epithelial-mesenchymal transition during interaction," *Cell Communication and Signaling*, vol. 16, no. 1, p. 54, 2018.

[57] F. Rolfs, M. Huber, A. Kuehne et al., "Nrf2 activation promotes keratinocyte survival during early skin carcinogenesis via metabolic alterations," *Cancer Research*, vol. 75, no. 22, pp. 4817–4829, 2015.

[58] C. Y. Choi, J. Y. Kim, S. Y. Wee et al., "Expression of nuclear factor erythroid 2 protein in malignant cutaneous tumors," *Archives of Plastic Surgery*, vol. 41, no. 6, pp. 654–660, 2014.

[59] E. V. Knatko, M. Higgins, J. W. Fahey, and A. T. Dinkova-Kostova, "Loss of Nrf2 abrogates the protective effect of Keap1 downregulation in a preclinical model of cutaneous squamous cell carcinoma," *Scientific Reports*, vol. 6, no. 1, article 25804, 2016.

[60] C. L. Saw, A. Y. Yang, M. T. Huang et al., "Nrf2 null enhances UVB-induced skin inflammation and extracellular matrix damages," *Cell & Bioscience*, vol. 4, no. 1, p. 39, 2014.

[61] K. S. Chun, J. Kundu, J. K. Kundu, and Y. J. Surh, "Targeting Nrf2-Keap1 signaling for chemoprevention of skin carcinogenesis with bioactive phytochemicals," *Toxicology Letters*, vol. 229, no. 1, pp. 73–84, 2014.

[62] X. Wang, A. K. Mandal, H. Saito et al., "Arsenic and chromium in drinking water promote tumorigenesis in a mouse colitis-associated colorectal cancer model and the potential mechanism is ROS-mediated Wnt/β-catenin signaling pathway," *Toxicology and Applied Pharmacology*, vol. 262, no. 1, pp. 11–21, 2012.

[63] A. Vallée and Y. Lecarpentier, "Crosstalk between peroxisome proliferator-activated receptor gamma and the canonical WNT/β-catenin pathway in chronic inflammation and oxidative stress during carcinogenesis," *Frontiers in Immunology*, vol. 9, p. 745, 2018.

[64] M. Rastrelli, S. Tropea, C. R. Rossi, and M. Alaibac, "Melanoma: epidemiology, risk factors, pathogenesis, diagnosis and classification," *In Vivo*, vol. 28, no. 6, pp. 1005–1011, 2014.

[65] R. W. Jenkins and R. J. Sullivan, "NRAS mutant melanoma: an overview for the clinician for melanoma management," *Melanoma Management*, vol. 3, no. 1, pp. 47–59, 2016.

[66] G. Comito, M. Calvani, E. Giannoni et al., "HIF-1α stabilization by mitochondrial ROS promotes Met-dependent invasive growth and vasculogenic mimicry in melanoma cells," *Free Radical Biology & Medicine*, vol. 51, no. 4, pp. 893–904, 2011.

[67] T. A. Yuan, V. Yourk, A. Farhat et al., "A case-control study of the genetic variability in reactive oxygen species-metabolizing enzymes in melanoma risk," *International Journal of Molecular Sciences*, vol. 19, no. 1, p. 242, 2018.

[68] S. J. Park, Y. T. Kim, and Y. J. Jeon, "Antioxidant dieckol downregulates the Rac1/ROS signaling pathway and inhibits Wiskott-Aldrich syndrome protein (WASP)-family verprolin-homologous protein 2 (WAVE2)-mediated invasive migration of B16 mouse melanoma cells," *Molecules and Cells*, vol. 33, no. 4, pp. 363–369, 2012.

[69] Y. L. Shih, H. M. Chou, H. C. Chou et al., "Casticin impairs cell migration and invasion of mouse melanoma B16F10 cells via PI3K/AKT and NF-κB signaling pathways," *Environmental Toxicology*, vol. 32, no. 9, pp. 2097–2112, 2017.

[70] S. P. Cannavò, A. Tonacci, L. Bertino, M. Casciaro, F. Borgia, and S. Gangemi, "The role of oxidative stress in the biology of melanoma: a systematic review," *Pathology, Research and Practice*, vol. 215, no. 1, pp. 21–28, 2019.

[71] T. R. Correia de Sá, R. Silva, and J. M. Lopes, "Basal cell carcinoma of the skin (part1): epidemiology, pathology and genetic syndromes," *Future Oncology*, vol. 11, no. 22, pp. 3011–3021, 2015.

[72] Z. Majidi, M. Djalali, M. H. Javanbakht, M. Fathi, M. Zarei, and K. Foladsaz, "Evaluation of the level of zinc and malondialdehyde in basal cell carcinoma," *Iranian Journal of Public Health*, vol. 46, no. 8, pp. 1104–1109, 2017.

[73] L. Chaisiriwong, R. Wanitphakdeedecha, P. Sitthinamsuwan et al., "A case-control study of involvement of oxidative DNA damage and alteration of antioxidant defense system in patients with basal cell carcinoma: modulation by tumor removal," *Oxidative Medicine and Cellular Longevity*, vol. 2016, Article ID 5934024, 12 pages, 2016.

[74] C. Pellegrini, M. Maturo, L. di Nardo, V. Ciciarelli, C. Gutiérrez García-Rodrigo, and M. Fargnoli, "Understanding the molecular genetics of basal cell carcinoma," *International Journal of Molecular Sciences*, vol. 18, no. 11, p. 2485, 2017.

[75] A. Yoshifuku, K. Fujii, and T. Kanekura, "Comparison of oxidative stress on DNA, protein and lipids in patients with actinic keratosis, Bowen's disease and squamous cell carcinoma," *The Journal of Dermatology*, vol. 45, no. 11, pp. 1319–1323, 2018.

[76] R. M. Brand, P. Wipf, A. Durham, M. W. Epperly, J. S. Greenberger, and L. D. Falo Jr., "Targeting mitochondrial oxidative stress to mitigate UV-induced skin damage," *Frontiers in Pharmacology*, vol. 9, p. 920, 2018.

[77] C. L. Benjamin and H. N. Ananthaswamy, "p53 and the pathogenesis of skin cancer," *Toxicology and Applied Pharmacology*, vol. 224, no. 3, pp. 241–248, 2007.

[78] R. Kumar, G. Deep, and R. Agarwal, "An overview of ultraviolet B radiation-induced skin cancer chemoprevention by silibinin," *Current Pharmacology Reports*, vol. 1, no. 3, pp. 206–215, 2015.

[79] L. Liu, H. R. Rezvani, J. H. Back et al., "Inhibition of p38 MAPK signaling augments skin tumorigenesis via NOX2 driven ROS generation," *PLoS One*, vol. 9, no. 5, article 97245, 2014.

[80] Y. Kitagishi and S. Matsuda, "Redox regulation of tumor suppressor PTEN in cancer and aging (Review)," *International Journal of Molecular Medicine*, vol. 31, no. 3, pp. 511–515, 2013.

[81] M. Ming, L. Feng, C. R. Shea et al., "PTEN positively regulates UVB-induced DNA damage repair," *Cancer Research*, vol. 71, no. 15, pp. 5287–5295, 2011.

[82] M. C. F. Simões, J. J. S. Sousa, and A. A. C. C. Pais, "Skin cancer and new treatment perspectives: a review," *Cancer Letters*, vol. 357, no. 1, pp. 8–42, 2015.

[83] Q. Cui, J. Q. Wang, Y. G. Assaraf et al., "Modulating ROS to overcome multidrug resistance in cancer," *Drug Resistance Updates*, vol. 41, pp. 1–25, 2018.

[84] Y. Rong, L. Zuo, L. Shang, and J. G. Bazan, "Radiotherapy treatment for nonmelanoma skin cancer," *Expert Review of Anticancer Therapy*, vol. 15, no. 7, pp. 765–776, 2015.

[85] M. W. Sung, D. Y. Lee, S. W. Park et al., "Celecoxib enhances the inhibitory effect of 5-FU on human squamous cell carcinoma proliferation by ROS production," *The Laryngoscope*, vol. 127, no. 4, pp. E117–E123, 2017.

[86] L. Metterle, C. Nelson, and N. Patel, "Intralesional 5-fluorouracil (FU) as a treatment for nonmelanoma skin cancer (NMSC): a review," *Journal of the American Academy of Dermatology*, vol. 74, no. 3, pp. 552–557, 2016.

[87] H. P. Tham, K. Xu, W. Q. Lim et al., "Microneedle-assisted topical delivery of photodynamically active mesoporous formulation for combination therapy of deep-seated melanoma," *ACS Nano*, vol. 12, no. 12, pp. 11936–11948, 2018.

[88] D. Bauer, F. Werth, H. A. Nguyen, F. Kiecker, and J. Eberle, "Critical role of reactive oxygen species (ROS) for synergistic enhancement of apoptosis by vemurafenib and the potassium channel inhibitor TRAM-34 in melanoma cells," *Cell Death & Disease*, vol. 8, no. 2, article 2594, 2017.

[89] M. Maio, K. Lewis, L. Demidov et al., "Adjuvant vemurafenib in resected, $BRAF^{V600}$ mutation-positive melanoma (BRIM8): a randomised, double-blind, placebo-controlled, multicentre, phase 3 trial," *The Lancet Oncology*, vol. 19, no. 4, pp. 510–520, 2018.

[90] K. K. Broman, L. A. Dossett, J. Sun, Z. Eroglu, and J. S. Zager, "Update on BRAF and MEK inhibition for treatment of melanoma in metastatic, unresectable, and adjuvant settings," *Expert Opinion on Drug Safety*, vol. 18, no. 5, pp. 381–392, 2019.

[91] X. Han, Y. Han, Y. Zheng et al., "Chaetocin induces apoptosis in human melanoma cells through the generation of reactive oxygen species and the intrinsic mitochondrial pathway, and exerts its anti-tumor activity in vivo," *PLoS One*, vol. 12, no. 4, article e0175950, 2017.

[92] S. Yu, C. Wang, J. Yu et al., "Injectable bioresponsive gel depot for enhanced immune checkpoint blockade," *Advanced Materials*, vol. 30, no. 28, article e1801527, 2018.

[93] C. Wang, J. Wang, X. Zhang et al., "In situ formed reactive oxygen species-responsive scaffold with gemcitabine and checkpoint inhibitor for combination therapy," *Science Translational Medicine*, vol. 10, no. 429, article eaan3682, 2018.

[94] P. Fonda-Pascual, O. M. Moreno-Arrones, A. Alegre-Sanchez et al., "In situ production of ROS in the skin by photodynamic therapy as a powerful tool in clinical dermatology," *Methods*, vol. 109, pp. 190–202, 2016.

[95] I. Baldea, L. Giurgiu, I. D. Teacoe et al., "Photodynamic therapy in melanoma—where do we stand?," *Current Medicinal Chemistry*, vol. 25, no. 40, pp. 5540–5563, 2018.

[96] W. P. Hu, K. K. Kuo, G. C. Senadi, L. S. Chang, and J. J. Wang, "Photodynamic therapy using indolines-fused-iriazoles induces mitochondrial apoptosis in human non-melanoma BCC cells," *Anticancer Research*, vol. 37, no. 10, pp. 5499–5505, 2017.

[97] N. Cheraghi, A. Cognetta, and D. Goldberg, "Radiation therapy in dermatology: non-melanoma skin cancer," *Journal of Drugs in Dermatology*, vol. 16, no. 5, pp. 464–469, 2017.

[98] Z. Zou, H. Chang, H. Li, and S. Wang, "Induction of reactive oxygen species: an emerging approach for cancer therapy," *Apoptosis*, vol. 22, no. 11, pp. 1321–1335, 2017.

[99] Q. Xie, Y. Zhou, G. Lan et al., "Sensitization of cancer cells to radiation by selenadiazole derivatives by regulation of ROS-mediated DNA damage and ERK and AKT pathways," *Biochemical and Biophysical Research Communications*, vol. 449, no. 1, pp. 88–93, 2014.

[100] S. Afrin, F. Giampieri, M. Gasparrini et al., "Dietary phytochemicals in colorectal cancer prevention and treatment: a focus on the molecular mechanisms involved," *Biotechnology Advances*, 2018.

[101] N. Shapira, "Nutritional approach to sun protection: a suggested complement to external strategies," *Nutrition Reviews*, vol. 68, no. 2, pp. 75–86, 2010.

[102] X. Wu, J. Cheng, and X. Wang, "Dietary antioxidants: potential anticancer agents," *Nutrition and Cancer*, vol. 69, no. 4, pp. 521–533, 2017.

[103] A. Godic, B. Poljšak, M. Adamic, and R. Dahmane, "The role of antioxidants in skin cancer prevention and treatment," *Oxidative Medicine and Cellular Longevity*, vol. 2014, Article ID 860479, 6 pages, 2014.

[104] C. Parrado, M. Mascaraque, Y. Gilaberte, A. Juarranz, and S. Gonzalez, "Fernblock (*Polypodium leucotomos* extract): molecular mechanisms and pleiotropic effects in light-related skin conditions, photoaging and skin cancers, a review," *International Journal of Molecular Sciences*, vol. 17, no. 7, p. 1026, 2016.

[105] J. R. Heo, S. M. Kim, K. A. Hwang, J. H. Kang, and K. C. Choi, "Resveratrol induced reactive oxygen species and endoplasmic reticulum stress-mediated apoptosis, and cell cycle arrest in the A375SM malignant melanoma cell line," *International Journal of Molecular Medicine*, vol. 42, no. 3, pp. 1427–1435, 2018.

[106] F. Khan, K. Niaz, F. Maqbool et al., "Molecular targets underlying the anticancer effects of quercetin: an update," *Nutrients*, vol. 8, no. 9, p. 529, 2016.

[107] N. Zeng, T. Hongbo, Y. Xu, M. Wu, and Y. Wu, "Anticancer activity of caffeic acid n-butyl ester against A431 skin carcinoma cell line occurs via induction of apoptosis and inhibition of the mTOR/PI3K/AKT signaling pathway," *Molecular Medicine Reports*, vol. 17, no. 4, pp. 5652–5657, 2018.

[108] C. W. Lee, F. L. Yen, H. H. Ko et al., "Cudraflavone C induces apoptosis of A375.S2 melanoma cells through mitochondrial ROS production and MAPK activation," *International Journal of Molecular Sciences*, vol. 18, no. 7, p. 1508, 2017.

[109] Y. S. Hah, J. G. Kim, H. Y. Cho, J. S. Park, E. P. Heo, and T. J. Yoon, "Procyanidins from *Vitis vinifera* seeds induce apoptotic and autophagic cell death via generation of reactive oxygen species in squamous cell carcinoma cells," *Oncology Letters*, vol. 14, no. 2, pp. 1925–1932, 2017.

[110] Q. Li, X. Wang, T. Dai et al., "Proanthocyanidins, isolated from *Choerospondias axillaris* fruit peels, exhibit potent antioxidant activities in vitro and a novel anti-angiogenic property in vitro and in vivo," *Journal of Agricultural and Food Chemistry*, vol. 64, no. 18, pp. 3546–3556, 2016.

[111] M. B. de Silva and T. Tencomnao, "The protective effect of some Thai plants and their bioactive compounds in UV light-induced skin carcinogenesis," *Journal of Photochemistry and Photobiology. B*, vol. 185, pp. 80–89, 2018.

Hindawi
Oxidative Medicine and Cellular Longevity
Volume 2019, Article ID 4120379, 14 pages
https://doi.org/10.1155/2019/4120379

Research Article

Presence of Stromal Cells Enhances Epithelial-to-Mesenchymal Transition (EMT) Induction in Lung Bronchial Epithelium after Protracted Exposure to Oxidative Stress of Gamma Radiation

Anna Acheva,[1,2] **Siamak Haghdoost**,[3,4] **Alice Sollazzo**,[3] **Virpi Launonen**,[1†] **and Meerit Kämäräinen**[1]

[1]*STUK-Radiation and Nuclear Safety Authority, Helsinki, Finland*
[2]*Department of Veterinary Biosciences, Section of Pathology, Faculty of Veterinary Medicine, University of Helsinki, Finland*
[3]*Department of Molecular Bioscience, Centre for Radiation Protection Research, The Wenner-Gren Institute, Stockholm University, Stockholm, Sweden*
[4]*University of Caen Normandy, Cimap-Laria, Advanced Resource Center for HADrontherapy in Europe (ARCHADE), Caen, France*
[†]*Deceased*

Correspondence should be addressed to Anna Acheva; anna.acheva@helsinki.fi

Received 15 April 2019; Revised 19 June 2019; Accepted 23 July 2019; Published 8 September 2019

Guest Editor: Jayeeta Ghose

The aim of the study was to investigate the role of a microenvironment in the induction of epithelial-to-mesenchymal transition (EMT) as a sign of early stages of carcinogenesis in human lung epithelial cell lines after protracted low-dose rate γ-radiation exposures. BEAS-2B and HBEC-3KT lung cell lines were irradiated with low-dose rate γ-rays (^{137}Cs, 1.4 or 14 mGy/h) to 0.1 or 1 Gy with or without adding TGF-β. TGF-β-treated samples were applied as positive EMT controls and tested in parallel to find out if the radiation has a potentiating effect on the EMT induction. To evaluate the effect of the stromal component, the epithelial cells were irradiated in cocultures with stromal MRC-9 lung fibroblasts. On day 3 post treatment, the EMT markers: α-SMA, vimentin, fibronectin, and E-cadherin, were analyzed. The oxidative stress levels were evaluated by 8-oxo-dG analysis in both epithelial and fibroblast cells. The protracted exposure to low Linear Energy Transfer (LET) radiation at the total absorbed dose of 1 Gy was able to induce changes suggestive of EMT. The results show that the presence of the stromal component and its signaling (TGF-β) in the cocultures enhances the EMT. Radiation had a minor cumulative effect on the TGF-β-induced EMT with both doses. The oxidative stress levels were higher than the background in both epithelial and stromal cells post chronic irradiation (0.1 and 1 Gy); as for the BEAS-2B cell line, the increase was statistically significant. We suggest that the induction of EMT in bronchial epithelial cells by radiation requires more than single acute exposure and the presence of stromal component might enhance the effect through free radical production and accumulation.

1. Introduction

Ionizing radiation has been pointed out as the second leading cause for lung cancer after smoking [1]. However, there are no detailed mechanistic models for the early stages of radiation-induced lung carcinogenesis so far.

Over the last fifteen years, the important role of the tissue microenvironment (stroma) for the early stages of carcinogenesis and particularly the role of microenvironment in radiation-induced breast cancer have been highlighted [2–5]. The stroma of the tissue provides the "soil" for the transformed cells to grow and invade distant from their origin causing metastasis. It also produces specific chemokines and signaling molecules such as transforming growth factor beta (TGF-β), epidermal growth factor (EGF), and hepatocyte growth factor (HGF) during tumorigenesis [2, 3].

An important step during the modification of the microenvironment is the induction of morphological and functional changes of the normal stromal fibroblasts. These

activated growth factor- and chemokine-secreting fibroblast cells are very often associated with the tumor microenvironment and are thus called cancer-associated fibroblasts (CAFs) [6, 7]. They are considered to be able to induce tumor growth and dissemination via secretion of different factors, stimulate angiogenesis, and interact with the tumors' growth factor receptors. CAFs have a set of common characteristics that allows for easy distinguishing from normal fibroblasts. The majority of these CAF markers have been identified as various tropic molecules and extracellular matrix remodeling enzymes: alpha-smooth muscle actin (α-SMA), matrix metalloproteinase-1 (MMP1), matrix metalloproteinase-3 (MMP3), and collagens [8, 9]. The expression of some myofibroblast markers, such as α-SMA, can be used as predictive markers for cancer recurrence and distant metastasis [7].

In the last decades, a process taking part in the epithelial cells has been described—epithelial-to-mesenchymal transition (EMT) [10–12]. It has a role not only in organogenesis and wound healing but also in disease pathogenesis like fibrosis and cancer. During EMT under microenvironmental stimulation, the epithelial cells change their shape and lose their polarity as well as expression of epithelial markers. At the same time, they acquire a spindle-shaped mesenchymal phenotype and gain expression of mesenchymal markers [13].

One of the important pathways shared by EMT and tumorigenesis is the activation of the TGF-β signaling pathway [11–14]. The TGF-β molecule affects the tumor microenvironment as it decreases the levels of active immune system cells, increases angiogenesis, and facilitates invasion by enhancing the cellular protease activity and the production of extracellular matrix components by the tumor microenvironment cells. It is interesting from the radiation point of view that the TGF-β pathway is induced by oxidative stress, which is one of the main cell-damaging conditions produced by low LET radiation [15] particularly at a low-dose rate [16]. The connection between oxidative stress, TGF-β signaling, and the role of the microenvironment in radiation-induced cancer has been studied in detail for breast models [4, 5, 17]. It was also proven that low dose and low-dose rate gamma radiation at mGy/h range induces oxidative stress by increasing the endogenous production of reactive oxygen species in primary human fibroblast cells (VH10), whole blood samples, and human lymphocytes [18]. Exposure to ionizing radiation (IR) is regarded as a sensitizing factor for cells to undergo TGF-β-induced EMT. Andarawewa et al. [19, 20] showed that a single exposure to IR sensitizes cells to TGF-β-mediated EMT. Neither radiation nor a chronic TGF-β secretion alone could induce EMT [19–22]. Radiation-induced secretion of TGF-β, not from the epithelial cells themselves, but from the surrounding stroma may increase the occurrence of EMT, which could be one of the early stages in the radiation-activated tumorigenic changes [23].

The latent TGF-β activation due to reactive oxygen species (ROS) is so efficient that it can be used as a sensor for the oxidative stress [17]. TGF-β is also upregulated in a NSCLC (non-small-cell lung cancer) patient's blood samples during radiotherapy [24]. The high TGF-β levels have been connected not only with severe late effects but also with insufficient response to radiotherapy. The TGF-β signaling pathway has been known for many years to be involved in the tissue remodeling and induction of late effects of radiotherapy in the lung, as it has been considered one of the main mediators of tissue fibrosis in the organ [12, 25].

In this pilot project, we tested the hypothesis that radiation modifies the lung stromal cells, thus creating an environment that facilitates EMT and promotes tumorigenesis. Our aim was to investigate the role of the microenvironment in the induction of EMT in human lung epithelial cells after protracted low-dose rate γ-ray exposures, which so far has not been explored. Such type of protracted radiation exposures with low-dose rates could occur in real life for example to workers at uranium mines or to individuals living in near proximity of contaminated areas [26–28]. To our knowledge, this is the first of its kind study of lung epithelial cells and the questions we address need further and more detailed investigation in the future to reveal the mechanisms of radiation-induced lung carcinogenesis.

2. Materials and Methods

2.1. Cell Culture. The human bronchial epithelial cell line BEAS-2B was purchased from the American Type Culture Collection (ATCC, Manassas, VA, USA) and maintained in serum-free Bronchial Epithelial Cell Growth Medium (BEGM) medium (Lonza, Walkersville, MD, USA), supplemented with Bronchial Epithelial Cell Growth Medium SingleQuots™ Supplements and Growth Factors (Lonza). The HBEC-3KT bronchial epithelial cell line was kindly provided by Professor Jerry Shay (UT Southwestern, TX, USA). The cells were immortalized in the laboratory of Prof. Shay and further cultured as described by Ramirez et al. [29]. In brief, the cells were cultured in KSF (Keratinocyte Serum-Free) media (Gibco, Carlsbad, CA, USA) supplemented with epidermal growth factor 1-53 (EGF 1-53) and Bovine Pituitary Extract (BPE) provided frozen from the manufacturer. The MRC-9 normal human lung fibroblasts were purchased from the ATTC. The cells were expanded and maintained in Eagle's Minimum Essential Medium (Sigma-Aldrich, St. Louise, MO, USA) supplemented with fetal bovine serum and L-glutamine as instructed by the supplier.

The cells were stimulated with 0.1-0.2 ng/ml recombinant human TGF-β1 (#240-B-002, R&D Systems, Minneapolis, USA).

2.2. Coculturing of the Cells. For the coculture experiments, 1×10^4 BEAS-2B or HBEC-3KT cells were plated on 0.42 cm^2 polycarbonate membrane inserts with a 0.4 μm pore size (Nunc, Thermo Fisher Scientific, Waltham, MA, USA) and placed into 35 mm plastic petri dishes (Corning, Tewksbury, MA, USA). For the coculturing, 1×10^5 MRC-9 normal human lung fibroblasts were plated on the bottom of the 35 mm plastic petri dishes, and the standing inserts, containing BEAS-2B or HBEC-3KT epithelial cells, were placed into the p35 dishes. The

cocultures were maintained in ALI (Air-Liquid Interface) media consisting of 1 : 1 KSF and DMEM supplemented with 10% FCS and further modified as described in [30]. The incubation time before analysis was three days.

2.3. Irradiation. The chronic exposures (1.4 or 14 mGy/h) were implemented in a sterile cell culture incubator (Sanyo, Japan) equipped with a ^{137}Cs source at the Centre for Radiation Protection Research, The Wenner-Gren Institute, Stockholm University. The total doses applied were 0.1 Gy (1.4 mGy/h) and 1 Gy (14 mGy/h) as both took 72 hrs. A separate Sanyo incubator was used for nonexposed cells. Three biological replicates were collected from each dose and treatment. The experiments were repeated two or three times as noted in the figure legends.

2.4. Immunofluorescence Staining. The cells were plated on membrane inserts on the starting day of the irradiation and cultured for three days until the cumulated dose reached 0.1 or 1 Gy. The cells were fixed with 4% paraformaldehyde for 20 min at room temperature (RT). The blocking was done with 5% FCS (GIBCO) and 0.3% Triton X-100 (Sigma-Aldrich) in PBS at RT for 30 min. The primary antibodies were added to the cells diluted in 1% FCS in 0.3% Triton-X-100-PBS: anti-vimentin (monoclonal mouse anti-human #V6630, Sigma-Aldrich) 1 : 200 for 1 h at RT; anti-E-cadherin 1 : 100 (monoclonal rabbit anti-human #3195, Cell Signaling, Denver, MA, USA) for overnight at 4°C; and anti-fibronectin 1 : 20 (polyclonal sheep anti-human #AF1918, R&D Systems, Minneapolis, MN, USA), again overnight at 4°C. The incubation with secondary Alexa-488-conjugated antibodies (Invitrogen, Carlsbad, CA, USA) was performed for 1 h at room temperature. The cells were mounted with propidium iodide containing antifading media Vectashield (Vector Laboratories, Burlingame, CA, USA). Imaging was performed with a Zeiss AxioImager Z1 fluorescence microscope using AxioVision image analysis software (Carl Zeiss, Göttingen, Germany). The EMT status of the immunofluorescence images was evaluated via blind scoring from two independent researchers following clear scoring criteria and TGF-β-treated samples as positive controls. The criteria for EMT-positive were increase in cell size and cell elongation, combined with (1) relocalization of vimentin (BEAS-2B cells) or (2) loss of E-cadherin (HBEC-3KT). The results from the blind scoring were combined and reported. For the cell size measurements, we used the manual cell analysis tool from the ImageJ 1.04 (National Institutes of Health, Bethesda, MD, USA, http://imagej.nih.gov/ij/, 1997-2016) software. Briefly, the cells were marked manually and included in the Region Of Interest (ROI) tool. The measure function from the ROI menu was used to create a table including the area information of each cell. One hundred cells were analyzed from each condition.

2.5. Western Blotting. On day 3 after the irradiation onset when the planned dose (0.1 or 1 Gy) has been cumulated, the cells were lysed in buffer containing 8 M Urea, 1 M Thiourea, 30 mM Tris, 4% Chaps buffer 1% protease inhibitor cocktail (Roche, Mannheim, Germany), and 1% phosphatase inhibitor mixture (Protein phosphatase inhibitor cocktail 2 and 3, Sigma-Aldrich). 10 μg of the protein solution was loaded per lane on 4-12% Bis-Tris Amersham precast gels (GE Healthcare Bio-Sciences, Uppsala, Sweden). The separated proteins were transferred onto a PVDF membrane (Bio-Rad Laboratories, Hertfordshire, UK). After incubating with the blocking buffer (5% skimmed milk, 0.5% Tween-20 in PBS or 5% BSA in 0.75% PBS-Tween-20) for 1 h at RT, the membranes were blotted with antibodies against fibronectin (polyclonal sheep anti-human #AF1918, R&D Systems) 1 : 30 000; E-cadherin (monoclonal rabbit anti-human #3195, Cell Signaling) 1 : 5 000; α-SMA 1 : 5 000 (monoclonal mouse anti-human #A5228, Sigma-Aldrich); TGF-β1 1 : 5000 (polyclonal rabbit anti-human #NB100-91995, Novus Biologicals, Littleton, CO, USA); and GAPDH 1 : 50 000 (monoclonal mouse anti-human #G8795, Sigma-Aldrich) overnight at 4°C. The blots were incubated with secondary HRP-conjugated antibodies (GE Healthcare) for 1 h at room temperature followed by treatment with Super-Signal ECL (Thermo Fisher Scientific, Rockford, IL, USA) and developed on an X-ray sensitive film (GE Healthcare, Buckinghamshire, UK). Protein expression was quantified using the semiquantitative gel analysis function of the ImageJ 1.04 (National Institutes of Health, Bethesda, MD, USA, http://imagej.nih.gov/ij/, 1997-2016) software. The results of each individual protein were normalized to the GAPDH expression.

2.6. 8-oxo-dG Analysis. For the 8-oxo-dG analysis, medium was collected simultaneously with cell harvesting and kept frozen at -20°C. The 8-oxo-dG was measured using a modified ELISA assay as described previously [31, 32]. The ELISA kit was provided by Health Biomarkers Sweden AB. Briefly, 1 ml medium was filtered once using a C18 solid phase extraction column (Varian, CA) as described previously [33]. This step is necessary to remove any products other than the 8-oxo-dG that could cross-react with the monoclonal antibody that was used in ELISA. The purified samples were freeze-dried and reconstituted in PBS. 90 μl of the purified sample was mixed with 50 μl of a primary antibody against 8-oxo-dG (Japan Institute for the Control of Aging, Japan) and transferred to a 96-well ELISA plate precoated with 8-oxo-dG. After overnight incubation at 4°C, the plates were washed three times with 250 μl of washing solution. 140 μl of HRP-conjugated secondary antibody (goat anti-mouse IgG-HRP, Scandinavian Diagnostic Services, Sweden) was added to each well and incubated for 2 hours at room temperature. The wells were washed three times with 250 μl of washing solution and finally with PBS (pH 7.4). Then, 140 μl of tetramethylbenzidine liquid substrate (ICN Biomedicals Inc., USA) was added to each well, and the plate was incubated for 15 min at room temperature. The reaction was terminated by adding 70 μl of 2 M H_3PO_4 (Merck, Germany). The absorbance was read at 450 nm using an automatic ELISA plate reader (UV-160A, Shimadzu, Kyoto, Japan). Each sample was analyzed in triplicate (variation = 2.5%), and the samples of each

experiment were analyzed using the same 96-well ELISA plate. A standard curve for 8-oxo-dG (0.05-10 ng/ml) was established for each plate covering the range of 8-oxo-dG in the samples. The validation of the modified ELISA method was performed by HPLC-EC (r^2: 0.87, $p < 0.05$) as described previously [32]. The comparisons between the ELISA and the HPLC-EC methods showed a linear correlation at the concentration range found in the human blood serum [32]. There was no correlation between the ELISA and the HPLC-EC results when unfiltered samples were used.

2.7. Statistical Analysis. Differences between groups were analyzed using paired two-sample Student's t-test, part of Excel, MS Office 2003 package, with nonequal assumption of variances or with one-way ANOVA, and Tukey's posttest, part of the statistical package of GraphPad Prism 4 (GraphPad, La Jolla, USA) as noted in the text.

3. Results

3.1. Protracted γ-Radiation with a Dose Rate of 14 mGy/h (1 Gy Total Dose) Induces Changes Connected with EMT in BEAS-2B and HBEC-3KT Bronchial Epithelial Cell Lines. A low-dose rate irradiation facility was used to perform a series of protracted irradiation experiments with two bronchial epithelial cell lines (BEAS-2B and HBEC-3KT). The cells were plated on membrane inserts and exposed to either 1.4 or 14 mGy/h up to 0.1 or 1 Gy cumulated doses, respectively, over a time period of three days as described in Materials and Methods. The cell lines were immunostained for vimentin (BEAS-2B) and E-cadherin (HBEC-3KT). These markers were selected after the two lines were screened for sensitivity to EMT-inducing stimuli and EMT marker expression levels [34]. BEAS-2B cells showed significant changes in vimentin expression and HBEC-3KT in E-cadherin expression, and these two markers were used in [34] and further as the most sensitive.

After exposure to protracted irradiation, we observed EMT-related changes (while vimentin levels increase and extend throughout the cytoplasm relative to control, the E-cadherin decreases at the plasma membrane relative to control) in both cell lines after treatment with a dose rate of 14 mGy/h and a total dose of 1 Gy (Figure 1). No EMT and change in the cell size were seen after treatment with 1.4 mGy/h (0.1 Gy total dose). With the higher applied dose (1 Gy), we observed both EMT and a statistically significant increase in the cell size compared to the control. The results show that the mesenchymal marker vimentin was relocalized in BEAS-2B cells undergoing EMT (Figure 1(a)). In the nontreated BEAS-2B cells, vimentin was forming a dense spot in the cytoplasm, while in the cells that had undergone EMT-consistent changes, vimentin was forming a fine intermediate filament network. The BEAS-2B cells changed from an epithelial cuboidal morphology to the elongated form of mesenchymal cells. Interestingly, the cells were exhibiting long cytoplasmic protrusions post irradiation (Figure 1(a), blue arrows). The right panels in Figure 1(a) visualise the changes in cell size and shape during the EMT process in BEAS-2B cells. The inserts have the same size; however, in EMT-positive fields 2, 3, and 4, they contain fewer but larger cells with an elongated shape. We have performed measurements of the elongation of the cells (Suppl. Fig 1). The white arrows show the level of cells which undergone EMT changes in each panel. The areas were selected to represent EMT negative control, positive control (TGF-β), irradiated only cells (EMT-positive), and irradiated plus TGF-β-treated cells (EMT-positive). When the cell area of the BEAS-2B cells was measured, there was a statistically significant increase in the size post 1 Gy compared to the nontreated controls (Figure 1(c), BEAS-2B graph).

In HBEC-3KT cells, the epithelial marker E-cadherin was decreasing in the cell-to cell-contacts in some, but not all cells. In addition, we observed changes in the cell size in the HBEC-3KT cells as marked in the right side panels containing again the same size insets (Figure 1(b), 1–4). At confluence before the exposure, the cells were small with cobblestone epithelial morphology (Figure 1(b), "No EMT" panels), while after irradiations, they had grown to large (Figure 1(b), "EMT" panels, white arrows) cells. The enlarged areas help to compare the cell size and shape changes between the control (Figure 1(b), 1) and 1 Gy irradiated cells (Figure 1(b), 4). We also performed the measurement of the cell size for the HBEC-3KT cells (Figure 1(c), HBEC-3KT graph). The results were similar as for the BEAS-2B, there are no increase of the size at 0.1 Gy and statistically significant increase at 1 Gy, compared to the control.

In addition to chronic irradiation, we treated the cells with a minimal EMT-inducing concentration of TGF-β (0.1-0.2 ng/ml) and the same protracted doses of ionizing radiation at dose rates of 1.4 and 14 mGy/h (total dose 0.1 and 1 Gy, respectively) (Figures 1(a) and 1(b), lower images). In this experimental setup, where we investigated the potentiating effect of radiation on TGF-β-induced EMT, a statistically significant additive effect was observed only with 1 Gy radiation for the BEAS-2B cells (Figure 1(c)).

While the effect of irradiation on the expression and relocalization of the EMT markers was clear when detected by immunofluorescence, western blotting and semiquantitative evaluation show significant changes to the control only at 0.1 Gy in BEAS-2B cells and 0.1 Gy +TGF-β treatments for the fibronectin marker (Figure 2) for both cell lines. Vimentin is a good marker for immunofluorescence studies but not expected to be quantitative for western blots because the concentration of the vimentin protein is not changed, rather distribution within the cytoplasm is more diffused during EMT. That is why we have compared only E-cadherin and fibronectin in the western blots.

Although the analysis failed to show a statistical significance in the majority of the western blot analyses (except BEAS-2B 0.1 Gy and 0.1 Gy+TGF-β and HBEC-3KT 0.1 Gy+TGF-β for fibronectin), a trend characteristic for EMT (increase of fibronectin and decrease of E-cadherin levels) and also enhancement of the TGF-β-induced

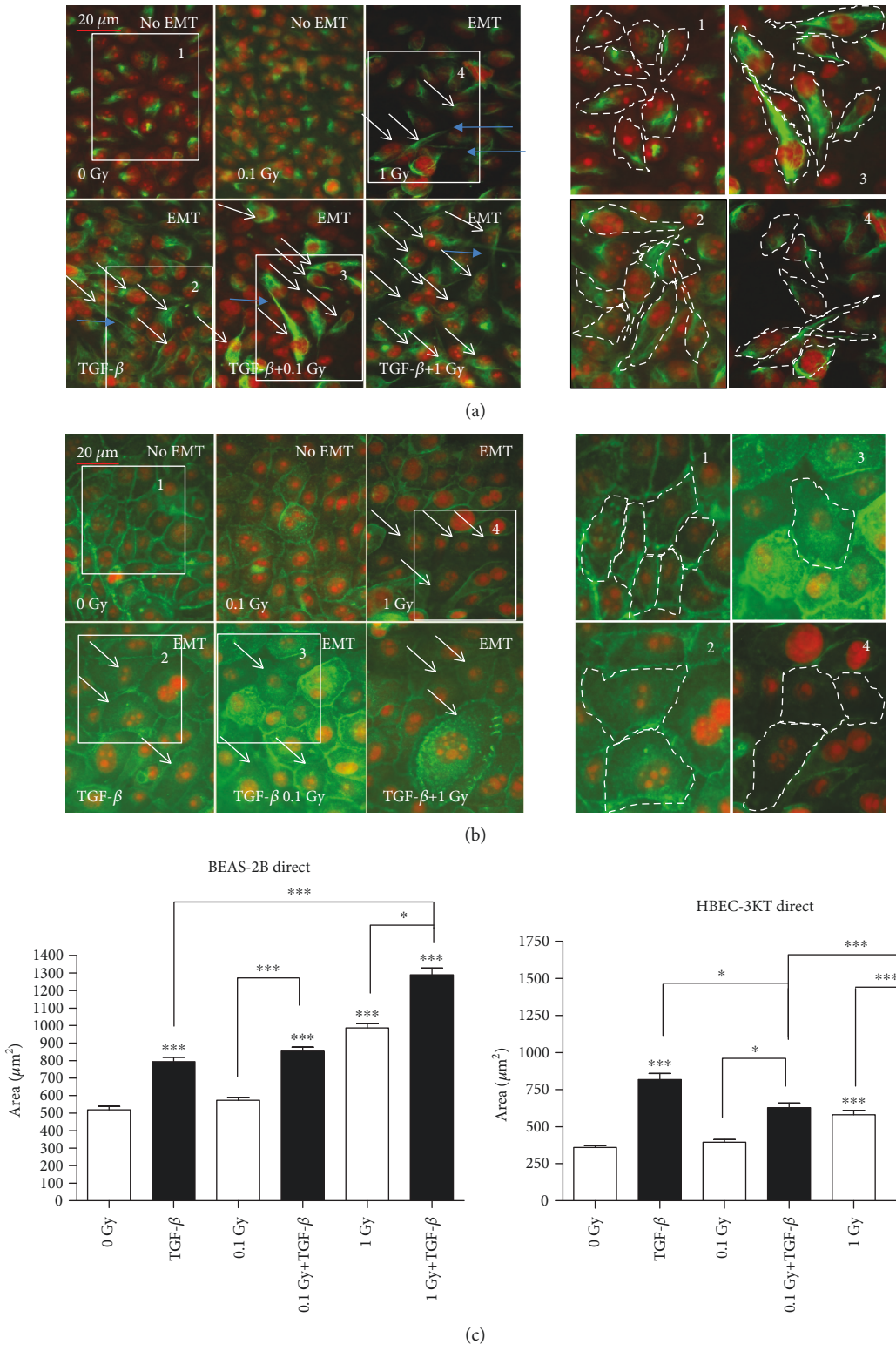

Figure 1: Immunofluorescence staining of EMT marker expression in lung epithelial cell lines: (a) in BEAS-2B with vimentin staining and (b) in HBEC-3KT with E-cadherin staining. The cells were exposed to 0.1 or 1 Gy protracted radiation at a dose rate of 1.4 or 14 mGy/h, upper panels. Lower panels: positive TGF-β control and EMT enhancement after combined treatment of the cells with TGF-β and 0.1 or 1 Gy of protracted radiation. Vimentin and E-cadherin are stained in green. The nuclei are counterstained with propidium iodide (red). White arrows indicate cells with changes consistent with EMT. Cytoplasmic protrusions are marked with blue arrows. The enlarged same size areas on the right side of (a) for vimentin and (b) for E-cadherin. Numbers 1-4 are visualising the change in cell shape and size: (1) control, (2) TGF-β, (3) TGF-β+0.1 Gy, and (4) 1 Gy. Scale bars: 20 μm. (c) ImageJ measurements of the cell size in the BEAS-2B and HBEC-3KT cells from the image series (a, b). $^{*}p < 0.05$ and $^{***}p < 0.001$; one-way ANOVA and Tukey's posttest ($n = 3$).

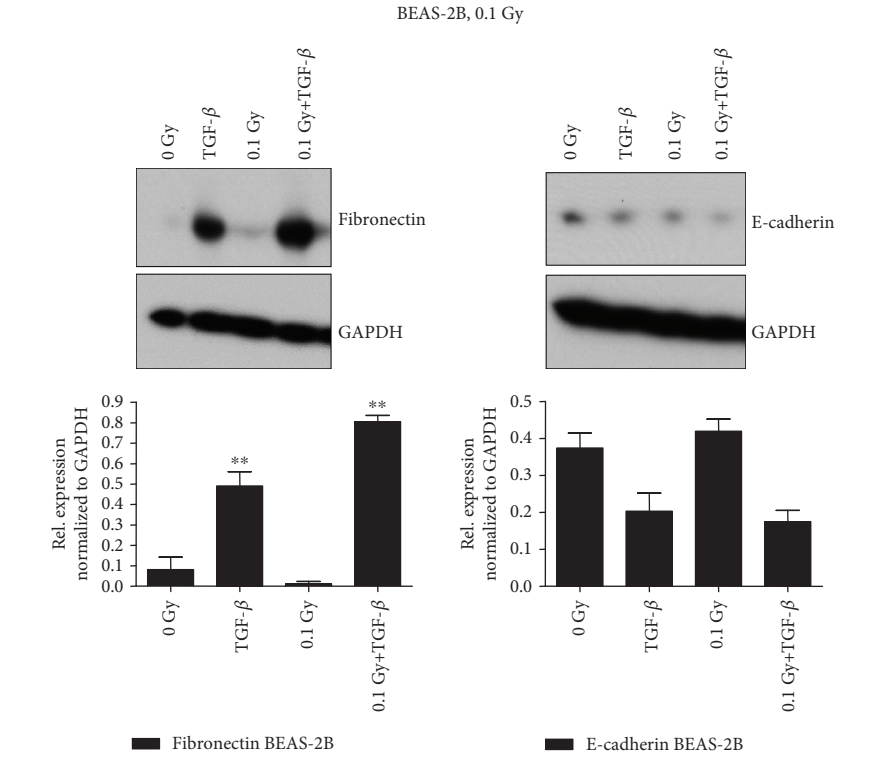

(a)

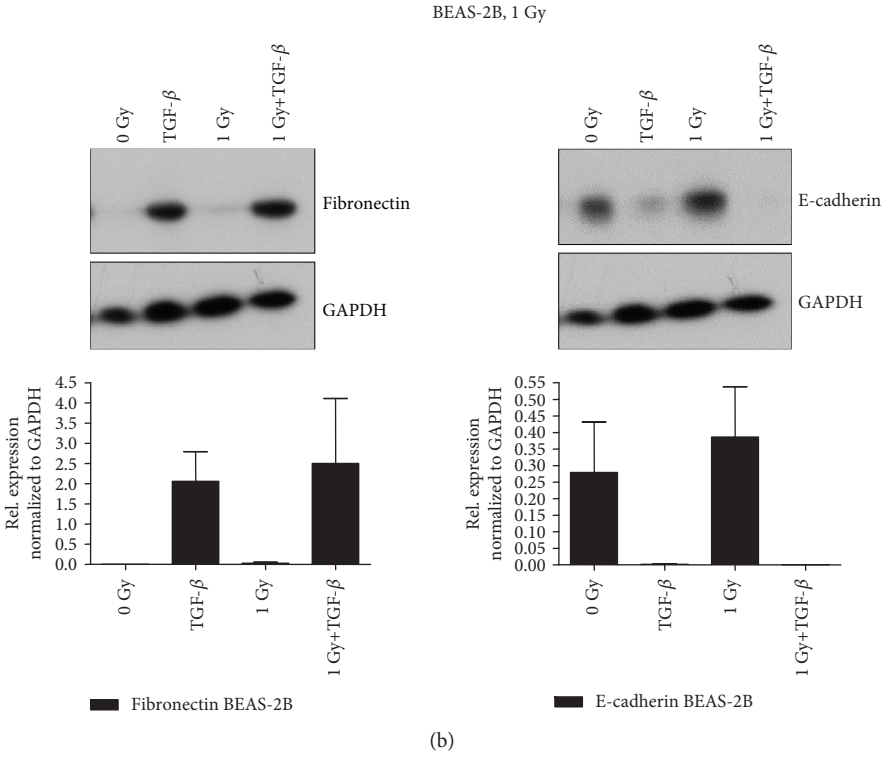

(b)

Figure 2: Continued.

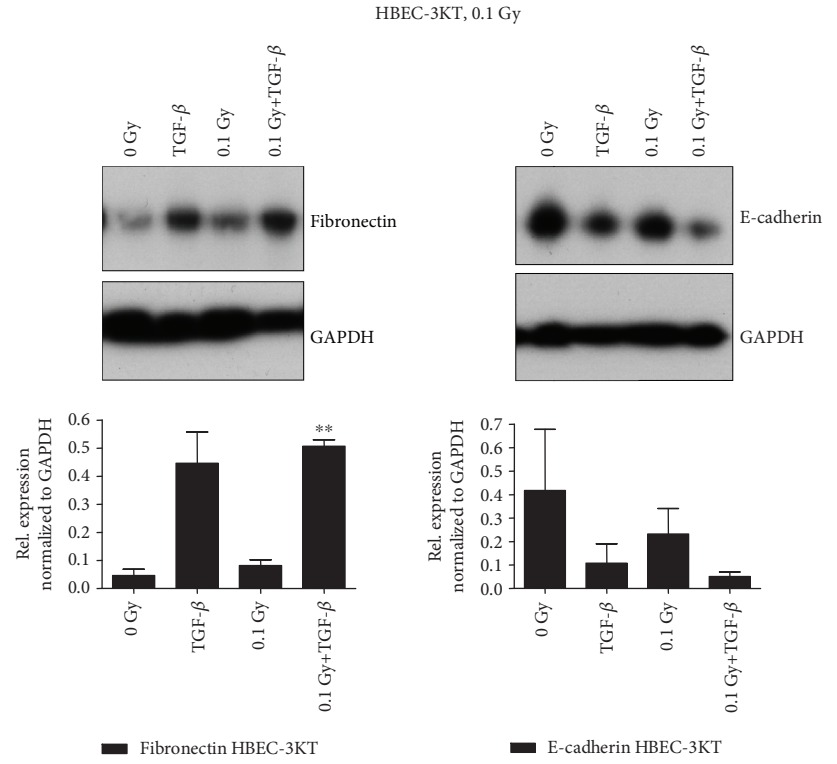

(c)

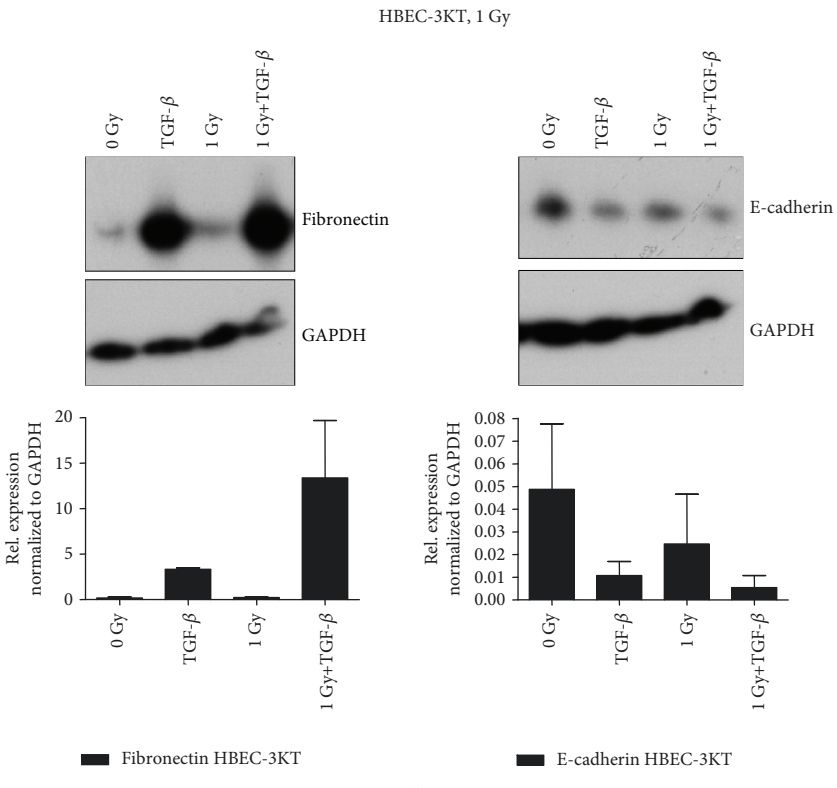

(d)

Figure 2: Western blotting analyses of EMT marker expression (a, b) in BEAS-2B and (c, d) HBEC-3KT cells chronically irradiated to a total dose of (a, c) 0.1 (at 1.4 mGy/h) or (b, d) 1 Gy (at 14 mGy/h). Representative western blot analyses of fibronectin expression (a–d, left side blots) and E-cadherin expression (a–d, right side blots). The graphs below are results of quantification of the protein expression as described in Materials and Methods. Error bars—standard deviation, comparison to untreated control. $^{**}p < 0.01$, one-way ANOVA and Tukey's posttest ($n = 3$).

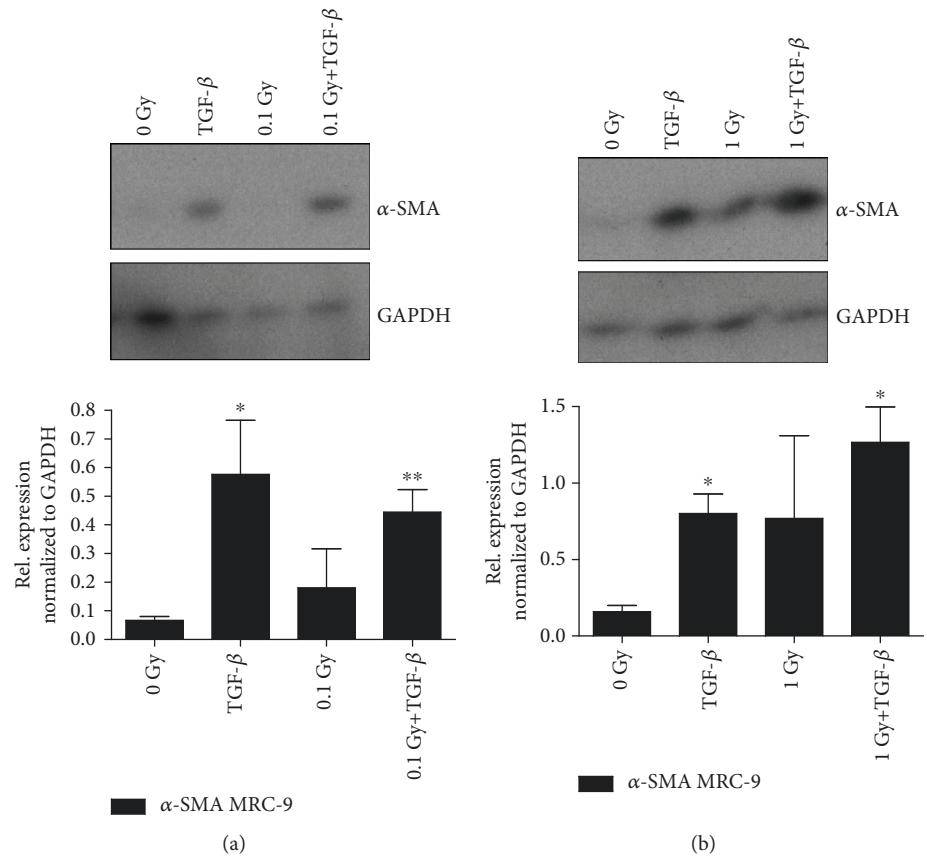

Figure 3: Myofibroblastic marker α-SMA expression in MRC-9 fibroblasts post chronic low LET irradiation at dose rates of (a) 1.4 mGy/h to 0.1 Gy or (b) 14 mGy/h to 1 Gy with or without TGF-β. The graphs below are the results of the semiquantification of the protein expression as described in Materials and Methods. Error bars—standard deviation. $^{*}p < 0.05$ and $^{**}p < 0.01$; one-way ANOVA and Tukey's posttest ($n = 3$).

EMT in combination with the IR (Figure 2) were observed in the HBEC-3KT cells. The other cell line BEAS-2B responded with EMT characteristic changes in the fibronectin and E-cadherin only to TGF-$\beta\pm$ irradiation.

3.2. Effect of the Microenvironment on EMT Characteristic Changes in Fibroblast-Epithelial Cell Cocultures. The microenvironment is involved in the TGF-β-induced EMT process via secretion of signaling molecules from the stromal cells [35, 36]. We observed that TGF-β induces higher expression of α-SMA, an actin isoform involved in the formation of stress fibers during myofibroblastic differentiation in MRC-9 cells (Figure 3) [7, 11]. There is also a trend in increased α-SMA with 1 Gy ionizing radiation in the MRC-9 cells.

As shown in Figure 3(a), a dose of 0.1 Gy delivered at 1.4 mGy/h was able to increase slightly the α-SMA expression. The 1 Gy exposures induced a higher level of the stress fiber protein in comparison to the 0.1 Gy (Figure 3). The combination of TGF-β treatment and 1 Gy radiation exposure had some cumulative effects on the α-SMA expression compared to the TGF-β only. However, we have to point that we could not show a statistically significant increase of the radiation and TGF-β effects in comparison to the TGF-β treatments alone (Figure 3).

In coculturing experiments the epithelial (BEAS-2B or HBEC-3KT) cells were plated in membrane inserts while the stromal cells were plated in 35 mm Petri dishes. The cocultures were either sham irradiated or exposed to the same cumulative doses of 0.1 and 1 Gy at 1.4 or 14 mGy/h, respectively. To test if the coculture ALI medium that contains 5% fetal calf serum (potentially containing minimal quantities of TGF-β) induces the EMT changes in the epithelial cells, we had a parallel negative control where the cells were incubated in the ALI medium without a coculture with the MRC-9 fibroblast. As shown in Suppl. Fig 2, the ALI medium was not able to induce the EMT. At the same time, the coculture and the same exposure time of 14 mGy/h irradiation had a higher EMT-inducing effect than radiation only (Figures 1 and 4).

In the BEAS-2B cells, enhanced EMT characteristic changes were detected when the cells were cocultured with fibroblasts and irradiated with a dose rate of 14 mGy/h up to a cumulative dose of 1 Gy, in comparison to those irradiated with a dose rate 1.4 mGy/h to a dose of 0.1 Gy over the same time period (Figure 4(a)). With the HBEC-3KT cells, coculturing with fibroblasts enhanced radiation and the TGF-β-induced EMT-specific changes with a dose of 1 Gy (Figure 4(b)). Interestingly, the features of the cocultured cells undergoing EMT-like transformation, for both BEAS-2B and HBEC-3KT, are different than those of the

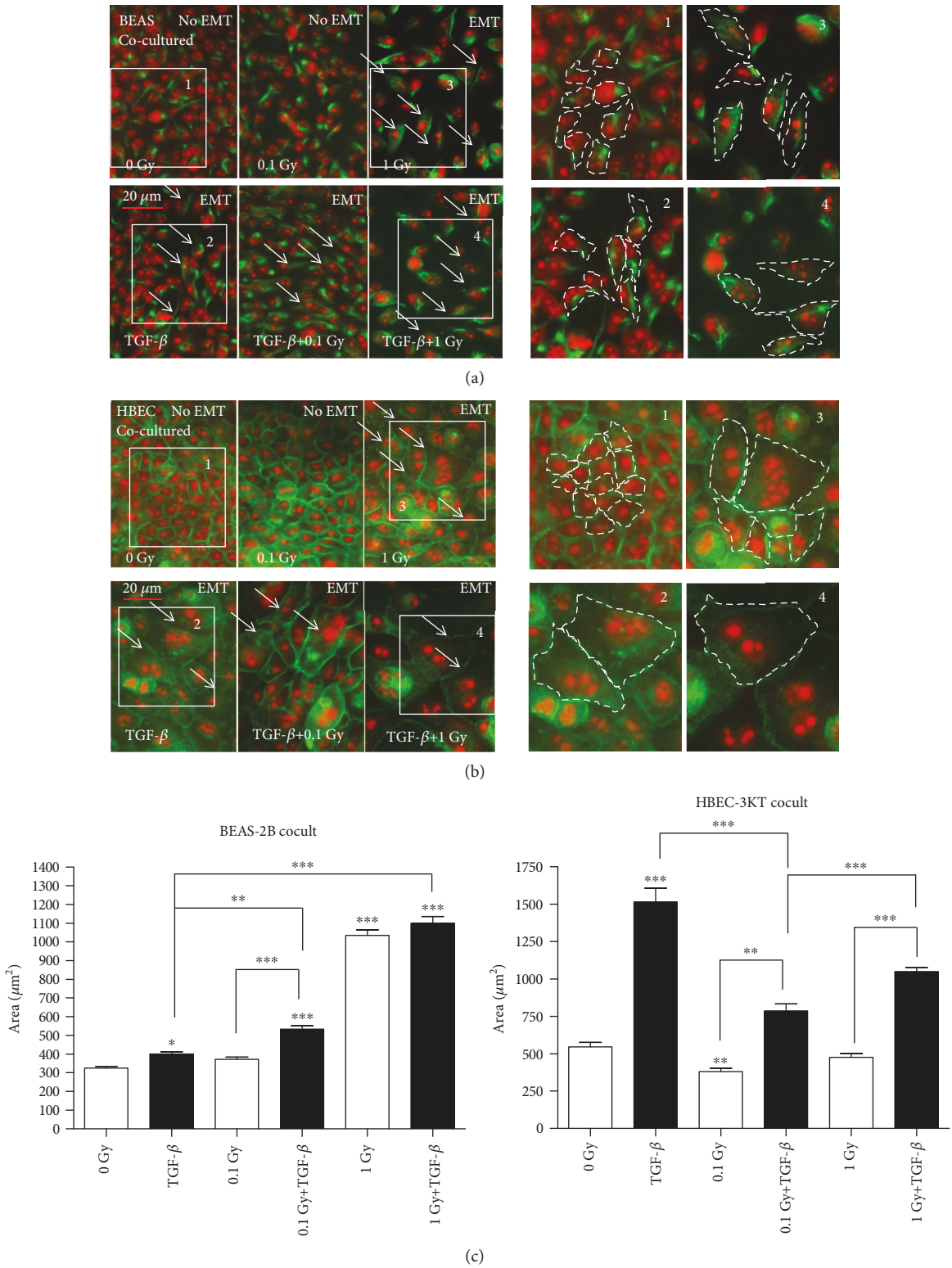

Figure 4: Immunofluorescence staining of EMT marker expression in lung epithelial cell lines cocultured with MRC-9 fibroblasts: (a) vimentin in BEAS-2B and (b) E-cadherin in HBEC-3KT. The cocultures were exposed to 0.1 or 1 Gy of protracted radiation at the dose rates of 1.4 or 14 mGy/h, upper panels. Lower panels: positive control TGF-β treatment and the EMT enhancement after the combined treatment of the TGF-β+0.1 cells or 1 Gy of protracted radiation. Vimentin and E-cadherin are stained in green. The nuclei are counterstained with propidium iodide (red). White arrows indicate the cells with consistent changes. Scale bars: 20 μm. The enlarged same size areas on the right side of (a) for vimentin and (b) for E-cadherin with numbers 1-4 are visualising the change in cell shape and size: (1) control, (2) TGF-β, (3) 1 Gy, and (4) TGF-β+1 Gy. (c) ImageJ measurements of the cell size in the BEAS-2B and HBEC-3KT cells from the image series (a, b). $^{*}p < 0.05$, $^{**}p < 0.01$, and $^{***}p < 0.001$; one-way ANOVA and Tukey's posttest ($n = 3$).

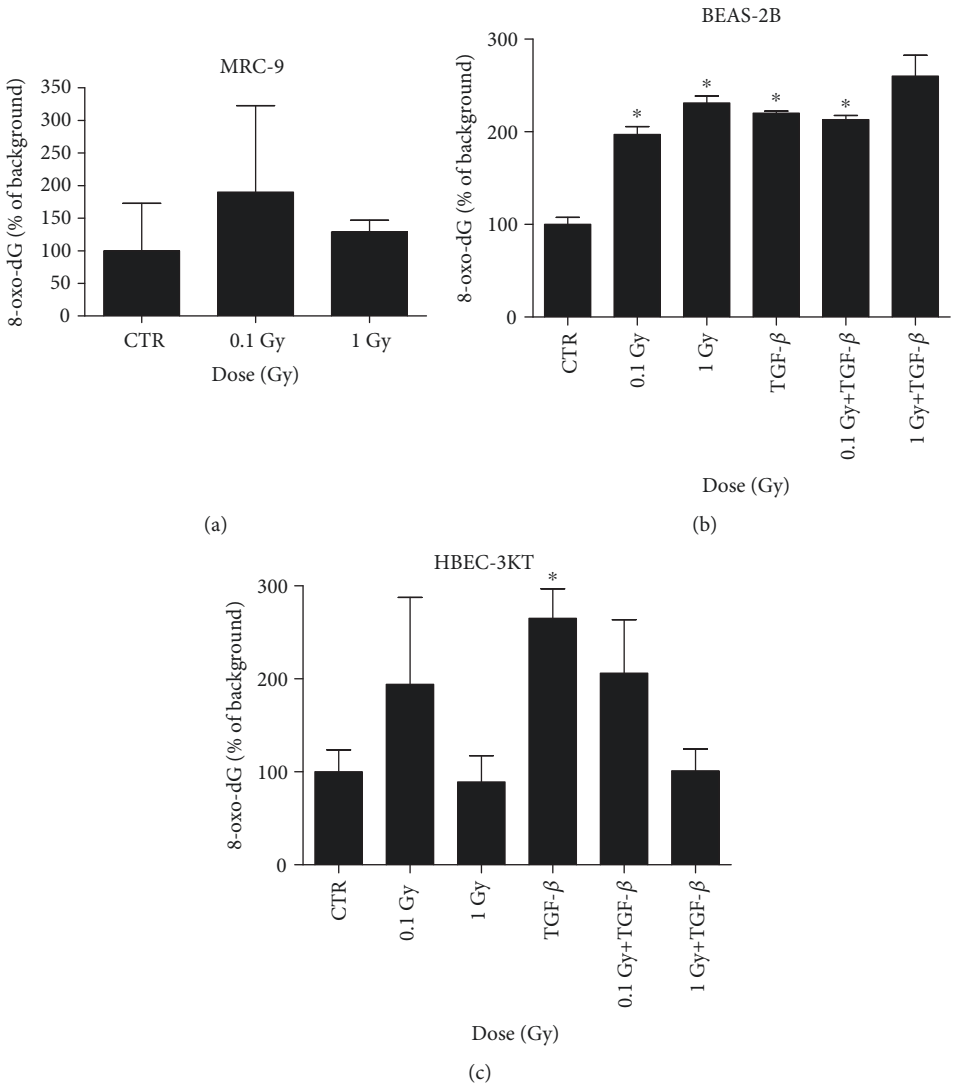

Figure 5: 8-oxo-dG secretion in chronically irradiated MRC-9 fibroblast cells (a), (b) BEAS-2B or (c) HBEC-3KT cells. The cells have been exposed to a total of 0.1 (at 1.4 mGy/h) or 1 Gy (14 mGy/h). Error bars—standard deviation. Statistical analysis—Student's t-test ($n = 2$) (a). In addition, the same cells were treated with the TGF-β in combination to radiation ((b) 0.1 or (c) 0.2 ng/ml) as described in Materials and Methods. Error bars—standard deviation. $^*p < 0.05$; one-way ANOVA and Tukey's posttest ($n = 2$).

monocultures (Figure 4 and Suppl. Fig 3). As could be seen in Figure 4 and the insets (Figures 4(a) and 4(b), 3 and 4), the irradiated and TGF-β-treated cells are both larger than control and compared to the TGF-β only (Figure 4(c)), and for the HBEC-3KT (Figure 4(b), 3 and 4), they are containing more than one nucleus (Figure 4(b)).

3.3. 8-oxo-dG Production from MRC-9, BEAS-2B, and HBEC-3KT Cells. Radiation-induced oxidative stress is one of the main cell-damaging conditions induced by low LET radiation such as X- or γ-rays. The reactive oxygen species generated during the exposure to radiation in aqueous solutions are able to damage biological molecules, including DNA and cytoplasmic DNA precursors (dNTP). One of the products from the oxidation of the deoxyribonucleotides, 8-oxo-dG, has proved to accumulate after irradiation. Radiation-induced extracellular 8-oxo-dG has been reported even after very low dose and low-dose rate exposures [18, 31]. In our study, chronic irradiation causes the increase of 8-oxo-dG from the MRC-9 fibroblasts in comparison with the background levels (Figure 5(a)). However, the induction was very small and not statistically significant. On the other hand, radiation-induced oxidative stress levels were increased in the chronically irradiated epithelial cell lines as in one of them, BEAS-2B we observed a statistically significant dose-dependent increase (Figure 5(b)).

Also, the combination of TGF-β treatment and irradiation had a slight cumulative effect on the 1 Gy delivered at 14 mGy/h. The second cell line, HBEC-3KT, although showing a statistically significant induction of 8-oxo-dG in the TGF-β treated cells, failed to respond to radiation or to a combination of radiation and TGF-β in the same statistically significant manner (Figure 5(c)). This might be explained with the differences in the genetic background and antioxidant properties of the two cell lines [29].

4. Discussion

Based on the data for synergy between TGF-β signaling and radiation exposure in a mouse mammary gland model [19, 37], we introduce a new mechanistic model for the lung in which protracted exposure to low-dose radiation activates the stromal TGF-β pathway and leads to the radiation-induced EMT of the lung epithelial cells. We have previously reported that low doses of gamma radiation induce oxidative stress in a nonlinear manner [31, 32] with a peak already at doses of about 5 mGy. In our earlier studies, cells exposed to low-dose chronic irradiation have constantly elevated oxidative stress [16]. We have also shown that the main target for radiation-induced oxidative stress is the intracellular nucleotide pool, dNTP, where different types of modified dNTP can be produced, e.g., 8-oxo-dGTP. 8-oxo-dGTP release from cells such as 8-oxo-dG can be detected as a measurement of oxidative stress [31, 32]. In this study, the results suggest that the low-dose rate radiation might induce oxidative stress and that this possibly activates TGF-β and leads to EMT-connected cell transformation, even with low cumulative dose exposure (0.1 Gy delivered at 1.4 mGy/h). We detected an increased level of the oxidative markers (8-oxo-dG) in the culture media of the irradiated and double treated (radiation and TGF-β) lung epithelial cells. Oxidative stress has been previously described to play a crucial role in the TGF-β activation [7, 31, 38]. We hypothesize that the elevated oxidative stress and the TGF-β signaling in lung epithelium and microenvironment are co-operating and acting synergistically leading to the observed enhanced EMT-consistent changes particularly for a dose of 1 Gy in the BEAS-2B cell line. In further studies, there should also be considered other important and more sensitive indicators of the TGF-β signaling activation such as p-smad 2/3 or the Pai-1 luciferase assay [10–12].

In our study, the additional treatment of the cells with a low concentration of TGF-β had a potentiating effect on the protracted low-dose radiation-induced EMT only when the cumulative dose reached 1 Gy for the BEAS-2B cell line. Earlier publications by Ehrhart et al. [39] showed that TGF-β is activated after low doses of low LET radiation in the *in vivo* mouse mammary gland model. Although they found a dose-dependent relationship for the activation of the factors, the observed effects were the strongest at the lowest dose applied (0.1 Gy). We observed a similar trend in our experiments for oxidative stress induction in the epithelial cell line (BEAS-2B) at 0.1 Gy. Earlier, we detected an increase in the TGF-β levels in the MRC-9 fibroblasts after acute exposure to doses of 0.1-2 Gy [34]. Other scientists have reported a significant role of TGF-β in the activation of oxidative stress response, especially in myofibroblastic cells during their invasive transformation [40].

The activation of TGF-β signaling in the MRC-9 cells post radiation is plausible as the molecule is one of the main fibroblast activators responsible for their transition into myofibroblasts or CAFs [36, 41]. As TGF-β is also an important factor produced by stromal cells post irradiation and involved in cancer progression, it has been widely considered a potential therapeutic target for reducing metastases and formation of secondary cancers after radiotherapy. Blocking its expression or application of functional inhibitors could be a potential therapy for secondary cancer dissemination [42, 43].

We investigated the effects of low-dose protracted radiation in two immortalized bronchial epithelial cell lines, which are commonly used as a model of lung epithelium. An interesting finding after the protracted low-dose rate irradiations was the detection of various EMT features in the epithelial cells that differed after irradiation compared to TGF-β induction. For example, the analysis of the BEAS-2B cells showed that the radiation-induced EMT was characterized by an elongated shape with single cilium-like cytoplasmic protrusions (Figure 1(a); 1 Gy, blue arrows), while the typical TGF-β-induced EMT phenotype was more spindle-shaped with a well-defined vimentin network (Figure 1(a); TGF-β, white arrows). The vimentin behavior could be connected with its functionality—the dense perinuclearly concentrated vimentin in the nontreated cells is nonactive, while the well-spread intermediate filament network has a crucial role for EMT and motility in many mesenchymal type cells [44]. The additive effect of radiation and TGF-β was observed only after the higher cumulated dose of 1 Gy for both cell lines. The role of the long protrusions in the irradiated cells is not clear. It is possible that the cells are being transformed into fibroblasts, which described a spindle shape and are expressing a high level of the mesenchymal marker fibronectin. Accumulation of EMT-generated fibroblasts could accelerate the radiation-induced lung fibrosis in agreement with Guarino et al. [25] and Lee and Nelson [13]. This should be studied further in more detail in a different setup that involves *in vivo* experiments.

In the coculturing experiments (Figure 4), we show an increase between TGF-β vs. 0.1 Gy+TGF-β and TGF-β vs. 1 Gy+TGF-β EMT-related changes only in BEAS-2B cells. The 8-oxo-dG is increasing in response to chronic irradiation or to TGF-β again only in the BEAS-2B cells (Figure 5(b)). However, the two effects do not appear to be additive except to small extent for the 1 Gy+TGF-β in the BEAS-2B cells.

In our prestudies with acute radiation exposures, some of the classical features of the EMT were not affected, although some of the markers or phenotypic features were changed. For example, the ZO-1 and β-catenin expression were not affected (data not shown), while the vimentin and E-cadherin were, respectively, up- or downregulated [34]. In the earlier study, we could not prove any clear EMT induction with low or moderate doses of α-particles and γ-rays. Also, no significant additive effect with radiation and TGF-β was observed. However, the results from the current study suggest that (1) radiation may induce partial EMT features; (2) the radiation and particularly the protracted radiation-induced EMT potentially have their own distinguishable features; (3) the combination of radiation and TGF-β has an additive effect on the EMT, but this particular feature very likely depends on the antioxidative properties of the cell line; and finally (4) stromal/epithelial cell cocultures enhance the induction of EMT in one of the two cell lines studied (BEAS-2B) suggesting that chronic *in vivo* exposures

can influence precarcinogenic changes in the normal epithelium via signals from the microenvironment.

In the two epithelial cell lines that have been used, there is a clear difference in the oxidative stress product levels post irradiation (Figures 5(b) and 5(c)). The BEAS-2A cells are more prone to accumulation of 8-oxo-dG than the HBEC-3KT cells. This can be connected to the viral oncoprotein (SV40 large T antigen) immortalization of the BEAS-2B cells [45]. While the immortalized HBEC-3KT cells are not carcinogenic, the BEAS-2B cells are closer in their genetic properties to tumor cells and can undergo malignant transformations after repetitive passaging [29]. The BEAS-2B cells are reported also to have lower antioxidant activities, e.g., for MnSOD [45]. This is compromising their defense against free radicals, leads to elevated extracellular 8-oxo-dG, and explains the dose response relation for radiation-induced extracellular 8-oxo-dG presented in Figure 5(b). For HBEC-3KT, no clear dose response relation for radiation-induced extracellular 8-oxo-dG was observed (Figure 5(c)). The response of HBEC-3KT cells at the levels of radiation-induced 8-oxo-dG in the medium suggests that HBEC-3KT cells might have a problem to release 8-oxo-dGTP from the cytoplasm to the medium as similar pattern of results were previously observed in primary fibroblast knockdown in the hMTH1 (Figure 5(c), [18]).

To our knowledge, there are no other studies describing how a chronic exposure to low doses and dose rates ionizing radiation affects both the microenvironment and the epithelial cells. We focused on the EMT process as one of the potential precarcinogenic stages undergone by the epithelial cells during malignant transformation. What we found was a partial EMT, concerning only some of the EMT features in the epithelial cells, when they were exposed to radiation without the stromal component. Further, some enhanced EMT-consistent changes were monitored in the TGF-β-treated and cocultured irradiated BEAS-2B epithelial cells. These observations suggest how the cellular transformation after low-dose radiation exposures depends on the cell-to-cell interactions.

Data Availability

The data used to support the findings of this study are available from the corresponding author upon request.

Conflicts of Interest

The authors declare that there is no conflict of interest regarding the publication.

Authors' Contributions

V.L. and S.H. introduced the concept of the project. A.A. and M.K. conceived and planned the experiments. A.A., M.K., and A.S. carried out the experiments. A.A. and M.K. analyzed the data. A.A. wrote the manuscript. S.H. and M.K. critically read and advised how to improve the manuscript.

Acknowledgments

This work has been supported by an EPIRADBIO grant (FP7-FI-2010-269553) under the Euratom-specific program for research and training on nuclear energy, 7th Framework Program, the Swedish Radiation Protection Authority (SSM) and the Swedish Cancer Society. The authors would like to thank Prof. Jerry Shay, UT Southwestern Medical Center, Dallas, TX, USA, for kindly providing the HBEC-3KT cell line, and to the team at CRPR, Stockholm University, Stockholm, Sweden, for the help with the protracted irradiations. The authors would like to express their deep grief from the early loss of V.L. She was the engine of this project and at the same time a respected colleague and supportive supervisor. Her joyful personality and positive attitude to the work-related challenges are greatly missed by all her colleagues.

Supplementary Materials

Supplementary Figure 1: elongation in lung epithelial cell lines BEAS-2B (A) and HBEC-3KT (B) post chronic irradiation with or without MRC-9 fibroblasts. Elongation factor (cell length by cell diameter) was calculated manually by ImageJ in 50 cells from each sample. Supplementary Figure 2: immunofluorescence staining of vimentin expression in lung epithelial cell line BEAS-2B cocultured with MRC-9 fibroblasts after protracted irradiation at 1.4 and 14 mGy/h to 0.1 or 1 Gy. Negative control without the fibroblast cells is shown on panel 0 Gy/-MRC-9. Supplementary Figure 3: comparison between the EMT markers' expression in monocultures of bronchial epithelial cells (A) BEAS-2B and vimentin and (B) HBEC-3K and E-cadherin upper panels; (A and B, lower panels) and cocultures of the same cells and MRC-9 fibroblasts, after a protracted irradiation at 1.4 and 14 mGy/h to 0.1 or 1 Gy. Vimentin and E-cadherin are stained in green. The nuclei are counterstained with propidium iodide (red). White arrows indicate the EMT undergone cells. Scale bars: 20 μm. *(Supplementary Materials)*

References

[1] D. R. Youlden, S. M. Cramb, and P. D. Baade, "The international epidemiology of lung cancer: geographical distribution and secular trends," *Journal of Thoracic Oncology*, vol. 3, no. 8, pp. 819–831, 2008.

[2] A. Östman and M. Augsten, "Cancer-associated fibroblasts and tumor growth – bystanders turning into key players," *Current Opinion in Genetics & Development*, vol. 19, no. 1, pp. 67–73, 2009.

[3] M. Allen and J. Louise Jones, "Jekyll and Hyde: the role of the microenvironment on the progression of cancer," *The Journal of Pathology*, vol. 223, no. 2, pp. 163–177, 2011.

[4] M. H. Barcellos-Hoff, "Stromal mediation of radiation carcinogenesis," *Journal of Mammary Gland Biology and Neoplasia*, vol. 15, no. 4, pp. 381–387, 2010.

[5] D. H. Nguyen, H. A. Oketch-Rabah, I. Illa-Bochaca et al., "Radiation acts on the microenvironment to affect breast carcinogenesis by distinct mechanisms that decrease cancer

latency and affect tumor type," *Cancer Cell*, vol. 19, no. 5, pp. 640–651, 2011.

[6] T. D. Tlsty and P. W. Hein, "Know thy neighbor: stromal cells can contribute oncogenic signals," *Current Opinion in Genetics & Development*, vol. 11, no. 1, pp. 54–59, 2001.

[7] O. De Wever, P. Demetter, M. Mareel, and M. Bracke, "Stromal myofibroblasts are drivers of invasive cancer growth," *International Journal of Cancer*, vol. 123, no. 10, pp. 2229–2238, 2008.

[8] P. Cirri and P. Chiarugi, "Cancer associated fibroblasts: the dark side of the coin," *American Journal of Cancer Research*, vol. 1, no. 4, pp. 482–497, 2011.

[9] M.-J. Tsai, W.-A. Chang, M.-S. Huang, and P.-L. Kuo, "Tumor Microenvironment: A New Treatment Target for Cancer," *ISRN Biochemistry*, vol. 2014, 8 pages, 2014.

[10] K. B. Ewan, R. L. Henshall-Powell, S. A. Ravani et al., "Transforming growth factor-beta1 mediates cellular response to DNA damage in situ," *Cancer Research*, vol. 62, no. 20, pp. 5627–5631, 2002.

[11] B. Kaminska, A. Wesolowska, and M. Danilkiewicz, "TGF beta signalling and its role in tumour pathogenesis," *Acta Biochimica Polonica*, vol. 52, no. 2, pp. 329–337, 2005.

[12] J. Zavadil and E. P. Böttinger, "TGF-β and epithelial-to-mesenchymal transitions," *Oncogene*, vol. 24, no. 37, pp. 5764–5774, 2005.

[13] K. Lee and C. M. Nelson, "New insights into the regulation of epithelial-mesenchymal transition and tissue fibrosis," *International Review of Cell and Molecular Biology*, vol. 294, pp. 171–221, 2012.

[14] M. K. Wendt, T. M. Allington, and W. P. Schiemann, "Mechanisms of the epithelial–mesenchymal transition by TGF-β," *Future Oncology*, vol. 5, no. 8, pp. 1145–1168, 2009.

[15] D. I. Portess, G. Bauer, M. A. Hill, and P. O'Neill, "Low-dose irradiation of nontransformed cells stimulates the selective removal of precancerous cells via intercellular induction of apoptosis," *Cancer Research*, vol. 67, no. 3, pp. 1246–1253, 2007.

[16] S. Shakeri Manesh, T. Sangsuwan, A. Pour Khavari, A. Fotouhi, S. N. Emami, and S. Haghdoost, "MTH1, an 8-oxo-2′-deoxyguanosine triphosphatase, and MYH, a DNA glycosylase, cooperate to inhibit mutations induced by chronic exposure to oxidative stress of ionising radiation," *Mutagenesis*, vol. 32, no. 3, pp. 389–396, 2017.

[17] M. H. Barcellos-Hoff and T. A. Dix, "Redox-mediated activation of latent transforming growth factor-beta 1," *Molecular Endocrinology*, vol. 10, no. 9, pp. 1077–1083, 1996.

[18] T. Sangsuwan and S. Haghdoost, "The nucleotide pool, a target for low-dose *s*-ray-induced oxidative stress," *Radiation Research*, vol. 170, no. 6, pp. 776–783, 2008.

[19] K. L. Andarawewa, A. C. Erickson, W. S. Chou et al., "Ionizing Radiation Predisposes Nonmalignant Human Mammary Epithelial Cells to Undergo Transforming Growth Factor β–Induced Epithelial to Mesenchymal Transition," *Cancer Research*, vol. 67, no. 18, pp. 8662–8670, 2007.

[20] K. L. Andarawewa, S. V. Costes, I. Fernandez-Garcia et al., "Lack of radiation dose or quality dependence of epithelial-to-mesenchymal transition (EMT) mediated by transforming growth factor β," *International Journal of Radiation Oncology Biology Physics*, vol. 79, no. 5, pp. 1523–1531, 2011.

[21] M. WANG, M. HADA, J. HUFF et al., "Heavy ions can enhance TGFβ mediated epithelial to mesenchymal transition," *Journal of Radiation Research*, vol. 53, no. 1, pp. 51–57, 2012.

[22] M. Wang, M. Hada, J. Saha, D. M. Sridharan, J. M. Pluth, and F. A. Cucinotta, "Protons sensitize epithelial cells to mesenchymal transition," *PLoS One*, vol. 7, no. 7, article e41249, 2012.

[23] M. H. Barcellos-Hoff and D. H. Nguyen, "Radiation carcinogenesis in context: how do irradiated tissues become tumors?," *Health Physics*, vol. 97, no. 5, pp. 446–457, 2009.

[24] Z. Vujaskovic and H. J. M. Groen, "TGF-beta, radiation-induced pulmonary injury and lung cancer," *International Journal of Radiation Biology*, vol. 76, no. 4, pp. 511–516, 2000.

[25] M. Guarino, A. Tosoni, and M. Nebuloni, "Direct contribution of epithelium to organ fibrosis: epithelial-mesenchymal transition," *Human Pathology*, vol. 40, no. 10, pp. 1365–1376, 2009.

[26] H. Vandenhove, L. Sweeck, D. Mallants et al., "Assessment of radiation exposure in the uranium mining and milling area of Mailuu Suu, Kyrgyzstan," *Journal of Environmental Radioactivity*, vol. 88, no. 2, pp. 118–139, 2006.

[27] K. Yajima, K. Iwaoka, S. Kamada et al., "Dose rate survey inside and outside three public buildings located approximately 40 km northwest of the Fukushima Daiichi Nuclear Power Stations," in *Proceedings of international symposium on environmental monitoring and dose estimation of residents after accident of TEPCO's Fukushima Daiichi Nuclear Power Stations, KUR Research Program for Scientific Basis of Nuclear Safety*, Shiran Hall, Kyoto, Japan, 2012 Dec 14.

[28] N. Matsuda, S. Mikami, T. Sato, and K. Saito, "Measurements of air dose rates in and around houses in the Fukushima Prefecture in Japan after the Fukushima accident," *Journal of Environmental Radioactivity*, vol. 166, pp. 427–435, 2017.

[29] R. D. Ramirez, S. Sheridan, L. Girard et al., "Immortalization of human bronchial epithelial cells in the absence of viral oncoproteins," *Cancer Research*, vol. 64, no. 24, pp. 9027–9034, 2004.

[30] M. L. Fulcher, S. Gabriel, K. A. Burns, J. R. Yankaskas, and S. H. Randell, "Well-differentiated human airway epithelial cell cultures," *Methods in Molecular Medicine*, vol. 107, pp. 183–206, 2005.

[31] S. Haghdoost, S. Czene, I. Näslund, S. Skog, and M. Harms-Ringdahl, "Extracellular 8-oxo-dG as a sensitive parameter for oxidative stressin vivoandin vitro," *Free Radical Research*, vol. 39, no. 2, pp. 153–162, 2005.

[32] S. Haghdoost, L. Sjölander, S. Czene, and M. Harms-Ringdahl, "The nucleotide pool is a significant target for oxidative stress," *Free Radical Biology and Medicine*, vol. 41, no. 4, pp. 620–626, 2006.

[33] S. Haghdoost, P. Svoboda, I. Näslund, M. Harms-Ringdahl, A. Tilikides, and S. Skog, "Can 8-oxo-dG be used as a predictor for individual radiosensitivity?," *International Journal of Radiation Oncology Biology Physics*, vol. 50, no. 2, pp. 405–410, 2001.

[34] A. Acheva, E. Eklund, E. Lemola, T. Siiskonen, V. Launonen, and M. Kämäräinen, "Lack of epithelial-to-mesenchymal transition induction in two bronchial epithelial cell lines after alpha and gamma irradiation," *International Journal of Low Radiation*, vol. 10, no. 2, pp. 116–133, 2015.

[35] A. Calon, D. V. F. Tauriello, and E. Batlle, "TGF-beta in CAF-mediated tumor growth and metastasis," *Seminars in Cancer Biology*, vol. 25, pp. 15–22, 2014.

[36] Y. Yu, C.-H. Xiao, L.-D. Tan, Q.-S. Wang, X.-Q. Li, and Y.-M. Feng, "Cancer-associated fibroblasts induce epithelial–mesenchymal transition of breast cancer cells through paracrine TGF-β signalling," *British Journal of Cancer*, vol. 110, no. 3, pp. 724–732, 2014.

[37] C. C. Park, R. L. Henshall-Powell, A. C. Erickson et al., "Ionizing radiation induces heritable disruption of epithelial cell interactions," *Proceedings of the National Academy of Sciences*, vol. 100, no. 19, pp. 10728–10733, 2003.

[38] M. F. Jobling, J. D. Mott, M. T. Finnegan et al., "Isoform-specific activation of latent transforming growth factor β (LTGF-β) by reactive oxygen species," *Radiation Research*, vol. 166, no. 6, pp. 839–848, 2006.

[39] E. J. Ehrhart, P. Segarini, M. L. Tsang, A. G. Carroll, and M. H. Barcellos-Hoff, "Latent transforming growth factor beta1 activation in situ: quantitative and functional evidence after low-dose gamma-irradiation," *The FASEB Journal*, vol. 11, no. 12, pp. 991–1002, 1997.

[40] C. D. Bondi, N. Manickam, D. Y. Lee et al., "NAD(P)H Oxidase Mediates TGF-β1–Induced Activation of Kidney Myofibroblasts," *Journal of the American Society of Nephrology*, vol. 21, no. 1, pp. 93–102, 2010.

[41] T. M. Casey, J. Eneman, A. Crocker et al., "Cancer associated fibroblasts stimulated by transforming growth factor beta1 (TGF-β1) increase invasion rate of tumor cells: a population study," *Breast Cancer Research and Treatment*, vol. 110, no. 1, pp. 39–49, 2008.

[42] S. Lonning, J. Mannick, and J. M. McPherson, "Antibody Targeting of TGF-β in Cancer Patients," *Current Pharmaceutical Biotechnology*, vol. 12, no. 12, pp. 2176–2189, 2011.

[43] M. Zhang, S. Kleber, M. Röhrich et al., "Blockade of TGF-β Signaling by the TGFβR-I Kinase Inhibitor LY2109761 Enhances Radiation Response and Prolongs Survival in Glioblastoma," *Cancer Research*, vol. 71, no. 23, pp. 7155–7167, 2011.

[44] M. G. Mendez, S.-I. Kojima, and R. D. Goldman, "Vimentin induces changes in cell shape, motility, and adhesion during the epithelial to mesenchymal transition," *The FASEB Journal*, vol. 24, no. 6, pp. 1838–1851, 2010.

[45] V. L. Kinnula, J. R. Yankaskas, L. Chang et al., "Primary and immortalized (BEAS 2B) human bronchial epithelial cells have significant antioxidative capacity in vitro," *American Journal of Respiratory Cell and Molecular Biology*, vol. 11, no. 5, pp. 568–576, 1994.

Hindawi
Oxidative Medicine and Cellular Longevity
Volume 2019, Article ID 2647068, 15 pages
https://doi.org/10.1155/2019/2647068

Research Article

NRF1 and NRF2 mRNA and Protein Expression Decrease Early during Melanoma Carcinogenesis: An Insight into Survival and MicroRNAs

Mari Hämäläinen,[1,2] Hanna-Riikka Teppo,[1] Sini Skarp,[3] Kirsi-Maria Haapasaari,[1] Katja Porvari,[1] Katri Vuopala,[4] Thomas Kietzmann,[5] and Peeter Karihtala[2]

[1]*Cancer Research and Translational Medicine Research Unit, University of Oulu, Oulu University Hospital and University of Oulu, Oulu, Finland*
[2]*Department of Oncology and Radiotherapy, Medical Research Center Oulu, Oulu University Hospital and University of Oulu, Oulu, Finland*
[3]*Infrastructure for Population Studies, Faculty of Medicine, University of Oulu, Oulu, Finland*
[4]*Department of Pathology, Lapland Central Hospital, Rovaniemi, Finland*
[5]*Faculty of Biochemistry and Molecular Medicine, Biocenter Oulu, University of Oulu, Oulu, Finland*

Correspondence should be addressed to Peeter Karihtala; peeter.karihtala@oulu.fi

Received 10 March 2019; Revised 7 June 2019; Accepted 25 June 2019; Published 4 September 2019

Guest Editor: Kanhaiya Singh

The prognostic significance of the major redox regulator nuclear factor erythroid-2-related factor (NRF2) is recognized in many cancers, but the role of NRF1 is not generally well understood in cancer. Our aim was to investigate these redox transcription factors in conjunction with redox-related microRNAs in naevi and melanoma. We characterized the immunohistochemical expression of NRF1 and NRF2 in 99 naevi, 88 primary skin melanomas, and 67 lymph node metastases. In addition, NRF1 and NRF2 mRNA and miR-23B, miR-93, miR-144, miR-212, miR-340, miR-383, and miR-510 levels were analysed with real-time qPCR from 54 paraffin-embedded naevi and melanoma samples. The immunohistochemical expression of nuclear NRF1 decreased from benign to dysplastic naevi ($p < 0.001$) and to primary melanoma ($p < 0.001$) and from primary melanoma to metastatic lesions ($p = 0.012$). Also, NRF1 mRNA levels decreased from benign naevi to dysplastic naevi ($p = 0.034$). Similarly, immunopositivity of NRF2 decreased from benign to dysplastic naevi ($p = 0.02$) and to primary lesions ($p = 0.018$). NRF2 mRNA decreased from benign to dysplastic naevi and primary melanomas ($p = 0.012$). Analysis from the Gene Expression Omnibus datasets supported the mRNA findings. High nuclear immunohistochemical NRF1 expression in pigment cells associated with a worse survival ($p = 0.048$) in patients with N0 disease at the time of diagnosis, and high nuclear NRF2 expression in pigment cells associated with a worse survival ($p = 0.033$) in patients with M0 disease at the time of diagnosis. In multivariate analysis, neither of these variables exceeded the prognostic power of Breslow. The levels of miR-144 and miR-212 associated positively with ulceration ($p = 0.012$ and $p = 0.027$, respectively) while miR-510 levels associated positively with lymph node metastases at the time of diagnosis ($p = 0.004$). Furthermore, the miRNAs correlated negatively with the immunohistochemical expression of NRF1 and NRF2 but positively with their respective mRNA. Together, this data sheds new light about NFE2L family factors in pigment tumors and suggests that these factors are worth for further explorations.

1. Introduction

Nuclear factor erythroid-2-related factor 2 (NRF2) is the most studied member of the Cap 'n' collar basic leucine zipper (CNC-bZIP) family of transcription factors. It is a main inductor of genes of antioxidant proteins and phase II detoxifying enzymes [1]. In addition, due to activating mutations, growth signalling and epigenetic dysregulation NRF2 was

also found be aberrantly activated in several cancers [2, 3]. From the same family of transcription factors, NRF1 is generally far less studied and its role in carcinogenesis is insufficiently explored. Similar to NRF2, it is responsive to oxidative stress and activates antioxidant responsive element- (ARE-) driven genes [4]. Both, NRF1 and NRF2 reside outside of the nucleus under unstressed conditions: NRF1 in the endoplasmic reticulum (ER) and NRF2 in the cytoplasm [5]. Several events contribute to NRF1 and NRF2 activation, among them the proteolytic cleavage of NRF1 from the ER membrane and the phosphorylation of NRF2. As a consequence, both factors are transported to the nucleus to induce the expression of their target genes.

MicroRNAs (miRNAs) are small noncoding RNAs that posttranscriptionally regulate gene expression by imperfect matching of mRNA [6]. The so-called redoximiRs represent an additional regulatory mechanism for redox homeostasis. In particular, miR-23B, miR-93, miR-144, and miR-212 were found to play a role as NRF2 inhibitors, while miR-340 appears to have a role as an NRF1 and MAPK inhibitor with miR-383 and miR-510 having a less clear role in the regulation of NRF1 and NRF2 levels [7]. Furthermore, it has been shown that miRNAs have a substantial role in melanocyte and melanoma biology [8] and that they affect, for instance, melanoma cell proliferation, invasion, and migration [9]. A total of 63 differentially expressed miRNAs have been previously linked to metastatic melanoma, many of which are known to be associated with multiple different cancers [10]. Previous studies also show that miRNA expression differs in healthy patients as compared to patients with melanoma and that miRNA expression associates with patient survival rate. All in all, miRNAs could be used as potential diagnostic, prognostic, and predictive markers in the future [11].

We have previously described the expression and prognostic role of the NRF2 immunohistochemical expression in primary and metastatic melanoma [12, 13]. Here, we have extended those studies and investigated the activated state of both factors in an enlarged sample set of naevi and melanoma. To do this, we explored active NRF2 with a phosphorylation-specific antibody [14] and NRF1 with two different antibodies targeting its N- and C-terminal domains to reflect its inactive and active location and activation, respectively [5]. In addition, NRF1 and NRF2 mRNAs and the redox-related miRNAs miR-23B, miR-93, miR-144, miR-212, miR-340, miR-383, and miR-510 were analysed from the same material and three Gene Expression Omnibus (GEO) datasets, and the results were correlated to the clinical and histopathological factors.

2. Materials and Methods

The study included 172 patients and 255 patient samples (Table 1) collected from the paraffin block archives stored in the Department of Pathology at Oulu University Hospital between 2001 and 2016 and in the Department of Pathology at Lapland Central Hospital between 2010 and 2016. All samples were fixed in neutral buffered formalin and embedded in paraffin. Cases were randomly collected based on the diagnosis and the adequacy of the samples for RNA extraction. The series consisted of 53 benign naevi (25 compositus, 28 intradermal), 46 dysplastic naevi, 48 nodular melanomas, 32 superficially spreading melanomas, and 9 acral melanomas. Out of all malignant samples, 59 were metastatic melanomas with, respectively, 67 lymph node metastases available (one or several per case). All samples were used for immunohistochemical analysis, but for RNA isolation and qPCR analysis, only selected cases were included based on the estimated sufficiency of the tumorous tissue ($n = 54$, Table 1). Diagnoses were according to the current WHO classification. Clinical data and pathologists' reports of the cases were collected retrospectively from the patient records of Oulu University Hospital and Lapland Central Hospital. We also collected data on adjuvant therapy or treatment at a possible metastatic stage, but only a few patients received oncological treatments, and therefore, no statistical analyses on the predictive power of the markers were able to be used.

2.1. NRF1 and NRF2 Immunohistochemistry. Sections of 3-4 μm thickness were cut from samples routinely fixed in formalin and embedded in paraffin. Tissue sections were deparaffinised in xylene (2 min, 4 times) and rehydrated through graded ethanol. Antigen retrieval was performed according to Table 2 by boiling with microwaves at 95°C for either 12 minutes (sodium citrate buffer) or 20 minutes (TrisEDTA). After boiling, the sections were allowed to cool at room temperature (RT) and washed using PBS 3 times. The sections were incubated in 3% hydrogen peroxide for 5 minutes to inactivate endogenous peroxidases. After washing repeatedly by PBS for 5 minutes, sections were incubated with the primary antibody (Table 2), then washed repeatedly by PBS for 5 minutes and incubated with a secondary antigen retrieval system at RT (Table 2). After washing repeatedly by PBS, the labelled secondary antibody was visualised according to the manufacturer's instructions. Sections were then counterstained with haematoxylin, dehydrated, and mounted. To evaluate the immunohistochemical data, the staining intensity was evaluated from the tumorous cells as one of the following expressions: negative, weak positive, or strong positive. The quantity of each intensity level was recorded (0-100%). Subsequently, a modified Histoscore was used with the following algorithm: $0 \times$ negative expression percentage + $1 \times$ weak expression percentage + $3 \times$ strong expression percentage (range 0-300).

2.2. RNA Isolation and qPCR Analysis. Tumorous tissue was macrodissected from 2 to 6 sections of 10 μm thickness. Samples were estimated to represent melanocytic proliferation for >80% of the volume. Macrodissected samples were collected into Eppendorf tubes and deparaffinised using deparaffinisation solution (Qiagen, Hilden, Germany), and total RNA was extracted from paraffin samples using the miRNeasy FFPE Kit (Qiagen). cDNA synthesis was done using the miScript II Reverse Transcription Kit (Qiagen). The miScript SYBR Green PCR Kit (Qiagen) was used for cDNA amplification by the Rotor-Gene Q real-time quantitative PCR equipment (Qiagen). Amplicon length was checked by gel electrophoresis.

Table 1: Patient cohort.

			IHC analysis	RNA analysis
Total number of patients			172	54
Age median (years)			60	67
Samples per diagnosis	Compound naevus		25	5
	Intradermal naevus		28	4
	Dysplastic naevus		46	4
	Nodular melanoma		48	15
	Superficially spreading melanoma		32	5
	Acral melanoma		9	1
	Metastasis		67	20
Number of patients with malignant melanoma			68	21
	Median age (years)		70	71
	Males		53	14
	Females		15	7
	Ulceration		19	11
	No ulceration or not defined		49	10
	Breslow	≤1 mm	11	1
		1–1.9 mm	20	0
		2–3.9 mm	13	3
		>4 mm	24	17
	Breslow mean		3.6 mm	9.2 mm
	Breslow median		2.5 mm	6.0 mm

For mRNA and miRNA quantification, both specially designed (Sigma) and commercial miScript Primer Assays (Qiagen) were used for amplification, respectively (Table 3). GAPDH mRNA and miScript Primer Assay for RNU6B were used for normalization of qPCR results. Cycling was carried out as recommended in the PCR Kit with annealing temperatures of 60–68°C or 55°C for mRNA and miRNA, respectively. Fluorescence signals were measured continuously during repetitive cycles to detect Ct values for target RNA and reference (GAPDH or RNU6B) in the samples. Relative expression levels of mRNA or miRNA targets were calculated using the $2^{-\Delta\Delta Ct}$ method [15], where $\Delta\Delta Ct = (Ct_{\text{target RNA}} - Ct_{\text{GAPDH or RNU6B}})_{\text{sample}} - (Ct_{\text{target RNA}} - Ct_{\text{GAPDH or RNU6B}})_{\text{reference sample}}$. Representative cell culture samples were run and analysed in parallel with the patient samples (Figure 1(b)). RNA from melanocytes was used as a reference sample (with a given value of 1) in relative expression level calculations.

2.3. GEO Datasets. The three microarray datasets GSE8401, GSE46517, and GSE53223 first described in original articles [16–18] were downloaded in .CEL-file format from the Gene Expression Omnibus (National Center for Biotechnology Information). Data was analysed using Chipster v3.14 software [19]. Datasets were first normalized individually and then, when combining the datasets, the batch effect was corrected using ComBat. The differential mRNA expression levels of NFE2L1 and NFE2L2 (NRF1 and NRF2) were determined and tested with the empirical Bayes *T*-test between the diagnostical groups. The combined data contained normal skin samples ($n = 13$), benign and dysplastic naevi ($n = 21$), primary melanoma lesions ($n = 62$), and metastatic melanoma lesions ($n = 104$). The respective results were plotted with GraphPad Prism 7.05.

2.4. Cell Lines. Cell lines representing human primary melanoma IPC-298 (ACC 251), metastatic melanoma SK-MEL-30 (ACC 151), and adult primary epidermal melanocytes (PCS-200-013) were ordered from Leibniz-Institut, DSMZ (Braunschweig, Germany) and ATCC (LGC Standards GmbH, Germany). Melanoma cells were cultured in RPMI-1640 with 10% foetal bovine serum and 100 IU/ml penicillin and streptomycin (Pen-Strep solution HyClone laboratories Inc., UT, USA). Melanocytes were cultured in a Dermal Cell Basal Medium supplemented with an Adult Melanocyte Growth Kit (PCS-200-030 and PCS-200-042 from ATCC). Cells were cultured in 37°C 5% CO_2.

2.5. Western Blot Analysis. The fractionated lysates were prepared by using the Subcellular Protein Fractionation Kit for Cultured Cells (Thermo Scientific, IL, USA). Protein concentrations were measured using the Bio-Rad Protein Assay (Bio-Rad; CA, USA), and the concentration in individual samples was equalized before adding 4x Laemmli buffer to a final concentration of 1x. Equal amounts of protein were run on 7.5% SDS-PAGE gels, transferred to PVDF membranes, probed with the antibodies (Table 2), and diluted with 5% bovine serum albumin in tris-buffered saline with 0.1% Tween 20. Primary antibodies were incubated

Table 2: Antibodies used in immunohistochemical staining and western blot.

Immunohistochemistry								
Antigen	1st antibody	Dilution	Revealing of antigen	Incubation	Detection of 1st AB	Colour development	Product	Clone
NRF1	Rabbit polyclonal anti-NRF1 (C-terminal)	1 : 500	Tris-EDTA pH 9.0	2 h RT	Dako EnVision	DAB	Sigma, HPA065424	Not reported
NRF1	Mouse monoclonal anti-NRF1 (N-terminal)	1 : 500	10 mM sodium citrate buffer pH 6.0	45 min RT	Dako EnVision	Fast Red	Santa Cruz Biotechnology, sc-365651	E-4
NRF2	Rabbit monoclonal anti-NRF2 phospho S40	1 : 600	10 mM sodium citrate buffer pH 6.0	30 min RT	Dako EnVision	DAB	Abcam, 76086	EP1809Y
Western blot								
Antigen	1st antibody	Dilution					Product	Clone
NRF1	Rabbit polyclonal anti-NRF1 (C-terminal)	1 : 2500					Sigma, HPA065424	Not reported
NRF1	Mouse monoclonal anti-NRF1 (N-terminal)	1 : 1000					Santa Cruz Biotechnology, sc-365651	E-4
NRF2	Rabbit monoclonal anti-NRF2 phospho S40	1 : 10000					Abcam, 76086	EP1809Y
β-Actin	Mouse monoclonal anti-β-actin	1 : 5000					Novus Biologicals, NB600-501SS	AC-15
PCNA	Mouse monoclonal anti-PCNA	1 : 2000					Cell Signalling Technology, #2586	PC10
	HRP-conjugated goat-anti-mouse	1 : 5000					Santa Cruz Biotechnology, sc-2055	—
	HRP-conjugated goat-anti-rabbit	1 : 5000					Santa Cruz Biotechnology, sc-2054	—

RT = room temperature, DAB = diaminobenzidine.

Table 3: Primers used in qPCR.

RNA target	Product company	Primer sequences	Amplicon length (base pairs)	Function related to oxidative stress (references)
mRNA NRF2	Sigma	Forward: 5′-CAATGAGGTTTCTTCGGCTACG-3′ Reverse: 5′-AAGACTGGGCTCTCGATGTG-3′	72	Major redox response regulator [1]
mRNA NRF1	Sigma	Forward: 5′-ATGGAAATGCAGGCCATGGAAG-3′ Reverse: 5′-GAGGGGCACTGTACAGGATTT-3′	61	Redox response regulator [5]
GAPDH	Sigma	Forward: 5-TGGAAGGACTCATGACCACA-3′ Reverse: 5-CCATCACGCCACAGTTT-3′		—
miR-23B-3p	Qiagen	5′AUCACAUUGCCAGGGAUUACC		Predicted NRF2 inhibition [40]
miR-93-5p	Qiagen	5′CAAAGUGCUGUUCGUGCAGGUAG		Predicted NRF2 inhibition [40]
miR-144-3p	Qiagen	5′UACAGUAUAGAUGAUGUACU		Predicted NRF2 inhibition [8, 40, 52]
miR-212-3p	Qiagen	5′UAACAGUCUCCAGUCACGGCC		NRF1 and NRF2 inhibition, interaction with Mn-SOD
miR-340-3p	Qiagen	5′UCCGUCUCAGUUACUUUAUAGC		MAPK signalling, predicted NRF1 inhibition [40]
miR-383-5p	Qiagen	5′AGAUCAGAAGGUGAUUGUGGCU		No predicted inhibition of NRF1/NRF2
miR-510-5p	Qiagen	5′UACUCAGGAGAGUGGCAAUCAC		No predicted inhibition of NRF1/NRF2
RNU-6B	Qiagen	(Not reported, product no. 218300 cat. no. MS00014000)		—

overnight, and appropriate HRP-conjugated secondary antibodies were incubated at RT for one hour (Table 2). Blots were detected with the ECL chemiluminescence system (Pierce ECL Western Blotting Substrate, Thermo Scientific, IL, USA) on radiographic films, which were then scanned to an electronic format.

2.6. Statistical Analyses. Statistical analyses were performed by using IBM SPSS Statistics software, v. 25.0.0.0 (IBM Corporation, Armonk, NY, USA). The significance of associations was defined by using the Mann–Whitney *U* test and Spearman's rho test with a correlation coefficient. The Kaplan-Meier curves with the log-rank test were applied in survival analyses, along with Cox regression to perform multivariate analysis. In determining a two-classed variable for survival analysis, a Histoscore cut-off value (32.5) was chosen using a Receiver Operating Characteristic Curve (ROC) analysis for NRF1, the highest Histoscore quartal for NRF2, and the median for mRNA and miRNA levels. Disease-specific survival (DSS) was calculated from the time of diagnosis to the time of confirmed melanoma-related death. Values of p of less than 0.05 were considered significant.

2.7. Ethical Approval. The study was approved by Valvira, the Finnish National Supervisory Authority for Welfare and Health, and the Local Ethics Committee of the Northern Ostrobothnia Hospital District. During data collection and management, the principles of the Helsinki Declaration were followed. The authors declare that they have no competing interests and that funding sources had no involvement in the study.

3. Results

3.1. Immunohistochemical and mRNA Expression of NRF1 and NRF2 in Naevi, Primary Melanomas, and Melanoma Metastases and Their Association with Histopathological and Clinical Parameters. First, we tested whether the antibodies against the N-terminal domain of NRF1 and the C-terminus of NRF1 as well as against phosphorylated NRF2 detect the respective localization and activity status of the proteins. To do this, we performed western blot analyses where we detected the proteins in respective subcellular fractions of primary melanomas. According to expectations, the antibody detecting the N-terminal domain of NRF1, i.e., the inactive ER localized protein, displayed NRF1 in the membranous fraction, whereas the antibody against the C-terminus primarily detecting the active protein showed positive staining in the nuclear fraction. Active NRF2 (p40-NRF2) was detected in all fractions, in line with the fact that its activation by phosphorylation can occur outside the nucleus (Figure 2). Thus, these data indicate that the antibodies are suitable to detect NRF1 and NRF2 by immunohistochemistry in patient samples.

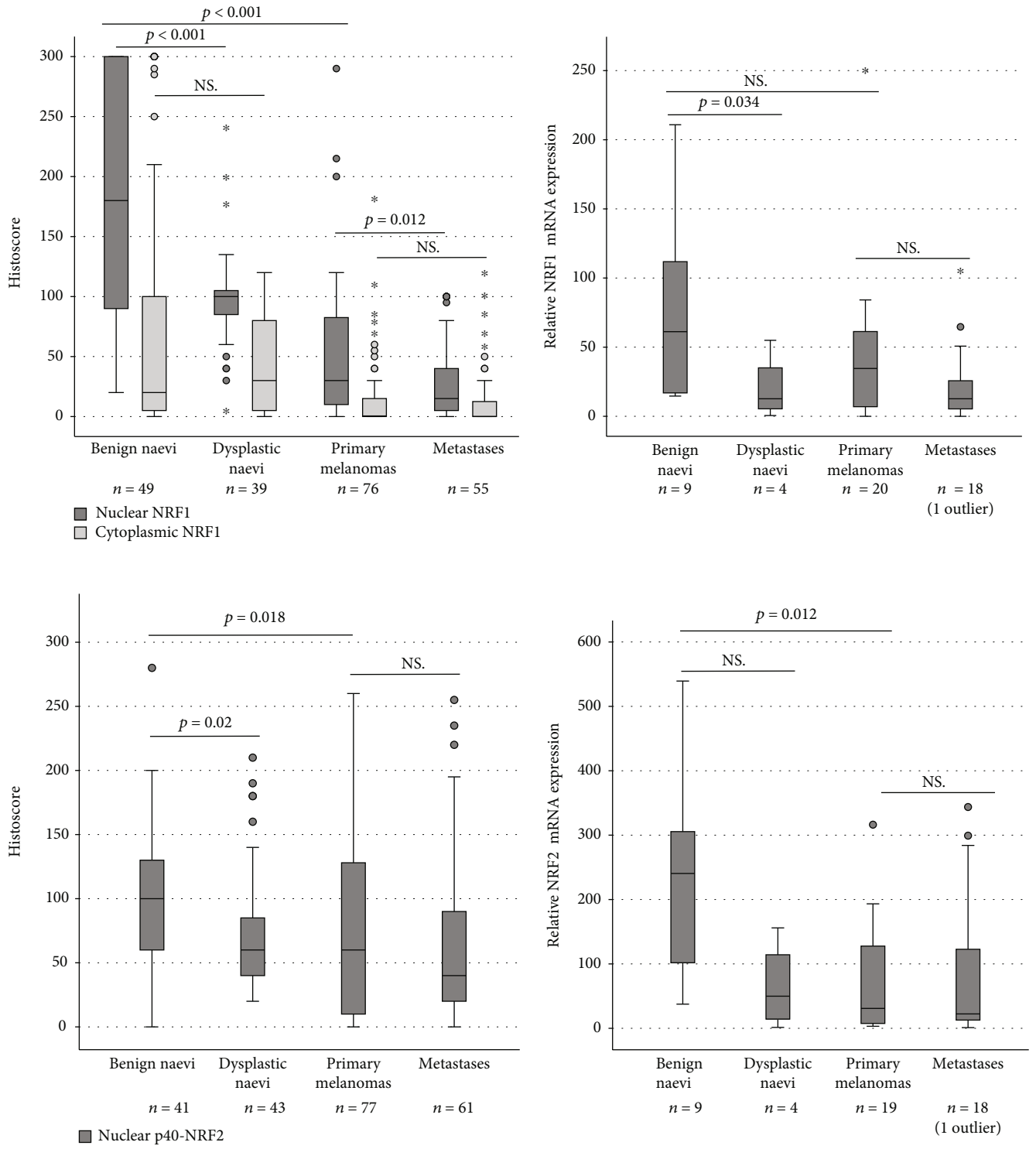

(a)

Figure 1: Continued.

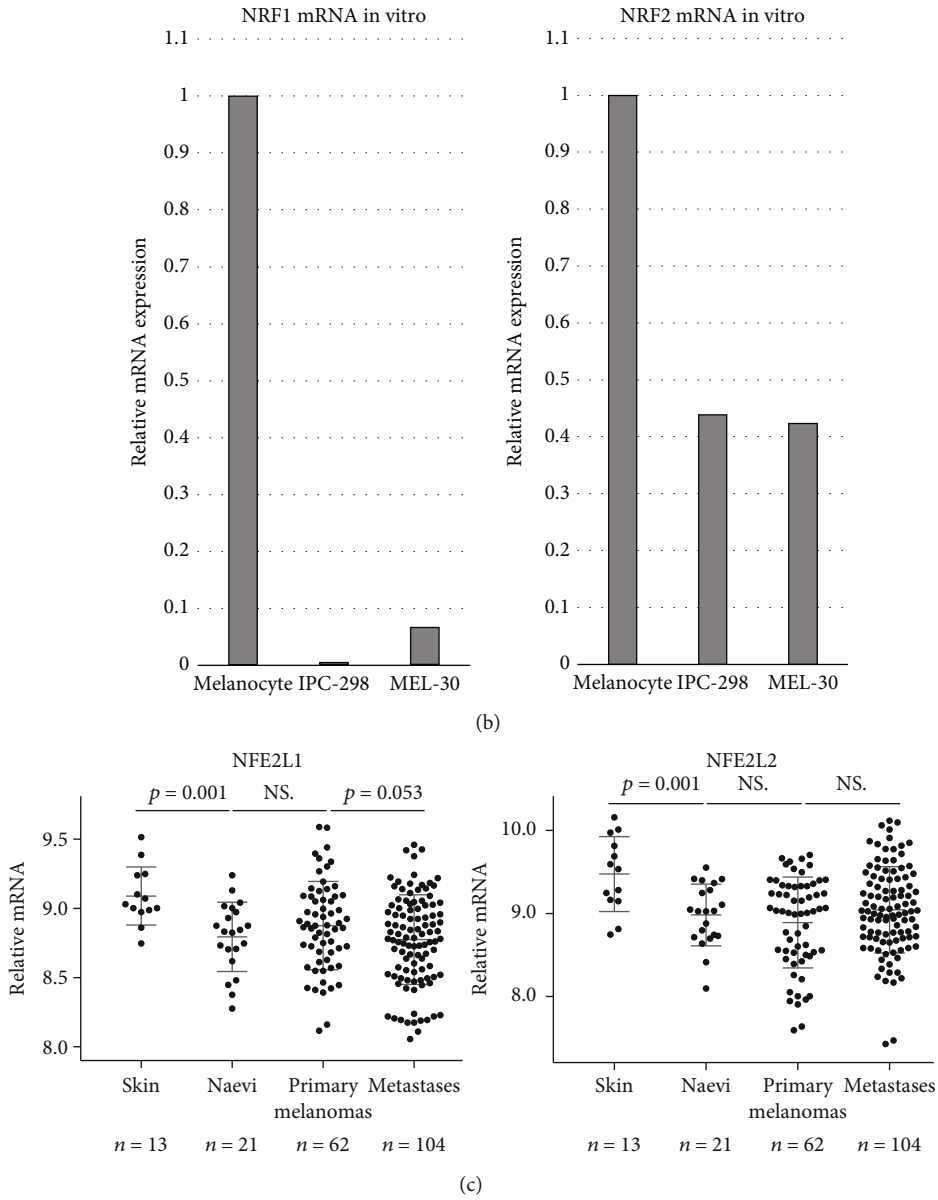

Figure 1: Immunohistochemical and mRNA expression of NRF1 and NRF2. (a) Boxplots representing the Histoscore of the immunohistochemical expression of NRF1 and p40-NRF2 and relative mRNA levels of NRF1 and NRF2 from paraffin-embedded patient samples, (b) expression levels of NRF1 and NRF2 mRNA from representative cell culture samples, and (c) Pooled GEO data from three different cDNA microarray studies including the expression levels of NFE2L1 and NFE2L2 (NRF1 and NRF2). Outliers of the figures are reported.

The immunohistochemistry revealed that, in line with western blots and according to the activity status, the antibody against the N-terminal domain of NRF1 detected the protein in the cytoplasm around the nucleus and never in the nuclei. The antibody against the C-terminal domain detected the protein mostly in the nuclei and rarely in the cytoplasm. The expression of both NRF1 antibodies showed a significant NRF1 decrease from benign to dysplastic naevi ($p < 0.001$ and $p = 0.034$, Supplementary Table 1, Figures 1(a) and 3) and from naevi to primary melanoma, as well as to metastatic lesions ($p < 0.001$, Figures 1(a) and 3) [20]. Nuclear NRF1 further decreased from primary to metastatic lesions ($p = 0.012$, Figures 1(a) and 3). Similarly, NRF1 mRNA levels were decreased from benign to dysplastic naevi ($p < 0.001$ and $p = 0.034$, Supplementary Table 1 and Figure 1(a)) but not from primary to metastatic lesions.

Immunopositivity of p40-NRF2 was detected mainly in the nuclei, and its expression decreased from benign to dysplastic naevi ($p = 0.02$) and then further to primary lesions ($p = 0.018$, Figures 1(a) and 3). The p40-NRF2 expression had a notable intersample variation in primary melanomas. The levels of NRF2 mRNA decreased from its highest levels in benign naevi to intermediate levels in dysplastic naevi, and its lowest levels occurred in primary melanomas ($p = 0.012$). The decrease of p40-NRF2 immunopositivity and NRF2 mRNA levels from primary to metastatic lesions

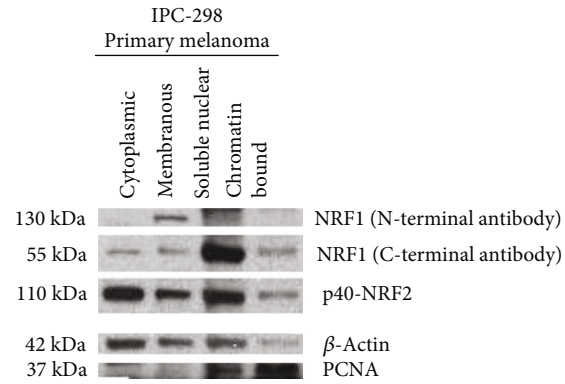

Figure 2: Protein expression of NRF1 and p40-NRF2 in western blot, fractionated cell lysates from IPC-298 melanoma cells, β-actin, and PCNA (proliferating cell nuclear antigen) serve as loading and fractioning controls. NRF1 detected with an antibody targeting N-terminal domain is expressed in membranous fraction, and NRF1 detected with an antibody targeting C-terminal domain is expressed mostly in the nuclear fraction. p40-NRF2 is expressed in the cytoplasmic, membranous, and nuclear fractions.

was not considered significant. In addition, the decline in NRF1 and NRF2 mRNA levels from benign naevi to melanomas could be reproduced when comparing the NRF1 and NRF2 mRNA levels in cell culture lysates in the qPCR, showing a decrease of relative mRNA levels between benign melanocyte and malignant melanoma cells (Figure 1(b)).

The immunohistochemical expressions of NRF1 and p40-NRF2 did not associate with the melanoma patients' age, gender, lesion location, Breslow's thickness, ulceration, mitotic activity, or pigmentation. However, NRF1 and NRF2 mRNA correlated with melanoma patients' gender (higher mRNA levels in males, $p = 0.037$ and $p = 0.017$, $n = 20$ and $n = 19$, respectively), and NRF1 mRNA also correlated positively with the presence of ulceration ($p = 0.016$, $n = 18$).

3.2. Correlations of Immunohistochemical and mRNA Expression of NRF1 and NRF2. Nuclear and cytoplasmic NRF1 correlated positively in the complete series of samples ($p = 4.7 \times 10^{-13}$, 219 samples, Figure 4). Nuclear and cytoplasmic NRF1 and p40-NRF2 had a positive correlation in the complete series of samples ($p = 0.0020$ and $p = 0.018$, $n = 204$ and $n = 203$, respectively). Also, nuclear NRF1 and p40-NRF2 correlated positively in malignant samples ($p = 0.032$, $n = 103$, Figure 4). p40-NRF2 associated positively with our previously described NRF2 expression in the melanoma cohort with a different antibody ($p = 0.021$, $n = 49$) [12, 13]. The immunostainings did not correlate with mRNA expression levels. However, NRF1 and NRF2 mRNA expression correlated both in the complete cohort and separately in malignant samples ($p = 0.010$ and $p = 0.037$, $n = 49$ and $n = 36$, respectively, Figure 4).

3.3. miRNA Expression in Naevi, Primary Melanomas, and Melanoma Metastases and Association with Histopathological and Clinical Parameters. Significant miRNA expression alterations (Supplementary Table 1) were not detected between benign and dysplastic naevi. However, the levels of miR-93 and miR-340 increased significantly from all naevi to primary melanomas and to metastases ($p = 0.023$ and $p = 0.045$, respectively, Figure 5). In contrast, the levels of miR-383 and miR-510 showed a decreasing trend between the three groups ($p = 0.024$, $p = 0.002$, respectively, $n = 31$, Figure 5). Moreover, significant changes in miRNA levels could not be detected between primary and metastatic melanoma lesions.

The miRNA levels did not associate with melanoma patients' gender, lesion location, or Breslow's thickness. The miR-510 levels associated positively with melanoma patients' age ($p = 0.025$, $n = 19$) and nodal disease at the time of diagnosis ($p = 0.004$, $n = 19$). In addition, the levels of miR-212 and miR-340 associated positively with pigmentation ($p = 0.024$ and $p = 0.012$, $n = 11$, respectively). Furthermore, miR-144 and miR-212 levels were found to associate positively with ulceration ($p = 0.012$ and $p = 0.027$, $n = 18$, respectively).

3.4. Respective Correlations of Immunohistochemical and mRNA Expression of NRF1 and NRF2 and miRNAs. There was an ample amount of significant correlation between protein and mRNA expression with different miRNAs, and this data is thoroughly presented in Supplementary Table 1 in all cases and separately in malignant samples including primary and metastatic melanoma lesions. Significant correlations between protein expression and miRNAs were always negative, except for the cytoplasmic NRF1 and miR-510, whereas correlations between mRNA and miRNAs were always positive.

3.5. GEO Data. Levels of NRF1 and NRF2 mRNA decreased from normal skin samples to pooled benign and dysplastic naevi ($p = 0.001$). There was no significant difference in levels between naevi and primary melanomas. Although the level of NRF1 mRNA decreased nearly significantly between primary melanomas and metastases ($p = 0.053$), the difference in NRF2 mRNA levels was not significant between primary melanomas and metastases (Figure 1(c)).

3.6. Survival and Cox Regression Analysis. A high nuclear NRF1 immunohistochemical expression in pigment cells correlated with a worse survival ($p = 0.048$) in patients without nodal metastases at the time of diagnosis ($n = 45$, Figure 6(a)). When N1-3 cases were considered, nuclear NRF1 had no prognostic significance ($p = 0.72$, Figure 6(b)). When analysing the NRF2 expression in patients with M0 disease at the time of diagnosis ($n = 71$, Figure 6(c)), we found that the highest quartile of the nuclear NRF2 expression in pigment cells correlated with a significantly worse survival rate ($p = 0.033$). mRNAs or miRNAs had no prognostic significance. In multivariate analysis, neither of these variables exceeded the prognostic power of Breslow thickness.

4. Discussion

In this work, we studied for the first time the protein level of the redox-sensitive transcription factor NRF1 together with NRF2. Very early on in melanoma carcinogenesis, both NRF1 and NRF2 were found to be downregulated at the protein level as well as at the mRNA level. The results of the mRNA expression from our own patient cohort are further

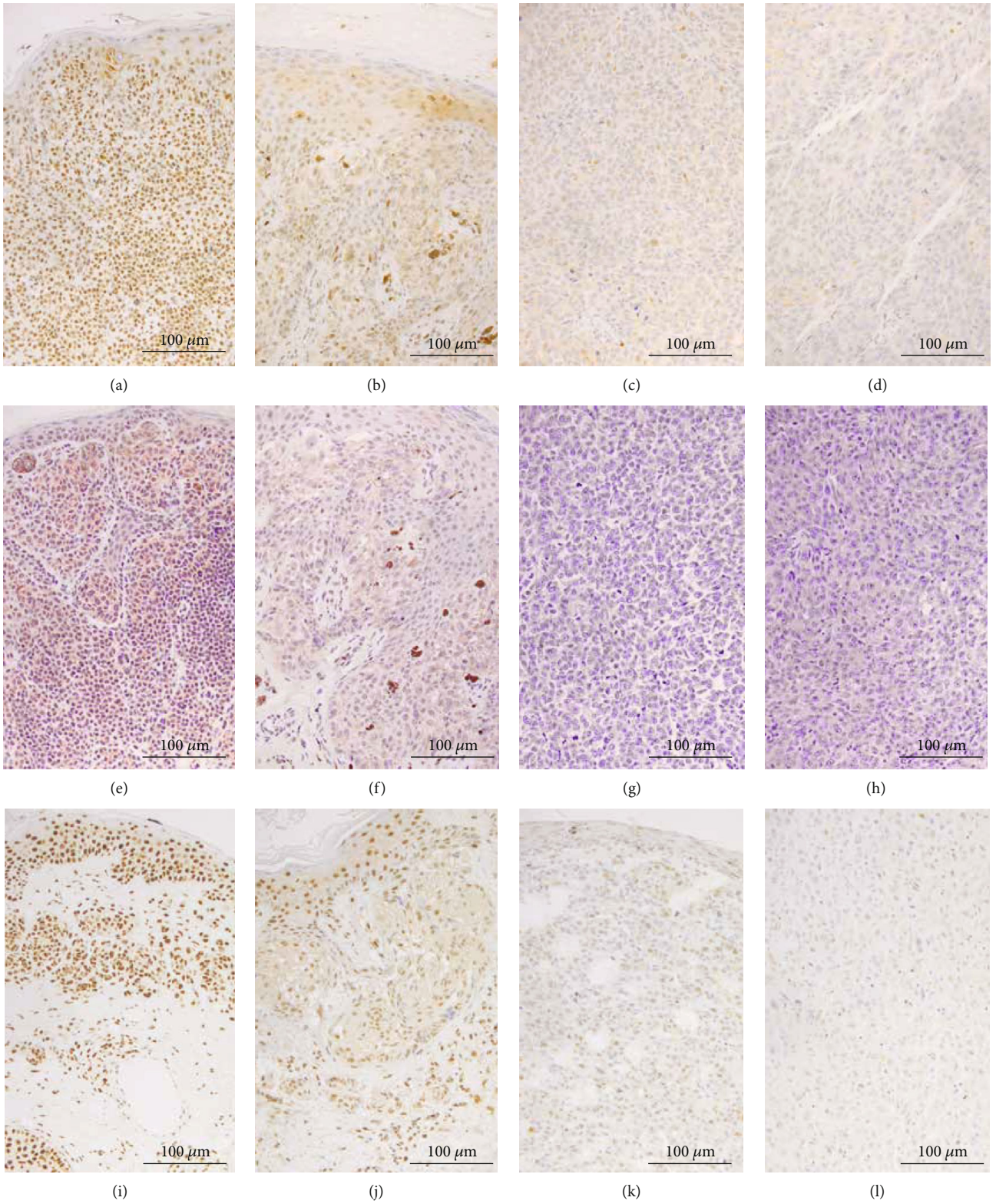

Figure 3: Immunohistochemical expression in patient samples. (a-d) NRF1 C-terminal antibody, benign naevus, dysplastic naevus, primary melanoma, and metastatic melanoma from a lymph node, respectively, diaminobenzidine and haematoxylin, (e-h) NRF1 N-terminal antibody, benign naevus, dysplastic naevus, primary melanoma, and metastatic melanoma from a lymph node, respectively, Fast Red and haematoxylin, and (i-l) p40-NRF2, benign naevus, dysplastic naevus, primary melanoma, and metastatic melanoma from a lymph node, respectively, diaminobenzidine and haematoxylin.

	NRF1 n IHC	NRF1 sp IHC	NRF2 IHC	NRF1 mRNA	NRF2 mRNA	miR-23B	miR-93	miR-144	miR-212	miR-340	miR-383	miR-510
NRF1 n IHC		4.7×10^{-13}	0.0020				0.023		0.038	0.0094		
NRF1 sp IHC			0.018									0.033
NRF2 IHC	0.032									0.016		
NRF1 mRNA					0.010							0.039
NRF2 mRNA				0.037		0.0230						0.00036
miR-23B			0.041				2.9×10^{-6}	0.002	0.00014	9.8×10^{-6}		
miR-93	0.048					2.4×10^{-9}		8.26×10^{-9}	3.37×10^{-16}	4.88×10^{-15}		
miR-144						0.00052	4.7×10^{-7}		$2{,}4 \times 10^{-10}$	6.1×10^{-5}		
miR-212	0.042					2.3×10^{-5}	2×10^{-13}	2.67×10^{-8}		1.2×10^{-8}		
miR-340	0.0083		0.011			1.6×10^{-8}	6×10^{-11}	0.00055	7.7×10^{-7}			
miR-383										0.036		
miR-510	0.023					0.001	0.015			0.004		

Correlations in all samples

Correlations in malignant samples

Figure 4: Significant correlations between studied parameters in all samples (top) and in malignant samples (bottom), p value. Blue box indicates negative and brown box positive correlation.

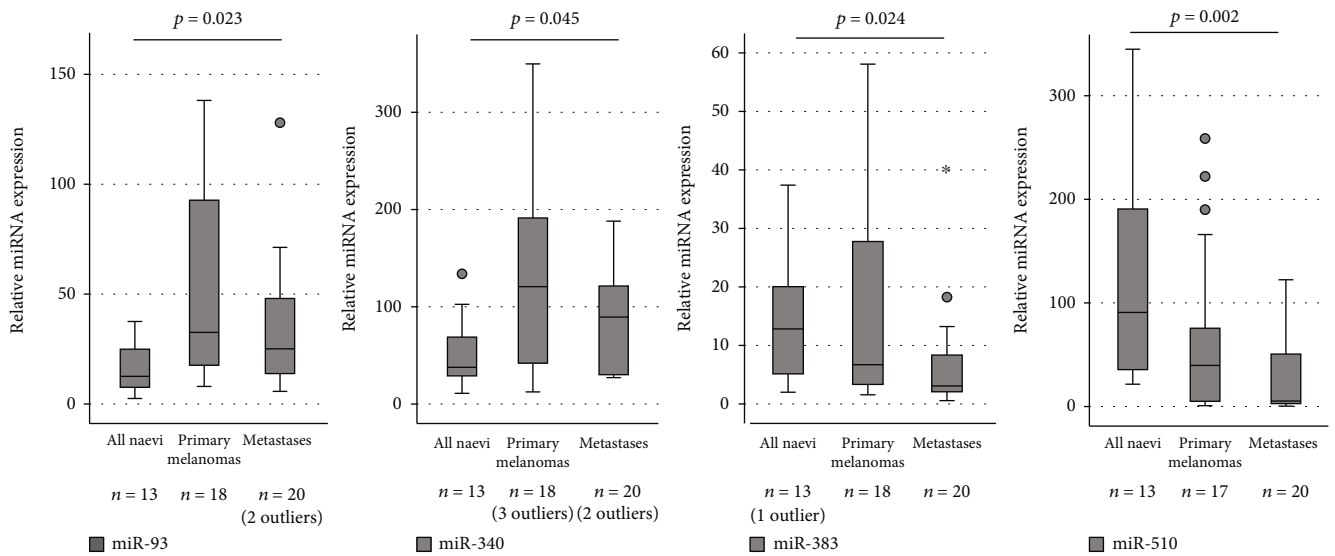

Figure 5: Expression levels of miR-93, miR-340, miR-383, and miR-510 in paraffin-embedded patient samples. Outliers of the figures are reported.

supported by analyses from three independent melanoma patient sample sets from the GEO database [16–18]. We also studied the expression of some redoximiRNAs from the same sample set and described some new data on their expression level changes in melanoma carcinogenesis and correlation with immunohistochemical and mRNA expression levels of NRF1 and NRF2.

4.1. NRF1 and NRF2 in Melanoma. We carefully examined the expression of NRF1 with two different antibodies targeting the N-terminal and C-terminal sites of the protein. As NRF1 binds the ER membrane with its N-terminal domain and is cleaved upon activation [21], it is logical that the antibody targeting the N-terminus showed a perinuclear staining pattern under light microscopy and a strong expression in the membranous fraction in the immunoblot. By contrast, the antibody recognizing the C-terminus showed predominantly a nuclear staining pattern and a strong expression in the nuclear fraction in the immunoblot resembling active NRF1. In immunohistochemistry, the protein level of NRF1 had a decreasing trend during melanoma carcinogenesis. We also observed that the NRF1 mRNA level decreased from benign naevi to dysplastic naevi and to melanomas and that their levels associate with ulceration. There is human sample set data showing that NRF1 mRNA levels

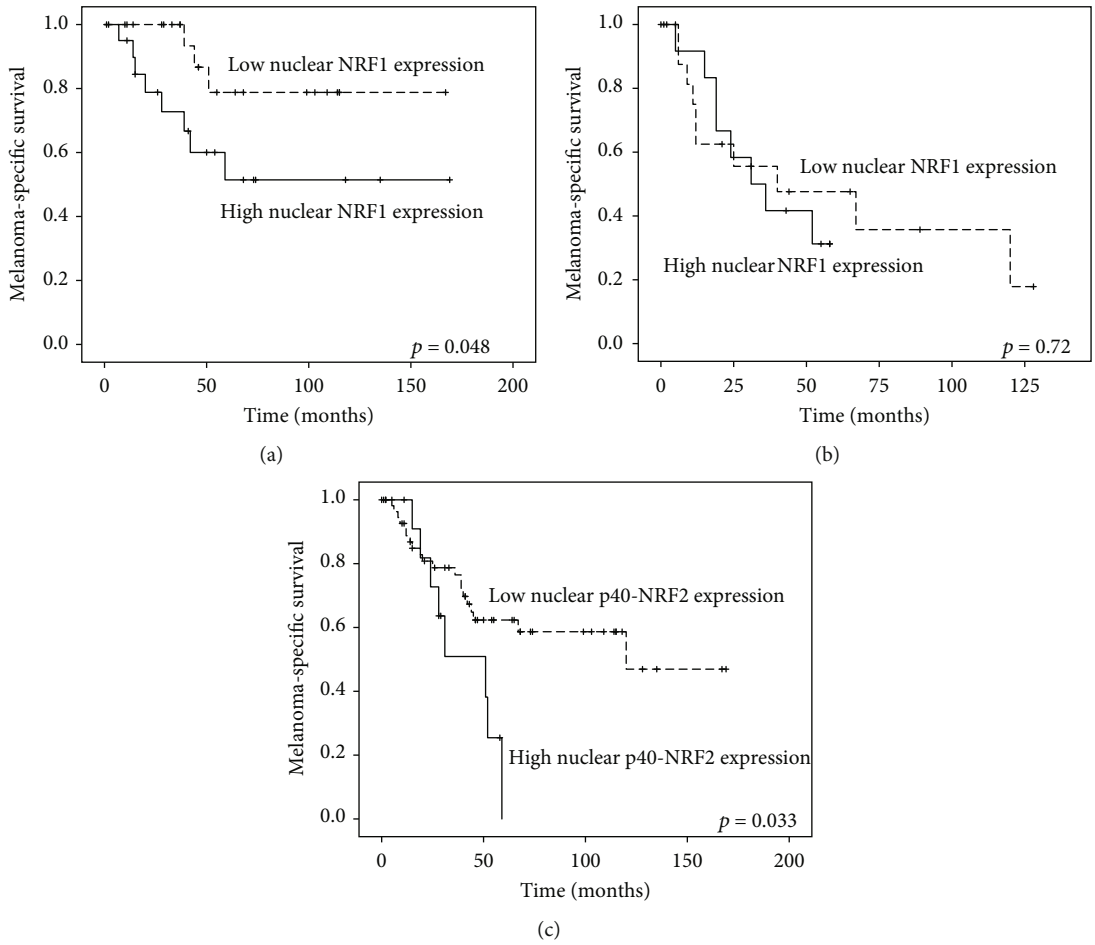

Figure 6: (a) High nuclear NRF1 expression (cut-off 32.5 based on ROC analysis) associated with worse melanoma-specific survival in those patients without nodal metastases at the time of diagnosis. (b) NRF1 did not separate the groups in cases with nodal metastases at the time of diagnosis. (c) High nuclear p40-NRF2 expression (highest quartile in Histoscore) predicted poor outcome within the patients with M0 disease at the time of diagnosis.

are also downregulated in prostate carcinoma [22] but they are upregulated in oesophageal squamous cell carcinoma [23]. Conditions such as oxidative stress, proteasomal inhibition, ER stress, and hypoxia activate NRF1 to function as a transcription factor [4]. An early increase of ER stress in melanomas and adaptation to it as a driver of malignancy was discussed a decade ago [24]. Therefore, the dysregulated NRF1 might be a mere surrogate marker for more robust biological processes behind the pigment cell malignancy, but it can also play a significant role in carcinogenesis, as its deficiency can lead to genomic instability [25]. Indeed, there is some experimental evidence from a study using keratinocyte cell culture, mouse model, and patient samples that NRF1 functions as a tumor suppressor in the skin by activating DNA damage repair after ultraviolet (UV) B irradiation and is downregulated in human squamous cell carcinoma compared to normal skin [26]. Nuclear NRF1 expression, which predicted exceptionally poor melanoma-specific outcome in those patients without nodal metastases at the time of diagnosis, might benefit the carcinogenetic process by alleviating oxidative and ER stress accumulated in the aggressive disease [24]. To the best of our knowledge, there is no further published data on the prognostic role of NRF1 in cancers yet, except for our recent report pointing out that low nuclear and high cytoplasmic NRF1 is associated with poor overall survival in diffuse large B-cell lymphoma [27].

An elevated protein expression level of NRF2 has been noted in solid cancers as a prognostic feature, as has been summarized in a previous meta-analysis [28]. Alterations of NRF2 mRNA in different cancers have been reported, for example, its decrease in breast and oesophageal squamous cell carcinoma compared to normal tissue [23, 29]. We have described the prognostic role of NRF2 in a melanoma sample set recently [12, 13] and reported that the NRF2 expression increased from benign to dysplastic naevi to primary and metastatic melanomas. While those studies were rather hampered by the unspecific antibody against NRF2 (clone C-20), as also discussed in detail in another study [30], here, we used an antibody against NRF2 that is phosphorylation-specific. Phosphorylation of the amino acid serine in position 40 by protein kinase C in response to oxidative stress dissociates NRF2 from its inhibitor Keap1, promoting its translocation into the nucleus [14]. Thus, the signal detected with this antibody represents an active transcription factor and is

mainly seen in the nuclei with a decreasing trend of expression in melanoma compared to nonmalignant lesions. The differences in the expression trends seen between the previous and the current report could be explained by the specificity of these two antibodies. Despite the contradictory result in the expression trends, current p40-NRF2 results support our previous observation, namely, that the NRF2 expression favours worse disease-specific survival, and the role of NRF2 in melanoma carcinogenesis seems to be rather consistent with NRF1.

4.2. MicroRNAs in Melanoma. We described the expression of seven different miRNAs in our naevi and melanoma sample set which was selected based on their NFE2L family and redox association. Expression levels of miR-93 and miR-340 increased significantly from all naevi to primary melanomas and metastases. Apart from NRF2, miR-93 associates with lung cancer proliferation, migration, and invasion *in vitro* and is upregulated in multiple cancers [31, 32]; our data complements this background. The miR-340 is also described to regulate the master regulator of melanocyte development and melanoma progression, microphthalmia-associated transcription factor (MITF) [33], and MAPK-signalling by modulating the expression of multiple components of this pathway *in vitro*. Our data is in line with these findings, since miR-340 expression levels were significantly elevated in several tested melanoma cell lines compared to normal human epidermal melanocytes [34].

Based on the available literature, miR-510 may have either cancer promoting or suppressing properties, depending on the cancer type. Overexpression of miR-510 can increase cell growth and migration as well as invasion and colony formation of breast cancer *in vitro* [35], while the effect is just the opposite in renal cell carcinoma [36]. In ovarian cancer, high miR-510 expression associates with early stage and predicts prolonged survival [37, 38]. In our material, miR-510 expression strongly correlated with the presence of lymph node metastases at the time of diagnosis and, on the other hand, showed a decreasing expression from all naevi to primary melanomas and further to metastases. Similarly, primary gastric cancers were found to have higher miR-510 expression than lymph node metastases [39].

4.3. Correlation of miRNAs with NRF1 and NRF2. The post-transcriptional regulation of gene expression by imperfect matching of miRNA leads to the inhibition of mRNA translation and eventually to mRNA degradation [6], and therefore, the effect of miRNA would be generally negative when seen typically on a protein level. Thus, it is logical that miRNA levels correlate negatively with protein levels rather than mRNA levels. From the studied miRNAs, miR-23b-3p, miR-93-5p, and miR-144-3p are predicted inhibitors of NRF2 mRNA, miR-212-3p of both NRF1 and NRF2 mRNA, and miR-340 of NRF1 mRNA, based on the miRmap database [40]. The miR-383 and miR-510 were not predicted to bind NRF1 or NRF2 mRNA. In our material, only miR-23b-3p correlated positively with NRF2 mRNA in the whole material and significantly with NRF2 immunohistochemical expression in malignant cases. Interestingly, according to this database, miR23b-5p, the complementary sequence of the same miRNA hairpin structure, would be an inhibitor to NRF1. miR-340 negatively correlated with both nuclear NRF1 and p40-NRF2 protein expression. Additionally, miR-510 correlated negatively with the expression of nuclear NRF1 in malignant samples. Although miR-93-5p, miR-144, and miR-212 had a predicted relation with NRF1 and NRF2, apparently, this is not the case in melanoma and the lack of correlation may reflect the general discoordination within a cancer cell.

4.4. miRNAs in respect to Clinical Variates. miR-144 and miR-212 associated positively with melanoma ulceration, a highly important prognostic and predictive factor of melanoma. Previously, let-7b-5p, miR-16, miR-106b, and miR-137 were described to be associated with melanoma ulceration that can be linked to anchorage-independent growth, aggressive disease, and progression [41–44]. Also, miR-212 and miR-340 associated with pigmentation. The association of miR-340 to pigmentation could be explained by the relation to melanocyte differentiation regulator MITF [33]. Other pigmentation-related miRNAs reported are miR-16, miR-125b, miR-155, miR-203, miR-204, and miR-211 [45–49]. In univariate analysis, mRNAs or miRNAs had no prognostic significance, possibly due to the small amount of tested primary melanomas (n = 17-20).

Although the current study addresses for the first time the association of NRF1 in melanoma, its retrospective nature causes also some weaknesses. In particular, despite the material was sufficient to produce the current results, the size of effect may have been different with the larger sample size. Moreover, we did not have data on ethnicity, UV exposure, skin type, or the number of blistering sunburns available, which is a confounding factor in the study.

5. Conclusions

This data suggests that there is a loss of NRF1 and NRF2 mRNA and protein levels during different stages of melanoma carcinogenesis. This early change can be seen between the groups of benign and dysplastic proliferative naevi that are known to harbour oncogenic mutations [50]. High nuclear NRF1 and NRF2 protein expression may also predict a dismal outcome in patients before nodal or distant metastases occur, respectively. Thus, it is plausible that even if these redox-regulating and stress-sensing transcription factors have a protective role against melanoma carcinogenesis, they can be exploited as tumor-progressing factors in the malignant phase, as suggested earlier in other tumor types [51]. Additionally, redoxmiRs miR-144, miR-212, and miR-510 appear to associate with aggressive melanoma features, and their possible prognostic value should be evaluated in larger cohorts.

Data Availability

The data used to support the findings of this study are available from the corresponding author upon request.

Conflicts of Interest

All authors declare that there are none.

Authors' Contributions

HRT and PK designed the study. MH and HRT collected the patient sample set, analysed immunohistochemistry, dissected and ran RNA samples, and finally, analysed qPCR data. KMH guided and participated in the immunohistochemical analysis. KP guided all the RNA work. HRT and SS analysed the GEO data, and SS guided the analysis. KV assisted MH in the collection of the patient sample set. TK provided HRT additional laboratory facilities and guidance with cell culture and analysis. HRT, MH, and PK analysed the statistical data and compiled the manuscript, and all authors participated in writing the manuscript. HRT, KMH, KP, TK, and PK provided the financial support for this study. Mari Hämäläinen and Hanna-Riikka Teppo contributed equally to this work.

Acknowledgments

We thank the Thelma Mäkikyrö Foundation, the Finnish Cancer Society, the Finnish Medical Society Duodecim, the Finnish Medical Foundation, the Finnish Society for Oncology, and its melanoma group for financial support in the form of personal grants (HRT). We also received funding from the Academy of Finland (SA296027), the Jane and Aatos Erkko Foundation, the Sigrid Juselius Foundation, and the Finnish Cancer Society (TK). We thank Riitta Vuento, Erja Tomperi, Mirja Mäkeläinen, and Päivi Sortti for their technical knowledge in immunohistochemistry and qPCR work.

Supplementary Materials

Supplementary Table 1: association between variables and diagnoses. *(Supplementary Materials)*

References

[1] M. R. de la Vega, E. Chapman, and D. D. Zhang, "NRF2 and the Hallmarks of Cancer," *Cancer Cell*, vol. 34, no. 1, pp. 21–43, 2018.

[2] C. Geismann, A. Arlt, S. Sebens, and H. Schafer, "Cytoprotection "gone astray": Nrf2 and its role in cancer," *OncoTargets and Therapy*, vol. 2014, no. 7, pp. 1497–1518, 2014.

[3] G. M. DeNicola, F. A. Karreth, T. J. Humpton et al., "Oncogene-induced Nrf2 transcription promotes ROS detoxification and tumorigenesis," *Nature*, vol. 475, no. 7354, pp. 106–109, 2011.

[4] W. Tian, M. R. de la Vega, C. J. Schmidlin, A. Ooi, and D. D. Zhang, "Kelch-like ECH-associated protein 1 (KEAP1) differentially regulates nuclear factor erythroid-2-related factors 1 and 2 (NRF1 and NRF2)," *Journal of Biological Chemistry*, vol. 293, no. 6, pp. 2029–2040, 2018.

[5] W. Wang and J. Y. Chan, "Nrf1 Is Targeted to the Endoplasmic Reticulum Membrane by an N-terminal Transmembrane Domain," *Journal of Biological Chemistry*, vol. 281, no. 28, pp. 19676–19687, 2006.

[6] L. Fattore, S. Costantini, D. Malpicci et al., "MicroRNAs in melanoma development and resistance to target therapy," *Oncotarget*, vol. 8, no. 13, pp. 22262–22278, 2017.

[7] X. Cheng, C.-H. Ku, and R. C. M. Siow, "Regulation of the Nrf2 antioxidant pathway by microRNAs: new players in micromanaging redox homeostasis," *Free Radical Biology & Medicine*, vol. 64, pp. 4–11, 2013.

[8] P. E. Bennett, L. Bemis, D. A. Norris, and Y. G. Shellman, "miR in melanoma development: miRNAs and acquired hallmarks of cancer in melanoma," *Physiological Genomics*, vol. 45, no. 22, pp. 1049–1059, 2013.

[9] C. L. Ross, S. Kaushik, R. Valdes-Rodriguez, and R. Anvekar, "MicroRNAs in cutaneous melanoma: role as diagnostic and prognostic biomarkers," *Journal of Cellular Physiology*, vol. 233, no. 7, pp. 5133–5141, 2018.

[10] J. Y. Li, L. L. Zheng, T. T. Wang, and M. Hu, "Functional Annotation of Metastasis-associated MicroRNAs of Melanoma," *Chinese Medical Journal*, vol. 129, no. 20, pp. 2484–2490, 2016.

[11] A. Mohammadpour, M. Derakhshan, H. Darabi, P. Hedayat, and M. Momeni, "Melanoma: Where we are and where we go," *Journal of Cellular Physiology*, vol. 234, no. 4, pp. 3307–3320, 2018.

[12] H. R. Hintsala, E. Jokinen, K. M. Haapasaari et al., "Nrf2/Keap1 Pathway and Expression of Oxidative Stress Lesions 8-hydroxy-2'-deoxyguanosine and Nitrotyrosine in Melanoma," *Anticancer Research*, vol. 36, no. 4, pp. 1497–1506, 2016.

[13] H. R. Hintsala, K. M. Haapasaari, Y. Soini, and P. Karihtala, "An immunohistochemical study of NFE2L2, KEAP1 and 8-hydroxy-2'-deoxyguanosine and the EMT markers SNAI2, ZEB1 and TWIST1 in metastatic melanoma," *Histology and Histopathology*, vol. 32, no. 2, pp. 129–136, 2017.

[14] H.-C. Huang, T. Nguyen, and C. B. Pickett, "Phosphorylation of Nrf2 at Ser-40 by protein kinase C regulates antioxidant response element-mediated transcription," *Journal of Biological Chemistry*, vol. 277, no. 45, pp. 42769–42774, 2002.

[15] K. J. Livak and T. D. Schmittgen, "Analysis of relative gene expression data using real-time quantitative PCR and the 2(-delta delta C(T)) method," *Methods*, vol. 25, no. 4, pp. 402–408, 2001.

[16] L. Xu, S. S. Shen, Y. Hoshida et al., "Gene expression changes in an animal melanoma model correlate with aggressiveness of human melanoma metastases," *Molecular Cancer Research*, vol. 6, no. 5, pp. 760–769, 2008.

[17] O. Kabbarah, C. Nogueira, B. Feng et al., "Integrative genome comparison of primary and metastatic melanomas," *PLoS ONE*, vol. 5, no. 5, p. e10770, 2010.

[18] H. Mitsui, F. Kiecker, A. Shemer et al., "Discrimination of dysplastic nevi from common melanocytic nevi by cellular and molecular criteria," *Journal of Investigative Dermatology*, vol. 136, no. 10, pp. 2030–2040, 2016.

[19] M. A. Kallio, J. T. Tuimala, T. Hupponen et al., "Chipster: user-friendly analysis software for microarray and other high-throughput data," *BMC Genomics*, vol. 12, no. 1, 2011.

[20] American Joint Committee on Cancer, "Melanoma of the skin," in *AJCC Cancer Staging Manual*, M. B. Amin, S. Edge, F. Greene, D. R. Byrd, and R. K. Brookland, Eds., Springer, New York, NY, 8th ed edition, 2016.

[21] H. Digaleh, M. Kiaei, and F. Khodagholi, "Nrf2 and Nrf1 signaling and ER stress crosstalk: implication for proteasomal

degradation and autophagy," *Cellular and Molecular Life Sciences*, vol. 70, no. 24, pp. 4681–4694, 2013.

[22] A. S. Nikitina, E. I. Sharova, S. A. Danilenko et al., "Novel RNA biomarkers of prostate cancer revealed by RNA-seq analysis of formalin-fixed samples obtained from Russian patients," *Oncotarget*, vol. 8, no. 20, pp. 32990–33001, 2017.

[23] Y. Zhao, L. Min, C. Xu et al., "Construction of disease-specific transcriptional regulatory networks identifies co-activation of four gene in esophageal squamous cell carcinoma," *Oncology Reports*, vol. 38, no. 1, pp. 411–417, 2017.

[24] P. Hersey and X. D. Zhang, "Adaptation to ER stress as a driver of malignancy and resistance to therapy in human melanoma," *Pigment Cell & Melanoma Research*, vol. 21, no. 3, pp. 358–367, 2008.

[25] D. H. Oh, D. Rigas, A. Cho, and J. Y. Chan, "Deficiency in the nuclear-related factor erythroid 2 transcription factor (Nrf1) leads to genetic instability," *The FEBS Journal*, vol. 279, no. 22, pp. 4121–4130, 2012.

[26] W. Han, M. Ming, R. Zhao, J. Pi, C. Wu, and Y.-Y. He, "Nrf1 CNC-bZIP protein promotes cell survival and nucleotide excision repair through maintaining glutathione homeostasis," *Journal of Biological Chemistry*, vol. 287, no. 22, pp. 18788–18795, 2012.

[27] E. Kari, H.-R. Teppo, K.-M. Haapasaari et al., "Nuclear factor erythroid 2-related factors 1 and 2 are able to define the worst prognosis group among high-risk diffuse large B cell lymphomas treated with R-CHOEP," *Journal of Clinical Pathology*, vol. 72, no. 4, pp. 316–321, 2019.

[28] L. Wang, C. Zhang, L. Qin et al., "The prognostic value of NRF2 in solid tumor patients: a meta-analysis," *Oncotarget*, vol. 9, no. 1, pp. 1257–1265, 2018.

[29] B. Wolf, G. Goebel, H. Hackl, and H. Fiegl, "Reduced mRNA expression levels of NFE2L2 are associated with poor outcome in breast cancer patients," *BMC Cancer*, vol. 16, no. 1, p. 821, 2016.

[30] A. Lau, W. Tian, S. A. Whitman, and D. D. Zhang, "The predicted molecular weight of Nrf2: it is what it is not," *Antioxid Redox Signal*, vol. 18, no. 1, pp. 91–93, 2013.

[31] C. Li, J. Lyu, and Q. H. Meng, "MiR-93 Promotes Tumorigenesis and Metastasis of Non-Small Cell Lung Cancer Cells by Activating the PI3K/Akt Pathway via Inhibition ofLKB1/PTEN/CDKN1A," *Journal of Cancer*, vol. 8, no. 5, pp. 870–879, 2017.

[32] Y. Gao, K. Deng, X. Liu et al., "Molecular mechanism and role of microRNA-93 in human cancers: a study based on bioinformatics analysis, meta-analysis, and quantitative polymerase chain reaction validation," *Journal of Cellular Biochemistry*, vol. 120, no. 4, pp. 6370–6383, 2019.

[33] S. Goswami, R. S. Tarapore, A. M. Poenitzsch Strong et al., "MicroRNA-340-mediated degradation of microphthalmia-associated transcription factor (MITF) mRNA is inhibited by coding region determinant-binding protein (CRD-BP)," *J Biol Chem*, vol. 290, no. 1, pp. 384–395, 2015.

[34] A. M. Poenitzsch Strong, V. Setaluri, and V. S. Spiegelman, "MicroRNA-340 as a modulator of RAS-RAF-MAPK signaling in melanoma," *Archives of Biochemistry and Biophysics*, vol. 563, pp. 118–124, 2014.

[35] Q. J. Guo, J. N. Mills, S. G. Bandurraga et al., "MicroRNA-510 promotes cell and tumor growth by targeting peroxiredoxin1 in breast cancer," *Breast Cancer Research*, vol. 15, no. 4, p. R70, 2013.

[36] D. Chen, Y. Li, Z. Yu et al., "Downregulated microRNA-510-5p acts as a tumor suppressor in renal cell carcinoma," *Molecular Medicine Reports*, vol. 12, no. 2, pp. 3061–3066, 2015.

[37] X. Yu, X. Zhang, T. Bi et al., "MiRNA expression signature for potentially predicting the prognosis of ovarian serous carcinoma," *Tumour Biology*, vol. 34, no. 6, pp. 3501–3508, 2013.

[38] X. Zhang, G. Guo, G. Wang et al., "Profile of differentially expressed miRNAs in high-grade serous carcinoma and clear cell ovarian carcinoma, and the expression of miR-510 in ovarian carcinoma," *Molecular Medicine Reports*, vol. 12, no. 6, pp. 8021–8031, 2015.

[39] W. Chen, Z. Tang, Y. Sun et al., "miRNA expression profile in primary gastric cancers and paired lymph node metastases indicates that miR-10a plays a role in metastasis from primary gastric cancer to lymph nodes," *Experimental and Therapeutic Medicine*, vol. 3, no. 2, pp. 351–356, 2012.

[40] C. E. Vejnar, M. Blum, and E. M. Zdobnov, "miRmap web: comprehensive microRNA target prediction online," *Nucleic Acids Research*, vol. 41, no. W1, pp. W165–W168, 2013.

[41] S. Babapoor, R. Wu, J. Kozubek, D. Auidi, J. M. Grant-Kels, and S. S. Dadras, "Identification of microRNAs associated with invasive and aggressive phenotype in cutaneous melanoma by next-generation sequencing," *Lab Invest*, vol. 97, no. 6, pp. 636–648, 2017.

[42] S. Guo, W. Guo, S. Li et al., "Serum miR-16: a potential biomarker for predicting melanoma prognosis," *Journal of Investigative Dermatology*, vol. 136, no. 5, pp. 985–993, 2016.

[43] N. Lin, Y. Zhou, X. Lian, and Y. Tu, "Expression of microRNA-106b and its clinical significance in cutaneous melanoma," *Genetics and Molecular Research*, vol. 14, no. 4, pp. 16379–16385, 2015.

[44] N. Li, "Low expression of Mir-137 predicts poor prognosis in cutaneous melanoma patients," *Medical Science Monitor*, vol. 22, pp. 140–144, 2016.

[45] P. Dietrich and A. K. Bosserhoff, "Melanoma sponge on pigmentation gene to reduce tumour-suppressive microRNAs," *Pigment Cell & Melanoma Research*, vol. 31, no. 3, pp. 350-351, 2018.

[46] K.-H. Kim, B.-H. Bin, J. Kim et al., "Novel inhibitory function of miR-125b in melanogenesis," *Pigment Cell & Melanoma Research*, vol. 27, no. 1, pp. 140–144, 2014.

[47] S. Noguchi, M. Kumazaki, Y. Yasui, T. Mori, N. Yamada, and Y. Akao, "MicroRNA-203 regulates melanosome transport and tyrosinase expression in melanoma cells by targeting kinesin superfamily protein 5b," *The Journal of Investigative Dermatology*, vol. 134, no. 2, pp. 461–469, 2014.

[48] M. Vitiello, A. Tuccoli, R. D'Aurizio et al., "Context-dependent miR-204 and miR-211 affect the biological properties of amelanotic and melanotic melanoma cells," *Oncotarget*, vol. 8, no. 15, pp. 25395–25417, 2017.

[49] X. Dai, C. Rao, H. Li et al., "Regulation of pigmentation by microRNAs: MITF-dependent microRNA-211 targets TGF-β receptor 2," *Pigment Cell & Melanoma Research*, vol. 28, no. 2, pp. 217–222, 2015.

[50] A. H. Shain, I. Yeh, I. Kovalyshyn et al., "The genetic evolution of melanoma from precursor lesions," *The New England Journal of Medicine*, vol. 373, no. 20, pp. 1926–1936, 2015.

[51] J. Xu, J. T. F. Wise, L. Wang, K. Schumann, Z. Zhang, and X. Shi, "Dual roles of oxidative stress in metal carcinogenesis," *Journal of Environmental Pathology, Toxicology and Oncology*, vol. 36, no. 4, pp. 345–376, 2017.

[52] C. Sangokoya, M. J. Telen, and J. T. Chi, "microRNA miR-144 modulates oxidative stress tolerance and associates with anemia severity in sickle cell disease," *Blood*, vol. 116, no. 20, pp. 4338–4348, 2010.

Hindawi
Oxidative Medicine and Cellular Longevity
Volume 2019, Article ID 6470950, 9 pages
https://doi.org/10.1155/2019/6470950

Research Article

Nitric Oxide Metabolites and Lung Cancer Incidence: A Matched Case-Control Study Nested in the ESTHER Cohort

Xīn Gào,[1,2] Yang Xuan,[1,2] Axel Benner,[3] Ankita Anusruti,[1,2] Hermann Brenner,[1,2,4,5] and Ben Schöttker[1,2]

[1]*Division of Clinical Epidemiology and Aging Research, German Cancer Research Center, Heidelberg, Germany*
[2]*Network Aging Research, Heidelberg University, Germany*
[3]*Division of Biostatistics, German Cancer Research Center, Heidelberg, Germany*
[4]*Division of Preventive Oncology, German Cancer Research Center and National Center for Tumor Diseases (NCT), Heidelberg, Germany*
[5]*German Cancer Consortium (DKTK), German Cancer Research Center, Heidelberg, Germany*

Correspondence should be addressed to Ben Schöttker; b.schoettker@dkfz.de

Received 26 May 2019; Revised 18 July 2019; Accepted 26 July 2019; Published 2 September 2019

Guest Editor: Jayeeta Ghose

Studies suggest that nitric oxide (NO) may have a possible role in lung carcinogenesis. This study is aimed to evaluate the association of the NO metabolites, namely, nitrite and nitrate, with lung cancer incidence. We conducted a matched case-control study ($n = 245$ incident lung cancer cases and $n = 735$ controls) based on the German ESTHER cohort ($n = 9{,}940$). Controls were matched to cases on age, sex, smoking status (never/former/current smoking), and pack-years of smoking. The sum of nitrite and nitrate was measured in urine samples using a colorimetric assay and was standardized for renal function by urinary creatinine. Conditional logistic regression models, adjusted for lifestyle factors, asthma prevalence, and family history of lung cancer, were used to estimate odds ratios (ORs) and 95% confidence intervals (95% CI). Among incident lung cancer cases, high nitrite/nitrate levels were statistically significantly associated with current smoking, a low BMI, and the oxidative stress biomarker 8-isoprostane levels. Nitrite/nitrate levels in the top quintile were statistically significantly associated with lung cancer incidence: the OR (95% CI) was 1.37 (1.04-1.82) for comparison with the bottom quintile. This association was unaltered after additional adjustment for 8-isoprostane levels and C-reactive protein (CRP). In conclusion, this large cohort study suggested that subjects with high urinary nitrite/nitrate concentrations had an increased risk of lung cancer and this association was independent of smoking, CRP, 8-isoprostane levels, and other established lung cancer risk factors. Further studies are needed to validate these findings and to confirm the hypothesis that pathologically high levels of NO are involved in lung cancer development.

1. Introduction

Lung cancer is one of the most common causes of cancer death worldwide with a poor prognosis [1, 2]. Oxidative stress is suggested to mediate chronic inflammation-induced lung cancer development [3]. Inflammatory cells are recruited to the site of inflammation leading to respiratory burst, during which the inflammatory cells produce more reactive oxygen species (ROS). The sustained oxidative environment results in the transformation of normal cells to cancer cells [4, 5]. In addition, smokers have a much higher risk of developing lung cancer than nonsmokers [6]. It has been shown that cigarette smoking leads to oxidative stress and inflammation in an acute cigarette smoking model [7]. Therefore, oxidative stress and inflammation might partially mediate the effect of smoking on lung cancer development.

Endogenous nitric oxide (NO) is a multifunctional inflammatory molecule and promotes inflammation under physiological condition [8]. It is synthesized by 3 isoforms of NO synthase (NOS). The neuronal NOS and endothelial NOS constitutively catalyze the formation of NO, while the inducible NOS (iNOS) is being induced by inflammatory cytokines and produces larger, toxic amounts of NO [9]. NO is also a free radical. It has one unpaired electron, which

makes it susceptible for reactions with other radical species [10]. For instance, the reaction of NO with the superoxide anion (O_2^-) leads to peroxynitrite ($ONOO^-$) formation [11]. Thus, excessive formation of NO results in elevated generation of reactive oxygen/nitrogen species, which may induce oxidative stress.

NO plays a pivotal role in cancer development. On the one hand, excessive NO is toxic and can prevent tumor growth by increasing the apoptosis rate of cells. While on the other hand, NO is a mediator of signaling pathways, which promote cancer progression and metastasis [9]. In summary, NO plays an important role in the complex interrelationships of ROS, inflammation, and cancer development and growth [12].

However, it is difficult to detect NO in tissues and biological fluids directly due to its highly reactive nature and low concentration. The end-products of NO metabolism, nitrite and nitrate, are much more stable and can be used to reflect the systemic NO production [11]. To our knowledge, no previous study has investigated the association between nitrite/nitrate levels and lung cancer development in a prospective, population-based study. We addressed this research question by performing a matched case-control study nested in a large, prospective cohort study from Germany.

2. Materials and Methods

2.1. Study Population. This investigation was based on the ESTHER cohort study (Epidemiologische Studie zu Chancen der Verhütung, Früherkennung und optimierten Therapie chronischer Erkrankungen in der älteren Bevölkerung [German]), which is a population-based, longitudinal study, with repeated investigation of inhabitants in the German federal state Saarland. The details of the ESTHER cohort study have been reported elsewhere [13]. In brief, 9940 individuals, aged 50-75 years, were invited to participate during a routine health checkup between 2000 and 2002. So far, those participants were recontacted 5 times: 2, 5, 8, 11, and 14 years after baseline. Information on sociodemographic characteristics, lifestyle, smoking habits, and diet was investigated by using a comprehensive questionnaire at baseline as well as at follow-ups. The ESTHER study was approved by the ethics committees of the University of Heidelberg and the state medical board of Saarland, Germany. Written informed consent was issued by all participants.

2.2. Cancer Follow-Up. Information on lung cancer was provided by the Saarland Cancer Registry up to the end of the year 2014. Linkage of ESTHER participants with data of the Saarland Cancer Registry was possible for 99.7% of the cohort's participants. Lung cancer cases were ascertained according to the 10^{th} revision of the International Statistical Classification of Diseases (ICD-10) code C34.

2.3. Selection of Case and Control Subjects. From 252 incident lung cancer cases, during a mean follow-up time of 13.4 years, 245 could be included in the present analysis because they donated a blood sample and a urine sample at baseline of the ESTHER cohort. Each of the lung cancer cases was matched with three controls from the same cohort on sex, age (±5 years), smoking status (never/former/current smoker), and pack-years of smoking (±10 years).

2.4. Laboratory Analyses. At baseline, a blood sample and a spontaneous spot urine sample were collected by general practitioners (GPs) during the health checkup and then shipped to the study center and maintained at -80°C until further processing. Urinary concentrations of nitrite/nitrate were determined using the nitrite/nitrate Colorimetric Assay Kit of Cayman Chemical (Ann Arbor, Michigan, USA). This method detects the sum of nitrate and nitrite. Urine samples were used directly after dilution to a proper concentration (1 : 5, 1 : 25, or 1 : 50 depending on the levels of nitrite/nitrate in the urine sample). For renal function adjustment of the spot urine samples, urinary creatinine was determined by the kinetic Jaffe method. In addition, the acute-phase inflammatory protein C-reactive protein (CRP) was measured in serum samples by immunoturbidimetry with the wrCRP antibody (Bayer, Leverkusen, Germany) on the ADVIA 2400. Furthermore, the levels of an established oxidative stress marker, urinary 8-isoprostane, were determined by the 8iso1 ELISA kit from Detroit R&D (Detroit, Michigan, USA).

2.5. Covariates. Information on sociodemographic characteristics, including age, sex, smoking status, pack-years of smoking, education, physical activity, vegetable consumption, meat consumption, family history of lung cancer, and individual history of asthma, was collected by a standardized self-administered questionnaire. To calculate body mass index (BMI), height and weight were measured by the GPs during the health checkup and documented on a standardized form.

2.6. Statistical Analyses. Baseline characteristics of cases and controls were expressed as medians (interquartile ranges) or proportions. Differences between the two groups were determined by the Wilcoxon tests for continuous variables and by the chi-square tests for categorical variables. To assess the determinants of nitrite/nitrate concentrations, distributions of nitrite/nitrate concentrations across categories of baseline characteristics were compared using the Wilcoxon-Mann-Whitney tests.

To evaluate the association of nitrite/nitrate levels and lung cancer incidence, conditional logistic regression was used to compute odds ratios (ORs) and 95% confidence intervals (CIs). The main model was adjusted for body mass index (BMI), education, family history of lung cancer, asthma prevalence, physical activity, and vegetable and meat consumption. In sensitivity models, the inflammatory marker CRP and the oxidative stress marker 8-isoprostane were additionally added to the main model. In order to address possible reverse causality, a sensitivity analysis was conducted, in which cancer cases that occurred in the first 5 years of follow-up were excluded. A dose-response analysis was conducted using restricted cubic spline (RCS) functions with five knots at the 10^{th}, 30^{th}, 50^{th}, 70^{th}, and 90^{th} percentiles of the nitrite/nitrate distribution.

Multiple imputation was applied to impute covariates with missing values [14]. All covariates had less than 3.7% missing values in study population. Briefly, five data sets were imputed with the SAS procedure PROC MI. The conditional logistic regression models were performed in the five imputed data sets, and the results were combined by the SAS procedure PROC MIANALYZE. Restricted cubic splines were produced from one of the five imputed data sets.

All statistical tests were two-sided using a significant level of 0.05. All analyses were performed with the Statistical Analysis System (SAS) version 9.4 (SAS Institute Inc., Cary, NC).

3. Results

Table 1 presents the sociodemographic and lifestyle characteristics of the 245 lung cancer patients and the 735 controls at baseline. Age, sex, smoking status, and pack-years of smoking were almost identically distributed among cases and controls due to the matching. In addition, there was no statistically significant difference between cases and controls in school education, physical activity, vegetable and meat consumption frequency, asthma prevalence, family history of lung cancer, and CRP and 8-isoprostane levels. This is likely also a result of the matching by age, sex, and smoking. The only statistically significantly difference between cases and controls was observed for BMI. Study participants who developed lung cancer during follow-up were more frequently lean (BMI < 25 kg/m^2) and less frequently obese (BMI > 30 kg/m^2) compared to matched control subjects. Nitrite/nitrate levels were higher in study participants who were diagnosed with lung cancer during follow-up (median (IQR) = 122 (80-206)) than among controls (median (IQR) = 114 (75-170)), but the median difference was not statistically significant.

Table 2 shows median (IQR) nitrite/nitrate levels across the categories of baseline characteristics. High nitrite/nitrate levels were statistically significantly associated with current smoking and high 8-isoprostane concentrations among cases and controls. Among cases, they were additionally statistically significantly associated with a low BMI. Among controls, nitrite/nitrate levels were statistically significantly higher among subjects aged < 65 years compared to older subjects.

Table 3 presents the association between nitrite/nitrate levels and lung cancer incidence. The top quintile of nitrite/nitrate levels (≥192.8 μmol/mmol creatinine) was statistically significantly associated with lung cancer incidence, when compared to the bottom quintile (<66.9 μmol/mmol creatinine): the OR (95% CI) was 1.37 (1.04-1.82) in the main model. Additional adjustments for CRP and 8-isoprostane levels did not change this finding. Furthermore, the strength of the observed association remained similar after excluding lung cancer cases within the first 5 years of follow-up (Table 4).

The dose-response relationship between nitrite/nitrate concentrations and lung cancer incidence is presented in Figure 1. It shows that the association is not linear and that a statistically significant association is only present at high nitrite/nitrate concentrations (approx. >200 μmol/mmol creatinine). This is in agreement with the findings from the logistic models, in which only an increased lung cancer risk was found in the highest nitrite/nitrate quintile (≥192.8 μmol/mmol creatinine).

4. Discussion

In this prospective matched case-control study from Germany, we investigated the determinants of urinary nitrite/nitrate levels and the association between nitrite/-nitrate levels and lung cancer incidence. We observed that high nitrite/nitrate levels were associated with lower age in controls and a lower BMI among cases. Current smoking and high 8-isoprostane levels were associated with high nitrite/nitrate levels in both groups. Furthermore, the association of nitrite/nitrate levels was not linear, and only participants with nitrite/nitrate levels greater than approximately 200 μmol/mmol creatinine had an increased lung cancer risk.

Previous studies have demonstrated that NO is a mediator and regulator in inflammatory responses. Whereas low NO is anti-inflammatory, excessively elevated NO promotes inflammation and oxidative stress under pathological conditions [15, 16]. This could explain why we only observed an association of nitrite/nitrate levels and lung cancer incidence at high nitrite/nitrate concentrations. Interestingly, this association was independent from CRP and 8-isoprostane levels, which suggests that the pathway from NO to lung cancer is independent from the inflammatory and oxidative stress processes that are reflected by these biomarkers.

Figure 2 illustrates the observed associations of nitrite/nitrate, 8-isoprostane, and CRP levels with each other and with lung cancer incidence and puts them into context with reactive oxygen species (ROS) and NO. Previous studies have shown urinary 8-isoprostane levels and CRP to be associated with lung cancer risk [17, 18]. Nitrite/nitrate levels were associated with 8-isoprostane levels in our study but not with CRP. However, we showed in a previous analysis of the ESTHER study that 8-isoprostane levels and CRP are associated with each other. In the context of these close associations of these oxidative stress and inflammatory biomarkers, the observed independent association of nitrite/nitrate levels with lung cancer incidence was surprising. However, adjustment for other biomarkers of oxidative stress or inflammation (e.g., interleukin-6) might have led to stronger attenuations of the strength of the association and should be investigated in future studies.

The following mechanisms could explain the observed association of nitrite/nitrate concentrations in urine with lung cancer incidence. NO can react with other reactive oxygen species (ROS) which is converted to reactive nitrogen species (RNS), which are subsequently metabolized to nitrite and nitrate [3]. NO can be oxidized to nitrite in the presence of oxygen. Nitrate is produced by the reaction of NO and singlet oxygen, in which peroxynitrite ($ONOO^-$) is generated as a midproduct. Peroxynitrite is a strong oxidant and may exert negative effects on DNA, proteins, and lipids initiating cancer cell transition [14, 19]. In addition, RNS/ROS-

Table 1: Baseline characteristics of the incident lung cancer cases and matched controls, the ESTHER study (2000-2014).

Characteristics	Incident lung cancer cases			Controls			$P_{difference}$
	n (cases)	%	Median (IQR)	*n* (controls)	%	Median (IQR)	
Age (years)	245	—	62 (59-68)	735	—	63 (59-68)	0.885
Sex							
Female	75	30.6		226	30.7	—	
Male	170	69.4		509	69.3	—	
Smoking status							0.937
Never smoker	29	12.1		93	13.0	—	
Former smoker	87	36.2		260	36.2	—	
Current smoker	124	51.7		365	50.8	—	
Pack-years of smoking	221	—	34.8 (19.3-48.0)	624	—	33.8 (14.0-47.4)	0.423
School education (years)							0.077
≤9	198	83.2	—	551	77.0	—	
10-11	19	8.0	—	82	11.4	—	
≥12	21	8.8	—	83	11.6	—	
Physical activity							0.182
Inactive	67	27.6	—	165	22.5	—	
Sedentary	110	45.3	—	351	48.0	—	
Vigorously active	66	27.1	—	216	29.5	—	
BMI (kg/m^2)							**0.037**
<25	83	33.9	—	202	27.0	—	
25 - <30	103	42.0	—	330	44.2	—	
≥30	59	24.1	—	215	28.8	—	
Meat consumption							0.711
<once/week	81	36.0	—	259	37.4	—	
Once/week	133	54.2	—	369	53.3	—	
>once/week	22	9.8	—	65	9.4	—	
Vegetable consumption							0.338
<once/week	25	10.6	—	110	15.6	—	
Once/week	160	68.1	—	442	62.5	—	
>once/week	50	21.3	—	155	21.9	—	
Asthma							0.292
Yes	21	8.9	—	49	6.8	—	
No	216	91.1	—	671	93.2	—	
Family history of lung cancer							0.709
Yes	27	11.4	—	76	10.5	—	
No	210	88.6	—	646	89.5	—	
CRP (mg/L)	243	—	2.6 (1.3-5.8)	729	—	2.2 (1.1-5.1)	0.164
8-Isoprostane (nmol/mmol creatinine)	240		0.25 (0.18-0.33)	729		0.23 (0.17-0.31)	0.059
Nitrite/nitrate (μmol/mmol creatinine)	245	—	122 (80-206)	733	—	114 (75-170)	0.081

Abbreviation: BMI: body mass index; CRP: C-reactive protein. Note: lung cancer cases and controls were 1 : 3 matched for age, sex, smoking status, and pack-years of smoking.

sensitive pathways may be activated to promote cell growth/-proliferation, differentiation, and angiogenesis in cancer [9].

To the best of our knowledge, the associations of NO metabolites and the risk of lung or any other cancer site have not been investigated by prospective, population-based studies before. However, a case-control study nested in a prostate cancer cohort from Sweden observed that high compared to low/negative iNOS immunoreactivity in prostate tumor epithelial cells was associated with a strongly increased 10-year prostate cancer mortality (OR (95% CI), 3.80 (1.45-9.97)) [20]. These findings for prostate cancer suggest that elevated NO production may also be a useful prognostic marker in cancer research, which deserves attention in future studies.

In addition to 8-isoprostane levels, nitrite/nitrate levels were associated with current smoking and a low BMI among cases. This might be explained by the long latency period of

Table 2: Median (IQR) of a nitrite/nitrate concentration according to population characteristics in cases and controls, the ESTHER study (2000-2014).

Characteristics	Cases		Controls	
	n (cases)	Nitrite/nitrate (μmol/mmol creatinine)	*n* (controls)	Nitrite/nitrate (μmol/mmol creatinine)
Age (year)				
50-60	79	122.1 (85.2-202.1)	245	122.0 (88.0-182.9)
60-64	62	130.3 (79.4-256.5)	184	120.9 (80.4-187.2)
65-69	60	103.2 (69.7-160.6)	176	98.9 (64.9-158.8)
70-75	44	136.2 (88.7-237.5)	130	97.1 (62.7-147.0)
P value		0.323		**<0.001**
Sex				
Female	75	121.5 (67.8-227.0)	226	117.6 (78.8-184.0)
Male	170	120.8 (81.4-181.7)	509	111.2 (71.9-164.3)
P value		0.595		0.199
Smoking status				
Never smoker	29	104.7 (60.4-125.5)	93	108.9 (74.7-146.3)
Former smoker	87	112.6 (70.0-172.7)	260	102.2 (64.8-151.4)
Current smoker	124	139.3 (92.8-231.1)	365	127.2 (87.0-188.7)
P value		**0.009**		**<0.001**
Pack-years of smoking				
≤15.0	73	107.1 (60.4-167.1)	274	106.9 (71.8-158.1)
15.0 - ≤34.0	59	117.7 (69.4-204.8)	160	114.5 (74.6-162.5)
34.0 - ≤47.5	56	141.7 (89.5-198.6)	148	114.6 (75.9-171.7)
>47.5	57	136.5 (94.5-248.1)	153	122.0 (79.4-197.1)
P value		0.071		0.105
Education levels (years)				
≤9	198	122.0 (78.7-195.8)	551	113.7 (74.1-168.6)
10-11	19	112.6 (79.9-235.3)	82	112.7 (67.7-163.5)
≥12	21	145.7 (93.4-250.4)	83	122.7 (92.6-211.9)
P value		0.788		0.103
Physical activity				
Inactive	67	121.6 (77.9-193.6)	165	118.6 (76.7-183.5)
Sedentary	110	123.7 (78.7-227.2)	351	110.8 (72.5-170.6)
Vigorously active	66	121.2 (94.1-216.0)	216	118.3 (74.6-167.7)
P value		0.846		0.510
BMI (kg/m^2)				
<25	83	135.8 (85.9-222.0)	199	118.4 (83.2-168.8)
25 - <30	103	134.4 (86.4-229.2)	325	114.3 (72.1-173.8)
≥30	59	98.7 (58.6-170.7)	211	105.0 (70.4-162.5)
P value		**0.022**		0.337
Meat intake frequency				
<once/week	81	125.5 (85.0-191.6)	259	114.3 (75.2-177.2)
Once/week	122	112.9 (79.4-207.5)	369	113.8 (74.3-165.7)
>once/week	22	121.8 (64.6-195.8)	65	120.5 (76.2-170.0)
P value		0.933		0.877
Vegetable consumption frequency				
<once/week	25	108.5 (71.3-181.7)	108	111.6 (75.7-152.3)
Once/week	160	125.4 (86.1-202.0)	435	113.8 (72.5-163.8)
>once/week	50	105.8 (67.0-188.3)	152	134.6 (80.8-227.3)
P value		0.240		0.134

Table 2: Continued.

Characteristics	Cases		Controls	
	n (cases)	Nitrite/nitrate (μmol/mmol creatinine)	*n* (controls)	Nitrite/nitrate (μmol/mmol creatinine)
Asthma prevalence				
No	216	121.5 (79.4-200.6)	671	114.0 (74.7-170.0)
Yes	21	107.2 (80.7-229.7)	49	112.7 (78.9-147.0)
P value		0.520		0.921
Family history of lung cancer				
No	210	121.2 (79.9-217.7)	646	113.9 (74.7-168.7)
Yes	27	132.3 (71.3-191.6)	76	111.3 (72.0-186.0)
P value		0.870		0.907
CRP (mg/L)				
≤1.175	52	114.3 (63.5-236.5)	191	118.0 (78.1-178.3)
1.175 - ≤2.325	59	148.9 (85.9-229.7)	184	108.9 (70.8-162.2)
2.325 - ≤5.140	67	113.0 (89.4-207.5)	177	111.2 (78.2-165.7)
>5.140	65	118.1 (76.0-171.5)	177	114.8 (70.3-174.6)
P value		0.520		0.739
8-Isoprostane (nmol/mmol creatinine)				
≤0.175	54	108.3 (69.4-158.0)	189	105.0 (70.5-155.7)
0.174 - ≤0.231	54	112.6 (79.5-193.6)	188	108.4 (73.4-162.5)
0.231 - ≤0.308	59	107.9 (67.1-176.9)	182	114.1 (75.7-175.5)
>0.308	73	167.0 (112.0-267.3)	170	138.9 (88.3-195.9)
P value		**0.001**		**0.026**

Abbreviations: BMI: body mass index; CRP: C-reactive protein.

Table 3: Associations of nitrite/nitrate concentration quintiles with lung cancer incidence, the ESTHER study (2000-2014).

	Nitrite/nitrate levels (μmol/mmol creatinine)	$n_{case}/n_{control}$	Main model[a] OR (95% CI)	Sensitivity model 1[b] OR (95% CI)	Sensitivity model 2[c] OR (95% CI)
Quintile 1	<66.9	48/147	Ref.	Ref.	Ref.
Quintile 2	66.9 - <97.2	39/147	0.81 (0.59-1.12)	0.81 (0.59-1.12)	0.82 (0.60-1.12)
Quintile 3	97.2 - <134.1	43/147	0.88 (0.65-1.20)	0.89 (0.65-1.21)	0.88 (0.65-1.20)
Quintile 4	134.1 - <192.8	48/147	1.00 (0.74-1.36)	1.01 (0.75-1.37)	1.01 (0.74-1.36)
Quintile 5	≥192.8	67/147	**1.37 (1.04-1.82)**	**1.38 (1.04-1.82)**	**1.36 (1.03-1.80)**

[a]Adjusted for body mass index (BMI), education, family history of lung cancer, asthma, physical activity, and vegetable and meat consumption frequency. In addition, potential confounding by the following factors was controlled by matching age, sex, smoking status, and pack-years of smoking. [b]Adjusted for variables of the main model+C-reactive protein. In addition, potential confounding by the following factors was controlled by matching age, sex, smoking status, and pack-years of smoking. [c]Adjusted for variables of the main model+8-isoprostane. In addition, potential confounding by the following factors was controlled by matching age, sex, smoking status, and pack-years of smoking. Note: numbers in bold: statistically significant estimates compared to the quintile 1 ($P < 0.05$).

lung cancer, and some lung cancer cases diagnosed during follow-up may have already been subclinical at the baseline examination. Lung cancer patients often experience loss of appetite and weight for a long period of time before they are diagnosed [21]. The association of a nitrite/nitrate concentration with current smoking was expected because cigarette smoke itself contains NO, which can cross the alveolar-capillary membrane. NO may also dilate the constricted respiratory tract, making more smoke get into the lung [15]. A previous study demonstrated that smoking led to increased nitrite/nitrate levels in exhaled breath condensate of subjects [21].

Furthermore, we observed that nitrite/nitrate levels were inversely associated with age in the control group, which confirms previous observations in healthy individuals [22]. This inverse association could be explained by the increased plasma concentrations of the NO synthase inhibitor, asymmetric dimethylarginine (ADMA), in older subjects [23]. However, the mechanism for these findings is not clear so far.

It has been shown that NO has pathophysiological effects on asthma and COPD. Elevated NO can lead to nitrosative stress in the airway epithelium, which may be responsible for steroid resistance or ineffectiveness in inflammatory pulmonary diseases [24]. Furthermore, cancer-cell-derived NO

Table 4: Associations of a nitrite/nitrate concentration with lung cancer incidence in a sensitivity analyses excluding lung cancer cases which occurred in the first 5 years of follow-up, the ESTHER study (2000-2014).

	Nitrite/nitrate levels (μmol/mmol creatinine)	$n_{case}/n_{control}$	Main model[a] OR (95% CI)	Sensitivity model 1[b] OR (95% CI)	Sensitivity model 2[c] OR (95% CI)
Quintile 1	<67.7	37/101	Ref.	Ref.	Ref.
Quintile 2	67.7 - <97.4	29/101	0.88 (0.60-1.29)	0.88 (0.602-1.29)	0.88 (0.60-1.29)
Quintile 3	97.4 - <133.7	31/101	0.95 (0.65-1.38)	0.95 (0.66-1.39)	0.95 (0.66-1.39)
Quintile 4	133.7 - <188.8	26/101	0.81 (0.55-1.18)	0.80 (0.55-1.18)	0.81 (0.55-1.19)
Quintile 5	≥188.77	45/100	1.36 (0.97-1.92)	1.36 (0.97-1.92)	1.34 (0.95-1.90)

[a]Adjusted for body mass index (BMI), education, family history of lung cancer, asthma, physical activity, and vegetable and meat consumption frequency. In addition, potential confounding by the following factors was controlled by matching age, sex, smoking status, and pack-years of smoking. [b]Adjusted for variables of the main model+C-reactive protein (CRP). In addition, potential confounding by the following factors was controlled by matching age, sex, smoking status, and pack-years of smoking. [c]Adjusted for variables of the main model+8-isoprostane. In addition, potential confounding by the following factors was controlled by matching age, sex, smoking status, and pack-years of smoking.

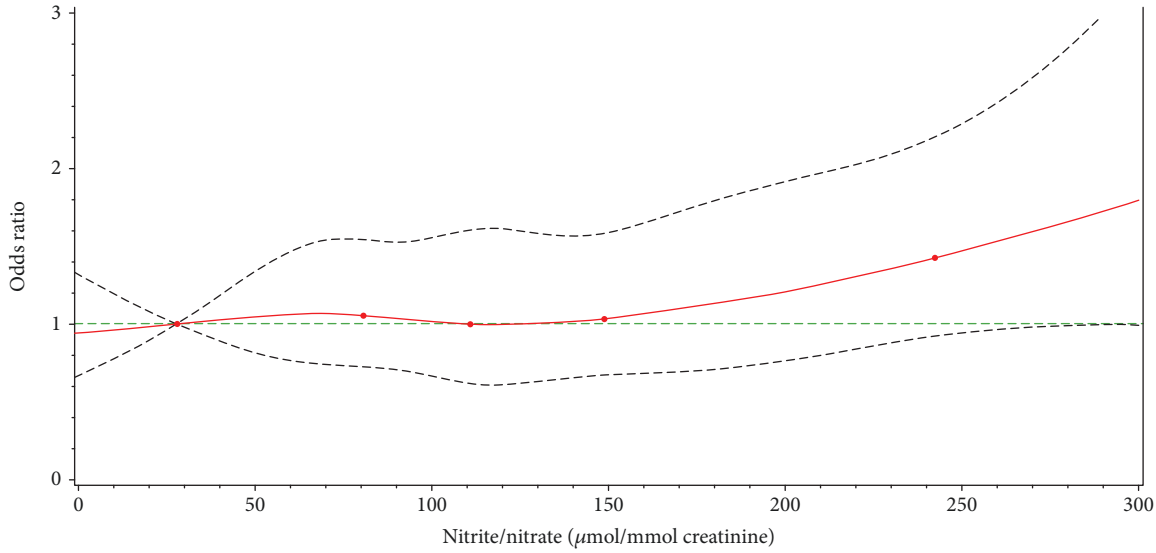

Figure 1: Dose-response relationship of a nitrite/nitrate concentration and lung cancer incidence, the ESTHER study (2000-2014). Notes: results of a logistic regression model adjusted for BMI, education, family history of lung cancer, asthma, physical activity, and vegetable and meat consumption frequency. In addition, potential confounding by the following factors was controlled by matching age, sex, smoking status, and pack-years of smoking. Knots: 10th, 30th, 50th, 70th, and 90th percentile. Solid red line: estimation for the odds ratio. Dashed grey lines: 95% confidence interval bands. Dashed green line: odds ratio = 1 as reference.

may promote cancer-cell invasion, proliferation, and angiogenesis [25]. Therefore, the link between NO and lung cancer suggests that inhibiting NO production might be a potential preventive and/or therapeutic strategy for lung cancer. The major approach to NO inhibition is suppressing NOS activity. A randomized preclinical trial reported that L-NMMA, a competitive NOS inhibitor, decreased lung tumor growth in a mouse model [26]. There is also evidence showing that inhaled steroid treatment reduces exhaled NO as well as the risk of lung cancer [27, 28]. However, the NOS inhibition approaches should be used with caution. Potential side effects, such as endothelial dysfunction, may be caused by inhibiting the NOS [29].

Our study has several strengths. First, a prospective matched case-control study design was used, and subjects with a history of lung cancer before baseline were excluded from the analyses to avoid reverse causality. In addition, cancer cases diagnosed within the first 5 years of follow-up were excluded in a sensitivity analysis to address the lag time of lung cancer development, and the results were consistent with the main results. Second, linkage to cancer registries ensured high certainty regarding lung cancer diagnoses and minimized attrition bias, which often affects cohort studies with long-term follow-up. Third, in order to control for confounding, cases were matched to controls for age, sex, smoking status, and pack-years of smoking, and models were comprehensively adjusted for other potential confounders, including 8-isoprostane levels and CRP. Nevertheless, several limitations in our study need to be considered when interpreting the results. First, the sampling of controls

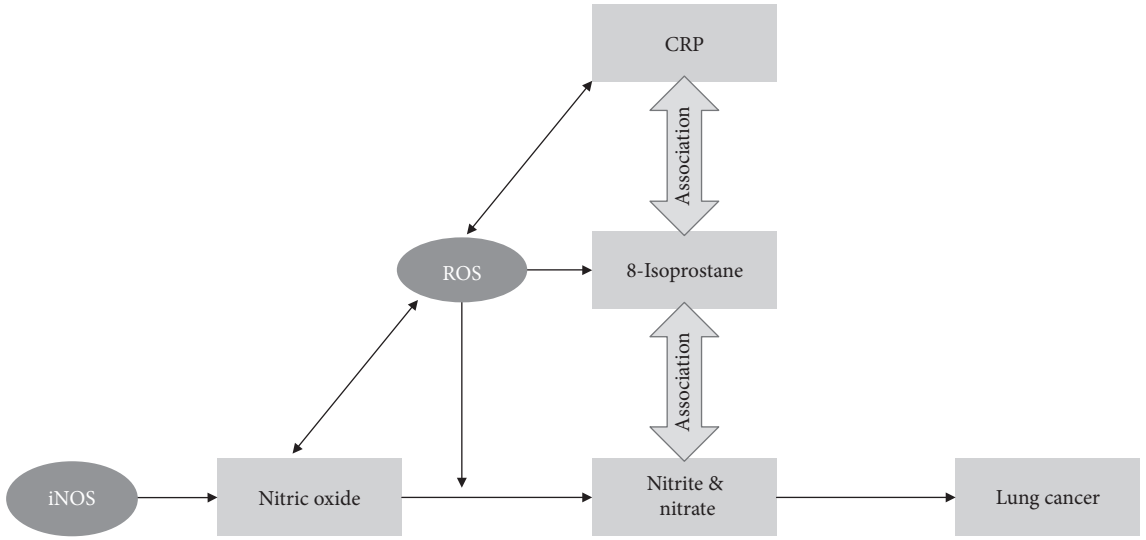

Figure 2: Schematic illustration of observed associations of nitrite/nitrate, 8-isoprostane, and CRP concentrations with lung cancer incidence. Abbreviation: CRP: C-reactive protein; iNOS: inducible nitric oxide synthase; ROS: reactive oxygen species.

reduces precision and power compared to a cohort design. Second, residual confounding can generally not be excluded in an observational study. Third, the number of cases in each quintile was relatively small and led to a rather low statistical power for quintile comparisons. Fourth, urinary nitrite/nitrate concentrations may also be influenced by a nitrate-rich diet [30, 31]. Although the logistic regression models were adjusted for vegetable consumption and meat consumption frequency, we cannot exclude residual confounding by diet in our analyses because no detailed food frequency questionnaire asking for specific nitrate-rich vegetables was used in our study. Lastly, urine samples were collected only once at baseline. Further studies with repeated measurements are needed because urinary nitrite/nitrate levels might vary during follow-up.

In conclusion, the current study observed that high urinary nitrite/nitrate levels were associated with high lung cancer incidence although the comparison between cases and controls was matched for age, sex, and smoking and controlled for other biomarkers of oxidative stress and inflammation. This suggests an independent mechanism that links pathologically high levels of NO to lung cancer development.

Data Availability

The total ESTHER study data cannot be made freely available due to data security regulations. Requests for access to the data used for this publication can be made to the corresponding author, Dr. Ben Schöttker (b.schoettker@dkfz.de).

Conflicts of Interest

The authors have no conflicts of interest to disclose.

Acknowledgments

This study was funded by a grant from the German Research Foundation (grant No. SCHO 1545/3-1) and by the China Scholarship Council (grant No. 201506010268 to Xīn Gào). The ESTHER study was funded by grants from the Ministry of Science, Research and the Arts Baden-Württemberg (Stuttgart, Germany), the German Federal Ministry of Education and Research (Berlin, Germany), the Federal Ministry of Family Affairs, Senior Citizens, Women and Youth (Berlin, Germany), and the Saarland State Ministry of Social Affairs, Health, Women and Family. The authors gratefully thank the study participants and their general practitioners as well as the laboratory and administrative staff of the ESTHER study team. The authors also gratefully acknowledge Prudence R. Carr for her effort to improve the English of the manuscript as well as her comments on the manuscript.

References

[1] J. Ferlay, M. Colombet, I. Soerjomataram et al., "Estimating the global cancer incidence and mortality in 2018: GLOBOCAN sources and methods," *International Journal of Cancer*, vol. 144, no. 8, pp. 1941–1953, 2019.

[2] F. Bray, J. Ferlay, I. Soerjomataram, R. L. Siegel, L. A. Torre, and A. Jemal, "Global cancer statistics 2018: GLOBOCAN estimates of incidence and mortality worldwide for 36 cancers in 185 countries," *CA: a Cancer Journal for Clinicians*, vol. 68, no. 6, pp. 394–424, 2018.

[3] S. Reuter, S. C. Gupta, M. M. Chaturvedi, and B. B. Aggarwal, "Oxidative stress, inflammation, and cancer: how are they linked?," *Free Radical Biology & Medicine*, vol. 49, no. 11, pp. 1603–1616, 2010.

[4] X. Gào, T. Wilsgaard, E. H. Jansen et al., "Pre-diagnostic derivatives of reactive oxygen metabolites and the occurrence of lung, colorectal, breast and prostate cancer: an individual

participant data meta-analysis of two large population-based studies," *International Journal of Cancer*, vol. 145, no. 1, pp. 49–57, 2019.

[5] X. Gào, T. Wilsgaard, E. Jansen et al., "Serum total thiol levels and the risk of lung, colorectal, breast and prostate cancer: a prospective case-cohort study," *International Journal of Cancer*, 2019.

[6] P. N. Lee, B. A. Forey, and K. J. Coombs, "Systematic review with meta-analysis of the epidemiological evidence in the 1900s relating smoking to lung cancer," *BMC Cancer*, vol. 12, no. 1, article 385, 2012.

[7] H. van der Vaart, D. S. Postma, W. Timens, and N. H. ten Hacken, "Acute effects of cigarette smoke on inflammation and oxidative stress: a review," *Thorax*, vol. 59, no. 8, pp. 713–721, 2004.

[8] J. N. Sharma, A. Al-Omran, and S. S. Parvathy, "Role of nitric oxide in inflammatory diseases," *Inflammopharmacology*, vol. 15, no. 6, pp. 252–259, 2007.

[9] X. Gào and B. Schöttker, "Reduction–oxidation pathways involved in cancer development: a systematic review of literature reviews," *Oncotarget*, vol. 8, no. 31, pp. 51888–51906, 2017.

[10] J. R. Lancaster Jr., "Nitric oxide: a brief overview of chemical and physical properties relevant to therapeutic applications," *Future Science OA*, vol. 1, no. 1, 2015.

[11] M. Kelm, "Nitric oxide metabolism and breakdown," *Biochimica et Biophysica Acta (BBA) - Bioenergetics*, vol. 1411, no. 2-3, pp. 273–289, 1999.

[12] F. Masri, "Role of nitric oxide and its metabolites as potential markers in lung cancer," *Annals of Thoracic Medicine*, vol. 5, no. 3, pp. 123–127, 2010.

[13] E. Raum, D. Rothenbacher, M. Low, C. Stegmaier, H. Ziegler, and H. Brenner, "Changes of cardiovascular risk factors and their implications in subsequent birth cohorts of older adults in Germany: a life course approach," *European Journal of Cardiovascular Prevention & Rehabilitation*, vol. 14, no. 6, pp. 809–814, 2007.

[14] S. Sinharay, H. S. Stern, and D. Russell, "The use of multiple imputation for the analysis of missing data," *Psychological Methods*, vol. 6, no. 4, pp. 317–329, 2001.

[15] W. Vleeming, B. Rambali, and A. Opperhuizen, "The role of nitric oxide in cigarette smoking and nicotine addiction," *Nicotine & Tobacco Research*, vol. 4, no. 3, pp. 341–348, 2002.

[16] J. W. Coleman, "Nitric oxide in immunity and inflammation," *International Immunopharmacology*, vol. 1, no. 8, pp. 1397–1406, 2001.

[17] M. S. Shiels, R. M. Pfeiffer, A. Hildesheim et al., "Circulating inflammation markers and prospective risk for lung cancer," *Journal of the National Cancer Institute*, vol. 105, no. 24, pp. 1871–1880, 2013.

[18] X. Gào, H. Brenner, B. Holleczek et al., "Urinary 8-isoprostane levels and occurrence of lung, colorectal, prostate, breast and overall cancer: results from a large, population-based cohort study with 14 years of follow-up," *Free Radical Biology & Medicine*, vol. 123, pp. 20–26, 2018.

[19] G. Y. Liou and P. Storz, "Reactive oxygen species in cancer," *Free Radical Research*, vol. 44, no. 5, pp. 479–496, 2010.

[20] A. Erlandsson, J. Carlsson, S. O. Andersson et al., "High inducible nitric oxide synthase in prostate tumor epithelium is associated with lethal prostate cancer," *Scandinavian Journal of Urology*, vol. 52, no. 2, pp. 129–133, 2018.

[21] J. Polanski, B. Jankowska-Polanska, J. Rosinczuk, M. Chabowski, and A. Szymanska-Chabowska, "Quality of life of patients with lung cancer," *OncoTargets and Therapy*, vol. 9, pp. 1023–1028, 2016.

[22] M. Toprakci, D. Ozmen, I. Mutaf et al., "Age-associated changes in nitric oxide metabolites nitrite and nitrate," *International Journal of Clinical & Laboratory Research*, vol. 30, no. 2, pp. 83–85, 2000.

[23] A. L. Sverdlov, D. T. Ngo, W. P. Chan, Y. Y. Chirkov, and J. D. Horowitz, "Aging of the nitric oxide system: are we as old as our NO?," *Journal of the American Heart Association*, vol. 3, no. 4, 2014.

[24] S. A. Kharitonov, "Influence of different therapeutic strategies on exhaled NO and lung inflammation in asthma and COPD," *Vascular Pharmacology*, vol. 43, no. 6, pp. 371–378, 2005.

[25] D. Fukumura, S. Kashiwagi, and R. K. Jain, "The role of nitric oxide in tumour progression," *Nature Reviews Cancer*, vol. 6, no. 7, pp. 521–534, 2006.

[26] N. L. Pershing, C. F. J. Yang, M. Xu, and C. M. Counter, "Treatment with the nitric oxide synthase inhibitor L-NAME provides a survival advantage in a mouse model of Kras mutation-positive, non-small cell lung cancer," *Oncotarget*, vol. 7, no. 27, pp. 42385–42392, 2016.

[27] J. Beck-Ripp, M. Griese, S. Arenz, C. Koring, B. Pasqualoni, and P. Bufler, "Changes of exhaled nitric oxide during steroid treatment of childhood asthma," *The European Respiratory Journal*, vol. 19, no. 6, pp. 1015–1019, 2002.

[28] Y. M. Lee, S. J. Kim, J. H. Lee, and E. Ha, "Inhaled corticosteroids in COPD and the risk of lung cancer," *International Journal of Cancer*, vol. 143, no. 9, pp. 2311–2318, 2018.

[29] V. W. Wong and E. Lerner, "Nitric oxide inhibition strategies," *Future Science OA*, vol. 1, no. 1, 2015.

[30] S. T. J. McDonagh, L. J. Wylie, J. M. A. Webster, A. Vanhatalo, and A. M. Jones, "Influence of dietary nitrate food forms on nitrate metabolism and blood pressure in healthy normotensive adults," *Nitric Oxide*, vol. 72, pp. 66–74, 2018.

[31] A. C. Olin, A. Aldenbratt, A. Ekman et al., "Increased nitric oxide in exhaled air after intake of a nitrate-rich meal," *Respiratory Medicine*, vol. 95, no. 2, pp. 153–158, 2001.

Hindawi
Oxidative Medicine and Cellular Longevity
Volume 2019, Article ID 6793957, 12 pages
https://doi.org/10.1155/2019/6793957

Research Article

Prooxidative Activity of Celastrol Induces Apoptosis, DNA Damage, and Cell Cycle Arrest in Drug-Resistant Human Colon Cancer Cells

Helena Moreira, Anna Szyjka, Kamila Paliszkiewicz, and Ewa Barg

Department of Basic Medical Sciences, Wroclaw Medical University, Borowska 211 street, 50-556 Wroclaw, Poland

Correspondence should be addressed to Helena Moreira; helena.moreira@umed.wroc.pl

Received 19 April 2019; Revised 12 June 2019; Accepted 18 July 2019; Published 14 August 2019

Guest Editor: Kanhaiya Singh

Cancer resistance to chemotherapy is closely related to tumor heterogeneity, i.e., the existence of distinct subpopulations of cancer cells in a tumor mass. An important role is assigned to cancer stem cells (CSCs), a small subset of cancer cells with high tumorigenic potential and capacity of self-renewal and differentiation. These properties of CSCs are sustained by the ability of those cells to maintain a low intracellular reactive oxygen species (ROS) levels, via upregulation of ROS scavenging systems. However, the accumulation of ROS over a critical threshold disturbs CSCs—redox homeostasis causing severe cytotoxic consequences. In the present study, we investigated the capacity of celastrol, a natural pentacyclic triterpenoid, to induce the formation of ROS and, consequently, cell death of the colon cancer cells with acquired resistant to cytotoxic drugs (LOVO/DX cell line). LOVO/DX cells express several important stem-like cell features, including a higher frequency of side population (SP) cells, higher expression of multidrug resistant proteins, overexpression of CSC-specific cell surface marker (CD44), increased expression of DNA repair gene (PARP1), and low intracellular ROS level. We found that celastrol, at higher concentrations (above 1 μM), significantly increased ROS amount in LOVO/DX cells at both cytoplasmic and mitochondrial levels. This prooxidant activity was associated with the induction of DNA double-strand breaks (DSBs) and apoptotic/necrotic cell death, as well as with inhibition of cell proliferation by S phase cell cycle arrest. Coincubation with NAC, a ROS scavenger, completely reversed the above effects. In summary, our results provide evidence that celastrol exhibits effective cytotoxic effects via ROS-dependent mechanisms on drug-resistant colon cancer cells. These findings strongly suggest the potential of celastrol to effectively kill cancer stem-like cells, and thus, it is a promising agent to treat severe, resistant to conventional therapy, colon cancers.

1. Introduction

Reactive oxygen species (ROS) are highly reactive, oxygen-containing, chemical molecules produced intracellularly through multiple mechanisms. The major endogenous sources of ROS are NADPH oxidase (NOX) complex in the cell membrane, mitochondria, peroxisomes, and endoplasmic reticulum. At low and moderate levels, cellular and mitochondrial ROS are implicated in various important cellular processes such as proliferation, differentiation, and survival. Excessive ROS levels interfere with redox homeostasis leading to a significant modification of the structure and function of cellular macromolecules that determine the fate of the cell. Importantly, chronically increased endogenous ROS is linked to the adaptive changes in cells that lead to cellular transformation and tumorigenesis [1–5]. Compared to normal cells, cancer cells display higher levels of ROS as a result of higher energy metabolism rate, oncogene activation, and loss of tumor suppressors [2, 6]. For instance, Haklar et al. have reported significantly increased levels of all ROS, especially hypochlorite, NO, and peroxynitrite in cancerous colon tissues [7]. Despite elevated intracellular ROS levels, cancer cells are sensitive to oxidative stress and ROS amplification over a critical threshold selectively kill tumor cells [8]. Most cytotoxic effects of chemotherapy are associated with the induction of cellular ROS generation. However, chronical exposure of cancer cells to ROS induced by chemotherapeutics, such as doxorubicin, daunorubicin, epirubicin, or

camptothecin, leads to the development of drug-resistant phenotype which is associated with the overexpression of ATP-dependent transmembrane efflux pumps and reduced ROS level [9, 10].

Resistance to chemotherapy is closely related to tumor heterogeneity, i.e., the existence of distinct subpopulations of cancer cells in a tumor mass. An important role is assigned to cancer stem cells (CSCs), a small subset of cancer cells with high tumorigenic potential and capacity of self-renewal and differentiation. Compared to differentiated cancer cells, CSCs are quiescent and present lower energy metabolism rate that consequently results in a significantly lower level of basal ROS [4]. This is also achieved by upregulation of ROS scavenging systems such as glutathione (GSH) [11]. In gastrointestinal CSCs, increased intracellular GHS synthesis is maintained by CD44v, a cellular adhesion molecule. CD44v is overexpressed in CSC and is a critical regulator of cancer stemness, including self-renewal, tumor initiation, and metastasis [12, 13]. A growing amount of evidence indicates that CSCs and non-CSCs can be bidirectionally converged, i.e., non-CSCs can be reprogrammed into CSCs and conversely CSCs into non-CSCs phenotypes [8, 12]. In view of these abilities of cancer cells, anticancer therapy strategies should target both bulk differentiated cells and CSCs. The treatment that impairs ROS defense and/or induces ROS generation provides a potential approach for killing CSCs.

Celastrol (tripterine) is a natural polyphenolic compound; one of the most biologically active product isolated from the Celastraceae family plants. Celastrol has been shown to exhibit important antioxidant and anti-inflammatory activities. It also inhibits the secretion of proinflammatory cytokines. In the past decade, it has also been found to inhibit tumor proliferation and growth in various cancer models as well as tumor capacity to metastasis. Anticancer properties of celastrol arise from its pleiotropic activities on multiple cellular signal pathways, including multidrug resistance mechanisms [14–18]. It has been reported that celastrol synergistically enhances the cytotoxicity of radiotherapy and chemotherapeutic agents [19]. We have also demonstrated that celastrol was able to enhance the sensitivity of the doxorubicin-resistant colon cancer cells via direct binding to P-glycoprotein1 (P-gp), a multidrug resistance protein belonging to ATP-dependent transporters. Interestingly, a few recent reports have indicated that celastrol has the potential to induce intracellular ROS generation in lung, osteosarcoma, melanoma, and ovarian cancer cells [20–23]. This prooxidative activity of celastrol was associated with the induction of cytotoxic effects in these tumors. In addition, Seo et al. showed that celastrol augmented ROS production induced by ionizing radiation in lung cancer as a result of celastrol-induced thiol reactivity of antioxidant enzymes [24].

In this work, for the first time, the effect of celastrol on ROS amounts in colon cancer cells displaying a high level of resistance to cytotoxic drugs (LOVO/DX cell line) was investigated.

These cells express several important features of CSCs, such as increased frequency of side population (SP) cells, high efflux capacity through ATP-dependent transporters (mainly P-gp glycoprotein), overexpression of CD44 and PARP1, a DNA repair gene, and significantly lower intracellular ROS level. We demonstrated that celastrol was able to generate oxidative stress in LOVO/DX cells at both cytoplasmic and mitochondrial levels. This prooxidant activity was associated with the induction of ROS-dependent DNA double-strand breaks (DSBs), the strongly deleterious and harmful DNA damages. The high level of phosphorylated H2A.X histone (γ-H2A.X), a biomarker of DSBs, was related to inhibition of cell proliferation by S phase cell cycle arrest and induction of apoptotic cell death in these cancer cells. Coincubation with N-Acetyl-L-cysteine (NAC), a ROS scavenger, completely reversed above effects. These results provide evidence that celastrol exhibits effective cytotoxic effects via ROS-dependent mechanisms on drug-resistant colon cancer cells.

2. Materials and Methods

2.1. Materials. DMEM F12 (Dulbecco's Modified Eagle's Medium: Nutrient Mixture F-12), HBSS (Hank's Balanced Salt Solution), FBS (fetal bovine serum), ultraglutamine 1, and gentamicin sulfate were purchased from Lonza (Basel, Switzerland). Accutase™ Cell Detachment and FITC Annexin V Apoptosis Detection Kit were obtained from BD Biosciences (Franklin Lakes, New Jersey, USA). TrypLE™ Express was from Gibco (Waltham, MA, USA). MitoPy1 [4-[4-[3-Oxo-6′-(4,4,5,5-tetramethyl-1,3,2-dioxaborolan-2-yl)spiro [isobenzofuran-1(3H), 9′-[9H]xanthen]-3′-yl]-1-piperazinyl]butyl]-triphenyl-phosphonium iodide) was from Tocris Bioscience (Bristol, United Kingdom). Bovine serum albumin (BSA), DCF-DA (2,7-dichlorofluorescin diacetate), NAC (N-Acetyl-L-cysteine), DMSO (Dimethyl Sulfoxide), paraformaldehyde (PFA), propidium iodide, and DAPI (4′,6-Diamidino-2-phenylindole dihydrochloride) were purchased from Sigma-Aldrich (St. Louis, MO, USA). Ethanol 96% was from Chempur. Celastrol, with purity more than 98%, was purchased from Cayman Chemical Company (Ann Arbor, MI, USA). Phospho-histone H2A.X (Ser139) monoclonal antibody (CR55T33) Alexa Fluor 488 eBioscience™ was obtained from Invitrogen (Carlsbad, CA, USA).

2.2. Methods

2.2.1. Cell Line and Culture Conditions. The doxorubicin-resistant colon cell line (LOVO/DX) was derived from LOVO cell line (ATCC collection) by 3-month cultivation in the presence of a low concentration of doxorubicin. LOVO cell line originates from the metastatic site of colon adenocarcinoma. The LOVO/DX cells were cultured in DMEM F12 medium supplemented with 10% FBS, 2 mM L-glutamine, and 25 μg/ml of gentamicin at 37°C in a humidified atmosphere with 5% CO_2. The cells were subcultured twice a week using TrypLE™ Express.

2.3. Drug Solution. Celastrol was dissolved in DMSO as 10 mM stock solution and stored at -20°C. The working solution was freshly prepared before each experiment by 10x dilution of stock solution in a culture medium. The

final DMSO concentration in the cell culture did not exceed 0.02%.

2.4. Detection of Intracellular ROS. The DCF-DA assay was carried out with flow cytometry according to the protocol previously described [25, 26]. The working DCF-DA solution was freshly prepared before each experiment by dissolving in 100% ethanol and further 10x dilution in HBSS. The final DCF-DA concentration in cell culture was 20 μM.

The LOVO/DX cells were removed from the culture flask using TrypLE™ Express solution, spun down, and pelleted. Cells (1×10^6/ml) were then resuspended in 1 ml of freshly prepared DCF-DA/HBSS solution in plastic Falcon tubes, and celastrol was immediately added to the samples to the final concentrations of 0.1-20 μM. The samples were incubated for 1 h at 37°C in a CO_2 incubator. Following incubation time, the cells were washed in HBSS and stained with propidium iodide (PI) for dead cell exclusion from the analysis. Afterwards, all samples were placed on ice and immediately analyzed for intracellular content of DCF using flow cytometer.

2.5. Detection of Mitochondrial H_2O_2. The mitochondria peroxy yellow 1 (MitoPY1), a fluorescent probe that selectively tracks to the mitochondria, was used to measure mitochondrial hydrogen peroxide (H_2O_2) [27]. MitoPY1 was dissolved in DMSO as 5 mM stock solution and aliquoted into PCR tubes. The aliquots (20 μl) were placed in a desiccator under weak vacuum until the solvent was removed and then stored at -20°C. Working solution (10 μM) was freshly prepared before each experiment by dissolving the aliquot in 20 μl of DMSO and then by adding 10 ml of HBSS.

The LOVO/DX cells were removed from the culture flask using TrypLE™ Express solution, spun down, and pelleted. Then, the cell pellets (1×10^6 cells/sample) were resuspended in 1 ml of freshly prepared MitoPY1 solution in plastic Falcon tubes. Afterwards, celastrol solution was immediately added to the cells to the final concentrations of 0.1-20 μM. The samples were incubated for 1 h at 37°C in a CO_2 incubator and then washed in HBSS. For dead cell exclusion from analysis, the cells were costained with propidium iodide (PI). The cell-associated fluorescence was measured by flow cytometry.

2.6. Apoptosis and Necrosis Assay. Apoptosis and necrosis were detected with flow cytometry after staining of the cells with fluorochrome mixture: Annexin V-FITC and PI, using the FITC Annexin V Apoptosis Detection Kit. The staining allows to discriminate between early and late apoptotic cells and necrotic cells. LOVO/DX cells (7.5×10^5/ml) were seeded in a 12-well plate and incubated with various celastrol concentrations in the absence or presence of 5 mM NAC (N-Acetyl-L-cysteine) (37°C, 5% CO_2). Following 4 hours incubation, the cells were detached with Accutase™ Cell Detachment and washed with HBSS. The cells were resuspended in 100 μl of ice-cold 1x binding buffer and stained with 5 μl of Annexin V-FITC and 5 μl of PI for 15 minutes in the dark at room temperature. Samples were immediately analyzed with the flow cytometer.

2.7. Cell Cycle Analysis. The flow cytometric analysis of cell cycle was done by the means of propidium iodide (PI) staining according to the protocol described in the literature [28]. The PI staining solution was freshly prepared before each experiment and contained PI 0.1% (*v*/*v*) Triton X-100, 50 μg/ml PI (Molecular Probes Inc.), and 50 μg/ml DNase-free RNase A in PBS.

LOVO/DX cells (1×10^6/ml) were seeded in a 6-well plate and incubated with various celastrol concentrations (37°C, 5% CO_2). Following 18 hours of incubation, the cells were removed from wells using TrypLE™ Express solution and washed with cold HBSS. The cells were then fixed with ice-cold 70% ethanol and kept on ice for 1 hour. After two washing steps with cold HBSS, the cells were resuspended in 0.5 ml of PI staining solution and incubated for 30 minutes in the dark. Samples were then analyzed with the flow cytometer.

2.8. Detection of γ-H2A.X. Detection and quantification of γ-H2A.X$^+$ positive cells were done using phospho-histone H2A.X (Ser139) monoclonal antibody (CR55T33) Alexa Fluor 488, based on the protocol previously described by Kataoka et al. [29].

LOVO/DX cells (1×10^6/ml) were seeded in a 6-well plate and incubated for 4 hours with various celastrol concentrations (37°C, 5% CO_2). Then, the cells were removed with TrypLE™ Express solution, placed into plastic Falcon tubes, and washed twice with cold HBSS. The cells were fixed using 2% paraformaldehyde (PFA) for 10 minutes on ice. After two washing steps with cold HBSS containing 1% bovine-serum albumin (1% BSA-HBSS), the cells were permeabilized with ice-cold 70% ethanol (prepared in 1% BSA-HBSS). The samples were kept in this solution for 5-7 days at 4°C. Before staining with antibody, the cells were washed twice using 1% BSA-HBSS. The cell pellets were resuspended in 100 μl of 1% BSA-HBSS containing 2 μl of phospho-histone H2A.X (Ser139) monoclonal antibody (CR55T33) Alexa Fluor 488 and incubated for 30 minutes in the dark. Then, the cells were washed with 1% BSA-HBSS and counterstained with DAPI (1 μg/ml) for cell cycle analysis. Stained cells were analyzed by flow cytometry.

2.9. Flow Cytometric Analysis. In all assays, the cells were acquired on CyFlow® SPACE flow cytometer (Sysmex, Kobe, Prefektura Hyōgo, Japan). The laser excitation 488 nm (50 mW) and the filter 536/40 (BP) were used for fluorescence measurement of DCF, MitoPY1, FITC, and Alexa Fluor 488. Propidium iodide fluorescence was measured using laser excitation 488 nm (50 mW) and 675/20 (BP) filter and DAPI fluorescence with 375 nm (16 mW) laser excitation and 455/50 (BP) filter. The results were analyzed using FlowMax (Sysmex, Kobe, Prefektura Hyōgo, Japan) or FCS express 4 flow software (De Novo Software, Glendale, CA, USA). The MultiCycle™ DNA analysis model was used for cell cycle analysis.

2.10. Statistical Analysis. Statistical significance of the results was calculated using GraphPad Prism Version 6.05 (GraphPad Software, La Jolla, CA, USA).

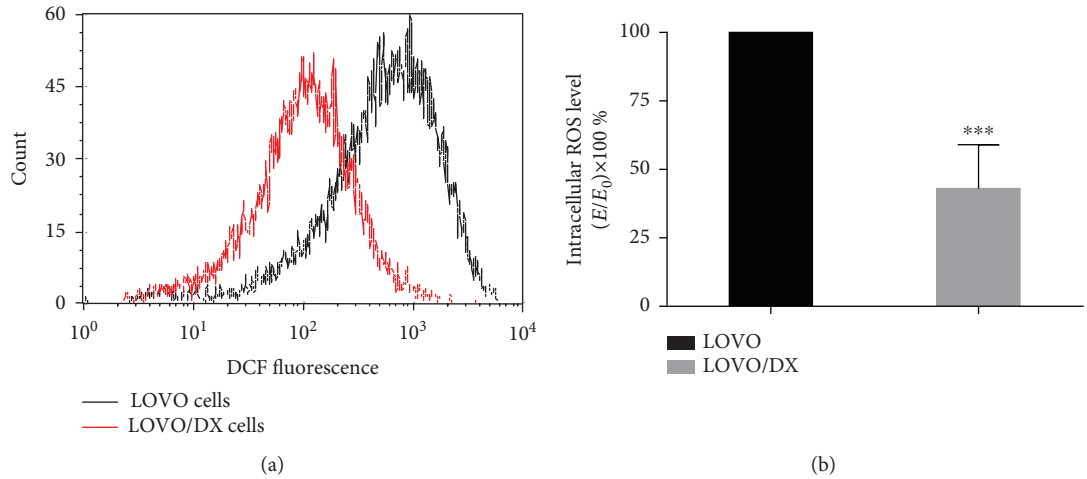

(a) (b)

Figure 1: Intracellular ROS level (DCF-DA assay) in LOVO/DX cells compared to LOVO cells. (a) Representative histograms of flow cytometric evaluation of the cell-associated DCF fluorescence. (b) The basal level of intracellular ROS in LOVO/DX cells compared to LOVO cells. Results are expressed as $E/E_0 \times 100\%$ (mean ± SD, $n = 5$, $^{***}p \leq 0.0001$), where the MFI (mean fluorescent intensity) of DCF in LOVO/DX cells (E) was compared to the MFI in LOVO cells (E_0).

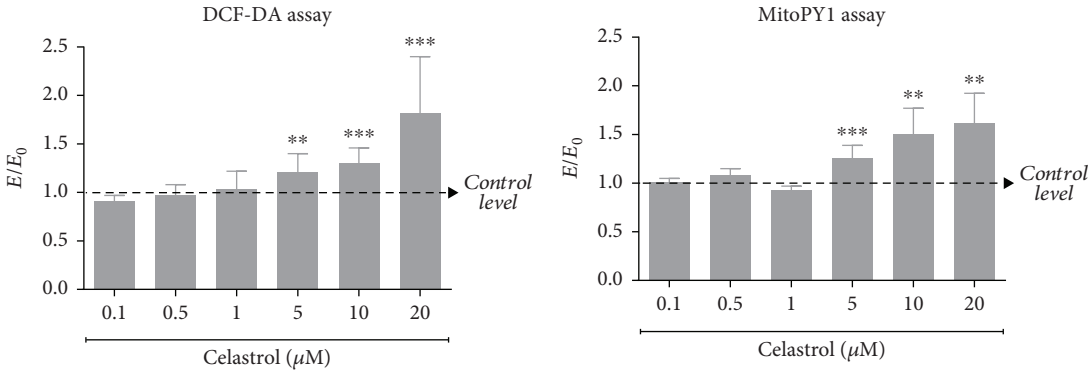

(a) (b)

Figure 2: Impact of celastrol on the intracellular ROS level (DCF-DA assay) (a) and the mitochondrial H_2O_2 level (MitoPY assay) (b) in LOVO/DX cell cultures. The results obtained in the presence of celastrol (E) were compared to the relevant control (E_0), i.e., cells incubated in the presence of the solvent (DMSO). The values are expressed as the mean ± SD, $n = 6$, $^{**}p \leq 0.01$, $^{***}p \leq 0.001$.

3. Results

3.1. Intracellular ROS Level in LOVO/DX Cells. Several reports indicate that drug-resistant cancer cells and CSCs present a reduced amount of ROS than drug-sensitive cancer cells. Therefore, we first evaluated the basal ROS level in LOVO/DX cells exhibiting high resistance to doxorubicin compared to sensitive cells (LOVO cells). Intracellular ROS amount was assessed by flow cytometry using DCF-DA assay. As shown in Figure 1, the endogenous ROS level in LOVO/DX cells is significantly lower (>50%) than in LOVO cells.

3.2. Effect of Celastrol on ROS Level in LOVO/DX Cells. To investigate whether celastrol is able to induce an increase in the amount of endogenous ROS in drug-resistant cells, the LOVO/DX cells were treated with various concentrations of celastrol. Since mitochondria are the major intracellular source of ROS, mitochondrial H_2O_2 content (MitoPY1 assay) was evaluated in addition to cytosol ROS amount (DCF-DA test). The influence of celastrol on ROS and H_2O_2 generation is shown in Figures 2(a) and 2(b), respectively. The results indicate that ROS levels did not change or slightly decreased following cell incubation with lower celastrol concentrations (0.1-1 μM). However, at higher concentrations (5-20 μM), it induces significant ROS accumulation at both cytosol and mitochondrial levels. This increase is dose-dependent and reaches up to 80% (DCF-DA) and 60% (MitoPY1) above the control level, at the highest concentration of 20 μM.

3.3. Cytotoxic Effect of Celastrol on LOVO/DX Cells. It is well known that excessive ROS production can affect the viability of cancer cells. Therefore, we investigated whether celastrol prooxidative activity could lead to cytotoxic effects in LOVO/DX cells. The celastrol-induced cytotoxicity was determined after 2 and 4 hours of the treatment by means of PI staining. In shorter incubation time, celastrol had no impact on LOVO/DX cell viability at the tested concentration range. Extending the incubation time to 4 hours led to the appearance of necrotic cells in a very small percentage

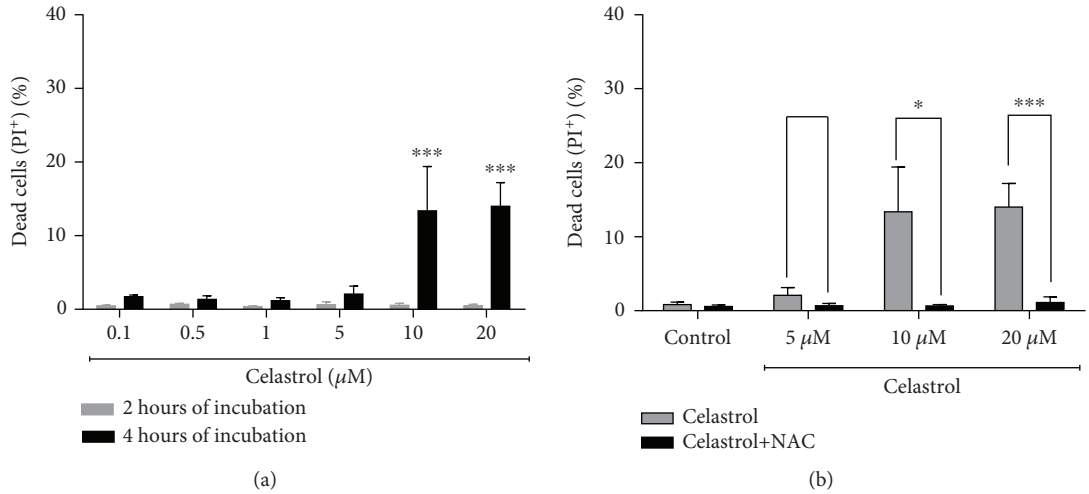

Figure 3: The frequency of necrotic cells in LOVO/DX cell cultures incubated with celastrol (a) and coincubated with celastrol and NAC (b). The cells were double stained with Annexin V-FITC and propidium iodide (PI) fluorescent dyes (FITC Annexin V Apoptosis Detection Kit) and analyzed by flow cytometry. Control: LOVO/DX cells incubated without celastrol (gray), LOVO/DX cells incubated without celastrol and NAC (black). The results are presented as a percentage of PI^+ cells (Annexin V-$FITC^-$ and PI^+ dead cells); mean ± SD, $n = 4$, $^*p < 0.05$, $^{***}p \leq 0.001$.

(1.2–2%) at lower concentrations. At the higher concentrations, 10 and 20 μM, the percentage of necrotic cells increases up to 14% (Figure 3(a)). This effect is completely abolished in cell culture incubated with celastrol in the presence of ROS scavenger: *N*-acetylcysteine (NAC, 5 mM) (Figure 3(b)).

3.4. Effects of Celastrol on Apoptotic Cell Death of LOVO/DX Cells. ROS and mitochondria play an important role in apoptosis induction. We evaluated whether the prooxidant activity of celastrol is associated with apoptosis induction in LOVO/DX cells. Proapoptotic effects of celastrol were studied after 2 and 4 hours of incubation with LOVO/DX cells using double staining with Annexin V-FITC and PI dye. The results are presented as a percentage of early apoptotic cells (Annexin V-$FITC^+$ and PI^-) and late apoptotic cells (Annexin V-$FITC^+$ and PI^+). As shown in Figures 4(a) and 4(b), the frequency of cells with early and late apoptotic features does not change after 2 hours of incubation regardless of the celastrol concentration. However, longer incubation time leads to a significant increase in the percentage of late apoptotic cells up to 41% at 5–20 μM concentrations of celastrol (Figure 4(b)). Moreover, there is a clear disproportion between the number of cells in early and late stages of apoptosis, i.e., the decrease of early apoptotic cells along with the increase of late apoptotic cells is observed (Figure 4(c)). The addition of NAC (5 mM) to the cell cultures entirely abolishes these effects of celastrol (Figures 5 and 6).

3.5. Impact of Celastrol on Cell Cycle and DNA Damage. In addition to apoptosis induction, ROS, at higher levels, cause oxidative DNA damage and subsequent cell cycle arrest. We thus investigated whether celastrol-induced apoptosis was associated with inhibition of cell cycle and induction of double-strand breaks in LOVO/DX cells. The cell cycle was evaluated by PI staining. Figure 7(a) depicts the distribution of LOVO/DX cells through the cell cycle after treatment with celastrol for 18 hours. The results reveal that celastrol causes cell cycle arrest by the accumulation of cells in the S phase together with a marked reduction in the number of cells in the G2/M phase (Figure 7(b)). Moreover, at 2.5 and 5 μM of celastrol, a marked increase in the generation of double-strand breaks was observed, as assessed by γ-H2AX (Table 1, Figure 8(a)). γ-H2A.X^+ positive cells were observed in all phases of the cell cycle; however, S phase cells revealed a lower frequency of γ-H2A.X^+ cells compared to G2/M phase cells (Table 2, Figure 8(b)). The addition of NAC (5 mM) to the cell culture incubated with celastrol results in the complete abolishment of γ-H2AX formation (Tables 1 and 2).

4. Discussion

Reactive oxygen species (ROS) play an important role in the anticancer activity of several agents used for the treatment of colon and other cancers. Amplification of the intracellular ROS level in tumor cells induces apoptosis and, in some cases, other types of cell death, i.e., autophagy or necrosis by damaging cellular components such as DNA and protein and lipid membranes. Recently, some naturally occurring polyphenols have been reported to act as selective cytotoxic agents against cancer cells by generation of toxic levels of ROS [30]. Celastrol is a plant triterpenoid that strongly inhibits the growth and development of cancer in various cancer cell models. Some molecular mechanisms responsible for its anticancer activity have been proposed. The celastrol structure holds a highly redox-active para-quinone methide moiety that can induce oxidative stress by forming ROS, such as superoxide or hydrogen peroxide [31, 32]. Some recent reports have indicated that celastrol induces antitumor effects by increasing the intracellular accumulation of ROS in lung, osteosarcoma, melanoma, and ovarian cancer cells [20–24]. However, the effect of celastrol on drug-resistant, stem-like colon cancer cells is still unexplored.

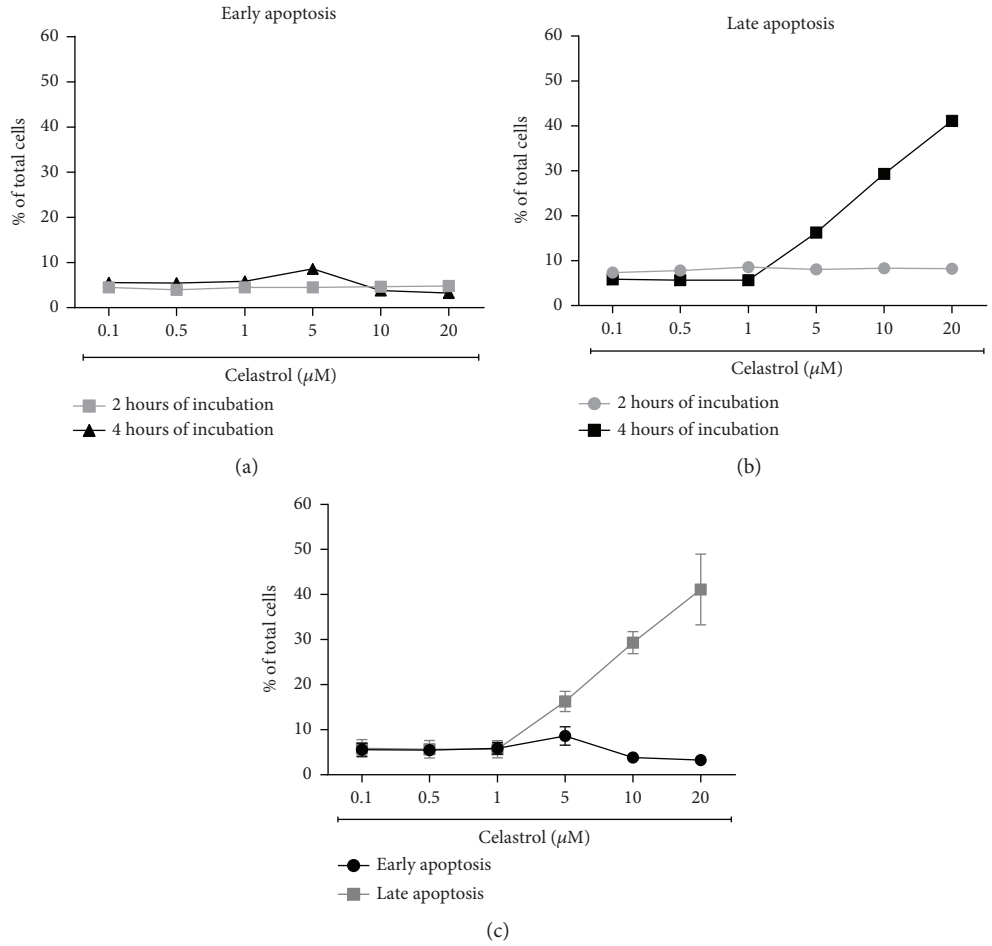

Figure 4: The effects of 2 and 4 hours of incubation of celastrol with LOVO/DX cells on the frequency of early and late apoptosis. The cells were double stained with Annexin V-FITC and PI fluorescent dyes (FITC Annexin V Apoptosis Detection Kit) and analyzed by flow cytometry. The results are presented as a percentage of early apoptotic cells (Annexin V-FITC$^+$ and PI$^-$) and late apoptotic cells (Annexin V-FITC$^+$ and PI$^+$); mean ± SD, $n = 4$.

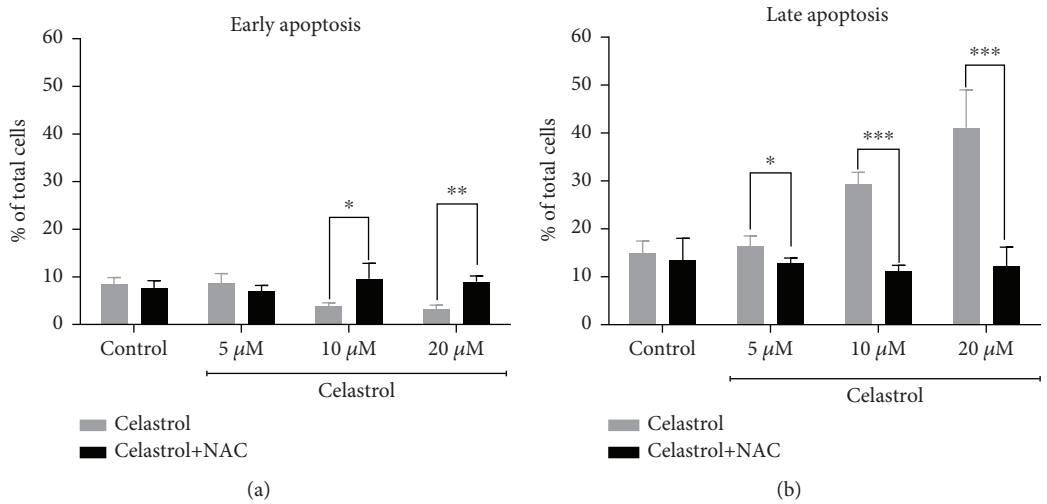

Figure 5: The frequency of early and late apoptotic cells in LOVO/DX cell cultures incubated with celastrol (a) and coincubated with celastrol and NAC (b). The cells were double stained with Annexin V-FITC and PI fluorescent dyes (FITC Annexin V Apoptosis Detection Kit) and analyzed by flow cytometry. Control: LOVO/DX cells incubated without celastrol (gray), LOVO/DX cells incubated without celastrol and NAC (black). The results are presented as a percentage of early apoptotic cells (Annexin V-FITC$^+$ and PI$^-$) and late apoptotic cells (Annexin V-FITC$^+$ and PI$^+$); mean ± SD, $n = 4$, $^*p < 0.05$, $^{**}p \leq 0.01$, and $^{***}p \leq 0.001$.

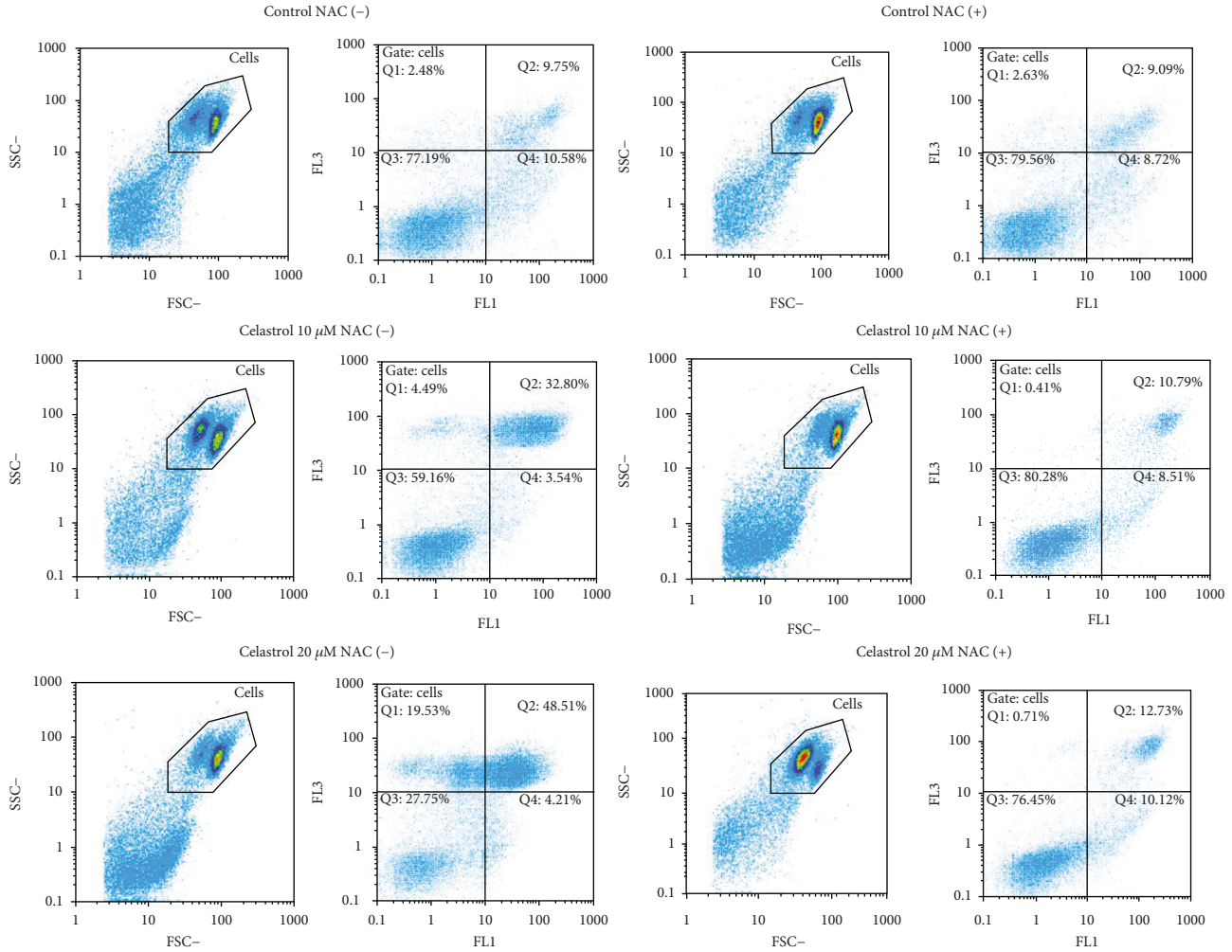

FIGURE 6: Flow cytometric analysis of early and late apoptosis in LOVO/DX cell cultures incubated with celastrol or coincubated with celastrol and NAC. Representative cytograms are shown. FSC = forward light scatter, SSC = side light scatter, FL1 = Annexin V-FITC, FL3 = PI, Q1 = necrotic cells (Annexin V-FITC$^-$ and PI$^+$), Q2 = late apoptotic cells (Annexin V-FITC$^+$ and PI$^+$), Q3 = live cells (Annexin V-FITC$^-$ and PI$^-$), Q4 = early apoptotic cells (Annexin V-FITC$^+$ and PI$^-$).

In the present study, we aimed to determine whether celastrol is able to induce the formation of ROS and consequently cell death in colon cancer cells with acquired resistant to cytotoxic drugs. For this purpose, we used human colon adenocarcinoma cell line (LOVO/DX) which shows cross-resistance to doxorubicin and other anthracyclines such as vinca alkaloids, epipodophyllotoxin derivatives, 4′-(9-acridinylamino-methanesulfon-*m*-aniside), and actinomycin D [33]. We compared the endogenous redox status of those cells with their sensitive counterpart (LOVO) and we found that LOVO/DX cells have a significantly lower level of cytoplasmic ROS. Maiti has reported that ovarian cancer cells resistant to chlorambucil (A2780/100) present reduced amount of ROS compared to sensitive cells and that decreased ROS level is one of the main reasons for developing and maintaining the resistance of those cells. In addition, the elevation of the cellular ROS by exogenous ROS generation increases the A2780/100 sensitivity [10]. In our previous paper, we have shown that celastrol exhibits significant chemopreventive and chemosensitizing activities on LOVO/DX cells, in part by inhibition of P-gp, a multidrug-resistant protein [34]. Although we demonstrated that celastrol has the ability to bind directly to P-gp, we hypothesized that ROS generation might be an additional mechanism by which celastrol exerts its anticancer effects in those cells. Indeed, celastrol was able to generate a significant amount of intracellular ROS at both cytoplasmic and mitochondrial level. The prooxidant activity of celastrol was limited to higher concentrations—above 1 μM. This is in agreement with literature data indicating that phenolic compounds can act as a prooxidant only under certain conditions, i.e., at elevated doses. In addition, celastrol-induced generation of ROS was significantly decreased by ROS scavenger, *N*-acetylcysteine (NAC) (Figure S1, supplementary data).

Cellular ROS, and particularly mitochondrial H_2O_2, have been identified as critical intermediates in the activation of the apoptotic process via the mitochondria-dependent and mitochondria-independent pathways [35]. Chen et al. demonstrated that in lung cancer cells (H1299 cell line) celastrol induced ROS generation by inhibiting the activity

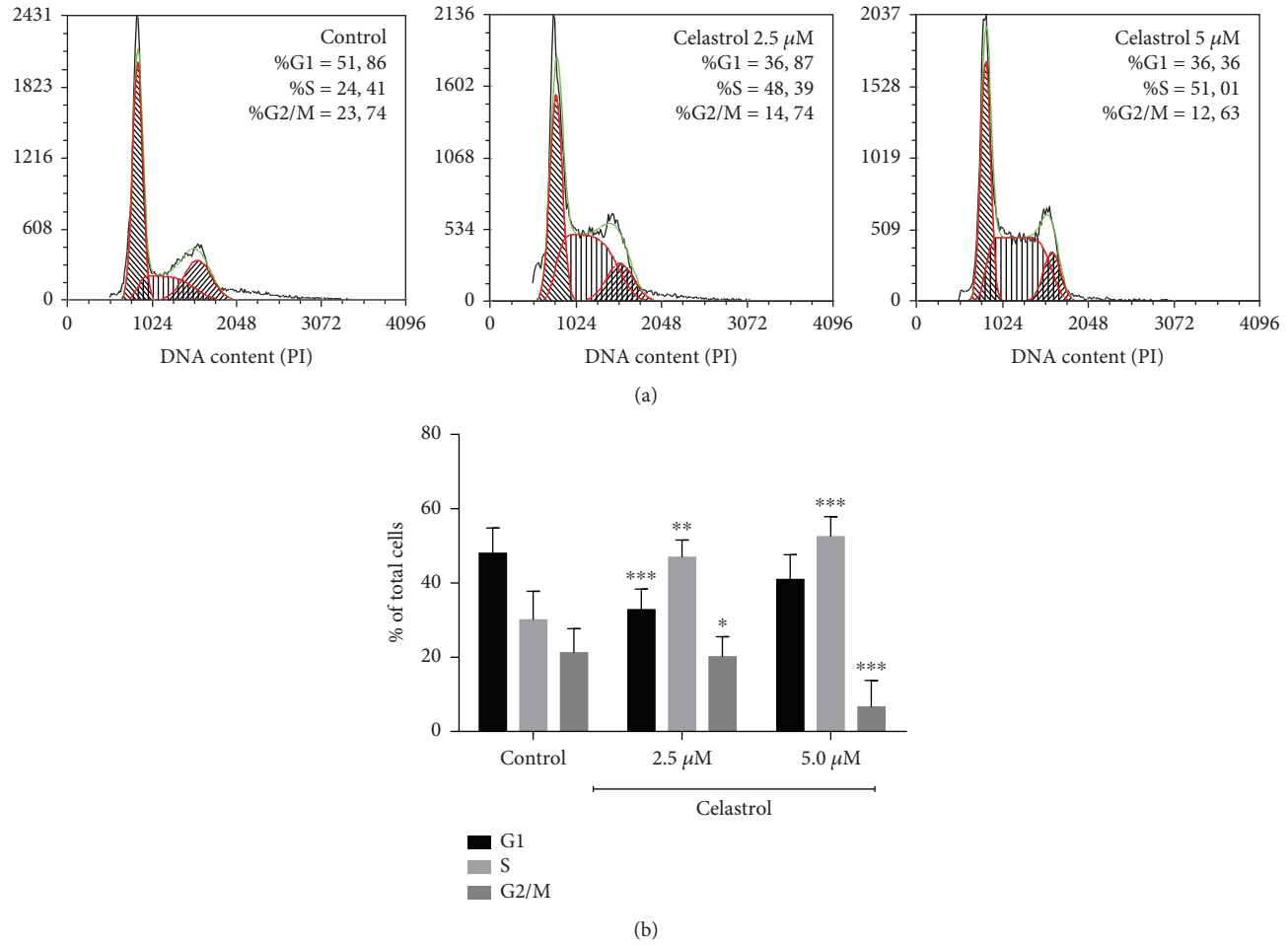

Figure 7: Impact of celastrol on cell cycle distribution in LOVO/DX cells. (a) Representative histograms of flow cytometric analysis of cell cycle. (b) Bar graph showing the percentage of LOVO/DX cells in each cell cycle phase after incubation with solvent (DMSO) or celastrol. The results are presented as mean ± SD, $n = 4$, $^{*}p < 0.05$, $^{**}p \leq 0.01$, and $^{***}p \leq 0.001$.

Table 1: Effect of celastrol on the percentage of γ-H2AX^{+} cells in LOVO/DX cell culture.

	γ-H2AX^{+} cells (%)
Control	1.18 ± 0.39
CEL 1 μM	3.37 ± 2.14
CEL 2.5 μM	***18.78 ± 6.65***
CEL 5 μM	***26.93 ± 1.99***
CEL 20 μM	2.17 ± 1.39
NAC	1.54 ± 0.11
CEL 5 μM+NAC	1.70 ± 0.62

of complex I MRC and not by inhibiting the expression of antioxidant proteins. Thus, ROS accumulation in H1299 cells was associated with apoptotic and necrotic cell death by downstream activation of JNK and downregulating client proteins HSP90 [20]. In our study, celastrol was also able to induce apoptotic and, in a smaller extent, necrotic cell death in doxorubicin-resistant colon cancer cells. Those effects were only observed at prooxidative concentrations and appeared after 4 hours of incubation. In addition, hydrogen peroxide (H_2O_2), one of the most important ROS, induces apoptosis of LOVO/DX cells, in a dose-dependent manner (Figure S2, supplementary data). Moreover, the coincubation with NAC significantly decreased celastrol- and hydrogen peroxide-induced cell death. These observations point that the generation of ROS plays an important role in the apoptotic/necrotic activity of this phenolic compound.

ROS, at higher levels, are known to induce oxidative DNA damage and subsequent cell cycle arrest [1, 36]. Previously, it has been shown that celastrol was able to induce cell cycle arrest at the G_2/M phase in ovarian cancer cells and at the G_0/G_1 phase in monocytic leukemia cells [23, 37]. In our study, we demonstrated that celastrol exerts growth-inhibitory effects via arresting the cell cycle at the S phase in doxorubicin-resistant cancer cells. The S phase is a crucial stage in the cell cycle progression as it allows for proper replication of DNA. Some anticancer drugs inhibit cell proliferation by inducing DNA double-strand breaks that result in cell cycle arrest at the S phase [36]. Increased level of intracellular free radicals, reacting with DNA and thereby modifying its structure and function, is one of the main causes of DNA damage [38]. Here, we showed that celastrol (at 2.5 and 5 μM) significantly increases the quantity of γ-H2AX, a

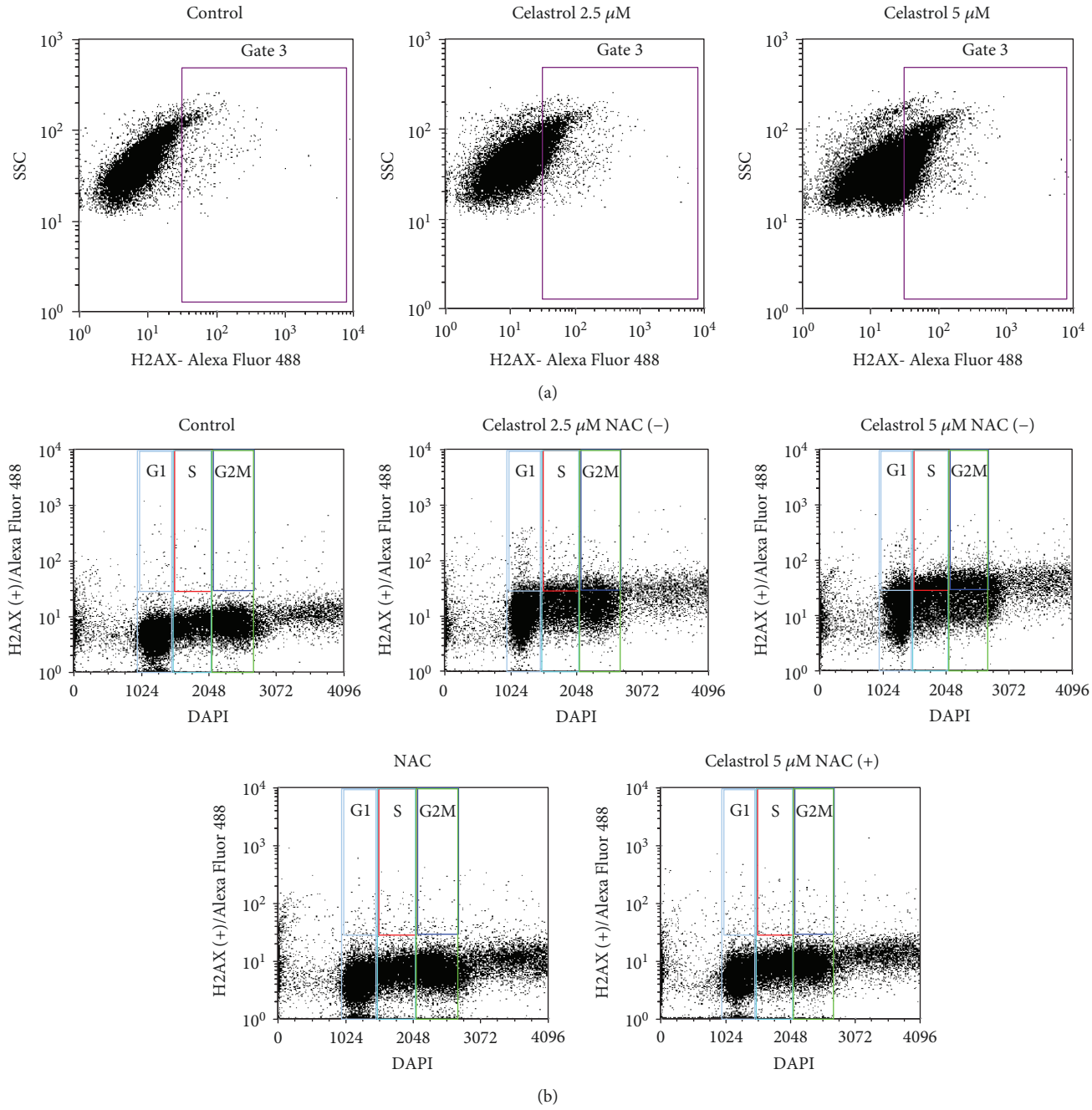

Figure 8: Representative histograms of flow cytometric analysis of DNA damages (γ-H2AX$^+$ cells) and cell cycle phases in LOVO/DX cells after treatment with celastrol. (a) Detection of γ-H2AX$^+$ cells using phospho-histone H2A.X (Ser139) monoclonal antibody (CR55T33) Alexa Fluor 488. SSC = side light scatter. (b) Bivariant cell cycle/DAPI-combined γ-H2AX analysis.

well-known marker of DNA damage, in LOVO/DX cells. The γ-H2AX formation showed no cell cycle-phase specificity and was completely abolished in the presence of NAC. Moreover, coincubation of celastrol (5 μM) with NAC restored normal diploid distribution of LOVO/DX cells in the relevant cell cycle phases. These observations confirm the role of celastrol-induced ROS in the S phase cell cycle arrest and DNA damage. Interestingly, the increase in the γ-H2AX level was not observed at 20 μM concentration of celastrol. Huang et al. have demonstrated that the drug-induced γ-H2AX appears very early during treatment, prior to caspase 3 activation, and decreases importantly at late stages of apoptosis which is characterized by increased levels of chromatin condensation [39]. In our study, celastrol at higher concentrations (10 and 20 μM) caused a significant increase in the number of cells with late apoptotic features together with a decrease in the cell number bearing early apoptotic characteristics. Thus, γ-H2AX could not be detected in LOVO/DX cells after cell treatment with these doses.

Our data show that celastrol possesses a significant anticancer potential against drug-resistant colon cancer cells. This activity is related to the induction of DNA double-

Table 2: Effect of celastrol on the number of γ-H2AX$^+$ cells in different phases of cell cycle in LOVO/DX cell culture.

	γ-H2AX$^+$ cells in cell cycle phases (%)		
	G1	S	G2/M
CEL 1 μM	0.29	0.18	0.32
CEL 2.5 μM	***3.85***	***4.95***	***7.48***
CEL 5 μM	***8.69***	***6.97***	***9.73***
CEL 20 μM	0.11	0.12	0.13
NAC	0.37	0.36	0.38
CEL 5 μM+NAC	0.58	0.53	0.57

strand breaks, S phase cell cycle arrest, and triggering apoptosis. The increase in intracellular production of ROS induced by celastrol appears to be an important mechanism of its cytotoxic activity. ROS are highly reactive and react with DNA and proteins inducing cancer cell death. It should be emphasized that celastrol was able to cause anticancer effects only at higher concentrations in which it acts as a prooxidant. In addition, these doses do not change the viability of normal human cells, suggesting its specificity for tumor cells (Figure S3, supplementary data). It seems also that the mechanisms of celastrol cytotoxicity might differ in drug-sensitive and drug-resistant cancer since we found that in LOVO cells, celastrol mainly induces necrosis and has only a small proapoptotic effect (Figure S4, supplemented data). However, both this issue and the impact of celastrol on normal epithelial cells of the colon mucosa require further investigation.

In summary, we demonstrated that ROS play an important role in the cytotoxic activity of celastrol in resistant colon cancer cells. The resistance of colon cancer to chemotherapy is linked to the content of the cancer stem cells (CSCs) [34, 40]. Our previous study indicated that LOVO/DX cells contain an almost 7-fold greater number of CSC (measured by the size of the SP cell subpopulation) than the LOVO cells, ordinarily sensitive to cytostatics [34]. Moreover, celastrol-induced inhibition of P-gp function significantly lowered the SP fraction. The high efflux capacity through ATP-depending transporters is one of the most important CSC features that prevents the accumulation of cytostatic drug within the cells [11]. Interestingly, the LOVO/DX cells carry other stem-cell characteristics such as higher expression of CD44, a CSC-specific cell surface marker, and PARP1, a DNA repair gene (data not shown). Also, significantly lower ROS content was found in LOVO/DX cells compared to sensitive cells, as was mentioned above. In CSCs, the low amount of ROS sustains their self-renew potential and improves the abilities of invasion and resistance against therapy. CSCs maintain lower intracellular ROS level in part as a consequence of the modulation of the redox systems. For instance, in gastrointestinal CSCs, increased CD44v variant isoform expression contributes to ROS defense through GSH-dependent antioxidant mechanism [41]. Interestingly, Peng et al. have shown that celastrol has the ability to directly react with a thiol such as NAC and GSH (when coincubated) which results in reversing G0/G1 cell cycle arrest in U937 cells [37]. This finding strongly suggests that celastrol might induce cytotoxic effects not only by the direct increase of the ROS level but also via GSH depletion. Evidence to date has shown that despite the low ROS level and elevated antioxidant defense mechanisms in CSCs, accumulating ROS over a critical threshold that alters redox-homeostasis selectively kills these cells [8]. Taken together, it may be assumed that celastrol plays an important role in CSC clearance in drug-resistant colon cancer cells via a ROS-dependent mechanism.

5. Conclusions

Drug-resistant colon cancer cells possess a large number of CSC-specific features. We found that celastrol demonstrates prooxidative activity on those cells and causes ROS-dependent DNA DSBs which results in the expression of γ-H2A.X$^+$. The ROS-induced DNA damage leads to inhibition of cell proliferation by S phase cell cycle arrest and induction of apoptotic cell death. These findings strongly suggest the potential of celastrol to effectively kill cancer stem-like cells, and thus, it is a promising agent to treat severe, resistant to conventional therapy, colon cancers. Further studies should be performed to confirm these results in *in vivo* models of colon cancer.

Data Availability

All data used to support the findings of this study are included within the article. The additional data, demonstrating the CD44 and PARP1 expression in LOVO/DX cells, are available from the corresponding author upon request.

Conflicts of Interest

The authors declare no conflicts of interest.

Acknowledgments

This work was supported by the Wroclaw Medical University Grant No. ST.D130.16.009.

Supplementary Materials

Figure S1: impact of celastrol and celastrol coincubation with NAC on the intracellular ROS level (DCF-DA assay) in LOVO/DX cells. Representative histograms of flow cytometric evaluation of the cell-associated DCF fluorescence. Figure S2: flow cytometric analysis of early and late apoptosis in LOVO/DX cell cultures incubated with H_2O_2 and coincubated with H_2O_2 and NAC. The cells were incubated with H_2O_2 for 4 hours (37°C, 5% CO_2) and then double stained with Annexin V-FITC and PI fluorescent dyes (FITC Annexin V Apoptosis Detection Kit). Representative cytograms are shown. FSC = forward light scatter, SSC = side light scatter, FL1 = Annexin V-FITC, FL3 = PI, Q1 = necrotic cells (Annexin V-FITC and PI$^+$), Q2 = late apoptotic cells (Annexin V-FITC$^+$ and PI+), Q3 = live cells (Annexin V-FITC and PI$^-$), Q4 = early apoptotic cells (Annexin V-FITC$^+$ and PI$^-$). Figure S3: effect of celastrol on the viability of NHDF cells (normal human dermal fibroblast) (A) and

PBMC cells (B). (A) The cells were incubated with celastrol for 4 hours (37°C, 5% CO_2). The cell viability was measured by the means of XTT proliferation assay. The mean optical density (OD, absorbance (A)) was used to calculate the percentage of viable cell viability as follows: percentage of viable cells = $(A_{\text{Celastrol}})/(A_{\text{control}}) \times 100\%$; mean ± SD, $n = 5$ (B). PBMC was activated with LPS and incubated with celastrol for 24 hours (37°C, 5% CO_2). The viability of cells was assessed with the Guava PCA-96 Nexin Kit by flow cytometry; mean ± SD, $n = 3$ (data from PhD thesis: "Study of the Molecular Mechanisms TNF-α Secretion, a Key Cytokine in Chronic Inflammation" by Helena Tabaka-Moreira, Université de Strasbourg, France). Figure S4: the frequency of apoptotic and necrotic cells in LOVO cell cultures incubated with celastrol. The cells were incubated with celastrol for 4 hours (37°C, 5% CO_2) and then double stained with Annexin V-FITC and PI fluorescent dyes (FITC Annexin V Apoptosis Detection Kit) and analyzed by flow cytometry. The results are presented as a percentage of early apoptotic cells (Annexin V-FITC$^+$ and PI$^-$), late apoptotic cells (Annexin V-FITC$^+$ and PI$^+$), and necrotic cells (Annexin V-FITC and PI$^+$); mean ± SD, $n = 5$. *(Supplementary Materials)*

References

[1] J. Boonstra and J. A. Post, "Molecular events associated with reactive oxygen species and cell cycle progression in mammalian cells," *Gene*, vol. 337, pp. 1–13, 2004.

[2] A. Phaniendra, D. B. Jestadi, and L. Periyasamy, "Free radicals: properties, sources, targets, and their implication in various diseases," *Indian Journal of Clinical Biochemistry*, vol. 30, no. 1, pp. 11–26, 2015.

[3] S. I. Dikalov and D. G. Harrison, "Methods for detection of mitochondrial and cellular reactive oxygen species," *Antioxidants & Redox Signaling*, vol. 20, no. 2, pp. 372–382, 2014.

[4] S. Ding, C. Li, N. Cheng, X. Cui, X. Xu, and G. Zhou, "Redox regulation in cancer stem cells," *Oxidative Medicine and Cellular Longevity*, vol. 2015, Article ID 750798, 11 pages, 2015.

[5] P. T. Schumacker, "Reactive oxygen species in cancer: a dance with the devil," *Cancer Cell*, vol. 27, no. 2, pp. 156-157, 2015.

[6] H. Yang, R. M. Villani, H. Wang et al., "The role of cellular reactive oxygen species in cancer chemotherapy," *Journal of Experimental & Clinical Cancer Research*, vol. 37, no. 1, p. 266, 2018.

[7] G. Haklar, E. Sayin-Özveri, M. Yüksel, A. Ö. Aktan, and A. S. Yalçin, "Different kinds of reactive oxygen and nitrogen species were detected in colon and breast tumors," *Cancer Letters*, vol. 165, no. 2, pp. 219–224, 2001.

[8] J. Liu and Z. Wang, "Increased oxidative stress as a selective anticancer therapy," *Oxidative Medicine and Cellular Longevity*, vol. 2015, Article ID 294303, 12 pages, 2015.

[9] H. Wang, Z. Gao, X. Liu et al., "Targeted production of reactive oxygen species in mitochondria to overcome cancer drug resistance," *Nature Communications*, vol. 9, no. 1, p. 562, 2018.

[10] A. K. Maiti, "Gene network analysis of oxidative stress-mediated drug sensitivity in resistant ovarian carcinoma cells," *The Pharmacogenomics Journal*, vol. 10, no. 2, pp. 94–104, 2010.

[11] C. I. Kobayashi and T. Suda, "Regulation of reactive oxygen species in stem cells and cancer stem cells," *Journal of Cellular Physiology*, vol. 227, no. 2, pp. 421–430, 2012.

[12] X. Shi, Y. Zhang, J. Zheng, and J. Pan, "Reactive oxygen species in cancer stem cells," *Antioxidants & Redox Signaling*, vol. 16, no. 11, pp. 1215–1228, 2012.

[13] L. Wang, X. Zuo, K. Xie, and D. Wei, "The role of CD44 and cancer stem cells," *Methods in Molecular Biology*, pp. 31–42, 2018.

[14] V. R. Yadav, S. Prasad, B. Sung, R. Kannappan, and B. B. Aggarwal, "Targeting inflammatory pathways by triterpenoids for prevention and treatment of cancer," *Toxins*, vol. 2, no. 10, pp. 2428–2466, 2010.

[15] N. S. Amirruddin, A. P. Kumar, A. K. K. Teo, and G. Sethi, "Role of celastrol in chemosensitization of cancer," in *Role of Nutraceuticals in Chemoresistance to Cancer, Volume 2*, pp. 141–150, Academic Press, 2017.

[16] P. Yadav, V. Jaswal, A. Sharma et al., "Celastrol as a pentacyclic triterpenoid with chemopreventive properties," *Pharmaceutical Patent Analyst*, vol. 7, no. 4, pp. 155–167, 2018.

[17] S. R. Chen, Y. Dai, J. Zhao, L. Lin, Y. Wang, and Y. Wang, "A mechanistic overview of triptolide and celastrol, natural products from *Tripterygium wilfordii* Hook F," *Frontiers in Pharmacology*, vol. 9, p. 104, 2018.

[18] R. Cascão, J. E. Fonseca, and L. F. Moita, "Celastrol: a spectrum of treatment opportunities in chronic diseases," *Frontiers in Medicine*, vol. 4, p. 69, 2017.

[19] X. Han, S. Sun, M. Zhao et al., "Celastrol stimulates hypoxia-inducible factor-1 activity in tumor cells by initiating the ros/akt/p70s6k signaling pathway and enhancing hypoxia-inducible factor-1α protein synthesis," *PLoS One*, vol. 9, no. 11, article e112470, 2014.

[20] G. Chen, X. Zhang, M. Zhao et al., "Celastrol targets mitochondrial respiratory chain complex I to induce reactive oxygen species-dependent cytotoxicity in tumor cells," *BMC Cancer*, vol. 11, no. 1, p. 170, 2011.

[21] H. Y. Li, J. Zhang, L. L. Sun et al., "Celastrol induces apoptosis and autophagy via the ROS/JNK signaling pathway in human osteosarcoma cells: an *in vitro* and *in vivo* study," *Cell Death & Disease*, vol. 6, no. 1, article e1604, 2015.

[22] J. H. Lee, Y. S. Won, K. H. Park et al., "Celastrol inhibits growth and induces apoptotic cell death in melanoma cells via the activation ROS-dependent mitochondrial pathway and the suppression of PI3K/AKT signaling," *Apoptosis*, vol. 17, no. 12, pp. 1275–1286, 2012.

[23] L.-N. Xu, N. Zhao, J.-Y. Chen et al., "Celastrol inhibits the growth of ovarian cancer cells in vitro and in vivo," *Frontiers in Oncology*, vol. 9, no. 2, 2019.

[24] H. R. Seo, W. D. Seo, B. J. Pyun et al., "Radiosensitization by celastrol is mediated by modification of antioxidant thiol molecules," *Chemico-Biological Interactions*, vol. 193, no. 1, pp. 34–42, 2011.

[25] E. Eruslanov and S. Kusmartsev, "Identification of ROS using oxidized DCFDA and flow-cytometry," *Methods in Molecular Biology*, vol. 594, pp. 57–72, 2010.

[26] A. Slezak, H. Moreira, A. Szyjka, J. Oszmianski, and K. Gasiorowski, "Condition of prooxidant activity of cistus and pomegranate polyphenols in V79 cell cultures," *Acta Poloniae Pharmaceutica*, vol. 74, no. 2, pp. 670–678, 2017.

[27] B. C. Dickinson, V. S. Lin, and C. J. Chang, "Preparation and use of MitoPY1 for imaging hydrogen peroxide in

mitochondria of live cells," *Nature Protocols*, vol. 8, no. 6, pp. 1249–1259, 2013.

[28] J. Szeberenyl, "Analysis of the cell cycle by flow cytometry," *Biochemistry and Molecular Biology Education*, vol. 35, no. 2, pp. 153-154, 2007.

[29] Y. Kataoka, V. P. Bindokas, R. C. Duggan, J. S. Murley, and D. J. Grdina, "Flow cytometric analysis of phosphorylated histone H2AX following exposure to ionizing radiation in human microvascular endothelial cells," *Journal of Radiation Research*, vol. 47, no. 3/4, pp. 245–257, 2006.

[30] A. J. León-González, C. Auger, and V. B. Schini-Kerth, "Pro-oxidant activity of polyphenols and its implication on cancer chemoprevention and chemotherapy," *Biochemical Pharmacology*, vol. 98, no. 3, pp. 371–380, 2015.

[31] A. C. Allison, R. Cacabelos, V. R. M. Lombardi, X. A. Álvarez, and C. Vigo, "Celastrol, a potent antioxidant and anti-inflammatory drug, as a possible treatment for Alzheimer's disease," *Progress in Neuro-Psychopharmacology & Biological Psychiatry*, vol. 25, no. 7, pp. 1341–1357, 2001.

[32] R. Kannaiyan, M. K. Shanmugam, and G. Sethi, "Molecular targets of celastrol derived from thunder of god vine: potential role in the treatment of inflammatory disorders and cancer," *Cancer Letters*, vol. 303, no. 1, pp. 9–20, 2011.

[33] M. Broggini, M. Grandi, P. Ubezio, C. Geroni, F. C. Giuliani, and M. D'Incalci, "Intracellular doxorubicin concentrations and drug-induced DNA damage in a human colon adenocarcinoma cell line and in a drug-resistant subline," *Biochemical Pharmacology*, vol. 37, no. 23, pp. 4423–4431, 1988.

[34] H. Moreira, A. Szyjka, and K. Gąsiorowski, "Chemopreventive activity of celastrol in drug-resistant human colon carcinoma cell cultures," *Oncotarget*, vol. 9, no. 30, pp. 21211–21223, 2018.

[35] M. Redza-Dutordoir and D. A. Averill-Bates, "Activation of apoptosis signalling pathways by reactive oxygen species," *Biochimica et Biophysica Acta (BBA) - Molecular Cell Research*, vol. 1863, no. 12, pp. 2977–2992, 2016.

[36] U. H. Preya, K. T. Lee, N. J. Kim, J. Y. Lee, D. S. Jang, and J. H. Choi, "The natural terthiophene α-terthienylmethanol induces S phase cell cycle arrest of human ovarian cancer cells via the generation of ROS stress," *Chemico-Biological Interactions*, vol. 272, pp. 72–79, 2017.

[37] B. Peng, L. Xu, F. Cao et al., "HSP90 inhibitor, celastrol, arrests human monocytic leukemia cell U937 at G0/G1 in thiol-containing agents reversible way," *Molecular Cancer*, vol. 9, no. 1, p. 79, 2010.

[38] U. S. Srinivas, B. W. Q. Tan, B. A. Vellayappan, and A. D. Jeyasekharan, "ROS and the DNA damage response in cancer," *Redox Biology*, vol. 1692, article 101084, pp. 31–42, 2018.

[39] X. Huang, M. Okafuji, F. Traganos, E. Luther, E. Holden, and Z. Darzynkiewicz, "Assessment of histone H2AX phosphorylation induced by DNA topoisomerase I and II inhibitors topotecan and mitoxantrone and by the DNA cross-linking agent cisplatin," *Cytometry*, vol. 58A, no. 2, pp. 99–110, 2004.

[40] H. Taniguchi, C. Moriya, H. Igarashi et al., "Cancer stem cells in human gastrointestinal cancer," *Cancer Science*, vol. 107, no. 11, pp. 1556–1562, 2016.

[41] O. Nagano, S. Okazaki, and H. Saya, "Redox regulation in stem-like cancer cells by CD44 variant isoforms," *Oncogene*, vol. 32, no. 44, pp. 5191–5198, 2013.

Hindawi
Oxidative Medicine and Cellular Longevity
Volume 2019, Article ID 8547846, 10 pages
https://doi.org/10.1155/2019/8547846

Review Article

Hypoxia-Inducible Factors as an Alternative Source of Treatment Strategy for Cancer

Musbau Adewumi Akanji,[1] Damilare Rotimi,[2] and Oluyomi Stephen Adeyemi[2]

[1]*Department of Biochemistry, University of Ilorin, Ilorin, Nigeria*
[2]*Department of Biochemistry, Medicinal Biochemistry, Nanomedicine & Toxicology Laboratory, Landmark University, Omu-Aran 251101, Nigeria*

Correspondence should be addressed to Oluyomi Stephen Adeyemi; yomibowa@yahoo.com

Received 11 April 2019; Revised 13 July 2019; Accepted 30 July 2019; Published 14 August 2019

Academic Editor: Mithun Sinha

Hypoxia-inducible factors (HIFs) are transcription factors that activate the transcription of genes necessary to circumvent to hypoxic (low oxygen level) environments. In carcinogenesis, HIFs play a critical role. Indeed, HIF-1α has been validated as a promising target for novel cancer therapeutics, even as clinical investigations have linked increased levels of HIF-1α with aggressive cancer progression as well as poor patient prognosis. More so, inhibiting HIF-1 activity restricted cancer progression. Therefore, HIF-1 is a viable target for cancer therapy. This may be expected considering the fact that cancer cells are known to be hypoxic. In order to survive the hypoxic microenvironment, cancer cells activate several biochemical pathways via the HIF-1α. Additionally, cellular and molecular insights have proved prospects of the HIF-1α pathway for the development of novel anticancer treatment strategies. The biochemical importance of hypoxia-inducible factors (HIFs) cannot be overemphasized as carcinogenesis, cancer progression, and HIFs are intricately linked. Therefore, this review highlights the significance of these linkages and also the prospects of HIFs as an alternative source of cancer therapies.

1. Introduction

The function and survival of living organisms are dependent on the adequate supply of oxygen available to the cells. Animals catabolize the sugar from plant using glycolysis, citric acids, and oxidative phosphorylation in an aerobic state. During these processes, oxygen is used as an electron acceptor. Inefficient transfer of electron results in a risk of oxygen species generation. Electron escape can lead to generation of superoxide anion and/or hydroxyl radicals, all of which are examples of reactive oxygen species (ROS) [1]. ROS have the potential to destroy the configuration of biomolecules, which could result in cellular damage or cell death [2]. Increased ROS production is associated with deviations from physiological oxygen pressure (PO_2) in the electron transport chain. Therefore, tight regulation of cellular oxygen concentration through homeostatic mechanisms is very essential. When the supply of oxygen fails to meet the demand from tissues and cells, it is called hypoxia. All solid tumors are characterized by hypoxia, as proliferation of the tumor cells results in deprivation of oxygen due to insufficient blood flow from abnormal tumor microvasculature. Hypoxia induces stress in organisms either through pathological or through nonpathological conditions [3].

The consequences of deregulation of hypoxia in cells include breakage of DNA strand, oxidative DNA damage, and gene aberration which hinder cell growth and eventual cellular death. It also affects the development of diseases such as chronic lung disease, cancer, diabetes, ischemic heart diseases, stroke, and advanced atherosclerosis [4]. Hypoxia signaling adaptation in a cell is facilitated by the transcriptional regulation family called hypoxia-inducible factor (HIF). HIF is an oxygen-labile DNA-binding transcriptional activator [5]. HIF controls multiple gene expression involved in a process of cancer cell adaptation and progression [6]. Therefore, a better understanding of the molecular mechanism of hypoxia in cancer cells could afford the development of more effective therapy for solid tumors [7]. Additionally,

the available cancer therapies have not been desirably effective [8], thus making research efforts aimed at identifying and developing newer cancer treatment strategies imperative. In light of this, the current review is aimed at discussing the prospects of hypoxia-inducible factors as alternative treatment strategy for cancer.

2. Cellular Response to Hypoxia

Hypoxia can simply be defined as a state of decreased oxygen level in the cell or tissue when the oxygen provided for use in the tissue is far less than what is actually needed. A cell can be said to be hypoxia when the overall oxygen pressure in the cell is less than 40 mmHg [9]. Oxygen is extremely important, especially in the cells and tissues of mammals, mostly because of its importance in respiration; it is extremely necessary in the final step of the electron transport chain, as the final electron acceptor in oxidative phosphorylation. Its presence increases the chances of reactive oxygen species (ROS) generation, which react with other biological molecules, resulting in the alteration of the biochemical and physical properties of the cell, causing either an upset of the delicate functions or cell death [1]. Therefore, it can be seen that hypoxia is a potentially lethal condition, for both the cell and the tissue at large, if it is allowed to persist long enough. It causes the oxygen-dependent process of respiration to either slow down or cease completely, particularly the oxidative phosphorylation process, which transfers the chemical energy stored in C-H bonds into the high-energy inorganic phosphate bonds found in ATP [10].

The stoppage of oxidative phosphorylation causes a decrease in ATP, ultimately leading to the stoppage of the ATP-dependent sodium potassium pump. This leads to an imbalance of ions, creating an unbalanced cell environment; the stoppage of the sodium potassium pump forces the cell into employing anaerobic respiration as a means of survival, as its oxygen is cut off. This causes a buildup of lactic acid in the cell, and the pH level drops, as the cell becomes increasingly acidic. The acidity of the cell causes it to swell, as it absorbs water from the environment in an attempt to stabilize its pH. When the cell swells, the permeability of the plasma membrane increases, allowing the leaking of soluble enzymes and coenzymes. If hypoxia persists, the continuing depletion of ATP leads to more serious and pronounced structural anomalies. The comprehensive cellular structure is upset, resulting in loss of the extracellular characteristics such as microvilli, and irregular bulges are formed in the plasma membrane of the cell and eventual cellular death.

Mammals have different mechanisms for surviving the events of hypoxia. The human response to a condition of hypoxia involves physiological changes in respiratory, hematopoietic, and cardiovascular systems. The intake of oxygen is maximized by increasing the functions of the cardiac systems, while the rate of oxygen distribution to individual cells is improved by the acceleration of erythropoiesis. At the cellular level, however, there are intricate factors that underlie these physiological changes in response to hypoxia. These factors seek to restore the oxygenation, minimizing hypoxic environment. These intricate factors are known as hypoxia-inducible factors (HIFs) [11, 12].

3. Hypoxia-Inducible Factors (HIFs)

Hypoxia-inducible factor 1 is the heterodimer protein of two subunits: HIF-1α and HIF-1β transcriptional factor [13, 14]. Each contains helix-loop- (HLS-) PER-ARNT-SIM (HLS-PAS) domains that facilitate DNA binding and heterodimerization. The beta subunit can also be referred to as the aryl hydrocarbon receptor nuclear translocator (ARNT). The alpha subunit is sensitive to oxygen, while the β subunit (HIF-1β) is oxygen dependent [4]. HIF transcription factor is the master regulator of the translational response, and it is produced as a result of oxygen deficiency in the cell [1, 6]. HIF-α consists of different alpha subunits: HIF-1α, HIF-2α, and HIF-3α. The α subunit of HIF is tightly regulated by HIF prolyl hydroxylases (PHDs). PHDs hydroxylate specific prolyl residues at the HIF-α subunits. von Hippel-Lindau (VHL) tumor suppressors E3 ligase recognize hydroxylated HIF-α subunit for degradation [4, 15]. In addition, there is reduced transcriptional activities when the factor inhibiting HIF (FIH) hydrolyses HIFs. Decreased activities of PHD and FIH stabilize HIF-α during hypoxia, leading to its translocation to the nucleus, where it subsequently binds with HIF-β to form a complex. This complex then binds target genes containing the hypoxia responsive element and transactivates the gene expression for different signaling pathways [4]. Essentially, HIF-1 can be referred to as a messenger which migrates towards the nucleus to activate transcription responses to hypoxia. HIF-1 has been involved in gene regulation involving metastasis, growth, tumorigenesis, angiogenesis, and invasion.

The vascular endothelial growth factor (VEGF) is an example of the HIF-1 target gene in which its expression is induced by hypoxia. Meanwhile, HIF-1 alone does not determine the specific gene expression by individual cells, as this is relatively determined by the functional interaction of HIF-1 with other transcriptional factors that control the activation of a selected subgroup of HIF-1 in hypoxic cells [13].

4. General Functions of Hypoxia-Inducible Factors (HIFs)

HIFs perform very essential roles, in a vast number of mammalian conditions and reactions (Figure 1), and any form of impairment of their functions can result in dire consequences. Briefly, few studies that highlight the roles of the HIFs are described in the following.

4.1. Metabolism

(a) HIF-1α has been shown to cause a transition from oxidative to glycolytic metabolism by inducing the transcription of genes which support glycolytic metabolism, PDK-1, coding for pyruvate

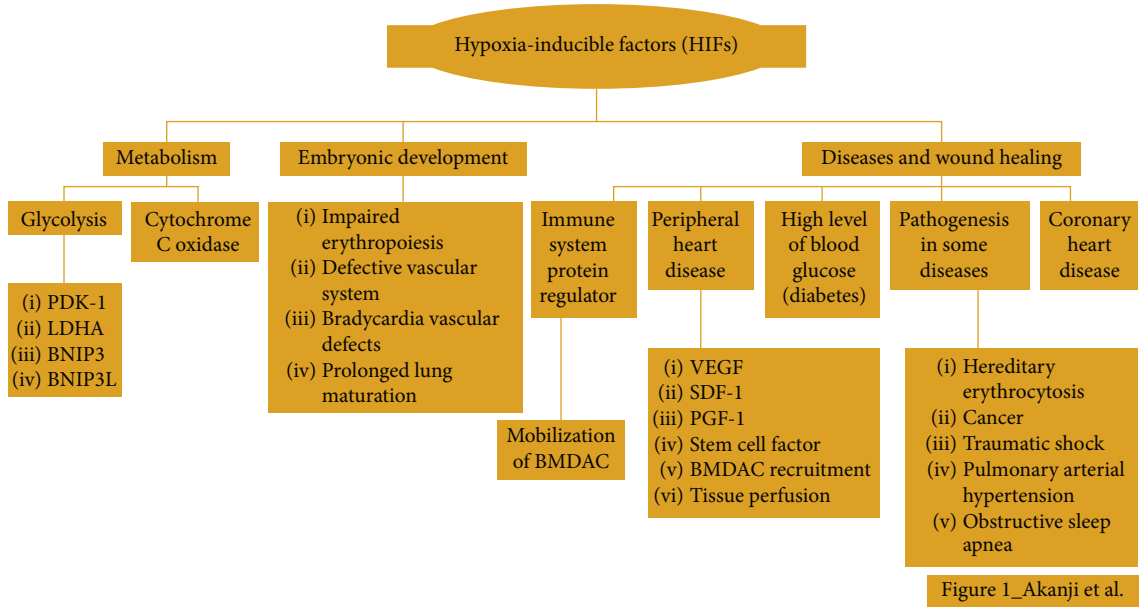

Figure 1: The general function of hypoxia-inducible factors (HIFs).

dehydrogenase kinase-1, which inactivates pyruvate dehydrogenase, inhibiting the reaction converting pyruvate dehydrogenase, inhibiting the reaction converting pyruvate to acetyl-CoA, preventing subsequent continuation into the Krebs cycle [16, 17], LDHA, which encodes for lactate dehydrogenase, that catalyzes the reaction converting pyruvate to lactate [18], BNIP3 and BNIP3L, which mediate mitochondrial autophagy [19, 20]

(b) HIF-1 also mediates a change in the proteinous configuration of the enzyme cytochrome c oxidase, facilitating improvement in the transfer of electrons in situations of hypoxia [21]

4.2. Embryonic Development. Most of the discoveries made concerning the role of HIFs in embryonic development were obtained from experiments conducted on mice by quite a number of scientists. From these experiments, it was discovered that

(a) the circulatory system depends on HIFs for normal development. For example, mouse embryos defective in the gene coding for the HIF (HIF-1α precisely) died on their 11th day due to impaired erythropoiesis and defective vascular system [22]

(b) mouse embryos which died on the 13th day due to bradycardia or vascular defects are usually defective in the genes coding for HIF-2α [23, 24]

(c) neonate mice may also die at birth due to prolonged lung maturation or at a few months after birth, due to reactive oxygen species- (ROS-) mediated organ failure, showing a role of HIFs in organ development [25]

(d) increased HIF concentration in fetuses due to a reduced blood flow, which brings about a state of prolonged hypoxia, could cause congenital malfunctions

4.3. Diseases and Wound Healing. HIFs mediate protective responses activated by the immune system response to disease or injury.

(a) In coronary heart disease, adenosine is extremely important as it mediates preconditioning, an initial immune response to hypoxia, where exposure of the heart to short periods of hypoxia is followed by reperfusion, protecting the heart against subsequent, long episodes of hypoxia. HIFs activate the transcription of the genes that code for adenosine, which offshoots the aforementioned process [26]

(b) In the process of healing wounds, HIFs regulate the release of regulatory protein of the immune system from the wound which facilitates the mobilization and direction of bone marrow-derived angiogenic cells (BMDACs) to the site of the wound. BMDACs then stimulate vasculogenesis or angiogenesis, enabling the wound to heal [27]

(c) The effect of HIFs in wound healing was found to be impaired in mice with a high level of blood glucose. It can be said that diabetes inhibits the action of HIFs [28, 29]

(d) In peripheral heart disease (PAD) of which limb ischaemia is a complication, HIFs mediate the activation of various target genes which encode for multiple angiogenic growth factors, including the vascular endothelial growth factor (VEGF), stromal-

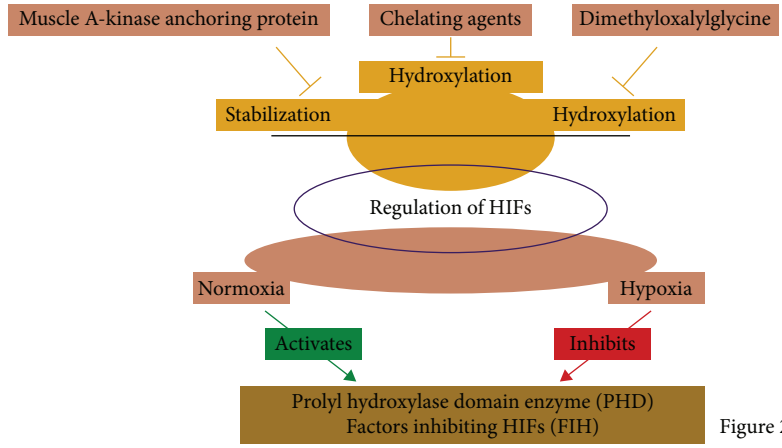

Figure 2: The regulation of HIFs by various cellular factors—cell proliferation and survival, invasion and metastasis, epithelial-mesenchymal transition, metabolic programming, and angiogenesis.

derived factor-1 (SDF-1), placental growth factor (PGF-1), and stem cell factor. HIFs also oversee the recruitment of BMDACs and recover tissue perfusion

(e) HIFs also contribute to pathogenesis in some diseases like hereditary erythrocytosis [22], cancer [30], traumatic shock, pulmonary arterial hypertension, and obstructive sleep apnea [27]

5. Regulation of HIFs

The expression of HIFs in the cellular environment is a closely regulated process, where a lot of factors and reactions are involved (Figure 2). Since HIFs have mainly to do with oxygen levels in tissues, their system of regulation can be considered under conditions of normal oxygen pressure (normoxia) and conditions of abnormal oxygen pressure (hypoxia).

In normoxic conditions, the HIF expression is constitutive or rather inhibited, as they are not required. HIFs are regulated in normoxic conditions by special oxygen sensitive enzymes called prolyl hydroxylase domain enzyme (PHDs). These enzymes regulate HIFs by hydroxylating the proline residues found in the oxygen-dependent degradation (ODD) domain of HIFs [31, 32]. The hydroxylation is carried out by inserting an oxygen molecule into proline and another into α-ketoglutarate, splitting it into succinate and carbon dioxide. Since the PHDs use oxygen as a substrate, if oxygen is not available, the process cannot take place [33]. The hydroxylation process is a precursor to another very important step, which is the ubiquitylation of the HIF by von Hippel-Lindau (VHL) protein. The β subunit of the VHL protein recognizes and binds the newly hydroxylated HIF. The α subunit of the pVHL then assembles the pVHL ubiquitin ligase, which marks the HIF for cleavage by the 26S proteasome [34].

HIFs are also regulated by factors inhibiting HIFs (FIHs) in normoxic conditions. They function by repressing the transactivation of the HIF-α subunit. They do this by hydroxylating asparagine residues in the C-terminal transactivation domain of the HIFs using oxygen and α-ketoglutarate as reactions, thus preventing the interaction of the hypoxia-inducible factor with the p300 coactivator protein [35, 36].

In hypoxic conditions, however, most of the above processes are reversed. The PHDs, for instance, require oxygen in order to hydroxylate the protein residues. The hydroxylation of the HIF is thus stopped under conditions of hypoxia, making it impossible for it to be recognized and marked for degradation by the pVHL ubiquitin ligase complex. As a result, HIFs are accumulated in the nucleus.

The FIH-mediated hydroxylation is also reduced in the conditions of hypoxia, allowing the HIFs react with the transcriptional coactivators p300/CREB-binding protein [37]. This transcriptional complex that is activated leads to the transcription of a particular set of genes, as a part of the cellular response to hypoxia, which includes, but is not limited to, SLC2A1 (glycolysis) and VEGFA (angiogenesis) [38].

HIFs may also be regulated in some other ways as follows:

(a) Muscle A-kinase anchoring protein (mAKAP): AKAPs are scaffolding proteins that mediate the assembly of multiprotein complexes. The mAKAPs arrange the E3 ubiquitin ligase complex, affecting the stability and positioning of HIF in the active site of the enzyme. A decrease in the availability of the mAKAP would alter the stability of the HIF complex

(b) Dimethyloxalylglycine (DMOG) is a well-known opponent of α-ketoglutarate, which, if inhibited, would abrogate the function of the hydroxylase, thereby supporting HIF transcription [39]

(c) HIF is also stimulated by chelating agents of iron, desferrioxamine and cobalt chloride (Adeyemi et al., 2017). These chelators inhibit the hydroxylases by displacing the iron ions present in their catalytic centers

(d) Doxorubicin (adriamycin) is a chemotherapeutic drug used for cancer treatment. HIF-1 transcriptional activity was inhibited by doxorubicin by preventing the binding of HIF-1 to DNA [40, 41]

6. HIF Regulation and Mitochondria Function in Cancer

The tricarboxylic acid (TCA) cycle catalyzes enzymatic reactions that provide electrons in the form of the reducing equivalents NADH and $FADH_2$ to the electron transport chain (ETC) in the mitochondrial matrix. Different intermediates enter the cycle at a different point from other pathways but under hypoxia; glucose and fatty acid-derived carbons are diverted from being broken down to acetyl-CoA, while glutamine-derived carbons are diverted from being catabolized to succinyl-CoA by the HIF-regulated genes.

Decreased oxidative phosphorylation could induce HIF to upregulate lactate dehydrogenase (LDHA), thus regenerating NAD to maintain ATP production from glycolysis, and thereby, divert pyruvate from breakdown into acetyl-CoA which adversely suppress both TCA and ETC activities [17].

Cells adapt their metabolic programme under hypoxia to maintain the reactions that rely on ATP produced by oxidative phosphorylation. Generally, HIF-1 signaling supports the production of ATP anaerobic and downregulation of oxidative phosphorylation, thereby reducing the cell's reliance on oxygen-dependent energy production [17]. In relation to mitochondrial function, it has been noted that the coexpression of HIF-1α and HIF-2α has some opposing roles; however, they both in a similar manner decrease a cell's dependence on mitochondrial oxidative phosphorylation [42].

Stress signaling pathways in the cell-like hypoxic response [43], redox signaling [44], and unfolded protein response [45] are activated in the mitochondria. As evident in previous studies using mitochondrial DNA- (mtDNA-) deficient $\rho 0$ cells in mouse xenograft models, it was observed that the growth of the tumor is accelerated by the mitochondria (Tan, et al., 2015; Yan et al., 2015). Cancer prognosis has been linked clinically to single nucleotide variants in mtDNA [46, 47]. However, mtDNA mutations or reduced mitochondrial content has caused decreased or low mitochondrial function noticeable in many cancer types, including pancreatic, kidney, thyroid, and colon cancer [48–50]. This suggests that there are some adaptive mechanisms during tumor development in which mitochondrial activity is decreased.

7. MicroRNAs and Cancer

MicroRNAs also called miRNAs or miRs are small noncoding RNAs which regulate gene expression at the posttranscriptional level. miRNAs repress mRNA translation and degrades RNA targets [51]. miRNAs give a new insight into cancer studies. miRNA genes are an important factor in the pathogenesis of human cancer as they form central nodal points in cancer development [52]. Understanding the mechanistic role of miRNAs in cancers still presents a challenge. Reports have shown that molecular pathways of cancer are regulated by miRNAs by targeting oncogenes and tumor suppressor genes, involving the cancer-stem-cell development pathway, angiogenesis, and drug resistance [53].

8. HIF-1 Responses in Tumor and Prospects for Targeted Therapies

Tumors are noticeably characterized by a low oxygen level of the tumor microenvironment. A partial pressure (PO_2) of less than 10 mm is exhibited in solid tumors compared to 45-65 mm in normal tissues. There is inadequate blood perfusion in acute or transient hypoxia, but chronic hypoxia limits diffusion of oxygen in enlarged tumors. This leads to the activation of both HIF-1 and HIF-2 with overexpression of HIF-1α which is linked to metastasis and mortality [4].

Cancer cells in humans have overexpression of HIF-1α, but this is dependent on the type of cancer. The overexpressed HIF-1α has resulted into high mortality rate in patient experiencing cancers of the breast, ovary, uterus, cervix, brain, and oropharynx, while overexpression of HIF-1α has been associated with decreased death rate with head and neck cancer patients [54]. Although studies have indicated that HIF-1α facilitates resistance to radiation and chemotherapy, the inhibition of HIF-1α activation may be useful in hindering cancer progression, thereby starving the growing tumor cell of oxygen and the required nutrient supply [54].

9. HIFs in Cancer Progression

The significances of HIFs in different stages in cancer cell formation cannot be overemphasized (Figure 3). The different stages include angiogenesis, metastasis, metabolic reprogramme, invasion, epithelial-mesenchymal transition, and cell proliferation and survival. With different clinical and experimental research establishing HIF as a cancer therapy target, HIF-1α and HIF-2α levels are associated with metastasis, vascularization, and tumor growth in both animal-based and clinical-based studies. Several HIF-regulated genes that are identified as important in cancer development are as follows [1].

(a) Increase proliferation and survival of cell: a major distinction between tumor cell and normal cell which is initiated by autocrine signaling increased cell proliferation and reduced cell death. The level of ATP is an important determinant of cell apoptosis as abundant glycolytic ATP leads to apoptosis during hypoxic. Besides, deprivation of oxygen leads to the inhibition of or decreased electron transport chain processes, thus reducing the mitochondrial membrane potential [55]. This results in the activation of survival/growth factors which are expressed by HIF-regulated genes such as insulin-like growth factor-2 (IGF2), erythropoietin (EPO), vascular endothelial growth factor (VEGF), Endothelin 1 (EDN1), transforming growth factor-α (TGFA), and adrenomedullin [1]. These genes are the

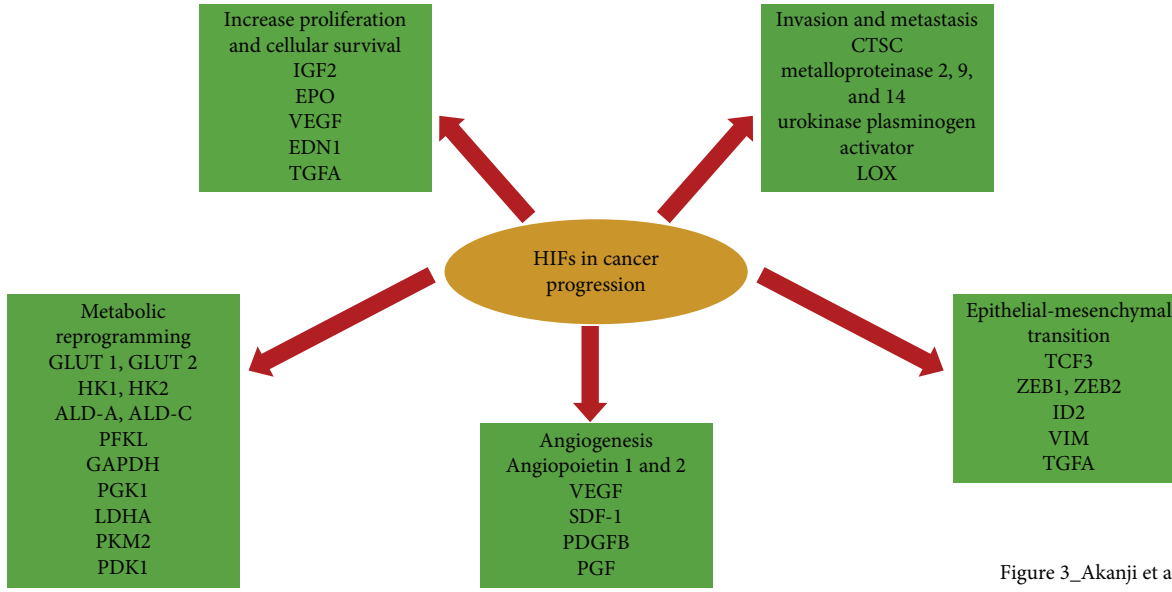

Figure 3: HIFs in cancer progression.

controlling hub of tumor pathways such as invasion, proliferation, angiogenesis, and colonization of far-off sites [5]

(b) Metabolic reprogramming: in order to meet cell energy demands, glucose uptake is highly upregulated in cancer cells compared to a normal cell. It is the basis to detect metastases by imaging using 18-F-fluorodeoxyglucose-positron emission tomography (FDG-PET). HIF-1 also moderate the tumor-related metabolic switch through the Warburg effect which is responsible for greater glucose oxidation in anaerobic condition than in oxidative phosphorylation. Critical effects of this shift are tumor microenvironment acidosis. The acidic environment and the metabolic switch are responsible for abundant metabolic intermediates that stimulates tumor progression and aggressiveness [55]. HIF-1 facilitates the gene expression encoding glucose transporter 1 and 3 and enzymes involved in glucose conversion to lactose different from those found in normal cells such as hexokinase 1 and 2 (HK1, HK2), aldolase A and C (ALD-A, ALD-C), phosphofructokinase L (PFKL), glyceraldehyde-3-phosphate dehydrogenase (GAPDH), enolase A, phosphoglycerate kinase 1 (PGK1), lactate dehydrogenase A (LDHA), and pyruvate kinase M2 (PKM2). HIF-1 increases the pyruvate dehydrogenase kinase-1 (PDK1) expression which inhibits pyruvate dehydrogenase responsible for converting pyruvate to acetyl-CoA before TCA cycle can occur, thereby suppressing mitochondria function and oxygen utilization [1]. Hexokinase and lactate dehydrogenase A are oncogenic transcription factors for MYC targets. Under physiological condition, c-MYC activities are inhibited by HIF-1α, but both c-MYC and HIF-1α work hand in hand to induce the pyruvate dehydrogenase kinase-1 (PDK1) and hexokinase expression which result in aerobic glycolysis and angiogenesis. Additionally, HIF-1α influences cytochrome c oxidase subunit 4 (COX4) switch under hypoxic condition to give a homeostatic response which improves respiration efficacy at different oxygen concentrations [5]. Semenza [27] also revealed that HIF-1 may also mediate the transketolase enzyme expression in the hexose monophosphate pathway required for nonoxidative production of ribose, a precursor for nucleic acid [5, 27]

(c) Angiogenesis: new capillaries formed from already existing vessels in response to low oxygen especially in cancerous cell to deliver oxygen to the cells and thereby encourage tumor growth [56]. The angiogenic switch regulated by HIF-1 in hypoxic tumor microenvironment may be connected with increased oxygen consumption, while reducing oxygen diffusion distance. Angiogenesis is an intricate, well-ordered process which is essential for neoplasm formation. The mechanism comprises of many genes, regulators, and pathways. Induction of angiogenesis results in enlarged vascular density and reduced oxygen diffusion distance [5]. Furthermore, HIF-1 also regulates the encoding genes for angiogenic growth factor expressions. These include angiopoietin 1 and 2, vascular endothelial growth factor (VEGF), stromal-derived factor-1 (SDF-1), platelet-derived growth factor B (PDGFB), and placenta growth factor (PGF) [27]. A critical link between hypoxia and angiogenesis is the discovery of vascular endothelial growth factor (VEGF)

(d) Epithelial-mesenchymal transition: HIF-1 triggers activation of repressor genes that inhibit proteins

Table 1: Some HIF inhibitors and targets.

Agents	Inhibitory mechanisms	Targeting HIF-1	Targeting HIF-2	Reference no.
EZN-2968	HIF-1 mRNA expression	√	—	Jeong, et al., [60]
EZN-2208	HIF-1 mRNA expression	√	—	Coltella, et al., [61]
Topotecan	HIF-1 mRNA translation	√	—	Rapisarda, et al., [62]
HIF-1α inhibitor	HIF-α transcriptional activity	√	√	Cui, et al., [63]
PX-12	HIF-α transcriptional activity	√	—	Raninga, et al., [64]
Acriflavine	HIF transcriptional activity	√	√	Lee, et al., [40, 41]
Echinomycin	HIF DNA binding	√	—	Yu, et al., [65]

responsible for cell to cell contact and rigid cytoskeleton. Examples of such repressor genes include transcription factor 3 (TCF3), zinc finger E-box-binding homeobox 1 and 2 (ZEB1, ZEB2), and inhibitor of differentiation 2 (ID2). HIF-1 also facilitates a gene expression that stimulates flexible cytoskeleton like TGFA and vimentin (VIM) [1]

(e) Invasion and metastasis: invasion and metastasis of tumor cells are regulated by hypoxia. Metastasis is a series of well-defined events which is the basic reason of cancer-related mortality. These events include the local spread of tumor cells, intravasation, survival of circulating tumor cells, and extravasation followed by proliferation that leads to colonization. Activation of genes regulated by HIF may improve metastasis in multiple tumors. HIF-1 stimulates genetic transcription such as proteases that degrade cathepsin C (CTSC), matrix metalloproteinase 2, 9, and 14, and the urokinase plasminogen activator receptor or remodel lysyl oxidase (LOX); the extracellular matrices within are of metastasis [5]

10. Inhibitors of HIF-1 in Cancer Therapy

Different chemical compounds or drugs have been revealed to block the activity of HIF through different molecular mechanisms (Table 1), including a reduced synthesis of HIF-1α protein (mTOR inhibitors, cardiac glycosides, topoisomerase inhibitor, and synthetic oligonucleotides), decreased HIF-1α mRNA levels (aminoflavone component of prodrug AFP-464), increased HIF-1α breakdown (HSP90 inhibitors, antioxidants, and Se-methylselenocysteine), reduced heterodimerization of HIF subunit (acriflavine), decreased DNA binding to the HIF (anthracyclines and echinomycin), and reduced transcriptional activity [1].

(a) Inhibitors of the HIF-1 mRNA expression: HIF-1 increase is regulated predominantly at the degradation or translation of protein, and these pathways are the targets of most HIF-1 inhibitors. However, under hypoxic conditions, HIF-1 mRNA levels can act as a limiting factor thereby affecting protein translation [57]. Aminoflavone (AF) is an agent that affects the HIF-1 mRNA expression. It acts as a ligand of aryl-hydrocarbon receptor (AhR) and presently being used in clinical trials in metastatic cancer patients [57]

(b) Inhibitors of HIF-1 protein translation: numerous agents may affect the HIF-1 protein synthesis rate, including tyrosine kinase inhibitor, topoisomerase I and II inhibitor, cyclin-dependent kinase inhibitor, oncogenic pathway inhibitor, and thioredoxin reductase inhibitor. One of the earlier agents used for HIF-1 protein translation is topotecan, a second line chemotherapy for lung cancer or ovarian cancer. Topotecan is a camptothecin analogue which in the presence of DNA replication generate double strand DNA breaks and cytotoxicity, thereby poisons topoisomerase I by inducing the formation of stable Top1-DNA cleavage complexes [57]. Another class of agents that affect HIF-1 protein translation is cardiac glycosides. Digoxin in particular has been identified as a HIF-1 potent inhibitor. Digoxin inhibits HIF-1 translation using mTOR-independent mechanism and also exhibits antitumor activity [55]. PX-478 is another HIF-1 inhibitor presently in phase I clinical trials in advanced metastatic cancer patients. It showed antitumor activity in tumor xenograft models, which correlate with the HIF-1 expression [57]

EZN-2968 is a RNA modulator composed of synthetic antisense oligonucleotide that binds and inhibits specifically the HIF-1α mRNA expression [6, 58]. There is a dose-dependent downregulation of HIF-1α mRNA after it binds to EZN-2968 leading to inhibition in both normoxia and hypoxia [58]. In mice implanted with DU-145 human prostate cancer cells, EZN-2968 treatment showed tumor reduction. Clinically, evaluation of EZN-2968 treatment of 4 out of 6 patients with paired tumor biopsies showed reduced HIF-1α mRNA in posttreatment biopsies while two patients had a reduced level of mRNA and HIF-1α protein of target genes in biopsies [59]. This revealed a pilot proof of HIF-1α mRNA and protein expression modulation in response to EZN-2968 thereby indicating inhibition of HIF-1α mRNA has potential as a target for cancer therapy [60].

11. Conclusion

The mechanism for cellular oxygen homeostasis and its response to a low oxygen state is basically facilitated by the

HIF pathway. Additionally, the regulation or dysregulation of the HIF pathway is a major determinant in cancer metastasis, and this correlates with a poor cancer prognosis. Because of the roles that it plays in cancer progression, HIF has become an attractive target for chemotherapy against cancerous cells. Perhaps, the combined usage of conventional treatment and HIF inhibitors may prove to be useful clinically.

Abbreviations

ALD-A and ALD-C: Aldolase A and aldolase C
AF: Aminoflavone
ARNT: Aryl hydrocarbon receptor nuclear translocator
AhR: Aryl-hydrocarbon receptor
BNIP3: BCL2/adenovirus E1B 19-kDa interacting protein 3
BNIP3L: BNIP3-like
BMDACs: Bone marrow-derived angiogenic cells
CTSC: Cathepsin C
COX4: Cytochrome c oxidase subunit 4
DMOG: Dimethyloxalylglycine
ETC: Electron transport chain
EDN1: Endothelin 1
EPO: Erythropoietin
FDG-PET: 18-F-fluorodeoxyglucose-positron emission tomography
FIH: Factor inhibiting HIF
GAPDH: Glyceraldehyde-3-phosphate dehydrogenase
HK1 and HK2: Hexokinase 1 and 2
ID2: Inhibitor of differentiation 2
IGF2: Insulin-like growth factor-2
LDHA: Lactate dehydrogenase A
LOX: Lysyl oxidase
miRNAs: MicroRNAs
mAKAP: Muscle A-kinase anchoring protein
ODD: Oxygen-dependent degradation
PO_2: Partial oxygen pressure
PAD: Peripheral heart disease
PFKL: Phosphofructokinase L
PGK1: Phosphoglycerate kinase 1
PGF: Placenta growth factor
PGF-1: Placental growth factor
PDGFB: Platelet-derived growth factor B
PHD: Prolyl hydroxylases
PDK1: Pyruvate dehydrogenase kinase-1
PKM2: Pyruvate kinase M2
ROS: Reactive oxygen species
SDF-1: Stroma-derived factor-1
TCF3: Transcription factor 3 (TCF3)
TGFA: Transforming growth factor-α
TCA: Tricarboxylic acid
VEGF: Vascular endothelial growth factor
VIM: Vimentin
VHL: Von Hippel-Lindau
ZEB1 and ZEB2: Zinc finger E-box-binding homeobox 1 and 2.

Conflicts of Interest

The authors declare no conflict of interest.

References

[1] G. L. Semenza, "Hypoxia-inducible factors in physiology and medicine," *Cell*, vol. 148, no. 3, pp. 399–408, 2012.

[2] G. L. Semenza, "Regulation of metabolism by hypoxia-inducible factor 1," *Cold Spring Harbor Symposia on Quantitative Biology*, vol. 76, pp. 347–353, 2011.

[3] D. C. Fuhrmann and B. Brüne, "Mitochondrial composition and function under the control of hypoxia," *Redox Biology*, vol. 12, pp. 208–215, 2017.

[4] K. Balamurugan, "HIF-1 at the crossroads of hypoxia, inflammation, and cancer," *International Journal of Cancer*, vol. 138, no. 5, pp. 1058–1066, 2016.

[5] S. Soni and Y. S. Padwad, "HIF-1 in cancer therapy: two decade long story of a transcription factor," *Acta Oncologica*, vol. 56, no. 4, pp. 503–515, 2017.

[6] C. Wigerup, S. Pahlman, and D. Bexell, "Therapeutic targeting of hypoxia and hypoxia-inducible factors in cancer," *Pharmacology & Therapeutics*, vol. 164, pp. 152–169, 2016.

[7] E. Poon, A. L. Harris, and M. Ashcroft, "Targeting the hypoxia-inducible factor (HIF) pathway in cancer," *Expert Reviews in Molecular Medicine*, vol. 11, article e26, 2009.

[8] O. S. Adeyemi and D. A. Otohinoyi, "Inorganic nanoparticles restrict viability of metastatic breast cancer cells in vitro," *Comparative Clinical Pathology*, vol. 28, no. 4, pp. 949–954, 2019.

[9] S. Sharma and D. Rawat, "Partial Pressure of Oxygen (PO2)," in *StatPearls*, StatPearls, Treasure Island, FL, USA, 2019, https://www.ncbi.nlm.nih.gov/books/NBK493219/.

[10] N. Lane and W. Martin, "The energetics of genome complexity," *Nature*, vol. 467, no. 7318, pp. 929–934, 2010.

[11] H. K. Eltzschig and P. Carmeliet, "Hypoxia and inflammation," *The New England Journal of Medicine*, vol. 364, no. 7, pp. 656–665, 2011.

[12] T. G. Smith, P. A. Robbins, and P. J. Ratcliffe, "The human side of hypoxia-inducible factor," *British Journal of Haematology*, vol. 141, no. 3, pp. 325–334, 2008.

[13] G. L. Semenza, "Targeting HIF-1 for cancer therapy," *Nature Reviews Cancer*, vol. 3, no. 10, pp. 721–732, 2003.

[14] N. Yewalkar, V. Deore, A. Padgaonkar et al., "Development of novel inhibitors targeting HIF-1α towards anticancer drug discovery," *Bioorganic & Medicinal Chemistry Letters*, vol. 20, no. 22, pp. 6426–6429, 2010.

[15] C. V. Dang, J. Kim, P. Gao, and J. Yustein, "The interplay between MYC and HIF in cancer," *Nature Reviews Cancer*, vol. 8, no. 1, pp. 51–56, 2008.

[16] J. Kim, I. Tchernyshyov, G. L. Semenza, and C. V. Dang, "HIF-1-mediated expression of pyruvate dehydrogenase kinase: a metabolic switch required for cellular adaptation to hypoxia," *Cell Metabolism*, vol. 3, no. 3, pp. 177–185, 2006.

[17] I. Papandreou, R. A. Cairns, L. Fontana, A. L. Lim, and N. C. Denko, "HIF-1 mediates adaptation to hypoxia by actively downregulating mitochondrial oxygen consumption," *Cell Metabolism*, vol. 3, no. 3, pp. 187–197, 2006.

[18] G. L. Semenza, B. H. Jiang, S. W. Leung et al., "Hypoxia response elements in the aldolase A, enolase 1, and lactate

dehydrogenase A gene promoters contain essential binding sites for hypoxia-inducible factor 1," *Journal of Biological Chemistry*, vol. 271, no. 51, pp. 32529–32537, 1996.

[19] G. Bellot, R. Garcia-Medina, P. Gounon et al., "Hypoxia-induced autophagy is mediated through hypoxia-inducible factor induction of BNIP3 and BNIP3L via their BH3 domains," *Molecular and Cellular Biology*, vol. 29, no. 10, pp. 2570–2581, 2009.

[20] H. Zhang, M. Bosch-Marce, L. A. Shimoda et al., "Mitochondrial autophagy is an HIF-1-dependent adaptive metabolic response to hypoxia," *Journal of Biological Chemistry*, vol. 283, no. 16, pp. 10892–10903, 2008.

[21] R. Fukuda, H. Zhang, J. W. Kim, L. Shimoda, C. V. Dang, and G. L. Semenza, "HIF-1 regulates cytochrome oxidase subunits to optimize efficiency of respiration in hypoxic cells," *Cell*, vol. 129, no. 1, pp. 111–122, 2007.

[22] D. Yoon, P. Ponka, and J. T. Prchal, "Hypoxia. 5. Hypoxia and hematopoiesis," *American Journal of Physiology-Cell Physiology*, vol. 300, no. 6, pp. C1215–C1222, 2011.

[23] J. Peng, L. Zhang, L. Drysdale, and G. H. Fong, "The transcription factor EPAS-1/hypoxia-inducible factor 2α plays an important role in vascular remodeling," *Proceedings of the National Academy of Sciences of the United States of America*, vol. 97, no. 15, pp. 8386–8391, 2000.

[24] H. Tian, R. E. Hammer, A. M. Matsumoto, D. W. Russell, and S. L. McKnight, "The hypoxia-responsive transcription factor EPAS1 is essential for catecholamine homeostasis and protection against heart failure during embryonic development," *Genes & Development*, vol. 12, no. 21, pp. 3320–3324, 1998.

[25] V. Compernolle, K. Brusselmans, T. Acker et al., "Loss of HIF-2α and inhibition of VEGF impair fetal lung maturation, whereas treatment with VEGF prevents fatal respiratory distress in premature mice," *Nature Medicine*, vol. 8, no. 7, pp. 702–710, 2002.

[26] T. Eckle, D. Köhler, R. Lehmann, K. C. el Kasmi, and H. K. Eltzschig, "Hypoxia-inducible factor-1 is central to cardioprotection: a new paradigm for ischemic preconditioning," *Circulation*, vol. 118, no. 2, pp. 166–175, 2008.

[27] G. L. Semenza, "Hypoxia-inducible factors: mediators of cancer progression and targets for cancer therapy," *Trends in Pharmacological Sciences*, vol. 33, no. 4, pp. 207–214, 2012.

[28] I. R. Botusan, V. G. Sunkari, O. Savu et al., "Stabilization of the HIF-1α is crucial to improve wound healing in diabetic mice," *Proceedings of the National Academy of Sciences of the United States of America*, vol. 105, no. 49, pp. 19426–19431, 2008.

[29] H. Thangarajah, D. Yao, E. I. Chang et al., "The molecular basis for impaired hypoxia-induced VEGF expression in diabetic tissues," *Proceedings of the National Academy of Sciences of the United States of America*, vol. 106, no. 32, pp. 13505–13510, 2009.

[30] G. L. Semenza, "Defining the role of hypoxia-inducible factor 1 in cancer biology and therapeutics," *Oncogene*, vol. 29, no. 5, pp. 625–634, 2010.

[31] P. Jaakkola, D. R. Mole, Y. M. Tian et al., "Targeting of HIF-α to the von Hippel-Lindau ubiquitylation complex by O_2-regulated prolyl hydroxylation," *Science*, vol. 292, no. 5516, pp. 468–472, 2001.

[32] M. Ivan, K. Kondo, H. Yang et al., "HIFα targeted for VHL-mediated destruction by proline hydroxylation: implications for 0_2 sensing," *Science*, vol. 292, no. 5516, pp. 464–468, 2001.

[33] W. G. Kaelin Jr. and P. J. Ratcliffe, "Oxygen sensing by metazoans: the central role of the HIF hydroxylase pathway," *Molecular Cell*, vol. 30, no. 4, pp. 393–402, 2008.

[34] P. H. Maxwell, M. S. Wiesener, G. W. Chang et al., "The tumour suppressor protein VHL targets hypoxia-inducible factors for oxygen-dependent proteolysis," *Nature*, vol. 399, no. 6733, pp. 271–275, 1999.

[35] D. Lando, D. J. Peet, J. J. Gorman, D. A. Whelan, M. L. Whitelaw, and R. K. Bruick, "FIH-1 is an asparaginyl hydroxylase enzyme that regulates the transcriptional activity of hypoxia-inducible factor," *Genes & Development*, vol. 16, no. 12, pp. 1466–1471, 2002.

[36] P. Mahon, K. Hirota, and G. Semenza, "FIH-1: a novel protein that interacts with HIF-1α and VHL to mediate repression of HIF-1 transcriptional activity," *Genes & Development*, vol. 15, no. 20, pp. 2675–2686, 2001.

[37] B. L. Ebert and H. F. Bunn, "Regulation of transcription by hypoxia requires a multiprotein complex that includes hypoxia-inducible factor 1, an adjacent transcription factor, and p300/CREB binding protein," *Molecular and Cellular Biology*, vol. 18, no. 7, pp. 4089–4096, 1998.

[38] S. N. Greer, J. L. Metcalf, Y. Wang, and M. Ohh, "The updated biology of hypoxia-inducible factor," *The EMBO Journal*, vol. 31, no. 11, pp. 2448–2460, 2012.

[39] A. C. R. Epstein, J. M. Gleadle, L. A. McNeill et al., "*C. elegans* EGL-9 and mammalian homologs define a family of dioxygenases that regulate HIF by prolyl hydroxylation," *Cell*, vol. 107, no. 1, pp. 43–54, 2001.

[40] K. Lee, D. Z. Qian, S. Rey, H. Wei, J. O. Liu, and G. L. Semenza, "Anthracycline chemotherapy inhibits HIF-1 transcriptional activity and tumor-induced mobilization of circulating angiogenic cells," *Proceedings of the National Academy of Sciences of the United States of America*, vol. 106, no. 7, pp. 2353–2358, 2009.

[41] K. Lee, H. Zhang, D. Z. Qian, S. Rey, J. O. Liu, and G. L. Semenza, "Acriflavine inhibits HIF-1 dimerization, tumor growth, and vascularization," *Proceedings of the National Academy of Sciences of the United States of America*, vol. 106, no. 42, pp. 17910–17915, 2009.

[42] J. D. Gordan, P. Lal, V. R. Dondeti et al., "HIF-α effects on c-Myc distinguish two subtypes of sporadic *VHL*-deficient clear cell renal carcinoma," *Cancer Cell*, vol. 14, no. 6, pp. 435–446, 2008.

[43] T. Klimova and N. S. Chandel, "Mitochondrial complex III regulates hypoxic activation of HIF," *Cell Death and Differentiation*, vol. 15, no. 4, pp. 660–666, 2008.

[44] S. E. Weinberg and N. S. Chandel, "Targeting mitochondria metabolism for cancer therapy," *Nature Chemical Biology*, vol. 11, no. 1, pp. 9–15, 2015.

[45] N. Haga, S. Saito, Y. Tsukumo et al., "Mitochondria regulate the unfolded protein response leading to cancer cell survival under glucose deprivation conditions," *Cancer Science*, vol. 101, no. 5, pp. 1125–1132, 2010.

[46] Y. Bai, Z. Guo, J. Xu et al., "Single nucleotide polymorphisms in the D-loop region of mitochondrial DNA is associated with renal cell carcinoma outcome," *Mitochondrial DNA*, vol. 26, no. 2, pp. 224–226, 2015.

[47] F. Navaglia, D. Basso, P. Fogar et al., "Mitochondrial DNA D-loop in pancreatic cancer: somatic mutations are epiphenomena while the germline 16519 T variant worsens

metabolism and outcome," *American Journal of Clinical Pathology*, vol. 126, no. 4, pp. 593–601, 2006.

[48] M. Brandon, P. Baldi, and D. C. Wallace, "Mitochondrial mutations in cancer," *Oncogene*, vol. 25, no. 34, pp. 4647–4662, 2006.

[49] A. Chatterjee, E. Mambo, and D. Sidransky, "Mitochondrial DNA mutations in human cancer," *Oncogene*, vol. 25, no. 34, pp. 4663–4674, 2006.

[50] D. C. Wallace, "Mitochondria and cancer," *Nature Reviews Cancer*, vol. 12, no. 10, pp. 685–698, 2012.

[51] J. S. Mattick and M. J. Gagen, "The evolution of controlled multitasked gene networks: the role of introns and other non-coding RNAs in the development of complex organisms," *Molecular Biology and Evolution*, vol. 18, no. 9, pp. 1611–1630, 2001.

[52] G. Di Leva, M. Garofalo, and C. M. Croce, "MicroRNAs in cancer," *Annual Review of Pathology*, vol. 9, no. 1, pp. 287–314, 2014.

[53] W. Tan, B. Liu, S. Qu, G. Liang, W. Luo, and C. Gong, "MicroRNAs and cancer: key paradigms in molecular therapy (Review)," *Oncology Letters*, vol. 15, no. 3, pp. 2735–2742, 2018.

[54] J.-W. Lee, S. H. Bae, J. W. Jeong, S. H. Kim, and K. W. Kim, "Hypoxia-inducible factor (HIF-1)α: its protein stability and biological functions," *Experimental & Molecular Medicine*, vol. 36, no. 1, pp. 1–12, 2004.

[55] G. N. Masoud and W. Li, "HIF-1α pathway: role, regulation and intervention for cancer therapy," *Acta Pharmaceutica Sinica B*, vol. 5, no. 5, pp. 378–389, 2015.

[56] L. Schito and G. L. Semenza, "Hypoxia-inducible factors: master regulators of cancer progression," *Trends in Cancer*, vol. 2, no. 12, pp. 758–770, 2016.

[57] B. Onnis, A. Rapisarda, and G. Melillo, "Development of HIF-1 inhibitors for cancer therapy," *Journal of Cellular and Molecular Medicine*, vol. 13, no. 9A, pp. 2780–2786, 2009.

[58] G. M. Burslem, H. F. Kyle, A. Nelson, T. A. Edwards, and A. J. Wilson, "Hypoxia inducible factor (HIF) as a model for studying inhibition of protein–protein interactions," *Chemical Science*, vol. 8, no. 6, pp. 4188–4202, 2017.

[59] T. Yu, B. Tang, and X. Sun, "Development of inhibitors targeting hypoxia-inducible factor 1 and 2 for cancer therapy," *Yonsei Medical Journal*, vol. 58, no. 3, pp. 489–496, 2017.

[60] W. Jeong, A. Rapisarda, S. R. Park et al., "Pilot trial of EZN-2968, an antisense oligonucleotide inhibitor of hypoxia-inducible factor-1 alpha (HIF-1α), in patients with refractory solid tumors," *Cancer Chemotherapy and Pharmacology*, vol. 73, no. 2, pp. 343–348, 2014.

[61] N. Coltella, R. Valsecchi, M. Ponente, M. Ponzoni, and R. Bernardi, "Synergistic leukemia eradication by combined treatment with retinoic acid and HIF inhibition by EZN-2208 (PEG-SN38) in preclinical models of PML-RARα and PLZF-RARα-driven leukemia," *Clinical Cancer Research*, vol. 21, no. 16, pp. 3685–3694, 2015.

[62] A. Rapisarda, B. Uranchimeg, O. Sordet, Y. Pommier, R. H. Shoemaker, and G. Melillo, "Topoisomerase I-mediated inhibition of hypoxia-inducible factor 1: mechanism and therapeutic implications," *Cancer Research*, vol. 64, no. 4, pp. 1475–1482, 2004.

[63] X. Y. Cui, M. Tinholt, B. Stavik et al., "Effect of hypoxia on tissue factor pathway inhibitor expression in breast cancer," *Journal of Thrombosis and Haemostasis*, vol. 14, no. 2, pp. 387–396, 2016.

[64] P. V. Raninga, G. Di Trapani, S. Vuckovic, M. Bhatia, and K. F. Tonissen, "Inhibition of thioredoxin 1 leads to apoptosis in drug-resistant multiple myeloma," *Oncotarget*, vol. 6, no. 17, pp. 15410–15424, 2015.

[65] W. Yu, R. A. Denu, K. A. Krautkramer et al., "Loss of SIRT3 provides growth advantage for B cell malignancies," *The Journal of Biological Chemistry*, vol. 291, no. 7, pp. 3268–3279, 2016.

Hindawi
Oxidative Medicine and Cellular Longevity
Volume 2019, Article ID 5357649, 15 pages
https://doi.org/10.1155/2019/5357649

Research Article

Label-Free Proteomics Revealed Oxidative Stress and Inflammation as Factors That Enhance Chemoresistance in Luminal Breast Cancer

Bruno R. B. Pires,[1] **Carolina Panis**,[1,2] **Vinícius Dias Alves**,[2] **Ana C. S. A. Herrera**,[3] **Renata Binato**,[1] **Luciana Pizzatti**,[4] **Rubens Cecchini**,[5] **and Eliana Abdelhay**[1]

[1]*Laboratório de Célula Tronco, Instituto Nacional de Câncer, Rio de Janeiro, RJ 20230-130, Brazil*
[2]*Laboratório de Mediadores Inflamatórios, Universidade Estadual do Oeste do Paraná, Francisco Beltrão, PR 85605-010, Brazil*
[3]*Instituto do Câncer de Londrina, Londrina, PR 86015-520, Brazil*
[4]*Laboratório de Biologia Molecular e Proteômica do Sangue, Instituto de Química, Universidade Federal do Rio de Janeiro, Rio de Janeiro, RJ 21941-598, Brazil*
[5]*Laboratório de Fisiopatologia e Radicais Livres, Universidade Estadual de Londrina, Londrina, PR 86057-970, Brazil*

Correspondence should be addressed to Carolina Panis; carolpanis@hotmail.com

Bruno R. B. Pires and Carolina Panis contributed equally to this work.

Received 15 April 2019; Revised 22 June 2019; Accepted 1 July 2019; Published 8 August 2019

Guest Editor: Kanhaiya Singh

Breast cancer is the leading cause of cancer-associated death among women worldwide. Its high mortality rate is related to resistance towards chemotherapies, which is one of the major challenges of breast cancer research. In this study, we used label-free mass spectrometry- (MS-) based proteomics to investigate the differences between circulating proteins in the plasma of patients with chemoresponsive and chemoresistant luminal A breast cancer. MS analysis revealed 205 differentially expressed proteins. Furthermore, we used in silico tools to build protein-protein interaction networks. Most of the upregulated proteins in the chemoresistant group were closely related and tightly linked. The predominant networks were related to oxidative stress, the inflammatory response, and the complement cascade. Through this analysis, we identified inflammation and oxidative stress as central processes of breast cancer chemoresistance. Furthermore, we confirmed our hypothesis by evaluating oxidative stress and performing cytokine profiling in our cohort. The connections among oxidative stress, inflammation, and the complement system described in our study seem to indicate a pivotal axis in breast cancer chemoresistance. Hence, these findings will have significant clinical implications for improving therapies to bypass breast cancer chemoresistance in the future.

1. Introduction

Breast cancer (BC) is the leading cause of cancer-associated death among women worldwide. In the U.S., approximately 270,000 new cases of female BC and more than 40,000 deaths are expected in 2019 [1]. More than 70% of all diagnosed BC cases are estrogen- and/or progesterone receptor-positive (ER+ and PR+, respectively), which is defined as the luminal subtype [2]. Over the past two decades, the investigation of BC biology has increased our understanding of BC at the molecular level. However, relevant issues remain to be addressed. In this context, resistance to treatment is considered the main critical challenge in BC research since resistance is responsible for treatment failure, especially in cases of metastatic disease [3].

Cytotoxic chemotherapy for BC treatment is based on a protocol that includes taxanes and anthracyclines, such as the combined paclitaxel/doxorubicin treatment. Paclitaxel belongs to the taxane family and acts by stabilizing microtubules, altering cell division and, consequently, causing cell death [4]. An additional mechanism of this drug is the generation of oxidative stress and inflammatory mediators [5].

Studies have shown that paclitaxel promotes cytotoxicity by reactive oxygen and nitrogen species (ROS and RNS, respectively) [6]. Doxorubicin is the most commonly used anthracycline in BC treatment. It disrupts DNA replication by binding to topoisomerase II and generating free radicals, resulting in DNA damage [7]. In both cases, oxidative stress is generated when there is an imbalance between the production of antioxidant substances by cancer cells and the production of ROS by chemotherapeutics. Approximately 50% of patients treated with cytotoxic chemotherapy develop resistance to treatment within a 6-month interval [8–11]. Chemoresistance is defined as tumor resistance intrinsic or extrinsic to the chemotherapeutic treatment leading to recurrence of the disease or its progression to metastasis [12]. Thus, chemoresistance poses one of the major challenges in BC research [13].

The early detection of chemoresistance has a significant effect on reducing mortality. Proteomics is a powerful high-throughput tool for screening circulating proteins and evaluating the response to treatment or disease recurrence [14, 15]; however, chemoresistance in BC has not been sufficiently explored. Many chemoresistance studies are cell line-based, which does not replicate the complexity of the human body. Hence, discovering proteomic signatures associated with chemoresistance is critical to differentiate chemoresistant and treatment-sensitive patients.

Our group recently suggested markers of BC progression through plasma proteomic profile analyses [16]. In the present study, resistance to combined paclitaxel/doxorubicin treatment in luminal A breast cancer patients was investigated using a label-free proteomic approach to acquire a comprehensive analysis of the crucial factors related to this phenomenon. Our findings revealed that most of the upregulated proteins in the chemoresistant group are closely related and tightly linked. Although our results showed a strong interplay between inflammation and oxidative stress in the chemoresistant condition, the complement system might be responsible for their connection, which has been well demonstrated in age-related macular degeneration [17], but not for breast cancer yet. Through this analysis, we identified inflammation and oxidative stress as central signaling pathways and possible markers associated with BC chemoresistance. In addition, to the best of our knowledge, this is the first in-depth proteomic study of the differentially circulating proteins in patients with BC chemoresistance. These findings will have critical implications for the development of more effective therapies for BC.

2. Materials and Methods

2.1. Design of the Study and Patient Characteristics. Two hundred women diagnosed with invasive breast carcinoma who attended a public Oncology Center in Brazil were enrolled in this study. This was a prospective study that started in 2014 with follow-up until 2018. Figure 1 displays a schematic design of this study, which was approved by the Research Ethics Committee of the Institution and the National Ethics Research Council (CAAE 23753014.3.0000.5231). All participants signed informed consent forms.

Patients were included in the study from the time of diagnosis. They were administered 5-6 cycles of combined paclitaxel (175 mg/m^2) and doxorubicin (60 mg/m^2) every 21 weeks. Samples were collected at diagnosis before starting treatment and posteriorly categorized according to the pattern of each patient's chemotherapy response in the first year of treatment. Thereafter, patients were categorized into the following groups according to the treatment response criteria established by the Response Evaluation Criteria in Solid Tumors (RECIST) guidelines [18]: (1) patients responsive to chemotherapy and (2) patients resistant to chemotherapy. All patients were subjected to the same treatment schedule, which included anthracyclines and taxanes, and were evaluated at the end of the first-choice treatment module (5-6 months). The following parameters in the cohort were considered for clinicopathological characterization: age at diagnosis, weight, height, comorbidities, International Union Against Cancer (UICC) tumor, node, metastasis (TNM) stage, hormonal status of the tumors, and chemotherapy protocol. Patients bearing tumors exhibiting amplification of the receptor of epidermal growth factor 2 (HER2) were excluded from this study due to the use of other treatment protocols (monoclonal anti-HER2 antibodies). Other exclusion criteria were a history of previous chemotherapy, smoking, hepatic, renal or cardiac dysfunction, diabetes, and other chronic conditions that could interfere in the analysis of the results. Clinicopathological data were obtained from medical records and are presented in Table 1.

2.2. Plasma Collection and In-Solution Tryptic Digestion. Whole blood samples (20 mL) were obtained by peripheral venipuncture and collected in sodium EDTA tubes. The tubes were centrifuged for 5 min at 1400 × g at 4°C, and the nondepleted plasma was then collected, supplemented with a 1 : 1000 (μL) protease inhibitor cocktail (GE Healthcare, USA), and stored at −80°C. Nondepleted plasma samples were used to prevent loss of information during the removal of the high-abundance proteins. Protein concentration was determined using the Bradford assay. Proteomic analysis was performed using pooled plasma samples (500 μL from each individual sample) for each group (responsive and chemoresistant patients), and 1 mg of nondepleted plasma samples were concentrated 39-fold and exchanged into 50 mM ammonium bicarbonate (NH_4HCO_3) using a 3 kDa ultrafiltration device (Millipore, USA). Then, 200 μg of protein was denatured (0.1% RapiGEST SF at 60°C for 15 min) (Waters, USA), reduced with 10 mM DTT (60°C for 30 min), alkylated with 10 mM iodoacetamide (30 min at room temperature in the dark), and, after that, enzymatically digested with trypsin at a 1 : 50 w/w enzyme/protein ratio (Promega, USA), according to the method described by Panis et al. [19]. Digestion was stopped by adding 10 μL of 5% TFA, and yeast alcohol dehydrogenase (ADH; P00330, Waters) was added to the digests at a final concentration of 10 fmol/μL as an internal standard for absolute quantification [20].

2.3. Label-Free Protein Quantitation via Mass Spectrometry. For qualitative and quantitative experiments, the nanoUPLC tandem nanoESI-HDMS^E proteomic approach was applied in

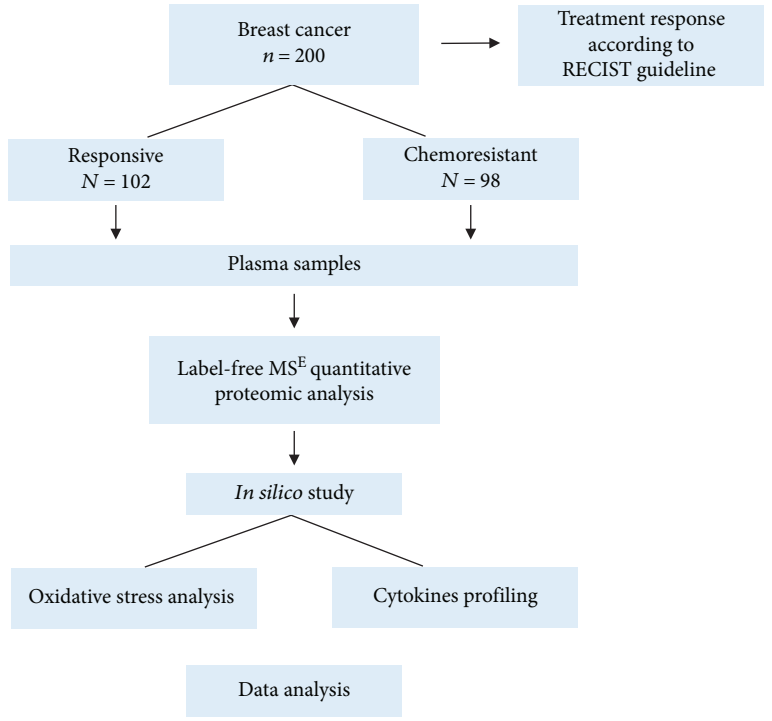

Figure 1: Schematic design of the study.

Table 1: Clinicopathological characteristics of the patients.

Variable	
Total number of patients	*n* = 200
Mean age at diagnosis (years)	56.3
TNM stage (%)	
I/II	30%
III/IV	70%
Tumor histological type (%)	
Infiltrative ductal carcinoma	100%
Tumor grade (n)	
1	5%
2	39%
3	56%
Tumor size (cm)	
≤2	15.5%
2–5	54.5%
>5	30%
Molecular receptor status	
Positive ER	72%
Positive PR	56%
Response to chemotherapy	52%

this study. A nanoACQUITY UPLC system (Waters, UK) was used according to the method described by Panis et al. [16].

For the first dimension, a strong cation exchange (SCX) column was used. The samples were eluted from the SCX column using nine salt gradient fractions that were followed by a reversed-phase (RP) gradient. The released peptides were captured by a downstream RP trap column. After all the peptides had been captured, the trap column was placed online with a different RP analytical column, and an RP gradient of 5–40% acetonitrile (containing 0.1% *v*/*v* formic acid) over 58 min with a flow rate of 600 nL/min was used as the second dimension. Analyses were performed using nanoelectrospray ionization in positive ion mode nanoESI (+) and a NanoLockSpray ionization source (Waters, UK). Multiplexed data-independent (DIA) scanning with specificity and selectivity based on nonlinear "T-wave" ion mobility (HDMS^E) experiments was performed with a Synapt HDMS mass spectrometer (Waters, UK) as previously described [16]. Full-scan orthogonal acceleration time-of-flight (oa-TOF) MSE was acquired from an *m*/*z* of 50 to 2000.

2.4. Database Searching, Protein Quantification, and In Silico Analysis. Database searching and protein quantification were performed as previously reported [16] using ProteinLynx Global Server v.2.5.2 (PLGS) and Expression^E informatics. Proteins present in all replicates of each condition were considered for expression analysis using the Expression^E tool. The identified proteins were organized into a statistically significant list corresponding to increased and decreased regulation ratios between samples from patients with the chemoresistant group vs. the chemosensitive group. Additional filtering procedure was performed to select only those proteins that presented differential expression levels (ratios) with *p* value less than 0.05. Next, in silico analysis was performed using STRING v.10 software (http://string-db.org) [21], the PANTHER (http://pantherdb.org) [22], KEGG (http://genome.jp/kegg) [23], and IPA (QIAGEN Inc., https://www.qiagenbioinformatics.com/products/ingenuity-pathway-analysis)

[24] to identify the main interaction networks, biological processes, and signaling pathways corresponding to the differentially expressed proteins.

2.5. Oxidative Stress Analyses. To evaluate oxidative stress in the plasma, we determined the carbonyl content, malondialdehyde (MDA), and nitrite levels as estimates of nitric oxide (NO) and the antioxidant profile by measuring the total reactive antioxidant potential (TRAP) and reduced glutathione (GSH) levels. Healthy control plasma samples ($n = 32$) were included as reference.

The carbonyl content was measured as an estimate of oxidative injury to proteins, as previously described [25]. Dinitrophenylhydrazine (DNPH 10 Mm in HCl 2.5 M) was added to 200 μL of plasma, which was incubated in an ice bath (1 hour) and successively incubated with trichloroacetic acid 20% on ice for 15 minutes. Next, the samples were centrifuged (3000 rpm, 15 min), the supernatants were discarded, and the pellets were treated twice with an ethanol/water (1 : 1) solution. The final precipitates were dissolved in guanidine 6 M pH 2.3 and incubated for 24 h at 37°C [26]. The carbonyl content was calculated by obtaining spectra from 355 to 390 nm of the DNPH-treated samples. The obtained peaks were employed to calculate the carbonyl concentration using a molar extinction coefficient of 22 M^{-1} cm^{-1}. The results are expressed in nmol/mL/mg total protein. To determine the carbonyl content, total protein levels were measured with Folin-Ciocalteu reagent [27].

Malondialdehyde (MDA) levels were determined by high-performance liquid chromatography (HPLC) by using an HPLC-20AT Shimadzu equipped with an LC20AT pump and SPDM20A UV diode array absorbance detector employing a C18 reversed-phase column, as previously described [28]. Aliquots of 160 μL of plasma samples or standard solution reacted with 100 μL of 0.5 M perchloric acid. Samples were centrifuged for 5 min at 5000 × g at 4°C. 180 μL of supernatant was recovered to react with 100 μL of thiobarbituric acid for 30 min at 95°C. Reaction was stopped by ice bath, and 100 μL of 1 M NaH_2PO_4, pH 7.0, was added to stabilize sample pH. Further, samples were centrifuged for 10 min at 5000 × g at 4°C. The mobile phase consisted of 65% 50 mM KH_2PO_4 buffer, pH 7.0, and 35% HPLC-grade methanol. To determine MDA concentration, a standard curve was performed. For preparation of standard solution of MDA, 10 mL of 0.1 M HCl was added in 10 mL of 1,1,3,3-tetraethoxypropane (TEP), and this solution was maintained for 5 min in boiling water, following ice bath to complete synthesis of MDA. Readings were taken at 535 nm for 12 min with an isocratic flow of 0.8 mL/minute, and the results are expressed as nM MDA.

Nitrite levels were determined as estimates of the NO content and determined as previously described by Herrera and colleagues [29]. Plasma aliquots of 60 μL were deproteinized by adding 50 μL of 75 mM $ZnSO_4$ solution and after centrifugation (9500 × g for 2 min at 25°C) were mixed with 55 mM NaOH. The supernatant was recovered and diluted in a glycine buffer 5 : 1 in 45 g/L glycine, pH 9.7, with further incubation with cadmium granules activated in 5 mM $CuSO_4$ in 15 g/L glycine-NaOH buffer, pH 9.7 by 5 min. Aliquots of the recovered supernatant were mixed with the same volume of Griess reagent. A calibration curve was prepared by dilution of $NaNO_2$ in distilled sterile water. The absorbance was measured at 550 nm on a standard microplate reader, and the results are expressed as μM nitrite.

For antioxidant profiling, the total reactive antioxidant potential (TRAP) was determined, as described by Repetto and colleagues [30]; 2,2′-azobis (ABAP) was employed as a radical generator, and luminol was used to amplify photon detection and light emission by chemiluminescence. ABAP basal emission (900 μL of glycine buffer 0.1 M pH 8.6, 50 μL of luminol and 50 μL of ABAP) and hydrosoluble vitamin E standard solution (trolox, 6-hydroxy-2,5,7,8-tetramethylchroman-2-carboxylic acid 25 μM, 830 μL of glycine buffer 0.1 M pH 8.6, 70 μL of trolox, 50 μL of luminol, and 50 μL ABAP) emissions were recorded as references. For sample analysis, plasma was diluted 1 : 50 (830 μL of glycine buffer 0.1 M pH 8.6, 70 μL of sample, 50 μL of luminol, and 50 μL of ABAP). All readings were performed in a GloMax luminometer (Promega, USA) during 30 minutes, 5 readings/second. Results were expressed as nM sample equivalents of trolox.

GSH content was determined as described by Sedlak and Lindsay [31]. Plasma aliquots (60 μL) were deproteinized with 250 μL of trichloroacetic acid 50% and centrifuged at 2400 × g for 15 min, and the supernatants were added to 2 mL of 0.4 M TRIS buffer, pH 8.9. This mixture reacted with 50 μL of 5,5′-dithiobis (2-nitrobenzoic acid) solution. A standard curve was performed in order to determine GSH concentration in samples. The absorbance was read at 412 nm, and results were expressed in nM.

2.6. Cytokine Analysis. Interleukin-12 (IL-12), interleukin-10 (IL-10), transforming growth factor beta (TGF-β1), and tumor necrosis factor alpha (TNF-α) levels in plasma samples were determined by using a commercial antibody-specific RSG ELISA kit (eBioscience, USA). The results were calculated in pg/mL by fitting to a standard curve obtained using recombinant human cytokines. Healthy control plasma samples ($n = 32$) were included as reference.

2.7. Statistical Analysis. Analyses were conducted in duplicate, and the data are expressed as the means ± error of the means. Oxidative stress and cytokine parameters were compared by unpaired Student's t-test (parametric data) or the Mann-Whitney test (nonparametric data). A p value < 0.05 indicated significance. All statistical analyses were performed using GraphPad Prism 7.0 software (GraphPad Software, San Diego, CA).

3. Results

3.1. Clinicopathological Data. Table 1 shows the clinicopathological data of the patients. The mean age at diagnosis was 56.3 years, and most of the patients presented advanced disease, poorly differentiated tumors, and hormone-positive breast tumors larger than 2 cm.

3.2. Proteomic Profile of Breast Cancer Chemoresistance. To identify the differentially expressed proteins in plasma samples from patients with chemoresistant BC vs. patients with chemosensitive BC treated with a combination of doxorubicin and paclitaxel, we used label-free protein quantitation by MS. Proteomic screening revealed 444 proteins in the plasma samples from chemoresistant patients and 482 proteins in plasma samples from chemosensitive patients, of which 205 were differentially expressed between the two conditions. The total number of identified protein was separated into unique (exclusive in each condition) and differentially expressed (Table 2).

To identify the main biological processes and signaling pathways associated with the differentially expressed proteins, we performed separate in silico analyses of the upregulated and downregulated proteins. The most relevant processes associated with the differentially expressed proteins were oxidative metabolism, immune response (including inflammation, the humoral response, and the complement system), blood coagulation, cytoskeleton remodeling/cell adhesion, and DNA repair/kinetochore assembly. The proteins associated with these processes are shown in Table 3 (upregulated) and Table 4 (downregulated).

We found increased levels of proteins relevant to migratory behavior, such as Rho GTPase-activating protein, fibronectin, and vitronectin, in the chemoresistant samples compared with their levels in the responsive samples. Changes in the levels of cytoskeleton proteins and proteins that interact with the extracellular matrix (ECM) play an essential role in the invasive phenotype and progression of cancer. Consistently, we observed decreased levels of the adhesion proteins collagen alpha-1(VII), integrin alpha V, and keratin type II. The levels of proteins associated with DNA repair and kinetochore assembly were also changed. We observed the increased expression of DnaJ homolog subfamily C member 10, LINE-1 type transposase domain-containing protein 1, and centromere/kinetochore protein zw10 homolog, although we identified the decreased expression of DNA polymerase alpha catalytic subunit and centromere protein F, among others. Blood coagulation was represented through upregulation of plasminogen, prothrombin, alpha 1-antitrypsin, antithrombin III, and kininogen 1, among others, and downregulation of fibrinogen α and fibrinogen β. We identified several oxidative metabolism-associated proteins with altered expression in the resistant samples, indicating that oxidative metabolism may be a critical biological process for chemoresistance. The levels of iron metabolism-related proteins haptoglobin, hemoglobin subunits α and β, hemopexin, serotransferrin, and ceruloplasmin were increased. We also observed augmented levels of proteins related to the modulation of oxidative stress and vitamins, such as afamin and vitamin D-binding protein. Another biological process that was shown to be relevant was the immune response. Several immunoglobulins were upregulated in the resistant samples compared with their expression in the responsive samples. The same was observed for complement cascade proteins, including cascade initiators (C1q subunits, C4, C3, and complement factor B) and effectors (C5). Inflammatory and acute phase proteins were also differentially expressed in the chemoresistant samples. We observed upregulation of lumican, C-reactive protein, and apolipoproteins, whereas AKT3 and RGS14 were downregulated.

Table 2: Differentially expressed proteins of label-free proteomic analysis.

Upregulated in chemoresistant patients	79
Downregulated in chemoresistant patients	13
Unique in chemoresistant patients	59
Unique in chemosensitive patients	54
Total	205

Based on the most relevant biological processes and pathways revealed in our analysis, STRING software was used to build networks for the lists of up- and downregulated proteins (Figures 2 and 3, respectively). We observed that most of the upregulated proteins were associated with more than one biological process. This provoked network connection among the processes in STRING analysis. The majority of the upregulated proteins could be classified into the 4 following biological networks directly associated with processes relevant to BC chemoresistance: "response to oxidative stress" (Figure 2(a)), "acute inflammatory response" (Figure 2(b)), "complement and coagulation cascades" (Figure 2(c)), and "innate immune system" (Figure 2(d)). In contrast, the same analysis of the downregulated proteins showed distinct roles for each member and clustered them into exclusive networks (Figure 3). Nevertheless, they revealed a direct connection by their association with different biological processes, such as the cytoskeleton organization-fibrinolysis axis. To obtain a more accurate view of the molecular changes in samples of chemoresistant patients, we used the IPA software to identify the networks and canonical pathways most altered in this condition. The data are shown in the Supplementary Figures S1-6.

3.3. Oxidative Stress and Inflammatory Profile of Chemoresistant Breast Cancer. Since the proteins identified by proteomic analysis revealed the significance of inflammation and oxidative stress, we sought to investigate whether such processes were altered in the chemoresistant group.

Figure 4 shows the prooxidant parameters. The carbonyl content (Figure 4(a)) was higher in the chemoresistant patients than in the responsive patients (79.24 ± 4.68 nM/mg total protein in the responsive group and 96.72 ± 5.27 nM/mg total protein in the chemoresistant group, $p = 0.0160$). No variations were found in the MDA levels (576.3 ± 38.15 nM in the responsive group and 600.4 ± 38.2 nM in the chemoresistant group, $p = 0.6456$, Figure 4(b)). NO levels (Figure 4(c)) were also augmented in the chemoresistant group compared with the responsive group ($18.59 \pm 1.19\,\mu$M in the responsive group and $24.15 \pm 2.0\,\mu$M in the chemoresistant group, $p = 0.0486$).

According to antioxidant profiling of the groups (Figure 5), the chemoresistant patients exhibited lower levels of TRAP (292.8 ± 29.6 nM trolox) than the responsive patients (380 ± 26.6 nM trolox, $p = 0.0314$, Figure 5(a)). No

Table 3: Representative biological processes related to proteins upregulated in chemoresistant breast cancer.

Cytoskeleton remodeling/cell adhesion
Collagen alpha-1(XII) chain, fibronectin, keratin type I cytoskeletal 10, myosin 7, Rho GTPase-activating protein 35, vitronectin
Blood coagulation
Alpha 1-antichymotrypsin, alpha 1-antitrypsin, alpha 2-macroglobulin, antithrombin III, kininogen-1, plasminogen, prothrombin
DNA repair/kinetochore assembly
Centromere/kinetochore protein zw10 homolog, DnaJ homolog subfamily C member 10, LINE-1 type transposase domain-containing protein 1
Oxidative metabolism
Acetyl-CoA carboxylase 1; activator of 90 kDa heat shock protein ATPase homolog 2; acylpyruvase FAHD1, mitochondrial; afamin; alpha 1B-glycoprotein; alpha 2 HS glycoprotein; angiotensinogen; apolipoprotein E; ceruloplasmin; clusterin; dynein heavy chain 10, axonemal; dynein heavy chain 3, axonemal; exocyst complex component 1; haptoglobin; haptoglobin-related protein; hemoglobin subunit alpha; hemoglobin subunit beta; hemopexin; inositol hexakisphosphate and diphosphoinositol-pentakisphosphate kinase 2; kinectin; nuclear pore complex protein Nup205; nuclear receptor corepressor 2; polypeptide N-acetylgalactosaminyltransferase 3; pregnancy zone protein; prolyl 4 hydroxylase subunit alpha-3; regulator of nonsense transcripts 2; ribose phosphate pyrophosphokinase 3; rod cGMP-specific $3'$,$5'$-cyclic phosphodiesterase subunit alpha; sarcoplasmic/endoplasmic reticulum calcium ATPase 3; serine/threonine protein kinase WNK2; serine/threonine protein phosphatase 2A, 55 kDa regulatory subunit B alpha isoform; serotransferrin; serum albumin; serum amyloid A-4 protein; serum amyloid P component; synembryn-B; transcriptional repressor p66-alpha; vitamin D-binding protein
Immune response_inflammation
Alpha-1 acid glycoprotein 1, alpha-1 acid glycoprotein 2, apolipoprotein A-I, apolipoprotein A-II, apolipoprotein B-100, C-reactive protein, inter-alpha-trypsin inhibitor heavy chain H1, inter-alpha-trypsin inhibitor heavy chain H2, inter-alpha-trypsin inhibitor heavy chain H4, lumican, son of sevenless homolog 1, transcription factor 4
Immune response_humoral immune response
Ig alpha-1 chain C region, Ig gamma-1 chain C region, Ig gamma-2 chain C region, Ig gamma-3 chain C region, Ig gamma-4 chain C region, Ig heavy chain VI region V35, Ig heavy chain V-II region ARH 77, Ig heavy chain V-III region GAL, Ig heavy chain V-III region TIL, Ig kappa chain C region, Ig kappa chain VI region AU, Ig kappa chain VI region EU, Ig kappa chain VI region Gal, Ig kappa chain VI region Rei, Ig kappa chain V-II region TEW, Ig kappa chain V-III region GOL, Ig kappa chain V-III region NG9 (fragment), Ig kappa chain V-III region SIE, Ig kappa chain V-III region Ti, Ig kappa chain V-III region VG (fragment), Ig lambda-1 chain C regions, Ig lambda-2 chain C regions, Ig lambda-3 chain C regions, Ig mu chain C region, immunoglobulin lambda such as polypeptide 5
Immune response_complement system
C4b-binding protein alpha chain, complement C1q subcomponent subunit B, complement C1q subcomponent subunit C, complement C3, complement C4A, Complement C5, complement component C7, complement factor B, complement factor H, plasma protease C1 inhibitor

Table 4: Representative biological processes related to downregulated proteins in breast cancer chemoresistance.

Cytoskeleton remodeling/cell adhesion
Collagen alpha-1(VII) chain; GRB2-associated-binding protein 1; integrin alpha V; keratin type II cytoskeletal 1; myosin regulatory light chain 2, skeletal muscle isoform; plectin
Blood coagulation
Fibrinogen alpha chain, fibrinogen beta chain
DNA repair/kinetochore assembly
Centromere protein F, centrosome-associated protein 350, DNA polymerase alpha catalytic subunit, microtubule-associated protein 1B, centrosomal protein of 290 kDa
Oxidative metabolism
ATPase family AAA domain-containing protein 3B; dynein heavy chain 1, axonemal; E3 ubiquitin protein ligase UBR5; ectonucleotide pyrophosphatase phosphodiesterase family member 1; glycogen phosphorylase, liver form; inorganic pyrophosphatase; sodium bicarbonate cotransporter 3; TBC1 domain family member 2A; tripeptidyl peptidase 2
Immune response_inflammation
Apolipoprotein C-II, RAC-gamma serine/threonine-protein kinase, regulator of G protein signaling 14
Immune response_humoral immune response
Ig heavy chain V-III region JON, Ig heavy chain V-III region VH26, Ig kappa chain VI region Roy, Ig lambda chain VI region WAH, Ig lambda chain V-VI region SUT, Ig mu heavy chain disease protein
Immune response_complement system
Complement C4B, complement component C8 gamma chain

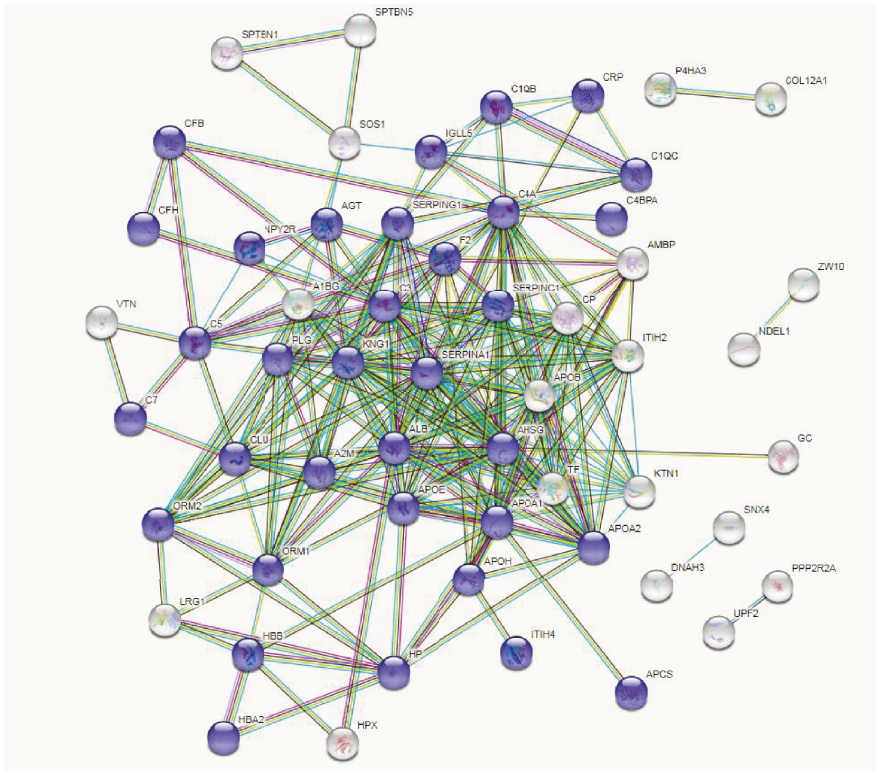

(a)

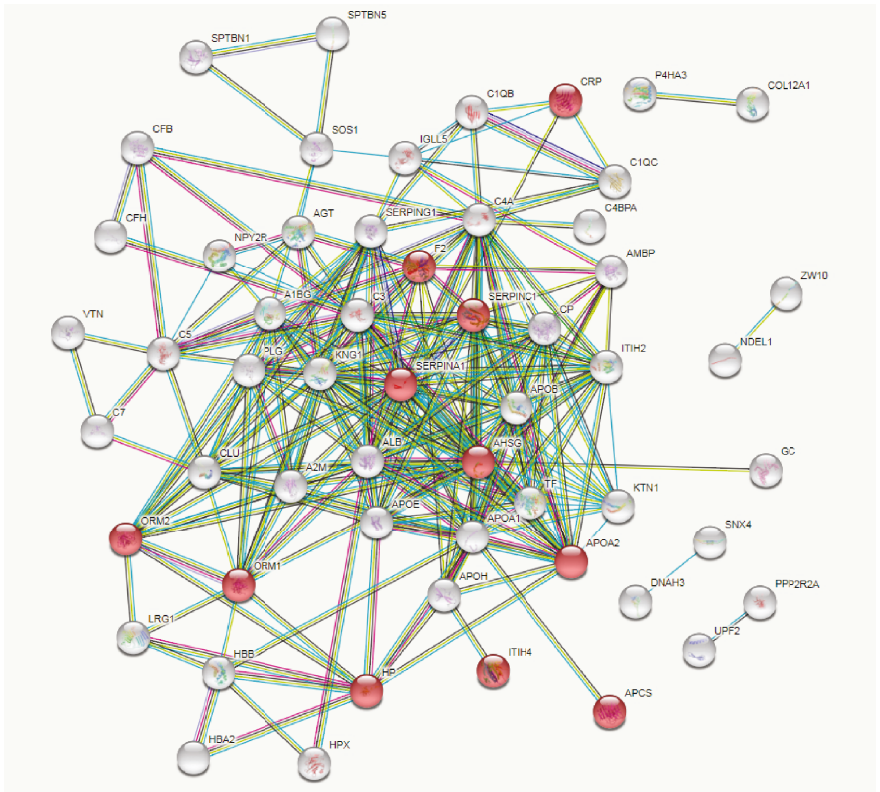

(b)

Figure 2: Continued.

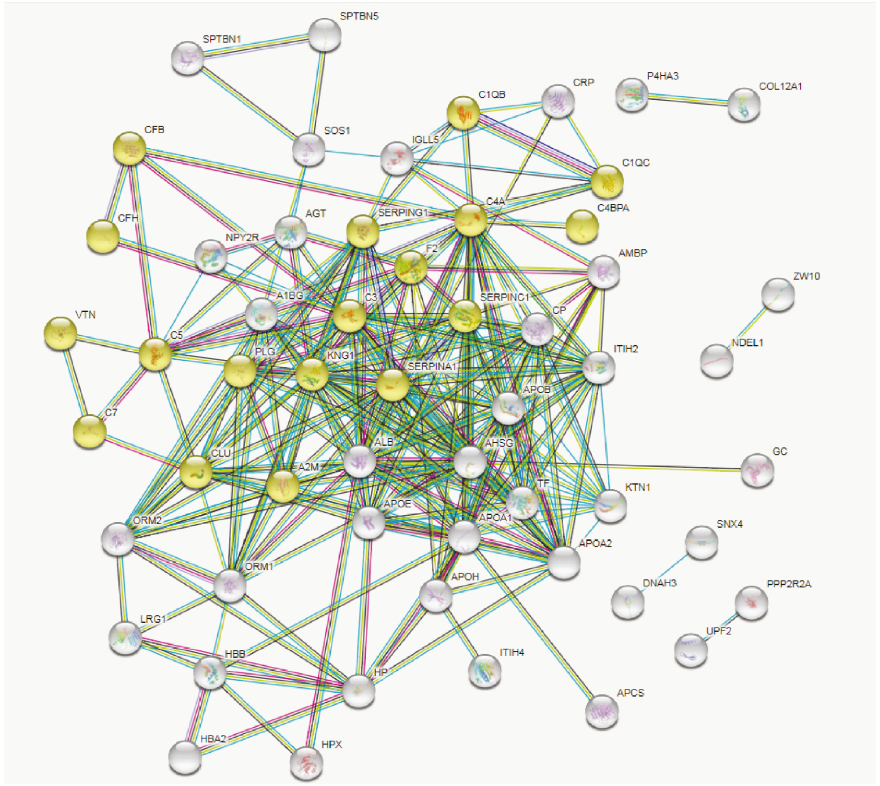

(c)

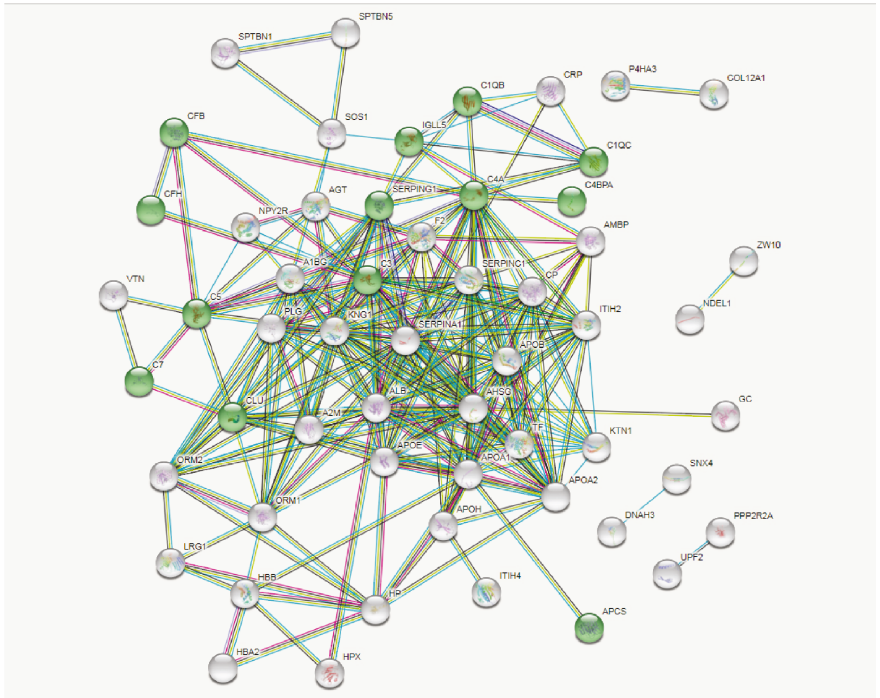

(d)

Figure 2: Network of interactions among the upregulated proteins in chemoresistant breast cancer identified by STRING software. (a) Proteins identified in the representative "response to oxidative stress" network are in blue. (b) Proteins identified in the representative "acute inflammatory response" network are in red. (c) Proteins identified in the representative "complement and coagulation cascades" network are in yellow. (d) Proteins identified in the representative "innate immune system" network are in green. The networks were generated with high interaction score > 0.9.

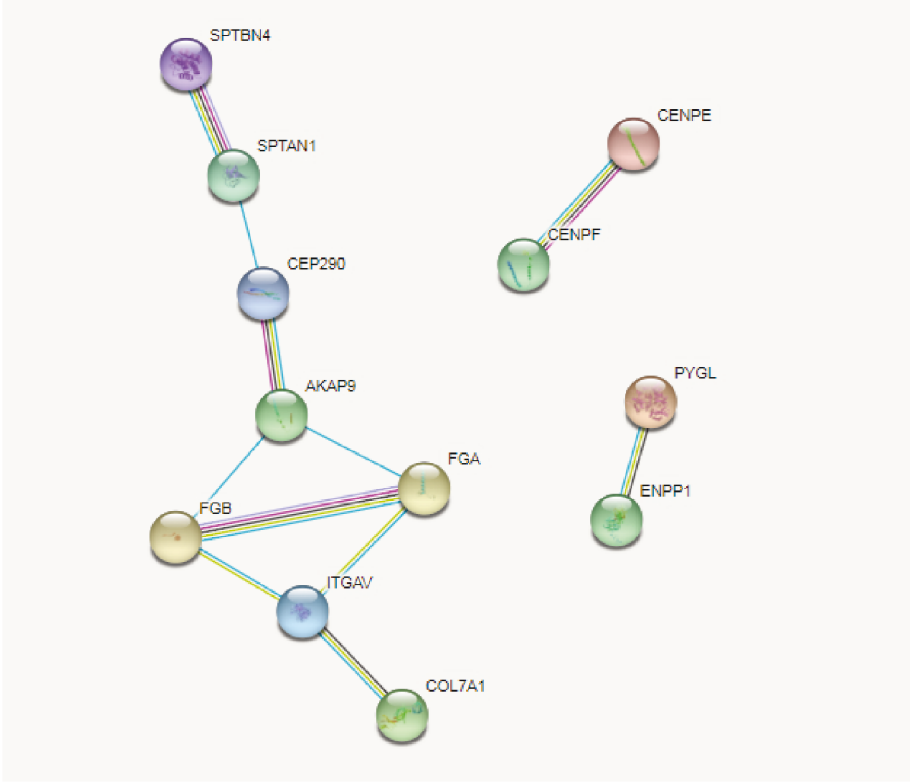

Figure 3: Network of interactions among the downregulated proteins in chemoresistant breast cancer identified by STRING software. Proteins were clustered according to the main representative networks identified. The networks were generated with high interaction score > 0.9.

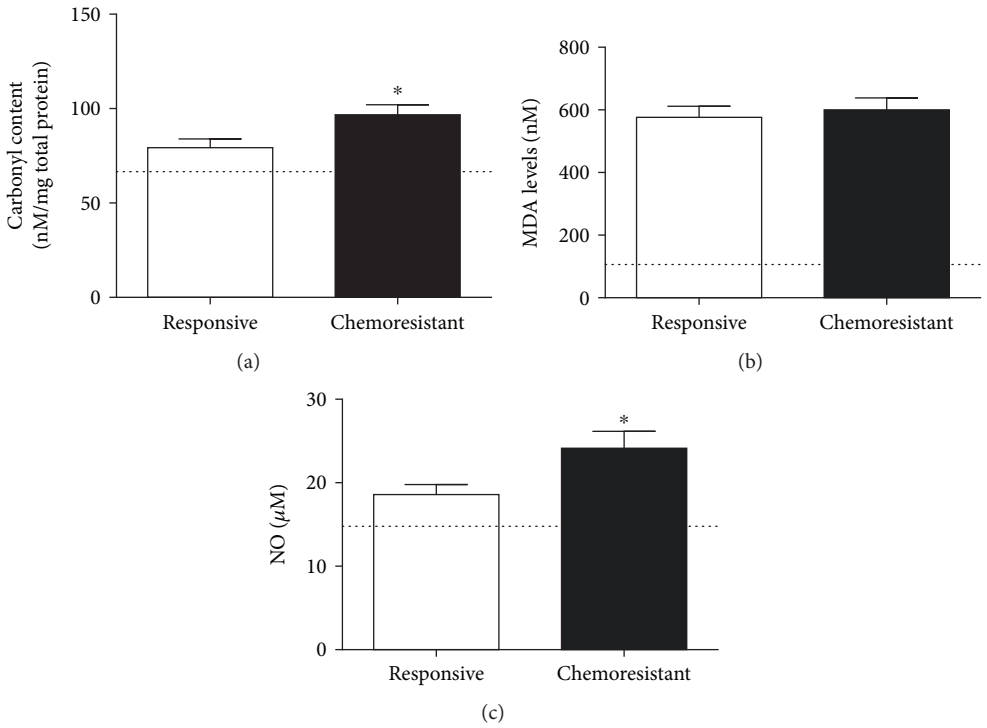

Figure 4: Prooxidant parameters in plasma samples from responsive and chemoresistant patients. Carbonyl content (a), malondialdehyde levels (MDA, (b)) and nitric oxide content (NO, (c)) were measured to determine the prooxidant profile of both groups. * indicates a significant difference ($p < 0.05$). The line illustrates the mean levels of each parameter as determined in healthy controls.

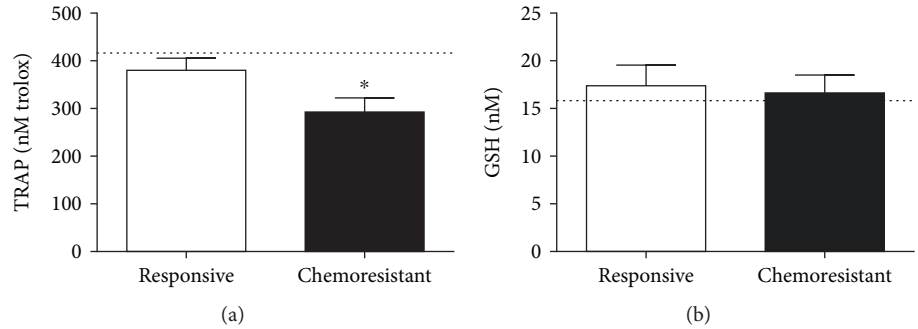

Figure 5: Antioxidant profiling of plasma samples from responsive and chemoresistant patients. The total radical antioxidant parameter (TRAP, (a)) and reduced glutathione (GSH, (b)) levels were measured to determine the antioxidant profile of both groups. * indicates a significant difference ($p < 0.05$). The line illustrates the mean levels of each parameter as determined in healthy controls.

differences were detected in GSH levels between the two groups ($17.4 \pm 2.16\,\mu$M in the responsive group and $16.7 \pm 1.9\,\mu$M in the chemoresistant group, $p = 0.7918$, Figure 5(b)).

Cytokine measurement (Figure 6) revealed that the chemoresistant patients presented higher levels of IL-10 (20.23 ± 4.8 pg/mL and 47.06 ± 13.5 pg/mL, respectively, $p = 0.0439$, Figure 6(a)), TGF-β1 (15.18 ± 2.2 pg/mL and 28.71 ± 5.7 pg/mL, respectively, $p = 0.025$, Figure 6(b)), and TNF-α (21.9 ± 7.6 pg/mL and 25 ± 5.8 pg/mL, respectively, $p = 0.0414$, Figure 6(c)) than the responsive patients. No differences were observed in the IL-12 levels between the two groups (34.5 ± 2.6 pg/mL in the responsive group and 30.23 ± 0.67 pg/mL in the chemoresistant group, $p = 0.41$, Figure 6(d)).

For reference, we included healthy control levels for each parameter, represented as a line in the graphs, and the means were 67.2 nM/mg total proteins for carbonyl content (Figure 4(a)), 106 nM for MDA (Figure 4(b)), 14.6 μM for NO (Figure 4(c)), 416 nM trolox for TRAP (Figure 5(a)), 15.6 nM for GSH (Figure 5(b)), 23 pg/mL for IL-10 (Figure 6(a)), 9.1 pg/mL for TGF-β1 (Figure 6(b)), 10.6 pg/mL for TNF-α (Figure 6(c)), and 31.9 pg/mL for IL-12 (Figure 6(d)).

In spite of one of the aims of the present study was to understand comparatively the differential redox profile between responsive and resistant patients, it can be noted that both groups exhibited different levels for all oxidative stress parameters when compared to the baseline of healthy controls. Moreover, chemoresistant patients presented important differences if compared to either responsive or healthy women.

4. Discussion

The main aspects associated with the high mortality rates of breast cancer are related to advanced stages of disease at diagnosis, the limited efficacy of treatment and resistance towards chemotherapy. Chemoresistance poses as one of the major challenges in breast cancer treatment [13], and its underlying molecular mechanisms remain unclear.

In the present study, we investigated the chemoresistance mechanisms in women with breast cancer carrying luminal A breast cancer by using the label-free proteomic approach. This strategy allows mapping the differential changes when comparing groups with distinct responses and indicates putative targets to further investigate and validate.

The main chemotherapy schedule used to treat the patients enrolled in this study was the combined paclitaxel/-doxorubicin protocol, largely employed as the first line of treatment for luminal breast cancer worldwide. Beyond its main mechanism of action on cell microtubules [4], paclitaxel is known by generating oxidative stress and promoting changes in inflammatory mediator patterns [5, 6]. In the same way, doxorubicin acts as a DNA replication disruptor and gives rise to free radicals that results in DNA damage and cell death [7]. Despite these mechanism of actions, some tumors possess adaptative mechanisms that allow cell surviving and chemoresistance development.

A large number of chemoresistance studies are based on cell lines, which does not replicate the complexity of the human body. Thus, to the best of our knowledge, this is the first in-depth proteomic study that exploits the differential profiling of circulating proteins in breast cancer patients that undergo chemoresistance. It is important to highlight that all included patients had their samples collected at diagnosis, prior to any therapeutic intervention, and were categorized as responsive or resistant of the chemotherapeutic treatment. The data presented here indicate that it is possible to distinguish the systemic profile of patients still at diagnosis, when clinicians do not know if the patient will respond or not to the treatment. The initial goal of the present study was to determine the differences between the circulating proteomic profiles of chemoresistant and chemosensitive breast cancer patients. Furthermore, the identification of relevant biological processes and signaling networks shows that most of the upregulated proteins clustered into network connections, related to inflammation, redox signaling, and immune responses. Thus, we decided to further validate such pathways by measuring some proteins and metabolites resulting from the inflammatory axis and investigate if such targets correlated with the chemoresistant phenotype in breast cancer patients diagnosed with luminal A breast cancer.

The luminal A phenotype is known as the tumor with the best prognosis in breast cancer. In spite of this, some patients may progress as nonresponsive to treatment, and the reasons why this phenomenon occurs are not clear yet.

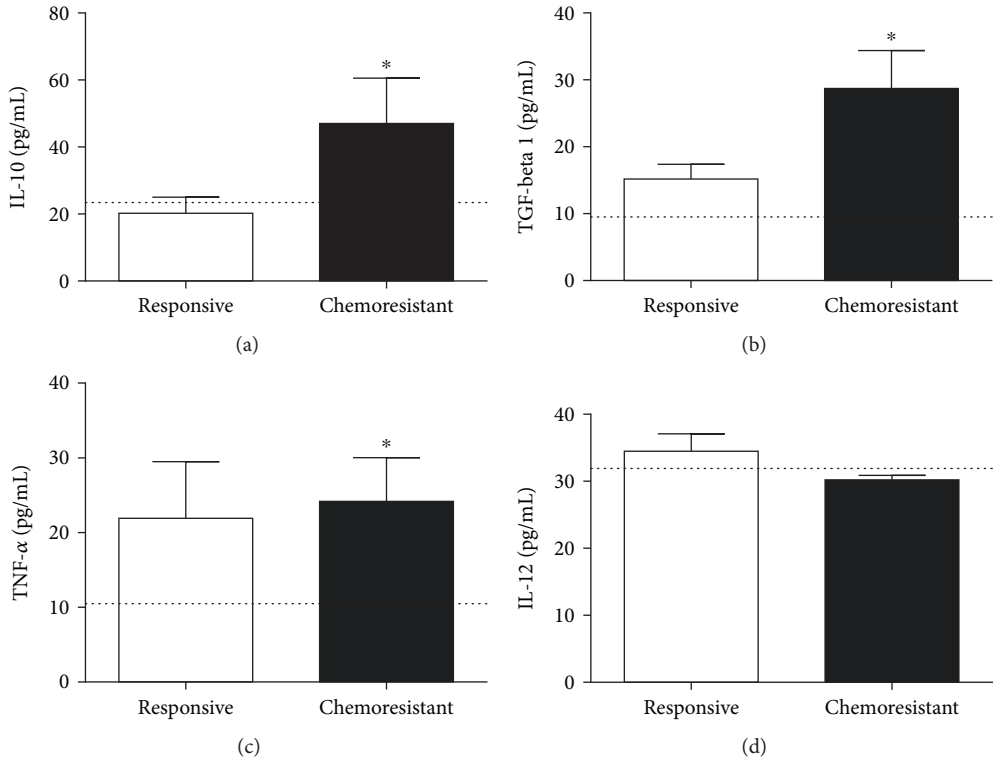

Figure 6: Cytokine profiling. The circulating levels of IL-10 (a), TGF-β1 (b), TNF-α (c), and IL-12 (d) were evaluated in both the responsive and resistant groups. * indicates statistical significance ($p < 0.05$). The line illustrates the mean levels of each parameter as determined in healthy controls.

A recent study from Zhang and colleagues reported some similarities with proteins found in our study. The authors compared plasma samples from ovarian cancer patients who were chemosensitive or chemoresistant by using a proteomic approach [32]. In accordance with our findings, the study found the upregulation of complement C4A, clusterin, and alpha 1-antitrypsin in the chemoresistant patients. These data suggest that some circulating proteins may be common players of chemoresistance, independent on the type of cancer.

In relation to the key processes identified in the present study, a body of evidence has shown the contribution of oxidative stress-related events to the physiopathology of breast cancer, including changes according to disease staging, types of treatment, and disease subtypes [11, 16, 19]. In the context of chemoresistance, the levels of antioxidants such as glutathione (GSH) play an essential role in the induction of chemoresistance. Reduced levels of GSH have been reported to enhance cellular sensitivity to anticancer-induced apoptosis. In contrast, elevated levels of antioxidant agents may confer resistance to drug-induced ROS [33]. Some abundant proteins identified here in the chemoresistant group, as albumin, ceruloplasmin, hemopexin, haptoglobins, and serotransferrin, play an important antioxidant role in plasma by sequestering iron ions [34]. Iron is a potent generator of oxidative stress, since it is a catalyst of Fenton's reaction that generates significant amounts of free radicals.

Several ROS and RNS can modulate signaling pathways that enhance the proinflammatory profile. Inflammatory cells liberate reactive species at the site of inflammation, as well as induce systemic changes in immune responses that lead to excessive oxidative stress [35]. Dysregulated inflammation is commonly associated with tissue damage, since in the inflammatory milieu, activated cells release proteases, reactive species, and chemical mediators (cytokines, chemokines, and complement components) [34]. As inflammation and oxidative stress can induce each other, a continuous, vicious cycle is commonly observed.

In the present study, oxidative stress analysis showed that the chemoresistant patients presented higher levels of carbonyls in association with augmented NO as well as impaired antioxidants. This scenario clearly indicates that these patients are more oxidatively/nitrosatively stressed than the responsive patients.

In recent years, redox signaling has been identified as a pivotal phenomenon in chemoresistance. In breast cancer, overexpression of the master regulator of redox homeostasis, NF-E2-related transcription factor 2 (Nrf2), in tumor cells was clearly implicated as a central mechanism of acquired chemoresistance [36]. The ability of Nrf2 to regulate chemotherapy sensitivity in BC is reflective of the antioxidant response element- (ARE-) bearing gene products regulated by this transcription factor, which function in cytoprotective responses [37]. Thus, antioxidant defense is the result of the balance between ARE-encoded enzymes and nonenzymatic antioxidants. Our results show that chemoresistant patients presented reduced levels of total nonenzymatic antioxidants in their plasma compared with their levels in chemosensitive

patients. This fact may reflect both augmented systemic consumption and the demands of the tumor.

Carbonylation is a marker of the systemic oxidation of proteins [38] and plays a role in cell signaling [39]. Antioxidant consumption in the presence of protein carbonylation is expected in resistant cancer cells, and nitrosative stress participates in the generation of such products [40]. In the presence of inflammation, NO can react with superoxide anions from the mitochondria, yielding the most powerful reactive species, peroxynitrite [41]. The augmentation of NO in chemoresistant patients compared with chemosensitive patients suggests the activation of nitrosative stress in chemoresistant patients.

NO is a pleiotropic molecule with multiple functions and a dual role in redox and immune responses. Although NO is a classical tumoricidal molecule, altered NO homeostasis is related to chemoresistance [42, 43], and this mechanism seems to involve the protective effects of tumor-associated macrophages (TAMs) against proapoptotic events [44].

The cytokine panel from chemoresistant patients revealed here represents the sum of systemic cytokine balance. Tumors, and even immune cells, are constantly stimulated to produce and secrete such cytokines in cancer, albeit in a disordered manner. Our data show that chemoresistant patients simultaneously exhibit significantly higher levels of IL-10, TGF-β1, and TNF-α than chemosensitive patients, which contradicts the classical concept of an equilibrium between Th1/Th2 cytokines.

During immune responses, TNF-α is initially produced to fight cancer cells. However, when immune cells infiltrate the tumor mass, this activity inverts, and the production of TNF-α benefits to the tumor progression [45]. This controversial behavior of TNF-α also suggests a role for this molecule in the acquisition of chemoresistance. ER-positive breast cancer cells that resist TNF-α-induced death are associated with a multidrug-resistant phenotype by epithelial-mesenchymal transition- (EMT-) driven mechanisms [46]. Furthermore, circulating TGF-β1 was also increased in chemoresistant patients compared with chemosensitive patients. In breast cancer, TGF-β1 antagonizes ER-α signaling by inducing EMT and chemoresistance [47]. Similarly, IL-10 produced by TAMs can induce breast cancer chemoresistance [48]. Collectively, these findings support the hypothesis that the sustained circulation of TNF-α, TGF-β1, and Il-10 observed here constitute a putative synergistic mechanism of chemoresistance induction and maintenance, in addition to strongly supporting the perpetuation of oxidative stress [11, 49].

Although inflammation and oxidative stress dominate the chemoresistant signature presented in our study, the complement system might be responsible for their connection. In recent years, the paradigm regarding the role of complement proteins in the context of cancer has been broken. Some studies found that these proteins may be associated with ovarian and BC progression. However, the mechanism of this has not yet been described [50, 51].

Dysregulation of the complement system leads to autologous damage, and the complement system has been implicated in the pathogenesis of a wide spectrum of diseases [50, 51]. We observed the upregulation of several complement proteins in chemoresistant samples compared with chemosensitive samples, including members of the classical (C1q, C4, and C4b) and alternative (C3, factor H) pathways and the C5 effector.

Complement C3 is a key complement protein. The deposition of C3 and C3b on the endothelium increased oxidative stress in retinal vessels [17]. Bonavita and colleagues reported that C3-deficient mice were protected against carcinogen-induced cancer because of reduced inflammation [52]. C5 also plays a central role in the complement cascade. Beyond forming the terminal complement complex, called the membrane-attack complex (MAC, C5b-9), C5 has been reported to play an essential proinflammatory role [53]. Conversely, C1 inhibitor (SERPING1) was upregulated in chemoresistant samples compared with chemosensitive samples, showing a balance between induction and repression of the complement cascade. This inhibitor forms stable complexes with C1 subunits, which results in the repression of classical complement pathways. In addition, SERPING1 inhibits the inflammation, clotting, and kinin pathways [54]. Complement factor H, an essential regulator of the alternative pathway, was also upregulated in chemoresistant samples compared with chemosensitive samples. *In vitro* studies showed decreased levels of this factor in oxidative stress conditions [17]. The interplay between the complement system and oxidative stress has been extensively investigated in age-related macular degeneration [17]. Thurman and colleagues demonstrated that cells exposed to oxidant stress from hydrogen peroxide exhibited decreased levels of complement inhibitors and increased the VEGF expression compared with control cells [55].

Defense mechanisms to avoid MAC (C5b-9 complex) accumulation include the action of vitronectin and clusterin, which were upregulated in the chemoresistant group. Vitronectin and clusterin play critical roles in cell aggregation, complement inhibition, immune signaling regulation, and tissue repair. Together with angiotensin, they may connect oxidative stress to the complement cascade and inflammatory signaling.

Recent findings have suggested that C3, C4, and C5 may aid the survival of tumors through immunosuppression. Other evidence has suggested that complement proteins induce the production of TNF-α [56] and TGF-β [57, 58] in pathological processes such as cancer. Additionally, complement proteins cooperate with extracellular matrix (ECM) remodeling through the degradation of collagens and gelatins and by activating matrix metalloproteinases (MMPs) [50, 51].

5. Conclusion

In summary, the connection among inflammation, the complement system, and oxidative stress described in our study seems to be a pivotal axis in chemoresistance of luminal A breast cancer subtype. These findings will have significant clinical implications for improving BC chemoresistance. Hence, further studies are necessary to determine the main triggers of those signaling pathways in the context of breast

cancer. Finally, studies to select molecules that simultaneously inhibit the oxidative and inflammatory pathways are indicated to bypass this chemoresistance in the future.

Data Availability

The high-throughput proteome data used to support the findings of this study are included within the supplementary information files.

Conflicts of Interest

The authors declare that there is no conflict of interest regarding the publication of this paper.

Authors' Contributions

Bruno R. B. Pires and Carolina Panis contributed equally to this work.

Acknowledgments

The authors are grateful to Dr. Everton Cruz dos Santos and Dr. Gerson Moura Ferreira for their relevant suggestions. This work was supported by grants from the Conselho Nacional de Desenvolvimento Científico e Tecnológico (CNPq), Ministério da Saúde (MS), Institutos Nacionais de Ciência e Tecnologia para o Controle do Câncer (INCT-CANCER), Fundação de Amparo à Pesquisa do Estado do Rio de Janeiro (FAPERJ), Fundação Araucária, and Programa Pesquisa Para o SUS (PPSUS).

Supplementary Materials

Supplementary Figure 1: interaction networks among the altered proteins in chemoresistant breast cancer identified by Ingenuity Pathway Analysis (IPA) software. Red arrows indicate upregulated proteins and green arrows indicate downregulated proteins in our data. Supplementary Figure 2: histogram from the top canonical pathways among the altered proteins in chemoresistant breast cancer generated using Ingenuity Pathway Analysis (IPA) software. p value is indicated on the left side of the histogram. Supplementary Figure 3: in silico analysis obtained with Ingenuity Pathway Analysis (IPA) software showed upregulated proteins in the chemoresistant breast cancer group identified in the complement system cascade pathway. Pink-shaded proteins were upregulated in chemoresistant patients. Supplementary Figure 4: Supplementary Figure Y: coagulation system pathway identified with Ingenuity Pathway Analysis (IPA) software. Shaded notes represented altered proteins presented in chemoresistant breast cancer. Pink-shaded objects indicate upregulated proteins, and green-shaded objects indicate downregulated proteins. Supplementary Figure 5: production of nitric oxide and reactive oxygen species signaling pathway identified using Ingenuity Pathway Analysis (IPA) software. Pink-shaded target indicates upregulated proteins and green-shaded target indicates downregulated proteins presented in chemoresistant breast cancer. Supplementary Figure 6: actin cytoskeleton signaling pathway identified using Ingenuity Pathway Analysis (IPA) software. Pink-shaded target indicates upregulated proteins and green-shaded target indicates downregulated proteins presented in chemoresistant breast cancer. *(Supplementary Materials)*

References

[1] R. L. Siegel, K. D. Miller, and A. Jemal, "Cancer statistics, 2019," *CA: A Cancer Journal for Clinicians*, vol. 69, no. 1, pp. 7–34, 2019.

[2] K. Polyak and O. Metzger Filho, "SnapShot: breast cancer," *Cancer Cell*, vol. 22, no. 4, pp. 562–562.e1, 2012.

[3] L. N. Abdullah and E. K.-H. Chow, "Mechanisms of chemoresistance in cancer stem cells," *Clinical and Translational Medicine*, vol. 2, no. 1, p. 3, 2013.

[4] R. Yusuf, Z. Duan, D. Lamendola, R. Penson, and M. Seiden, "Paclitaxel resistance: molecular mechanisms and pharmacologic manipulation," *Current Cancer Drug Targets*, vol. 3, no. 1, pp. 1–19, 2003.

[5] C. Panis, R. Binato, S. Correa et al., "Short infusion of paclitaxel imbalances plasmatic lipid metabolism and correlates with cardiac markers of acute damage in patients with breast cancer," *Cancer Chemotherapy and Pharmacology*, vol. 80, no. 3, pp. 469–478, 2017.

[6] B. Ramanathan, K. Y. Jan, C. H. Chen, T. C. Hour, H. J. Yu, and Y. S. Pu, "Resistance to paclitaxel is proportional to cellular total antioxidant capacity," *Cancer Research*, vol. 65, no. 18, pp. 8455–8460, 2005.

[7] C. F. Thorn, C. Oshiro, S. Marsh et al., "Doxorubicin pathways: pharmacodynamics and adverse effects," *Pharmacogenetics and Genomics*, vol. 21, no. 7, pp. 440–446, 2011.

[8] A. Acharya, I. Das, D. Chandhok, and T. Saha, "Redox regulation in cancer: a double-edged sword with therapeutic potential," *Oxidative Medicine and Cellular Longevity*, vol. 3, no. 1, 34 pages, 2010.

[9] G. Housman, S. Byler, S. Heerboth et al., "Drug resistance in cancer: an overview," *Cancers*, vol. 6, no. 3, pp. 1769–1792, 2014.

[10] P. C. Marinello, K. L. Machado, R. Cecchini, and A. L. Cecchini, "The participation of oxidative stress in breast cancer cells progression and treatment resistance," *American Journal of Immunology*, vol. 10, no. 4, pp. 207–214, 2014.

[11] C. Panis, V. J. Victorino, A. C. S. A. Herrera et al., "Can breast tumors affect the oxidative status of the surrounding environment? A comparative analysis among cancerous breast, mammary adjacent tissue, and plasma," *Oxidative Medicine and Cellular Longevity*, vol. 2016, Article ID 6429812, 9 pages, 2016.

[12] H.-C. Zheng, "The molecular mechanisms of chemoresistance in cancers," *Oncotarget*, vol. 8, no. 35, pp. 59950–59964, 2017.

[13] D. Longley and P. Johnston, "Molecular mechanisms of drug resistance," *The Journal of Pathology*, vol. 205, no. 2, pp. 275–292, 2005.

[14] E.-K. Y. Breuer and M. M. Murph, "The role of proteomics in the diagnosis and treatment of women's cancers: current trends in technology and future opportunities," *International Journal of Proteomics*, vol. 2011, Article ID 373584, 17 pages, 2011.

[15] C. Panis, L. Pizzatti, and E. Abdelhay, "How can proteomics reach cancer biomarkers?," *Current Proteomics*, vol. 10, no. 2, pp. 136–149, 2013.

[16] C. Panis, L. Pizzatti, A. C. Herrera, R. Cecchini, and E. Abdelhay, "Putative circulating markers of the early and advanced stages of breast cancer identified by high-resolution label-free proteomics," *Cancer Letters*, vol. 330, no. 1, pp. 57–66, 2013.

[17] S. Khandhadia, V. Cipriani, J. R. W. Yates, and A. J. Lotery, "Age-related macular degeneration and the complement system," *Immunobiology*, vol. 217, no. 2, pp. 127–146, 2012.

[18] S. J. Mandrekar, M. W. An, J. Meyers, A. Grothey, J. Bogaerts, and D. J. Sargent, "Evaluation of alternate categorical tumor metrics and cut points for response categorization using the RECIST 1.1 data warehouse," *Journal of Clinical Oncology*, vol. 32, no. 8, pp. 841–850, 2014.

[19] C. Panis, L. Pizzatti, A. C. Herrera, S. Correa, R. Binato, and E. Abdelhay, "Label-free proteomic analysis of breast cancer molecular subtypes," *Journal of Proteome Research*, vol. 13, no. 11, pp. 4752–4772, 2014.

[20] F. Mbeunkui and M. B. Goshe, "Investigation of solubilization and digestion methods for microsomal membrane proteome analysis using data-independent LC-MS^E," *Proteomics*, vol. 11, no. 5, pp. 898–911, 2011.

[21] D. Szklarczyk, A. Franceschini, S. Wyder et al., "STRING v10: protein–protein interaction networks, integrated over the tree of life," *Nucleic Acids Research*, vol. 43, no. D1, pp. D447–D452, 2015.

[22] H. Mi, A. Muruganujan, J. T. Casagrande, and P. D. Thomas, "Large-scale gene function analysis with the PANTHER classification system," *Nature Protocols*, vol. 8, no. 8, pp. 1551–1566, 2013.

[23] M. Kanehisa, M. Furumichi, M. Tanabe, Y. Sato, and K. Morishima, "KEGG: new perspectives on genomes, pathways, diseases and drugs," *Nucleic Acids Research*, vol. 45, no. D1, pp. D353–D361, 2017.

[24] A. Kramer, J. Green, J. Pollard Jr., and S. Tugendreich, "Causal analysis approaches in ingenuity pathway analysis," *Bioinformatics*, vol. 30, no. 4, pp. 523–530, 2014.

[25] R. L. Levine, D. Garland, C. N. Oliver et al., "[49] Determination of carbonyl content in oxidatively modified proteins," *Methods in Enzymology*, vol. 186, pp. 464–478, 1990.

[26] A. C. S. Herrera, V. J. Victorino, F. C. Campos et al., "Impact of tumor removal on the systemic oxidative profile of patients with breast cancer discloses lipid peroxidation at diagnosis as a putative marker of disease recurrence," *Clinical Breast Cancer*, vol. 14, no. 6, pp. 451–459, 2014.

[27] O. H. Lowry, N. J. Rosebrough, A. L. Farr, and R. J. Randall, "Protein measurement with the Folin phenol reagent," *The Journal of Biological Chemistry*, vol. 193, no. 1, pp. 265–275, 1951.

[28] V. J. Victorino, C. Panis, F. C. Campos et al., "Decreased oxidant profile and increased antioxidant capacity in naturally postmenopausal women," *Age*, vol. 35, no. 4, pp. 1411–1421, 2013.

[29] A. C. S. A. Herrera, C. Panis, V. J. Victorino et al., "Molecular subtype is determinant on inflammatory status and immunological profile from invasive breast cancer patients," *Cancer Immunology, Immunotherapy*, vol. 61, no. 11, pp. 2193–2201, 2012.

[30] M. Repetto, C. Reides, M. L. Gomez Carretero, M. Costa, G. Griemberg, and S. Llesuy, "Oxidative stress in blood of HIV infected patients," *Clinica Chimica Acta*, vol. 255, no. 2, pp. 107–117, 1996.

[31] J. Sedlak and R. H. Lindsay, "Estimation of total, protein-bound, and nonprotein sulfhydryl groups in tissue with Ellman's reagent," *Analytical Biochemistry*, vol. 25, no. 1, pp. 192–205, 1968.

[32] Z. Zhang, K. Qin, W. Zhang et al., "Postoperative recurrence of epithelial ovarian cancer patients and chemoresistance related protein analyses," *Journal of Ovarian Research*, vol. 12, no. 1, p. 29, 2019.

[33] A. Cort, T. Ozben, L. Saso, C. De Luca, and L. Korkina, "Redox control of multidrug resistance and its possible modulation by antioxidants," *Oxidative Medicine and Cellular Longevity*, vol. 2016, Article ID 4251912, 17 pages, 2016.

[34] S. K. Biswas, "Does the interdependence between oxidative stress and inflammation explain the antioxidant paradox?," *Oxidative Medicine and Cellular Longevity*, vol. 2016, Article ID 5698931, 9 pages, 2016.

[35] P. L. de Sa Junior, D. A. D. Camara, A. S. Porcacchia et al., "The roles of ROS in cancer heterogeneity and therapy," *Oxidative Medicine and Cellular Longevity*, vol. 2017, Article ID 2467940, 12 pages, 2017.

[36] T. Wu, B. G. Harder, P. K. Wong, J. E. Lang, and D. D. Zhang, "Oxidative stress, mammospheres and Nrf2–new implication for breast cancer therapy?," *Molecular Carcinogenesis*, vol. 54, no. 11, pp. 1494–1502, 2015.

[37] A. Raghunath, K. Sundarraj, R. Nagarajan et al., "Antioxidant response elements: discovery, classes, regulation and potential applications," *Redox Biology*, vol. 17, pp. 297–314, 2018.

[38] Y. J. Suzuki, M. Carini, and D. A. Butterfield, "Protein carbonylation," *Antioxidants & Redox Signaling*, vol. 12, no. 3, pp. 323–325, 2010.

[39] C. M. Wong, L. Marcocci, L. Liu, and Y. J. Suzuki, "Cell signaling by protein carbonylation and decarbonylation," *Antioxidants & Redox Signaling*, vol. 12, no. 3, pp. 393–404, 2010.

[40] A. Singh, M. Bodas, N. Wakabayashi, F. Bunz, and S. Biswal, "Gain of Nrf2 function in non-small-cell lung cancer cells confers radioresistance," *Antioxidants & Redox Signaling*, vol. 13, no. 11, pp. 1627–1637, 2010.

[41] R. Radi, "Oxygen radicals, nitric oxide, and peroxynitrite: redox pathways in molecular medicine," *Proceedings of the National Academy of Sciences of the United States of America*, vol. 115, no. 23, pp. 5839–5848, 2018.

[42] A. Porro, C. Chrochemore, F. Cambuli, N. Iraci, A. Contestabile, and G. Perini, "Nitric oxide control of MYCN expression and multi drug resistance genes in tumours of neural origin," *Current Pharmaceutical Design*, vol. 16, no. 4, pp. 431–439, 2010.

[43] B. Salimian Rizi, C. Caneba, A. Nowicka et al., "Nitric oxide mediates metabolic coupling of omentum-derived adipose stroma to ovarian and endometrial cancer cells," *Cancer Research*, vol. 75, no. 2, pp. 456–471, 2015.

[44] C. Perrotta, D. Cervia, I. di Renzo et al., "Nitric oxide generated by tumor-associated macrophages is responsible for cancer resistance to cisplatin and correlated with syntaxin 4 and acid sphingomyelinase inhibition," *Frontiers in Immunology*, vol. 9, p. 1186, 2018.

[45] H. Wajant, "The role of TNF in cancer," in *Death Receptors and Cognate Ligands in Cancer*, pp. 1–15, Springer, 2009.

[46] J. W. Antoon, R. Lai, A. P. Struckhoff et al., "Altered death receptor signaling promotes epithelial-to-mesenchymal transition and acquired chemoresistance," *Scientific Reports*, vol. 2, no. 1, p. 539, 2012.

[47] M. Tian and W. P. Schiemann, "TGF-β stimulation of EMT programs elicits non-genomic ER-α activity and anti-estrogen resistance in breast cancer cells," *Journal of Cancer Metastasis and Treatment*, vol. 3, no. 8, p. 150, 2017.

[48] C. Yang, L. He, P. He et al., "Increased drug resistance in breast cancer by tumor-associated macrophages through IL-10/STAT3/bcl-2 signaling pathway," *Medical Oncology*, vol. 32, no. 2, p. 14, 2015.

[49] C. Panis, A. C. Herrera, V. J. Victorino, A. M. Aranome, and R. Cecchini, "Screening of circulating TGF-β levels and its clinicopathological significance in human breast cancer," *Anticancer Research*, vol. 33, no. 2, pp. 737–742, 2013.

[50] V. Afshar-Kharghan, "The role of the complement system in cancer," *The Journal of Clinical Investigation*, vol. 127, no. 3, pp. 780–789, 2017.

[51] M. J. Rutkowski, M. E. Sughrue, A. J. Kane, S. A. Mills, and A. T. Parsa, "Cancer and the complement cascade," *Molecular Cancer Research*, vol. 8, no. 11, pp. 1453–1465, 2010.

[52] E. Bonavita, S. Gentile, M. Rubino et al., "PTX3 is an extrinsic oncosuppressor regulating complement-dependent inflammation in cancer," *Cell*, vol. 160, no. 4, pp. 700–714, 2015.

[53] J. M. Skeie, J. H. Fingert, S. R. Russell, E. M. Stone, and R. F. Mullins, "Complement component C5a activates ICAM-1 expression on human choroidal endothelial cells," *Investigative Ophthalmology & Visual Science*, vol. 51, no. 10, pp. 5336–5342, 2010.

[54] A. E. Davis III, P. Mejia, and F. Lu, "Biological activities of C1 inhibitor," *Molecular Immunology*, vol. 45, no. 16, pp. 4057–4063, 2008.

[55] J. M. Thurman, B. Renner, K. Kunchithapautham et al., "Oxidative stress renders retinal pigment epithelial cells susceptible to complement-mediated injury," *Journal of Biological Chemistry*, vol. 284, no. 25, pp. 16939–16947, 2009.

[56] M. M. Markiewski, R. A. DeAngelis, C. W. Strey et al., "The regulation of liver cell survival by complement," *The Journal of Immunology*, vol. 182, no. 9, pp. 5412–5418, 2009.

[57] P. Boor, A. Konieczny, L. Villa et al., "Complement C5 mediates experimental tubulointerstitial fibrosis," *Journal of the American Society of Nephrology*, vol. 18, no. 5, pp. 1508–1515, 2007.

[58] R. Derynck, R. J. Akhurst, and A. Balmain, "TGF-β signaling in tumor suppression and cancer progression," *Nature Genetics*, vol. 29, no. 2, pp. 117–129, 2001.

Hindawi
Oxidative Medicine and Cellular Longevity
Volume 2019, Article ID 6315034, 9 pages
https://doi.org/10.1155/2019/6315034

Review Article

Neuroglobin: A Novel Player in the Oxidative Stress Response of Cancer Cells

Marco Fiocchetti, Virginia Solar Fernandez, Emiliano Montalesi, and Maria Marino

Department of Science, University Roma Tre, Viale Guglielmo Marconi 446, I-00146 Roma, Italy

Correspondence should be addressed to Maria Marino; maria.marino@uniroma3.it

Received 19 April 2019; Accepted 11 June 2019; Published 1 July 2019

Guest Editor: Jayeeta Ghose

Reactive oxygen species (ROS) result from intracellular aerobic metabolism and/or extracellular stimuli. Although endogenous antioxidant systems exquisitely balance ROS production, an excess of ROS production, commonly found in diverse human degenerative pathologies including cancer, gives rise to the oxidative stress. Increased oxidative stress in cancer is related to the sustained proliferation and metabolism of cancer cells. However, cancer cells show an intrinsic higher antioxidant capacity with respect to the normal counterpart as well as an ability to cope with oxidative stress-induced cell death by establishing mechanisms of adaptation, which define a selective advantage against the adverse oxidative stress environment. The identification of survival factors and adaptive pathways, set up by cancer cells against oxidative stress, provides multiple targets for the therapeutic intervention against cancer. Neuroglobin (NGB), a globin primarily described in neurons as an oxidative stress sensor and cytoprotective factor against redox imbalance, has been recently recognized as a novel tumor-associated protein. In this review, the involvement of NGB in the cancer cell adaptation and resistance to oxidative stress will be discussed highlighting the globin role in the regulation of both the stress-induced apoptotic pathway and antioxidant systems activated by cancer cells.

1. Introduction

Reactive oxygen species (ROS), including superoxide anion (O_2^-), hydrogen peroxide (H_2O_2), and hydroxyl radical (OH^-), are abundant products of aerobic metabolism, and their levels set up the intracellular redox state [1]. However, excessive intracellular ROS levels, not balanced by endogenous antioxidant molecules (*e.g.*, glutathione), could lead to membrane lipid, protein, and DNA damage [1, 2] with the consequent cell death. Thus, the balance between prooxidant and antioxidant compounds influences the cell fate [1–3]. Aside from such a classical view of the intracellular ROS role, in the last two decades, mounting evidence sustained that low concentrations of ROS could promote cell growth and differentiation by regulating the activation status of enzymes, triggering signal transduction pathways as well as gene expression [1, 2].

Cancer cells represent a good example of these dual ROS effects. Actually, cancer cells, compared to their normal counterparts, live constantly or occasionally under an oxidative stress condition [3, 4]. Moreover, the increased ROS levels have been double linked with the tumor initiation and progression. Although the exact mechanism is still unclear, ROS represent the main selective pressure, which could induce cancer cell death or activate aberrant adaptation mechanisms involved in the acquisition of almost all the cancer hallmarks, including sustained cell proliferation, immortalization, cell death escape, metastasis, and chemo resistance [3]. These two faces played by ROS in cancer have been translated into two different strategies to develop anticancer agents. Antioxidant molecules have been predicted as a plausible tumor suppressor based on the tumorigenic role of ROS-activated signaling [3, 4]. However, the role of antioxidant deficit in increased cancer ROS generation and the actual anticancer effects of ROS scavenging are still debated [3]. On the other side, different ROS-inducing chemotherapeutic agents have been developed based on the idea that a further induction of intracellular ROS levels could

represent a way to kill selectively cancer cells without affecting the normal counterpart [3, 4]. Nonetheless, the cancer cells' adaptation to high levels of ROS and the consequent cancer resistance associated with the oxidative stress encourage the current research to define the survival factors and activated pathways devoted to increase cancer cell tolerability to ROS. Among different proteins that could serve as a compensatory element, here, we discuss the role of Neuroglobin (NGB), a monomeric heme-protein that operates as an oxidative stress biosensor and player in the context of the compensatory/adaptive systems of cancer cells.

2. Neuroglobin as a Stress Sensor in the Brain

NGB is a monomeric heme-protein [5, 6] that displays the classical 3/3 α-helical sandwich globin structure and is characterized by the presence of a hexa-coordinated heme-Fe atom in both the ferrous and ferric states [7–9]. Although its discovery date is quite recent, NGB shows a very slow evolutionary rate remaining largely unmodified throughout the evolution, suggesting a critical physiological role of the protein [5, 10, 11]. Due to its belonging to the globin superfamily, initially, it was assumed that NGB might play a role as an intracellular O_2 carrier [6, 12]. Although such a role could be possible in the retinal cells, where very high NGB concentration (100-200 μM) occurs ([13] and literature cited therein), the relatively low concentration ($\leq$1 μM) found in the other brain area ruled out on the function of NGB as an O_2 supply [5, 10, 11, 14]. Nonetheless, in the last two decades, the growing interest about NGB is raised from evidence that sustain a cytoprotective function of highly expressed globin in a wide range of neurological disorders and neuronal stressing conditions [5, 15]. In this context, several data have defined the close relationship between NGB and oxidative stress in the brain in terms of NGB ability to preserve cell survival of neuron and astrocytes, *in vitro* and *in vivo*, in the presence of high levels of ROS [16–23]. In addition, increased levels of NGB due to ectopic overexpression protect cultured neurons against hypoxia, oxygen-glucose deprivation (OGD), and neurotoxic challenges induced by sodium arsenite ($NaAsO_2$) and β-amyloid toxicity, which are directly or indirectly linked to intracellular ROS production [24–27].

In this regard, different hypotheses have been put forward and experimentally tested to define the protective mechanisms of the globin [5, 11, 13]. In particular, it has been proposed that NGB may act as a ROS/RNS scavenger to counteract the increased levels of oxidative stress [5, 28–31]. Nonetheless, the discovery of NGB-interacting proteins and the identification of specific subcellular expression profile (cytosol, mitochondria, nuclei) of the globin have widened the cellular functions in which NGB is involved. The NGB direct impact on the apoptotic pathway [17, 18, 32, 33], the NGB suppression of ROS production through the interaction with the cytochrome bc_1 complex (complex III) in the inner mitochondrial membrane [34], and the modulation of several intracellular signaling pathways devoted to the cell survival (*e.g.*, AKT and G protein) [5, 13, 35–39] have been described.

Intriguingly, diverse stress conditions like hypoxia [40], oxidative stress (H_2O_2) [17], oxygen and glucose deprivation [41], and lipopolysaccharide [42] increased NGB expression in neuron-derived cells suggesting a role of NGB as a stress-responsive sensor which transfers the stress condition to the signal transduction pathway [43]. On these findings, in neuron-derived cells exposed to oxidative stress, two different and interconnected functions of NGB have been demonstrated: the cytoprotective role, when an excessive intracellular ROS concentration occurs, and the globin involvement in the activated response to internal and external oxidative stress. Furthermore, it has been demonstrated that NGB expression is enhanced by endogenous factors, including hormones and growth factors. Among different hormones (*e.g.*, vascular endothelial growth factor and erythropoietin) [5, 44–46], 17β-estradiol (E2) induces, via estrogen receptor β (ERβ), high levels of NGB primarily involved in the E2-activated antiapoptotic pathway in neuron-derived cells [17, 18]. In particular, the demanding localization of NGB into mitochondria for its antiapoptotic function against oxidative stress has been demonstrated. Indeed, only the E2-induced mitochondrial reallocated NGB interacts with and impairs the cytosolic release of cytochrome *c* (Cyt-*c*) preventing the consequent activation of the apoptotic pathway during H_2O_2-induced stress condition [18, 47].

Altogether, such functions result in neuroprotection, and any approach able to upregulate NGB could preserve neurons/astrocytes from stress injury. On the other hand, NGB is now considered as an ubiquitary inducible protein, in which increased levels could guarantee the proper response and the adaptation to stress conditions that represent the main mechanisms activated by cancer cells to escape from necrosis and apoptosis in the presence of an imbalanced redox state [4, 48].

3. Neuroglobin in Cancer

Some evidence demonstrates the expression of human NGB in the nervous system neoplasm [49–52]. NGB expressions have been found higher in the mouse and the human astrocytoma cell line and in human astrocytoma tissues with respect to the normal astrocytes, sustaining a possible role of NGB in the adaptation of astrocytoma to the hypoxic and oxidative stress conditions [50]. Consistently, the analysis of both NGB mRNA and protein levels strongly sustained an upregulation of NGB levels in glioma tissue with respect to the normal counterpart. The correlation between NGB expression and the worse clinic-pathological feature, type/grade of glioma, poor prognosis, and shorter survival overall led to proposing NGB as a prognostic marker for glioma patients [51, 53]. In particular, Hu and colleagues provided different evidence, which supports the direct role of NGB as an antiapoptotic protein in glioma tumors against oxidative stress. On the one side, they proved that NGB overexpression protects U87 glioma cells against cell death induced by 4-hydroxy-2-nonenal (4-HNE), an end-product of the reaction between ROS and polyunsaturated fatty acids, which reflects a high oxidative stress inside cells. In addition, high levels of

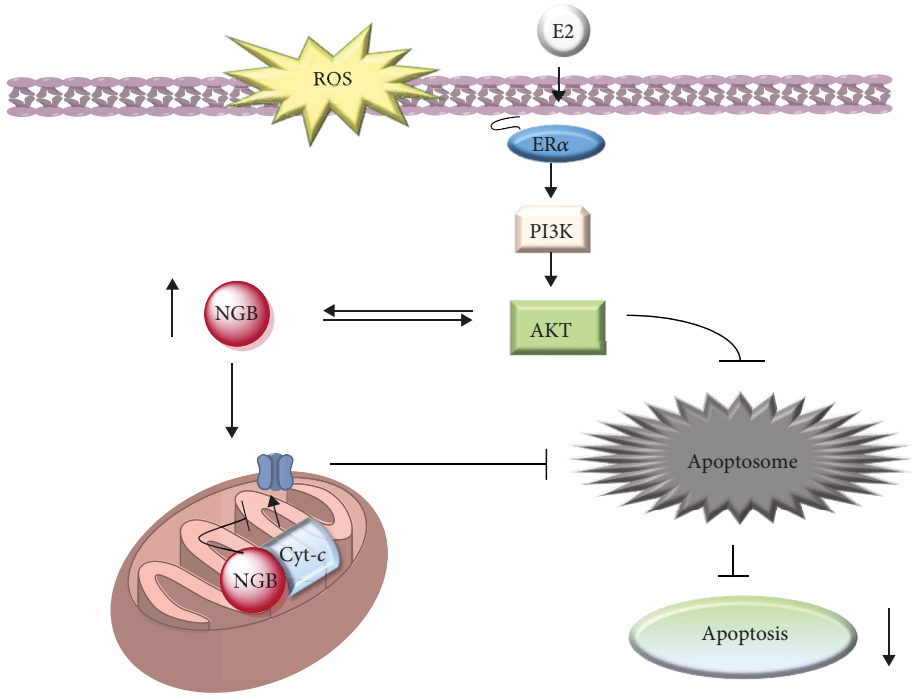

Figure 1: Schematic model of the E2 intracellular activated pathway impacting on NGB expression levels/intracellular localization and the related antiapoptotic role of both mitochondrial NGB and AKT which appears to be double linked with NGB function. E2: 17β-estradiol; ERα: estrogen receptor α; PI3K: phosphatidylinositol 3 kinase, Cyt-*c*: cytochrome *c*. For further detail, see the text.

the globin preserve glioma cells from the excessive ROS accumulation given by the activation of peroxisome proliferator-activated receptor γ (PPARγ) which, in turn, negatively regulates NGB expression to render glioma cells more susceptible to oxidative stress-induced cell death. Noteworthy, in such a contest of bidirectional negative cross-talk between NGB and PPARγ, the expression of such a receptor is lowered during cancer progression in parallel with the increase of NGB in high-grade glioma, strongly sustaining that NGB exerts a critical antiapoptotic function in glioma mainly by protecting cells exposed to accumulating oxidative pressure [54]. Mechanically, it has been proposed that NGB could favor glioma progression and a malignant phenotype by preserving cancer cells from apoptosis against oxidative pressure through the direct regulation of the antiapoptotic PI3K/AKT pathway [53, 54].

Similarly, in other independent studies, the analysis of NGB in matched normal and cancer tissues has demonstrated the enhanced expression of NGB in primary tumors and cancer cell line of brain and nonbrain origins and its positive correlation with a marker of hypoxia conditions [55]. In addition, Oleksiewicz and colleagues confirmed the overexpression of NGB in non-small cell lung cancer (NSCLC) specimens with respect to their matched normal tissue and in a panel of cell lines derived by lung cancer suggesting a NGB procancerous function even in extra-nervous tumors [56].

In line with the above reported results, we identified NGB as a 17β-estradiol- (E2-) inducible protein and key mediator of the hormone functions in various estrogen-responsive extra-nervous cancer cell lines [57–59]. Intriguingly, E2 upregulates NGB in diverse breast cancer cell lines (MCF-7, T47D, and ZR-75-1) expressing just the subtype α of the estrogen receptor (ERα), but not in the ERα-devoid MDA-MB-231 cell line [58, 59]. Although ERs are ligand-activated transcription factors, the *NGB* gene promoter does not contain any estrogen response element; thus, multiple and synergic cellular mechanisms underline the E2-induced NGB expression. Physiological E2 concentrations, in the presence of ERα, rapidly activate the pathway PI3K/AKT, which in turn prevents proteasome and lysosomal NGB degradation, and enhance *NGB* gene transcription via the phosphorylation of the nuclear transcription factor CREBP [58, 59]. Moreover, the persistent (24 h) AKT activation is necessary to reallocate NGB to the mitochondria (Figure 1) [58, 59]. Intracellular (*e.g.*, ROS) and extracellular stresses that cause the loss of mitochondrial membrane integrity and the release of Cyt-*c* from cardiolipin represent the main trigger event, which commits the cell to death [60]. Indeed, once released, Cyt-*c* binds to the apoptosis protease activation factor (APAF-1) to form the apoptosome that, in turn, activates effector caspases leading to apoptotic cell death [60]. Mitochondrial NGB localization, induced by E2, binds to free Cyt-*c* avoiding its release in the cytosol and the consequent apoptosome formation [18, 61]. Thus, NGB upregulation is one of the critical mechanisms triggered by the E2/ERα complex to protect breast cancer cells against oxidative stress by preventing, at mitochondrial levels, the triggering of the apoptotic cascade (Figure 1) [58, 59]. A similar E2-induced antiapoptotic function has also been reported in the hepatoma cell HepG2 [59] in contrast with the antiproliferative and tumor-suppressor function of the overexpressed NGB reported by other authors in these cells [39].

Overall, beyond the contradictory evidence about the expression of NGB in tumor cells and tissues [39, 62], mostly affected by experimental procedure, new perspectives regarding a possible role of the protein as a part of the defense mechanism against oxidative stress in cancer occurred.

4. Neuroglobin and Oxidative Stress Signaling in Cancer

A large number of positive and negative regulator systems affect the balance between oxidative stress and antioxidant capability, many of these systems are significantly modified in cancer cells leading to an aberrant regulation of redox homeostasis [3, 4]. Persistent ROS exposure in cancer cells may lead to cell adaptation via the abnormal activation of different redox-sensitive transcription factors including nuclear factor-κB (NF-κB), c-Jun, hypoxia-inducible factor-1 (HIF-1), and the nuclear factor erythroid 2-related factor 2 (NRF-2) whose functions are largely involved in the positive expression of different antioxidant enzymes (*e.g.*, SOD, catalase, and GSH antioxidant systems) [3, 4]. Aside from these redox-sensitive transcription factors, the forkhead box O (FOXO) family of transcription factors and p53 also have a major role in the regulation of antioxidant system expression. Both FOXO and p53 results are strongly modified during the onset and progression of cancer [1, 3].

In the classical stress response pathway consisting of sensors, signal transducers, and effectors, different proteins are regulated through redox-mediated mechanisms behaving, effectively, as an oxidative stress sensor [3]. ROS can change both the levels of proteins acting on their stability or expression and their functions through a direct regulation of structural conformation and reactivity by redox reaction on cysteine residues or an indirect posttranslational modification tightly regulated by redox-sensitive signaling proteins [3]. Altogether, upstream stress sensing and transducer systems, which are deeply modified during unbalanced and aberrant conditions, could represent good targets for the therapeutic approach direct to impact on cancer oxidative stress regulation.

Human NGB contains three cysteine residues; those at positions CD7 (cysteine 46) and D5 (cysteine 55) are sufficiently close to form a disulfide bond. This defines a redox-dependent conformational transition in NGB between a structure with intramolecular disulfide bond, oxidized form, and a disulfide-free NGB form in reduced condition [63–65]. Overall, NGB could sense the intracellular status, in terms of redox state or activation/inactivation of signaling cascade, by changing its three-dimensional structure, which mainly affects the protein affinity with an endogenous gaseous ligand, including oxygen [63–65], and, reasonably, could regulate NGB functional properties including its interaction with proteins (interactome) and intracellular localization as well.

In neuron-derived cells, Watanabe and colleagues demonstrated that oxidative stress imposes a large tertiary modification of the NGB fold allowing its interaction with flotillin-1 at the plasma membrane and favoring its inhibitory function on $G\alpha_i$ protein and the consequent oxidative stress-induced apoptosis, thus acting as an oxidative stress sensor able to impact on cellular response [43]. A similar oxidative stress-sensing activity has also been proposed in malignant tumor cells. In hepatoma cells, evidence suggests a role of NGB as on oxygen/ROS sensor, where it could act by coupling oxygen/ROS signals with a signal cascade, in particular, suppressing the Raf/MEK/ERK pathway via a regulatory machinery, which may involve other NGB-interacting proteins [39].

In this context, we recently confirmed NGB as a stress-inducible protein in breast cancer cells, where it acts as a sensing and compensatory protein activated in response to oxidative stress [59, 66]. As reported above, oxidative stress might affect the activity of sensor proteins by changing their levels via different ways. In our study, we demonstrated that oxidative stress mainly increases NGB levels by acting, like E2, through the inhibition of lysosomal protein degradation and the increase of the protein translation rate [66]. In particular, in breast cancer cells, our evidence demonstrated the transient activation of the PI3K/AKT signaling cascade by oxidative stress which culminates in NGB upregulation and in its localization mainly at the cytosolic compartment, where it could act as a direct ROS scavenger, behaving as a first barrier to the increased ROS levels (Figure 2) [58].

Conversely to the mitochondrial-gathered NGB induced by E2 (see the previous section), the oxidative stress-dependent increase in cytosolic NGB content does not correlate with a direct antiapoptotic function, opening new perspectives in the NGB function during an imbalanced stress condition depending on its intracellular localization [58].

Among the others, NRF-2 is the main regulator of the intracellular defense mechanism against oxidative stress controlling the transcription of ARE (antioxidant-responsive elements) containing genes encoding for proteins (*e.g.*, *glutamate-cysteine ligase modifier* (*GCLM*), *heme oxygenase (decycling) 1* (*HMOX1*), and *NADPH:quinone oxidoreductase 1* (*NQO1*)) involved in cell detoxification of reactive species [67, 68]. Under the resting condition, NRF-2 is targeted to the proteasome degradation by the binding with the oxidative sensor Kelch-like ECH-associated protein 1 (KEAP-1). KEAP-1 interaction with NRF-2 is mainly modulated by the intracellular redox state; indeed, high levels of oxidative stress oxidize KEAP-1 cysteine residues leading to the dissociation of its complex with NRF-2, which accumulates in cells and translocates to the nucleus where it induces the transcription of antioxidant genes [1, 69].

Some evidence addresses NRF-2 as a tumor suppressor function in normal and premalignant cells, according to the role of oxidative stress on cancer onset [4, 70]. Contrarily, a constitutive stabilization of NRF-2 and the consequent high levels of antioxidant enzymes are often found in malignant tumor cells and tissue, sustaining that an increased detoxifying intracellular system confers an advantage for the cancer progression and adaptation to microenvironment stressing conditions [1, 69]. In solid tumors, including those of the lung and liver, somatic missense mutations of the *KEAP-1* gene, which result in a mutant KEAP-1 protein unable to mediate the NRF-2 degradation, have been found. Consistently, mutations in the NRF-2 gene observed in cancer and

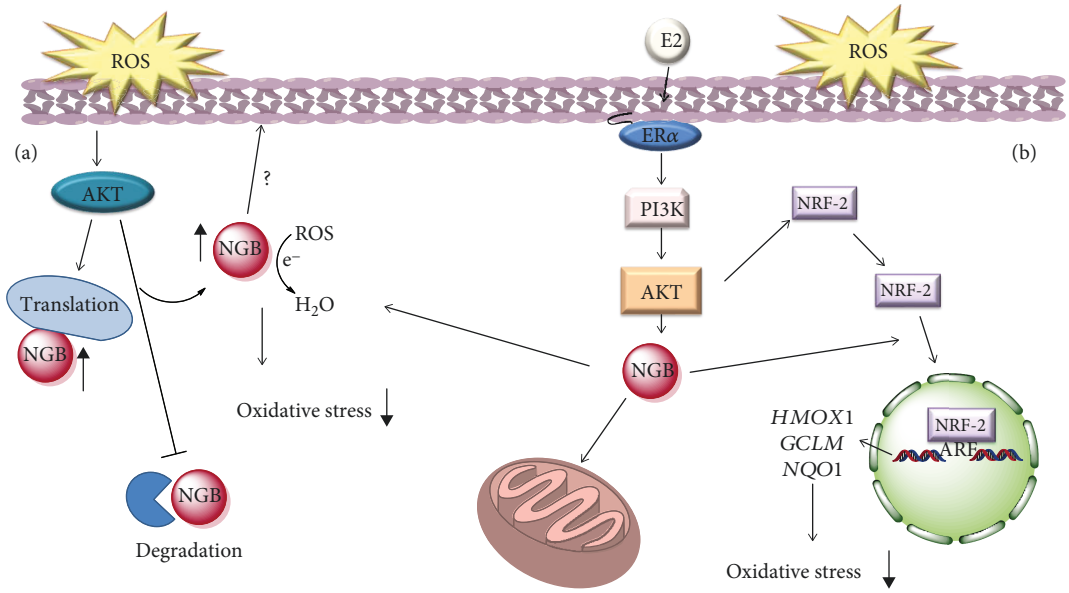

FIGURE 2: (a) Schematic model of ROS-activated signaling involved in the rapid modulation of NGB levels, its localization, and function on the redox balance outside mitochondria. (b) Schematic model of the E2 intracellular-activated pathway impacting on NGB expression, localization, and the NRF-2 pathway describing how NGB affects the E2-dependent activation of the antioxidant NRF-2 system. E2: 17β-estradiol; ERα: estrogen receptor α; PI3K: phosphatidylinositol 3 kinase. For further detail, see the text.

linked to a constitutive hyperactivation of the transcriptional function of the protein are totally related to the critical site for the formation of NRF-2 and KEAP-1 complex ([69] and literature cited therein).

Our latest results support a critical role of NGB as cytosolic signals intermediate in breast cancer cell stress response, taking part in the E2-dependent activation of the NRF-2 pathway and potentiation of the antioxidant system. Indeed, although the E2-dependent increase in the NRF-2 protein levels was not affected in NGB knockout MCF-7, the positive modulation of antioxidant genes under the direct control of the NRF-2 pathway (*NQO1*, *HMOX1*, and *GCLM*) was lost. As a consequence, obtained data strongly sustain a key function of NGB in the E2 and NRF-2-dependent high antioxidant capacity of estrogen-responsive breast cancer cells, and they suggest a possible role of the globin in the cytosolic signaling pathway involved in the NRF-2 nuclear translocation and transcriptional activity (Figure 2) [71].

The current understanding of NGB function, in particular regarding its involvement in oxidative stress response, is mainly focalized on the intracellular content of NGB and its subcompartmentalization. However, latest reported data propose an effect of subnanomolar concentration of extracellular NGB on the cellular function regulation, in terms of cytoprotection and modulation of antioxidant response [72]. In particular, authors found out that astrocyte cell treatment with extracellular NGB significantly reduced the H_2O_2 cell death by restoring the cell antioxidant systems, as demonstrated by the increase in SOD and catalase enzyme activity and transcription. The AKT phosphorylation appears to be the critical signaling pathway activated by exogenous NGB [52, 72, 73]. In addition, active AKT regulates the NGB expression and globin delivery inside cells in a time-dependent manner [58, 59]. Therefore, the story of the double cross link between AKT and NGB adds another piece of information widening the possible interaction between the globin and the PI3K/AKT signaling pathway. As a whole, such results open the fascinating possibility that, in cancer tissue, like in the brain, the NGB function in the cell adaptation response to oxidative stress might not be restricted to the intracellular environment but also spread to the extracellular microenvironemnt. In this context, the overproduced NGB in cancer cells by endogenous modulators (*e.g.*, E2) or stress conditions (*e.g.*, H_2O_2) may be, under proper circumstances, delivered outside the cells, participating in a cellular response to external stimuli which appear not confined to the cell itself but rather extended to the cell-microenvironment interface. However, further studies will be needed to properly support such a hypothesis and better understand the possible mechanism of action of NGB outside the cells.

5. Conclusion and Perspectives

The balance between ROS and the antioxidant-activated systems set up the levels of intracellular stress, and the fine regulation of this equilibrium is demanding for the correct function and survival of cells [4, 74]. At cellular levels, ROS-scavenging largely relies on the activation of enzymatic processes such as superoxide dismutase (SOD), glutathione peroxidase, catalase, glutaredoxin, and thioredoxin which, overall, constitute the antioxidant defense mechanism of the cells [3, 74]. When the intracellular antioxidant capability is overwhelmed by ROS, cytoprotective mechanisms are activated to impair, when possible, cell death due to the oxidative damage [74].

Given the aberrant ROS concentration, which commonly occurs in tumor progression, cancer cells establish several adaptive mechanisms, including antioxidant responses or activation of prosurvival pathways (*e.g.*, Bcl-2 and AKT), to cope with such stress and survive [3, 4]. Therefore, a greater understanding of pathways devoted to increase the threshold of ROS cellular tolerability appears to be demanding to overcome oxidative stress-associated cancer resistance and to improve the efficacy of therapeutic intervention in selectively killing cancer cells.

Since its discovery in 2000, NGB has been considered a specific globin expressed in the nervous system [6, 75, 76] where its neuroprotective function against different neurological disorders has been demonstrated in both *in vivo* and *in vitro* studies [17, 21, 22, 40, 77, 78]. Aside from this, different evidence sustain a role of NGB as a novel tumor-associated protein [39, 55, 56, 59]. Although the exact role of NGB as a cancer promotor or oncosuppressor is still debated [39, 55, 56, 59], the discovery of higher NGB expression in tumor tissues with respect to the normal counterpart in the brain and extra-nervous malignancies [55, 56] and the positive correlation between the globin expression and glioma tumor grade [54] lead to sustaining a critical NGB function in cancer progression. Consistently, NGB is directly correlated, at different levels, with the cancer cells' adaptation to the increased oxidative stress, which characterized the tumor microenvironment. On the one side, the globin interferes with the apoptotic cascade activated by ROS [53, 58, 59]; on the other side, it participates in the stress response to the detrimental redox imbalance [54, 55, 71].

In the last decade, increasing efforts have been made to define the molecular mechanisms behind the neuroprotective effects of NGB, which, overall, might also occur in tumors. Some of the proposed mechanisms, including O_2 carrier and ROS scavenger functions, have arisen looking at the typical globin structure of the protein [11, 31, 64, 79]. Furthermore, the involvement of NGB in regulating membrane/cytosolic transduction pathways devoted to increase cell survival [43, 53, 73, 80] and/or mitochondrial functionality [18, 21, 58, 59] has been demonstrated both in neurons/glial cells and cancer cells. The high reactivity of NGB protein in response to change in the intracellular redox state [5], its differential intracellular localization (*e.g.*, cytosol and mitochondria) depending on extracellular stimuli [58, 66], and the large spectrum of NGB-interacting proteins [13] sustain the idea that NGB functions may be finely regulated by the cross-action of all of these events. This intriguing vision is supported by evidence in cancer cells indicating that the anti-apoptotic role of NGB against oxidative stress required the protein mitochondrial localization [58, 59], and it is promoted by the change in reactivity and protein interactions (*e.g.*, Cyt-*c*) induced by oxidative stress itself [57]. In parallel, cytosolic NGB directly participates in the antioxidant system established by cancer cells to cope with enhanced ROS accumulation, so that one might predict that different pools of intracellular NGB may cooperate through different mechanisms to enhance cancer cell survival and promote cell adaptations to the stressful tumor microenvironment. In this regard, any stimulus able to change the NGB levels, intracellular localization, and reactivity in order to withdraw NGB prooncogenic functions might be promising to increase cancer cell susceptibility to oxidative stress-induced cell death.

Globins (i.e., myoglobin (MB), hemoglobin (HB), cytoglobin (CYGB), and NGB) are present in all kingdoms of living organisms where they display a variety of functions, including the O_2 sensing, transport, and storage; the synthesis and scavenging of RONS; and heme-based catalysis [81]. However, many studies demonstrated various other and additional roles of globins including the regulation of cancer progression. The rather low expression levels of these globins in tumor tissue seems to argue against a contribution to tumor oxygenation [62]. On the other hand, the reported functions of MB and CYGB in breast and lung tumors agree with the proposed role as a tumor suppressor for these globins [82, 83]. Contrarily, NGB is the unique globin identified as a critical player in cancer cell adaptations and resistance to detrimental oxidative stress conditions. Although further studies are needed to understand the complex regulating mechanisms of NGB functions, the NGB role in cancer could represent the new target for anticancer therapeutic interventions.

Conflicts of Interest

The authors declare no conflict of interest.

Acknowledgments

The authors want to thank past and present members of their laboratories who contributed with data and discussions to the ideas presented here. We apologize for the many authors of the outstanding papers that were not cited here due to space limitation. This work was supported by a grant from Associazione Italiana Ricerca sul Cancro (AIRC, IG#15221) to M.M. The grant of Excellence Departments, Italian Ministry of Education, University and Research (MIUR) (Legge 232/2016, Articolo 1, Comma 314-337), is gratefully acknowledged.

References

[1] M. Schieber and N. S. Chandel, "ROS function in redox signaling and oxidative stress," *Current Biology*, vol. 24, no. 10, pp. R453–R462, 2014.

[2] V. Sosa, T. Moliné, R. Somoza, R. Paciucci, H. Kondoh, and M. E. LLeonart, "Oxidative stress and cancer: an overview," *Ageing Research Reviews*, vol. 12, no. 1, pp. 376–390, 2013.

[3] D. Trachootham, J. Alexandre, and P. Huang, "Targeting cancer cells by ROS-mediated mechanisms: a radical therapeutic approach?," *Nature Reviews. Drug Discovery*, vol. 8, no. 7, pp. 579–591, 2009.

[4] C. Gorrini, I. S. Harris, and T. W. Mak, "Modulation of oxidative stress as an anticancer strategy," *Nature Reviews. Drug Discovery*, vol. 12, no. 12, pp. 931–947, 2013.

[5] P. Ascenzi, A. di Masi, L. Leboffe et al., "Neuroglobin: from structure to function in health and disease," *Molecular Aspects of Medicine*, vol. 52, pp. 1–48, 2016.

[6] T. Burmester, B. Weich, S. Reinhardt, and T. Hankeln, "A vertebrate globin expressed in the brain," *Nature*, vol. 407, no. 6803, pp. 520–523, 2000.

[7] B. G. Guimaraes, D. Hamdane, C. Lechauve, M. C. Marden, and B. Golinelli-Pimpaneau, "The crystal structure of wild-type human brain neuroglobin reveals flexibility of the disulfide bond that regulates oxygen affinity," *Acta Crystallographica. Section D, Biological Crystallography*, vol. 70, no. 4, pp. 1005–1014, 2014.

[8] A. Pesce, S. Dewilde, M. Nardini et al., "Human brain neuroglobin structure reveals a distinct mode of controlling oxygen affinity," *Structure*, vol. 11, no. 9, pp. 1087–1095, 2003.

[9] B. Vallone, K. Nienhaus, M. Brunori, and G. U. Nienhaus, "The structure of murine neuroglobin: novel pathways for ligand migration and binding," *Proteins*, vol. 56, no. 1, pp. 85–92, 2004.

[10] T. Burmester and T. Hankeln, "Neuroglobin: a respiratory protein of the nervous system," *News in Physiological Sciences*, vol. 19, no. 3, pp. 110–113, 2004.

[11] T. Burmester and T. Hankeln, "What is the function of neuroglobin?," *The Journal of Experimental Biology*, vol. 212, no. 10, pp. 1423–1428, 2009.

[12] M. Schmidt, A. Giessl, T. Laufs, T. Hankeln, U. Wolfrum, and T. Burmester, "How does the eye breathe? Evidence for neuroglobin-mediated oxygen supply in the mammalian retina," *Journal of Biological Chemistry*, vol. 278, no. 3, pp. 1932–1935, 2003.

[13] M. Fiocchetti, M. Cipolletti, V. Brandi, F. Polticelli, and P. Ascenzi, "Neuroglobin and friends," *Journal of Molecular Recognition*, vol. 30, no. 12, 2017.

[14] A. Giuffre, T. Moschetti, B. Vallone, and M. Brunori, "Neuroglobin: enzymatic reduction and oxygen affinity," *Biochemical and Biophysical Research Communications*, vol. 367, no. 4, pp. 893–898, 2008.

[15] D. A. Greenberg, K. Jin, and A. Khan, "Neuroglobin: an endogenous neuroprotectant," *Current Opinion in Pharmacology*, vol. 8, no. 1, pp. 20–24, 2008.

[16] R. Cabezas, E. Baez-Jurado, O. Hidalgo-Lanussa et al., "Growth factors and neuroglobin in astrocyte protection against neurodegeneration and oxidative stress," *Molecular Neurobiology*, vol. 56, no. 4, pp. 2339–2351, 2019.

[17] E. de Marinis, P. Ascenzi, M. Pellegrini et al., "17β-Estradiol – a new modulator of neuroglobin levels in neurons: role in neuroprotection against H_2O_2-induced toxicity," *Neurosignals*, vol. 18, no. 4, pp. 223–235, 2010.

[18] E. de Marinis, M. Fiocchetti, F. Acconcia, P. Ascenzi, and M. Marino, "Neuroglobin upregulation induced by 17β-estradiol sequesters cytocrome c in the mitochondria preventing H_2O_2-induced apoptosis of neuroblastoma cells," *Cell Death & Disease*, vol. 4, no. 2, article e508, 2013.

[19] R. C. Li, M. W. Morris, S. K. Lee, F. Pouranfar, Y. Wang, and D. Gozal, "Neuroglobin protects PC12 cells against oxidative stress," *Brain Research*, vol. 1190, pp. 159–166, 2008.

[20] A. A. Khan, Y. Wang, Y. Sun et al., "Neuroglobin-overexpressing transgenic mice are resistant to cerebral and myocardial ischemia," *Proceedings of the National Academy of Sciences of the United States of America*, vol. 103, no. 47, pp. 17944–17948, 2006.

[21] J. Liu, Z. Yu, S. Guo et al., "Effects of neuroglobin overexpression on mitochondrial function and oxidative stress following hypoxia/reoxygenation in cultured neurons," *Journal of Neuroscience Research*, vol. 87, no. 1, pp. 164–170, 2009.

[22] Y. Sun, K. Jin, A. Peel, X. O. Mao, L. Xie, and D. A. Greenberg, "Neuroglobin protects the brain from experimental stroke in vivo," *Proceedings of the National Academy of Sciences of the United States of America*, vol. 100, no. 6, pp. 3497–3500, 2003.

[23] X. Wang, J. Liu, H. Zhu et al., "Effects of neuroglobin overexpression on acute brain injury and long-term outcomes after focal cerebral ischemia," *Stroke*, vol. 39, no. 6, pp. 1869–1874, 2008.

[24] A. A. Khan, X. O. Mao, S. Banwait, K. Jin, and D. A. Greenberg, "Neuroglobin attenuates β-amyloid neurotoxicity *in vitro* and transgenic Alzheimer phenotype *in vivo*," *Proceedings of the National Academy of Sciences of the United States of America*, vol. 104, no. 48, pp. 19114–19119, 2007.

[25] X. Liu, Y. Gao, H. Yao, L. Zhou, D. Sun, and J. Wang, "Neuroglobin involvement in the course of arsenic toxicity in rat cerebellar granule neurons," *Biological Trace Element Research*, vol. 155, no. 3, pp. 439–446, 2013.

[26] Z. Yu, N. Liu, Y. Li, J. Xu, and X. Wang, "Neuroglobin overexpression inhibits oxygen-glucose deprivation-induced mitochondrial permeability transition pore opening in primary cultured mouse cortical neurons," *Neurobiology of Disease*, vol. 56, pp. 95–103, 2013.

[27] Y. Lin, B. Cai, X. H. Xue, L. Fang, Z. Y. Wu, and N. Wang, "TAT-mediated delivery of neuroglobin attenuates apoptosis induced by oxygen-glucose deprivation via the Jak2/Stat3 pathway *in vitro*," *Neurological Research*, vol. 37, no. 6, pp. 531–538, 2015.

[28] M. Brunori, A. Giuffre, K. Nienhaus, G. U. Nienhaus, F. M. Scandurra, and B. Vallone, "Neuroglobin, nitric oxide, and oxygen: functional pathways and conformational changes," *Proceedings of the National Academy of Sciences of the United States of America*, vol. 102, no. 24, pp. 8483–8488, 2005.

[29] S. Dewilde, L. Kiger, T. Burmester et al., "Biochemical characterization and ligand binding properties of neuroglobin, a novel member of the globin family," *The Journal of Biological Chemistry*, vol. 276, no. 42, pp. 38949–38955, 2001.

[30] E. Fordel, L. Thijs, L. Moens, and S. Dewilde, "Neuroglobin and cytoglobin expression in mice. Evidence for a correlation with reactive oxygen species scavenging," *FEBS Journal*, vol. 274, no. 5, pp. 1312–1317, 2007.

[31] S. Herold, A. Fago, R. E. Weber, S. Dewilde, and L. Moens, "Reactivity studies of the Fe(III) and Fe(II)NO forms of human neuroglobin reveal a potential role against oxidative stress," *The Journal of Biological Chemistry*, vol. 279, no. 22, pp. 22841–22847, 2004.

[32] W. B. Lan, J. H. Lin, X. W. Chen et al., "Overexpressing neuroglobin improves functional recovery by inhibiting neuronal apoptosis after spinal cord injury," *Brain Research*, vol. 1562, pp. 100–108, 2014.

[33] S. Raychaudhuri, J. Skommer, K. Henty, N. Birch, and T. Brittain, "Neuroglobin protects nerve cells from apoptosis by inhibiting the intrinsic pathway of cell death," *Apoptosis*, vol. 15, no. 4, pp. 401–411, 2010.

[34] Z. Yu, Y. Zhang, N. Liu et al., "Roles of neuroglobin binding to mitochondrial complex III subunit cytochrome *c*1 in oxygen-glucose deprivation-induced neurotoxicity in primary neurons," *Molecular Neurobiology*, vol. 53, no. 5, pp. 3249–3257, 2016.

[35] N. Takahashi, S. Watanabe, and K. Wakasugi, "Crucial roles of Glu60 in human neuroglobin as a guanine nucleotide dissociation inhibitor and neuroprotective agent," *PLoS One*, vol. 8, no. 12, article e83698, 2013.

[36] K. Wakasugi, T. Nakano, and I. Morishima, "Oxidized human neuroglobin acts as a heterotrimeric Galpha protein guanine nucleotide dissociation inhibitor," *The Journal of Biological Chemistry*, vol. 278, no. 38, pp. 36505–36512, 2003.

[37] S. Watanabe and K. Wakasugi, "Neuroprotective function of human neuroglobin is correlated with its guanine nucleotide dissociation inhibitor activity," *Biochemical and Biophysical Research Communications*, vol. 369, no. 2, pp. 695–700, 2008.

[38] S. Zara, M. de Colli, M. Rapino et al., "Ibuprofen and lipoic acid conjugate neuroprotective activity is mediated by Ngb/Akt intracellular signaling pathway in Alzheimer's disease rat model," *Gerontology*, vol. 59, no. 3, pp. 250–260, 2013.

[39] J. Zhang, S. J. Lan, Q. R. Liu, J. M. Liu, and X. Q. Chen, "Neuroglobin, a novel intracellular hexa-coordinated globin, functions as a tumor suppressor in hepatocellular carcinoma via Raf/MAPK/Erk," *Molecular Pharmacology*, vol. 83, no. 5, pp. 1109–1119, 2013.

[40] R. Schmidt-Kastner, M. Haberkamp, C. Schmitz, T. Hankeln, and T. Burmester, "Neuroglobin mRNA expression after transient global brain ischemia and prolonged hypoxia in cell culture," *Brain Research*, vol. 1103, no. 1, pp. 173–180, 2006.

[41] E. Fordel, L. Thijs, W. Martinet, D. Schrijvers, L. Moens, and S. Dewilde, "Anoxia or oxygen and glucose deprivation in SH-SY5Y cells: a step closer to the unraveling of neuroglobin and cytoglobin functions," *Gene*, vol. 398, no. 1-2, pp. 114–122, 2007.

[42] E. de Marinis, E. Acaz-Fonseca, M. A. Arevalo et al., "17β-Oestradiol anti-inflammatory effects in primary astrocytes require oestrogen receptor β-mediated neuroglobin up-regulation," *Journal of Neuroendocrinology*, vol. 25, no. 3, pp. 260–270, 2013.

[43] S. Watanabe, N. Takahashi, H. Uchida, and K. Wakasugi, "Human neuroglobin functions as an oxidative stress-responsive sensor for neuroprotection," *The Journal of Biological Chemistry*, vol. 287, no. 36, pp. 30128–30138, 2012.

[44] Y. Gao, Y. Mengana, Y. R. Cruz et al., "Different expression patterns of Ngb and EPOR in the cerebral cortex and hippocampus revealed distinctive therapeutic effects of intranasal delivery of neuro-EPO for ischemic insults to the gerbil brain," *The Journal of Histochemistry and Cytochemistry*, vol. 59, no. 2, pp. 214–227, 2011.

[45] K. Jin, X. Mao, L. Xie, and D. A. Greenberg, "Interactions between vascular endothelial growth factor and neuroglobin," *Neuroscience Letters*, vol. 519, no. 1, pp. 47–50, 2012.

[46] K. C. Oliveira, R. R. da Conceição, G. C. Piedade et al., "Thyroid hormone modulates neuroglobin and cytoglobin in rat brain," *Metabolic Brain Disease*, vol. 30, no. 6, pp. 1401–1408, 2015.

[47] M. Fiocchetti, E. De Marinis, P. Ascenzi, and M. Marino, "Neuroglobin and neuronal cell survival," *Biochimica et Biophysica Acta (BBA) - Proteins and Proteomics*, vol. 1834, no. 9, pp. 1744–1749, 2013.

[48] P. Storz, "Reactive oxygen species in tumor progression," *Frontiers in Bioscience*, vol. 10, no. 1-3, pp. 1881–1896, 2005.

[49] E. Fordel, L. Thijs, W. Martinet et al., "Neuroglobin and cytoglobin overexpression protects human SH-SY5Y neuroblastoma cells against oxidative stress-induced cell death," *Neuroscience Letters*, vol. 410, no. 2, pp. 146–151, 2006.

[50] H. Qin, Y. Guo, C. Zhang, L. Zhang, M. Li, and P. Guan, "The expression of neuroglobin in astrocytoma," *Brain Tumor Pathology*, vol. 29, no. 1, pp. 10–16, 2012.

[51] B. Zhang, M. Chang, J. Wang, and Y. Liu, "Neuroglobin functions as a prognostic marker and promotes the tumor growth of glioma via suppressing apoptosis," *Biomedicine & Pharmacotherapy*, vol. 88, pp. 173–180, 2017.

[52] B. Zhang, X. Ji, S. Zhang et al., "Hemin-mediated neuroglobin induction exerts neuroprotection following ischemic brain injury through PI3K/Akt signaling," *Molecular Medicine Reports*, vol. 8, no. 2, pp. 681–685, 2013.

[53] B. Zhang, Y. Liu, Y. Li, X. Zhe, S. Zhang, and L. Zhang, "Neuroglobin promotes the proliferation and suppresses the apoptosis of glioma cells by activating the PI3K/AKT pathway," *Molecular Medicine Reports*, vol. 17, no. 2, pp. 2757–2763, 2018.

[54] J. Hu, X. Cao, D. Pang et al., "Tumor grade related expression of neuroglobin is negatively regulated by PPARγ and confers antioxidant activity in glioma progression," *Redox Biology*, vol. 12, pp. 682–689, 2017.

[55] M. Emara, A. R. Turner, and J. Allalunis-Turner, "Hypoxic regulation of cytoglobin and neuroglobin expression in human normal and tumor tissues," *Cancer Cell International*, vol. 10, no. 1, p. 33, 2010.

[56] U. Oleksiewicz, N. Daskoulidou, T. Liloglou et al., "Neuroglobin and myoglobin in non-small cell lung cancer: expression, regulation and prognosis," *Lung Cancer*, vol. 74, no. 3, pp. 411–418, 2011.

[57] M. Fiocchetti, G. Camilli, F. Acconcia, S. Leone, P. Ascenzi, and M. Marino, "ERβ-dependent neuroglobin up-regulation impairs 17β-estradiol-induced apoptosis in DLD-1 colon cancer cells upon oxidative stress injury," *The Journal of Steroid Biochemistry and Molecular Biology*, vol. 149, pp. 128–137, 2015.

[58] M. Fiocchetti, M. Cipolletti, P. Ascenzi, and M. Marino, "Dissecting the 17β-estradiol pathways necessary for neuroglobin anti-apoptotic activity in breast cancer," *Journal of Cellular Physiology*, vol. 233, no. 7, pp. 5087–5103, 2018.

[59] M. Fiocchetti, M. T. Nuzzo, P. Totta, F. Acconcia, P. Ascenzi, and M. Marino, "Neuroglobin, a pro-survival player in estrogen receptor α-positive cancer cells," *Cell Death & Disease*, vol. 5, no. 10, article e1449, 2014.

[60] P. Caroppi, F. Sinibaldi, L. Fiorucci, and R. Santucci, "Apoptosis and human diseases: mitochondrion damage and lethal role of released cytochrome C as proapoptotic protein," *Current Medicinal Chemistry*, vol. 16, no. 31, pp. 4058–4065, 2009.

[61] Y. J. Wang, Q. Y. Peng, S. Y. Deng et al., "Hemin protects against oxygen-glucose deprivation-induced apoptosis activation via neuroglobin in SH-SY5Y cells," *Neurochemical Research*, vol. 42, no. 8, pp. 2208–2217, 2017.

[62] T. A. Gorr, D. Wichmann, C. Pilarsky et al., "Old proteins - new locations: myoglobin, haemoglobin, neuroglobin and cytoglobin in solid tumours and cancer cells," *Acta Physiologica*, vol. 202, no. 3, pp. 563–581, 2011.

[63] D. Hamdane, L. Kiger, S. Dewilde et al., "The redox state of the cell regulates the ligand binding affinity of human neuroglobin and cytoglobin," *The Journal of Biological Chemistry*, vol. 278, no. 51, pp. 51713–51721, 2003.

[64] S. Nicolis, E. Monzani, C. Ciaccio, P. Ascenzi, L. Moens, and L. Casella, "Reactivity and endogenous modification by nitrite and hydrogen peroxide: does human neuroglobin act only as a scavenger?," *The Biochemical Journal*, vol. 407, no. 1, pp. 89–99, 2007.

[65] M. Tiso, J. Tejero, S. Basu et al., "Human neuroglobin functions as a redox-regulated nitrite reductase," *The Journal of Biological Chemistry*, vol. 286, no. 20, pp. 18277–18289, 2011.

[66] M. Fiocchetti, M. Cipolletti, S. Leone et al., "Neuroglobin in breast cancer cells: effect of hypoxia and oxidative stress on protein level, localization, and anti-apoptotic function," *PLoS One*, vol. 11, no. 5, article e0154959, 2016.

[67] J. D. Hayes and A. T. Dinkova-Kostova, "The Nrf2 regulatory network provides an interface between redox and intermediary metabolism," *Trends in Biochemical Sciences*, vol. 39, no. 4, pp. 199–218, 2014.

[68] T. Nguyen, P. Nioi, and C. B. Pickett, "The Nrf2-antioxidant response element signaling pathway and its activation by oxidative stress," *The Journal of Biological Chemistry*, vol. 284, no. 20, pp. 13291–13295, 2009.

[69] Y. Mitsuishi, H. Motohashi, and M. Yamamoto, "The Keap1-Nrf2 system in cancers: stress response and anabolic metabolism," *Frontiers in Oncology*, vol. 2, p. 200, 2012.

[70] M. B. Sporn and K. T. Liby, "NRF2 and cancer: the good, the bad and the importance of context," *Nature Reviews. Cancer*, vol. 12, no. 8, pp. 564–571, 2012.

[71] V. C. M. Solar Fernandez, P. Ascenzi, M. Marino, and M. Fiocchetti, "Neuroglobin as key mediator in the E2-induced antioxidant cell response to the oxidative stress," *Antioxidants & Redox Signaling*, 2019, In press.

[72] F. Amri, I. Ghouili, M. Amri, A. Carrier, and O. Masmoudi-Kouki, "Neuroglobin protects astroglial cells from hydrogen peroxide-induced oxidative stress and apoptotic cell death," *Journal of Neurochemistry*, vol. 140, no. 1, pp. 151–169, 2017.

[73] Y. Li, Y. B. Dai, J. Y. Sun et al., "Neuroglobin attenuates beta amyloid-induced apoptosis through inhibiting caspases activity by activating PI3K/Akt signaling pathway," *Journal of Molecular Neuroscience*, vol. 58, no. 1, pp. 28–38, 2016.

[74] M. Liontos, I. S Pateras, K. Evangelou, and V. G Gorgoulis, "The tumor suppressor gene ARF as a sensor of oxidative stress," *Current Molecular Medicine*, vol. 12, no. 6, pp. 704–715, 2012.

[75] T. Burmester, M. Haberkamp, S. Mitz et al., "Neuroglobin and cytoglobin: genes, proteins and evolution," *IUBMB Life*, vol. 56, no. 11, pp. 703–707, 2004.

[76] P. P. A. Mammen, J. M. Shelton, S. C. Goetsch et al., "Neuroglobin, a novel member of the globin family, is expressed in focal regions of the brain," *The Journal of Histochemistry and Cytochemistry*, vol. 50, no. 12, pp. 1591–1598, 2016.

[77] K. Jin, Y. Mao, X. Mao, L. Xie, and D. A. Greenberg, "Neuroglobin expression in ischemic stroke," *Stroke*, vol. 41, no. 3, pp. 557–559, 2010.

[78] Y. Sun, K. Jin, X. O. Mao, Y. Zhu, and D. A. Greenberg, "Neuroglobin is up-regulated by and protects neurons from hypoxic-ischemic injury," *Proceedings of the National Academy of Sciences of the United States of America*, vol. 98, no. 26, pp. 15306–15311, 2001.

[79] K. Jin, X. O. Mao, L. Xie, A. A. Khan, and D. A. Greenberg, "Neuroglobin protects against nitric oxide toxicity," *Neuroscience Letters*, vol. 430, no. 2, pp. 135–137, 2008.

[80] S. Y. Deng, Y. H. Ai, L. N. Zhang et al., "The role of neuroglobin in oxygen-glucose deprivation and reoxygenation-induced mitochondrial depolarization and reactive oxygen species production in SH-SY5Y cells," *Zhonghua Nei Ke Za Zhi*, vol. 56, no. 1, pp. 44–48, 2017.

[81] P. Ascenzi, S. Gustincich, and M. Marino, "Mammalian nerve globins in search of functions," *IUBMB Life*, vol. 66, no. 4, pp. 268–276, 2014.

[82] A. Braganza, K. Quesnelle, J. Bickta et al., "Myoglobin induces mitochondrial fusion, thereby inhibiting breast cancer cell proliferation," *The Journal of Biological Chemistry*, vol. 294, no. 18, pp. 7269–7282, 2019.

[83] T. C. Bholah, V. S. Neergheen-Bhujun, N. J. Hodges, S. D. Dyall, and T. Bahorun, "Cytoglobin as a biomarker in cancer: potential perspective for diagnosis and management," *BioMed Research International*, vol. 2015, Article ID 824514, 6 pages, 2015.

Hindawi
Oxidative Medicine and Cellular Longevity
Volume 2019, Article ID 3150145, 16 pages
https://doi.org/10.1155/2019/3150145

Review Article

Unraveling the Potential Role of Glutathione in Multiple Forms of Cell Death in Cancer Therapy

Huanhuan Lv,[1,2,3,4,5] **Chenxiao Zhen**,[1,2,5] **Junyu Liu**,[1,2,5] **Pengfei Yang**,[1,2,4,5] **Lijiang Hu**,[3] **and Peng Shang**[2,4,5]

[1]*School of Life Sciences, Northwestern Polytechnical University, Xi'an, Shaanxi 710072, China*
[2]*Research & Development Institute of Northwestern Polytechnical University in Shenzhen, Shenzhen 518057, China*
[3]*Zhejiang Heye Health Technology Co. Ltd., Anji, Zhejiang 313300, China*
[4]*Research Centre of Microfluidic Chip for Health Care and Environmental Monitoring, Yangtze River Delta Research Institute of Northwestern Polytechnical University in Taicang, Suzhou, Jiangsu 215400, China*
[5]*Key Laboratory for Space Bioscience and Biotechnology, Northwestern Polytechnical University, Xi'an, Shaanxi 710072, China*

Correspondence should be addressed to Peng Shang; shangpeng@nwpu.edu.cn

Received 11 April 2019; Accepted 21 May 2019; Published 10 June 2019

Guest Editor: Kanhaiya Singh

Glutathione is the principal intracellular antioxidant buffer against oxidative stress and mainly exists in the forms of reduced glutathione (GSH) and oxidized glutathione (GSSG). The processes of glutathione synthesis, transport, utilization, and metabolism are tightly controlled to maintain intracellular glutathione homeostasis and redox balance. As for cancer cells, they exhibit a greater ROS level than normal cells in order to meet the enhanced metabolism and vicious proliferation; meanwhile, they also have to develop an increased antioxidant defense system to cope with the higher oxidant state. Growing numbers of studies have implicated that altering the glutathione antioxidant system is associated with multiple forms of programmed cell death in cancer cells. In this review, we firstly focus on glutathione homeostasis from the perspectives of glutathione synthesis, distribution, transportation, and metabolism. Then, we discuss the function of glutathione in the antioxidant process. Afterwards, we also summarize the recent advance in the understanding of the mechanism by which glutathione plays a key role in multiple forms of programmed cell death, including apoptosis, necroptosis, ferroptosis, and autophagy. Finally, we highlight the glutathione-targeting therapeutic approaches toward cancers. A comprehensive review on the glutathione homeostasis and the role of glutathione depletion in programmed cell death provide insight into the redox-based research concerning cancer therapeutics.

1. Introduction

Glutathione is a thiol-containing tripeptide consisting of L-glutamate, cysteine, and glycine [1]. It is abundantly distributed in mammalian cells and mainly exists in the forms of reduced glutathione (GSH) and oxidized glutathione (glutathione disulfide (GSSG)). GSH is predominately distributed in the cytosol and to a lesser content in the subcellular organelles, such as the mitochondria, nucleus, and endoplasmic reticulum (ER). GSH takes part in many cellular metabolic activities including reactive oxygen species (ROS) removal, DNA and protein syntheses, and signal transduction [2, 3].

As for cancer cells, they need a greater ROS level than normal cells for the enhanced metabolism and vicious proliferation [4, 5]. Nevertheless, the higher ROS level can also be counteracted by an increased activity of the antioxidant defense system which copes with the higher oxidant state. The GSH system is one of the major cellular antioxidant systems that cooperatively maintain and synergize the redox balance [6]. The increased GSH level has been observed in different human cancer cells and is an important contributor to cancer pathology and the resistance to anticancer therapy [7]. As a contrary, GSH depletion increases the susceptibility of cancer cells to various forms of programmed cell death and sensitivity to chemotherapies [8]. Consequently, the role of

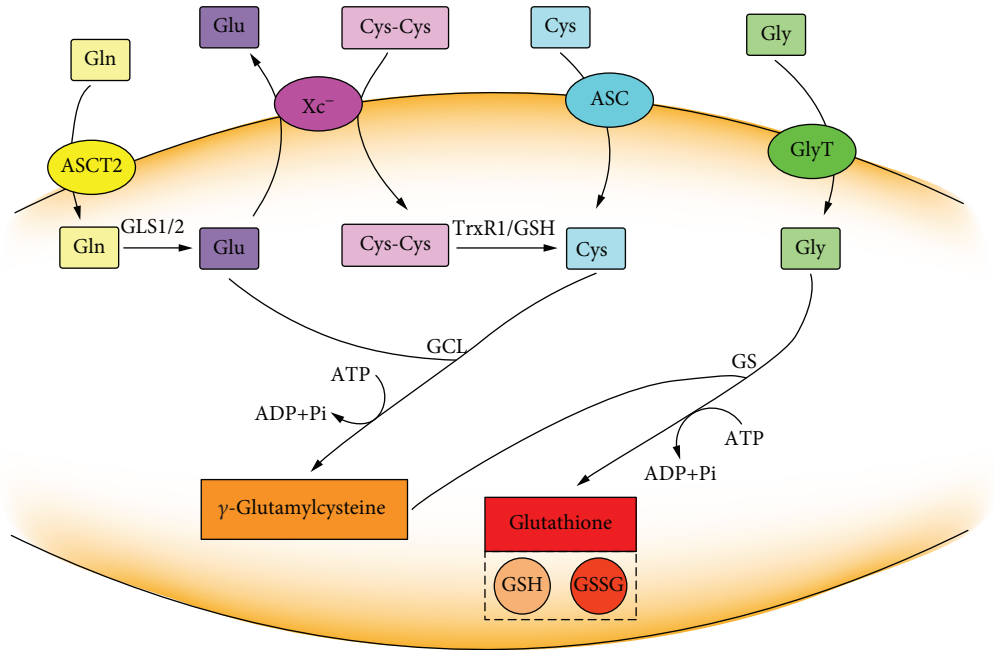

Figure 1: Two-step enzymatic reaction of glutathione synthesis. The first step is the coupling of L-glutamate and cysteine to produce γ-glutamylcysteine under the catalysis of glutamate-cysteine ligase (GCL). The second step is the coupling of γ-glutamylcysteine to glycine catalyzing by glutathione synthetase (GS). Each reaction consumes one ATP molecule. Glutathione exists in the forms of reduced GSH and oxidized GSSG.

GSH in the initiation of programmed cell death in cancer cells has been well implicated in accumulative studies. There are crosstalks and interrelationships between these different forms of programmed cell death induced by GSH.

Here, we highlight the GSH homeostasis, the relationship between GSH and oxidative stress, the recent findings of GSH depletion in multiple forms of programmed cell death, and GSH-targeting therapeutic approaches toward cancers. The review may help to better understand the role of GSH modulation in cell death and shed light on the possibility of finding new therapeutic approaches based on the redox system for cancers.

2. GSH Homeostasis

2.1. GSH Synthesis. The biosynthesis of glutathione was obtained by catalyzing of L-glutamate, cysteine, and glycine through continuous two-step enzymatic reactions which depend on ATP [9]. Glutamine is hydrolyzed by glutaminase (GLS1/2) to form glutamate after being absorbed into the cell via a transmembrane amino acid transporter (ASCT2). Cysteine can be directly absorbed by an amino acid transporter (ASC) or can be obtained by reduction of cystine absorbed by system X_c^-. The intracellular glycine can be directly absorbed by a glycine transporter (GlyT). The synthesis of glutathione is through two-step enzymatic reactions by glutamate-cysteine ligase (GCL) and glutathione synthetase (GS) (Figure 1). In the first step, GCL catalyzes the reaction of cysteine with glutamate to produce γ-glutamylcysteine; next step, γ-glutamylcysteine is combined with glycine to produce glutathione under the catalysis of GS [10]. Since the concentration of γ-glutamylcysteine is negligible when GS is present, GCL determines the rate of GSH synthesis during this process [11].

Glutathione exists in the reduced GSH form and oxidized GSSG form. The content of glutathione is in a dynamic balance through the regulation of synthesis, utilization, metabolism, and efflux. Under physiological condition, GSH is the predominant form which is more than 98%, while GSSG is less than 1% [12].

2.2. GSH Distribution. The glutathione-centered redox system participates in the redox signal network and controls cell growth, development, and oxidant defense [13]. In addition to the cytoplasm, glutathione also presents in various subcellular organelles, including the nucleus, mitochondria, and ER (Figure 2). There is a significant difference in glutathione distribution among these subcellular organelles [14, 15]. The distribution of glutathione in different intervals is critical because it establishes a redox environment that supports various metabolic and signaling events [16]. The maintenance of redox homeostasis of the nucleus, mitochondria, ER, and other organelles as well as the extracellular environment is inseparable from glutathione.

2.2.1. Cytosolic GSH. In mammalian cells, glutathione is exclusively synthesized in the cytosol and about 85% of it remains where it was synthesized [17, 18]. In the cytosol, glutathione is mainly in the reduced form. The ratio of GSH : GSSG in the cytosol is conservatively estimated at about 10000 : 1~50000 : 1 [19]. Reports show that the concentration of the cytosolic GSH is as high as 10 mM, while GSSG in the cytosol is as low as nanomolar concentration. The redox potential of E_{GSH} in the cytosol is about 320 mV

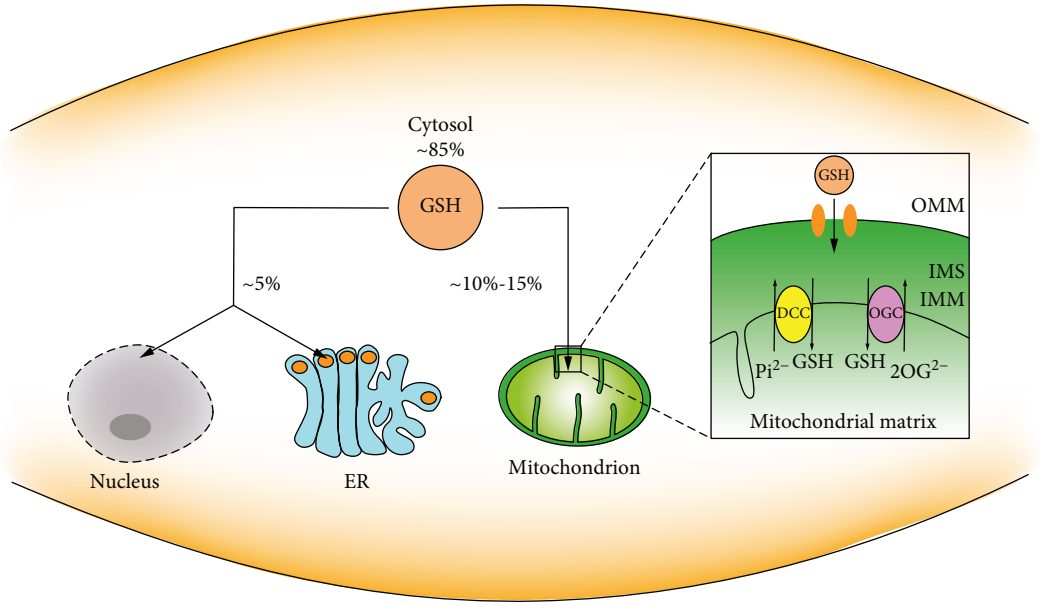

Figure 2: Distribution of intracellular GSH. GSH is distributed in the cytosol, nucleus, mitochondria, and ER.

[20]. The highly reduced GSH pool has also been found in a variety of species [21, 22]. The cytosol contains the largest GSH pool, which does not contradict its distribution of GSH in other subcellular organelles. Due to the lack of GS in subcellular compartmentation, GSH must be imported into the subcellular organelles from the cytosol.

2.2.2. Mitochondrial GSH. Mitochondria are coated by two membranes and separated into two spaces, the matrix surrounded by the inner mitochondrial membrane (IMM) and the intermembrane space (IMS) between the IMM and the outer mitochondrial membrane (OMM). Although the enzymes in these two separate chambers, the IMS and matrix, are not identical, each is providing NADPH and exchanging molecules through its mechanism. Mitochondria are the main sites for aerobic respiration and producing ROS, mainly $O_2^{\cdot-}$. Mn-dependent superoxide dismutase (MnSOD) reduces $O_2^{\cdot-}$ to H_2O_2, and the gradual accumulation of H_2O_2 further generates free radicals. In the mitochondria, catalase reduces H_2O_2 to H_2O and O_2 but due to the low catalase content, a certain amount of GSH is required to maintain the redox balance. During the oxidation of GSH to GSSG by glutathione peroxidase (GPX), H_2O_2 is reduced to H_2O, which can offset the H_2O_2 produced by MnSOD [23, 24].

The mitochondrial glutathione (mGSH) pool only accounts for 10%~15% of the total glutathione pool, and the internal glutathione is mainly present in a reduced state [25, 26]. Considering the mitochondrial volume, the concentration of mGSH per mitochondria is similar to that of cytosolic GSH and there is no concentration gradient in the mitochondrial inner membrane space. Mitochondria are not able to synthesize GSH as for lacking GS, but they can take up GSH from the cytosol [23]. GSH in the cytosol passes through the two layers of the OMM and IMM to reach the destination in the mitochondria. The monotonous uptake of GSH through the OMM is facilitated by the pore proteins, which allow molecules less than ~5 kDa to freely pass [27]. The concentration of small molecules in the IMS is equivalent to the concentration in the outer cytoplasm. Small molecules entering the IMS cannot penetrate into the mitochondrial matrix because of the different lipid composition between the IMM and OMM [28–30]. Since GSH exists in an anionic form at physiological pH [31], the task of GSH entering the mitochondrial matrix is borne by the two anion transporters localized on the IMM, dicarboxylate carrier (DCC), and 2-oxoglutarate carrier (OGC) [32]. DCC exchanges inorganic phosphate, Pi^{2-}, or OGC exchanges 2-oxoglutarate ($2\text{-}OG^{2-}$) when GSH enters the matrix [33]. These specialties in the IMM make it possible for GSH to transport into the mitochondria. Thus far, the exact mechanism of GSH transporting in mitochondria needs further verification.

2.2.3. Nucleus GSH. In spite of the minimal GSH concentration in the nucleus, studies have confirmed the important role of nuclear GSH in the cell cycle [16, 34, 35]. Cells that are ready for division have higher levels of nuclear GSH [13, 36]. Although there is no definitive proof for this mechanism, it cannot neglect the fact that GSH accumulates in the nucleus at an early stage of cell growth, and when the cells reach confluence, it is reuniformly distributed between the nucleus and the cytosol [34]. The study concerning the correlation between GSH and cell cycle may be helpful for us to better understand cell physiology and cellular metabolic processes.

Lower and medium levels of ROS are generally recognized as inducing mitosis and having beneficial effects in cell growth, while excessive ROS can cause DNA strand breaks, DNA mutations, and DNA double-strand aberrations, further leading to oxidative stress. The sulfhydryl group in GSH is essential in maintaining the status of DNA repair and expression in the nucleus [37]. In the process of

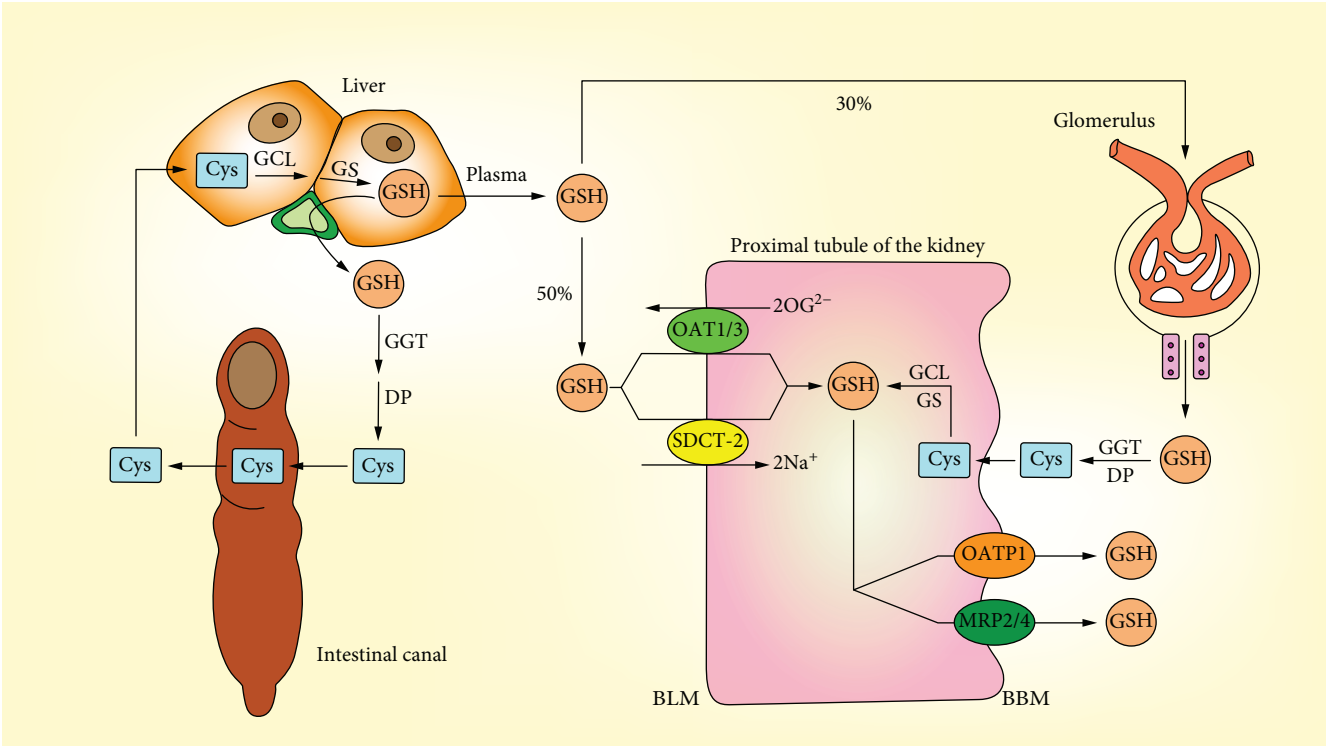

Figure 3: Transport of GSH. The liver is the main source of GSH, the kidney is the main organ that ingests and degrades GSH, and the small intestine participates in the GSH enterohepatic circulation. The renal proximal tubule is the place where the whole process of GSH transport, synthesis, and degradation is completed.

ribonucleic acid reduction, GSH acting as a donor of hydrogen catalyzes the reduction of ribonucleic acid to deoxyribonucleic acid, which plays a contributory role in DNA synthesis [38].

2.2.4. ER GSH. ER is interlaced in the cytoplasm and performs a variety of functions, including protein biosynthesis, folding, translocation, and glycosylation and formation of disulfide bonds [39]. The formation of disulfide bonds is the key process for the protein synthesis in ER and also benefits this highly oxidative environment. Accumulation of unfolded or misfolded proteins results in ER stress. The ER glutathione seems to be a special case where the oxidized form accounts for the most. The ratio of GSH : GSSG in ER is as high as 1~15 : 1 [40]. A highly oxidizing environment is a necessary condition for ER to perform its function [41]. Changes in the redox state of ER significantly affect the formation of disulfide bonds in which in this process, GSH is oxidized to GSSG.

2.3. GSH Transport. GSH in tissues is mainly derived from hepatocytes, which can only be synthesized in hepatocytes and cannot be degraded. Part of GSH is discharged to the blood through the transport proteins of the hepatocytes, and the other part is discharged to the bile through the bile duct [42, 43].

In mammalian tissues, the kidney is the main organ that takes up plasma GSH. 80% of GSH in the plasma is absorbed by the kidney, and 3/8 of them are rapidly decomposed by γ-glutamyltransferase (GGT) and dipeptidase (DP) which are located in the brush border membrane (BBM) of the renal tubule after glomerular filtration, and the amino acids absorbed by the renal cells are used to resynthesize proteins or GSH. In addition, the other 5/8 of GSH enters the renal tubule and is absorbed by the specific transporter on the basolateral plasma membrane (BLM) in the form of intact tripeptide [42, 44] (Figure 3). There are two main transporters that facilitate BLM to ingest GSH through a nonfiltering mechanism, and the difference between them is that whether or not they rely on Na^+ [31]. Organic anion transporter 1 (OAT1) and OAT3 can absorb GSH through exchanging 2-oxoglutarate (2OG). Probenecid and p-aminohippurate (PAH) are two classical inhibitors of OATs that significantly inhibit GSH uptake [45]. Dimethyl succinate (DMS) is a substrate of sodium-dicarboxylate 2 (SDCT2) which significantly inhibits the absorption of GSH by isolated proximal tubule cells [46]. The stoichiometry of Na^+-GSH cotransportation indicates that at least two Na^+ couplings are required for absorption per GSH molecule during transport through the SDOT-2 carrier [31].

The process of the GSH outflow in BBM is important for the overall GSH transport. Through the study on the vesicles isolated from the rat kidney cortex, it can be concluded that GSH transport in BBM is a process that is dependent on membrane potential. Unlike GSH transport through BLM, ion coupling is not involved in GSH transport through BBM [47]. Although there is still no evidence to prove the exact vectors that play the direct role in the GSH transport

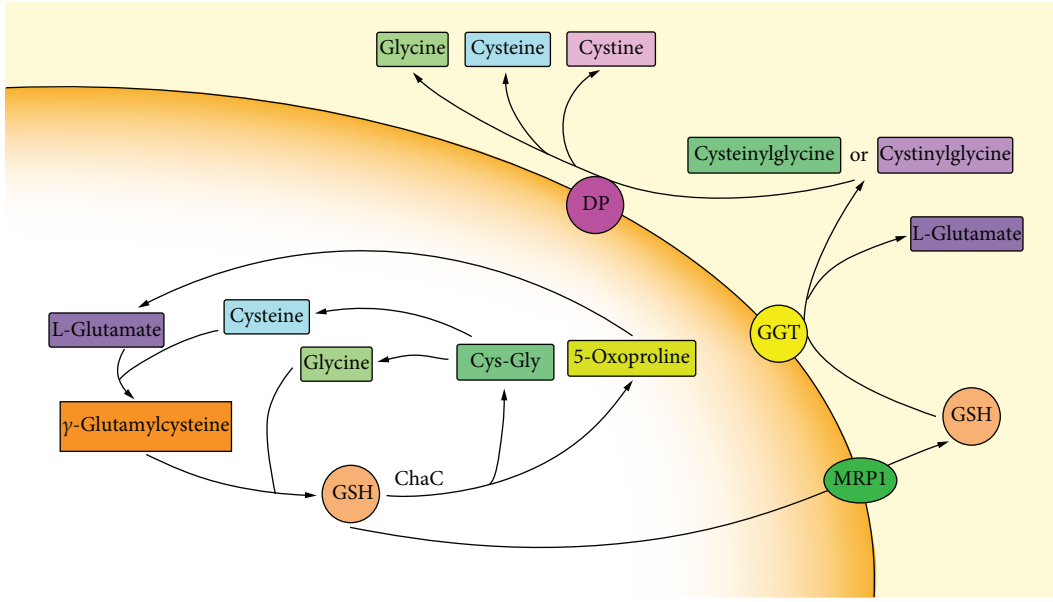

Figure 4: Two degradation pathways of GSH. One way occurs outside the cell where GSH is degraded by γ-glutamyltransferase (GGT) which is expressed only on the outer surface of particular cell; the other newly discovered pathway occurs in the cytoplasm where GSH is degraded through ChaC1 and ChaC2.

through BBM, it can lead to assumptions based on existing knowledge. There are two types of transporters that contribute to GSH transport [48]. One of the currently more convincing vectors is the organic anion-transporting polypeptide 1 (OATP1), which is expressed in the sinusoidal membrane and demonstrated to transport GSH [49]. Another type of vector that may play a role in the GSH efflux process is multidrug resistance proteins (MRPs) [50]. GSH excreted to the bile is hydrolyzed by GGT and DP on the surface of bile duct epithelial cells or small intestinal epithelial cells. The cysteine produced by hydrolysis can be reused by the small intestine to synthesize GSH and participate in the enterohepatic circulation.

2.4. GSH Metabolism. The structure of GSH is unique in the condensation of glutamate and cysteine producing a γ-carboxyl group rather than the usual α-carboxyl group. Most enzymes cannot hydrolyze γ-carboxyl groups. GGT is the only enzyme expressed on a specific cell surface that is capable of hydrolyzing this particular group [51]. GSH transported by the cell reaches to the GGT active site and is degraded to L-glutamate and cysteinylglycine or cystinylglycine and is then released as glutamate, cysteine, cystine, and glycine under the catalysis of DP. These single amino acids or dipeptides are taken up by the cells to complete the synthesis of GSH (Figure 4).

New pathways for GSH metabolism have also been discovered in recent years. Unlike GGT, the newly discovered ChaC family can enzymatically degrade GSH localized to the cytoplasm [52, 53]. ChaC1 is discovered in bacterial BtrG proteins and mammalian γ-GCT proteins, which hydrolyze GSH to produce cysteinyl-free Cys-Gly and 5-oxoproline [54]. It is worth noting that ChaC1 only works on reduced GSH. ChaC2 is another member of the ChaC family, which is found in E. *coli*, yeast, and humans. Its specificity for GSH is similar to that of ChaC1, producing 5-oxoproline and Cys-Gly. Enzyme kinetic studies showed that the catalytic activity of the two was significantly different. The efficiency of the ChaC2 enzyme in degrading GSH was 1/20~1/10 times higher compared to that of the ChaC1 enzyme [55]. GSH metabolism plays a key role in maintaining GSH homeostasis, nutrient recycling and recovery, and signal transduction.

3. Antioxidant Role of Cellular GSH

ROS is a product of normal cellular metabolism and involved in physiological and biochemical processes. Therefore, balancing the generation and elimination of ROS to maintain the favorable physiological and suitable environment is of great importance [56]. Oxidative stress is caused when the normal oxidation/antioxidant equilibrium state is destroyed. In general, cells are able to cope with mild oxidative stress, while the severe oxidative stress beyond the cell antioxidant capacity can cause damage to lipids, proteins, and DNA, even leading to cell death. There are two main possible strategies to inducing oxidative stress: one is to directly increase the level of ROS and the other is to impair the antioxidant defense system. The GSH system is one of the important antioxidant defense lines against ROS (Figure 5).

Maintenance of cellular redox balance is essential for cell fate. The cellular redox state is often referred to the balance of NAD^+/NADH, $NADP^+$/NADPH, and GSH/GSSG [57]. Among those redox-balancing partners, the two forms of glutathione can be interconverted by enzyme catalysis. Under normal physiological conditions, the vast majority of glutathione is the reduced form. Mitochondria are sites of cellular oxidative respiration, in which ROS are produced by enzymatic or nonenzymatic reactions [58]. Although

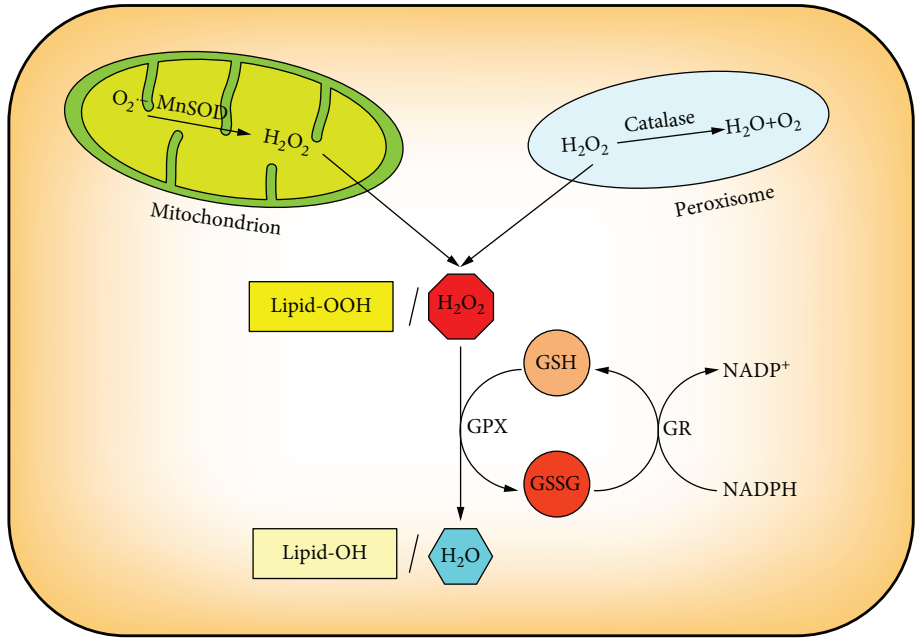

Figure 5: The antioxidant role of cellular GSH. Glutathione peroxidase (GPX) converts H_2O_2 and Lipid-OOH to H_2O and Lipid-OH where GSH is oxidized to GSSG, and glutathione reductase (GR) reduced GSSG to GSH dependent on NADPH, thereby forming a redox cycle to prevent oxidative damage.

mGSH accounts for only 10%~15% of the total GSH, its role as an antioxidant cannot be ignored. H_2O_2 is a product of aerobic metabolism and is primarily reduced by glutathione peroxidase (GPX) in which in this process, GSH is oxidized to GSSG. GPX is an important peroxide-degrading enzyme. It can catalyze the conversion of GSH to GSSG, reduce toxic peroxides to nontoxic hydroxyl compounds, and promote the decomposition of H_2O_2, thereby protecting the structure and function of cell membranes from peroxide interference and damage. GSSG is then reduced to GSH by glutathione reductase (GR) which is associated with NADPH which is oxidized to $NADP^+$, thereby forming a redox cycle to prevent oxidative damage [20]. At the same time, GPX reduces lipid peroxides (Lipid-OOH) to nontoxic lipid alcohols (Lipid-OH) with GSH as a substrate. This cycle of mutual transformation enables the continuous elimination of free radicals in the cells [7].

4. Role of GSH in Programmed Cell Death

Cancer cells exhibit a higher ROS level and also develop a greater GSH antioxidant system in order to avoid causing oxidative stress. Programmed cell death, including apoptosis, autophagy, necroptosis, and ferroptosis, is initiated by serials of intracellular programs [59]. In some cases, GSH depletion not only triggers one form of programmed cell death but also may initiate multiple forms of cell death. These different forms of cell death may be simultaneously or successively initiated and then interact with each other, and finally, one cell death form may mainly exist [60].

4.1. GSH and Apoptosis. Apoptosis is the most recognized form of programmed cell death which is initiated and executed by the caspase family. It is a genetically controlled and actively cascading cell death process that is characterized by membrane shrinkage, chromatin condensation, and formation of apoptotic bodies [61]. Studies have shown that the GSH/GSSG redox status is an important indicator of apoptosis in cancer cells. Apoptosis is consistently associated with a reduction in the GSH/GSSG ratio [62]. The decrease in GSH impairs the antioxidant system and leads to the increase in ROS generation which accelerates mitochondrial damage and induces apoptosis (Figure 6).

Intracellular GSH loss precedes the destruction of mitochondrial integrity, cytochrome c release, and caspase activation and is recognized as an early event in the progression of apoptosis in response to different stimuli. GSH depletion occurs in both intrinsic apoptosis and extrinsic apoptosis [63, 64]. A decline in GSH induced ROS generation and the release of cytochrome c, following depletion of the mitochondrial GSH level and caspase 3 activation [65]. Cellular GSH exported into the extracellular space is also demonstrated in the initiation of apoptotic signaling or promotion of apoptotic progression [66]. Cancer cells undergoing apoptosis release a large amount of intracellular GSH into the extracellular environment [67]. Reducing GSH efflux in the apoptotic process could attenuate cell death. Contrarily, stimulation of GSH synthesis could efficiently protect mitochondrial membrane potential loss and inhibit apoptosis [68]. In addition, the exogenous supply with N-acetyl-L-cysteine (NAC) restores the cellular GSH level and prevents the GSH depletion-induced apoptosis [69].

The elevated level of ROS and mGSH/GSSG imbalance can stimulate the intrinsic apoptosis pathway. Impairment of GSH uptake to the mitochondria directly affects the mitochondrial function. Depletion of mGSH leads to the

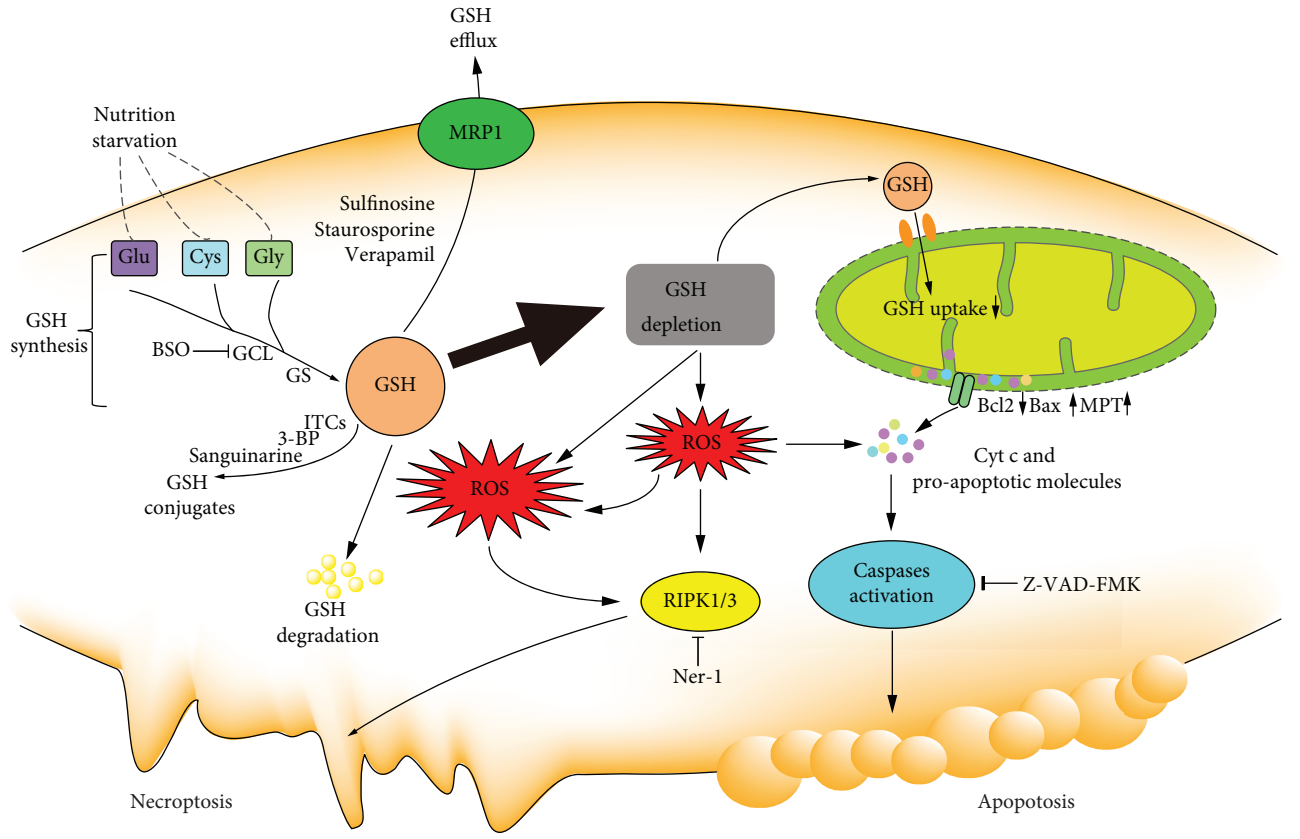

FIGURE 6: The role of cellular GSH in apoptosis and necroptosis. GSH depletion through nutrition starvation or GSH synthesis inhibition or conjugation with GSH or GSH efflux or GSH degradation induces ROS generation which results in the occurrence of proapoptotic signals, such as the disruption of MMP, increased bax, decreased bcl2, cytochrome c release, and caspase activation. Excess ROS accumulation induces necroptosis.

instability of the mitochondrial structure and release of proapoptotic proteins from the outer mitochondrial membrane [70]. The stimuli cause mitochondrial membrane permeabilization through mitochondrial permeability transition (MPT) opening or pores formed by bax and bcl2, resulting in apoptosis-inducing factor release, apoptosome complex formation, and caspase activation [71–73].

4.2. GSH and Necroptosis. Although necrosis is originally thought to be a passive and unregulated form of cell death, studies have shown that some form of necrosis can be regulated by intracellular proteins, which is also termed as necroptosis [74, 75]. Necroptosis is an alternative form of programmed cell death with distinct characters in the mitochondria, lysosome, and plasma membrane, exhibiting a translucent cytoplasm, swelling organelles, increased cell volumes, and disruption of the plasma membrane [76, 77]. Necroptosis could be initiated in a way that is similar to extrinsic apoptosis. Receptor-interacting protein kinases 1 (RIPK1) and 3 (RIPK3) are two key regulators involved in the execution of necroptosis. GSH depletion by pharmacological inhibition causes oxidative stress-induced necroptosis [78]. Necrostatin-1, an inhibitor of RIPK1, can protect cell from GSH depletion inducing cell death in HT-22 cells through inhibition on GCL [79]. Artesunate triggers necroptosis by decreasing the GSH/GSSG ratio and increasing ROS generation in human renal carcinoma cells which can be reduced by necrostatin-1 or knockdown of *RIPK1* [80]. To our knowledge, an excess level of ROS induces apoptosis, while massive ROS may lead to necroptosis. GSH depletion-induced ROS generation can simultaneously induce apoptosis and necrosis in cancer cells in some cases (Figure 6). Dimethyl fumarate (DMF) induced typical features of necroptosis-like excessive autophagy, disintegration of mitochondrial membrane potential, LDH release, and accumulation of ROS in colon cancer cells by depleting the cellular GSH level [81]. GSH depletion by cystine starvation or the GSH degradation results in oxidative stress which leads to necroptosis and ferroptosis by directly oxidizing lipids [82].

4.3. GSH and Ferroptosis. Ferroptosis, a kind of programmed cell death, is morphologically, biochemically, and genetically different from other well-known forms of cell death [83]. The characterized features of ferroptosis are iron dependent, GPX4 inactivation, and lipid ROS accumulation [84]. Ferroptosis can be induced by small molecules or GSH biosynthesis inhibitions or GPX4 impairment or some physiological conditions [85] (Figure 7). Cysteine starvation and further GSH depletion cooperate to elevate lipid ROS. Cystine deprivation induced GSH efflux and extracellular degradation for balancing the intracellular cysteine level

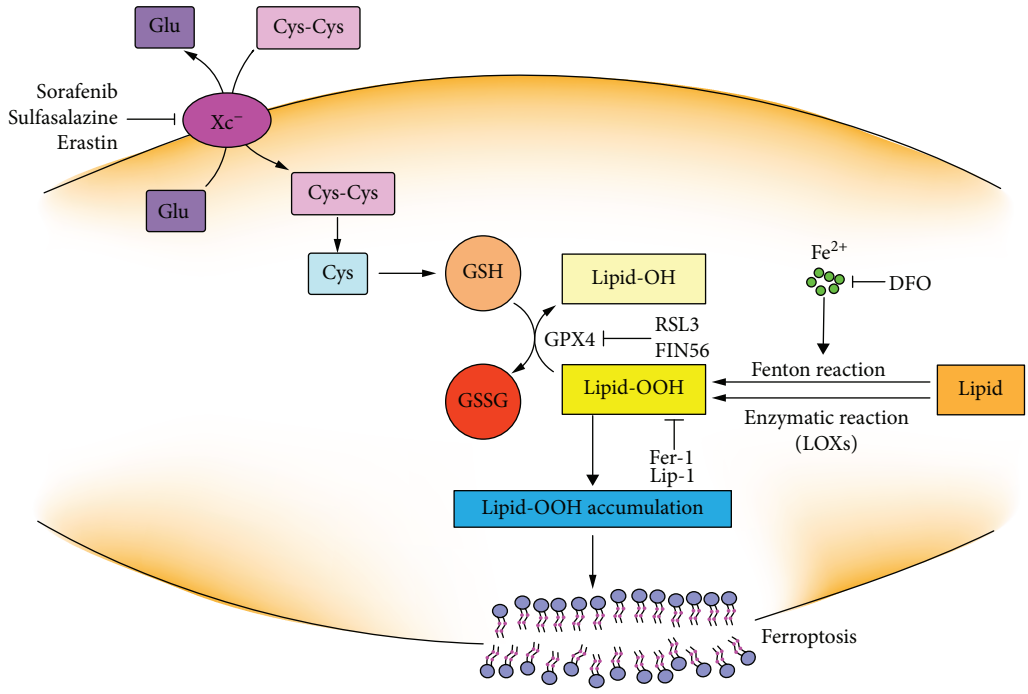

Figure 7: The mechanism of GSH depletion in induction of ferroptosis. Lipid-OOHs can be formed by autoxidation via Fenton reaction or by enzymatic reaction via lipoxygenases (LOXs). Lipid-OOHs are regulated by the balance between the activities of GPX4 and LOXs or Fenton reaction. System X_c^- impairment or GPX4 inactivation leads to Lipid-OOH accumulation which cannot be effectively cleared under the loss of GPX4 activity. Ultimately, the accumulation of Lipid-OOH triggers ferroptosis. Ferroptosis can be inhibited by DFO, liproxstatin-1 (Lip-1), and ferrostatin-1 (Fer-1).

[86]. GSH depletion through inhibition on cystine uptake is essential for erastin-induced ferroptosis. Additionally, the knockout of *GCL* could sensitize cells to ferroptosis induced by cysteine starvation [87]. Erastin treatment impairs the antioxidant defenses of the cell by indirectly inactivating GPX4 activity resulting in the increase in the cytoplasmic ROS and lipid ROS accumulation.

GPX4 can convert Lipid-OOH to nontoxic Lipid-OH. GPX4 reduced Lipid-OOH using GSH as a cosubstrate. Pharmacological inhibition or genetical depletion of *GPX4* promotes lipid ROS generation or, what is more, is lethal, while upregulation of *GPX4* can diminish lipid ROS [88–90]. Lipid-OOH formation and membrane damage are sufficient inducers in ferroptosis [91]. RSL3 is identified as a small molecule that enhances the lethality toward oncogene-harboring cancer cells by increasing oxidative stress through altering the iron regulatory proteins and genes [92]. Afterwards, RSL3 is proved to be a ferroptosis inducer by covalently targeting the active site of selenocysteine of GPX4 and resulting in the accumulation of lipid ROS. But the mechanism of RSL3-induced ferroptosis is not by depleting GSH but by inactivating GPX4. *GPX4* silence sensitizes cells to RSL3-induced ferroptosis which is accompanied by lipid ROS accumulation [93]. Consequently, direct inactivation of GPX4 can also induce ferroptotic cell death even when cellular cysteine and GSH levels are normal. FIN 56 is a special inducer of ferroptosis that can cause a slower accumulation of ROS as for the downregulation of GPX4 protein abundance [94]. Together, all these types of small molecules can induce ferroptosis by different modulatory profiles, while ultimately, all of them cause the loss of GPX4 activity and generation of lipid ROS. Therefore, it can conclude that GPX4 is the key regulator of ferroptosis and the GSH antioxidant system plays a central role in the regulation of ferroptosis [90, 95].

Ferroptotic oxidative signals are mainly produced by iron-mediated Fenton reaction or enzymatic reaction via lipoxygenases (LOXs) or when the GSH antioxidant system is impaired [96, 97]. GSH deficiency or GPX4 inactivation in inducing ferroptosis involves the enhanced production of oxygenated phosphatidylethanolamine (PE) species [98]. Suppression on the formation of oxygenated PE species can inhibit ferroptosis [99]. Depletion of GSH through the inhibiting system X_c^- induces ferroptosis that could be prevented by liproxstatin-1 (Lip-1), ferrostatin-1 (Fer-1), and iron chelator deferoxamine (DFO) [83, 100, 101].

4.4. GSH and Autophagy. Autophagy is a catabolic process by degrading cytoplasmic constituents or impaired organelles in autolysosomes for recycling under stress condition. Autophagy has long been considered a cell protective mechanism, while excessive autophagy can also trigger cell death and be regarded as a tumor suppressive mechanism [102, 103].

Growing evidence supports the role of ROS in the regulation of autophagy, but evidence about the mechanism and interplay between GSH and the initiation and promotion of autophagy is still elusive [104]. GSH, one of the principal molecules in the thiol network, has been indicated as the suspect for induction of autophagy [105]. The low level of GSH acts as a signal to activate autophagy as an adaptive

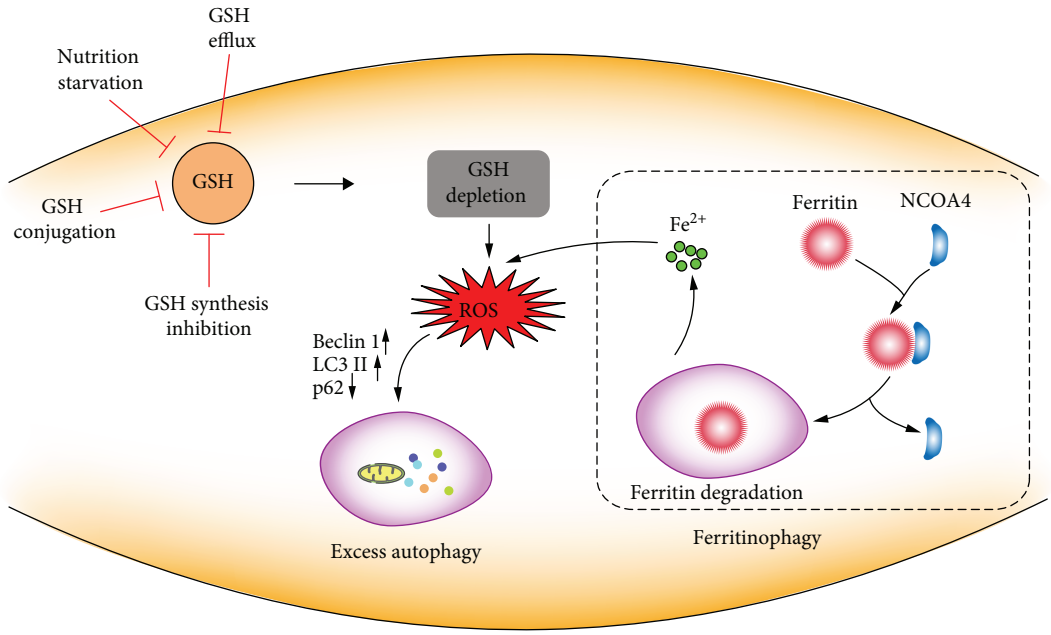

Figure 8: The role of cellular GSH in autophagy. GSH depletion through nutrition starvation or GSH synthesis inhibition or conjugation with GSH or GSH efflux induces ROS generation. ROS accumulation promotes changes in autophagy-related proteins, such as LC3 I/II conversion, p62 degradation, and autophagic vacuole formation. Additionally, ROS induce NCOA4-mediated ferritin degradation in an autophagy process, called ferritinophagy, which is promoting free iron release and accelerating ROS generation.

stress response [106, 107]. The ways that modulate the intracellular GSH state can drive autophagic response at multiple levels (Figure 8). The dysfunction of system X_c^- by pharmacologic inhibition (sulfasalazine) causes GSH decrease and ROS generation and triggers autophagic cell death [108]. Nutrition starvation can result in the modulation of the cellular GSH content which is mediated by GSH extrusion, GCL inhibition, and the formation of GS-R [109]. Under the GSH depletion case, H_2O_2 induced autophagic cell death with increased LC3 conversation and p62 degradation and enhanced autophagic vacuole formation [110]. Together, the decreased cellular GSH level contributes to autophagy and affects the autophagic process. Overall, the possible relationship between GSH and autophagy still deserves to be further investigated.

Ferroptosis is a form of cell death that is dependent on the induction of the autophagic process via a form of cargo-specific autophagy known as ferritinophagy [111]. Autophagy plays a decisive role in the degradation of cytosolic proteins. The impaired autophagic process can induce protein accumulation [112]. The proper function of lysosomes plays an essential role in ferroptotic cell death [113]. The activity of lysosomes is increased in ferroptosis in order to enhance chaperone-mediated autophagy to degrade GPX4 [114]. Inhibition of lysosomal function by bafilomycin A1 (BalfA1) and chloroquine (CQ) can significantly delay the ferroptosis process induced by erastin [115]. Autophagy flux is associated with ferroptosis for promoting the turnover of ferritin in erastin-treated cancer cells [116]. Ferritin degradation is dependent on autophagy where nuclear receptor coactivator 4 (NCOA4) acts as a cargo receptor targeting ferritin to autophagosome [117–119]. Dihydroartemisinin (DHA) induced ferroptosis in acute myeloid leukemia cells through activating the autophagy process with decreased GSH, ferritin degradation, and labile iron accumulation [120]. The exact mechanism of the connection between autophagy and ferroptosis still remains largely unknown.

5. GSH Depletion as a Means of Cancer Therapy

A relationship between the increased GSH level and resistance to chemotherapies was observed in many cancers [121]. Impairment in the GSH antioxidant defense system could sensitize cancer cells to current chemotherapeutics. It suggested that the moderate decline in the GSH level would be an effective strategy to improve the sensitivity of cancer cells to chemotherapies. Therefore, depletion of cellular GSH in cancer cells will make them more susceptible and sensitive to oxidative stress and chemotherapies. Cysteine insufficiency or glutamate sufficiency or pharmacological and genetic inhibition of system X_c^- can reduce the resistance of cancer cells to chemotherapies [122]. GSH depletion promotes cancer cell undergoing different forms of programmed cell death, such as apoptosis, necroptosis, autophagy, and ferroptosis. Ways for depleting the cellular GSH level to induce oxidative stress include the following: creation of the source shortage for GSH synthesis, inhibition of the GSH synthesis process, direct conjugation with GSH, and promotion of cellular GSH efflux [123–126].

5.1. Inhibition on System X_c^-. Cysteine is the main source for protein synthesis. Undoubtedly, it is of critical importance for maintaining the GSH level. Cysteine typically presents in its oxidized form in the extracellular space and can be

taken up into the intracellular space via a system X_c^- antiporter. System X_c^-, consisting of SLC3A2 (4F2, solute carrier family 3, membrane 2) and SLC7A11 (xCT, solute carrier family 7, membrane 11), forms as a glutamate/cysteine antiporter in the cell membrane [127]. xCT is the light chain of system X_c^-. Elevated expression of xCT has been demonstrated in many types of cancer and is related to chemoresistance and poor prognosis in cancer patients [128–133].

A reduction in the uptake of extracellular cysteine can directly cause intracellular GSH depletion. Inhibition on xCT expression triggers cysteine starvation and subsequently induces cell growth arrest in cancer cells. Stabilization of xCT promotes the uptake of cysteine for GSH synthesis and protects cancer cells from high levels of ROS [134]. Therefore, regulation of xCT is considered a promising therapeutic target for cancer therapy [135]. Pharmacological inhibition of system X_c^- inhibits cancer cells *in vitro* and delays tumor growth *in vivo*. Disruption on xCT function inhibits cell invasion and tumor metastasis [136]. The inhibitory effects on cancer cells can be ascribed for the rapid depletion of GSH by xCT dysfunction and subsequently increase in ROS generation.

Erastin is an inhibitor of system X_c^- that can lead to the depletion of GSH [83]. GSH-depleting effects of erastin could be reversed by supplying with GSH and N-acetylcysteine (NAC). Imidazole ketone erastin (IKE), a carbonyl erastin analogue, also exhibits system X_c^- inhibition activity and displays more potency to selective lethality to cancer cells than erastin [137]. Sorafenib promotes ferroptosis in HCC cells by its ability to inhibit system X_c^- and deplete GSH [101]. Sorafenib can also potentiate cisplatin cytotoxicity in resistant head and neck cancer cells through the inhibitory effect on xCT [138]. Sulfasalazine is an anti-inflammatory drug which can be used for the treatment of inflammatory bowel disease and rheumatoid arthritis and is also proved to be a potent inhibitor of system X_c^-. It can sensitize cancer cells not only to chemotherapies but also to radiotherapies [139–141]. Pseudolaric acid B, a natural diterpene acid isolated from the root and bark of *Pseudolarix kaempferi*, can trigger ferroptosis in glioma cells by depleting cellular GSH through inhibition of xCT [142, 143].

5.2. Inhibition on GCL. γ-GCL plays a key role in the synthesis and maintenance of the cellular GSH level. It is the first and rate-limiting enzyme in GSH synthesis consisting of the GCLC catalytic subunit and GCLM modifier subunit [144]. Overexpression of GCL increases the cellular GSH level, and cells exhibit more resistance to oxidative stress [145]. Adrenomedullin induces the expression of *GCLC* and protects cells against oxidative stress [146]. On the contrary, knockdown of *GCLC* could elevate the cellular ROS level [147]. L-Buthionine-(S,R)-sulfoximine (BSO) is an inhibitor of γ-GCL. It has been shown to increase the efficacy of nifurtimox against cancer cells and be an effective modulator of GSH-mediated chemoresistance by increasing the *in vitro* cytotoxicity of alkylating agents and radiation [148].

5.3. Conjugation with GSH. The most direct strategy to deprive GSH is to react with it. Some natural molecules exhibit good affinity to GSH. Sanguinarine directly reacts with cellular GSH and causes a rapid and sever depletion of GSH. It results in the subsequent modification of the membrane integrity and relates to a promotion of apoptotic response dependent on caspase 3 and caspase 7 activation in PC3 human prostatic adenocarcinoma cells [149]. 3-Bromopyruvate (3-BP), an alkylating agent, has high reactivity toward thiols and rapidly conjugates with GSH in the cell-free system and many cell types [150, 151]. It has been proved to have antitumor activities [152, 153]. Isothiocyanates (ITCs) are natural phytochemicals abundantly existing in cruciferous vegetables. The central carbon of the ITCs is highly electrophilic and can react with thiols. At physiological pH, ITCs react predominantly with the sulfhydryl group of cysteine residues in GSH. Accumulative evidence has proved that ITCs, such as sulforaphane (SFN), phenethyl isothiocyanate (PEITC), and ally isothiocyanate (AITC), are highly effective in chemoprevention and have antitumor activities *in vitro* and *in vivo* [154–158]. PEITC exhibits potential ability against not only solid tumor but also leukemia cells through the rapid deprive of mitochondrial GSH and elevation of ROS [70, 159].

5.4. Enhancement of GSH Efflux. The development of the multidrug resistance (MDR) phenotype poses as a major clinical problem that limits the curative potential of anticancer drugs. The characterized phenotype of MDR is the typically increased expressions of P-glycoprotein (P-gp) and MRPs. P-gp and MRPs can extrude anticancer agents out of cell consuming ATP and result in the chemotherapy failure. Inhibition of MRPs could reduce drug resistance in cancer cells, and MRPs act as a potential target in cancer therapy. MRP-1 is identified as a GSSG transporter. Evidence has shown that inhibition on MRP activity promotes the accumulation of GSSG which is cytotoxic to endothelial cell tumors [160]. Sulfinosine has the potential to induce apoptosis and autophagy by decreasing GSH, generating ROS, and inhibiting P-pg and then sensitizes cancer cells to chemotherapies [161]. Modulation of GSH efflux is also a potential strategy to induce cell death in cancers. Staurosporine causes apoptosis in cancer cells associated with exporting cellular GSH [162]. Cancer cells are sensitized to cell death when intracellular GSH is depleted through stimulation of GSH efflux pumps [163]. Natural compound chrysin induces GSH efflux by MRPs to maintain the depleted GSH level and sensitizes cancer cells to chemotherapeutic agents like doxorubicin [164]. Verapamil derivatives can effectively kill cancer cell through leading to apoptosis with the mechanism of stimulating GSH efflux by MRPs [126].

6. Conclusions

In this review, accumulative evidence has demonstrated the important role of GSH depletion in the initiation of multiple forms of programmed cell death in cancers and we have highlighted the GSH-based strategies for cancer therapies. As mentioned, some agents trigger not only one type of programmed cell death solely but also multiple forms of cell death simultaneously through altering cellular GSH in cancer

cells. While the crosstalks and interrelationships between the multiple forms of cell death induced by GSH modulation in cancer cells are still elusive, the exact death events along with GSH depletion in inducing cell death are still needed to be further explored. In the future work, a better understanding on the mechanism of GSH in triggering different forms of programmed cell death and whether GSH has a role in deciding cell fate will give more implications on the redox-based research concerning cancer therapeutics.

Conflicts of Interest

The authors declare no conflict of interest.

Authors' Contributions

Huanhuan Lv, Chenxiao Zhen, and Junyu Liu contributed equally.

Acknowledgments

This work was supported by the National Natural Science Fund of China (No. 81803032, No. 11872316, and No. 51777171), the Fundamental Research Funds for the Central Universities (No. 3102017OQD111), and the Northwestern Polytechnical University Foundation for Fundamental Research (No. 3102018JGC012).

References

[1] A. Meister and M. E. Anderson, "Glutathione," *Annual Review of Biochemistry*, vol. 52, no. 1, pp. 711–760, 1983.

[2] G. Wu, Y. Z. Fang, S. Yang, J. R. Lupton, and N. D. Turner, "Glutathione metabolism and its implications for health," *The Journal of Nutrition*, vol. 134, no. 3, pp. 489–492, 2004.

[3] H. Sies, "Glutathione and its role in cellular functions," *Free Radical Biology and Medicine*, vol. 27, no. 9-10, pp. 916–921, 1999.

[4] J. N. Moloney and T. G. Cotter, "ROS signalling in the biology of cancer," *Seminars in Cell & Developmental Biology*, vol. 80, pp. 50–64, 2018.

[5] S. Galadari, A. Rahman, S. Pallichankandy, and F. Thayyullathil, "Reactive oxygen species and cancer paradox: to promote or to suppress?," *Free Radical Biology and Medicine*, vol. 104, pp. 144–164, 2017.

[6] M. L. Circu and T. Y. Aw, "Reactive oxygen species, cellular redox systems, and apoptosis," *Free Radical Biology and Medicine*, vol. 48, no. 6, pp. 749–762, 2010.

[7] N. Traverso, R. Ricciarelli, M. Nitti et al., "Role of glutathione in cancer progression and chemoresistance," *Oxidative Medicine and Cellular Longevity*, vol. 2013, Article ID 972913, 10 pages, 2013.

[8] P. T. Schumacker, "Reactive oxygen species in cancer: a dance with the devil," *Cancer Cell*, vol. 27, no. 2, pp. 156-157, 2015.

[9] E. Hatem, N. el Banna, and M. E. Huang, "Multifaceted roles of glutathione and glutathione-based systems in carcinogenesis and anticancer drug resistance," *Antioxidants & Redox Signaling*, vol. 27, no. 15, pp. 1217–1234, 2017.

[10] M. E. Anderson, "Glutathione: an overview of biosynthesis and modulation," *Chemico-Biological Interactions*, vol. 111-112, pp. 1–14, 1998.

[11] T. P. Dalton, Y. Chen, S. N. Schneider, D. W. Nebert, and H. G. Shertzer, "Genetically altered mice to evaluate glutathione homeostasis in health and disease," *Free Radical Biology and Medicine*, vol. 37, no. 10, pp. 1511–1526, 2004.

[12] S. C. Lu, "Glutathione synthesis," *Biochimica et Biophysica Acta (BBA) - General Subjects*, vol. 1830, no. 5, pp. 3143–3153, 2013.

[13] P. Diaz Vivancos, T. Wolff, J. Markovic, F. V. Pallardó, and C. H. Foyer, "A nuclear glutathione cycle within the cell cycle," *Biochemical Journal*, vol. 431, no. 2, pp. 169–178, 2010.

[14] K. BRIVIBA, G. Fraser, H. Sies, and B. Ketterer, "Distribution of the monochlorobimane-glutathione conjugate between nucleus and cytosol in isolated hepatocytes," *Biochemical Journal*, vol. 294, no. 3, pp. 631–633, 1993.

[15] T. Söderdahl, M. Enoksson, M. Lundberg et al., "Visualization of the compartmentalization of glutathione and protein-glutathione mixed disulfides in cultured cells," *Journal of Biological Chemistry*, vol. 281, pp. 6372–6379, 2003.

[16] P. Diaz-Vivancos, A. de Simone, G. Kiddle, and C. H. Foyer, "Glutathione – linking cell proliferation to oxidative stress," *Free Radical Biology and Medicine*, vol. 89, pp. 1154–1164, 2015.

[17] M. J. Meredith and D. J. Reed, "Status of the mitochondrial pool of glutathione in the isolated hepatocyte," *The Journal of Biological Chemistry*, vol. 257, no. 7, pp. 3747–3753, 1982.

[18] C. Hwang, A. Sinskey, and H. Lodish, "Oxidized redox state of glutathione in the endoplasmic reticulum," *Science*, vol. 257, no. 5076, pp. 1496–1502, 1992.

[19] B. Morgan, D. Ezeriņa, T. N. E. Amoako, J. Riemer, M. Seedorf, and T. P. Dick, "Multiple glutathione disulfide removal pathways mediate cytosolic redox homeostasis," *Nature Chemical Biology*, vol. 9, no. 2, pp. 119–125, 2013.

[20] S. C. Lu, "Regulation of glutathione synthesis," *Molecular Aspects of Medicine*, vol. 30, no. 1-2, pp. 42–59, 2009.

[21] B. Morgan, "Reassessing cellular glutathione homoeostasis: novel insights revealed by genetically encoded redox probes," *Biochemical Society Transactions*, vol. 42, no. 4, pp. 979–984, 2014.

[22] A. J. Meyer, T. Brach, L. Marty et al., "Redox-sensitive GFP in arabidopsis thaliana is a quantitative biosensor for the redox potential of the cellular glutathione redox buffer," *The Plant Journal*, vol. 52, no. 5, pp. 973–986, 2007.

[23] G. Calabrese, B. Morgan, and J. Riemer, "Mitochondrial glutathione: regulation and functions," *Antioxidants & Redox Signaling*, vol. 27, no. 15, pp. 1162–1177, 2017.

[24] M. Marí, A. Morales, A. Colell, C. García-Ruiz, and J. C. Fernández-Checa, "Mitochondrial glutathione, a key survival antioxidant," *Antioxidants & Redox Signaling*, vol. 11, no. 11, pp. 2685–2700, 2009.

[25] L. H. Lash, T. M. Visarius, J. M. Sall, W. Qian, and J. J. Tokarz, "Cellular and subcellular heterogeneity of glutathione metabolism and transport in rat kidney cells," *Toxicology*, vol. 130, no. 1, pp. 1–15, 1998.

[26] R. G. Schnellmann, S. M. Gilchrist, and L. J. Mandel, "Intracellular distribution and depletion of glutathione in rabbit renal proximal tubules," *Kidney International*, vol. 34, no. 2, pp. 229–233, 1988.

[27] K. Kojer, M. Bien, H. Gangel, B. Morgan, T. P. Dick, and J. Riemer, "Glutathione redox potential in the mitochondrial intermembrane space is linked to the cytosol and impacts the

Mia40 redox state," *The EMBO Journal*, vol. 31, no. 14, pp. 3169–3182, 2012.

[28] T. Becker, M. Gebert, N. Pfanner, and M. van der Laan, "Biogenesis of mitochondrial membrane proteins," *Current Opinion in Cell Biology*, vol. 21, no. 4, pp. 484–493, 2009.

[29] T. Tatsuta, M. Scharwey, and T. Langer, "Mitochondrial lipid trafficking," *Trends in Cell Biology*, vol. 24, no. 1, pp. 44–52, 2014.

[30] S. Cogliati, J. A. Enriquez, and L. Scorrano, "Mitochondrial cristae: where beauty meets functionality," *Trends in Biochemical Sciences*, vol. 41, no. 3, pp. 261–273, 2016.

[31] L. H. Lash, "Role of glutathione transport processes in kidney function," *Toxicology and Applied Pharmacology*, vol. 204, no. 3, pp. 329–342, 2005.

[32] L. H. Lash, "Mitochondrial glutathione transport: physiological, pathological and toxicological implications," *Chemico-Biological Interactions*, vol. 163, no. 1-2, pp. 54–67, 2006.

[33] Z. Chen, D. A. Putt, and L. H. Lash, "Enrichment and functional reconstitution of glutathione transport activity from rabbit kidney mitochondria further evidence for the role of the dicarboxylate and 2-oxoglutarate carriers in mitochondrial glutathione transport," *Archives of Biochemistry and Biophysics*, vol. 373, no. 1, pp. 193–202, 2000.

[34] J. Markovic, C. Borras, A. Ortega, J. Sastre, J. Vina, and F. V. Pallardo, "Glutathione is recruited into the nucleus in early phases of cell proliferation," *Journal of Biological Chemistry*, vol. 282, no. 28, pp. 20416–20424, 2007.

[35] P. D. Vivancos, Y. Dong, K. Ziegler et al., "Recruitment of glutathione into the nucleus during cell proliferation adjusts whole-cell redox homeostasis in Arabidopsis thaliana and lowers the oxidative defence shield," *The Plant Journal*, vol. 64, no. 5, pp. 825–838, 2010.

[36] A. Holmgren, "Hydrogen donor system for Escherichia coli ribonucleoside-diphosphate reductase dependent upon glutathione," *Proceedings of the National Academy of Sciences of the United States of America*, vol. 73, no. 7, pp. 2275–2279, 1976.

[37] M. Valko, D. Leibfritz, J. Moncol, M. T. D. Cronin, M. Mazur, and J. Telser, "Free radicals and antioxidants in normal physiological functions and human disease," *The International Journal of Biochemistry & Cell Biology*, vol. 39, no. 1, pp. 44–84, 2007.

[38] A. Holmgren, "The function of thioredoxin and glutathione in deoxyribonucleic acid synthesis," *Biochemical Society Transactions*, vol. 5, no. 3, pp. 611-612, 1977.

[39] M. Wang and R. J. Kaufman, "Protein misfolding in the endoplasmic reticulum as a conduit to human disease," *Nature*, vol. 529, no. 7586, pp. 326–335, 2016.

[40] D. Montero, C. Tachibana, J. Rahr Winther, and C. Appenzeller-Herzog, "Intracellular glutathione pools are heterogeneously concentrated," *Redox Biology*, vol. 1, no. 1, pp. 508–513, 2013.

[41] S. S. Cao and R. J. Kaufman, "Endoplasmic reticulum stress and oxidative stress in cell fate decision and human disease," *Antioxidants & Redox Signaling*, vol. 21, no. 3, pp. 396–413, 2014.

[42] M. E. Anderson, R. J. Bridges, and A. Meister, "Direct evidence for inter-organ transport of glutathione and that the non-filtration renal mechanism for glutathione utilization involves γ-glutamyl transpeptidase," *Biochemical and Biophysical Research Communications*, vol. 96, no. 2, pp. 848–853, 1980.

[43] D. Häberle, A. Wahlländer, H. Sies, I. Linke, and C. Lachenmaier, "Assessment of the kidney function in maintenance of plasma glutathione concentration and redox state in anaesthetized rats," *FEBS Letters*, vol. 108, no. 2, pp. 335–340, 1979.

[44] R. Hahn, A. Wendel, and L. Flohé, "The fate of extracellular glutathione in the rat," *Biochimica et Biophysica Acta (BBA) - General Subjects*, vol. 539, no. 3, pp. 324–337, 1978.

[45] L. H. Lash and D. A. Putt, "Renal cellular transport of exogenous glutathione: heterogeneity at physiological and pharmacological concentrations," *Biochemical Pharmacology*, vol. 58, no. 5, pp. 897–907, 1999.

[46] X. Chen, H. Tsukaguchi, X. Z. Chen, U. V. Berger, and M. A. Hediger, "Molecular and functional analysis of SDCT2, a novel rat sodium-dependent dicarboxylate transporter," *The Journal of Clinical Investigation*, vol. 103, no. 8, pp. 1159–1168, 1999.

[47] M. Inoue and Y. Morino, "Direct evidence for the role of the membrane potential in glutathione transport by renal brush-border membranes," *Journal of Biological Chemistry*, vol. 260, no. 1, pp. 326–331, 1985.

[48] N. Ballatori, C. L. Hammond, J. B. Cunningham, S. M. Krance, and R. Marchan, "Molecular mechanisms of reduced glutathione transport: role of the MRP/CFTR/ABCC and OATP/SLC21A families of membrane proteins," *Toxicology and Applied Pharmacology*, vol. 204, no. 3, pp. 238–255, 2005.

[49] L. Li, T. K. Lee, P. J. Meier, and N. Ballatori, "Identification of glutathione as a driving force and leukotriene C_4 as a substrate for oatp1, the hepatic sinusoidal organic solute transporter," *Journal of Biological Chemistry*, vol. 273, no. 26, pp. 16184–16191, 1998.

[50] A. K. Bachhawat, A. Thakur, J. Kaur, and M. Zulkifli, "Glutathione transporters," *Biochimica et Biophysica Acta (BBA) - General Subjects*, vol. 1830, no. 5, pp. 3154–3164, 2013.

[51] M. H. Hanigan, "Gamma-glutamyl transpeptidase: redox regulation and drug resistance," *Advances in Cancer Research*, vol. 122, pp. 103–141, 2014.

[52] S. Kumar, A. Kaur, B. Chattopadhyay, and A. K. Bachhawat, "Defining the cytosolic pathway of glutathione degradation in *Arabidopsis thaliana*: role of the ChaC/GCG family of γ-glutamyl cyclotransferases as glutathione-degrading enzymes and AtLAP1 as the Cys-Gly peptidase," *Biochemical Journal*, vol. 468, no. 1, pp. 73–85, 2015.

[53] A. Kumar, S. Tikoo, S. Maity et al., "Mammalian proapoptotic factor ChaC1 and its homologues function as γ-glutamyl cyclotransferases acting specifically on glutathione," *EMBO Reports*, vol. 13, no. 12, pp. 1095–1101, 2012.

[54] A. J. Oakley, T. Yamada, D. Liu, M. Coggan, A. G. Clark, and P. G. Board, "The identification and structural characterization of C7orf24 as γ-glutamyl cyclotransferase: an essential enzyme in the γ-glutamyl cycle," *Journal of Biological Chemistry*, vol. 283, no. 32, pp. 22031–22042, 2008.

[55] A. Kaur, R. Gautam, R. Srivastava et al., "ChaC2, an enzyme for slow turnover of cytosolic glutathione," *Journal of Biological Chemistry*, vol. 292, no. 2, pp. 638–651, 2017.

[56] C. Gorrini, I. S. Harris, and T. W. Mak, "Modulation of oxidative stress as an anticancer strategy," *Nature Reviews Drug Discovery*, vol. 12, no. 12, pp. 931–947, 2013.

[57] A. L. Ortega, S. Mena, and J. M. Estrela, "Glutathione in cancer cell death," *Cancers*, vol. 3, no. 1, pp. 1285–1310, 2011.

[58] M. P. Murphy, "How mitochondria produce reactive oxygen species," *Biochemical Journal*, vol. 417, no. 1, pp. 1–13, 2009.

[59] L. Ouyang, Z. Shi, S. Zhao et al., "Programmed cell death pathways in cancer: a review of apoptosis, autophagy and programmed necrosis," *Cell Proliferation*, vol. 45, no. 6, pp. 487–498, 2012.

[60] Z. Su, Z. Yang, Y. Xu, Y. Chen, and Q. Yu, "Apoptosis, autophagy, necroptosis, and cancer metastasis," *Molecular Cancer*, vol. 14, no. 1, p. 48, 2015.

[61] S. Elmore, "Apoptosis: a review of programmed cell death," *Toxicologic Pathology*, vol. 29, no. 6, pp. 997–1003, 2012.

[62] Y. F. Zhao, C. Zhang, and Y. R. Suo, "MMPT as a reactive oxygen species generator induces apoptosis via the depletion of intracellular GSH contents in A549 cells," *European Journal of Pharmacology*, vol. 688, no. 1-3, pp. 6–13, 2012.

[63] R. Franco, M. I. Panayiotidis, and J. A. Cidlowski, "Glutathione depletion is necessary for apoptosis in lymphoid cells independent of reactive oxygen species formation," *Journal of Biological Chemistry*, vol. 282, no. 42, pp. 30452–30465, 2007.

[64] M. Khan, F. Yi, A. Rasul et al., "Alantolactone induces apoptosis in glioblastoma cells via GSH depletion, ROS generation, and mitochondrial dysfunction," *IUBMB life*, vol. 64, no. 9, pp. 783–794, 2012.

[65] J. S. Armstrong, K. K. Steinauer, B. Hornung et al., "Role of glutathione depletion and reactive oxygen species generation in apoptotic signaling in a human B lymphoma cell line," *Cell Death & Differentiation*, vol. 9, no. 3, pp. 252–263, 2002.

[66] L. Ghibelli, C. Fanelli, G. Rotilio et al., "Rescue of cells from apoptosis by inhibition of active GSH extrusion," *The FASEB Journal*, vol. 12, no. 6, pp. 479–486, 1998.

[67] C. L. Hammond, R. Marchan, S. M. Krance, and N. Ballatori, "Glutathione export during apoptosis requires functional multidrug resistance-associated proteins," *The Journal of Biological Chemistry*, vol. 282, no. 19, pp. 14337–14347, 2007.

[68] X. Zou, Z. Feng, Y. Li et al., "Stimulation of GSH synthesis to prevent oxidative stress-induced apoptosis by hydroxytyrosol in human retinal pigment epithelial cells: activation of Nrf2 and JNK-p62/SQSTM1 pathways," *The Journal of Nutritional Biochemistry*, vol. 23, no. 8, pp. 994–1006, 2012.

[69] M. J. Akhtar, M. Ahamed, H. A. Alhadlaq, and A. Alshamsan, "Nanotoxicity of cobalt induced by oxidant generation and glutathione depletion in MCF-7 cells," *Toxicology in Vitro*, vol. 40, pp. 94–101, 2017.

[70] G. Chen, Z. Chen, Y. Hu, and P. Huang, "Inhibition of mitochondrial respiration and rapid depletion of mitochondrial glutathione by β-phenethyl isothiocyanate: mechanisms for anti-leukemia activity," *Antioxidants & Redox Signaling*, vol. 15, no. 12, pp. 2911–2921, 2011.

[71] M. L. Circu and T. Yee Aw, "Glutathione and apoptosis," *Free Radical Research*, vol. 42, no. 8, pp. 689–706, 2008.

[72] P. Guha, A. Dey, R. Sen, M. Chatterjee, S. Chattopadhyay, and S. K. Bandyopadhyay, "Intracellular GSH depletion triggered mitochondrial Bax translocation to accomplish resveratrol-induced apoptosis in the U937 cell line," *Journal of Pharmacology and Experimental Therapeutics*, vol. 336, no. 1, pp. 206–214, 2011.

[73] T. Honda, S. Coppola, L. Ghibelli et al., "GSH depletion enhances adenoviral bax-induced apoptosis in lung cancer cells," *Cancer Gene Therapy*, vol. 11, no. 4, pp. 249–255, 2004.

[74] P. Vandenabeele, L. Galluzzi, T. vanden Berghe, and G. Kroemer, "Molecular mechanisms of necroptosis: an ordered cellular explosion," *Nature Reviews Molecular Cell Biology*, vol. 11, no. 10, pp. 700–714, 2010.

[75] T. V. Berghe, A. Linkermann, S. Jouan-Lanhouet, H. Walczak, and P. Vandenabeele, "Regulated necrosis: the expanding network of non-apoptotic cell death pathways," *Nature Reviews Molecular Cell Biology*, vol. 15, no. 2, pp. 135–147, 2014.

[76] D. E. Christofferson and J. Yuan, "Necroptosis as an alternative form of programmed cell death," *Current Opinion in Cell Biology*, vol. 22, no. 2, pp. 263–268, 2010.

[77] L. Galluzzi and G. Kroemer, "Necroptosis: a specialized pathway of programmed necrosis," *Cell*, vol. 135, no. 7, pp. 1161–1163, 2008.

[78] H. Nagai, K. Matsumaru, G. Feng, and N. Kaplowitz, "Reduced glutathione depletion causes necrosis and sensitization to tumor necrosis factor-alpha-induced apoptosis in cultured mouse hepatocytes," *Hepatology*, vol. 36, no. 1, pp. 55–64, 2002.

[79] X. Xu, C. C. Chua, J. Kong et al., "Necrostatin-1 protects against glutamate-induced glutathione depletion and caspase-independent cell death in HT-22 cells," *Journal of Neurochemistry*, vol. 103, no. 5, pp. 2004–2014, 2007.

[80] A. K. Chauhan, K. J. Min, and T. K. Kwon, "RIP1-dependent reactive oxygen species production executes artesunate-induced cell death in renal carcinoma Caki cells," *Molecular and Cellular Biochemistry*, vol. 435, no. 1-2, pp. 15–24, 2017.

[81] X. Xie, Y. Zhao, C. Y. Ma et al., "Dimethyl fumarate induces necroptosis in colon cancer cells through GSH depletion/ROS increase/MAPKs activation pathway," *British Journal of Pharmacology*, vol. 172, no. 15, pp. 3929–3943, 2015.

[82] M. S. Chen, S. F. Wang, C. Y. Hsu et al., "CHAC1 degradation of glutathione enhances cystine-starvation-induced necroptosis and ferroptosis in human triple negative breast cancer cells via the GCN2-eIF2α-ATF4 pathway," *Oncotarget*, vol. 8, no. 70, pp. 114588–114602, 2017.

[83] S. J. Dixon, K. M. Lemberg, M. R. Lamprecht et al., "Ferroptosis: an iron-dependent form of nonapoptotic cell death," *Cell*, vol. 149, no. 5, pp. 1060–1072, 2012.

[84] J. C. Reed and M. Pellecchia, "Ironing out cell death mechanisms," *Cell*, vol. 149, no. 5, pp. 963–965, 2012.

[85] W. S. Yang and B. R. Stockwell, "Ferroptosis: death by lipid peroxidation," *Trends in Cell Biology*, vol. 26, no. 3, pp. 165–176, 2016.

[86] X. Yu and Y. C. Long, "Crosstalk between cystine and glutathione is critical for the regulation of amino acid signaling pathways and ferroptosis," *Scientific Reports*, vol. 6, article 30033, no. 1, 2016.

[87] M. Gao, P. Monian, N. Quadri, R. Ramasamy, and X. Jiang, "Glutaminolysis and transferrin regulate ferroptosis," *Molecular Cell*, vol. 59, no. 2, pp. 298–308, 2015.

[88] X. Sui, R. Zhang, S. Liu et al., "RSL3 drives ferroptosis through GPX4 inactivation and ROS production in colorectal cancer," *Frontiers in Pharmacology*, vol. 9, p. 1371, 2018.

[89] J. P. Friedmann Angeli, M. Schneider, B. Proneth et al., "Inactivation of the ferroptosis regulator Gpx4 triggers acute

renal failure in mice," *Nature Cell Biology*, vol. 16, no. 12, pp. 1180–1191, 2014.

[90] T. M. Seibt, B. Proneth, and M. Conrad, "Role of GPX4 in ferroptosis and its pharmacological implication," *Free Radical Biology and Medicine*, vol. 133, pp. 144–152, 2019.

[91] T. Hirschhorn and B. R. Stockwell, "The development of the concept of ferroptosis," *Free Radical Biology and Medicine*, vol. 133, pp. 130–143, 2019.

[92] W. S. Yang and B. R. Stockwell, "Synthetic lethal screening identifies compounds activating iron-dependent, nonapoptotic cell death in oncogenic-RAS-harboring cancer cells," *Chemistry & Biology*, vol. 15, no. 3, pp. 234–245, 2008.

[93] W. S. Yang, R. SriRamaratnam, M. E. Welsch et al., "Regulation of ferroptotic cancer cell death by GPX4," *Cell*, vol. 156, no. 1-2, pp. 317–331, 2014.

[94] K. Shimada, R. Skouta, A. Kaplan et al., "Global survey of cell death mechanisms reveals metabolic regulation of ferroptosis," *Nature Chemical Biology*, vol. 12, no. 7, pp. 497–503, 2016.

[95] H. Miess, B. Dankworth, A. M. Gouw et al., "The glutathione redox system is essential to prevent ferroptosis caused by impaired lipid metabolism in clear cell renal cell carcinoma," *Oncogene*, vol. 37, no. 40, pp. 5435–5450, 2018.

[96] K. D'Herde and D. V. Krysko, "Ferroptosis: oxidized PEs trigger death," *Nature Chemical Biology*, vol. 13, no. 1, pp. 4-5, 2017.

[97] D. A. Stoyanovsky, Y. Y. Tyurina, I. Shrivastava et al., "Iron catalysis of lipid peroxidation in ferroptosis: regulated enzymatic or random free radical reaction?," *Free Radical Biology and Medicine*, vol. 133, pp. 153–161, 2019.

[98] V. E. Kagan, G. Mao, F. Qu et al., "Oxidized arachidonic and adrenic PEs navigate cells to ferroptosis," *Nature Chemical Biology*, vol. 13, no. 1, pp. 81–90, 2017.

[99] J. P. F. Angeli, R. Shah, D. A. Pratt, and M. Conrad, "Ferroptosis inhibition: mechanisms and opportunities," *Trends in Pharmacological Sciences*, vol. 38, no. 5, pp. 489–498, 2017.

[100] C. Louandre, Z. Ezzoukhry, C. Godin et al., "Iron-dependent cell death of hepatocellular carcinoma cells exposed to sorafenib," *International Journal of Cancer*, vol. 133, no. 7, pp. 1732–1742, 2013.

[101] C. Louandre, I. Marcq, H. Bouhlal et al., "The retinoblastoma (Rb) protein regulates ferroptosis induced by sorafenib in human hepatocellular carcinoma cells," *Cancer Letters*, vol. 356, no. 2, pp. 971–977, 2015.

[102] I. Dikic, T. Johansen, and V. Kirkin, "Selective autophagy in cancer development and therapy," *Cancer Research*, vol. 70, no. 9, pp. 3431–3434, 2010.

[103] D. R. Green and B. Levine, "To be or not to be? How selective autophagy and cell death govern cell fate," *Cell*, vol. 157, no. 1, pp. 65–75, 2014.

[104] G. Filomeni, D. De Zio, and F. Cecconi, "Oxidative stress and autophagy: the clash between damage and metabolic needs," *Cell Death & Differentiation*, vol. 22, no. 3, pp. 377–388, 2015.

[105] G. Filomeni, E. Desideri, S. Cardaci, G. Rotilio, and M. R. Ciriolo, "Under the ROS: Thiol network is the principal suspect for autophagy commitment," *Autophagy*, vol. 6, no. 7, pp. 999–1005, 2010.

[106] H. Mancilla, R. Maldonado, K. Cereceda et al., "Glutathione depletion induces spermatogonial cell autophagy," *Journal of Cellular Biochemistry*, vol. 116, no. 10, pp. 2283–2292, 2015.

[107] E. Ogier-Denis and P. Codogno, "Autophagy: a barrier or an adaptive response to cancer," *Biochimica et Biophysica Acta (BBA) - Reviews on Cancer*, vol. 1603, no. 2, pp. 113–128, 2003.

[108] W. Guo, Y. Zhao, Z. Zhang et al., "Disruption of xCT inhibits cell growth via the ROS/autophagy pathway in hepatocellular carcinoma," *Cancer Letters*, vol. 312, no. 1, pp. 55–61, 2011.

[109] E. Desideri, G. Filomeni, and M. R. Ciriolo, "Glutathione participates in the modulation of starvation-induced autophagy in carcinoma cells," *Autophagy*, vol. 8, no. 12, pp. 1769–1781, 2012.

[110] G. Seo, S. K. Kim, Y. J. Byun et al., "Hydrogen peroxide induces Beclin 1-independent autophagic cell death by suppressing the mTOR pathway via promoting the ubiquitination and degradation of Rheb in GSH-depleted RAW 264.7 cells," *Free Radical Research*, vol. 45, no. 4, pp. 389–399, 2011.

[111] R. Kang and D. Tang, "Autophagy and ferroptosis - what's the connection?," *Current Pathobiology Reports*, vol. 5, no. 2, pp. 153–159, 2017.

[112] C. Ott, J. Konig, A. Hohn, T. Jung, and T. Grune, "Reduced autophagy leads to an impaired ferritin turnover in senescent fibroblasts," *Free Radical Biology and Medicine*, vol. 101, pp. 325–333, 2016.

[113] S. Torii, R. Shintoku, C. Kubota et al., "An essential role for functional lysosomes in ferroptosis of cancer cells," *Biochemical Journal*, vol. 473, no. 6, pp. 769–777, 2016.

[114] Z. Wu, Y. Geng, X. Lu et al., "Chaperone-mediated autophagy is involved in the execution of ferroptosis," *Proceedings of the National Academy of Sciences of the United States of America*, vol. 116, no. 8, pp. 2996–3005, 2019.

[115] M. Gao, P. Monian, Q. Pan, W. Zhang, J. Xiang, and X. Jiang, "Ferroptosis is an autophagic cell death process," *Cell Research*, vol. 26, no. 9, pp. 1021–1032, 2016.

[116] W. Hou, Y. Xie, X. Song et al., "Autophagy promotes ferroptosis by degradation of ferritin," *Autophagy*, vol. 12, no. 8, pp. 1425–1428, 2016.

[117] N. Santana-Codina and J. D. Mancias, "The role of NCOA4-mediated ferritinophagy in health and disease," *Pharmaceuticals*, vol. 11, no. 4, p. 114, 2018.

[118] J. D. Mancias, X. Wang, S. P. Gygi, J. W. Harper, and A. C. Kimmelman, "Quantitative proteomics identifies NCOA4 as the cargo receptor mediating ferritinophagy," *Nature*, vol. 509, no. 7498, pp. 105–109, 2014.

[119] W. E. Dowdle, B. Nyfeler, J. Nagel et al., "Selective VPS34 inhibitor blocks autophagy and uncovers a role for NCOA4 in ferritin degradation and iron homeostasis in vivo," *Nature Cell Biology*, vol. 16, no. 11, pp. 1069–1079, 2014.

[120] J. Du, T. Wang, Y. Li et al., "DHA inhibits proliferation and induces ferroptosis of leukemia cells through autophagy dependent degradation of ferritin," *Free Radical Biology and Medicine*, vol. 131, pp. 356–369, 2019.

[121] H. H. W. Chen and M. T. Kuo, "Role of glutathione in the regulation of cisplatin resistance in cancer chemotherapy," *Metal-Based Drugs*, vol. 2010, Article ID 430939, 7 pages, 2010.

[122] J. L. Roh, E. H. Kim, H. J. Jang, J. Y. Park, and D. Shin, "Induction of ferroptotic cell death for overcoming cisplatin resistance of head and neck cancer," *Cancer Letters*, vol. 381, no. 1, pp. 96–103, 2016.

[123] K. J. Habermann, L. Grunewald, S. van Wijk, and S. Fulda, "Targeting redox homeostasis in rhabdomyosarcoma cells: GSH-depleting agents enhance auranofin-induced cell death," *Cell Death & Disease*, vol. 8, no. 10, article e3067, 2017.

[124] M. Lo, Y. Z. Wang, and P. W. Gout, "The x_c^- cystine/glutamate antiporter: a potential target for therapy of cancer and other diseases," *Journal of Cellular Physiology*, vol. 215, no. 3, pp. 593–602, 2008.

[125] J. Wang, B. Luo, X. Li et al., "Inhibition of cancer growth in vitro and in vivo by a novel ROS-modulating agent with ability to eliminate stem-like cancer cells," *Cell Death & Disease*, vol. 8, no. 6, p. e2887, 2017.

[126] R. Barattin, T. Perrotton, D. Trompier et al., "Iodination of verapamil for a stronger induction of death, through GSH efflux, of cancer cells overexpressing MRP1," *Bioorganic & Medicinal Chemistry*, vol. 18, no. 17, pp. 6265–6274, 2010.

[127] J. Lewerenz, S. J. Hewett, Y. Huang et al., "The cystine/glutamate antiporter system x_c^- in health and disease: from molecular mechanisms to novel therapeutic opportunities," *Antioxidants & Redox Signaling*, vol. 18, no. 5, pp. 522–555, 2013.

[128] F. Wada, H. Koga, J. Akiba et al., "High expression of CD44v9 and xCT in chemoresistant hepatocellular carcinoma: potential targets by sulfasalazine," *Cancer Science*, vol. 109, no. 9, pp. 2801–2810, 2018.

[129] M. Toyoda, K. Kaira, Y. Ohshima et al., "Prognostic significance of amino-acid transporter expression (LAT1, ASCT2 and xCT) in surgically resected tongue cancer," *British Journal of Cancer*, vol. 110, no. 10, pp. 2506–2513, 2014.

[130] E. Habib, K. Linher-Melville, H. X. Lin, and G. Singh, "Expression of xCT and activity of system x_c^- are regulated by NRF2 in human breast cancer cells in response to oxidative stress," *Redox Biology*, vol. 5, pp. 33–42, 2015.

[131] K. Sugano, K. Maeda, H. Ohtani, H. Nagahara, M. Shibutani, and K. Hirakawa, "Expression of xCT as a predictor of disease recurrence in patients with colorectal cancer," *Anticancer Research*, vol. 35, no. 2, pp. 677–682, 2015.

[132] M. Lo, V. Ling, Y. Z. Wang, and P. W. Gout, "The x_c^- cystine/glutamate antiporter: a mediator of pancreatic cancer growth with a role in drug resistance," *British Journal of Cancer*, vol. 99, no. 3, pp. 464–472, 2008.

[133] S. Okuno, H. Sato, K. Kuriyama-Matsumura et al., "Role of cystine transport in intracellular glutathione level and cisplatin resistance in human ovarian cancer cell lines," *British Journal of Cancer*, vol. 88, no. 6, pp. 951–956, 2003.

[134] T. Ishimoto, O. Nagano, T. Yae et al., "CD44 variant regulates redox status in cancer cells by stabilizing the xCT subunit of system x_c^- and thereby promotes tumor growth," *Cancer Cell*, vol. 19, no. 3, pp. 387–400, 2011.

[135] N. E. Savaskan, E. Hahnen, and I. Y. Eyüpoglu, "The x_c^- cystine/glutamate antiporter (xCT) as a potential target for therapy of cancer: yet another cytotoxic anticancer approach?," *Journal of Cellular Physiology*, vol. 220, no. 2, pp. 531-532, 2009.

[136] R. S. Chen, Y. M. Song, Z. Y. Zhou et al., "Disruption of xCT inhibits cancer cell metastasis via the caveolin-1/beta-catenin pathway," *Oncogene*, vol. 28, no. 4, pp. 599–609, 2009.

[137] M. H. Larraufie, W. S. Yang, E. Jiang, A. G. Thomas, B. S. Slusher, and B. R. Stockwell, "Incorporation of metabolically stable ketones into a small molecule probe to increase potency and water solubility," *Bioorganic & Medicinal Chemistry Letters*, vol. 25, no. 21, pp. 4787–4792, 2015.

[138] J. L. Roh, E. H. Kim, H. Jang, and D. Shin, "Aspirin plus sorafenib potentiates cisplatin cytotoxicity in resistant head and neck cancer cells through xCT inhibition," *Free Radical Biology and Medicine*, vol. 104, pp. 1–9, 2017.

[139] M. Z. Ma, G. Chen, P. Wang et al., "Xc^- inhibitor sulfasalazine sensitizes colorectal cancer to cisplatin by a GSH-dependent mechanism," *Cancer Letters*, vol. 368, no. 1, pp. 88–96, 2015.

[140] L. Sleire, B. S. Skeie, I. A. Netland et al., "Drug repurposing: sulfasalazine sensitizes gliomas to gamma knife radiosurgery by blocking cystine uptake through system Xc^-, leading to glutathione depletion," *Oncogene*, vol. 34, no. 49, pp. 5951–5959, 2015.

[141] V. S. Narang, G. M. Pauletti, P. W. Gout, D. J. Buckley, and A. R. Buckley, "Sulfasalazine-induced reduction of glutathione levels in breast cancer cells: enhancement of growth-inhibitory activity of Doxorubicin," *Chemotherapy*, vol. 53, no. 3, pp. 210–217, 2007.

[142] Z. Wang, Y. Ding, X. Wang et al., "Pseudolaric acid B triggers ferroptosis in glioma cells via activation of Nox4 and inhibition of xCT," *Cancer Letters*, vol. 428, pp. 21–33, 2018.

[143] B. N. Zhou, B. P. Ying, G. Q. Song, Z. X. Chen, J. Han, and Y. F. Yan, "Pseudolaric acids from pseudolarix kaempferi," *Planta Medica*, vol. 47, no. 1, pp. 35–38, 1983.

[144] Y. Chen, H. G. Shertzer, S. N. Schneider, D. W. Nebert, and T. P. Dalton, "Glutamate cysteine ligase catalysis," *Journal of Biological Chemistry*, vol. 280, no. 40, pp. 33766–33774, 2005.

[145] S. Shi, F. N. Hudson, D. Botta et al., "Over expression of glutamate cysteine ligase increases cellular resistance to H2O2-induced DNA single-strand breaks," *Cytometry Part A*, vol. 71, no. 9, pp. 686–692, 2007.

[146] J. Y. Kim, J. H. Yim, J. H. Cho et al., "Adrenomedullin regulates cellular glutathione content via modulation of γ-glutamate-cysteine ligase catalytic subunit expression," *Endocrinology*, vol. 147, no. 3, pp. 1357–1364, 2006.

[147] M. Liu, Y. Zhao, and X. Zhang, "Knockdown of glutamate cysteine ligase catalytic subunit by siRNA causes the gold nanoparticles-induced cytotoxicity in lung cancer cells," *Plos One*, vol. 10, no. 3, article e0118870, 2015.

[148] Y. D. Hoang, A. P. Avakian, and U. Luderer, "Minimal ovarian upregulation of glutamate cysteine ligase expression in response to suppression of glutathione by buthionine sulfoximine," *Reproductive Toxicology*, vol. 21, no. 2, pp. 186–196, 2006.

[149] E. Debiton, J. C. Madelmont, J. Legault, and C. Barthomeuf, "Sanguinarine-induced apoptosis is associated with an early and severe cellular glutathione depletion," *Cancer Chemotherapy and Pharmacology*, vol. 51, no. 6, pp. 474–482, 2003.

[150] E. Ehrke, C. Arend, and R. Dringen, "3-bromopyruvate inhibits glycolysis, depletes cellular glutathione, and compromises the viability of cultured primary rat astrocytes," *Journal of Neuroscience Research*, vol. 93, no. 7, pp. 1138–1146, 2015.

[151] S. M. El Sayed, H. Baghdadi, M. Zolaly, H. H. Almaramhy, M. Ayat, and J. G. Donki, "The promising anticancer drug 3-bromopyruvate is metabolized through glutathione conjugation which affects chemoresistance and clinical practice: an evidence-based view," *Medical Hypotheses*, vol. 100, pp. 67–77, 2017.

[152] S. Cardaci, E. Desideri, and M. R. Ciriolo, "Targeting aerobic glycolysis: 3-bromopyruvate as a promising anticancer drug," *Journal of Bioenergetics and Biomembranes*, vol. 44, no. 1, pp. 17–29, 2012.

[153] Y. H. Ko, B. L. Smith, Y. Wang et al., "Advanced cancers: eradication in all cases using 3-bromopyruvate therapy to deplete ATP," *Biochemical and Biophysical Research Communications*, vol. 324, no. 1, pp. 269–275, 2004.

[154] A. I. Amjad, R. A. Parikh, L. J. Appleman, E. R. Hahm, K. Singh, and S. V. Singh, "Broccoli-derived sulforaphane and chemoprevention of prostate cancer: from bench to bedside," *Current Pharmacology Reports*, vol. 1, no. 6, pp. 382–390, 2015.

[155] K. L. Cheung and A. N. Kong, "Molecular targets of dietary phenethyl isothiocyanate and sulforaphane for cancer chemoprevention," *The AAPS Journal*, vol. 12, no. 1, pp. 87–97, 2010.

[156] P. Gupta, B. Kim, S. H. Kim, and S. K. Srivastava, "Molecular targets of isothiocyanates in cancer: recent advances," *Molecular Nutrition & Food Research*, vol. 58, no. 8, pp. 1685–1707, 2014.

[157] P. Gupta, S. E. Wright, S. H. Kim, and S. K. Srivastava, "Phenethyl isothiocyanate: a comprehensive review of anticancer mechanisms," *Biochimica et Biophysica Acta (BBA) - Reviews on Cancer*, vol. 1846, no. 2, pp. 405–424, 2014.

[158] J. D. Clarke, R. H. Dashwood, and E. Ho, "Multi-targeted prevention of cancer by sulforaphane," *Cancer Letters*, vol. 269, no. 2, pp. 291–304, 2008.

[159] S. H. Huang, M. H. Hsu, S. C. Hsu et al., "Phenethyl isothiocyanate triggers apoptosis in human malignant melanoma A375.S2 cells through reactive oxygen species and the mitochondria-dependent pathways," *Human & Experimental Toxicology*, vol. 33, no. 3, pp. 270–283, 2013.

[160] G. M. Gordillo, A. Biswas, S. Khanna, J. M. Spieldenner, X. Pan, and C. K. Sen, "Multidrug resistance-associated protein-1 (MRP-1)-dependent glutathione disulfide (GSSG) efflux as a critical survival factor for oxidant-enriched tumorigenic endothelial cells," *Journal of Biological Chemistry*, vol. 291, no. 19, pp. 10089–10103, 2016.

[161] M. Dačević, A. Isaković, A. Podolski-Renić et al., "Purine nucleoside analog - sulfinosine modulates diverse mechanisms of cancer progression in multi-drug resistant cancer cell lines," *Plos One*, vol. 8, no. 1, article e54044, 2013.

[162] M. L. Circu, S. Stringer, C. A. Rhoads, M. P. Moyer, and T. Y. Aw, "The role of GSH efflux in staurosporine-induced apoptosis in colonic epithelial cells," *Biochemical Pharmacology*, vol. 77, no. 1, pp. 76–85, 2009.

[163] M. Benlloch, A. Ortega, P. Ferrer et al., "Acceleration of glutathione efflux and inhibition of γ-glutamyltranspeptidase sensitize metastatic B16 melanoma cells to endothelium-induced cytotoxicity," *Journal of Biological Chemistry*, vol. 280, no. 8, pp. 6950–6959, 2005.

[164] H. M. Brechbuhl, R. Kachadourian, E. Min, D. Chan, and B. J. Day, "Chrysin enhances doxorubicin-induced cytotoxicity in human lung epithelial cancer cell lines: the role of glutathione," *Toxicology and Applied Pharmacology*, vol. 258, no. 1, pp. 1–9, 2012.

Hindawi
Oxidative Medicine and Cellular Longevity
Volume 2019, Article ID 3264858, 11 pages
https://doi.org/10.1155/2019/3264858

Research Article

The NADPH Oxidase Nox4 Controls Macrophage Polarization in an NFκB-Dependent Manner

V. Helfinger,[1] K. Palfi,[1] A. Weigert,[2] and K. Schröder[1]

[1]*Institute for Cardiovascular Physiology, Goethe-University, Frankfurt, Germany*
[2]*Institute for Biochemistry I, Goethe-University, Frankfurt, Germany*

Correspondence should be addressed to K. Schröder; schroeder@vrc.uni-frankfurt.de

Received 13 December 2018; Revised 4 March 2019; Accepted 21 March 2019; Published 18 April 2019

Academic Editor: Mithun Sinha

The family of NADPH oxidases represents an important source of reactive oxygen species (ROS) within the cell. Nox4 is a special member of this family as it constitutively produces H_2O_2 and its loss promotes inflammation. A major cellular component of inflammation is the macrophage population, which can be divided into several subpopulations depending on their phenotype, with proinflammatory M(LPS+IFNγ) and wound-healing M(IL4+IL13) macrophages being extremes of the functional spectrum. Whether Nox4 is expressed in macrophages is discussed controversially. Here, we show that macrophages besides a high level of Nox2 indeed express Nox4. As Nox4 contributes to differentiation of many cells, we hypothesize that Nox4 plays a role in determining the polarization and the phenotype of macrophages. In bone marrow-derived monocytes, ex vivo treatment with LPS/IFNγ or IL4/IL13 results in polarization of the cells into M(LPS+IFNγ) or M(IL4+IL13) macrophages, respectively. In this ex vivo setting, Nox4 deficiency reduces M(IL4+IL13) polarization and forces M(LPS+IFNγ). Nox4-/- M(LPS+IFNγ)-polarized macrophages express more Nox2 and produce more superoxide anions than wild type M(LPS+IFNγ)-polarized macrophages. Mechanistically, Nox4 deficiency reduces STAT6 activation and promotes NFκB activity, with the latter being responsible for the higher level of Nox2 in Nox4-deficient M(LPS+IFNγ)-polarized macrophages. According to those findings, *in vivo*, in a murine inflammation-driven fibrosarcoma model, Nox4 deficiency forces the expression of proinflammatory genes and cytokines, accompanied by an increase in the number of proinflammatory $Ly6C^+$ macrophages in the tumors. Collectively, the data obtained in this study suggest an anti-inflammatory role for Nox4 in macrophages. Nox4 deficiency results in less M(IL4+IL13) polarization and suppression of NFκB activity in monocytes.

1. Introduction

Reactive oxygen species (ROS) regulate a variety of complex cellular processes including angiogenesis, inflammation, differentiation, and proliferation. The family of NADPH oxidases (Nox) consists of 7 members with tissue- and cell type-specific expression profiles. The main function of all family members is a controlled ROS production [1]. Importantly, the NADPH oxidases differ in the type of ROS produced. While Nox2 upon activation produces $\cdot O_2^-$, Nox4 is constitutively active and predominantly produces H_2O_2 [2, 3].

Inflammation and wound healing are processes that strongly depend on the function of macrophages. Macrophages are quite heterogeneous and represent a group of diversely polarized cells from the same monocyte origin [4]. The nomenclature of polarized macrophages has been changed recently. In particular, the M1 and M2 phenotypes have now been replaced by M(LPS+IFNγ) and M(IL4+IL13), respectively, according to the stimulation by cytokines forcing in vitro polarization to one or the other phenotype [5]. We followed this new nomenclature throughout the manuscript.

Nox2 and its product $\cdot O_2^-$ promote an M(LPS+IFNγ) phenotype with phagocytic activity and proinflammatory properties [6, 7]. In contrast, in tissue remodeling and wound healing, M(IL4+IL13) polarization of macrophages is characterized by both reduced Nox2 activity and reduced superoxide anion production [8]. H_2O_2 is a second messenger that enforces the polarization of monocytes to the M(IL4+IL13) phenotype (despite a lower Nox2-dependent

ROS production observed in other studies [9]). Although, there is evidence that Nox4 is expressed in macrophages [10], this is rather inconsistent throughout the literature, leading to the conclusion that Nox4 expression is dynamic over the course of a macrophage life. Nox4 is a major determinant of differentiation of a number of cells, including adipocytes [11] and osteoclasts [12]. Therefore, we hypothesize that Nox4 plays a role in macrophage polarization. With the aid of an *in vivo* model of tumorigenesis, as well as isolated murine bone marrow and human blood monocytes, we analyzed the contribution of Nox4 in macrophage polarization.

2. Material and Methods

2.1. Material. The following chemicals were used: 3-methylcholanthrene (MCA), NaCl, NH_4Cl, $NaHCO_3$ Hank's BSS without Ca^{2+} and Mg^{2+}, Trypsin-EDTA solution (T3924) and LPS from Sigma-Aldrich (Munich, Germany), Dulbecco's PBS (Gibco, Life Technologies, Carlsbad, CA, USA), Hank's buffer, Sybr Green from Bio-Rad (California, USA), Tris (Carl Roth) NFκB inhibitor #sc-3060 from Santa Cruz (Texas, USA), and GKT 137928 from Genkyotex (Switzerland). IL4, IL13, and IFNγ were purchased from PeproTech (NJ, USA). The following antibodies were used: anti-β-actin (AC-15) from Sigma-Aldrich (Munich, Germany), pSTAT6, STAT6, pSTAT1, and STAT1 from Cell Signaling (Danvers, MA, USA), and p65, β-tubulin, and topoisomerase from Santa Cruz (Texas, USA). YM1 was from Chemicon-Millipore (Darmstadt, Germany), and YY1 was from Bethyl Laboratories (Texas, USA).

2.2. Animals and Animal Procedures. All animal experiments were approved by the local governmental authorities (approval numbers: F28/27 and F28/46) and were performed in accordance with the animal protection guidelines. C57Bl/6J and Nox2y/- mice were purchased from Jackson Laboratories (Bar Harbor, Maine). Nox4-/- mice were generated by targeted deletion of the translation initiation site and of exons 1 and 2 of the Nox4 gene [13] and backcrossed into C57Bl/6J for more than 10 generations. Nox1y/- mice, kindly provided by Karl-Heinz Krause and previously characterized, were used for the same experiments [14]. Mice were housed in a specified pathogen-free facility with 12/12 hours day and night cycle and free access to water and chow. All experiments were performed with male mice at the age of 10-12 weeks. To induce fibrosarcomas, the chemical carcinogen MCA was injected subcutaneously into the right flank of the mice. In response to this, tumors were formed within the next three to four months. Once the tumors reached a diameter of 1.5 cm (around 100 days), mice were sacrificed by isoflurane anesthesia and subsequent decapitation. Subsequently, the tumor tissue was processed for biochemical analysis.

2.3. Cell Culture. Cell populations were isolated using the tumor dissociation kit for the mouse and the gentleMACS Dissociator (Miltenyi Biotec, Bergisch Gladbach, Germany), following the manufacturer instructions. Briefly, tumor tissue was homogenized enzymatically, erythrocytes were lysed, and only fibrosarcoma cells were cultured whereas the rest of the cell suspension was only used for FACS analysis. Murine monocytes were isolated from bone marrow by flushing the bones with PBS containing 1% of PenStrep. Cells were filtered (Falcon; #340605, BD) and centrifuged, and erythrocytes were lysed. Erythrocyte depletion buffer contained 155 mM NH_4Cl, 10 nM $NaHCO_3$, and 100 nM EDTA in double distilled water,pH = 7.4. For isolation of human monocytes, whole blood samples were centrifuged (400 ×g for 30 minutes) on a Ficoll gradient (Bicoll separation solution #L6115, Millipore) without brake. In order to force macrophage development, human peripheral blood mononuclear cells (PBMCs) and murine bone marrow-derived monocytes were cultured in Dulbecco's modified Eagle's medium (DMEM+glutaMAX) (Gibco, Life Technologies, Carlsbad, CA, USA), supplemented with 10% fetal calf serum (FCS), 1% penicillin (50 U/ml), and streptomycin (50 μg/ml), as well as 20% conditioned medium of L929 cells (contains M-CSF) for one week. Media were changed every 4 days. Before polarization, medium was exchanged to an unsupplemented DMEM/FCS. Polarization to M(LPS+IFNγ) was induced by 1 μg/ml LPS and 100 U/ml IFNγ; and M(IL4+IL13) polarization by IL4 and IL13 100 ng/ml each. After 4 hours, cells were used for nuclear extraction, Western Blot, PCR, or ROS measurements.

2.4. mRNA Isolation and RT-qPCR. Total mRNA from frozen homogenized tissue and isolated cells was obtained with an RNA-Mini-kit (Bio&Sell, Feucht, Germany) according to the manufacturers' protocol. Random hexamer primers (Promega, Madison, WI, USA) and SuperScript III Reverse Transcriptase (Invitrogen, Darmstadt, Germany) were used for cDNA synthesis. Semi-quantitative real-time PCR was performed with the Mx3500P qPCR cycler (Agilent Technologies, Santa Clara, CA, USA) using the PCR Sybr Green qPCR Mix with ROX (Bio&Sell, Feucht, Germany) and appropriate primers. Relative expression of target genes was normalized to eukaryotic translation elongation factor 2 (EF2), analyzed by the delta-delta-ct method. Primer sequences are listed in Table 1.

2.5. Protein and Western Blot Analysis. For protein isolation, cells were lysed in a buffer containing 20 mM Tris/cl pH 7.5, 150 mM NaCl, 10 mM $NaPP_i$, 20 nM NaF, 1% Triton, 10 nM okadaic acid (OA), 2 mM orthovanadate (OV), protein inhibitor mix (PIM), and 40 μg/ml phenylmethylsulfonylfluorid (PMSF). Separation of nucleus and cytosol was achieved by lysing the cells in hypotonic buffer (10 nM HEPES pH 7.9, 10 nM KCl, 0.1 mM EDTA, 0.1 mM EGTA, 1% Nonidet, 10 mM DTT, protein inhibitor mix (PIM), and 40 μg/ml phenylmethylsulfonylfluorid (PMSF)). Cells were centrifuged at 17000 g, and the supernatant was collected as the cytosolic fraction. The pellet was further lysed with a hypertonic buffer (20 mM HEPES pH 7.9, 0.4 M NaCl, 1 mM EDTA, 1 mM EGTA, 10 mM DTT, protein inhibitor mix (PIM), and 40 μg/ml phenylmethylsulfonylfluorid (PMSF)). After centrifugation at 17000 g, the supernatant contained most soluble nuclear proteins, while membranes, organelles, and DNA were collected in the pellet. Protein

Table 1: Primer sequences used.

Gene	Forward (5′ to 3′)	Reverse (5′ to 3′)
m TNFα	CCCGACTACGTGCTCCTCACC	CTCCAGCTGGAAGACTCCTCCCAG
m IL1β	GACCTTCCAGGATGAGGACATGAG	GGTGGGTGTGCCGTCTTTCATTAC
m ICAM-1	TGGCCTGGGGGATGCACACT	GGCTGTAGGTGGGTCCGGGT
m iNOS	TGAAGAAAACCCCTTGTGCT	TTCTGTGCTGTCCCAGTGAG
m YM1	CTGGAATTGGTGCCCCTACAA	TCATAACCAACCCACTCATTACC
m FIZZ1	GCAACTGCCTGTGCTTACTC	AGAAGCAGGGTAAATGGGCAA
m ARG1	GACAGGGCTCCTTTCAGGAC	CTTGGGAGGAGAAGGCGTTT
m Nox2	GTGCACCATGATGAGGAGAA	TTGCAATGGTCTTGAACTCG
m Nox1	CGCTCCCAGCAGAAGGTCGTGATTACCAAGG	GGAGTGACCCCAATCCCTGCCCCAACCA
m Nox4	TGTTGGGCCTAGGATTGTGTT	AGGGACCTTCTGTGATCCTCG
h Nox2	GTCACACCCTTCGCATCCATTCTCAAGTCAGT	CTGAGACTCATCCCAGCCAGTGAGGTAG
h Nox1	TTCACCAATTCCCAGGATTGAAGTGGATGGTC	GACCTGTCACGATGTCAGTGGCCTTGTCAA
h Nox4	CTGGAGGAGCTGGCTCGCCAACGAAG	GTGATCATGAGGAATAGCACCACCACCATGCAG
h iNOS	GACCTGGGACCCGCACCACT	AGGATGGTGGCACGGCTGGA
h TNFα	TGGAGAAGGGTGACCGACTC	TCCTCACAGGGCAATGATCC
h IL1β	CTGTACGATCACTGAACTGC	CACCACTTGTTGCTCCATATC
h ARG1	TTCTCAAAGGGACAGCCACG	AGCACCAGGCTGATTCTTCC
h MRC1	GGAGTGATGGAACCCCAGTG	CTGTCCGCCCAGTATCCATC
h TGM2	TTCAGGGTACAAACTGAGGCTGCT	TATTCAAGTTCACCCACTGGCCCT

content was determined with the Bradford assay [15]. Samples were boiled in reducing the Laemmli sample buffer and were subjected to SDS-PAGE followed by Western Blotting. After incubation with first antibodies, membranes were analyzed with an infrared-based detection system, using fluorescent dye-conjugated secondary antibodies from LI-COR Biosciences.

2.6. Electrophoretic Mobility Shift Assay. The electrophoretic mobility shift assay (EMSA) was performed according to the manufacturer protocol (LI-COR). Shortly, cells were lysed, and nuclear extract was gained as described above. 5 μg nuclear extract (14 μl including water and sample) was incubated with 2 μl 10x binding buffer (100 mM Tris, 500 mM KCl, and 10 mM DTT; pH 7.5), 1 μl poly(dI·dC) (1 μg/μl in 10 mM Tris and 1 mM EDTA; pH 7.5), 2 μl 25 mM DTT/2.5% Tween® 20 (all components of the Odyssey® EMSA Buffer Kit #829-07910), and 1 μl IRDye® NFκB Oligonucleotide for 30 min in the dark. After that, 10x Orange loading buffer was added, and the total mixture was loaded onto a 4% native polyacrylamide gel. Detection was performed with an Odyssey® Infrared Imaging System at 700 nm.

2.7. ROS Measurements with Chemiluminescence. After polarization, macrophages were dissociated from the plate with Ca^{2+}-free EDTA/EGTA (Versene). ROS levels were assessed in intact cells with either L-012 (200 μmol/l) or luminol (100 μmol/l)/horseradish peroxidase (HRP at 1 U/ml) in a Berthold 6-channel luminometer (LB9505, Berthold, Wildbad, Germany). All measurements were performed in the HEPES-Tyrode (HT) buffer containing (in mmol/l) 137 NaCl, 2.7 KCl, 0.5 $MgCl_2$, 1.8 $CaCl_2$, 5 glucose, 0.36 NaH_2PO_4, and 10 HEPES. Substances added during the experiment were used as follows: PMA 100 nM, DPI 10 μM, L-NAME 300 μM, PEG-catalase 250 U/ml, and PEG-SOD 50 U/ml.

2.8. Flow Cytometry. Tumor tissue was lysed with the aid of the tumor dissociation kit, mouse (Miltenyi) according to the manufacturer protocol. 3*10*E*6 cells were used for flow cytometry. Cells were pelleted by centrifugation at 500 g and resuspended in 100 μl PBS+0.5% BSA. CD16/32 blocking antibody was added to the cells for 15 minutes subsequently followed by a 15-minute incubation with the prepared mastermix of all antibodies indicated in Table 2. After staining, FACS flow was added; cells were centrifuged and resuspended in FACS flow for measurement. Samples were acquired with a LSRII/Fortessa flow cytometer (BD Biosciences) and analyzed using FlowJo software Vx (Treestar).

2.9. Statistics. All values are displayed as mean ± SEM. Statistical analysis was performed by ANOVA followed by LSD post hoc testing or by the t test if appropriate. Densitometry was performed with the aid of the Odyssey software. A p value of less than 0.05 was considered statistically significant.

3. Results

3.1. Nox4 Deficiency Promotes Inflammation in Murine Fibrosarcomas. In a murine fibrosarcoma model, the absence of Nox4 forces tumor growth [16]. Simultaneously, mRNA abundance of proinflammatory cytokines such as IL1β and TNFα and other markers of inflammation, such as ICAM-1, was elevated (Figure 1(a)). Accordingly, IL1β and TNFα

Table 2: Antibodies used.

Antigen	Dye
CD3	PE-CF594
CD4	V500
CD8	BV650
CD11b	eFluor 605
CD11c	Alexa Fluor 700
CD19	APC-H7
CD45	VioBLue
CD49b	PE-CF594
F4/80	PE-Cy7
HLA-DR (MHCII)	APC-H7
Ly-6C	PerCP-Cy5.5
Ly-6G	APC-Cy7
Siglec H	FITC

were elevated, when measured with an ELISA or a cytometric bead assay, respectively. In contrast, the anti-inflammatory cytokine IL10 was strongly reduced in tumors of Nox4-deficient mice (Figure 1(b)). These data point towards a more severe inflammation in tumors of Nox4-/- mice. However, the total number of immune cells per tissue was similar in wild type and Nox4-/- mice (Supplemental Figure 1) as measured by flow cytometry. Therefore, we analyzed the number of proinflammatory macrophages, identified by high expression of the surface marker Ly6C [17], and found a substantial increase in $Ly6C^{hi}$ monocytes in the tumors of Nox4-/- mice (Figure 1(c)). When we further analyzed the tumor tissue for pro- and anti-inflammatory markers, we observed a trend towards more inflammation, together with lower expression of markers typical for M(IL4+IL13)-polarized macrophages (Supplemental Figure 2). Accordingly, we conclude that the absence of Nox4 favors the polarization of macrophages towards a proinflammatory phenotype, which was further investigated.

3.2. Loss of Nox4 Promotes M(LPS+IFNγ) Polarization of Macrophages. Human and murine macrophages were generated and analyzed for the expression of individual NADPH oxidases. As expected, Nox2 expression was the highest in both macrophage populations, followed by Nox4 and Nox1 (Supplemental Figure 3). In order to analyze if Nox4 influences macrophage polarization, we isolated monocytes from bone marrow of wild type and Nox4-deficient mice, challenged them (with M-CSF) to become macrophages, and eventually polarized them to either M(LPS+IFNγ) or M(IL4+IL13) phenotype. Nox4 knockout promoted the expression of M(LPS+IFNγ) macrophage markers including TNFα and IL1β (Figure 2(a)), whereas typical M(IL4+IL13) markers were significantly downregulated (Figure 2(b)). This effect was mediated by H_2O_2, the product of Nox4: external H_2O_2 or increased intracellular H_2O_2 formation via PMA-induced activation of Nox2 and conversion of the resulting $\cdot O_2^-$ into H_2O_2 by SOD induced M(IL4+IL13) polarization. Depletion of H_2O_2 by catalase forces the expression of M(LPS+IFNγ) markers, both without any further treatment with cytokines (Supplemental Figure 4). Exemplary verification of the PCR results on the protein level revealed the same effect for the M(IL4+IL13) marker YM1 (Figure 2(c)). STAT6 is one of the main transcription factors involved in the expression of M(IL4+IL13) markers. In line with the decreased level of M(IL4+IL13) markers in Nox4-/- cells, phosphorylation of STAT6 was attenuated (Figure 2(d)). In order to analyze whether or not the effects seen are specific for Nox4, macrophage polarization was determined in Nox2- and Nox1-deficient macrophages as well. In contrast to Nox4-/- macrophages, loss of Nox2 induced a small but significant reduction in M(LPS+IFNγ) polarization with no effect on M(IL4+IL13) polarization or STAT6 phosphorylation (Supplemental Figure 5). Knockout of Nox1 had no effect on macrophage polarization, compared to wild type littermates (Supplemental Figure 6).

3.3. Formation of Reactive Oxygen Species upon M(LPS+IFNγ) Polarization Is Elevated in the Absence of Nox4. Several publications indicate that polarization of macrophages is dependent on ROS production and simultaneously forces ROS formation [18]. Polarization of macrophages towards the proinflammatory M(LPS+IFNγ) phenotype resulted in an increase in superoxide anion as well as in hydrogen peroxide production compared to M(IL4+IL13)-polarized macrophages (Figures 3(a) and 3(b)). Surprisingly, the absence of Nox4 further increased ROS formation in M(LPS+IFNγ)-polarized macrophages (Figures 3(a) and 3(b)). A major source of ROS in M(LPS+IFNγ)-polarized macrophages is Nox2, whose expression was elevated in Nox4-deficient M(LPS+IFNγ)-polarized macrophages (Figure 3(c)). Accordingly, when measuring $\cdot O_2^-$ in a more specific way with the aid of L-012 in intact cells, we found that both LPS and IFNγ separately increase the level of $\cdot O_2^-$ production in macrophages as well as the combination of both (Figure 3(d)). Knockout of Nox2 in macrophages completely abolished L-012 detectable $\cdot O_2^-$ formation (Figure 3(e)). In conclusion, the increase in Nox2 expression, which predominantly produces $\cdot O_2^-$ over H_2O_2, indicates that Nox2 is the major source of ROS in M(LPS+IFNγ)-polarized macrophages.

3.4. Nox4 Mediates the Proinflammatory Macrophage Polarization via Activation of NFκB. Inflammation is often associated with an increased activity of NFκB [19]. Indeed, TNFα and IL1β as well as ICAM-1 and Nox2 are target genes of NFκB. Therefore, we analyzed the potential role of Nox4 in NFκB activation in the course of macrophage polarization.

M(LPS+IFNγ) polarization was accompanied by an increased translocation of p65 from the cytosol to the nucleus in the Nox4-deficient macrophages when compared to wild type cells (Figures 4(a) and 4(b)). However, nuclear translocation alone is not sufficient as the indicator of a transcription factor activity. In order to test for both, NFκB nuclear translocation and DNA binding activity, an electro mobility shift assay (EMSA) was utilized. Activity of NFκB was enhanced in M(LPS+IFNγ) macrophages in the absence

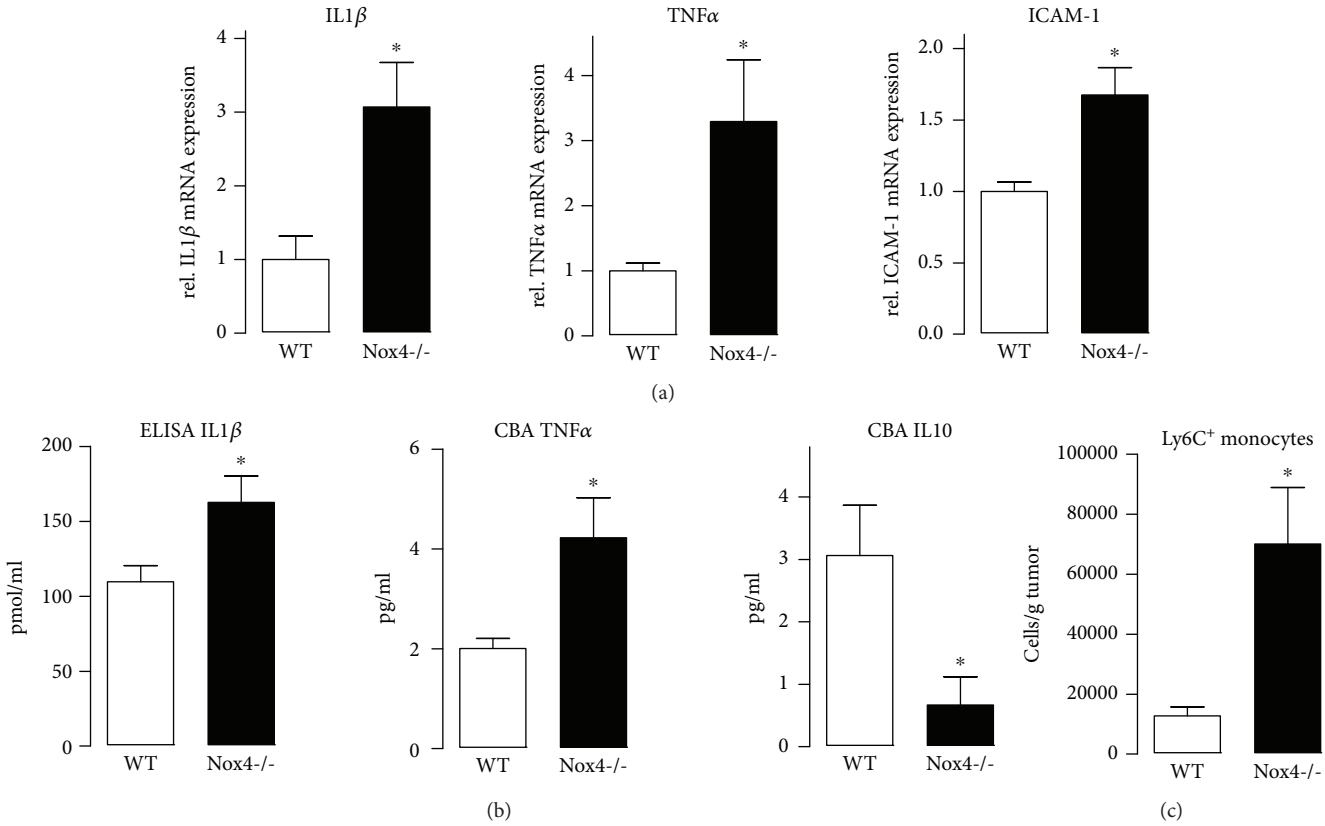

Figure 1: Nox4 deficiency favors inflammation in a murine tumor model. (a) Proinflammatory markers including the cytokines IL1β and TNFα and the adhesion molecule ICAM-1 were quantified by RT-qPCR in tumor tissue of WT and Nox4-/- mice. (b) Proinflammatory markers IL1β (ELISA) and TNFα as well as IL10 (CBA: cytometric bead assay) as anti-inflammatory markers were measured in tumor tissue, $n = 3$; $^*p < 0.05$. (c) Single-cell suspension of tumor tissue was analyzed by FACS for Ly6C$^+$ monocytes; $^*p < 0.05$, $n = 5$-10.

of Nox4 (Figure 4(c)). In M(IL4+IL13)-polarized macrophages, no such effect of Nox4 was observed.

3.5. Activated NFκB Promotes Nox2 Expression in the Absence of Nox4. NFκB is one of the transcription factors that control Nox2 expression. We therefore hypothesized that elevated activation of NFκB in the absence of Nox4 promotes Nox2 expression during macrophage M(LPS+IFNγ) polarization. The upregulation of Nox2 however is not accompanied by an elevated expression of its cytosolic subunits or antioxidative enzymes such as SOD1 or 3 in wild type vs. Nox4-/- cells (Supplemental Figure 7). Treatment of the cells with an NFκB inhibitor prevented the increase in p65 nuclear translocation (Supplemental Figure 8), and Nox2 expression was reduced in Nox4-/- macrophages to the level similar to that of the wild type, when cells were pretreated with the NFκB inhibitor prior to M(LPS+IFNγ) polarization (Figure 4(d)). NFκB acts in concert with other transcription factors to regulate the expression of Nox2 [20]. One of which is the redox-sensitive zinc-finger transcription factor Yin Yang 1 (YY1), which directly controls the activity of NFκB [21]. As such, YY1 represents a potential target of Nox4-derived ROS, which is upstream of NFκB and controls Nox2 expression. A significant increase in the YY1 protein level was observed in M(LPS+IFNγ)-polarized Nox4-/- macrophages; which was not the case for M(IL4+IL13)-polarized macrophages (Supplemental Figure 9A). Inhibition of Nox4 with GKT137928 in Nox2-deficient macrophages results in a small but significant increase in LPS and IFNγ-induced M(LPS+IFNγ) polarization. Under basal conditions, treatment with GKT only increased iNOS, compared to DMSO-treated samples. Those results indicate that inhibition of Nox4 favors M(LPS+IFNγ) polarization even in the absence of Nox2 (Supplemental Figure 10). The interpretation of this result could be that NFκB even in the absence of Nox2 promotes M(LPS +IFNγ) polarization in macrophages. Although many studies provide evidence for the involvement of NFκB in macrophage polarization, the exact role of NFκB and its effects besides induction of Nox2 are unclear. Therefore, investigation of how NFκB triggers M(LPS+IFNγ) polarization in the absence of Nox2 would be worth a second study. Another transcription factor involved in M(LPS+IFNγ) polarization is STAT1 [22]. We therefore checked for a potential effect of Nox4 on phosphorylation of STAT1 in M(LPS+IFNγ) polarization without observing any effect of Nox4 (Supplemental Figure 9B). Thus, Nox4 appears to selectively regulate the activity of NFκB and potentially YY1. In conclusion, the absence of Nox4 promotes Nox2 expression and subsequently M(LPS+IFNγ) polarization of macrophages.

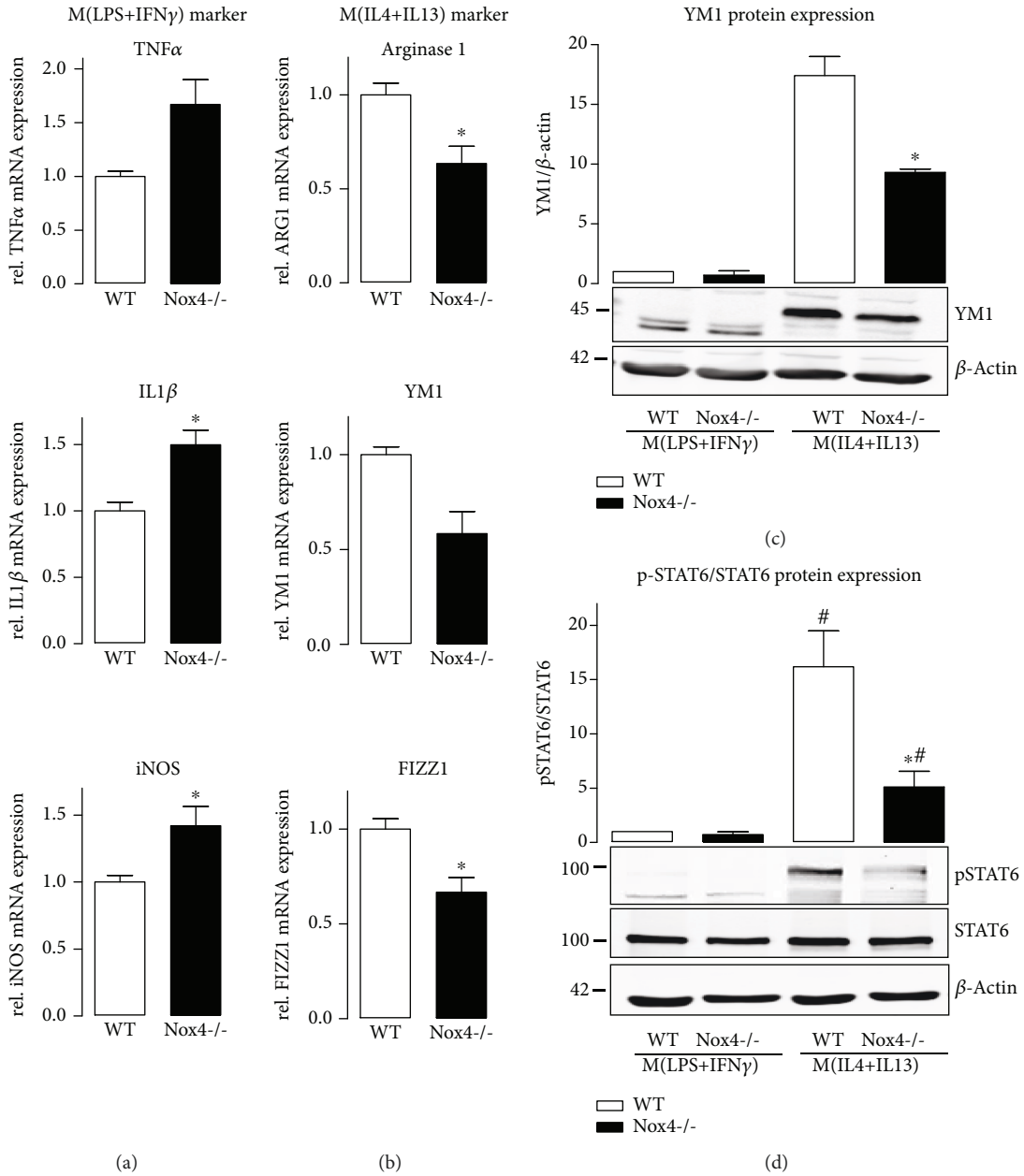

Figure 2: Nox4 knockout leads to a decreased M(IL4+IL13) polarization of macrophages. The specific M(LPS+IFNγ) markers IL1β, TNFα, and iNOS (a) and specific M(IL4+IL13) markers arginase 1, YM1, and FIZZ1 (b) were quantified by RT-qPCR after stimulation with cytokines polarizing the bone marrow-derived macrophages from WT and Nox4-/- mice to M(LPS+IFNγ) or M(IL4+IL13) phenotype. Protein expression of the M(IL4+IL13) marker YM1 (c) and the ratio of pSTAT6 to STAT6 (d) as determined by Western Blot; $^{*}p < 0.05$ WT vs. Nox4-/- and $\#p < 0.05$ WT/Nox4-/- M(LPS+IFNγ) vs. WT/Nox4-/- M(IL4+IL13), $n = 5$-6.

3.6. Pharmacological Inhibition of Nox4 Promotes M(LPS+IFNγ) Polarization of Human Macrophages. In order to determine whether our findings in a mouse can be translated to human cells, human macrophages generated from peripheral blood of healthy donors were analyzed. Inhibition of Nox4 was achieved by treatment of the cells with the Nox1/Nox4 inhibitor GKT137928. Upon treatment of the macrophages with GKT137928, an increased M(LPS+IFNγ) polarization was observed. This was accompanied by a decrease in M(IL4+IL13) polarization (Figure 5). As shown above in the murine system, knockout of Nox1 has no influence on macrophage polarization. Therefore, we assume that usage of the inhibitor will mainly affect Nox4-mediated signaling in the process of polarization. We conclude that the findings in the murine system also apply to the human system.

4. Discussion

Macrophages are a heterogeneous population of cells. Generally, they can be categorized into two discrete subsets as either classically activated M1 or alternatively activated

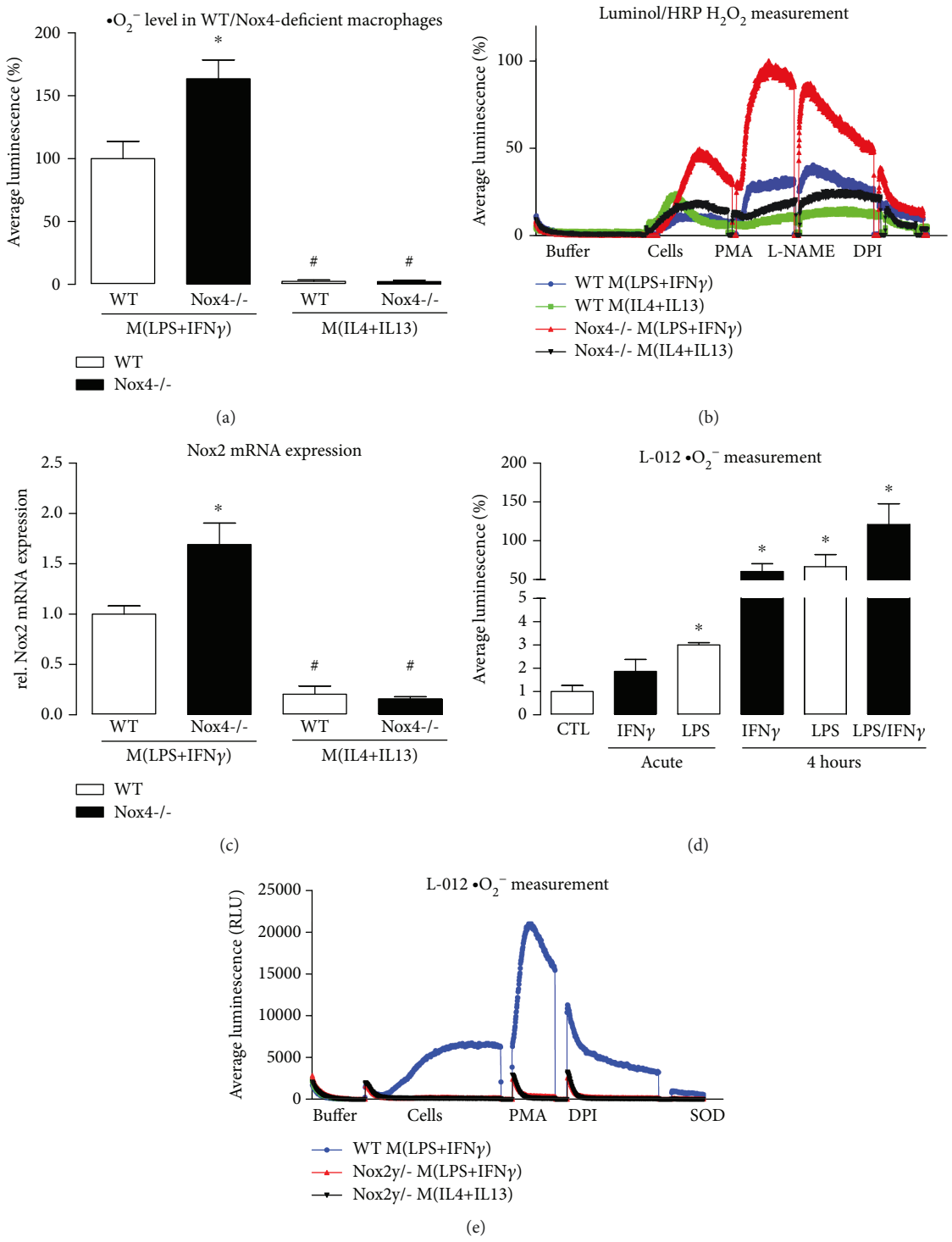

Figure 3: ROS measurements reveal increased ROS production in Nox4-deficient cells due to an increase in Nox2. Superoxide anion production measured with L-012 (a) and hydrogen peroxide levels measured with luminol and HRP (b) in polarized macrophages of wild type and Nox4 knockout mice. (c) RT-qPCR for Nox2 mRNA expression in polarized macrophages of WT and Nox4-deficient animals; $^{*}p < 0.05$ ($n = 3 - 8$). (d) Superoxide anion production, as measured with L-012 in WT macrophages with or without LPS (10 μg/ml) and IFNγ (100 U/ml) directly after stimulation or 4 hours after addition. (e) Superoxide anion production in polarized WT and Nox2-deficient macrophages; $^{*}p < 0.05$ WT vs. Nox4-/- or treated vs. CTL and $\#p < 0.05$ WT/Nox4-/- M(LPS+IFNγ) vs. WT/Nox4-/- M(IL4+IL13) ($n = 3$-5).

M2 macrophages, herein referred to as M(LPS+IFNγ) or M(IL4+IL13). In this context, M(LPS+IFNγ) macrophages represent proinflammatory "killers," while M(IL4+IL13) macrophages serve as "builders" in inflammatory wound repair. This polarization of the macrophage population results from interactions with other cells or molecules within

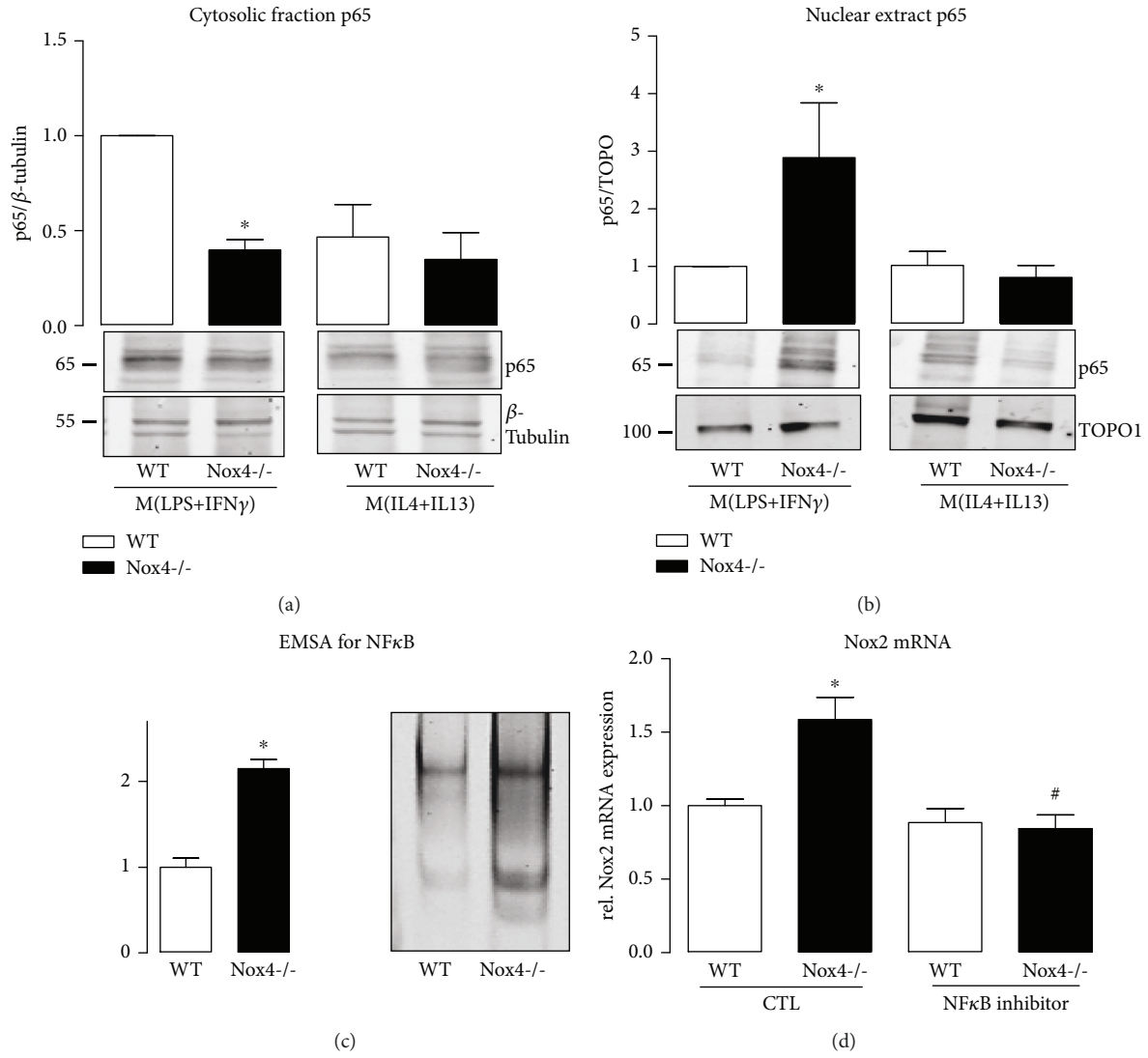

Figure 4: Increased NFκB activation in M(LPS+IFNγ)-polarized macrophages of Nox4-/- is responsible for elevated Nox2 expression. Translocation of p65 was analyzed by Western Blot in the cytosol (a) and nuclear fraction (b) of M(LPS+IFNγ)- and M(IL4+IL13)-polarized macrophages of WT and Nox4-/- mice. (c) Electrophoretic mobility shift assay for NFκB was performed in M(LPS+IFNγ)-polarized macrophages of WT and Nox4-/- animals. The left bar graph shows quantification, and the right bar graph representative shift. (d) Nox2 mRNA expression was quantified by RT-qPCR after M(LPS+IFNγ) polarization with and without an NFκB inhibitor (30 ng/ml, 1 h pretreatment before polarization); $^*p < 0.05$ WT vs. Nox4-/- and $\#p < 0.05$ CTL vs. NFκB inhibitor ($n = 3$-8). TOPO: topoisomerase I.

the host tissues [23]. In previous work, we found that knockout of the NADPH oxidase Nox4 enhances inflammation and tumorigenesis [16, 24]. In an angiotensin II-induced model of vascular dysfunction, loss of Nox4 promoted the expression of the proinflammatory cytokines IL6 and IL1β [12]. The present study underlines the protective potential of Nox4 in inflammation, as it promotes M(IL4+IL13) polarization of macrophages. Our results were confirmed in a very recent study in a myocardial infarction model, where overexpression of Nox4 promoted M(IL4+IL13) polarization of cardiac macrophages and protects from postinfarction remodeling [25].

The balance between activation of STAT1 and STAT3/STAT6 plays a crucial role in macrophage polarization: a predominance of STAT1 activation promotes M(LPS+IFNγ), while STAT3/STAT6 activation increases M(IL4+IL13) macrophage polarization [26]. In fact, STAT6 is the most important transcription factor regulating M(IL4+IL13) polarization of macrophages [27], and phosphorylation of STAT6 can be regulated by redox-sensitive phosphatases [28]. Therefore, it is likely that Nox4-derived H_2O_2 at least contributes to STAT6 phosphorylation and thereby to M(IL4+IL13) polarization. Importantly, STAT6 suppresses NFκB activation via Klf4. Here, we provide evidence that Nox4 deficiency prevents STAT6 phosphorylation and supports NFκB activation. NFκB has been shown to promote M(LPS+IFNγ) polarization of phagocytes [29]. Besides regulation by STAT6/Klf4, the activity of NFκB is redox sensitive and potentially regulated by NADPH oxidases [30]. Both, increased NFκB and reduced phosphorylation of STAT6,

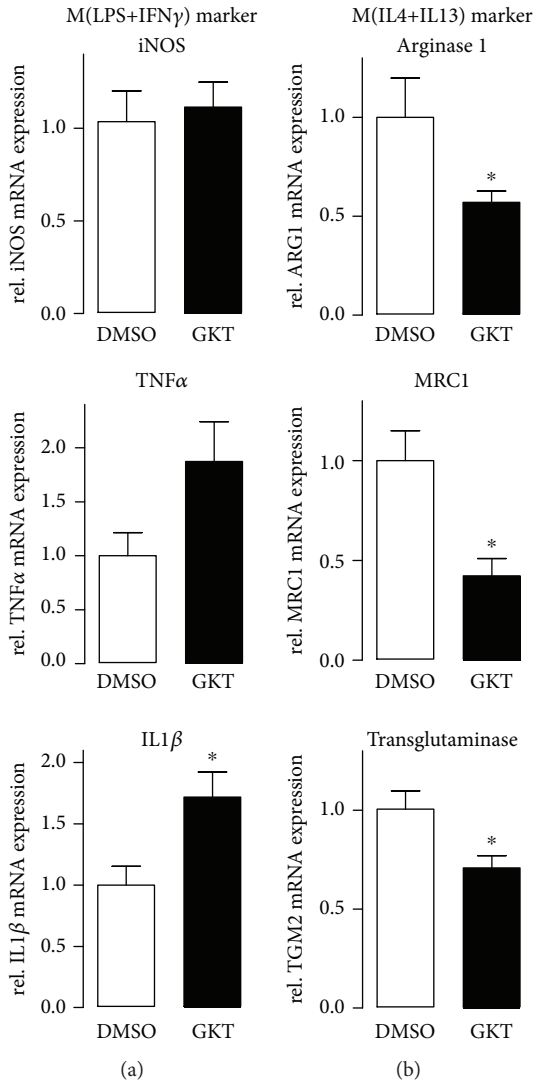

Figure 5: Treatment of human macrophages with the Nox4 inhibitor GKT137928 forces M(LPS+IFNγ) polarization. The specific M(LPS+IFNγ) markers iNOS, TNFα, and IL1β (a) and M(IL4+IL13) markers arginase 1, MRC1, and transglutaminase 2 (b) were quantified by RT-qPCR. Cells were preincubated with Nox4 inhibitor GKT (10 μM, 2 h) followed by stimulation with cytokines polarizing human macrophages; $^*p < 0.05$ ($n = 6$).

inhibit the polarization of macrophages towards the M(IL4+IL13) phenotype. Consequently, since there exists an intrinsic balance, less force in the direction of M(IL4+IL13) will lead to more M(LPS+IFNγ) polarization, as observed in the current study. Since Nox4 produces H_2O_2, a Nox4 knockout would naturally lead to a reduced production of H_2O_2. Therefore, our data can be supported by a finding concerning CuZn-SOD, an enzyme catalyzing the conversion of superoxide anion to hydrogen peroxide. Consequently, less H_2O_2 is formed in the absence of CuZn-SOD. Knockout of this enzyme promotes M(IL4+IL13) polarization of macrophages [8], favoring the hypothesis that indeed H_2O_2 mediates the effect of Nox4.

Different to Nox4, Nox2 produces superoxide anions ($\cdot O_2^-$), and knockout of Nox2 results in a decreased M(LPS+IFNγ) polarization. In contrast, Nox2, via production of superoxide anions, contributes to M(LPS+IFNγ) polarization [6]. We observed not only a reduced M(LPS+IFNγ) polarization in Nox2-deficient macrophages but also an increase in Nox2 expression and subsequently $\cdot O_2^-$ formation, in Nox4 knockout macrophages. This is potentially a consequence of the abovementioned enhanced NFκB activation in the absence of Nox4, as Nox2 expression is enhanced by NFκB [31].

We conclude that the specific types of ROS, such as H_2O_2 or $\cdot O_2^-$, differentially contribute to M(LPS+IFNγ) or M(IL4+IL13) macrophage polarization. Importantly, knockout of Nox4 not only favors M(LPS+IFNγ) polarization but also results in an increased expression of Nox2 in M(LPS+IFNγ)-polarized macrophages.

Data Availability

All data used to support the findings of this study are included within the article or the supplements.

Conflicts of Interest

The authors declare no conflict of interest.

Acknowledgments

This research was supported by the Else KrÖner-Fresenius-Stiftung Foundation (EKFS), Research Training Group Translational Research Innovation–Pharma (TRIP), and Cardio-Pulmonary Institute (CPI), EXC 2026, Project ID: 390649896 and by grants from the Deutsche Forschungsgemeinschaft (DFG) (to KS; SCHR1241/1-1, SFB815/TP1, and SFB834/TPA2).

Supplementary Materials

Supplemental Figure 1: FACS analysis of tumor tissue revealed only a tendency for differences in B cells within Nox4-deficient tumors. (A) Fibrosarcoma tissues of wild type and Nox4-/- mice were analyzed for cell composition with FACS using specific antibodies for cells indicated. The table contains the different T cell populations in cells/g tumor tissue, no statistical differences ($n = 6$-10). Supplemental Figure 2: tumor tissue was analyzed for different inflammatory and anti-inflammatory markers. (A) Fibrosarcoma tissues of wildtype and Nox4-/- mice were analyzed for proinflammatory markers iNOS and CD163, anti-inflammatory markers FIZZ1, arginase 1, and YM1, and tissue remodeling markers MMP9 and collagens I and III with RT-qPCR; $^*p < 0.05$ ($n = 6$-10). Supplemental Figure 3: NADPH oxidase expression in isolated murine and human macrophages. Nox1, Nox2, and Nox4 expressions were determined by RT-qPCR in isolated murine (A) and human (B) macrophages, and corresponding CT values were included ($n = 3$). Supplemental Figure 4: H_2O_2 mediates polarization of macrophages without cytokine stimulation. (A) WT macrophages were treated with basal medium or IL4 and IL13 to polarize. For polarization without cytokines, cells were treated with 5 μM H_2O_2 or PEG-SOD (50 U/ml) and PMA (100 nM) for 4 h,

and polarization markers ARG1, FIZZ1, and YM1 were quantified with RT-qPCR; $^{*}p < 0.05$ ($n = 6$). (B) WT macrophages were treated with basal medium or LPS and IFNγ or PEG-catalase (500 U/ml) for 4 h to polarize, followed by subsequent analysis of polarization markers TNFα, IL1β, and iNOS; $^{*}p < 0.05$ ($n = 3$). Supplemental Figure 5: Nox2 knockout decreases M(LPS+IFNγ) polarization of macrophages. The specific M(LPS+IFNγ) markers IL1β, TNFα, and iNOS (A) and specific M(IL4+IL13) markers arginase 1, YM1, and FIZZ1 (B) were quantified by RT-qPCR after stimulation with cytokines polarizing the bone marrow-derived macrophages from Nox2KO/C57Bl6J mice to M(LPS+IFNγ) or M2(IL4+IL13) phenotype. Protein expression of the M(IL4+IL13) marker YM1 (C) and the ratio of pSTAT6 to STAT6 (D) as determined by Western Blot; $^{*}p < 0.05$ and $\#p < 0.05$ WT/Nox2y/- M(LPS+IFNγ) vs. WT/Nox2y/- M(IL4+IL13) ($n = 4 - 8$). Supplemental Figure 6: deficiency in Nox1 does not affect polarization of macrophages. The specific M(LPS+IFNγ) markers IL1β, TNFα, and iNOS (A) and specific M(IL4+IL13) markers arginase 1, YM1, and FIZZ1 (B) were quantified by RT-qPCR after stimulation with cytokines polarizing the bone marrow-derived macrophages from Nox1KO/C57Bl6J mice to M(LPS+IFNγ) or M2(IL4+IL13) phenotype. Protein expression of the M(IL4+IL13) marker YM1 (C) and the ratio of pSTAT6 to STAT6 (D) as determined by Western Blot; $^{*}p < 0.05$ and $\#p < 0.05$ WT/Nox1y/- M(LPS+IFNγ) vs. WT/Nox1y/- M(IL4+IL13) ($n = 3 - 6$). Supplemental Figure 7: SOD and Nox2 cytosolic subunit expressions in WT and Nox4-deficient macrophages. SOD1 (A) and SOD3 (B) expressions were analyzed in WT and Nox4-/- M(LPS+IFNγ)- and M(IL4+IL13)-polarized macrophages by RT-qPCR. Expressions of cytosolic Nox2 subunits (C: p40phox, D: p47phox, and E: p67phox) and Nox1 (F) were analyzed in WT and Nox4-/- M(LPS+IFNγ)- and M(IL4+IL13)-polarized macrophages using RT-qPCR; $^{*}p < 0.05$ WT/Nox4-/- M(LPS+IFNγ) vs. WT/Nox4-/- M(IL4+IL13) ($n = 5$-8). Supplemental Figure 8: NFκB inhibition prevents p65 translocation into the nucleus in M(LPS+IFNγ)-polarized macrophages of Nox4-/-. P65 expression in cytosol (A) and nucleus (B) was assessed with Western Blot after M(LPS+IFNγ) polarization with and without treatment of NFκB inhibitor (30 ng/ml, 1 h pretreament before M(LPS+IFNγ) polarization); $^{*}p < 0.05$ WT vs. Nox4-/- and $\#p < 0.05$ CTL vs. NFκB inhibitor ($n = 3$-8). TOPO: topoisomerase I. Supplemental Figure 9: YY1 is increased in Nox4-deficient macrophages after M(LPS+IFNγ) polarization. (A) YY1 expression was determined by Western Blot after polarization of WT and Nox4-/- macrophages. (B) Phosphorylation of pSTAT1 and total STAT1 quantified by Western Blot in M(LPS+IFNγ)- and M(IL4+IL13)-polarized macrophages of WT and Nox4-deficient animals; $^{*}p < 0.05$ WT vs. Nox4-/- and $\#p < 0.05$ WT/Nox4-/- M(LPS+IFNγ) vs. WT/Nox4-/- M(IL4+IL13) ($n = 3$-5). Supplemental Figure 10: inhibition of Nox4 in Nox2-deficient macrophages elevates M(LPS+IFNγ) polarization in M(LPS+IFNγ)-polarized macrophages. Nox2-deficient macrophages were treated with Nox4 inhibitor GKT (10 μM) 2 h prior to cell polarization to M(LPS+IFNγ) or only control medium (CTL). M(LPS+IFNγ) markers TNFγ, IL1β, and iNOS were evaluated using RT-qPCR; $^{*}p < 0.05$ DMSO vs. GKT and $\#p < 0.05$ DMSO/GKT CTL vs. DMSO/GKT M(LPS+IFNγ) ($n = 3$). *(Supplementary Materials)*

References

[1] M. Ushio-Fukai and Y. Nakamura, "Reactive oxygen species and angiogenesis: NADPH oxidase as target for cancer therapy," *Cancer Letters*, vol. 266, no. 1, pp. 37–52, 2008.

[2] L. Serrander, L. Cartier, K. Bedard et al., "NOX4 activity is determined by mRNA levels and reveals a unique pattern of ROS generation," *The Biochemical Journal*, vol. 406, no. 1, Part 1, pp. 105–114, 2007.

[3] K. Bedard and K.-H. Krause, "The NOX family of ROS-generating NADPH oxidases: physiology and pathophysiology," *Physiological Reviews*, vol. 87, no. 1, pp. 245–313, 2007.

[4] A. Weigert, A. von Knethen, D. Fuhrmann, N. Dehne, and B. Brüne, "Redox-signals and macrophage biology," *Molecular Aspects of Medicine*, vol. 63, pp. 70–87, 2018.

[5] P. J. Murray, J. E. Allen, S. K. Biswas et al., "Macrophage activation and polarization: nomenclature and experimental guidelines," *Immunity*, vol. 41, no. 1, pp. 14–20, 2014.

[6] A. Kumar, J. P. Barrett, D.-M. Alvarez-Croda, B. A. Stoica, A. I. Faden, and D. J. Loane, "NOX2 drives M1-like microglial/macrophage activation and neurodegeneration following experimental traumatic brain injury," *Brain, Behavior, and Immunity*, vol. 58, pp. 291–309, 2016.

[7] D. Sanmun, E. Witasp, S. Jitkaew et al., "Involvement of a functional NADPH oxidase in neutrophils and macrophages during programmed cell clearance: implications for chronic granulomatous disease," *American Journal of Physiology-Cell Physiology*, vol. 297, no. 3, pp. C621–C631, 2009.

[8] D. R. Balce, B. Li, E. R. O. Allan, J. M. Rybicka, R. M. Krohn, and R. M. Yates, "Alternative activation of macrophages by IL-4 enhances the proteolytic capacity of their phagosomes through synergistic mechanisms," *Blood*, vol. 118, no. 15, pp. 4199–4208, 2011.

[9] C. He, A. J. Ryan, S. Murthy, and A. B. Carter, "Accelerated development of pulmonary fibrosis via Cu,Zn-superoxide dismutase-induced alternative activation of macrophages," *The Journal of Biological Chemistry*, vol. 288, no. 28, pp. 20745–20757, 2013.

[10] C. F. Lee, M. Qiao, K. Schröder, Q. Zhao, and R. Asmis, "Nox4 is a novel inducible source of reactive oxygen species in monocytes and macrophages and mediates oxidized low density lipoprotein-induced macrophage death," *Circulation Research*, vol. 106, no. 9, pp. 1489–1497, 2010.

[11] K. Schroder, K. Wandzioch, I. Helmcke, and R. P. Brandes, "Nox4 acts as a switch between differentiation and proliferation in preadipocytes," *Arteriosclerosis, Thrombosis, and Vascular Biology*, vol. 29, no. 2, pp. 239–245, 2009.

[12] C. Goettsch, A. Babelova, O. Trummer et al., "NADPH oxidase 4 limits bone mass by promoting osteoclastogenesis," *The Journal of Clinical Investigation*, vol. 123, no. 11, pp. 4731–4738, 2013.

[13] K. Schröder, M. Zhang, S. Benkhoff et al., "Nox4 is a protective reactive oxygen species generating vascular NADPH oxidase," *Circulation Research*, vol. 110, no. 9, pp. 1217–1225, 2012.

[14] G. Gavazzi, C. Deffert, C. Trocme, M. Schäppi, F,. R. Herrmann, and K. H. Krause, "NOX1 deficiency protects

from aortic dissection in response to angiotensin II," *Hypertension*, vol. 50, no. 1, pp. 189–196, 2007.

[15] M. M. Bradford, "A rapid and sensitive method for the quantitation of microgram quantities of protein utilizing the principle of protein-dye binding," *Analytical Biochemistry*, vol. 72, no. 1-2, pp. 248–254, 1976.

[16] V. Helfinger, F. F. von Gall, N. Henke et al., "Hydrogen peroxide formation by Nox4 limits malignant transformation," http://arxiv.org/abs/2017:177055. https://www.biorxiv.org/content/early/2017/08/16/177055.full.pdf.

[17] F. Geissmann, M. G. Manz, S. Jung, M. H. Sieweke, M. Merad, and K. Ley, "Development of monocytes, macrophages, and dendritic cells," *Science*, vol. 327, no. 5966, pp. 656–661, 2010.

[18] H.-Y. Tan, N. Wang, S. Li, M. Hong, X. Wang, and Y. Feng, "The reactive oxygen species in macrophage polarization: reflecting its dual role in progression and treatment of human diseases," *Oxidative Medicine and Cellular Longevity*, vol. 2016, Article ID 2795090, 16 pages, 2016.

[19] Y. Zhou, T. Zhang, X. Wang et al., "Curcumin modulates macrophage polarization through the inhibition of the Toll-like receptor 4 expression and its signaling pathways," *Cellular Physiology and Biochemistry*, vol. 36, no. 2, pp. 631–641, 2015.

[20] J. D. Lambeth, "Nox enzymes, ROS, and chronic disease: an example of antagonistic pleiotropy," *Free Radical Biology & Medicine*, vol. 43, no. 3, pp. 332–347, 2007.

[21] W. Zhu, S. Y. Olson, and H. J. Garbán, "Transcription regulator Yin-Yang 1: from silence to cancer," *Critical Reviews in Oncogenesis*, vol. 16, no. 3-4, pp. 227–238, 2011.

[22] Y.-B. Liang, H. Tang, Z.-B. Chen et al., "Downregulated SOCS1 expression activates the JAK1/STAT1 pathway and promotes polarization of macrophages into M1 type," *Molecular Medicine Reports*, vol. 16, no. 5, pp. 6405–6411, 2017.

[23] L. Parisi, E. Gini, D. Baci et al., "Macrophage polarization in chronic inflammatory diseases: killers or builders?," *Journal of Immunology Research*, vol. 2018, Article ID 8917804, 25 pages, 2018.

[24] C. Schürmann, F. Rezende, C. Kruse et al., "The NADPH oxidase Nox4 has anti-atherosclerotic functions," *European Heart Journal*, vol. 36, no. 48, pp. 3447–3456, 2015.

[25] H. Mongue-Din, A. S. Patel, Y. H. Looi et al., "NADPH oxidase-4 driven cardiac macrophage polarization protects against myocardial infarction–induced remodeling," *JACC: Basic to Translational Science*, vol. 2, no. 6, pp. 688–698, 2017.

[26] A. Sica and A. Mantovani, "Macrophage plasticity and polarization: in vivo veritas," *Journal of Clinical Investigation*, vol. 122, no. 3, pp. 787–795, 2012.

[27] T. Lawrence and G. Natoli, "Transcriptional regulation of macrophage polarization: enabling diversity with identity," *Nature Reviews. Immunology*, vol. 11, no. 11, pp. 750–761, 2011.

[28] S. Hirakawa, R. Saito, H. Ohara, R. Okuyama, and S. Aiba, "Dual oxidase 1 induced by Th2 cytokines promotes STAT6 phosphorylation via oxidative inactivation of protein tyrosine phosphatase 1B in human epidermal keratinocytes," *Journal of Immunology*, vol. 186, no. 8, pp. 4762–4770, 2011.

[29] N. Wang, H. Liang, and K. Zen, "Molecular mechanisms that influence the macrophage M1–M2 polarization balance," *Frontiers in Immunology*, vol. 5, p. 614, 2014.

[30] G. Bonizzi, J. Piette, S. Schoonbroodt et al., "Reactive oxygen intermediate-dependent NF-kappaB activation by interleukin-1beta requires 5-lipoxygenase or NADPH oxidase activity," *Molecular and Cellular Biology*, vol. 19, no. 3, pp. 1950–1960, 1999.

[31] J. Anrather, G. Racchumi, and C. Iadecola, "NF-kappaB regulates phagocytic NADPH oxidase by inducing the expression of gp91phox," *The Journal of Biological Chemistry*, vol. 281, no. 9, pp. 5657–5667, 2006.